January 2010

Revision 40

NAC-LWT

Legal Weight Truck Cask System

SAFETY ANALYSIS REPORT

Volume 1 of 2

Docket No. 71-9225

NAC INTERNATIONAL

Atlanta Corporate Headquarters: 3930 East Jones Bridge Road, Norcross, Georgia 30092 USA
Phone 770-447-1144, Fax 770-447-1797, www.nacintl.com

RECORD OF REVISIONS

Issue Date	Revision Number	Change	Description of Change
March 1988	0	N/A	Initial Release.
August 1988	1	2.10.8	Incorporate Drop Test Results.
July 1989	2	Throughout	General rewrite and reissue to incorporate NAC responses to NRC comments.
September 1989	3	Throughout	Provide revised stress tables. Clarify post-drop test revisions. Change from Fissile Class I to Fissile Class III. Vacuum drying required for PWR and BWR fuels.
November 1989	4	Throughout	Revise to Type B(U). Clarification of side and end drop analyses for the neutron shield and expansion tank. Correct containment calculations. Revise operating procedures.
June 1990	5		Deleted.
July 1990	6	2.10.14 and throughout	Incorporate failed metallic fuel as permissible contents of the packaging.
September 1990	6 (supplement)	7.1	Incorporate operational changes to 7/1990, Revision 6.

RECORD OF REVISIONS (continued)

Issue Date	Revision Number	Change	Description of Change
December 1990	7	2.10.13 and throughout	Renumber 2.10.14 as 2.10.13. Revise to include evaluation of three failed metallic fuel rods per canister.
August 1991	8	2.10.13	Revise to permit use of shipment of severely failed research reactor metallic fuel that has been accumulated in filters using failed fuel cans.
October 1991	9	1.0, 1.1, 1.2, 4.2, 4.4.3, 7.0, 7.1	Revise to incorporate response to NRC questions on Revision 8.
October 1994	10	1.4	Revise License Drawings to modify radiographic acceptance criteria.
November 1994	11	Throughout	Revise to permit shipment of MTR fuel.
January 1995	12	1.4	Revised License Drawings to incorporate new weld and inspection requirements.
March 1995	13	1.2, 2.2, 2.2.12.6, 5.1, 5.3.4, 6.4.4, 7.1.4	Submittal of consolidated SAR. Revised to incorporate responses to NRC questions on MTR fuel contents.
May 1995	14	1.4	Minor editorial corrections to consolidated SAR.

RECORD OF REVISIONS (continued)

Issue Date	Revision Number	Change	Description of Change
June 1995	15	Throughout	Revised to incorporate up to 25 individual PWR fuel rods as permissible contents.
August 1995	16	2.6.12.2	Revised to incorporate a description of the canister for individual intact PWR rods.
August 1995	17	2.6.12, 5.0, 5.1, 5.3, Table 6.2-1	Revised to incorporate shielding analysis for 25 PWR rods and editorial corrections.
October 1995	18	1,4,5 and 6	Revise to incorporate LEU MTR fuel elements as permissible contents.
December 1995	19	1.4	Submit revised MTR basket drawings incorporating additional fabrication details.
March 1996	20	1.2, 1.4, 7.1 and 7.2	Submit revised drawings for alternate drain configuration.
December 1997	21	1.2, 2.1.3, 2.4.3, 2.6, 2.7, 3.1, 3.4, 4.4, 5.0, 7.1.4, 7.1.5, 8.2, 9.0	Incorporates HEU MTR analysis for varying burnup and cool time. Incorporates note to clarify bolt thread chrome-plate requirements.
May 1998	22	1.0, 1.1, 1.2, 2.1, 2.6.12, 2.7.7, 2.9 (various), 3.1, 3.4, 3.5, 4.0 (all), 5.0, 5.1, 5.3, 6.0 (various), 7.0 (all), 8.1, 9.0	Incorporates 120 element TRIGA fuel analysis.
November 1998	23	1.0, 1.2.3, 2.7.1.6, 2.7.3, 2.7.5, 2.10.13.8, 3.2, 3.4, 3.5, 4.2, 4.3, 4.4, 5.1, 6 (all), 7.1, 8.1, 9.0	Incorporates changes for B(U)F-85 certification.

RECORD OF REVISIONS (continued)

Issue Date	Revision Number	Change	Description of Change
December 1998	24	1.2.3, 2.2.0, 2.3.0, 2.6.12, 2.7.7, 4.2, 4.3, 4.5.3, 5.1, 5.3.4, 6.4.3, 7.1, 7.2	Incorporates MTR-35 basket configuration, failed MTR fuel containment analysis, and various minor editorial changes.
February 1999	25	6.2.3 and 6.4.3	Added additional MTR configuration.
April 1999	26	1.0, 1.1, 1.2.2, 1.2.3, 2.6.12.7, 2.7.7.6, 2.7.7.9, 3.4.1.5, 3.4.1.6, 3.5.3.4, 4.2.1, 4.5.3, 5.0, 5.1, 5.3.6, 5.3.7, 6.0, 6.1, 6.2, 6.2.5, 6.2.6, 6.2.7, 6.3, 6.3.5, 6.4.5, 6.4.6, 6.6.5, 6.6.6, 7.0, 7.1.6, 8.1.7, 8.2	Incorporates TRIGA fuel cluster rod contents and TRIGA poisoned basket configuration.
June 1999	27	1.2.3.1.1.2 and 6.4.6.5	Incorporates increased fuel parameters for TRIGA fuel cluster rod contents.
December 1999	28	License drawings, 1.2, 2.3, 2.7, 2.10.8, 2.10.13, 3.2, 3.5, 5.4, 6.2, 6.4, 8.3, 9.0	Incorporates minor changes to numerous drawings to reflect changes facilitating fabrication and to increase the uranium loading of NISTR MTR fuel contents.
January 2000	29	Complete consolidation of SAR for CoC Renewal Application	Consolidated SAR, removed all shading and revision bars and numbered all pages to Revision 29.
		Chapter 7	Incorporated miscellaneous corrections and clarifications in the cask operating procedures based on cask operating experience.
		License Drawings 315-40-01, 02, and 03	Incorporated changes in Name Plate attachment and information (for corporate name and B(U)F-85 designation). Revised slot dimension on shield tank (Section G-G, sheet 4).

RECORD OF REVISIONS (continued)

Issue Date	Revision Number	Change	Description of Change
January 2000 (continued)	29	License drawings 315-40-05 and 06	Corrected material callout to 6061-T651 AL ALY for Items 10, 17, and 19 on 315-04-05 and Item 5 on 315-40-06.
July 2000	30	Throughout	Revised to incorporate high burnup PWR and BWR fuel rods and McMaster MTR fuel as authorized contents; to incorporate a revised specification for the Ball-Lok impact limiter attachment pins; and to incorporate an alternate fabrication method for the impact limiter shells.
		License Drawing 315-40-03	Corrected slot dimension for neutron shield gusset.
		License Drawings 315-40-01, -048, -052, -079, -084, and -094	Incorporated revised Ball-Lok pin specification.
		License Drawings 315-40-05 and –06	Incorporated alternate fabrication method for the impact limiter shells.
		License Drawings 315-40-098 through –105	Added to define the components used for shipment of high burnup fuel rods.
November 2000	31	Throughout Licensing Drawings 315-40-03, -04, -08, -099, -102, -105, and -106	Revised to incorporate drawing changes due to fabrication comments, as well as specific HEU-MTR fuel for Argentina research reactor.
January 2001	32	Throughout Licensing Drawings 315-40-05 and -06	Incorporated MEU-MTR fuel elements bounding MTR fuel element including tolerances for fabrication, enrichment, burnups and cool times. Incorporated revised dimensional tolerances for impact limiter shell dimensions and acceptance criteria for local scratches/gouges in the shells.

RECORD OF REVISIONS (continued)

Issue Date	Revision Number	Change	Description of Change
September 2001	33	Throughout; Licensing Drawings 315-40-02, -03, -04, -08, -10, -074, -108, -109, -110, -111, -113	Incorporated Alternate Port Cover design, alternate PWR fuel basket configuration and DIDO/Petten fuel
November 2002	34	Throughout	Incorporated 02A (LEU MTR) and 02B (MTR)
May 2004	35	Throughout	Incorporated 03A, 03C, 03D, 03F & 03G (GA IFM) and 03B, 03E & 03H (EPRI/Framatome)
December 2004	36	Complete consolidation of SAR for CoC renewal application. License drawings: 315-40-02 315-40-03 315-40-08 315-40-10 315-40-087 315-40-127 315-40-128	General update incorporating LWT-03I (TPBAR), LWT-04B (updated drawings for obsolete part numbers), LWT-04C (TPBAR RAI), LWT-04D (-96 changes), and LWT-04F (updates to TPBAR RAI for tritium release limits). Additional changes to the SAR have been incorporated in accordance with NRC/NAC discussions: Section 1.1, Page 1.1-1, clarified that fuel rod insert may also be referred to as a rod holder and that encapsulated fuel rods are not rod holders; Section 1.2.3, clarified that fuel rod capsules may be placed in a rod holder and added sketch of typical fuel rod capsule in Figure 1.2-11 to replace Framatome drawings; Section 1.2.3.1.2, added "intact" before "TRIGA fuel elements" in five places to clarify the TRIGA contents; Section 1.2.3.6, added "stainless steel" before "consolidation canister" in last paragraph to identify the TPBAR consolidation canister material; Figure 1.2-10 revised to eliminate unnecessary

RECORD OF REVISIONS (continued)

Issue Date	Revision Number	Change	Description of Change
December 2004 (continued)	36	Complete consolidation of SAR for CoC renewal application. License drawings: 315-40-02 315-40-03 315-40-08 315-40-10 315-40-087 315-40-127 315-40-128	detail; added drawing 315-40-03, revision 6, to cover LWT units 1 through 5 per CoC specification; revised drawing 315-40-128, per revision 1, to delete the reference to the Westinghouse TPBAR consolidation canister drawing; Figures 2.10.2-4a through –4d and Figure 2.10.2-5 renumbered with consecutive numbers; Table 5.1-1 simplified to only specify the Transport Index that is based on shielding per IAEA –96 regulations; Tables 5.3-3a through –3d, Table 5.3-6a, Table 5.3-7a and Table 5.3-9a renumbered consecutively; Section 5.3.6, moved Figures 5.3-9 through 5.3-15 and Figures 5.3-19 through 5.3-23 to the end of the section; Section 5.3.7.1, added references to Tables 5.3-26 and 5.3-27; Section 5.3.9, added reference to Figure 5.3-24; Figure 5.3-46, corrected MCNP input for 300 TPBARS at 30 days cool times. Files were updated to take advantage of automatic TOC, LOF, & LOT numbering, correct preface page numbers to chp# + pg number, delete extra section breaks, and except for Chapter 2 change page numbering to two levels. Pagination corrected, "x" changed to "x" in formulas, format for continued figures and tables made consistent, some footnotes put into true format and made consistent, and some automatic cross references set up.

RECORD OF REVISIONS (continued)

Issue Date	Revision Number	Change	Description of Change
June 2005	37	Incorporation of LWT-04E, LWT-05A, LWT-05B, LWT-05C, LWT-05D & LWT-05E License drawings: 315-40-01, Rev. 5 315-40-086, Rev. 1 315-40-098, Rev. 3 315-40-100, Rev. 3 315-40-104, Rev. 1 315-40-129, Rev. 1 315-40-130, Rev. 1 315-40-133, Rev. 0 315-40-134, Rev. 1 315-40-135, Rev. 1	Added PULSTAR fuel, screened can option & TPBAR dunnage approved amendments to Revision 36.
November 2007	38	Incorporation of LWT-05F, LWT-06A, LWT-06B, LWT-06C, LWT-06E, LWT-06F, LWT-06G, LWT-07A, LWT-07B, LWT-07C, LWT-07D & LWT-07F License drawings: 315-40-01, Rev. 6; 315-40-02, Rev. 20; 315-40-03, Rev. 6; 315-40-03, Rev. 22; 315-40-08, Rev. 17; 315-40-048, Rev. 3; 315-40-052, Rev. 3; 315-40-079, Rev. 3; 315-40-084, Rev. 3; 315-40-085, Rev. 0; 315-40-094, Rev. 4; 315-40-104, Rev. 2; 315-40-111, Rev. 1; 315-40-124, Rev. 1; 315-40-125, Rev. 3; 315-40-127, Rev. 2; 315-40-128, Rev. 2; 315-40-133, Rev. 1; 315-40-139, Rev. 0; 315-40-140, Rev. 0; 315-40-141, Rev. 0; 315-40-142, Rev. 0; 315-40-145; Rev. 0 The following license drawings were deleted: 315-40-13, 315-40-14, 315-40-15, 315-40-17, 315-40-18 & 315-40-20	Added ANSTO, TPBAR, TRIGA & Petten approved amendments to Revision 37.

RECORD OF REVISIONS (continued)

Issue Date	Revision Number	Change	Description of Change
October 2008	39	Incorporation of LWT-07G, LWT-08A, LWT-08B, LWT-08C & LWT-08E	Added Romanian TRIGA fuel & MOX fuel approved amendments to Revision 38.
		License drawings: 315-40-01, Rev. 7; 315-40-02, Rev. 22; 315-40-70, Rev. 4; 315-40-71, Rev. 4; 315-40-72, Rev. 4; 315-40-79, Rev. 5; 315-40-084, Rev. 4; 315-40-096, Rev. 3; 315-40-104, Rev. 3	
		The following license drawings were deleted: 315-40-74, 315-40-75 & 315-40-76	
January 2010	40	Incorporation of LWT-08D, LWT-08F, LWT-08G, LWT-09A, LWT--09C, LWT-09D & LWT-09E	Added ANSTO HIFAR, TPBAR & Impact Limiter Gusset Weld Repair amendments to Revision 39.
		License drawings: 315-40-02, Rev. 24; 315-40-05, Rev. 10; 315-40-06, Rev. 10; 315-40-08, Rev. 18; 315-40-10, Rev. 8; 315-40-045, Rev. 6; 315-40-046, Rev. 6; 315-40-047, Rev. 6; 315-40-049, Rev. 6; 315-40-050, Rev. 6; 315-40-051, Rev. 6; 315-40-070, Rev. 6; 315-40-071, Rev. 6; 315-40-072, Rev. 6; 315-40-080, Rev. 4; 315-40-081, Rev. 4; 315-40-082, Rev. 4; 315-40-087, Rev. 6; 315-40-090, Rev. 4, 315-40-091, Rev. 4; 315-40-092, Rev. 4; 315-40-098, Rev. 6; 315-40-100, Rev. 4; 315-40-102, Rev. 2; 315-40-104, Rev. 5; 315-40-111, Rev. 2; 315-40-128, Rev. 3; 315-40-139, Rev. 1; 315-40-140, Rev. 1; 315-40-141, Rev. 1; 315-40-142, Rev. 1; 315-40-148, Rev. 0	

LIST OF EFFECTIVE PAGES

Chapter 1

1-i thru 1-iv ..... Revision 40
1-1 thru 1-6 ..... Revision 40
1.1-1 thru 1.1-3 ..... Revision 40
1.2-1 thru 1.2-51 ..... Revision 40
1.3-1 ..... Revision 40
1.4-1 ..... Revision 40
1.5-1 ..... Revision 40

74 drawings in the
Chapter 1 List of Drawings

Chapter 1 Appendices 1-A
through 1-G

Chapter 2

2-i thru 2-xxiv ..... Revision 40
2-1 ..... Revision 40
2.1.1-1 thru 2.1.1-2 ..... Revision 40
2.1.2-1 thru 2.1.2-3 ..... Revision 40
2.1.3-1 thru 2.1.3-8 ..... Revision 40
2.2.1-1 thru 2.2.1-4 ..... Revision 40
2.3-1 ..... Revision 40
2.3.1-1 thru 2.3.1-13 ..... Revision 40
2.4-1 ..... Revision 40
2.4.1-1 ..... Revision 40
2.4.2-1 ..... Revision 40
2.4.3-1 ..... Revision 40
2.4.4-1 ..... Revision 40
2.4.5-1 ..... Revision 40
2.4.6-1 ..... Revision 40
2.5.1-1 thru 2.5.1-11 ..... Revision 40
2.5.2-1 thru 2.5.2-17 ..... Revision 40
2.6.1-1 thru 2.6.1-7 ..... Revision 40
2.6.2-1 thru 2.6.2-7 ..... Revision 40
2.6.3-1 ..... Revision 40
2.6.4-1 ..... Revision 40
2.6.5-1 thru 2.6.5-2 ..... Revision 40
2.6.6-1 ..... Revision 40
2.6.7-1 thru 2.6.7-137 ..... Revision 40
2.6.8-1 ..... Revision 40
2.6.9-1 ..... Revision 40
2.6.10-1 thru 2.6.10-15 ..... Revision 40
2.6.11-1 thru 2.6.11-12 ..... Revision 40
2.6.12-1 thru 2.6.12-95 ..... Revision 40
2.7-1 ..... Revision 40
2.7.1-1 thru 2.7.1-117 ..... Revision 40
2.7.2-1 thru 2.7.2-23 ..... Revision 40
2.7.3-1 thru 2.7.3-5 ..... Revision 40
2.7.4-1 ..... Revision 40
2.7.5-1 thru 2.7.5-5 ..... Revision 40
2.7.6-1 thru 2.7.6-4 ..... Revision 40
2.7.7-1 thru 2.7.7-74 ..... Revision 40
2.8-1 ..... Revision 40
2.9-1 thru 2.9-20 ..... Revision 40
2.10.1-1 thru 2.10.1-3 ..... Revision 40
2.10.2-1 thru 2.10.2-49 ..... Revision 40
2.10.3-1 thru 2.10.3-18 ..... Revision 40
2.10.4-1 thru 2.10.4-11 ..... Revision 40
2.10.5-1 ..... Revision 40
2.10.6-1 thru 2.10.6-19 ..... Revision 40
2.10.7-1 thru 2.10.7-66 ..... Revision 40
2.10.8-1 thru 2.10.8-67 ..... Revision 40
2.10.9-1 thru 2.10.9-9 ..... Revision 40
2.10.10-1 thru 2.10.10-97 ..... Revision 40
2.10.11-1 thru 2.10.11-10 ..... Revision 40
2.10.12-1 thru 2.10.12-31 ..... Revision 40
2.10.13-1 thru 2.10.13-17 ..... Revision 40

LIST OF EFFECTIVE PAGES (Continued)

2.10.14-1 thru 2.10.14-38 ..... Revision 40
2.10.15-1 thru 2.10.15-10 ..... Revision 40
2.10.16-1 thru 2.10.16-5 ..... Revision 40

Chapter 3
3-i thru 3-v ..... Revision 40
3.1-1 thru 3.1-2 ..... Revision 40
3.2-1 thru 3.2-11 ..... Revision 40
3.3-1 ..... Revision 40
3.4-1 thru 3.4-98 ..... Revision 40
3.5-1 thru 3.5-36 ..... Revision 40
3.6-1 thru 3.6-12 ..... Revision 40

Chapter 4
4-i thru 4-iii ..... Revision 40
4.1-1 thru 4.1-3 ..... Revision 40
4.2-1 thru 4.2-4 ..... Revision 40
4.3-1 thru 4.3-4 ..... Revision 40
4.4-1 ..... Revision 40
4.5-1 thru 4.5-41 ..... Revision 40

Chapter 5
5-i thru 5-xii ..... Revision 40
5-1 thru 5-3 ..... Revision 40
5.1.1-1 thru 5.1.1-17 ..... Revision 40
5.2.1-1 thru 5.2.1-7 ..... Revision 40
5.3.1-1 thru 5.3.1-2 ..... Revision 40
5.3.2-1 ..... Revision 40
5.3.3-1 thru 5.3.3-8 ..... Revision 40
5.3.4-1 thru 5.3.4-19 ..... Revision 40
5.3.5-1 thru 5.3.5-4 ..... Revision 40
5.3.6-1 thru 5.3.6-18 ..... Revision 40
5.3.7-1 thru 5.3.7-19 ..... Revision 40
5.3.8-1 thru 5.3.8-25 ..... Revision 40
5.3.9-1 thru 5.3.9-26 ..... Revision 40
5.3.10-1 thru 5.3.10-14 ..... Revision 40
5.3.11-1 thru 5.3.11-48 ..... Revision 40
5.3.12-1 thru 5.3.12-26 ..... Revision 40
5.3.13-1 thru 5.3.13-18 ..... Revision 40
5.3.14-1 thru 5.3.14-21 ..... Revision 40
5.3.15-1 thru 5.3.15-9 ..... Revision 40
5.3.16-1 thru 5.3.16-5 ..... Revision 40
5.3.17-1 thru 5.3.17-40 ..... Revision 40
5.3.18-1 thru 5.3.18-2 ..... Revision 40
5.3.19-1 thru 5.3.19-9 ..... Revision 40
5.4.1-1 thru 5.4.1-6 ..... Revision 40

Chapter 6
6-i thru 6-xiv ..... Revision 40
6-1 ..... Revision 40
6.1-1 thru 6.1-5 ..... Revision 40
6.2-1 ..... Revision 40
6.2.1-1 thru 6.2.1-3 ..... Revision 40
6.2.2-1 thru 6.2.2-3 ..... Revision 40
6.2.3-1 thru 6.2.3-7 ..... Revision 40
6.2.4-1 ..... Revision 40
6.2.5-1 thru 6.2.5-5 ..... Revision 40
6.2.6-1 thru 6.2.6-3 ..... Revision 40
6.2.7-1 thru 6.2.7-2 ..... Revision 40
6.2.8-1 thru 6.2.8-3 ..... Revision 40
6.2.9-1 thru 6.2.9-4 ..... Revision 40
6.2.10-1 thru 6.2.10-3 ..... Revision 40
6.2.11-1 thru 6.2.11-3 ..... Revision 40
6.2.12-1 thru 6.2.12-4 ..... Revision 40
6.3.1-1 thru 6.3.1-6 ..... Revision 40
6.3.2-1 thru 6.3.2-4 ..... Revision 40
6.3.3-1 thru 6.3.3-9 ..... Revision 40
6.3.4-1 thru 6.3.4-10 ..... Revision 40
6.3.5-1 thru 6.3.5-12 ..... Revision 40
6.3.6-1 thru 6.3.6-9 ..... Revision 40

LIST OF EFFECTIVE PAGES (Continued)

6.3.7-1 thru 6.3.7-4 ..... Revision 40
6.3.8-1 thru 6.3.8-7 ..... Revision 40
6.3.9-1 thru 6.3.9-7 ..... Revision 40
6.3.10-1 thru 6.3.10-2 ..... Revision 40
6.4.1-1 thru 6.4.1-10 ..... Revision 40
6.4.2-1 thru 6.4.2-10 ..... Revision 40
6.4.3-1 thru 6.4.3-34 ..... Revision 40
6.4.4-1 thru 6.4.4-24 ..... Revision 40
6.4.5-1 thru 6.4.5-32 ..... Revision 40
6.4.6-1 thru 6.4.6-23 ..... Revision 40
6.4.7-1 thru 6.4.7-14 ..... Revision 40
6.4.8-1 thru 6.4.8-14 ..... Revision 40
6.4.9-1 thru 6.4.9-10 ..... Revision 40
6.4.10-1 thru 6.4.10-18 ..... Revision 40
6.4.11-1 thru 6.4.11-7 ..... Revision 40
6.5.1-1 thru 6.5.1-13 ..... Revision 40
6.5.2-1 thru 6.5.2-4 ..... Revision 40
6.5.3-1 thru 6.5.3-2 ..... Revision 40
6.7.1-1 thru 6.7.1-19 ..... Revision 40
6.7.2-1 thru 6.7.2-47 ..... Revision 40

Appendix 6.6

6.6-i thru 6.6-iii ..... Revision 40
6.6-1 ..... Revision 40
6.6.1-1 thru 6.6.1-111 ..... Revision 40
6.6.2-1 thru 6.6.2-56 ..... Revision 40
6.6.3-1 thru 6.6.3-73 ..... Revision 40
6.6.4.-1 thru 6.6.4-77 ..... Revision 40
6.6.5-1 thru 6.6.5-101 ..... Revision 40
6.6.6-1 thru 6.6.6-158 ..... Revision 40
6.6.7-1 thru 6.6.7-84 ..... Revision 40
6.6.8-1 thru 6.6.8-183 ..... Revision 40
6.6.9-1 thru 6.6.9-52 ..... Revision 40
6.6.10-1 thru 6.6.10-33 ..... Revision 40
6.6.11-1 thru 6.6.11-47 ..... Revision 40
6.6.12-1 thru 6.6.12-20 ..... Revision 40
6.6.13-1 thru 6.6.13-22 ..... Revision 40
6.6.14-1 thru 6.6.14-7 ..... Revision 40
6.6.15-1 thru 6.6.15-45 ..... Revision 40
6.6.16-1 thru 6.6.16-30 ..... Revision 40

Chapter 7

7-i thru 7-ii ..... Revision 40
7.1-1 thru 7.1-57 ..... Revision 40
7.2-1 thru 7.2-14 ..... Revision 40
7.3-1 thru 7.3-2 ..... Revision 40

Chapter 8

8-i ..... Revision 40
8.1-1 thru 8.1-11 ..... Revision 40
8.2-1 thru 8.2-5 ..... Revision 40
8.3-1 thru 8.3-4 ..... Revision 40

Chapter 9

9-i ..... Revision 40
9-1 thru 9-11 ..... Revision 40

Table of Contents

1 GENERAL INFORMATION 1-1

1.1 Introduction 1.1-1

1.2 Package Description 1.2-1
1.2.1 Packaging 1.2-1
1.2.2 Operational Features 1.2-4
1.2.3 Contents of Packaging 1.2-5

1.3 Quality Assurance 1.3-1

1.4 License Drawings 1.4-1

1.5 Unclassified DOE Reference Documents and Drawings 1.5-1

Chapter 1 Appendices

Appendix 1-A – TTQP-1-015, "Description of the Tritium-Producing Burnable Absorber Rod for the Commercial Light Water Reactor," Revision 14

Appendix 1-B – TTQP-1-091, "Unclassified TPBAR Releases, Including Tritium," Revision 11

Appendix 1-C – TTQP-1-111, "Unclassified Bounding Source Term, Radionuclide Concentrations, Decay Heat, and Dose Rates for the Production TPBAR," Revision 5

Appendix 1-D – DOE Drawing H-3-307845, "Production TPBAR Reactor Interface Dimensions Watts Bar," Revision 10, Sheet 1 of 2

Appendix 1-E – DOE Drawing H-3-308875, "Production TPBAR Reactor Interface Dimensions Sequoyah," Revision 5, Sheet 1 of 2

Appendix 1-F – DOE Drawing H-3-310568, "Mark 8 Multi-Pencil TPBAR – Watts Bar Reactor Interface," Revision 0, Sheet 1 of 2

Appendix 1-G – PNNL Letter, TTP-06-056, Subject: Exposure of Shipping Casks to Tritium, February 21, 2006

List of Figures

Figure 1.2.3-1 Aluminum Clad TRIGA Fuel Element 1.2-19
Figure 1.2.3-2 Aluminum Clad Instrumented Fuel Element 1.2-20
Figure 1.2.3-3 Stainless Steel Clad TRIGA Fuel Element 1.2-21
Figure 1.2.3-4 Stainless Steel Clad Instrumented Fuel Element 1.2-22
Figure 1.2.3-5 Standard Fuel Follower Control Rod Element 1.2-23
Figure 1.2.3-6 TRIGA Fuel Cluster and Rod Details 1.2-24
Figure 1.2.3-7 HTGR Fuel Handling Unit 1.2-25
Figure 1.2.3-8 RERTR Fuel Handling Unit 1.2-26
Figure 1.2.3-9 Typical TPBAR Assembly 1.2-27
Figure 1.2.3-10 TPBAR Consolidation Canister Sketch 1.2-28
Figure 1.2.3-11 Failed PWR/BWR Fuel Rod Capsule 1.2-29
Figure 1.2.3-12 NAC-LWT with TPBAR Consolidation Canister Payload 1.2-30
Figure 1.2.3-13 PULSTAR Fuel Assembly 1.2-31
Figure 1.2.3-14 Spiral Fuel Assembly Cross-Section Sketch 1.2-32
Figure 1.2.3-15 MOATA Plate Bundle Sketches 1.2-33
Figure 1.2.3-16 TPBAR Waste Container and Extension Weldment Sketch 1.2-34
Figure 1.2.3-17 NAC-LWT with TPBAR Waste Container Payload 1.2-35
Figure 1.2.3-18 ANSTO Damaged Fuel Can (DFC) 1.2-36

List of Tables

Table 1.1-1 Terminology and Notation 1-3
Table 1.2-1 Characteristics of Design Basis TRIGA Fuel Elements Acceptable for Loading in the Poisoned TRIGA Basket 1.2-37
Table 1.2-2 Characteristics of Design Basis TRIGA Fuel Elements Acceptable for Loading in the Nonpoisoned TRIGA Basket 1.2-38
Table 1.2-3 Characteristics of Design Basis TRIGA Fuel Cluster Rods 1.2-39
Table 1.2-4 Fuel Characteristics 1.2-40
Table 1.2-5 PWR Fuel Characteristics 1.2-43
Table 1.2-6 BWR Fuel Characteristics 1.2-44
Table 1.2-7 Characteristics of General Atomics Irradiated Fuel Material (GA IFM) 1.2-45
Table 1.2-8 Typical Production TPBAR Characteristics 1.2-46
Table 1.2-9 PULSTAR Fuel Characteristics 1.2-47
Table 1.2-10 Spiral Fuel Assembly Characteristics 1.2-48
Table 1.2-11 MOATA Plate Bundle Characteristics 1.2-49
Table 1.2-12 Typical TPBAR Segment Characteristics in Waste Container 1.2-50
Table 1.2-13 Solid, Irradiated Hardware Characteristics 1.2-51

List of Drawings

315-40-01		Rev 7	Legal Weight Truck Transport Cask Assembly
315-40-02	Sheets 1 – 2	Rev 24	NAC-LWT Cask Body Assembly
315-40-03	Sheets 1 – 6	Rev 6*	NAC-LWT Transport Cask Body
315-40-03	Sheets 1 – 7	Rev 22	NAC-LWT Transport Cask Body
315-40-04		Rev 10	NAC-LWT Transport Cask Lid Assembly
315-40-05	Sheets 1 – 2	Rev 10	NAC-LWT Transport Cask Upper Impact Limiter
315-40-06		Rev 10	NAC-LWT Transport Cask Lower Impact Limiter
315-40-08	Sheets 1 – 5	Rev 18	NAC-LWT Transport Cask Parts Detail
315-40-09		Rev 2	NAC-LWT PWR Basket Spacer
315-40-10	Sheets 1 – 2	Rev 8	NAC-LWT Cask PWR Basket
315-40-11		Rev 2	NAC-LWT BWR Fuel Basket Assembly
315-40-12		Rev 3	NAC-LWT Metal Fuel Basket Assembly
315-40-045		Rev 6	Weldment, 7 Element Basket, 42 MTR Fuel Base Module
315-40-046		Rev 6	Weldment, 7 Element Basket, 42 MTR Fuel Intermediate Module
315-40-047		Rev 6	Weldment, 7 Element Basket, 42 MTR Fuel Top Module
315-40-048		Rev 3	Legal Weight Truck Transport Cask Assembly, 42 MTR Element
315-40-049		Rev 6	Weldment, 7 Element Basket, 28 MTR Fuel Base Module
315-40-050		Rev 6	Weldment, 7 Element Basket, 28 MTR Fuel Intermediate Module
315-40-051		Rev 6	Weldment, 7 Element Basket, 28 MTR Fuel Top Module
315-40-052		Rev 3	Legal Weight Truck Transport Cask Assembly, 28 MTR Element
315-40-070		Rev 6	Weldment, 7 Cell Basket, TRIGA Fuel Base Module
315-40-071		Rev 6	Weldment, 7 Cell Basket, TRIGA Fuel Intermediate Module
315-40-072		Rev 6	Weldment, 7 Cell Basket, TRIGA Fuel Top Module
315-40-079		Rev 5	Legal Weight Truck Transport Cask Assy, 120 TRIGA Fuel Elements or 480 Cluster Rods
315-040-080		Rev 4	Weldment, 7 Cell Poison Basket, TRIGA Fuel Base Module
315-040-081		Rev 4	Weldment, 7 Cell Poison Basket, TRIGA Fuel Intermediate Module
315-040-082		Rev 4	Weldment, 7 Cell Poison Basket, TRIGA Fuel Top Module
315-040-083		Rev 0	Spacer, LWT Cask Assembly, TRIGA Fuel
315-40-084		Rev 4	Legal Weight Truck Transport Cask Assy, 140 TRIGA Elements
315-40-085		Rev 0	Axial Fuel and Cell Block Spacers, MTR and TRIGA Fuel Baskets, NAC-LWT Cask
315-40-086		Rev 1	Assembly, Sealed Failed Fuel Can, TRIGA Fuel
315-40-087		Rev 6	Canister Lid Assembly, Sealed Failed Fuel Can, TRIGA Fuel
315-40-088		Rev 2	Canister Body Assembly, Sealed Failed Fuel Can, TRIGA Fuel
315-40-090		Rev 4	Weldment, 7 Element Basket, 35 MTR Fuel Base Module
315-40-091		Rev 4	Weldment, 7 Element Basket, 35 MTR Fuel Intermediate Module
315-40-092		Rev 4	Weldment, 7 Element Basket, 35 MTR Fuel Top Module
315-40-094		Rev 4	Legal Weight Truck Transport Cask Assembly, 35 MTR Element
315-40-096		Rev 3	Fuel Cluster Rod Insert, TRIGA Fuel
315-40-098	Sheets 1 - 3	Rev 6	PWR/BWR Rod Transport Canister Assembly
315-40-099	Sheets 1 - 3	Rev 3	Can Weldment, PWR/BWR Transport Canister

* Packaging Unit Nos. 1, 2, 3, 4 and 5 are constructed in accordance with this revision of drawing.

List of Drawings (continued)

315-40-100	Sheets 1 - 5	Rev 4	Lids, PWR/BWR Transport Canister
315-40-101		Rev 0	4 X 4 Insert, PWR/BWR Transport Canister
315-40-102		Rev 2	5 X 5 Insert, PWR/BWR Transport Canister
315-40-103		Rev 0	Pin Spacer, PWR/BWR Transport Canister
315-40-104	Sheets 1 - 3	Rev 5	Legal Weight Truck Transport Cask Assy, PWR/BWR Rod Transport Canister
315-40-105	Sheets 1 - 2	Rev 3	PWR Insert PWR/BWR Transport Canister
315-40-106	Sheets 1 - 3	Rev 1	MTR Plate Canister, LWT Cask
315-40-108	Sheets 1 - 3	Rev 1	Weldment, 7 Cell Basket, Top Module, DIDO Fuel
315-40-109	Sheets 1 - 3	Rev 1	Weldment, 7 Cell Basket, Intermediate Module, DIDO Fuel
315-40-110	Sheets 1 - 3	Rev 1	Weldment, 7 Cell Basket, Base Module, DIDO Fuel
315-40-111		Rev 2	Legal Weight Truck, Transport Cask Assy, DIDO Fuel
315-40-113		Rev 0	Spacers, Top Module, DIDO Fuel
315-40-120	Sheets 1 - 3	Rev 2	Top Module, General Atomics IFM, LWT Cask
315-40-123	Sheets 1 - 2	Rev 1	Spacer, General Atomics IFM, LWT Cask
315-40-124		Rev 1	Transport Cask Assembly, General Atomics IFM, LWT Cask
315-40-125	Sheets 1 - 3	Rev 3	Transport Cask Assembly, Framatome/EPRI, LWT Cask
315-40-126	Sheets 1 - 2	Rev 2	Weldments, Framatome/EPRI, LWT Cask
315-40-127	Sheets 1 - 2	Rev 2	Spacer Assembly, TPBAR Shipment, LWT Cask
315-40-128	Sheets 1 - 2	Rev 3	Legal Weight Truck, Transport Cask Assy, TPBAR Shipment
032230		Rev A	RERTR Secondary Enclosure, General Atomics
032231		Rev A	HTGR Secondary Enclosure, General Atomics
032236		Rev B	RERTR Primary Enclosure, General Atomics
032237		Rev B	HTGR Primary Enclosure, General Atomics
315-40-129		Rev 1	Canister Body Assembly, Failed Fuel Can, PULSTAR
315-40-130		Rev 1	Assembly, Failed Fuel Can, PULSTAR
315-40-133	Sheets 1 - 2	Rev 1	Transport Cask Assembly, PULSTAR Shipment, LWT Cask
315-40-134		Rev 1	Body Weldment, Screened Fuel Can, PULSTAR Fuel
315-40-135		Rev 1	Assembly, Screened Fuel Can, PULSTAR Fuel
315-40-139		Rev 1	Legal Weight Truck Transport Cask Assy, ANSTO Fuel
315-40-140	Sheets 1 - 2	Rev 1	Weldment, 7 Cell Basket, Top Module, ANSTO Fuel
315-40-141	Sheets 1 - 2	Rev 1	Weldment, 7 Cell Basket, Intermediate Module, ANSTO Fuel
315-40-142	Sheets 1 - 2	Rev 1	Weldment, 7 Cell Basket, Base Module, ANSTO Fuel
315-40-145		Rev 0	Irradiated Hardware Lid Spacer, LWT Cask
315-40-148		Rev 0	Legal Weight Truck Transport Cask Assembly, ANSTO-DIDO Combination Basket

1 GENERAL INFORMATION

This chapter of the NAC International, Legal Weight Truck spent fuel shipping cask (NAC-LWT) Safety Analysis Report (SAR) presents a general introduction to, and description of, the NAC-LWT cask. Terminology used throughout this report is presented in Table 1.1-1.

Shipment of the NAC-LWT cask by truck, ISO container, and/or by railcar, as a Type B(U)F-96 package, as defined in 10 CFR 71.4, is authorized for the following contents:

- PWR and BWR fuel assemblies[1];
- MTR fuel assemblies and plates;
- DIDO fuel assemblies;
- metallic fuel rods;
- 25 high burnup PWR and BWR fuel rods (including up to 14 fuel rods classified as damaged)[2];
- 16 PWR MOX fuel rods (or mixed load of up to 16 PWR MOX and UO_2 PWR fuel rods) and up to 9 burnable poison rods (BPRs);
- TRIGA fuel elements and TRIGA fuel cluster rods;
- General Atomics (GA) High-Temperature Gas-Cooled Reactor (HTGR) and Reduced-Enrichment Research and Test Reactor (RERTR) Irradiated Fuel Materials (IFM);
- up to 700 PULSTAR fuel elements;
- spiral fuel assemblies; and
- MOATA plate bundles.

The authorized contents previously listed include both irradiated and unirradiated forms of the materials.

Irradiated hardware is also authorized to be shipped in the NAC-LWT cask by truck, ISO container, and/or by railcar, as a Type B(U)F-96 package, as defined in 10 CFR 71.4. Irradiated hardware is defined as solid, irradiated and contaminated fuel assembly structural or reactor internal component hardware, which may include fissile material, provided the quantity of fissile material does not exceed a Type A quantity and does not exceed the exemptions of 10 CFR 71.15, paragraphs (a), (b) and (c).

Shipment of the NAC-LWT cask by truck, ISO container, and/or by railcar, as a Type B(M)-96 package, as defined in 10 CFR 71.4, is also authorized for the following contents:

- up to 300 Tritium Producing Burnable Absorber Rods (TPBARs), of which two can be prefailed; and
- up to 55 TPBARs segmented during PIE, including segmentation debris.

[1] NAC-LWT casks containing PWR and BWR fuel assemblies are to be transported on an open trailer with a personnel barrier.

[2] PWR and BWR fuel rods may be transported in either a fuel assembly lattice (skeleton) or in a fuel rod insert. The fuel rod insert may contain PWR instrument/guide tubes and BWR water/inert rods in addition to the fuel rods.

In accordance with 10 CFR 71.59, the NAC-LWT cask is assigned a Criticality Safety Index (CSI) for criticality control of the approved contents as follows:

Approved Contents	CSI
PWR fuel assemblies	100
BWR fuel assemblies	5.0
MTR fuel elements	0.0
Metallic fuel rods	0.0
TRIGA fuel elements (in poisoned TRIGA fuel baskets)	0.0
TRIGA fuel elements (in nonpoisoned TRIGA fuel baskets)	12.5
TRIGA fuel cluster rods	0.0
High burnup PWR rods	0.0
High burnup BWR rods	0.0
PWR MOX rods	0.0
DIDO fuel elements	12.5
General Atomic Irradiated Fuel Material (GA IFM)	0.0
TPBARS and segmented TPBARS	0.0
Intact (uncanned) PULSTAR fuel	0.0
Canned PULSTAR fuel	33.4
ANSTO fuel	0.0
Solid irradiated hardware	0.0
ANSTO-DIDO fuel combination	0.0

TPBARs do not contain fissile material and criticality assessments are not required. Solid, irradiated and contaminated hardware contents could include fissile material not exceeding a Type A quantity and the exemptions of 10 CFR 71.15, paragraphs (a), (b) and (c). A CSI of 0 is assigned for these contents for documentation purposes.

The estimated Transport Index (TI) for shielding for the prior listed contents is shown in Table 5.1.1-1. The actual TI for individual shipments will be determined in accordance with 10 CFR 71.4 by the licensee.

Table 1.1-1 Terminology and Notation

Cask Model	NAC-LWT
Package	The Packaging with its radioactive contents (payload), as presented for transportation (10 CFR 71.4). Within this report, the Package is denoted as the NAC-LWT cask or simply as the cask.
Packaging	The assembly of components necessary to ensure compliance with packaging requirements (10 CFR 71.4). Within this report, the Packaging is denoted as the NAC-LWT cask.
NAC-LWT Cask	This packaging consists of a spent-fuel shipping cask body and closure lid with energy absorbing impact limiters.
Contents (Payload)	• 1 PWR assembly • up to 2 BWR assemblies • up to 25 PWR or BWR rods (including high burnup fuel rods and up to 14 fuel rods classified as damaged)[1] • up to 16 PWR MOX fuel rods (or mixed contents of up to 16 PWR MOX and UO_2 PWR fuel rods) and up to 9 BPRs • up to 42 MTR fuel elements (including plates) • up to 42 DIDO fuel assemblies • up to 7 degraded clad DIDO fuel assemblies in damaged fuel cans (DFCs) in ANSTO top basket module • up to 15 sound (cladding intact) metallic fuel rods • up to 9 damaged metallic fuel rods or 3 severely damaged metallic fuel rods in filters • up to 140 intact or damaged TRIGA fuel elements/debris • up to 560 intact or damaged TRIGA fuel cluster rods • 2 GA IFM packages • up to 300 TPBARs (including up to 2 prefailed TPBARs) • up to 55 TPBARs segmented into individual segments and segmentation debris • up to 700 intact or damaged PULSTAR fuel elements in either assembly or element form, including fuel debris • up to 42 intact spiral fuel assemblies (also referred to as Mark III spiral fuel), including up to 7 degraded clad spiral fuel assemblies in DFCs. Spiral fuel assemblies may be cropped. • up to 42 intact MOATA plate bundles, including up to 7 MOATA plate bundles in DFCs

[1] PWR and BWR fuel rods may be transported in either a fuel assembly lattice (skeleton) or in a fuel rod insert. The fuel rod insert may contain PWR instrument/guide tubes and BWR water/inert rods in addition to the fuel rods.

Table 1.1-1 Terminology and Notation (cont'd)

	• any combination of individual ANSTO basket modules containing either spiral fuel assemblies or MOATA plate bundles up to a total of 42 assemblies/bundles, including up to 7 degraded clad DIDO, spiral or MOATA elements/ bundles in DFCs placed in an ANSTO top basket module • combination ANSTO-DIDO basket assembly (one ANSTO top module and five DIDO intermediate and base basket modules) containing up to 42 DIDO, spiral or MOATA elements/bundles with up to 7 degraded clad elements/bundles in the ANSTO top module in DFCs • up to 4,000 lbs of solid, irradiated and contaminated hardware, which may include fissile material less than a Type A quantity and meeting the exemptions of 10 CFR 71.15, paragraphs (a), (b) and (c). Total allowed mass includes the weight of spacers, shoring and dunnage.
Impact Limiters	Aluminum honeycomb energy absorbers located at the ends of the cask.
Intact LWR Fuel (Assembly or Rod)	Spent nuclear fuel that is not Damaged LWR Fuel, as defined herein. To be classified as intact, fuel must meet the criteria for both intact cladding and structural integrity. An intact fuel assembly can be handled using normal handling methods, and any missing fuel rods have been replaced by solid filler rods that displace a volume equal to, or greater than, that of the original fuel rod.
Damaged LWR Fuel (Assembly or Rod)	Spent nuclear fuel that includes any of the following conditions that result in either compromise of cladding confinement integrity or recognition of fuel assembly geometry. 1. The fuel contains known or suspected cladding defects greater than a pinhole leak or a hairline crack that have the potential for release of significant amounts of fuel particles. 2. The fuel assembly: i. is damaged in such a manner as to impair its structural integrity; ii. has missing or displaced structural components such as grid spacers;

Table 1.1-1 Terminology and Notation (cont'd)

	iii. is missing fuel pins that have not been replaced by filler rods that displace a volume equal to, or greater than, that of the original fuel rod; iv. cannot be handled using normal handling methods. 3. The fuel is no longer in the form of an intact fuel assembly and consists of, or contains, debris such as loose pellets, rod segments, etc.
Damaged Fuel (TRIGA)	TRIGA fuel (elements and cluster rods) with known or suspected clad breach (i.e., cladding defects that permit the release of gas from the interior of the rod and/or allow water intrusion into the clad to fuel gap while submerged).
Fuel Debris (TRIGA)	TRIGA damaged fuel that does not maintain its structural integrity, including fuel particles, fuel debris, and broken fuel rods.
Degraded ANSTO Fuel	ANSTO fuel elements (Mark II MOATA, Mark III Spiral, and Mark IV DIDO fuel) that have corrosion, destructive examination and/or mechanical damage to the fuel plates, but are structurally acceptable for transport (i.e., will not result in appreciable fuel debris formation under transport conditions). Fuel elements may be disassembled and plates may contain significant corrosion or mechanical damage in nonfueled plate areas; fuel elements may have sections of the fueled plate removed for examination; or fuel elements may have fuel core exposure due to through-clad corrosion or mechanical damage. The fuel (core material) area exposed may not exceed 5% of the total fueled cross-sectional area of the element.
Undamaged Aluminum-Based Fuel	Aluminum-based reactor fuel plates/elements that are structurally sound, but may have fuel core exposure due to corrosion or mechanical damage of the clad. Through-clad corrosion and/or mechanical damage is limited to 5% of the fueled surface area of the element.
TPBAR	Tritium Producing Burnable Absorber Rod

Irradiated Fuel Material (IFM)	High-Temperature Gas-Cooled Reactor (HTGR/IFM) and Reduced-Enrichment Research and Test Reactor (RERTR/IFM) type TRIGA fuel entities produced by General Atomics.
PULSTAR Fuel Element	PULSTAR fuel rod. May be contained in either assembly, rod holder or can form for shipment. PULSTAR fuel elements may be intact or damaged.
Damaged PULSTAR Fuel Element	PULSTAR fuel rods having cladding failures greater than hairline cracks or pinhole leaks. The damaged fuel definition for PULSTAR fuel elements includes fuel debris. Damaged PULSTAR fuel elements may also be referred to as failed and must be transported in either of two types of PULSTAR cans.
Irradiated Hardware	Solid, irradiated and contaminated fuel assembly structural or reactor internal component hardware, which may include fissile material, provided the quantity of fissile material does not exceed a Type A quantity and does not exceed the exemptions of 10 CFR 71.15, paragraphs (a), (b) and (c). Authorized quantity of irradiated hardware and components is limited to 4,000 lbs (including spacers, dunnage and containers) and a gamma source term as defined in Table 1.2-13.
MOX Fuel Rods	The term as used in this SAR is defined as irradiated or unirradiated mixed uranium-plutonium oxide (MOX) fuel rods. The MOX fuel rods can be made with plutonium having various compositions of plutonium isotopes. The evaluated mixes of the various grades of plutonium are defined in the shielding (Chapter 5) and criticality (Chapter 6) evaluations.

1.1 Introduction

The NAC-LWT spent-fuel shipping cask has been developed by NAC International (NAC) as a safe means of transporting radioactive materials authorized as approved contents. The cask design is optimized for legal weight over the road transport, with a gross weight of less than 80,000 pounds. The cask provides maximum safety during the loading, transport, and unloading operations required for spent-fuel shipment. The NAC-LWT cask assembly is composed of a package that provides a containment vessel that prevents the release of radioactive material. The actual containment boundary provided by the package consists of a 4.0-inch thick bottom plate, a 0.75-inch thick, 13.375-inch inner diameter shell, an upper ring forging, and an 11.3-inch thick closure lid. The cask lid closure is accomplished using twelve, 1-inch diameter bolts. The cask has an outer shell, 1.20 inches thick, to protect the containment shell and also to enclose the 5.75-inch thick lead gamma shield. Neutron shielding is provided by a 5.0-inch thick neutron shield tank with a 0.24-inch (6mm) thick outer wall, containing a water/ethylene glycol mixture and 1.0 minimum weight percent (wt %) boron (58 wt % ethylene glycol; 39 wt % demineralized water; 3 wt % potassium tetraborate [$K_2B_4O_7$]). The neutron shield tank system includes an expansion tank to permit the expansion and contraction of the shield tank liquid without compromising the shielding or overstressing the shield tank structure. Aluminum honeycomb impact limiters are attached to each end of the cask to absorb kinetic energy developed during a cask drop, and limit the consequences of normal operations and hypothetical accident events.

The NAC-LWT is a legal weight truck cask designed to transport the following contents:

- 1 PWR assembly;
- up to 2 BWR assemblies;
- up to 15 sound metallic fuel rods;
- up to 42 MTR fuel elements;
- up to 42 DIDO fuel assemblies;
- up to 25 high burnup PWR fuel rods (including up to 14 rods classified as damaged)[1];
- up to 25 high burnup BWR fuel rods (including up to 14 rods classified as damaged)[1];
- up to 16 PWR MOX fuel rods (or a combination of 16 PWR MOX and UO_2 PWR rods) and up to 9 BPRs
- up to 9 damaged metallic fuel rods;
- up to 3 severely damaged metallic fuel rods in filters;
- up to 140 TRIGA intact or damaged fuel elements/fuel debris ("TRIGA" is a Trademark of General Atomics);
- up to 560 TRIGA intact or damaged fuel cluster rods/fuel debris;
- 2 GA IFM packages;
- up to 300 TPBARs (of which two can be prefailed) in a consolidation canister;

[1] PWR and BWR fuel rods may be transported in either a fuel assembly lattice (skeleton) or in a fuel rod insert. The fuel rod insert may contain PWR instrument/guide tubes and BWR water/inert rods in addition to the fuel rods.

- Up to 25 TPBARs (of which two can be prefailed) in a rod holder;
- up to 55 TPBARs segmented during post-irradiation examination (PIE), including segmentation debris; ,
- up to 700 PULSTAR fuel elements (intact or damaged);
- up to 42 spiral fuel assemblies;
- up to 42 MOATA plate bundles; or
- up to 4,000 lbs of solid, irradiated and contaminated hardware, which may include fissile material less than a Type A quantity and meeting the exemptions of 10 CFR 71.15, paragraphs (a), (b) and (c). Total allowed mass includes the weight of spacers, shoring and dunnage.

PWR or BWR fuel rods may be placed in a fuel rod insert (also referred to as a rod holder) or in a fuel assembly lattice. The fuel rod holder is composed of a 4×4 or a 5×5 rod array. An alternate 5×5 rod holder is designed to contain an oversize nonfuel-bearing component (e.g., CE guide tube or BWR water rod). The alternative configuration reduces fuel-bearing capacity to a maximum of 21 fuel rods. The lattice may be irradiated or unirradiated. Up to 14 of the fuel rods may be classified as damaged. Damaged fuel rods must be placed in a rod holder. Damaged fuel rods or rod sections may be encapsulated to facilitate handling prior to placement in the rod holder. PWR rods may include Integral Fuel Burnable Absorber (IFBA) rods.

PWR MOX fuel rods (or a combination of PWR MOX and UO_2 PWR fuel rods) are required to be loaded in a screened or free flow PWR/BWR Rod Transport Canister with a 5×5 insert. PWR MOX/UO_2 rods may include Integral Fuel Burnable Absorber (IFBA) rods.

Damaged TRIGA fuel elements, cluster rods and fuel debris are required to be loaded in a sealed damaged fuel canister (DFC).

PULSTAR fuel elements may be configured as intact fuel assemblies, may be placed into a fuel rod insert, i.e., a 4×4 rod holder (intact elements only), or may be loaded into one of two can designs, designated as the PULSTAR screened fuel can or the PULSTAR failed fuel can. Damaged PULSTAR fuel elements and nonfuel components of PULSTAR fuel assemblies must be loaded into cans. PULSTAR fuel cans may only be loaded into the top or base module of the 28 MTR basket assembly. Intact PULSTAR fuel assemblies and intact PULSTAR fuel elements in a TRIGA fuel rod insert may be loaded in any basket module.

Irradiated hardware may be loaded directly into the NAC-LWT cavity or preloaded into a canister or cage. Stainless steel dunnage may be used to limit the movement of the irradiated hardware within the cask cavity. The maximum gamma source term of the irradiated hardware shall be limited to that defined for the authorized PWR content condition as described in Chapter 5.

The NAC-LWT cask provides a testable containment for the contents during both normal operations and hypothetical accident conditions, satisfying the requirements of 10 CFR 71.51. Any number of NAC-LWT casks may be shipped at one time, each on its own vehicle.

The NAC-LWT has two leaktight configurations as defined by ANSI N14.5. The standard configuration is provided by a closure lid with a metal containment seal and alternate vent and drain port covers provided with Viton® containment O-rings. The second configuration is provided by a closure lid with a metal containment seal and Alternate B vent and drain port covers provided with metal seals. The metal port cover seal containment configuration is required to be utilized for all TPBAR contents and may be used for other contents. The NAC-LWT standard, Viton® O-ring containment configuration is not authorized for TPBAR contents.

NAC-LWT casks may be shipped in a closed International Shipping Organization (ISO) container when containing all fuel contents other than PWR and BWR fuel assemblies. NAC-LWT casks containing PWR and BWR fuel assemblies are to be transported on an open trailer with a personnel barrier.

The terminology of MTR, DIDO and TRIGA fuel elements will be used independent of whether the element contains low, medium or high enriched uranium (i.e., LEU, MEU or HEU), except when required for analysis or loading purposes.

TPBAR contents may be placed into a consolidation canister, waste container or 5×5 rod insert (also referred to as a rod holder) in a PWR/BWR Rod Transport Canister. Segmented TPBARs are only permitted within the waste container. The three TPBAR shipping configurations are individually placed within one of the two TPBAR basket assemblies (one with a 7-inch bottom sspacer and the alternative TPBAR basket assembly with a 6.5-inch alternative bottom spacer), depending on container configuration.

1.2 Package Description

This section presents a basic description of the NAC-LWT cask and the contents that may be transported. Drawings of the cask are presented within Section 1.4.

1.2.1 Packaging

1.2.1.1 Gross Weight

Gross shipping weight of the NAC-LWT spent-fuel shipping cask is approximately 52,000 pounds for the package. When mounted on the transport vehicle, the cask and vehicle weight is less than the 80,000-pound maximum for legal weight transport. A summary of overall component weights, detailed in Table 2.2.1-1, is listed below:

Component	Weight (pounds)
Cask Body	43,412
Closure Lid and Bolts	941
Payload and Basket	4,000 maximum
Impact Limiters	2,855
Total	51,208
SAR Analysis Weight	52,000

1.2.1.2 Materials of Construction, Dimensions, and Fabrication

The NAC-LWT cask body consists of Type 304 stainless steel forgings and closure lid with Type XM-19 stainless steel shells. Type XM-19 is a high strength stainless steel and is used in the inner and outer structural shells, which are more highly stressed than other cask components that use the more common Type 304 stainless steel. A lead gamma shield and a borated ethylene glycol/water solution neutron shield are utilized for radiation shielding. The cask provides the containment boundary for the payload and also acts as an environmental barrier. The cask is protected at each end by energy absorbing impact limiters, which consist of crushable aluminum honeycomb material with a thin aluminum shell. The impact limiters also provide thermal insulation, which protects the lid seals during the hypothetical fire transient event, although this thermal protection is conservatively neglected in this report. The cask is passively cooled because of its relatively low maximum heat loading of 2.5 kilowatts (kW). The overall arrangement of the NAC-LWT cask and design details are presented in the drawings within Section 1.4. The cask body, closure lid, and impact limiters are more fully described in the following sections.

1.2.1.2.1 Cask Body

The cask body is fabricated from Type 304 and Type XM-19 stainless steel. A poured lead gamma shield forms an annulus 5.75 inches thick and 174.9 inches long. The lead is enclosed between a 0.75-inch thick, 13.375-inch inner diameter Type XM-19 stainless steel inner shell and a 1.20-inch thick, 28.78-inch outer diameter Type XM-19 stainless steel outer shell. The Type 304 stainless steel bottom end forging of the cask is 4.0 inches thick, and the bottom also contains a 3.0-inch thick, 20.75-inch diameter lead disk enclosed by a 3.5-inch thick Type 304 stainless steel end cover.

As discussed in Chapter 8, installation of the lead into the cask is done in a carefully controlled manner. Temperatures of the inner and outer shells are continuously monitored and controlled during the lead pour and cooldown process. In addition, the welds connecting the inner and outer shells to the bottom end forging are not made until after the cooldown process is complete and the entire cask has reached a uniform temperature. Dimensional checks for straightness and ovality are also made before and after lead pour.

The upper ring forging is a Type 304 stainless steel ring 14.25 inches thick. This forging is machined to accept the closure lid and contains the penetrations to the cask cavity for the vent and fill/drain valves. Four lifting trunnions are welded to the forging to permit cask lifting and handling with a nonredundant or redundant lifting yoke.

Neutron shielding is provided by an ethylene glycol/water jacket that surrounds the 1.20-inch thick Type XM-19 stainless steel outer shell and is designed to axially blanket the active fuel length of the more common light water reactor fuels. The neutron shield region is 5.00 inches thick and 164.0 inches long. The external surface of the shield tank is a 0.24-inch thick Type 304 stainless steel shell with 0.50-inch thick end plates. An expansion tank for the neutron shield is provided to allow for thermal expansion and contraction of the liquid and is connected to the shield tank by a siphon tube. The liquid contains a solution of ethylene glycol/water and 1.0 wt % boron, which is added to reduce the secondary gamma radiation component.

The inner shell, end forgings, and the closure lid establish a cask cavity that is 177.9 inches long and 13.375 inches in diameter.

The weight of the cask body is approximately 43,412 pounds. The overall length of the cask body is 199.8 inches, and the maximum outside diameter is 44.24 inches at the neutron shield expansion tank.

1.2.1.2.2 Closure Lid

The cask closure lid is a Type 304 stainless steel forging 11.3 inches thick. The lid is machined to recess into the upper ring forging when it is installed on the cask. The closure lid and upper end forging are machined to provide a series of steps to prevent radiation streaming through the gap between the components. The closure lid attaches to the cask using 12 bolts with a 1-inch diameter. The containment boundary seal is achieved by a metallic O-ring captured in a groove machined on the underside of the closure lid (a second O-ring is provided to allow seal testing of the containment boundary O-ring). The O-rings mate against a machined sealing surface of the cask upper ring forging.

1.2.1.2.3 Impact Limiters

The impact limiters are fabricated from aluminum. The aluminum "honeycomb" has a crush strength of 3,500 psi. The honeycomb is a multidirectional crushable material that does not actually resemble a hexagonal honeycomb structure. The impact limiter is attached to the cask body at four locations. The outside diameter of the top end impact limiter is 65.25 inches and the bottom end impact limiter has a 60.25-inch diameter. The top and bottom impact limiters are 27.8 and 28.3 inches long, respectively, and both overlap the ends of the cask body by 12.0 inches.

1.2.1.3 Valves and Testing

The closure lid and the alternate and Alternate B drain and vent port covers each have a seal test port. The seal test port accesses the volume between the two O-ring seals on the cover or lid permitting leakage testing to verify proper sealing. The vent and drain valves are not considered part of the containment boundary and are used during in-plant loading operations to access the cask cavity for water filling and draining, vacuum drying, helium backfilling, etc.

1.2.1.4 Heat Dissipation

There are no special devices utilized on the NAC-LWT cask for the transfer or dissipation of heat. The package is passively cooled, which is possible because of its relatively low maximum heat load of 2.5 kW. A more detailed discussion of the package thermal characteristics is provided in Chapter 3.

1.2.1.5 Coolants

There are no coolants utilized within the package other than the normal transportation atmosphere of air or helium, depending on content conditions.

1.2.1.6 Protrusions

There are no outer protrusions on the package other than the four external lifting trunnions, the longitudinal shear ring at the upper end of the cask, and the eight impact limiter attachment lugs, four near each end of the package. All of these protrusions are located within the envelope protected by the impact limiters. The closure lid and valve port covers are recessed into the cask body and do not protrude from the cask surface. Refer to the drawings in Section 1.4 for more detail.

1.2.1.7 Lifting and Tiedown Devices

Of the four trunnions located on the exterior of the package at the upper end forging, two are intended for lifting with a nonredundant lifting yoke and the other two are used with a redundant lifting yoke. The package lifting and tiedown features are described in more detail in Section 2.5.

1.2.1.8 Shielding

A 5.75-inch annulus of lead and 2.19 inches of steel are maintained between the cask contents and the exterior radial surface of the package for the attenuation of radiation. Five inches of borated water are also provided for neutron shielding. The bottom end of the cask provides 7.5 inches of steel and 3.0 inches of lead shielding, and the closure lid provides 11.3 inches of steel shielding. Further detail is provided in Chapter 5.

1.2.2 Operational Features

The NAC-LWT cask is intended to be simple to operate. The cask is designed to be easily loaded and handled at any nuclear facility. The outer surface of the cask is electropolished and the configuration of the exposed surfaces aids in decontamination. An optional sleeving arrangement is available to limit contact between the cask and the contaminated pool water during wet loading and unloading.

The closure lid of the cask and the two valve port covers (alternate and Alternate B designs) are one-piece fixtures designed for ease of handling and to maintain personnel dose rates as low as reasonably achievable (ALARA). The closure lid has built-in alignment grooves (i.e. key ways) to facilitate installation. The alternate and Alternate B port cover designs provide clearance for valves underneath the port cover. The inner O-rings on the closure lid and the vent and drain valve port covers are components of the cask containment boundary. For the transport of TPBAR contents and other contents requiring both leaktight and high-pressure containment capabilities (i.e., damaged TRIGA fuel in sealed DFCs or PWR MOX fuel rods), the cask is

required to be configured with Alternate B drain and vent port covers incorporating metallic seals. For all other contents, the leaktight capable (i.e., no credible leakage) alternate port covers incorporating Viton O-ring seals can be used. The transport arrangement drawings for approved contents are presented in Section 1.4.

An alternative drain tube, including a drain tube alignment ring, is required to be installed and utilized when loading and transporting modular fuel baskets (i.e., not full length) and canisters.

The impact limiters and the personnel barrier are designed to be removed and installed without the aid of supplemental lifting gear or fixtures. All approved content may be transported in an International Shipping Organization (ISO) container, except for PWR and BWR fuel assemblies. All operational features are readily apparent from the drawings provided in Section 1.4. Operational procedures are delineated in Chapter 7.

1.2.3 Contents of Packaging

The NAC-LWT cask is analyzed, as presented in this SAR, for the transport of the contents listed in Table 1.1-1 and Section 1.1.

Shipments in the NAC-LWT package shall not exceed the following limits:

1. The maximum contents weight shall not exceed 4,000 pounds.
2. The limits specified in Table 1.2-1 through Table 1.2-13 for the fuel and other radioactive contents shall not be exceeded.
3. Any number of casks may be shipped at one time, one cask per tractor/trailer vehicle.
4. The maximum decay heat shall not exceed the following: 2.5 kW for PWR fuel assemblies; 2.2 kW for BWR fuel assemblies; 2.3 kW for 25 high burnup PWR fuel rods; 2.1 kW for 25 high burnup BWR fuel rods; 2.3 kW for 16 PWR MOX/UO_2 fuel rods; 1.26 kW for MTR fuel; 1.05 kW for DIDO fuel assemblies with top spacer and 0.756 kW without top spacer; 1.05 kW for TRIGA fuel elements or fuel cluster rods; 13.05 W for GA IFM packages; 0.693 kW for 300 TPBARs; 0.127 kW for TPBAR segments; 0.058 kW for 25 TPBARs; 0.84 kW for the PULSTAR fuel contents; 0.659 kW for spiral fuel assemblies (0.109 kW per basket); 0.126 kW for MOATA plate bundles (21 W per basket); and 1.26 kW for solid, nonfissile, irradiated hardware.
5. Radiation levels shall meet the requirements delineated in 10 CFR 71.47 or 49 CFR 173.441. The neutron shield tank may be drained for shipment of metallic fuel rods.
6. Surface contamination levels shall meet the requirements of 10 CFR 71.87(i) or 49 CFR 173.443.
7. Damaged TRIGA fuel elements and fuel debris (up to two equivalent elements) will be shipped in a sealed damaged fuel canister.
8. Damaged TRIGA cluster rod and fuel debris will be transported in a sealed damaged fuel canister (maximum of up to six equivalent fuel cluster rods).

9. MTR fuel elements may consist of any combination of intact or damaged highly enriched uranium (HEU), medium enriched uranium (MEU) or low enriched uranium (LEU) fuel elements that are enveloped by the parameters listed in Table 1.2-4 as supported by information presented in Table 5.1.1-2, Table 6.4.3-21, Table 6.4.3-22, Table 6.4.3-25 and Table 6.4.3-28. MTR fuel elements will be transported in a leaktight configuration NAC-LWT cask.
10. High burnup PWR fuel rods will be shipped in either a sealed, free flow or screened can.
11. High burnup BWR fuel rods will be shipped in either a sealed, free flow or screened can.
12. Up to 25 high burnup PWR or BWR fuel rods in a fuel assembly lattice or rod holder. Up to 14 of the fuel rods in a rod holder may be classified as damaged. Damaged fuel rods or rod sections may be placed into fuel rod capsules prior to placing them in the fuel rod holder. Typical failed fuel rod capsule configuration is shown in Figure 1.2-11.
13. Production TPBARs will either be shipped in an open top consolidation canister as shown in Figure 1.2.3-10 and assembled in the cask as shown in Figure 1.2.3-12, or shipped in a PWR/BWR Rod Transport Canister in accordance with License Drawing No. 315-40-104.
14. Intact PULSTAR fuel elements may be loaded into a fuel rod insert or the PULSTAR screened or failed fuel can.
15. Damaged PULSTAR fuel elements and nonfuel components of PULSTAR fuel assemblies shall be loaded into either a PULSTAR failed fuel or screened fuel can, and placed into the top or base module of the 28 MTR fuel basket. Damaged fuel, including fuel debris, may be placed in an encapsulating rod prior to loading in a PULSTAR can.
16. Any combination of spiral fuel assemblies or MOATA plate bundles, each loaded into separate ANSTO basket modules containing up to a total of 42 assemblies/bundles.
17. Segmented TPBARs will be shipped in a sealed, dry Waste Container as shown in Figure 1.2.3-16 and assembled in the cask as shown in Figure 1.2.3-17.
18. Solid, irradiated and contaminated hardware containing less than a Type A quantity of fissile material and meeting the exemptions of 10 CFR 71.15, paragraphs (a), (b) and (c), loaded directly into the cask or contained in a secondary container or basket. The irradiated hardware spacer will be installed to limit the axial movement of the hardware above the lead shielded region of the cask body. As needed, additional secondary containers, dunnage and shoring may be used to limit the movement of the contents during normal and accident conditions of transport.
19. PWR MOX fuel rods (or a combination of PWR MOX and UO_2 PWR fuel rods) are required to be loaded in a screened or free flow PWR/BWR Rod Transport Canister provided with a 5 × 5 insert.
20. Any combination of up to 7 degraded clad DIDO, spiral or MOATA plate elements/ bundles loaded into an aluminum screened DFC as shown Figure 1.2.3-18 placed in an ANSTO top basket module, with remainder of either ANSTO basket modules containing MOATA plate bundles or spiral fuel elements or ANSTO-DIDO combination basket containing DIDO elements. Degraded aluminum-clad DIDO, spiral or MOATA plate elements/bundles will be transported in a leaktight configuration NAC-LWT cask.

1.2.3.1 TRIGA Fuel and Basket Description

Two basic types of TRIGA fuel are to be transported in the NAC-LWT cask: TRIGA fuel elements and smaller fuel rods from TRIGA fuel cluster assemblies. TRIGA fuel elements are approximately 1-1/2 inches in diameter and are described in Section 1.2.3.1.1. TRIGA fuel cluster rods are smaller; approximately 1/2-inch in diameter and are also described in Section 1.2.3.1.1.

Up to 140 TRIGA fuel elements in the form of: a) standard fuel elements – either aluminum clad or stainless steel clad; b) instrumented fuel elements – similar to standard fuel elements (aluminum clad or stainless steel clad), but containing thermocouple instrumentation; and c) fuel follower control rod elements (aluminum or stainless steel clad) – poison rods with a fuel follower in a single tube may be shipped in the NAC-LWT cask. Up to 560 TRIGA fuel cluster rods may be shipped.

Up to six equivalent TRIGA fuel cluster rods may be loaded and transported in a sealed damaged fuel can (DFC). Up to the equivalent of two TRIGA damaged fuel elements and debris may be loaded and shipped in a sealed DFC. The TRIGA transport baskets and DFCs are described in Section 1.2.3.1.2.

1.2.3.1.1 TRIGA Fuel

TRIGA Fuel Elements

The characteristics of the design basis TRIGA fuel element are presented in Table 1.2-4 and in Table 1.2-1 for the poisoned basket and in Table 1.2-2 for the nonpoisoned basket.

The fuel material in a TRIGA fuel element is a solid, homogeneous mixture of uranium-zirconium hydride alloy, i.e., a metal alloy fuel. Both the aluminum-clad and the stainless steel-clad TRIGA fuel elements are approximately 1.5-inch diameter rods by approximately 30 inches long. The fuel follower control rod elements range in length from 45 inches to 66.5 inches and are cut, as required, to fit the basket length. Instrumented fuel elements are identical to standard fuel elements with the exception of thermocouples and wires and lead-out tubing. The lead-out tubing needs to be detached prior to shipment in order for the instrumented fuel elements to fit into the standard element height envelope. The aluminum-clad TRIGA fuel element and instrumented fuel element, the stainless steel-clad TRIGA fuel element and instrumented fuel element, and the standard fuel follower control rod element are shown in Figure 1.2.3-1 through Figure 1.2.3-5, respectively.

TRIGA Fuel Cluster Rods

The fuel material in TRIGA fuel cluster rods is a solid, homogeneous mixture of uranium-zirconium-erbium hydride alloy, i.e., a metal alloy fuel. Erbium is a burnable neutron poison that is used in the fuel to enhance the flux profile along the length of the fuel rod, and conservatively ignored in the nuclear evaluations. The rods have a nominal diameter of 0.54 inch and are approximately 31 inches long. The rod cladding is Incoloy 800 material and is 0.015-inch thick, minimum. Instrumented rods are identical to the standard rods, with the exception of thermocouples and wires. A diagram of the TRIGA fuel cluster rods, and the individual fuel pin (cluster rod) making up the cluster, is shown in Figure 1.2.3-6.

The active fuel region of a TRIGA fuel cluster rod is a maximum of 0.53 inch in diameter, 22.5 inches in length, and has an initial uranium enrichment of up to 95 percent for HEU material and 20percent for LEU material. A compression spring is utilized to fill the space in the plenum region of the rod, and top and bottom plugs are used to seal the fuel within the rod. The design-basis TRIGA fuel cluster rod characteristics are summarized in Table **1.2-3**, Table 1.2-4, and Tables 5.1.1-1, 5.1.1-2, 6.2.6-1 and 6.2.6-2.

Axial fuel spacers, as shown on Drawing 315-40-085, may be used to axially position the TRIGA fuel elements, fuel inserts and DFCs. The axial spacers do not provide a safety function and are dunnage used to position the fuel elements to facilitate fuel handling. The total weight per basket module cell for the TRIGA fuel elements or cluster rods, inserts, spacer(s) and fuel cans, as applicable, shall be limited to a maximum of 80 pounds.

TRIGA Fuel Classification

The TRIGA fuel contents are divided into three categories based on fuel condition for evaluation, loading configuration and transport in the NAC-LWT:

1. Intact fuel (i.e., no cladding breach) is loaded directly into the TRIGA fuel basket modules (Section 1.2.3.1.2) with a maximum of four TRIGA fuel elements per loading position. Up to 16 intact cluster rods are loaded into fuel rod inserts (Drawing 315-40-096) that are inserted into the TRIGA fuel basket module cell openings. Intact TRIGA fuel elements and cluster rods may be loaded into a sealed DFC, if length permits.
2. Damaged TRIGA fuel elements and TRIGA fuel debris (up to the equivalent of two fuel elements) shall be loaded into a sealed DFC (Section 1.2.3.1.2), and then loaded into a top or base basket module.
3. Damaged TRIGA cluster rods and cluster rod fuel debris (up to the equivalent of six cluster rods) shall be loaded into a sealed DFC and then loaded into a top or base basket module.

1.2.3.1.2 TRIGA Fuel Baskets and Damaged Fuel Cans

The TRIGA fuel basket assembly configurations consist of five modules – a base module, three intermediate modules, and a top module. The three intermediate modules are interchangeable, but the base and top modules are required to be in their proper positions. Two basket configurations are available, "nonpoisoned" and "poisoned," where the poisoned basket configuration utilizes borated steel plates for additional criticality control. Each module has up to seven cells (fuel positions) for loading TRIGA fuel elements or cluster rods. The center cell of each module of the nonpoisoned basket configuration is blocked by a welded stainless steel baffle that prevents loading of that cell. The nonpoisoned configuration is also referred to as the 24-element basket or the 120-element loading, based on the maximum of 120 intact TRIGA fuel elements that may be loaded into the baskets in this configuration. The poisoned configuration is also referred to as the 28-element basket or the 140-element loading, based on the maximum of 140 intact TRIGA fuel elements that may be loaded into the baskets in this configuration. Additionally, the nonpoisoned configuration can accommodate up to 480 intact TRIGA fuel cluster rods, while the poisoned basket can hold up to 560 intact TRIGA fuel cluster rods.

Each basket module is a Type 304 stainless steel weldment consisting of longitudinal divider plates with circular support plates near each end; the top module also has a support plate at its midpoint due to its longer length. The poisoned basket modules contain four borated stainless steel plates that are seal welded to surfaces of the divider plates in the central region of the basket cross-section. The nonpoisoned basket modules are shown in Drawings 315-40-070, -071, and -072 and the poisoned basket modules are shown in Drawings 315-40-080, -081, and -082.

The nonpoisoned TRIGA fuel basket assembly in the NAC-LWT cask is shown in Drawing 315-40-079. The poisoned basket assembly in the NAC-LWT cask is shown in Drawing 315-40-084. In the poisoned basket configuration, an alternate assembly is presented that utilizes one base module and four intermediate modules, along with a spacer (Drawing 315-40-083). The spacer is utilized to fill the space differential in the cask cavity resulting from the use of an additional intermediate module, rather than a top module. This additional assembly configuration is provided for flexibility in situations where the extra length provided by the top module is not needed. The fuel basket modules are described in further detail in Section 2.6.12.8. Damaged TRIGA fuel and fuel debris shall be loaded into sealed DFCs.

The sealed DFC is a 3.25-inch outside diameter tube with a 0.065-inch thick wall. The bottom of the sealed fuel can includes a check valve and drain plug to facilitate draining of the can. The top of the sealed DFC is closed by a bolted lid that is sealed with a metallic O-ring and includes a diaphragm valve to facilitate draining, drying, and helium backfilling of the can. The sealed

DFC is constructed of austenitic stainless steels as shown on Drawings 315-40-086, -087, and-088.

1.2.3.2 MTR and DIDO Fuel and Basket Description

The MTR fuel elements to be shipped are 33 to 57 inches long, including the upper and lower nonfuel-bearing hardware, which may be removed from the element prior to transport. The MTR element fuel plates consist of a U-Al, U_3O_8-Al, or U_3Si_2-Al fuel meat clad with aluminum. The fuel plates are held in a parallel arrangement with two thick aluminum slotted pieces to form a fuel element. The active fuel region is typically 22.75 inches in height, and the fuel meat is typically 0.023-inch thick. MTR elements/plates may contain cadmium wires. A maximum 100-gram cadmium source is addressed in the shielding evaluations documented in Chapter 5. Axial fuel spacers and plates may be used in the cells of the basket modules to position MTR elements to facilitate fuel unloading and handling. The axial fuel spacers do not perform a safety function and are considered dunnage. The axial fuel spacers and plates are shown on Drawing 315-40-085.

A maximum of 42 MTR fuel elements has been analyzed for transport in the NAC-LWT cask. This configuration consists of up to seven fuel elements placed radially in each of the six axial fuel basket modules. Two alternate configurations of MTR fuel element loading provide for loads of 35 elements in five basket modules or 28 elements in four basket modules. HEU MTR fuel elements having > 380 g ^{235}U, but less than 460 g ^{235}U, shall have a minimum of 2.0 cm (0.8 inch) of nonfuel hardware and/or spacers/plates at both ends of the fuel element. The minimum 2.0 cm nonfuel hardware and/or spacer/plate dimension assures criticality control. The axial fuel spacer and plate design is shown on Drawing 315-40-085. For the shipment of MTR fuel elements (or an equivalent number of plates in a plate canister) having ^{235}U greater than 470 g per element, or greater than 22 g per plate (up to a maximum of 640 g per element or 32 g per plate), the maximum quantity of elements per basket module is limited to four, which are to be loaded in basket positions 4, 5, 6 and 7. Cell block spacers shall be installed in basket openings 1, 2 and 3 to block these cells from being inadvertently loaded with fuel elements. The cell block spacer design is shown on Drawing 315-40-085. Therefore, for the transport of elements of greater than 470 g ^{235}U, if only one element exceeds the 470 g (22 g per plate) limit, a maximum of four elements shall be loaded into the seven-element basket module and cell block spacers shall be placed in basket opening positions 1, 2 and 3.

Loose MTR fuel plates may be shipped in an MTR plate canister to facilitate handling. The contents of the canister are limited to the number of plates in the original intact fuel assembly, and the fuel plate dimensions and fuel masses must be bounded by the MTR fuel element limits

in Table 1.2-4. The total weight per basket module cell for the fuel element, spacer(s) and fuel plate canister, as applicable, shall be limited to a maximum of 80 pounds.

A maximum of 42 DIDO fuel assemblies has been analyzed for transport in the NAC-LWT cask. Again, up to seven fuel assemblies may be placed radially in each of six axial fuel basket modules.

DIDO fuel assemblies are similar to MTR fuel elements in that the fuel bearing hardware consists of plates of fuel meat sandwiched by cladding. However, in DIDO fuel, the plates have been formed into tubular elements that are arranged in a concentric configuration. Typical DIDO assemblies contain four of the concentric tubes.

MTR and DIDO fuel characteristics are presented in Table 1.2-4.

1.2.3.3 General Atomics Irradiated Fuel Material (GA IFM) and Basket Description

The GA IFM is made up of two separate types of fuel material—the High-Temperature Gas-Cooled Reactor (HTGR) type fuel and the Reduced-Enrichment Research and Test Reactor (RERTR) type fuel. Each type of IFM is packaged in its own unique Fuel Handling Unit (FHU). Figures 1.2-7 and 1.2-8 illustrate the HTGR and RERTR FHUs. Detailed drawings for the GA and IFM FHUs are in Section 1.4.

The HTGR IFM is comprised of fuel in four forms: fuel particles (kernels), fuel particles (coatings), fuel compacts (rods), and fuel pebbles. Fuel kernels are solid, spheridized, high-temperature sintered fully-densified, ceramic kernel substrate, composed of: UC_2, UCO, UO_2, $(Th,U)C_2$, or $(Th,U)O_2$. The as-manufactured enrichment of the HTGR fuel varies from ~10.0 to 93.15 wt % ^{235}U. Fuel coatings are solid, spheridized, isotropic, discrete multi-layered fuel particle coatings with chemical composition including pyrolitic-carbon (PyC) and silicon carbide (SiC). Fuel compacts are multi-coated ceramic fuel particles, bound in solid, cylindrical, injection-molded, high-temperature heat-treated compacts. The fuel compact matrix is composed of carbonized graphite shim, coke, and graphite powder. Fuel pebbles are multi-coated fuel particles, bound in solid, spherical injection-molded, high-temperature heat-treated pebbles. The fully-cured binding matrix is composed of carbonized graphite shim, coke , and graphite powder.

The RERTR IFM is comprised of 20 irradiated TRIGA fuel elements; 13 of the elements are intact and the remaining seven have been previously sectioned for examination purposes. Parameters characterizing the RERTR/TRIGA fuel elements are shown in Table 6.2.9-1. Three distinct mass loadings of uranium were used in the 20 TRIGA elements: 20, 30, and 45 wt % U; the average mass of the fueled portion of these elements is 551g with an enrichment of 19.7 wt %

^{235}U. The RERTR IFM consists of U-ZrH metal alloy fuel material and as a solid meets the requirement of 10 CFR 71.63.

Two GA IFM Fuel Handling Units (FHU) are intended for a single shipment in the NAC-LWT. The first IFM FHU contains HTGR type fuel and the second contains RERTR type fuel. Each IFM FHU consists of stainless steel weld-encapsulated primary and secondary enclosures. The FHUs are filled and sealed with air at atmospheric pressure. The two IFM FHUs are placed in the top of the NAC-LWT cavity with a bottom spacer to facilitate unloading of the IFM packages.

The GA IFM fuel characteristics are presented in Table 1.2-7.

1.2.3.4 PWR Fuel Assembly

The NAC-LWT cask is analyzed for the PWR fuel assemblies listed in Table 1.2-5. This table provides the dimensional and enrichment constraints for the PWR fuel. The burnup and decay heat limits are specified in Table 1.2-4.

The PWR fuel rod cladding is a zirconium alloy type (Zircaloy-2, Zircaloy-4, Zirlo, M-5, etc.). Minor variations of alloy composition have no impact on performance of cladding material.

1.2.3.5 BWR Fuel Assembly

The NAC-LWT cask is analyzed for the BWR fuel assemblies listed in Table 1.2-6. This table provides the dimensional constraints for the BWR fuel. The enrichment, burnup and decay heat limits are specified in Table 1.2-4.

The BWR fuel rod cladding is a zirconium alloy type (Zircaloy-2, Zircaloy-4, Zirlo, M-5, etc.). Minor variations of alloy composition have no impact on performance of cladding material.

1.2.3.6 TPBARs

The NAC-LWT cask is analyzed for the transport of three separate Tritium Producing Burnable Absorber Rod (TPBAR) content configurations. For the transport of production TPBARs from the reactor facility to the DOE processing facility, an open (i.e., unsealed) stainless steel consolidation canister is utilized to contain up to 300 TPBARs, two of which can be prefailed. The characteristics of the production TPBARs are listed in Table 1.2-8. The consolidation canister assembly is shown in Figure 1.2.3-10. Up to 25 TPBARs may also be transported within the 5×5 rod holder located within the PWR/BWR Rod Ttransport Canister. For a TPBAR shipment, the transport canister is located within the TPBAR basket. Up to two of the 25 TPBARs located within the rod holder may be classified as prefailed.

The third transport configuration is for the shipment of segmented TPBARs, following post-irradiation examination (PIE), contained in a welded stainless steel waste container containing segments and debris from up to 55 TPBARs. The characteristics of the TPBAR PIE segments are provided in Table 1.2-12. The waste container and extension weldment assembly is shown in Figure 1.2.3-16.

TPBARs are similar in size and nuclear characteristics to standard, commercial PWR, stainless steel-clad burnable absorber rods. The exterior of a typical TPBAR is a stainless steel clad tube. The internal components of the TPBAR are designed and selected to produce and retain tritium. Internal configurations differ for various TPBAR designs (see DOE reports provided in the Chapter 1 Appendices). The internal components of a typical TPBAR include a plenum spacer tube (getter tube), a spring clip or a plenum (compression) spring, pellet stack assemblies (pencils), and a bottom spacer tube. A pencil consists of a zirconium alloy liner around which lithium aluminate absorber pellets are stacked and then confined in a getter tube as shown in Figure 1.2.3-9. The unclassified design details of the various TPBAR designs are provided in the unclassified DOE documents and drawings provided in the Chapter 1 Appendices.

The transport assembly arrangements for the consolidation canister and waste container TPBAR content configurations are identical and include a closure lid spacer assembly, a TPBAR basket and Alternate B port covers with bolting installed. The detailed requirements for the NAC-LWT assembly are provided in license drawing 315-40-128 in Section 1.4. The overall payload arrangement for the NAC-LWT with the consolidation canister and waste container are shown in Figure 1.2.3-12 and Figure 1.2.3-17, respectively. For the transport of fewer than 300 TPBARs in the consolidation canister, stainless steel dunnage may be used to align and protect the contents. The weight and volume of the dunnage and the reduced TPBAR contents of the consolidation canister must be less than, or equal to, the weight and volume of 300 TPBARs. Up to 25 TPBPAR rods may also be transported in a PWR/BWR Rod Transport Canister in a NAC-LWT assembly as shown in License Drawing No. 315-40-104 (assembly 95).

The TPBAR content conditions are analyzed and evaluated for compliance with structural, thermal, containment and shielding conditions of the NAC-LWT in the appropriate SAR chapters. TPBARs do not contain fissile material and, therefore, criticality evaluations have not been performed. The operating procedures for the wet and dry loading and dry unloading of the TPBAR contents are provided in Chapter 7. The special leakage and pressure testing requirements for NAC-LWT casks intended for the transport of TPBAR contents are provided in Chapter 8.

1.2.3.7 PWR/BWR Fuel Rods

PWR and BWR fuel rods are transported within the fuel lattice (skeleton) or 4×4 or 5×5 inserts (rod holder). The rod holder is located within a free flow, screened or sealed PWR/BWR transport canister. (The rod holder may also contain a nonfuel-bearing irradiated hardware component [e.g., BWR water rod, PWR instrument/guide tube].)

The PWR and BWR fuel rod cladding is of Zirconium alloy type (Zircaloy-2, Zircaloy-4, Zirlo, M-5, etc.). Minor variations of alloy composition have no impact on performance of cladding material.

1.2.3.8 PULSTAR Fuel Element and Transport Configuration Description

PULSTAR fuel elements are transported in the NAC-LWT in the 28 MTR fuel basket assembly, which contains four modules with seven cells per module. The basket assembly is composed of a top module, a base module, and two intermediate modules (Dwgs 315-40-051, -049, and -050, respectively).

PULSTAR fuel elements may be loaded into the module cells in one of four configurations: a) intact PULSTAR fuel assemblies b) intact PULSTAR fuel elements loaded into the 4×4 TRIGA fuel rod insert (Dwg. 315-40-096); c) intact or damaged PULSTAR fuel elements, fuel debris and nonfuel-bearing components of PULSTAR fuel assemblies in the PULSTAR screened can (Dwg. 315-40-135); or d) intact or damaged PULSTAR fuel elements, fuel debris and nonfuel-bearing components of PULSTAR fuel assemblies in the PULSTAR sealed can (Dwg. 315-40-130). The contents of either can type are restricted to a quantity of fissile material and a total volume of material equivalent to 25 PULSTAR fuel elements. The sealed cask contents are restricted to the displaced volume of 25 intact PULSTAR fuel elements. The total cask payload shall not exceed 700 PULSTAR fuel elements. Loading of modules with mixed PULSTAR payload configurations is allowed, but PULSTAR cans, either screened or sealed, are restricted to loading in the base and top modules.

PULSTAR fuel elements are low enriched (< 7 wt %) uranium oxide rods, with zirconium alloy cladding. During reactor operation, 25 PULSTAR fuel elements are arranged in a rectangular 5×5 lattice, surrounded by a zirconium alloy box, and capped by top- and bottom-end fittings to form a PULSTAR fuel assembly. The nonfuel components of a PULSTAR fuel assembly are primarily aluminum and zirconium alloy and do not contain a significant activation source. A sketch of a PULSTAR fuel assembly is provided in Figure 1.2.3-13. Key physical, radiation protection and thermal characteristics of the PULSTAR fuel assembly/elements are listed in Table 1.2-9.

The sealed and screened PULSTAR cans are stainless steel containers that: a) minimize the dispersal of gross fuel particles that may escape from damaged fuel element cladding and/or fuel debris; b) facilitate retrieval of the contents from the transportation cask; and c) confine damaged fuel and/or debris within a known volume to facilitate criticality control, maintain dose limits, and control thermal loads within the cask. PULSTAR fuel pellets, pieces, and debris may be placed in an encapsulating rod for handling purposes prior to placement into either a sealed or screened can. The encapsulating rod is not required and has no safety significance. In addition to fuel elements, the cans may contain fuel assembly hardware up to the total content weight limit specified in Table 1.2-9. For operational/retrievability purposes, stainless steel rod inserts may be used to position the PULSTAR fuel elements within the fuel rod insert. Total content weight shall not exceed the total weight limit specified in Table 1.2-9. The fuel rod insert is composed of a 4×4 grid of 0.75-inch OD × 0.065-inch wall stainless steel tubes. The tubes provide structural support for individual intact PULSTAR fuel elements during transport in the NAC-LWT.

Spacers may be used to axially position PULSTAR fuel contents near the top of the module for ease of loading and unloading operations. The spacers are provided for ease of operations and do not provide a safety function.

1.2.3.9 ANSTO Basket and Payload Description

Three basic fuel types are to be transported in the ANSTO baskets within the NAC-LWT cask: spiral fuel assemblies, MOATA plate bundles and DIDO elements. Spiral fuel assemblies are composed of cylindrical aluminum inner and outer shells connected by curved metallic fuel plates. Further detail on the spiral fuel assemblies is provided in Section 1.2.3.9.1. MOATA plate bundles are comprised of up to 14 MTR fuel plates. Further detail on the plate bundles is provided in Section 1.2.3.9.2. DIDO elements are described in Section 1.2.3.2. The spiral fuel assemblies, MOATA plate bundles and DIDO elements may be intact or may have degraded cladding and be disassembled. Note that spiral assemblies may be cropped by removing nonfuel-bearing hardware to fit within the basket tubes. Cropped spiral fuel assemblies are classified as intact fuel. Spiral, MOATA and DIDO having degraded cladding or disassembled may be placed in aluminum DFCs as shown on Figure 1.2.3-18 prior to loading into the top ANSTO basket module or assembly to facilitate handling during loading and unloading operations. DFCs containing fuel elements shall be limited to loading in the 7 cells of the top ANSTO basket module of a standard six-module ANSTO basket assembly or in the top ANSTO basket module of the ANSTO-DIDO combination basket assembly. The ANSTO-DIDO combination basket is an assembly of a top ANSTO module, four intermediate DIDO modules and one base DIDO

module. As the interfaces, weight and overall dimensions of the ANSTO and DIDO basket modules are essentially identical, the combination basket assembly is bounded by the structural, thermal and criticality analyses for the separate DIDO and ANSTO basket assemblies.

Up to 42 spiral fuel assemblies or 42 MOATA plate bundles may be loaded in an ANSTO basket assembly. Up to 7 intact DIDO, spiral or MOATA plate elements/bundles and/or degraded clad DIDO, spiral or MOATA plate elements/bundles in DFCs may be loaded in an ANSTO top module in either the standard ANSTO basket assembly or in the ANSTO-DIDO combination basket assembly. DIDO fuel elements loaded into an ANSTO top module in either the ANSTO basket assembly or the ANSTO-DIDO combination basket assembly will be limited to a maximum decay heat load of 10 W per element whether with or without a DFC. Spiral fuel elements loaded into DFCs shall be limited to a maximum decay heat load of 10 W per element. MOATA plate bundles loaded into DFCs shall be limited to a maximum decay heat of 1 W per bundle. The remaining 35 cells of the ANSTO-DIDO combination basket may be loaded with up to 35 intact DIDO fuel elements.

A full cask load of either the ANSTO basket assembly or the ANSTO-DIDO combination basket assembly contains 6 baskets of up to 7 fuel assemblies or plate bundles per basket. The mixed loading of ANSTO and ANSTO-DIDO combination basket assemblies as described previously containing spiral fuel assemblies, MOATA plate bundles or DIDO elements is authorized.

1.2.3.9.1 Spiral Fuel Assemblies

The design basis characteristics of spiral fuel assemblies are presented in Table 1.2-10. The fuel material in spiral fuel assembly plates is a solid, homogeneous mixture of uranium-aluminum alloy, i.e., a metal alloy fuel. The fuel meat of each plate is clad in aluminum. A set of 10 curved fuel plates is located between an inner and outer cylindrical aluminum shell. Fuel elements are cropped to fit axially within the basket envelope. Fuel material is not cut during the cropping operation. The fuel plates are located in a spiral pattern, maintaining a constant pitch between fuel plate centers. A sketch of the assembly cross-section is provided in Figure 1.2.3-14.

1.2.3.9.2 MOATA Plate Bundles

The design basis characteristics of MOATA plate bundles are presented in Table 1.2-4. The fuel material in the plate bundle is a solid, homogeneous mixture of uranium-aluminum alloy, i.e., a metal alloy fuel. Each plate is clad in aluminum. A plate bundle is comprised of up to 14 fuel plates. Two thick (0.635 cm) aluminum nonfuel side plates support the fuel plate stack from two sides, making a possible total of 16 plates per bundle. At each axial end, the plates in the stack

are connected by a pin. Spacing between plates is maintained by disk spacers placed onto the top and bottom pins between each fuel plate and the aluminum side plates. A sketch of a typical MOATA plate bundle is provided in Figure 1.2.3-15.

1.2.3.10 Solid, Irradiated and Contaminated Hardware

The design basis characteristics of the solid, irradiated and contaminated hardware are provided in Table 1.2-13. As described in the content definition, the solid, irradiated and contaminated hardware may contain small quantities of fissile materials. Fissile materials in the irradiated hardware contents are acceptable if the quantity of fissile material does not exceed a Type A quantity and does not exceed the exemptions of 10 CFR 71.15, paragraphs (a), (b) and (c).

The irradiated hardware may be directly loaded into the NAC-LWT cask cavity, or may be contained in a secondary container or basket. As needed, appropriate component spacers, dunnage and shoring may be used to limit the movement of the contents during normal and accident conditions of transport.

To ensure that the movement of the irradiated hardware contents above the lead shielded length of the NAC-LWT cask body (i.e., the approximately upper 6.25 inches of the cavity length) is precluded, an Irradiated Hardware Lid Spacer as shown on Drawing No. 315-40-145 shall be installed for all irradiated hardware content configurations. The total installed height of the spacer is 6.5 inches. Therefore, the available cavity length for the irradiated hardware is approximately 171 inches. The NAC-LWT cask shall be assembled for transport as shown on NAC Drawing No. 315-40-01 with the irradiated hardware spacer installed on the lid.

A comparative shielding evaluation for a conservatively selected irradiated hardware transport configuration (i.e., a single line source with no self-shielding) or consideration of the additional shielding provided by additional spacers, dunnage, inserts or secondary containers is presented in Chapter 5. The evaluations show that the regulatory dose rate requirements per 10 CFR 71.47 for normal conditions of transport, or 10 CFR 71.51(b) under hypothetical accident conditions, are not exceeded.

1.2.3.11 PWR MOX Fuel Rods

The NAC-LWT cask is analyzed and evaluated for the transport of up to 16 PWR MOX fuel rods (or a combination of up to 16 PWR MOX and UO_2 fuel rods) loaded into a 5 × 5 insert placed in a screened or free flow PWR/BWR Rod Transport Canister. The authorized characteristics of the evaluated PWR MOX fuel rods are provided in Table 1.2-4. For mixed PWR MOX and UO_2

PWR fuel rod combinations, the UO_2 PWR fuel rods may have the identical heat load, burnup and cool time characteristics as the PWR MOX fuel rods.

In addition to the 16 PWR MOX fuel rods (or a combination of PWR MOX and UO_2 PWR fuel rods), up to 9 burnable poison rods (BPRs) may be loaded in the remaining openings in the 5 × 5 insert in the PWR/BWR Rod Transport Canister.

Figure 1.2.3-1 Aluminum Clad TRIGA Fuel Element

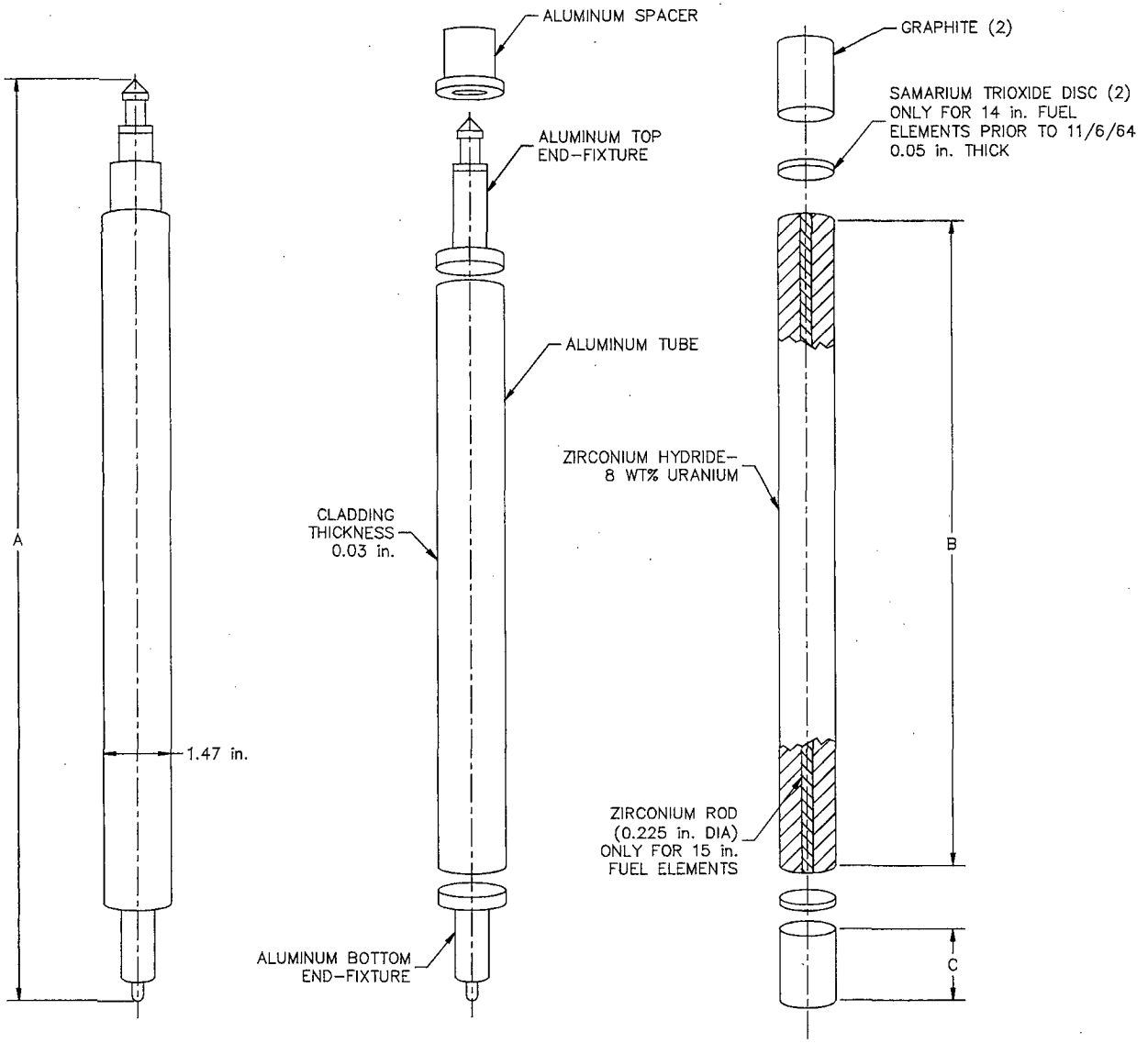

Figure 1.2.3-2 Aluminum Clad Instrumented Fuel Element

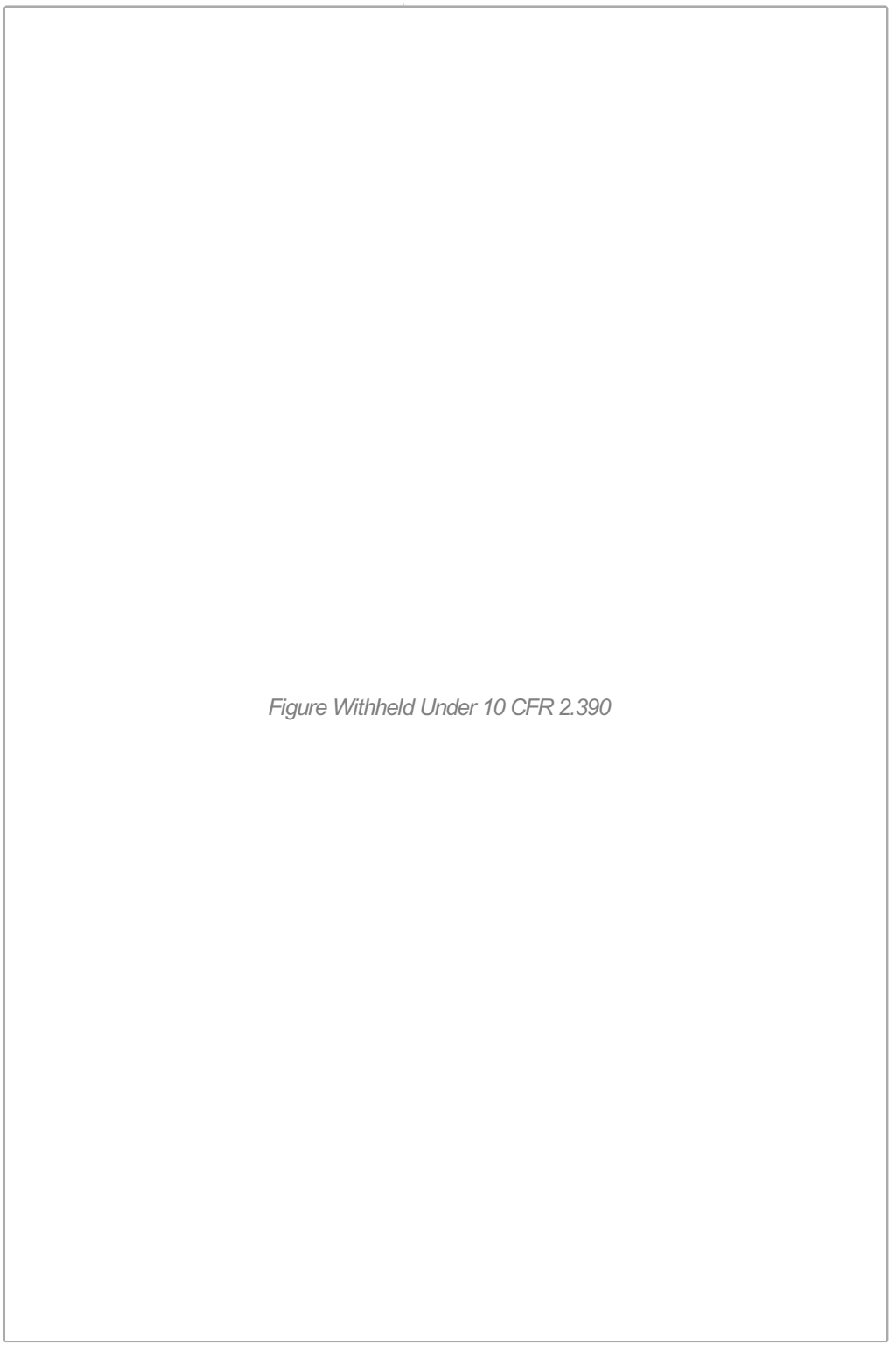

Figure 1.2.3-3 Stainless Steel Clad TRIGA Fuel Element

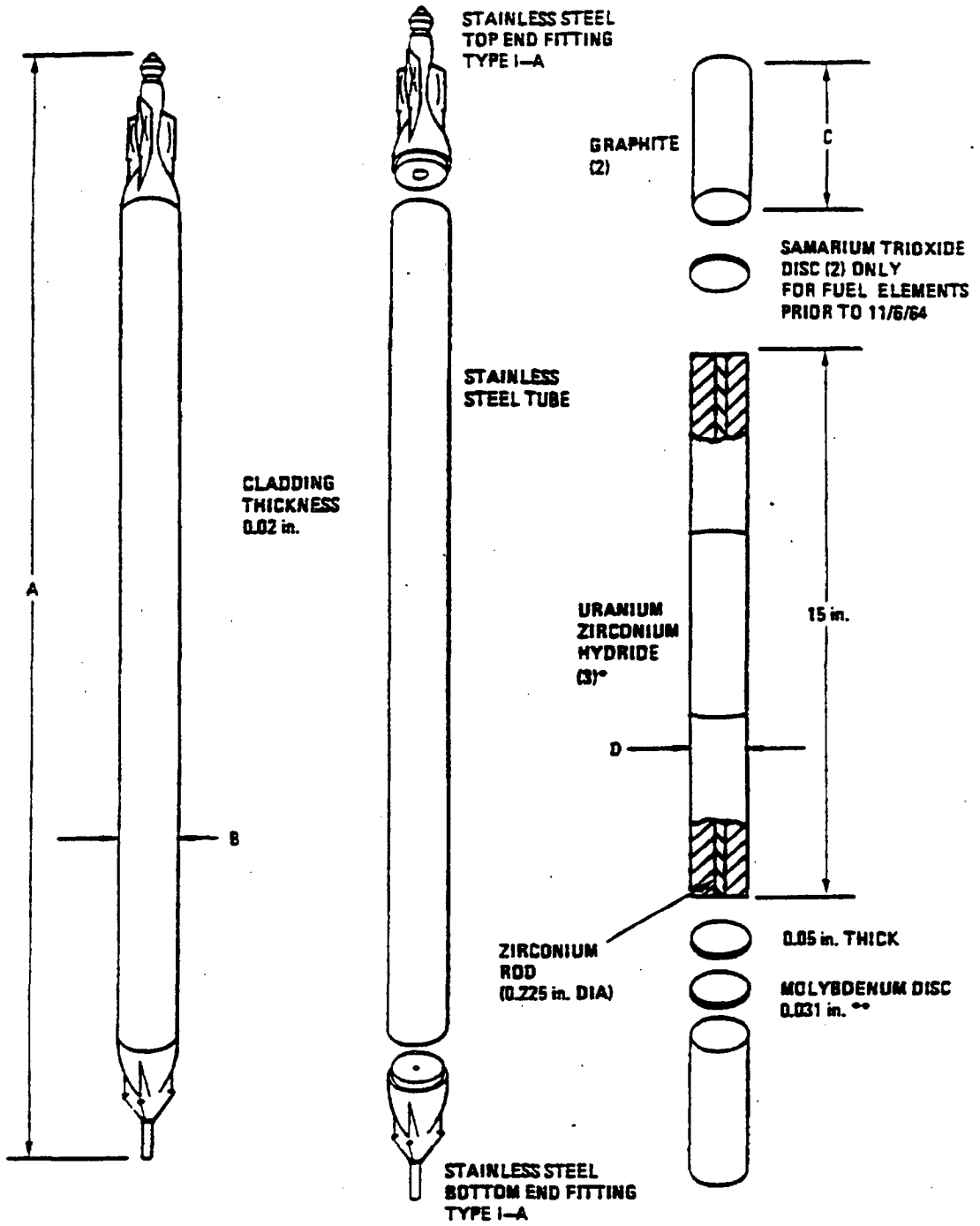

Figure 1.2.3-4 Stainless Steel Clad Instrumented Fuel Element

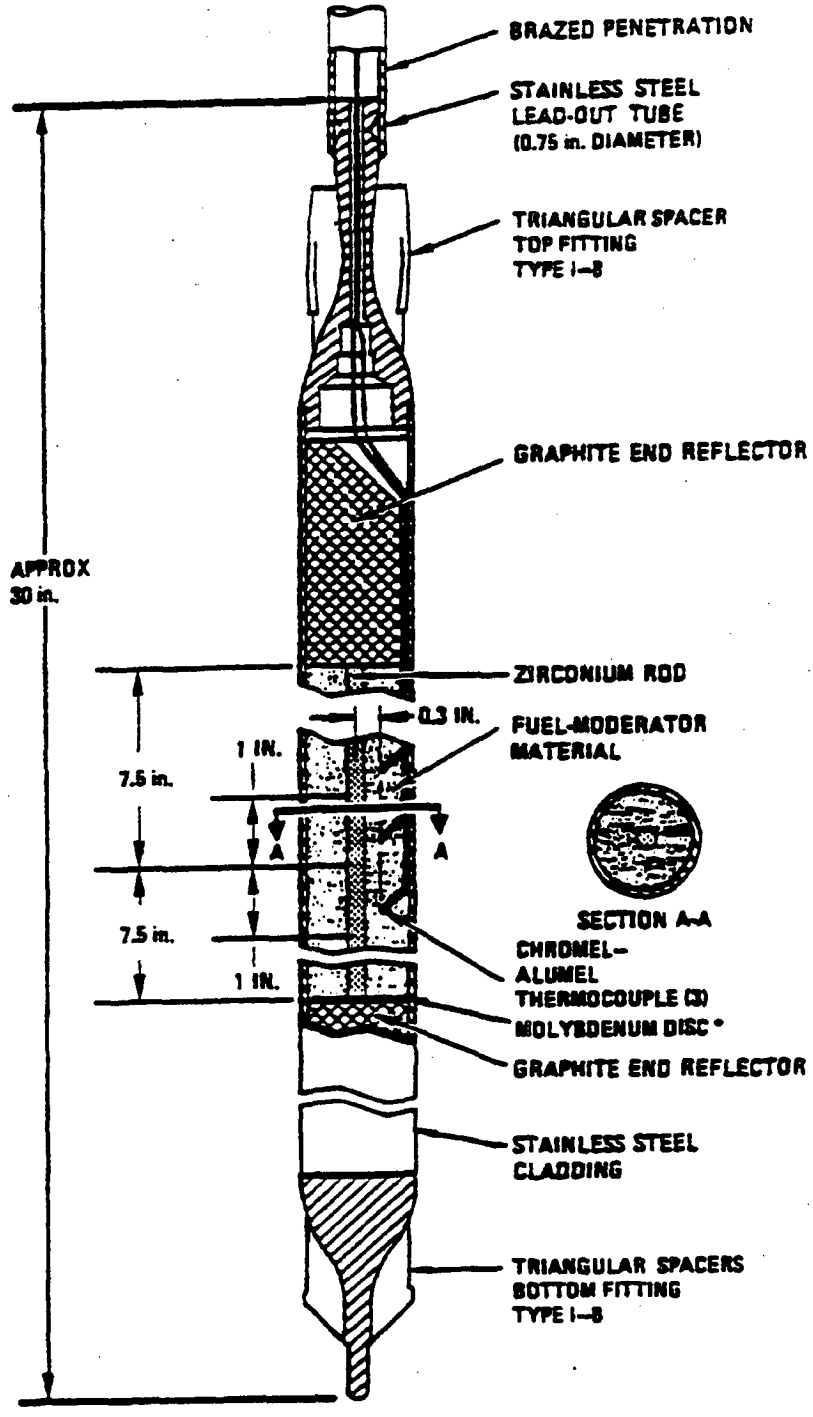

Figure 1.2.3-5 Standard Fuel Follower Control Rod Element

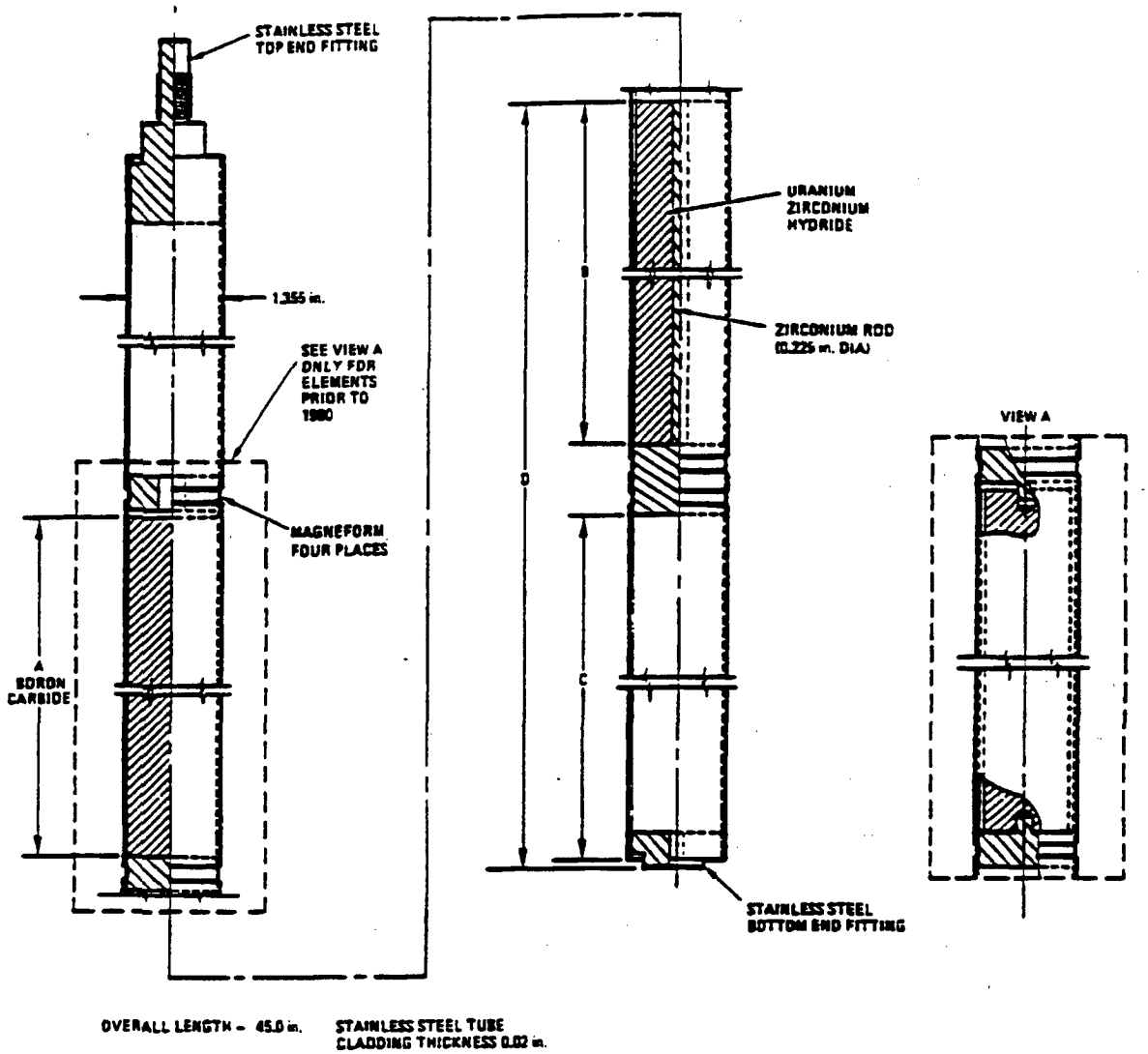

Figure 1.2.3-6 TRIGA Fuel Cluster and Rod Details

TRIGA *FUEL CLUSTER*

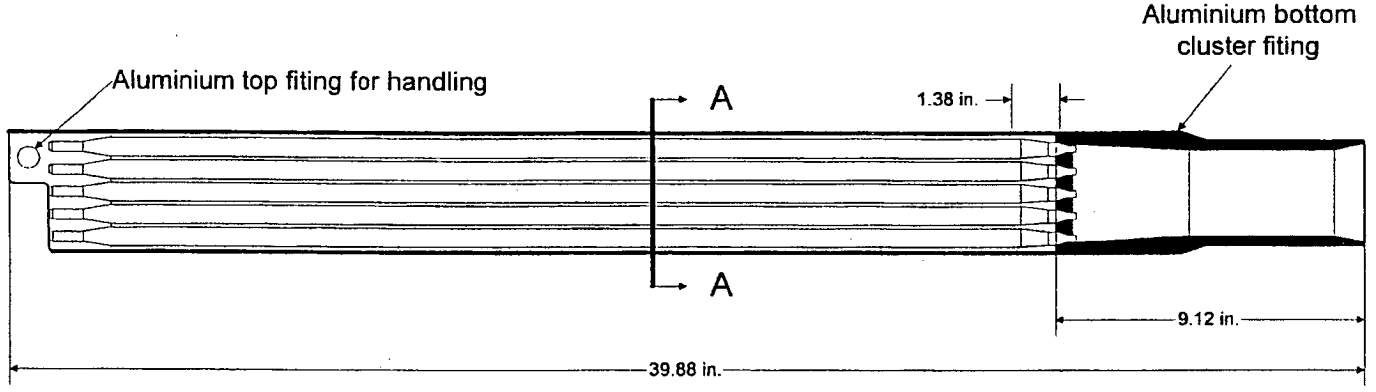

FUEL ROD

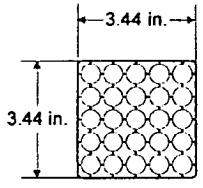

SECTION A:A

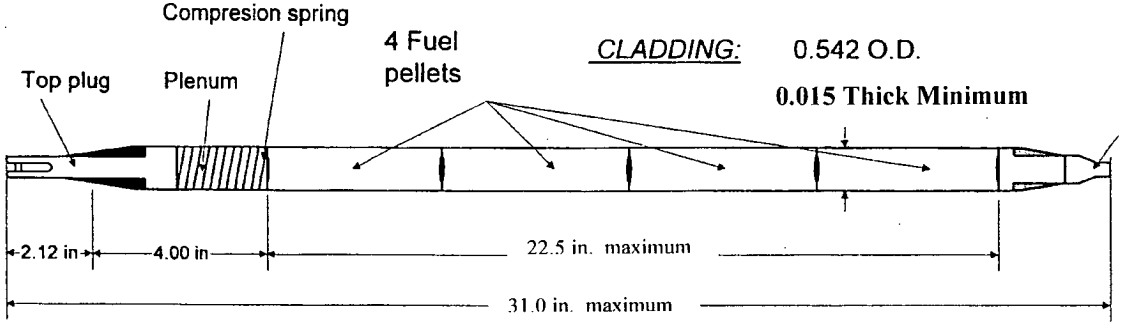

Fuel bundle and fuel element

Figure 1.2.3-7 HTGR Fuel Handling Unit

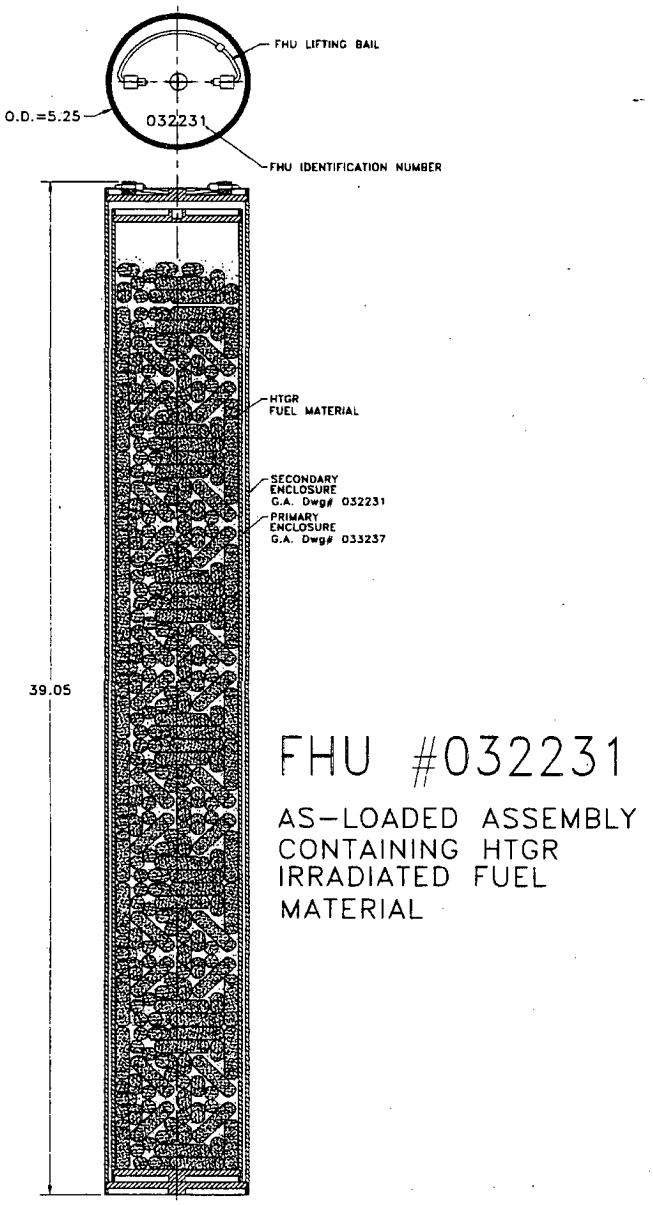

Figure 1.2.3-8 RERTR Fuel Handling Unit

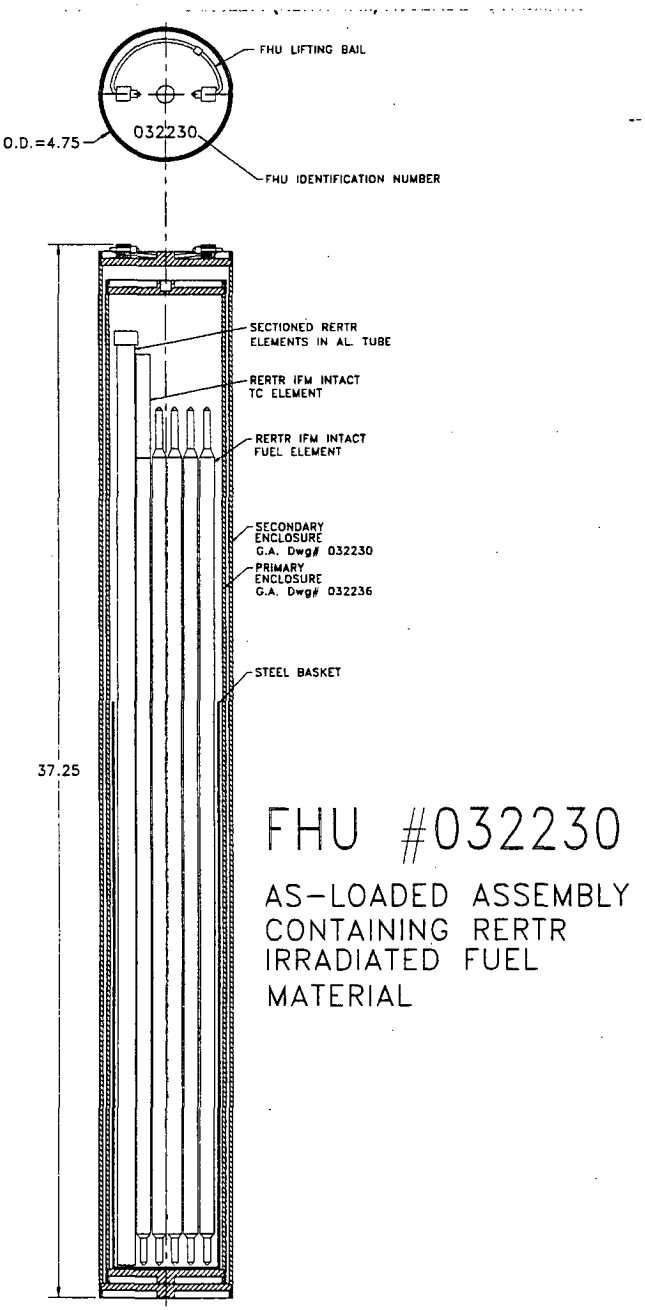

Figure 1.2.3-9 Typical TPBAR Assembly

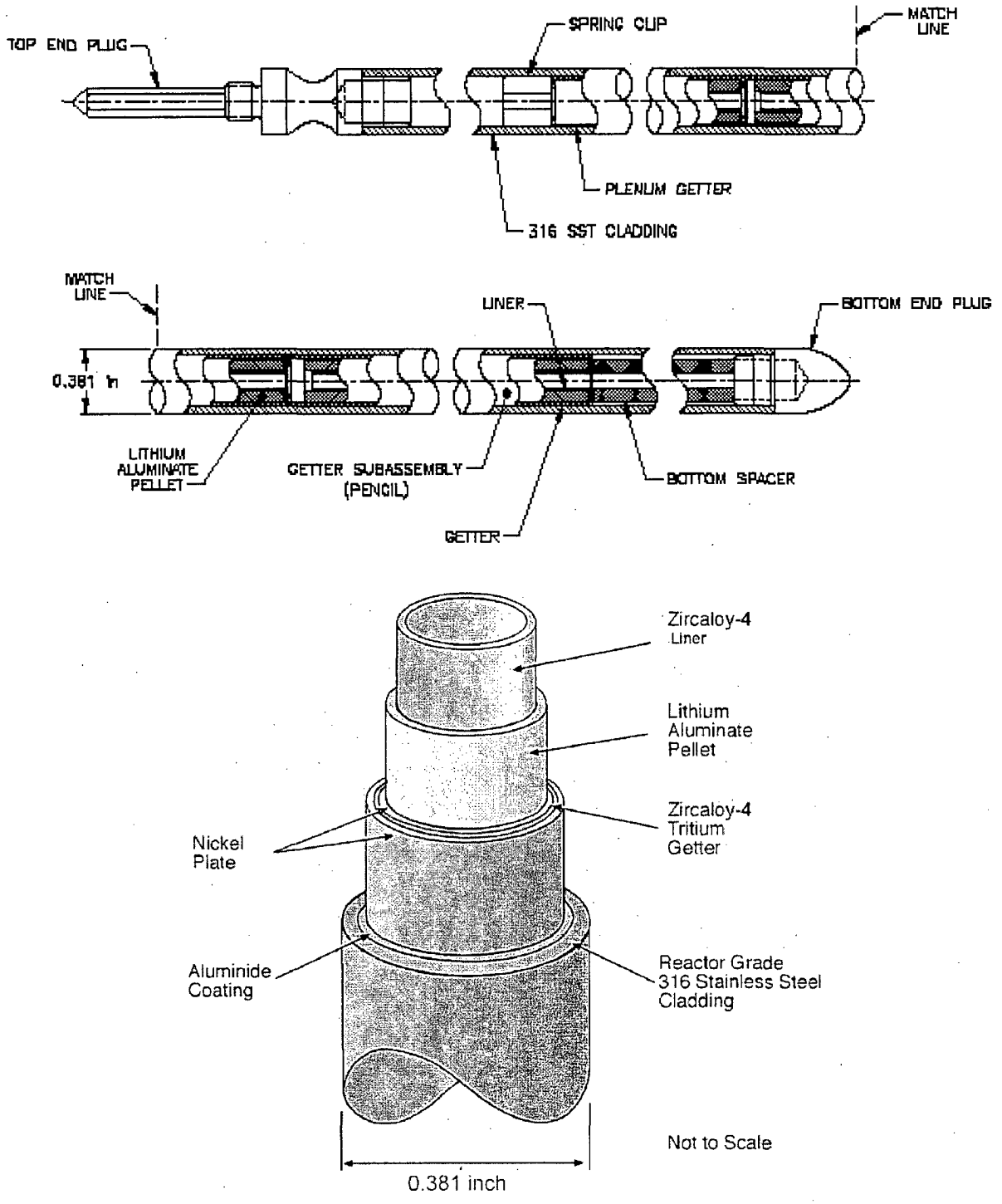

Figure 1.2.3-10 TPBAR Consolidation Canister Sketch

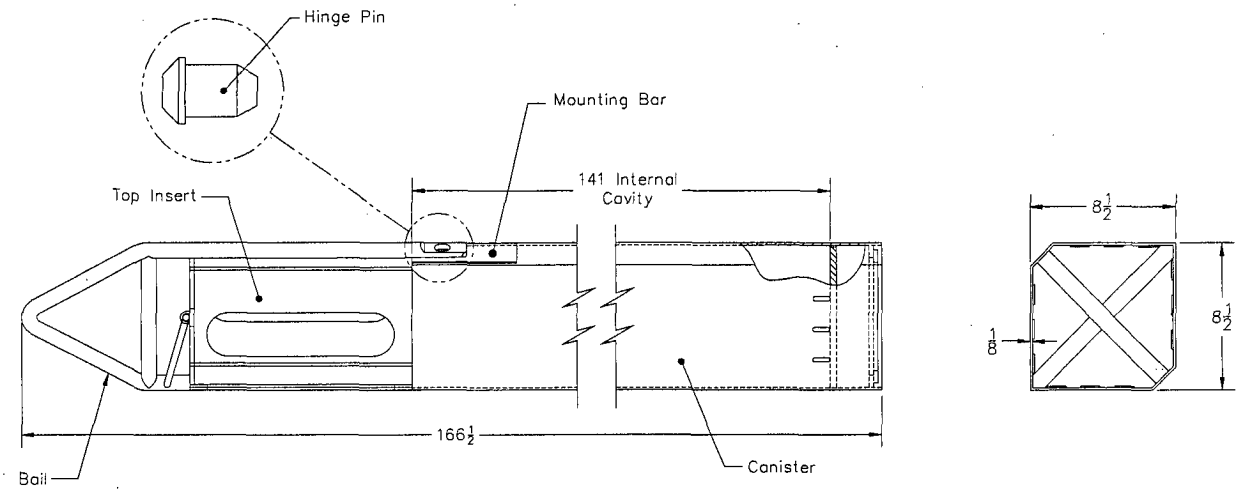

Conceptual Layout with Approximate Dimensions

Note: Material of construction is stainless steel.

Figure 1.2.3-11 Failed PWR/BWR Fuel Rod Capsule

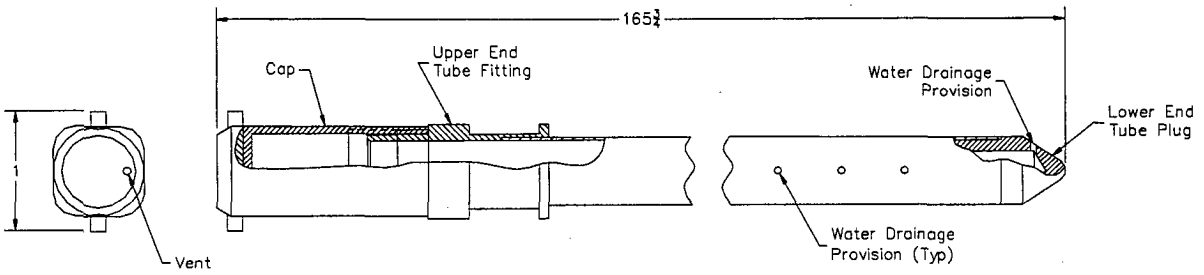

Failed Fuel Rod Capsule Conceptual Layout

All Dimensions Approximate

Note: Material of construction is stainless steel.

Figure 1.2.3-12 NAC-LWT with TPBAR Consolidation Canister Payload

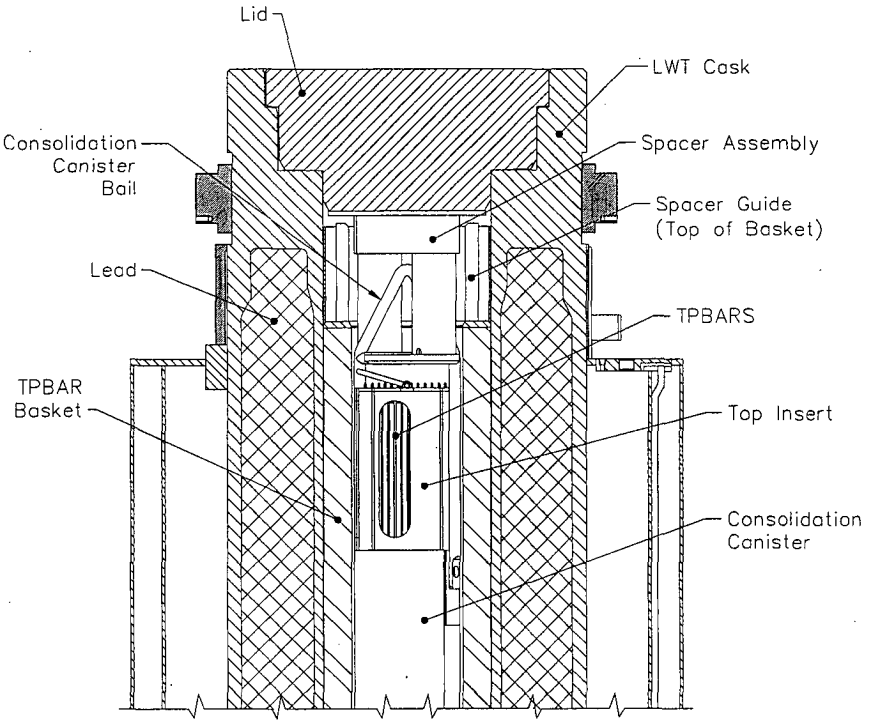

Figure 1.2.3-13 PULSTAR Fuel Assembly

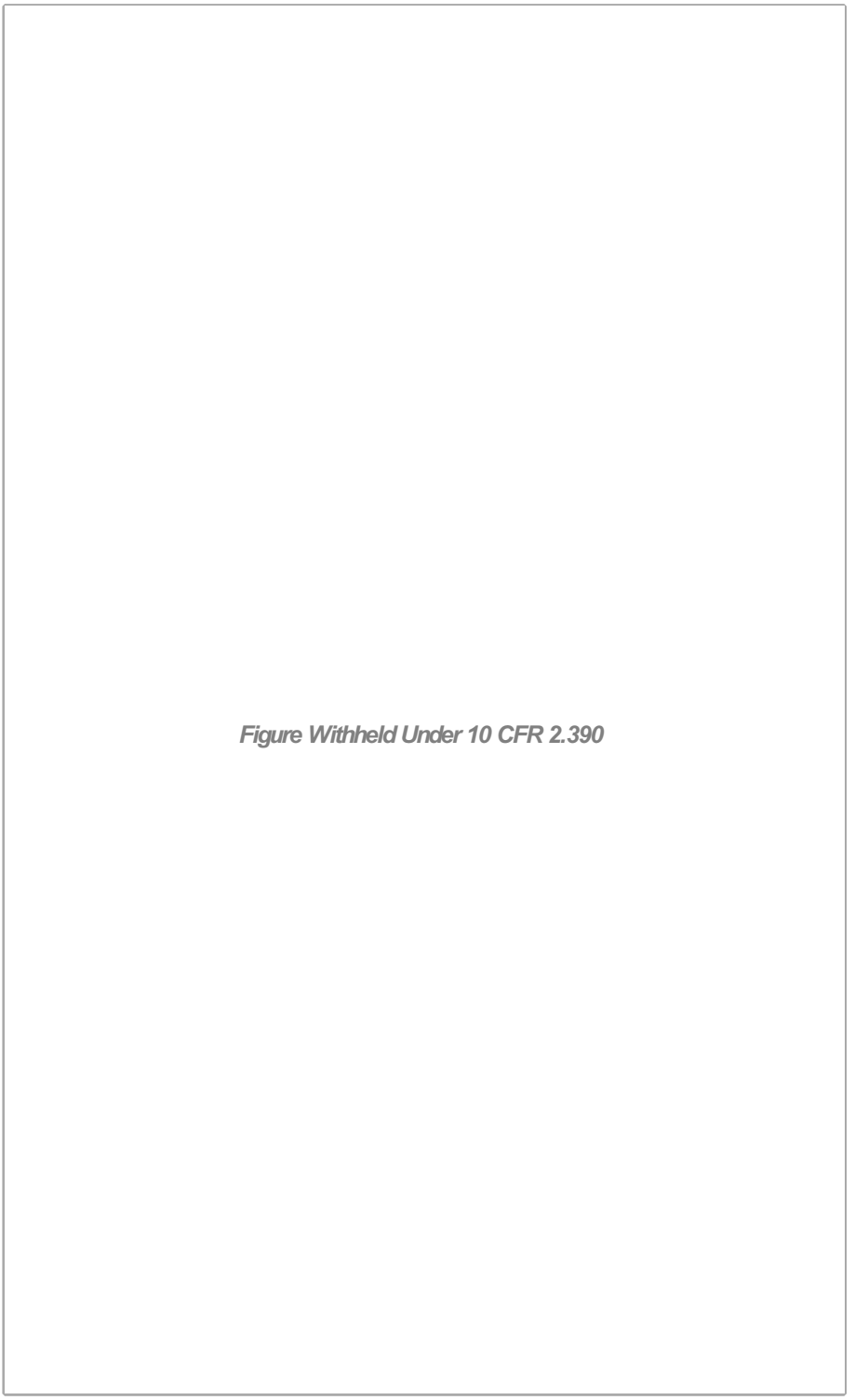

Figure 1.2.3-14 Spiral Fuel Assembly Cross-Section Sketch

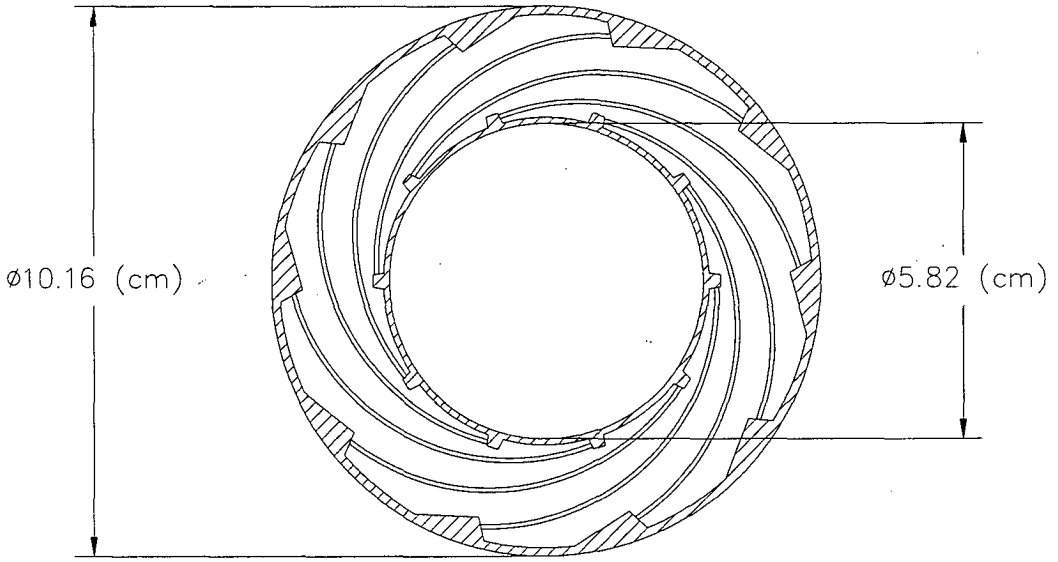

Note: Nominal dimensions

Figure 1.2.3-15 MOATA Plate Bundle Sketches

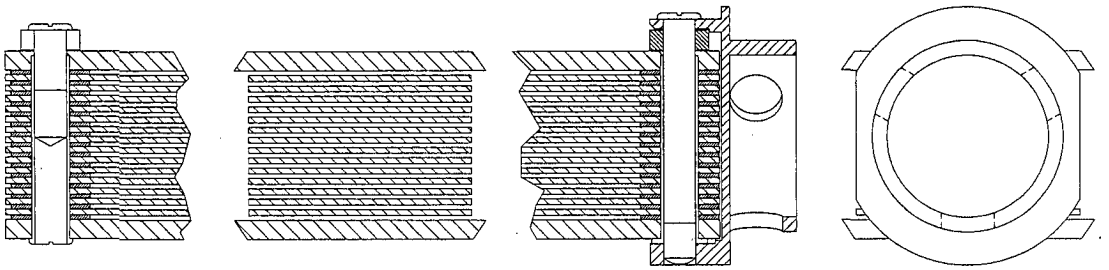

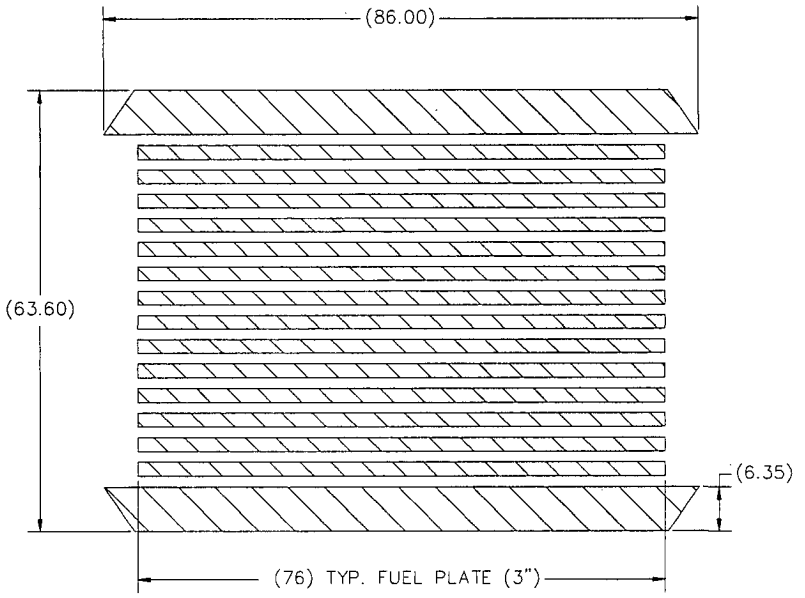

Note: 14-plate bundle configuration. Dimensions are reference values. Bundles with a reduced number of plates retain the plate pitch and compensate by wider side plates and outside spacers to retain overall bundle dimensions.

Figure 1.2.3-16 TPBAR Waste Container and Extension Weldment Sketch

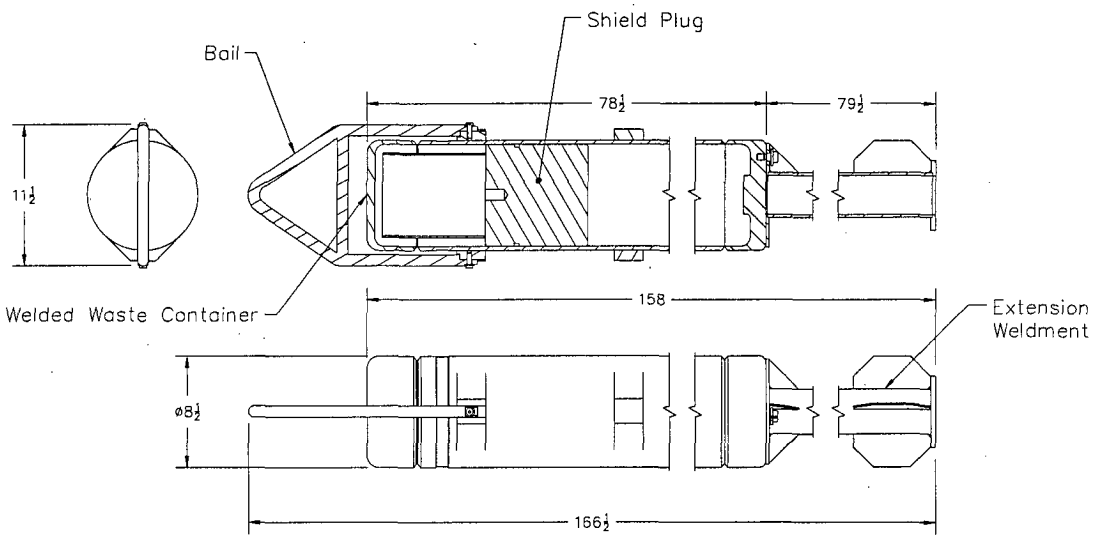

Conceptual Layout with Approximate Dimensions

Note: Material of construction is stainless steel.

Figure 1.2.3-17 NAC-LWT with TPBAR Waste Container Payload

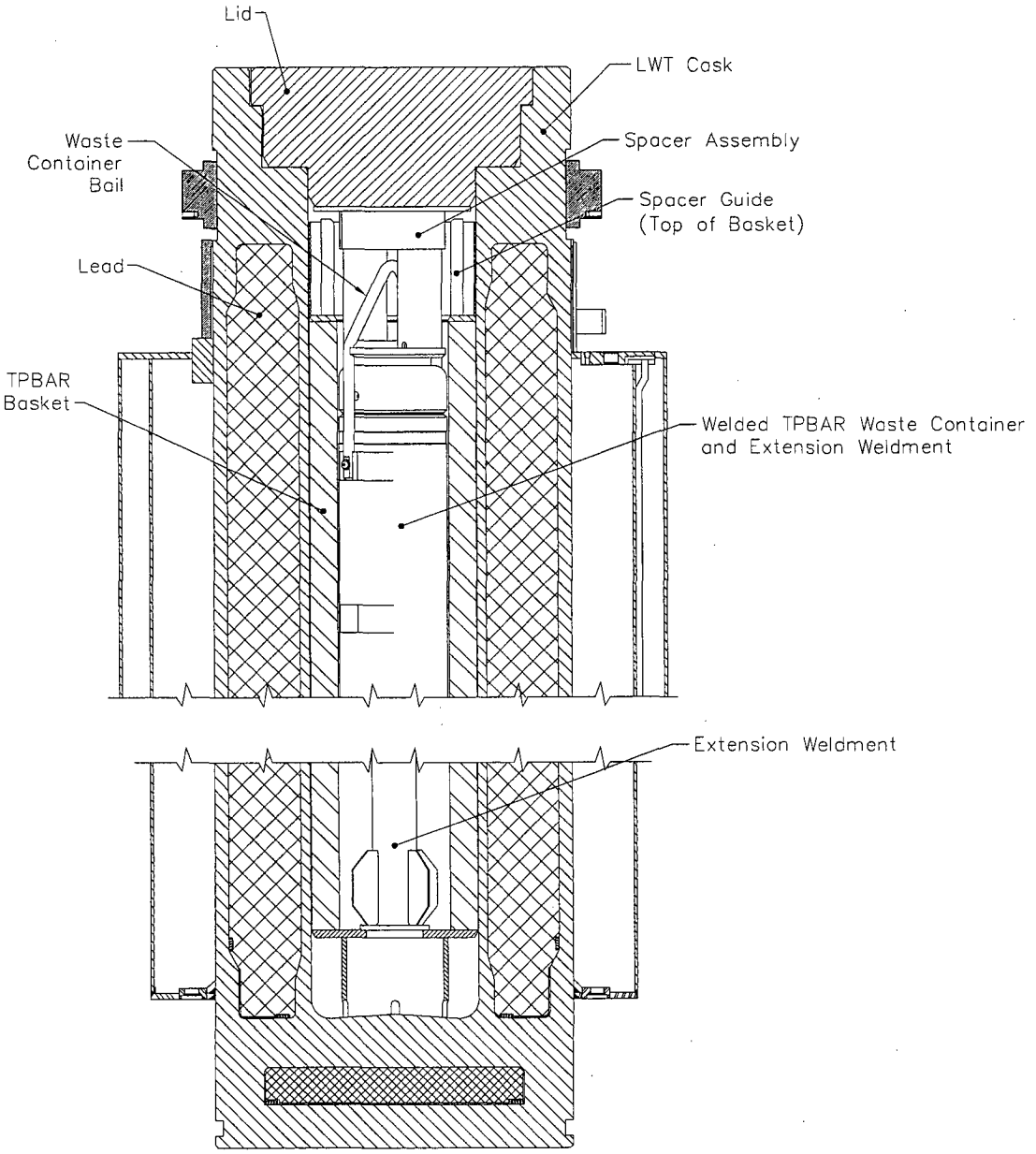

Figure 1.2.3-18 ANSTO Damaged Fuel Can (DFC)

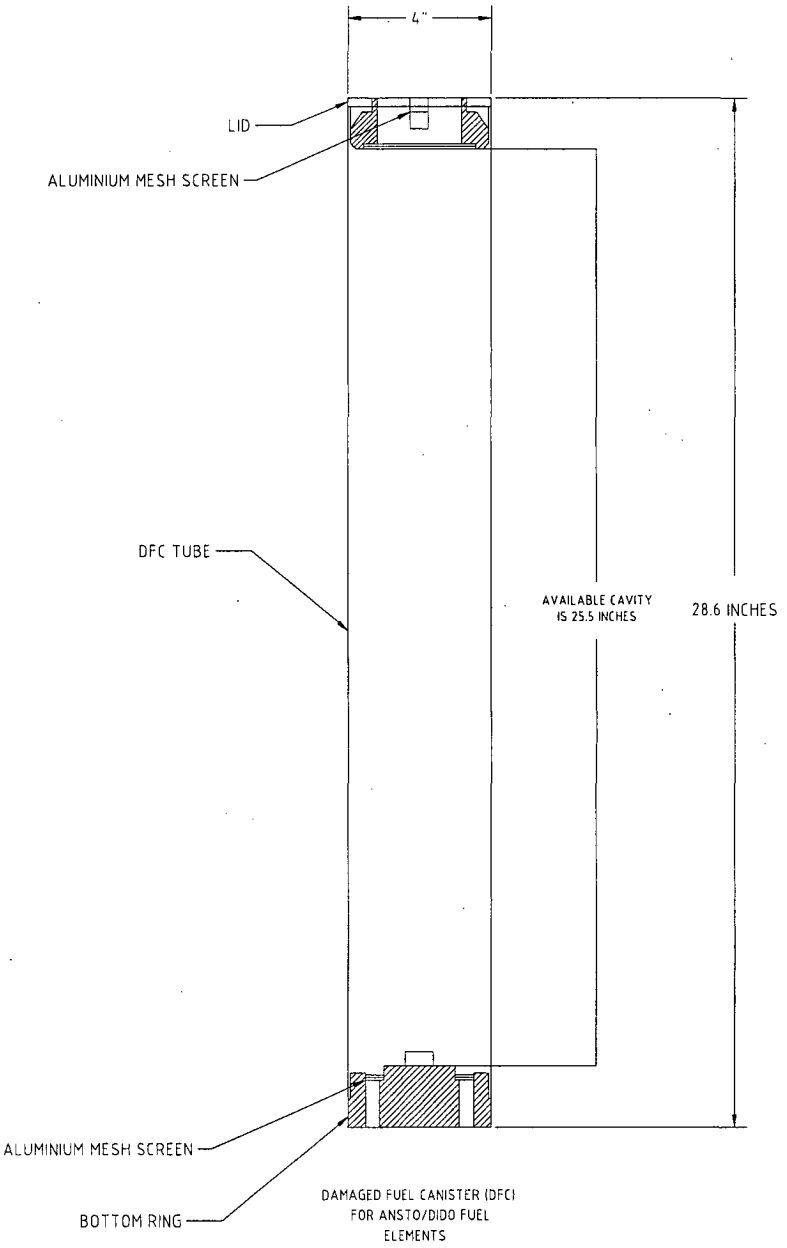

NOTES:
1. DFC MATERIAL - 6061 ALUMINIUM
2. DIMENSIONS NOMINAL

Table 1.2-1 Characteristics of Design Basis TRIGA Fuel Elements Acceptable for Loading in the Poisoned TRIGA Basket

	TRIGA HEU (Notes 1, 2, 6 & 7)	TRIGA LEU (Notes 1, 2, 6 & 7)	TRIGA LEU (Notes 1, 2, 6 & 7)
Fuel Form	Clad U-ZrH rod	Clad U-ZrH rod	Clad U-ZrH rod
Maximum Element Weight, lbs	13.2	13.2	13.2
Maximum Element Length, in	47.74	47.74	47.74
Element Cladding	Stainless Steel	Stainless Steel	Aluminum
Clad Thickness, in	0.02	0.02	0.03
Active Fuel Length, in	15	15	14-15 (Note 4)
Element Diameter, in	1.478 max.	1.478 max.	1.47 max.
Fuel Diameter, in	1.435 max.	1.435 max.	1.41 max.
Maximum Initial U Content/Element, kilograms	0.196	0.845	0.205
Maximum Initial ^{235}U Mass, grams	137	169	41
Maximum Initial ^{235}U Enrichment, weight percent	70	20	20
Zirconium Mass, grams (Note 5)	2060	1886-2300	2300
Hydrogen to Zirconium Ratio, max. (Note 5)	1.6	1.7	1.0
Maximum Average Burnup, MWd/MTU	460,000 (80% ^{235}U)	151,100 (80% ^{235}U)	151,100 (80% ^{235}U)
Minimum Cooling Time	90 days (Note 3)	90 days (Note 3)	90 days (Note 3)

Notes:

1. Mixed TRIGA LEU and HEU contents authorized.
2. TRIGA Standard, instrumented and fuel follower control rod type elements authorized.
3. Maximum decay heat of any element is 7.5 watts.
4. Aluminum clad fuel with 14-inch active fuel is solid and has no central hole with a zirconium rod.
5. Zirconium mass and H/Zr ratio apply to the fuel material (U-Zr-H_x) and do not include the center zirconium rod.
6. Listed TRIGA fuel elements have a 0.225-inch diameter zirconium rod in the center.
7. Dimensions listed are as-fabricated (unirradiated) nominal values.

Table 1.2-2 Characteristics of Design Basis TRIGA Fuel Elements Acceptable for Loading in the Nonpoisoned TRIGA Basket

	TRIGA HEU (Notes 1, 2, 6)	TRIGA LEU (Notes 1, 2, 6)	TRIGA LEU (Notes 1, 2, 6)
Fuel Form	Clad U-ZrH rod (Note 4)	Clad U-ZrH rod (Note 4)	Clad U-ZrH rod (Note 4)
Maximum Element Weight, lbs	13.2	13.2	13.2
Maximum Element Length, in	47.74	47.74	47.74
Element Cladding	Stainless Steel	Stainless Steel	Aluminum
Minimum Clad Thickness, in	0.01	0.01	0.01
Active Fuel Length, in	(Note 5)	(Note 5)	(Note 5)
Maximum Element Diameter, in	1.5 max.	1.5 max.	1.5 max.
Fuel Diameter, in	(Note 5)	(Note 5)	(Note 5)
Maximum Initial U Content/Element, kilograms	0.196	0.845	0.205
Maximum Initial ^{235}U Mass, grams	137	169	41
Maximum Initial ^{235}U Enrichment, weight percent	70	20	20
Zirconium Mass, grams	(Note 5)	(Note 5)	(Note 5)
Hydrogen to Zirconium Ratio, max.	(Note 5)	(Note 5)	(Note 5)
Maximum Average Burnup, MWd/MTU	460,000 (80% ^{235}U)	151,100 (80% ^{235}U)	151,100 (80% ^{235}U)
Minimum Cooling Time	90 days (Note 3)	90 days (Note 3)	90 days (Note 3)

Notes:

1. Mixed TRIGA LEU and HEU contents authorized.
2. TRIGA Standard, instrumented and fuel follower control rod type elements authorized.
3. Maximum decay heat of any element is 7.5 watts.
4. Element may contain zirconium rod in the center.
5. See criticality analyses in Chapter 6, Section 6.4.5.6, for the evaluations determining critical fuel characteristics.
6. Dimensions listed are as-fabricated (unirradiated) nominal values.

Table 1.2-3 Characteristics of Design Basis TRIGA Fuel Cluster Rods

Element Type	TRIGA Fuel Cluster Rod
Max. Rod Length (in)	31.0
Max. Active Length (in)	22.5
Clad Material	Incoloy 800
Min. Clad Thickness (in)	0.015
Fuel Material	U-ZrH
Max. Pellet Diameter (in)	0.53
Max. Rod Weight (kg)	0.65
Min. U in U-ZrH (wt %)	43.0 (LEU) or 9.5 (HEU)[1]
Max. ^{235}U in U (wt %)	19.9 to 93.3
^{235}U Mass (g)	55.0 (LEU) or 46.5 (HEU)
Max. H to Zr Ratio	1.7

[1] Equivalent to a maximum zirconium mass of 357 g for LEU fuel and 457 g for HEU fuel material. Lower weight percents are permitted, provided the maximum zirconium mass limits are not exceeded.

Table 1.2-4 Fuel Characteristics

Parameter	PWR Fuel Assembly	BWR Fuel Assembly	PWR Rods	High Burnup PWR Rods	PWR MOX Fuel Rods[6]	High Burnup BWR Rods 7 × 7	High Burnup BWR Rods[1] 8 × 8[2]
Maximum Number of Assemblies, Elements or Rods	[1]	[2]	25 rods	25 rods	16 rods	25 rods	25 rods
Maximum Overall Weight, lbs	1650	750	N/A	N/A	N/A	N/A	N/A
Maximum Overall Length, in	178.25	176.1	162	162	162	176.1	176.1
Maximum Active Fuel Length, in	150	150	150	150	153.5	150	150
Fuel Rod Cladding	Zirc	Zirc	Zirc	Zirc	Zirc	Zirc	Zirc
Maximum Uranium, kg U	475	198	58.2	65.6	41.6[7]	198	198
Maximum Initial ^{235}U, wt %	*See below*[3]	4.0	5.0	5.0	7.0 max/2.0 min, fissile Pu[8]	5.0	5.0
Maximum Burnup, MWd/MTU	35,000	30,000	60,000[4]	80,000	62,500	60,000 - 80,000	80,000
Maximum Unit Decay Heat, kW	2.5	1.1	0.564	0.92	0.143	0.84	0.84
Maximum Cask Decay Heat, kW	2.5	2.2	1.41	2.3	2.3	2.1	2.1
Minimum Cool Time, yr	2	2	150 days	150 days	90 days	210 - 270 days[5]	150 days

[1] High burnup rods are loaded in a fuel assembly lattice or rod holder. Up to 14 rods, loaded in a rod holder, may be classified as damaged. The lattice may be irradiated.
[2] Includes rods from all larger BWR assembly arrays (e.g., 9×9, 10×10).
[3] See Table 1.2-5 for maximum PWR fuel enrichment by fuel type.
[4] Up to 2 of the 25 PWR rods may have a maximum burnup of 65,000 MWd//MTU.
[5] Minimum cool time for high burnup BWR 7×7 rods is determined by extent of burnup. See Section 5.3.8 and Table 5.3.8-23.
[6] Up to 16 PWR MOX fuel rods or a combination of up to 16 MOX PWR and UO_2 PWR fuel rods can be loaded.
[7] Maximum fuel mass is 2.6 kg HM/rod.
[8] Maximum 5.0 wt % ^{235}U for UO_2 rods.

Table 1.2-4 Fuel Characteristics (Continued)

Parameter	Metallic Fuel	Metallic Fuel	Metallic Fuel	MTR HEU	MTR MEU	MTR LEU	TRIGA LEU Element	TRIGA HEU Element	TRIGA Cluster Rod
Maximum Number of Assemblies, Elements or Rods	15 rods (sound)	9 rods (failed)	3 rods (severely failed in filters)	42[1]	42	42[2]	140	140	560
Maximum Overall Weight, lbs	1805	1805	1805	30 (max)[3]	30 (max)[3]	30 (max)[3]	13.2 (max)[3]	8.82 (nom.) 13.2 (max)[3]	1.5[3]
Maximum Overall Length, in	120.5	120.5	120.5	25.4[4]	26.1[4]	26.1[4]	47.74[5]	47.74[5]	31.0
Maximum Active Fuel Length, in	120.0	120.0	120.0	24.8	25.6	25.6	15	15	22.5
Fuel Rod Cladding	Al	Al	Al	Al	Al	Al	Al or SS	Al or SS	Incoloy 800
Maximum Uranium, kg U	54.5	54.5	54.5	0.422 0.511	0.950	2.474 3.368[2]	0.824	0.196	0.0505 (HEU) 0.2894 (LEU)
Maximum Initial ^{235}U, wt %	Natural	Natural	Natural	94	94[6]	25	20	70	95 (HEU)/20 (LEU)
Maximum Burnup, MWd/MTU	1,600	1,600	1,600	Variable up to 660,000[7]	Variable up to 293,300	Variable up to 139,300	151,100 (80% ^{235}U)	460,000 (80% ^{235}U)	600,000 (HEU)/ 140,000 (LEU) (80% ^{235}U)
Maximum Unit Decay Heat, kW	0.036	0.036	0.036	Variable[8]	0.030[8]	0.030[8]	0.0075	0.0075	0.001875
Maximum Cask Decay Heat, kW	0.54	0.54	0.54	1.26	1.26	1.26	1.05	1.05	1.05
Minimum Cool Time, yr	1	1	1	Variable[8]	Variable[8]	Variable[8]	Variable[9]	Variable[9]	Variable[9]

[1] For NISTR fuel, 42 assemblies may be cut in half, producing 84 fuel-bearing pieces. Each fuel-bearing piece may contain up to 0.211 kgU.

[2] MTR fuel elements having ^{235}U content >470 g (>22 g per plate) are limited to a total of 4 elements in a 7-element basket. Basket openings 1, 2 and 3 shall be blocked by cell block spacers to ensure that MTR elements are not loaded in these openings. Therefore, depending on the number of such 4-element baskets, the maximum number of elements per cask will be reduced accordingly.

[3] Maximum weight of fuel element(s), spacer(s) and fuel can, as applicable, per basket module cell shall be 80 pounds.

[4] For MTR fuel elements, which are cut to remove nonfuel-bearing hardware prior to transport, a nominal 0.28 inch of nonfuel or spacer hardware will remain above and below the active fuel region to allow for fuel handling operations. The HFBR element, with an element length of 57.24 inches, must be cut prior to shipment. For HEU MTR elements having >380 g ^{235}U but less than 460 g ^{235}U, a minimum of 2.0 cm (0.8 inch) of nonfuel hardware and/or spacers/plates shall be provided at the ends of the element.

[5] Permissible fuel element length is limited to basket cavity length, which is a minimum 47.74 inches for the basket top module, 30.94 inches for the intermediate modules, and 32.64 inches for thebottom module.

[6] Typical MEU enrichment is 45 wt% ^{235}U. Criticality analysis supports up to 94 wt% under the MEU fuel definition.

[7] Maximum burnup is 660,000 MWd/MTU for 380g ^{235}U and 577,500 MWd/MTU for 460g ^{235}U.

[8] Minimum cool times for MTR fuel, down to 30 days, shall be determined using the procedure presented in Section 7.1.5..

[9] Minimum cool times for TRIGA fuel elements and fuel cluster rods, down to 90 days, are determined so that the maximum decay heat of any element to be shipped is $\leq$ 7.5 watts and any fuel cluster rod is $\leq$ 1.875 watts.

Table 1.2-4 Fuel Characteristics (Continued)

Parameter	DIDO HEU	DIDO MEU	DIDO LEU
Number of Fuel Cylinders per Assembly	4	4	4
Maximum Overall Weight (lb)[1]	15	15	15
Minimum Plate Thickness, in	0.051	0.051	0.051
Minimum Clad Thickness (Al), in	0.00984	0.00984	0.00984
Maximum ^{235}U per Element, g	190	190	190
Maximum Initial ^{235}U, wt %	94	94	94
Minimum Initial ^{235}U, wt %	90	40	19
Maximum Uranium, kg U	0.2111	0.4750	1.0000
Minimum Active Fuel Height, in	23.13	23.13	23.13
Minimum Element Height[2], in	24.21	24.21	24.21
Maximum Burnup, MWd/MTU	577,460	256,650	121,910
Maximum Unit Decay Heat[3], kW	0.025	0.025	0.025
Maximum Cask Decay Heat, kW	1.05	1.05	1.05
Minimum Cool Time[4], yr	Variable	Variable	Variable

1 Maximum weight of fuel element(s), spacer(s) and fuel can, as applicable, per basket module cell shall be 80 pounds.

2 Element height provides for spacing of fissile material. An optional spacer may be used to maintain spacing if the element is cut shorter than 24.21 inches.

3 Maximum unit decay heat of 0.025 kW allowed only in conjunction with spacers for top basket (see Section 7.1.4). The per element heat load is limited to 0.018 kW with no top basket spacer. For DIDO fuel elements loaded into a top ANSTO basket module, the maximum decay heat load is limited to 0.010 kW per element (with or without DFC).

4 Minimum cool times for DIDO fuel assemblies, down to 180 days, shall be determined using the procedure presented in Section 7.1.4.

Table 1.2-5 PWR Fuel Characteristics

Fuel Type	No. of Fuel Rods	Max. Assembly Length (in.)	Max. Assembly Weight (lb)	Max. Enrich. (wt %)	Max. MTU	Pitch (in.)	Rod Dia. (in.)	Clad Thick. (in.)	Pellet Dia.(in.)	Max. Active Length (in.)
B&W 15 x 15	208	165.63	1515	3.5	0.4750	0.5680	0.430	0.0265	0.3686	144.0
B&W 17 x 17	264	165.72	1505	3.5	0.4658	0.5020	0.379	0.0240	0.3232	143.0
CE 14 x 14	176	157.00	1270	3.7	0.4037	0.5800	0.440	0.0280	0.3765	137.0
CE 16 x 16	236	178.25	1430	3.7	0.4417	0.5060	0.382	0.0250	0.3250	150.0
WE 14 x 14 Std	179	159.71	1302	3.7	0.4144	0.5560	0.422	0.0225	0.3674	145.2
WE 14 x 14 OFA	179	159.71	1177	3.7	0.3612	0.5560	0.400	0.0243	0.3444	144.0
WE 15 x 15	204	159.71	1472	3.5	0.4646	0.5630	0.422	0.0242	0.3659	144.0
WE 17 x 17 Std	264	159.77	1482	3.5	0.4671	0.4960	0.374	0.0225	0.3225	144.0
WE 17 x 17 OFA	264	160.10	1373	3.5	0.4282	0.4960	0.360	0.0225	0.3088	144.0
Ex/ANF 14 x 14 WE	179	160.13	1271	3.7	0.3741	0.5560	0.424	0.0300	0.3505	144.0
Ex/ANF 14 x 14 CE	176	157.24	1292	3.7	0.3814	0.5800	0.440	0.0310	0.3700	134.0
Ex/ANF 15 x 15 WE	204	159.70	1433	3.7	0.4410	0.5630	0.424	0.0300	0.3565	144.0
Ex/ANF 17 x 17 WE	264	159.71	1348	3.5	0.4123	0.4960	0.360	0.0250	0.3030	144.0

Table 1.2-6 BWR Fuel Characteristics

Fuel Type	No. of Fuel Rods	No. of Water Rods	Max. Assembly Length (in.)	Max. Assembly Weight (lb)	Max. MTU	Pitch (in.)	Rod Dia. (in.)	Clad Thick. (in.)	Pellet Dia. (in.)	Max. Active Length (in.)
GE 7 x 7	49	0	175.9	678.9	0.1923	0.738	0.563	0.037	0.477	146
GE 8 x 8-1	63	1	175.9	681.0	0.1880	0.640	0.493	0.034	0.416	146
GE 8 x 8-2	62	2	175.9	681.0	0.1847	0.640	0.483	0.032	0.410	150[1]
GE 8 x 8-4	60	4	176.1	665.0	0.1787	0.640	0.484	0.032	0.410	150[1,2]
GE 9 x 9	74	2[3]	176.1	646.0	0.1854	0.566	0.441	0.028	0.376	150[1,4]
	79	2	176.1	646.0	0.1979	0.566	0.441	0.028	0.376	150[1,4]
Ex/ANF 7 x 7	49	0	171.3	619.1	0.1960	0.738	0.570	0.036	0.490	144
Ex/ANF 8 x 8-1	63	1	171.3	562.3	0.1764	0.641	0.484	0.036	0.4045	145.2
Ex/ANF 8 x 8-2	62	2	176.1	587.8	0.1793	0.641	0.484	0.036	0.4045	150
Ex/ANF 9 x 9	79	2	176.1	575.3	0.1779	0.572	0.424	0.03	0.3565	150
	74	2[3]	176.1	575.3	0.1666	0.572	0.424	0.03	0.3565	150

[1] 6" natural uranium blankets on top and bottom.
[2] May have 1 large water hole - 3.2 cm ID, 0.1 cm thickness.
[3] 2 large water holes occupying 7 fuel rod locations - 2.5 cm ID, 0.07 cm thickness.
[4] Shortened active fuel length in some rods.

Table 1.2-7 Characteristics of General Atomics Irradiated Fuel Material (GA IFM)

Parameter	RERTR	HTGR
Maximum Number of Assemblies, Elements or Rods	13 intact; 7 sectioned	N/A
Maximum Loaded Enclosure Weight, lbs	76.0	71.5
Maximum Fuel Weight, lbs	23.73	23.52
Maximum Overall Length, in	29.92	N/A
Maximum Active Fuel Length, in	22.05	N/A
Fuel Material	U-ZrH	UC_2, UCO, UO_2, $(Th,U)C_2$, $(Th,U)O_2$
Fuel Rod Cladding	Incoloy 800	N/A
Maximum Uranium, kg U	3.86	0.21
Maximum Initial ^{235}U, wt %	19.7	93.15
Maximum Burnup, MWd/MTU	N/A	N/A
Maximum Unit Decay Heat, W	11.0	2.05
Maximum Cask Decay Heat, W	13.05	13.05
Earliest Shipment Date	1/1/96	1/1/96
Maximum Activity, Ci	2920	483

Table 1.2-8 Typical Production TPBAR Characteristics[1]

Parameter Description	Value
Maximum Number of TPBARs per Consolidation Canister	300
Number of Consolidation Canisters per Cask	1
TPBAR Clad Material	316 L Stainless Steel
Rod Length[2], in	153.04
Rod Diameter[2], in	0.381
Maximum Rod Heat Load, W	2.31
Maximum Cask Heat Load, kW	0.693
Maximum Tritium Content per Rod, gram	1.2
Maximum Activity per Cask[3], Ci	3.84×10^6
Loaded TPBAR Consolidation Canister Maximum Weight, pounds[4]	1,000
Maximum Event Failed Tritium Release (Ci/rod)	<55
Minimum Cooling Time, days	30

1 Refer to Section 1.5, Chapter 1 Appendices, Unclassified DOE Reference Documents and Drawings.
2 Beginning of life, nominal, unirradiated dimensions.
3 Primary dose contribution: 1.1×10^4 Ci ^{60}Co/cask
4 The bounding weight employed in the structural analysis.

Table 1.2-9 PULSTAR Fuel Characteristics

Description	Value
Maximum Pellet Diameter (inch)	0.423
Minimum Element (Rod) Cladding Thickness (inch)	0.0185
Minimum Element (Rod) Diameter (inch)	0.470
Maximum Active Fuel Height (inch)	24.1
Element (Rod) Length (inch)	26.2
Rod Pitch (inch)	0.525 × 0.607
Assembly Length (inch)	38
Box Outside Width (inch)	2.745 × 3.155
Box Thickness (inch)	0.06
Maximum Assembly or Loaded Can Weight (lb) [1]	80
Maximum PULSTAR Can Content Weight (lb)[2]	39.6
Maximum Enrichment (wt % ^{235}U)	6.5
Maximum ^{235}U Content per Element (g)	33
No. of Elements (Rods) per Assembly	25
No. of Elements (Rods) per Can[2]	25
Maximum Depletion (%^{235}U)	45
Minimum Cool Time (yrs)	1.5
Maximum Heat Load per Assembly (W)	30
Maximum Heat Load per Element (W)	1.2

[1] Listed weight is the maximum weight evaluated for the structural calculation to bound all payload configurations, including loaded cans, and spacers. Nominal PULSTAR assembly weight is 45 pounds.

[2] The contents of a PULSTAR can are restricted to the equivalent of the fuel material in 25 PULSTAR fuel elements and of the displaced volume of 25 intact PULSTAR fuel elements. Fuel material may be in damaged form including fuel debris. The listed weight represents the can content limit established by the structural analyses.

Spiral Fuel Assembly Characteristics

Parameter	Value
Number of elements per assembly	10
Fuel element type	Curved plate
Nominal dimensions of element (cm)	0.147 × 7.33 × 63.5 (individual plate)
Chemical form of fuel meat	U-Al_x-alloy
Cladding material	Aluminum
Nominal over-all dimensions (cm)	63.818 (height) × 10.16 diameter[1]
Max total weight of ^{235}U (g)	160 (total per assembly)
Maximum enrichment (wt % ^{235}U)	95
Side plate material	Aluminum (inner and outer tubes)
Nominal side plate – dimensions (cm)	Inner 6.045 OD, 5.82 ID x 63.818 Outer 10.16 OD, 9.85 ID x 63.818[2]
Max. assembly weight (lb)	18[3]
Assembly maximum heat load (W)	15.7[4]
Burnup/cool time limit	Variable[5]

1 Cropped to fit within ANSTO fuel basket module nominal height of 28.3 inches.

2 Criticality evaluations reduced inner and outer shell thickness to 0.01 cm to provide additional moderator within the assembly.

3 Typical assembly weight is 7.9 pounds. Bounding structural analysis weight is listed. Bounding weight includes DFC and fuel plates.

4 Thermal and shielding evaluation employed 18 W per element. Based on cool time constraint, 15.7 W represents maximum heat load. Spiral fuel elements with degraded cladding loaded into aluminum DFCs shall be limited to a maximum decay heat of 10 W per element.

5 Spiral fuel is constrained to DIDO MEU cool time limits as a function of burnup. Minimum cool times for the spiral assembly, down to 270 days, shall be determined using the procedure presented in Section 7.1.4 for 18 W DIDO MEU fuel.

Table 1.2-11 MOATA Plate Bundle Characteristics

Parameter	Value
Maximum number of elements per assembly	14
Nominal dimensions of element (cm)	66 cm long, 7.6 cm wide and 0.203 cm thick
Nominal dimensions of fuel meat (cm)	58.4 cm long, 6.99 cm wide and 0.1016 cm thick (bounding active fuel width evaluated to a maximum of 7.32 cm)
Chemical form of fuel meat	U-Al_x-alloy
Cladding material	Aluminum
Nominal clad thickness (cm)	0.05 cm (evaluated to 0.01 cm minimum)
Plate spacer thickness (cm)	0.147 min, 0.152 max (evaluated to 0.18 maximum)
Maximum weight of ^{235}U (g) per plate	22.3
Maximum enrichment (wt % ^{235}U)	92
Nominal side plate thickness (cm)	0.635 (bounding evaluation replaced by cavity moderator)
Max. assembly weight (lb)	18[1]
Maximum heat load per assembly (W)[2]	3 (total for 14 fuel plates)
Maximum burnup	30,000 MWd/MTU or 4.1 % depletion ^{235}U
Minimum cool time (years)	10

[1] Typical assembly weight is 13.6 pounds. Bounding structural analysis weight is listed. Bounding weight includes DFC and fuel plates.

[2] Actual heat load at limiting burnup and cool time < 1 Watt. Thermal evaluations at 3 Watt per bundle.

Table 1.2-12 Typical TPBAR Segment Characteristics in Waste Container

Parameter/Description	Value
Maximum Number of TPBAR Segments and Debris per Waste Container, equivalent number of TPBARs	55
Number of Waste Containers per Cask	1
Waste Container Material	316L Stainless Steel
Maximum Tritium Content per TPBAR equivalent, gram	1.2
Maximum Activity per Cask, Ci	6.66 x10+5
Maximum Heat Load per Waste Container, watts	127
Maximum Loaded Waste Container Weight, pounds	700[1]
Minimum Cooling Time, years	90

[1] Design basis weight of a loaded waste container is 700 pounds. Applying a maximum payload of 55 TPBARs, with storage canister, yields a maximum weight of 662 pounds. Use of shrouds to contain segments and/or TPBAR debris reduces overall waste container weight due to a reduction in TPBAR payload capacity resulting from the reduced container free volume.

Table 1.2-13 Solid, Irradiated Hardware Characteristics[1]

Parameter	Value
Maximum Content Weight	4,000 pounds [2]
Maximum Content Length	171.5 inches [3]
Hardware Material	Solid, irradiated and contaminated fuel assembly structural or reactor internal component hardware [4]
Maximum Cask Heat Load	1.0 KW
Maximum Activity per Cask, Ci	6.0 x 10E+6
Maximum Source Term, gamma/sec	6.0 x 10E+15
Maximum Source Term, MeV/sec	1.0 x 10E+15

1 Maximum content weight includes any spacers, containers or dunnage loaded in the cavity with the irradiated hardware.

2 Length of cavity is limited to 171.5 inches by the installation and use of an irradiated hardware spacer bolted to the underside of the closure lid.

3 Appropriate secondary containers will be used to prevent any contact and cross-contamination between the carbon steel contents and the stainless steel internals of the cask cavity.

4 The irradiated hardware contents may contain fissile material, provided the quantity of fissile material does not exceed a Type A quantity and does not exceed the mass limits of 10 CFR 71.53.

1.3 Quality Assurance

The Nuclear Regulatory Commission (NRC) has assigned Approval Number 18 to the Nuclear Assurance Corporation Quality Assurance program that satisfies the provisions of Subpart H of 10 CFR 71.

The Quality Assurance program provides control over all activities that are important to safety that are applicable to the design, fabrication, assembly, testing, maintenance, repair, modification, and use of the packaging for transportation of radioactive materials. The program applies controls to the various activities in a graded approach, such that the effort expended on an activity is consistent with its importance to safety. The program is consistent in approach and method with Regulatory Guide 7.10 and satisfies the specific requirements of 10 CFR 71.101 (a), (b), and (c).

In accordance with the requirements of 10 CFR 71.37(a), the approved Quality Assurance program has been applied to the design, analysis, package fabrication, assembly, testing, maintenance, and repair or modification of the NAC-LWT package. An equivalent NRC approved program maintained by a Registered User would be applied to use of the package.

1.4 License Drawings

This section contains the license drawings pertinent to the NAC-LWT cask (refer to the List of Drawings in the Table of Contents for Chapter 1).

Figure Withheld Under 10 CFR 2.390

NAC INTERNATIONAL

LEGAL WEIGHT TRUCK TRANSPORT
CASK ASSEMBLY
SAFETY ANALYSIS
REPORT

PROJECT 315-40		DRAWING 01	REV 7
SCALE	WEIGHT	SH 1 OF 1	1:32PM 10-31-2001

Figure Withheld Under 10 CFR 2.390

NAC INTERNATIONAL

LEGAL WEIGHT TRUCK CASK
BODY ASSEMBLY
SAFETY ANALYSIS REPORT

PROJECT 315-40		DRAWING 02	REV 24
SCALE	EST. WT.	SH 1 OF 2	1:25PM 11-10-2008

Figure Withheld Under 10 CFR 2.390

NAC INTERNATIONAL

LEGAL WEIGHT TRUCK CASK
BODY ASSEMBLY
SAFETY ANALYSIS REPORT

PROJECT	DRAWING	REV
315-40	02	24
	SH 2 OF 2	1:24PM 11-10-2008

Figure Withheld Under 10 CFR 2.390

NUCLEAR ASSURANCE CORPORATION
ENGINEERING SERVICES DIVISION
NORCROSS, GEORGIA 30092

LEGAL WEIGHT TRUCK
TRANSPORT CASK BODY
SAFETY ANALYSIS
REPORT

PROJECT	DESIGN PACKAGE	DRAWING	REV
LWT	315-40	03	6

LWT 315-40 03

Figure Withheld Under 10 CFR 2.390

NUCLEAR ASSURANCE CORPORATION
ENGINEERING SERVICE DIVISION
NORCROSS GEORGIA 30092

LEGAL WEIGHT TRUCK
TRANSPORT CASK BODY
SAFETY ANALYSIS
REPORT

PROJECT	DESIGN PACKAGE	DRAWING	REV
LWT	315-40	03	0

SCALE 1/4 & NOTED WEIGHT | SHT. 2 OF 6 | LOC.

LWT 315-40 03

Figure Withheld Under 10 CFR 2.390

NUCLEAR ASSURANCE CORPORATION
ENGINEERING SERVICE DIVISION
NORCROSS GEORGIA 30087

LEGAL WEIGHT TRUCK
TRANSPORT CASK BODY
SAFETY ANALYSIS
REPORT

PROJECT	DESIGN PACKAGE	DRAWING	REV.
LWT	315-40	03	6

PROJ. LWT | DESIGN PAC. 315-40 | DWG. 03

Figure Withheld Under 10 CFR 2.390

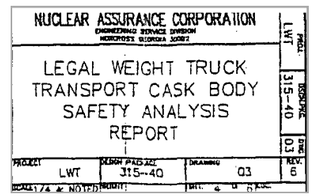

Figure Withheld Under 10 CFR 2.390

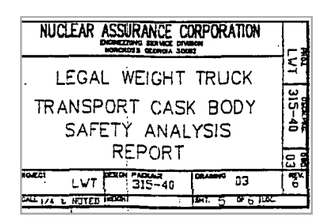

Figure Withheld Under 10 CFR 2.390

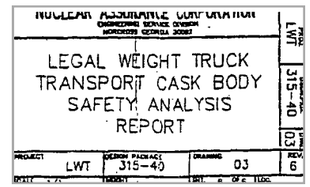

Figure Withheld Under 10 CFR 2.390

NAC INTERNATIONAL

LEGAL WEIGHT TRUCK
TRANSPORT CASK BODY
SAFETY ANALYSIS
REPORT

PROJECT	DRAWING	REV
315-40	03	22
	SH 1 OF 7	

Figure Withheld Under 10 CFR 2.390

NAC INTERNATIONAL

LEGAL WEIGHT TRUCK
TRANSPORT CASK BODY
SAFETY ANALYSIS
REPORT

PROJECT	DRAWING	REV
315-40	03	22
	SH 2 OF 7	11-28-2005

Figure Withheld Under 10 CFR 2.390

NAC INTERNATIONAL

LEGAL WEIGHT TRUCK
TRANSPORT CASK BODY
SAFETY ANALYSIS
REPORT

PROJECT 315-40	DRAWING 03	REV 22
	SH 3 OF 7	11:33PM 11-29-2005

Figure Withheld Under 10 CFR 2.390

NAC INTERNATIONAL

LEGAL WEIGHT TRUCK
TRANSPORT CASK BODY
SAFETY ANALYSIS
REPORT

PROJECT 315-40	DRAWING 03	REV 22
	SH 4 OF 7	1:53PM 11-18-2005

Figure Withheld Under 10 CFR 2.390

NAC INTERNATIONAL

LEGAL WEIGHT TRUCK
TRANSPORT CASK BODY
SAFETY ANALYSIS
REPORT

PROJECT	DRAWING	REV
315-40	03	22
	SH 5 OF 7	11-29-2006

Figure Withheld Under 10 CFR 2.390

NAC INTERNATIONAL

LEGAL WEIGHT TRUCK
TRANSPORT CASK BODY
SAFETY ANALYSIS
REPORT

PROJECT	DRAWING	REV
315-40	03	22
	SH 6 OF 7	

Figure Withheld Under 10 CFR 2.390

NAC INTERNATIONAL

LEGAL WEIGHT TRUCK
TRANSPORT CASK BODY
SAFETY ANALYSIS
REPORT

PROJECT 315-40	DRAWING 03	REV 22
	SH 7 OF 7	1:53PM 11-26-2003

Figure Withheld Under 10 CFR 2.390

NUCLEAR ASSURANCE CORPORATION
ENGINEERING SERVICE DIVISION
NORCROSS GEORGIA 30092

PROJ: LWT

LEGAL WEIGHT TRUCK
TRANSPORT CASK LID ASSY
SAFETY ANALYSIS
REPORT

DSGN PKG: 315-40

DWG: 04

PROJECT	DESIGN PACKAGE	DRAWING	REV
D LWT	315-40	04	10

SCALE 1/4 | WEIGHT 936 LBS. | SH 1 OF 1 | LOC

Figure Withheld Under 10 CFR 2.390

NAC INTERNATIONAL

LEGAL WEIGHT TRUCK
TRANSPORT CASK
UPPER IMPACT LIMITER
SAFETY ANALYSIS
REPORT

PROJECT	315-40	DRAWING	05	REV 10
SCALE N.T.S.	EST.WT.1535 LBS.	SH 1 OF 2		

Figure Withheld Under 10 CFR 2.390

NAC INTERNATIONAL

LEGAL WEIGHT TRUCK
TRANSPORT CASK
UPPER IMPACT LIMITER
SAFETY ANALYSIS
REPORT

PROJECT	315-40	DRAWING	05	REV 10
SCALE N. T. S.	WEIGHT AS NOTED	SH 2 OF 2	9:57AM 10-27-2001	

Figure Withheld Under 10 CFR 2.390

NAC INTERNATIONAL

LEGAL WEIGHT TRUCK
TRANSPORT CASK
LOWER IMPACT LIMITER
SAFETY ANALYSIS
REPORT

PROJECT	315-40	DRAWING	06	REV 10
SCALE N.T.S.	EST.WT.1320 LBS	SH 1 OF 1	TO DRAW 10-22-2009	

Figure Withheld Under 10 CFR 2.390

NUCLEAR ASSURANCE CORPORATION ENGINEERING SERVICE DIVISION NORCROSS GEORGIA 30092			PROJ LWT
LEGAL WEIGHT TRUCK TRANSPORT CASK PARTS DETAIL SAFETY ANALYSIS REPORT			DESIGNATOR 315-40 DWG 08
PROJECT LWT	DESIGN PACKAGE 315-40	DRAWING 08	REV 18
SCALE 1/1	WEIGHT	SH 1 OF 5 LOC	

Figure Withheld Under 10 CFR 2.390

NUCLEAR ASSURANCE CORPORATION ENGINEERING SERVICE DIVISION NORCROSS GEORGIA 30092			LWT
LEGAL WEIGHT TRUCK TRANSPORT CASK PARTS DETAIL SAFETY ANALYSIS REPORT			315-40 08
PROJECT: LWT	DESIGN PACKAGE: 315-40	DRAWING: 08	REV: 18
SCALE: 1/1	WEIGHT	SHT. 2 OF 5	LOC.

Figure Withheld Under 10 CFR 2.390

NUCLEAR ASSURANCE CORPORATION ENGINEERING SERVICE DIVISION NORCROSS GEORGIA 30092			PROJ. LWT
LEGAL WEIGHT TRUCK TRANSPORT CASK PARTS DETAIL SAFETY ANALYSIS REPORT			DRAWING NO. 315-40
			DRG. 08
PROJECT LWT	DESIGN PACKAGE 315-40	DRAWING 08	REV. 18
SCALE 1/4	WEIGHT	SHT. 3 OF 5	DOC.

Figure Withheld Under 10 CFR 2.390

NUCLEAR ASSURANCE CORPORATION ENGINEERING SERVICE DIVISION NORCROSS GEORGIA 30092			LWT
LEGAL WEIGHT TRUCK TRANSPORT CASK PARTS DETAIL SAFETY ANALYSIS REPORT			315-40
			08
PROJECT: LWT	DESIGN PACKAGE: 315-40	DRAWING: 08	REV: 18
SCALE: 1/1	WEIGHT	SHT. 4 OF 5	DOC.

Figure Withheld Under 10 CFR 2.390

NUCLEAR ASSURANCE CORPORATION
ENGINEERING SERVICE DIVISION
NORCROSS GEORGIA 30092

LWT 315-40 08

LEGAL WEIGHT TRUCK
TRANSPORT CASK
PARTS DETAIL
SAFETY ANALYSIS REPORT

PROJECT	DESIGN PACKAGE	DRAWING	REV
LWT	315-40	08	12
SCALE 1/1	WEIGHT	SHT. 5 OF 5	DOC.

Figure Withheld Under 10 CFR 2.390

NUCLEAR ASSURANCE CORPORATION
ENGINEERING SERVICE DIVISION
NORCROSS GEORGIA 30092

LEGAL WEIGHT TRUCK
TRANSPORT CASK
PWR BASKET SPACER
SAFETY ANALYSIS
REPORT

PROJ: LWT
DESIGN PAC: 315-40
DWG: 09

PROJECT	DESIGN PACKAGE	DRAWING	REV
LWT	315-40	09	2
SCALE 1/2	WEIGHT 34 LBS	SH 1 OF 1	LOC

Figure Withheld Under 10 CFR 2.390

NAC INTERNATIONAL

LWT CASK
PWR BASKET
SAFETY ANALYSIS
REPORT

PROJECT 315-40		DRAWING 10	REV 8
SCALE 1/4	WEIGHT NOTED	SH 1 OF 2	1-26-2009

Figure Withheld Under 10 CFR 2.390

NAC INTERNATIONAL

LWT CASK
PWR BASKET
SAFETY ANALYSIS
REPORT

PROJECT 315-40		DRAWING 10	REV 8
SCALE 1/4	EST.WT. NOTED	SH 2 OF 2	3:24PM 1-26-2009

Figure Withheld Under 10 CFR 2.390

NUCLEAR ASSURANCE CORPORATION ENGINEERING SERVICE DIVISION NORCROSS GEORGIA 30092			LWT
BWR FUEL BASKET ASSEM LWT CASK SAFETY ANALYSIS REPORT			315-390
			18
PROJECT LWT	DESIGN PACKAGE 315-40	DRAWING 11	REV 2
SCALE 1/2	WEIGHT 1174 LBS	SH 1 OF 1	UNC

Figure Withheld Under 10 CFR 2.390

NUCLEAR ASSURANCE CORPORATION
ENGINEERING SERVICE DIVISION
NORCROSS GEORGIA 30092

LWT CASK
METAL FUEL
BASKET ASSEMBLY
SAFETY ANALYSIS REPORT

PROJECT	DESIGN PACKAGE	DRAWING	REV
315	40	12	3

SCALE 1/4 WEIGHT 128 LBS SH 1 OF 1 LOC

PROJ. 315 DSGN PKG. 40 DWG. 12

Figure Withheld Under 10 CFR 2.390

NAC INTERNATIONAL

WELDMENT,
7 ELEMENT BASKET,
42 MTR FUEL BASE MODULE
SAFETY ANALYSIS REPORT

PROJECT 315	DESIGN PACKAGE 40	DRAWING 045	REV 6
SCALE 1/3	EST.WT. 174#	SH 1 OF 1	11:27AM 4-14-2008

Figure Withheld Under 10 CFR 2.390

NAC INTERNATIONAL

WELDMENT,
7 ELEMENT BASKET, 42
MTR FUEL INTERMEDIATE MODULE,
SAFETY ANALYSIS REPORT

PROJECT	DESIGN PACKAGE	DRAWING	REV
315	40	046	6
SCALE 1/3	EST.WT. 165#	SH 1 OF 1	11:51AM 4-14-2009

Figure Withheld Under 10 CFR 2.390

NAC INTERNATIONAL

WELDMENT,
7 ELEMENT BASKET, 42
MTR FUEL TOP MODULE,
SAFETY ANALYSIS REPORT

PROJECT 315	DESIGN PACKAGE 40	DRAWING 047	REV 6
SCALE 1/3	EST.WT. 165#	SH 1 OF 1	11:09AM 4-14-2011

Figure Withheld Under 10 CFR 2.390

NAC INTERNATIONAL

LEGAL WEIGHT TRUCK
TRANSPORT CASK ASSY
42 MTR ELEMENT
SAFETY ANALYSIS REPORT

PROJECT	DRAWING	REV
315-40	048	3
SCALE	WEIGHT	SH 1 OF 1

Figure Withheld Under 10 CFR 2.390

NAC INTERNATIONAL

WELDMENT,
7 ELEMENT BASKET,
28 MTR FUEL BASE MODULE
SAFETY ANALYSIS REPORT

PROJECT 315	DESIGN PACKAGE 40	DRAWING 049	REV 6
SCALE 1/3	EST. WT. 250#	SH 1 OF 1	12:00PM 4-14-2009

Figure Withheld Under 10 CFR 2.390

NAC INTERNATIONAL

WELDMENT,
7 ELEMENT BASKET, 28
MTR FUEL INTERMEDIATE MODULE
SAFETY ANALYSIS REPORT

PROJECT 315	DESIGN PACKAGE 40	DRAWING 050	REV 6
SCALE 1/3	EST. WT. 240#	SH 1 OF 1	12:27PM 4-14-2004

Figure Withheld Under 10 CFR 2.390

NAC INTERNATIONAL			
WELDMENT, 7 ELEMENT BASKET, 28 MTR FUEL TOP MODULE, SAFETY ANALYSIS REPORT			
PROJECT 315	DESIGN PACKAGE 40	DRAWING 051	REV 6
SCALE 1/3	EST.WT. 240#	SH 1 OF 1	12:26PM 4-14-2000

Figure Withheld Under 10 CFR 2.390

NAC INTERNATIONAL			
LEGAL WEIGHT TRUCK TRANSPORT CASK ASSY 28 MTR ELEMENT SAFETY ANALYSIS REPORT			
PROJECT 315-40		DRAWING 052	REV 3
SCALE	WEIGHT	SH 1 OF 1	11:40AM

Figure Withheld Under 10 CFR 2.390

NAC INTERNATIONAL

WELDMENT,
7 CELL BASKET,
TRIGA FUEL BASE MODULE

PROJECT 315-40		DRAWING 070	REV 5
SCALE 1/3	EST.WT. 197 LBS	SH 1 OF 1	10:55AM 4-14-2009

Figure Withheld Under 10 CFR 2.390

NAC INTERNATIONAL

WELDMENT,
7 CELL BASKET,
TRIGA FUEL INTERMEDIATE MODULE

PROJECT 315-40		DRAWING 071	REV 6
SCALE 1/3	EST.WT. 187 LBS	SH 1 OF 1	11:DAAM 4-16-2008

Figure Withheld Under 10 CFR 2.390

NAC INTERNATIONAL

WELDMENT,
7 CELL BASKET,
TRIGA FUEL TOP MODULE

PROJECT 315-40		DRAWING 072	REV 6
SCALE 1/3	EST.WT. 275 LBS	SH 1 OF 1	11:20AM 4-14-2005

Figure Withheld Under 10 CFR 2.390

NAC INTERNATIONAL

LEGAL WEIGHT TRUCK
TRANSPORT CASK ASSY,
120 TRIGA FUEL ELEMENTS
OR 480 CLUSTER RODS

PROJECT 315-40		DRAWING 079	REV 5
SCALE 1/8	WEIGHT	SH 1 OF 1	2:15PM 2-20-2008

Figure Withheld Under 10 CFR 2.390

NAC INTERNATIONAL			
WELDMENT, 7 CELL POISON BASKET, TRIGA FUEL BASE MODULE			
PROJECT 315	DESIGN PACKAGE 40	DRAWING 080	REV 4
SCALE 1/3	EST. WT. 197 LBS	SH 1 OF 1	10:41 AM 4-14-2009

Figure Withheld Under 10 CFR 2.390

NAC INTERNATIONAL

WELDMENT,
7 CELL POISON BASKET,
TRIGA FUEL INTERMEDIATE MODULE

PROJECT	DESIGN PACKAGE	DRAWING	REV
315	40	081	4
SCALE 1/3	EST.WT. 187 LBS	SH 1 OF 1	12:43PM 1-14-2009

Figure Withheld Under 10 CFR 2.390

NAC INTERNATIONAL

WELDMENT,
7 CELL POISON BASKET,
TRIGA FUEL TOP MODULE

PROJECT	DESIGN PACKAGE	DRAWING	REV
315	40	082	4

SCALE	EST.WT.	SH	OF	
1/3	275 LBS	1	1	12:47PM 4-14-2003

Figure Withheld Under 10 CFR 2.390

NAC INTERNATIONAL

SPACER,
LWT CASK ASSEMBLY
TRIGA FUEL

PROJECT	DESIGN PACKAGE	DRAWING	REV
315	040	083	0
SCALE 1/2	EST. WT.	SH 1 OF 1	3.21PM 12-11-97

Figure Withheld Under 10 CFR 2.390

NAC INTERNATIONAL

LEGAL WEIGHT TRUCK
TRANSPORT CASK ASSY
140 TRIGA ELEMENTS

PROJECT	DRAWING	REV
315-40	084	4
1/12	SH 1 OF 1	2-24PM 2-21-2008

Figure Withheld Under 10 CFR 2.390

NAC INTERNATIONAL

AXIAL FUEL AND CELL BLOCK SPACERS, MTR AND TRIGA FUEL BASKETS, NAC-LWT CASK SAR

PROJECT 315-40		DRAWING 085	REV 0
SCALE 1/1	WEIGHT NOTED	SH 1 OF 1	8:29AM 10-11-2007

Figure Withheld Under 10 CFR 2.390

NAC INTERNATIONAL

ASSEMBLY,
SEALED FAILED FUEL CAN,
TRIGA FUEL

PROJECT 315-40	DRAWING 086	REV 1
	SH 1 OF 1	2:02PM 2-24-2005

Figure Withheld Under 10 CFR 2.390

NAC INTERNATIONAL

CANISTER LID ASSEMBLY,
SEALED FAILED FUEL CAN,
TRIGA FUEL

PROJECT 315-40		DRAWING 087	REV 6
SCALE FULL	WEIGHT 5#	SH 1 OF 1	1:10PM 5-16-2006

Figure Withheld Under 10 CFR 2.390

NAC INTERNATIONAL

CANISTER BODY ASSEMBLY,
SEALED FAILED FUEL CAN,
TRIGA FUEL

PROJECT 315-40		DRAWING 088	REV 2
SCALE FULL	EST.WT. NOTED	SH 1 OF 1	3:15PM 5-20-98

Figure Withheld Under 10 CFR 2.390

NAC INTERNATIONAL

WELDMENT,
7 ELEMENT BASKET,
35 MTR FUEL BASE MODULE,

PROJECT 315-40		DRAWING 090	REV 4
SCALE 1/3	EST.WT.	SH 1 OF 1	12:55PM 4-14-2009

Figure Withheld Under 10 CFR 2.390

NAC INTERNATIONAL

WELDMENT,
7 ELEMENT BASKET, 35
MTR FUEL INTERMEDIATE MODULE

PROJECT 315-40		DRAWING 091	REV 4
SCALE 1/3	EST. WT.	SH 1 OF 1	1:02PM 4-14-2009

Figure Withheld Under 10 CFR 2.390

NAC INTERNATIONAL

WELDMENT,
7 ELEMENT BASKET,
35 MTR FUEL TOP MODULE

PROJECT	DRAWING	REV
315-40	092	4

SCALE	EST. WT.	SH	OF	
1/3		1	1	4-14-2009

Figure Withheld Under 10 CFR 2.390

NAC INTERNATIONAL

LEGAL WEIGHT TRUCK
TRANSPORT CASK ASSY
35 MTR ELEMENT

PROJECT 315-40		DRAWING 094	REV 4
SCALE 1/8	WEIGHT	SH 1 OF 1	11:44AM 10-11-2007

Figure Withheld Under 10 CFR 2.390

NAC INTERNATIONAL

FUEL CLUSTER ROD
INSERT,
(3)
TRIGA FUEL

PROJECT 315-40		DRAWING 096	REV 3
SCALE FULL	WEIGHT 11#	SH 1 OF 1	2:1 NAV 1-2-2008

Figure Withheld Under 10 CFR 2.390

NAC INTERNATIONAL

PWR/BWR ROD
TRANSPORT CANISTER
ASSEMBLY

PROJECT 315-40		DRAWING 098	REV 6
SCALE	WEIGHT	SH 1 OF 3	X:\DWG 2-11-2009

Figure Withheld Under 10 CFR 2.390

NAC INTERNATIONAL

PWR/BWR ROD
TRANSPORT CANISTER
ASSEMBLY

PROJECT	DRAWING	REV
315-40	098	6
	SH 2 OF 3	1:36PM 2-11-2009

Figure Withheld Under 10 CFR 2.390

NAC INTERNATIONAL

PWR/BWR ROD
TRANSPORT CANISTER
ASSEMBLY

PROJECT		DRAWING		REV
315-40		098		6
1/2	NOTED	SH 3 OF 3	1:54PM 2-11-2009	

Figure Withheld Under 10 CFR 2.390

NAC INTERNATIONAL

CAN WELDMENT
PWR/BWR TRANSPORT
CANISTER

PROJECT 315-40	DRAWING 099	REV 3
SCALE 1/2	EST.WT. NOTED	SH 1 OF 3

Figure Withheld Under 10 CFR 2.390

NAC INTERNATIONAL

CAN WELDMENT
PWR/BWR TRANSPORT
CANISTER

PROJECT 315-40	DRAWING 099	REV 3
SCALE 1/1	EST.WT. NOTED	SH 2 OF 3	11:09AM 8-23-2000

Figure Withheld Under 10 CFR 2.390

NAC INTERNATIONAL

CAN WELDMENT
PWR/BWR TRANSPORT
CANISTER

PROJECT 315-40		DRAWING 099	REV 3
SCALE 1/1	EST.WT. NOTED	SH 3 OF 3	11:10AM 8-23-2000

Figure Withheld Under 10 CFR 2.390

NAC INTERNATIONAL

LIDS,
PWR/BWR ROD TRANSPORT
CANISTER (4)

PROJECT 315-40		DRAWING 100	REV 4
SCALE	WEIGHT	SH 1 OF 5	1:23PM 7-24-2008

Figure Withheld Under 10 CFR 2.390

NAC INTERNATIONAL

LIDS,
PWR/BWR ROD TRANSPORT
CANISTER

4

PROJECT	DRAWING	REV
315-40	100	4
	SH 2 OF 5	1:21PM 7-24-2008

Figure Withheld Under 10 CFR 2.390

NAC INTERNATIONAL

LIDS,
PWR/BWR ROD TRANSPORT
CANISTER

4

PROJECT	DRAWING	REV
315-40	100	4
	SH 3 OF 5	1:20PM 1-24-2006

Figure Withheld Under 10 CFR 2.390

NAC INTERNATIONAL

LIDS,
PWR/BWR ROD TRANSPORT
CANISTER

PROJECT	DRAWING	REV
315-40	100	4
	SH 4 OF 5	1:20PM 3-24-2006

Figure Withheld Under 10 CFR 2.390

NAC INTERNATIONAL

LIDS,
PWR/BWR ROD TRANSPORT
CANISTER

PROJECT 315-40	DRAWING 100	REV 4
	SH 5 OF 5	1:20PM 7-24-2008

Figure Withheld Under 10 CFR 2.390

NAC INTERNATIONAL

4 X 4 INSERT
PWR/BWR TRANSPORT
CANISTER

PROJECT 315-40		DRAWING 101	REV 0
SCALE 1/1	EST.WT. NOTED	SH 1 OF 1	11:39 AM 2-7-2000

Figure Withheld Under 10 CFR 2.390

NAC INTERNATIONAL

5 X 5 INSERT
PWR/BWR TRANSPORT
CANISTER

PROJECT 315-40		DRAWING 102	REV 2
SCALE 1/1	EST. WT. NOTED	SH 1 OF 1	12:28PM 2-25-2009

Figure Withheld Under 10 CFR 2.390

NAC INTERNATIONAL

PIN SPACER
PWR/BWR TRANSPORT
CANISTER

PROJECT 315-40		DRAWING 103	REV 0
SCALE 2/1	EST.WT.	SH 1 OF 1	11:39 AM 2-7-200

Figure Withheld Under 10 CFR 2.390

NAC INTERNATIONAL

LEGAL WEIGHT TRUCK
TRANSPORT CASK ASSY,
PWR/BWR ROD
TRANSPORT CANISTER

PROJECT 315-40		DRAWING 104	REV 5
SCALE	WEIGHT	SH 1 OF 3	3:25PM 1-26-2007

Figure Withheld Under 10 CFR 2.390

NAC INTERNATIONAL

LEGAL WEIGHT TRUCK
TRANSPORT CASK ASSY
PWR/BWR ROD
TRANSPORT CANISTER

PROJECT	DRAWING	REV
315-40	104	5

Figure Withheld Under 10 CFR 2.390

NAC INTERNATIONAL

LEGAL WEIGHT TRUCK
TRANSPORT CASK ASSY
PWR/BWR ROD
TRANSPORT CANISTER

PROJECT	DRAWING	REV
315-40	104	5
	SH 3 OF 3	3:27PM 1-26-2009

Figure Withheld Under 10 CFR 2.390

NAC INTERNATIONAL		
PWR INSERT, PWR/BWR TRANSPORT CANISTER		
PROJECT 315-40	DRAWING 105	REV 3
SCALE 1/4	EST.WT NOTED	SH 1 OF 2

Figure Withheld Under 10 CFR 2.390

NAC INTERNATIONAL

PWR INSERT,
PWR/BWR TRANSPORT
CANISTER

PROJECT 315-40	DRAWING 105	REV 3
SCALE 1/4	EST.WT. NOTED	SH 2 OF 2

Figure Withheld Under 10 CFR 2.390

NAC INTERNATIONAL

MTR PLATE CANISTER,
LWT CASK

PROJECT 315-40		DRAWING 106	REV 1
SCALE 1/1	EST.WT. NOTED	SH 1 OF 3	4:34PM 8-29-2000

Figure Withheld Under 10 CFR 2.390

NAC INTERNATIONAL

MTR PLATE CANISTER,
LWT CASK

PROJECT 315-40		DRAWING 106	REV 1
SCALE 1/1	EST.WT. NOTED	SH 2 OF 3	1:54PM 8-29-2000

Figure Withheld Under 10 CFR 2.390

NAC INTERNATIONAL

MTR PLATE CANISTER,
LWT CASK

PROJECT 315-40		DRAWING 106	REV 1
SCALE 2/1	EST.WT. NOTED	SH 3 OF 3	2:09PM 6-29-2000

Figure Withheld Under 10 CFR 2.390

NAC INTERNATIONAL

WELDMENT,
7 CELL BASKET,
TOP MODULE,
DIDO FUEL

PROJECT 315-40		DRAWING 108	REV 1
SCALE 1/2.5	EST. WT. NOTED	SH 1 OF 3	11:54PM 8-6-2001

Figure Withheld Under 10 CFR 2.390

NAC INTERNATIONAL

WELDMENT,
7 CELL BASKET,
TOP MODULE,
DIDO FUEL

PROJECT 315-40		DRAWING 108	REV 1
SCALE 1/2	EST. WT. NOTED	SH 2 OF 3	1:34PM 8-6-2001

Figure Withheld Under 10 CFR 2.390

NAC INTERNATIONAL

WELDMENT,
7 CELL BASKET,
TOP MODULE,
DIDO FUEL

PROJECT 315-40		DRAWING 108	REV 1
SCALE 1/2	EST.WT. NOTED	SH 3 OF 3	J.McPhe 8-5-2001

Figure Withheld Under 10 CFR 2.390

NAC INTERNATIONAL

WELDMENT,
7 CELL BASKET,
INTERMEDIATE MODULE,
DIDO FUEL

PROJECT 315-40		DRAWING 109	REV 1
SCALE 1/2.5	EST.WT. NOTED	SH 1 OF 3	2:18PM 9-6-2001

Figure Withheld Under 10 CFR 2.390

NAC INTERNATIONAL

WELDMENT,
7 CELL BASKET,
INTERMEDIATE MODULE,
DIDO FUEL

PROJECT 315-40		DRAWING 109	REV 1
SCALE 1/2	EST.WT. NOTED	SH 2 OF 3	2:16PM 9-6-2001

Figure Withheld Under 10 CFR 2.390

INTERNATIONAL

WELDMENT,
7 CELL BASKET,
INTERMEDIATE MODULE,
DIDO FUEL

PROJECT	DRAWING	REV
315-40	109	1

Figure Withheld Under 10 CFR 2.390

NAC INTERNATIONAL

WELDMENT,
7 CELL BASKET,
BASE MODULE,
DIDO FUEL

PROJECT 315-40	DRAWING 110	REV 1
SCALE 1/2.5 EST.WT. NOTED	SH 1 OF 3	2:37PM 9-6-2001

Figure Withheld Under 10 CFR 2.390

NAC INTERNATIONAL

WELDMENT,
7 CELL BASKET,
BASE MODULE,
DIDO FUEL

PROJECT 315-40		DRAWING 110	REV 1
SCALE 1/2	EST.WT. NOTED	SH 2 OF 3	2:54PM 9-6-2001

Figure Withheld Under 10 CFR 2.390

NAC INTERNATIONAL

WELDMENT,
7 CELL BASKET,
BASE MODULE,
DIDO FUEL

PROJECT 315-40		DRAWING 110	REV 1
SCALE 1/2	EST.WT. NOTED	SH 3 OF 3	2:37PM 9-6-2001

Figure Withheld Under 10 CFR 2.390

NAC INTERNATIONAL

LEGAL WEIGHT TRUCK
TRANSPORT CASK ASSY
DIDO FUEL

PROJECT	DRAWING	REV
315-40	111	2
	SH 1 OF 1	10:13AM 7-29-2009

Figure Withheld Under 10 CFR 2.390

NAC INTERNATIONAL

SPACERS,
TOP MODULE
DIDO FUEL

PROJECT 315-40		DRAWING 113	REV 0
SCALE 1/2	EST.WT. NOTED	SH 1 OF 1	12:44PM 3-3-2001

Figure Withheld Under 10 CFR 2.390

NAC INTERNATIONAL

TOP MODULE,
GENERAL ATOMICS IFM,
LWT CASK

PROJECT 315-40	DRAWING 120	REV 2
SCALE 1/3	TEST WT NOTED	SH 1 OF 3

Figure Withheld Under 10 CFR 2.390

NAC INTERNATIONAL

TOP MODULE,
GENERAL ATOMICS IFM,
LWT CASK

PROJECT 315-40		DRAWING 120	REV 2
SCALE 1/3	EST.WT. NOTED	SH 2 OF 3	1:35PM 4-29-2003

Figure Withheld Under 10 CFR 2.390

NAC INTERNATIONAL

TOP MODULE,
GENERAL ATOMICS IFM,
LWT CASK

PROJECT 315-40		DRAWING 120	REV 2
SCALE 1/1	EST. WT. NOTED	SH 3 OF 3	1:35PM 4-29-2003

Figure Withheld Under 10 CFR 2.390

NAC INTERNATIONAL

SPACER,
GENERAL ATOMICS IFM,
LWT CASK

PROJECT 315-40	DRAWING 123	REV 1
SCALE 1/3	FST.WT NOTED	SH 1 OF 2

Figure Withheld Under 10 CFR 2.390

NAC INTERNATIONAL

SPACER,
GENERAL ATOMICS IFM,
LWT CASK

PROJECT 315-40		DRAWING 123	REV 1
SCALE 1/3	EST.WT. NOTED	SH 2 OF 2	11:05AM 4-20-2003

Figure Withheld Under 10 CFR 2.390

NAC INTERNATIONAL

TRANSPORT CASK ASSEMBLY,
GENERAL ATOMICS IFM,
LWT CASK

PROJECT		DRAWING	REV
315-40		124	1
1/8	N/A	SH 1 OF 1	8:34AM 5-16-2006

Figure Withheld Under 10 CFR 2.390

NAC INTERNATIONAL

TRANSPORT CASK ASSEMBLY,
FRAMATOME/EPRI,
LWT CASK

PROJECT	315-40	DRAWING	125	REV 3
		SH 1 OF 3	TS SAAR 5-19-2006	

Figure Withheld Under 10 CFR 2.390

NAC INTERNATIONAL

TRANSPORT CASK ASSEMBLY,
FRAMATOME/EPRI,
LWT CASK

PROJECT	DRAWING	REV
315-40	125	3

SH 2 OF 3

Figure Withheld Under 10 CFR 2.390

NAC INTERNATIONAL

TRANSPORT CASK ASSEMBLY,
FRAMATOME/EPRI,
LWT CASK

PROJECT	DRAWING	REV
315-40	125	3
	SH 3 OF 3	8:53AM 5-18-2006

Figure Withheld Under 10 CFR 2.390

NAC INTERNATIONAL

WELDMENTS,
FRAMATOME/EPRI,
LWT CASK

PROJECT 315-40	DRAWING 126	REV 2
SCALE 1/2	EST.WT. NOTED	SH 1 OF 2

2:18PM 9-23-2003

Figure Withheld Under 10 CFR 2.390

NAC INTERNATIONAL

WELDMENTS,
FRAMATOME/EPRI,
LWT CASK

PROJECT 315-40		DRAWING 126	REV 2
SCALE 1/2	EST.WT. NOTED	SH 2 OF 2	2:32PM 8-23-2003

Figure Withheld Under 10 CFR 2.390

NAC INTERNATIONAL

SPACER ASSEMBLY,
TPBAR SHIPMENT,
LWT CASK.

PROJECT 315-40		DRAWING 127	REV 2
		SH 1 OF 2	5-19-200

Figure Withheld Under 10 CFR 2.390

NAC INTERNATIONAL

SPACER ASSEMBLY,
TPBAR SHIPMENT,
LWT CASK

PROJECT 315-40	DRAWING 127	REV 2
	SH 2 OF 2	9:36 AM 5-24-2006

Figure Withheld Under 10 CFR 2.390

NAC INTERNATIONAL

LEGAL WEIGHT TRUCK
TRANSPORT CASK ASSY
TPBAR SHIPMENT
SAFETY ANALYSIS REPORT

PROJECT	DRAWING	REV
315-40	128	3

Figure Withheld Under 10 CFR 2.390

NAC INTERNATIONAL

LEGAL WEIGHT TRUCK
TRANSPORT CASK ASSY
TPBAR SHIPMENT
SAFETY ANALYSIS REPORT

PROJECT	DRAWING	REV
315-40	128	3
1/8	SH 2 OF 2	9/6AM 1-29-2009

Figure Withheld Under 10 CFR 2.390

GENERAL ATOMICS
SAN DIEGO, CALIFORNIA

TITLE RERTR SECONDARY ENCLOSURE

SIZE	SCM NO	DWG NO	REV
C	32334	032230	A

SCALE 1=1 | QAL 1B | SHEET 1 OF 1

Figure Withheld Under 10 CFR 2.390

GENERAL ATOMICS
SAN DIEGO CALIFORNIA

TITLE HTGR SECONDARY ENCLOSURE

SIZE	SCM NO	DWG NO	REV
C	32334	032231	A

SCALE 1=1 CAL 1B SHEET 1 OF 1

Figure Withheld Under 10 CFR 2.390

S M	GENERAL ATOMICS SAN DIEGO, CALIFORNIA		
TITLE	RERTR PRIMARY ENCLOSURE		
SIZE C	SCM NO 32334	DWG NO 032236	REV B
SCALE 1=1	QAL 1B	SHEET 1 OF 1	

Figure Withheld Under 10 CFR 2.390

GENERAL ATOMICS
SAN DIEGO, CALIFORNIA

TITLE: HTGR PRIMARY ENCLOSURE			
SIZE: C	SCM NO: 32334	DWG NO: 032237	REV: B
SCALE: 1=1	DAL: 1B	SHEET 1 OF 1	

Figure Withheld Under 10 CFR 2.390

NAC INTERNATIONAL

CANISTER BODY ASSEMBLY,
FAILED FUEL CAN,
PULSTAR

PROJECT	DRAWING	REV
315-40	129	1
	SH 1 OF 1	4:09PM 10-5-2004

Figure Withheld Under 10 CFR 2.390

NAC INTERNATIONAL

ASSEMBLY,
FAILED FUEL CAN,
PULSTAR

PROJECT	DRAWING	REV
315-40	130	1
	SH 1 OF 1	8:16AM 10-6-2004

Figure Withheld Under 10 CFR 2.390

NAC INTERNATIONAL

TRANSPORT CASK ASSEMBLY,
PULSTAR SHIPMENT,
LWT CASK

PROJECT	DRAWING	REV
315-40	133	1
	SH 1 OF 2	8:56 AM 5-18-2006

Figure Withheld Under 10 CFR 2.390

NAC INTERNATIONAL

TRANSPORT CASK ASSEMBLY,
PULSTAR SHIPMENT,
LWT CASK

PROJECT	DRAWING	REV
315-40	133	1
	SH 2 OF 2	8:58AM 4-18-2008

Figure Withheld Under 10 CFR 2.390

NAC INTERNATIONAL

BODY WELDMENT,
SCREENED FUEL CAN,
PULSTAR FUEL

PROJECT 315-40	DRAWING 134	REV 1
	SH 1 OF 1	2:04PM 2-3-2005

Figure Withheld Under 10 CFR 2.390

NAC INTERNATIONAL

ASSEMBLY,
SCREENED FUEL CAN,
PULSTAR FUEL

PROJECT	DRAWING	REV
315-40	135	1
	SH 1 OF 1	2:11PM 2-3-2005

Figure Withheld Under 10 CFR 2.390

NAC INTERNATIONAL

LEGAL WEIGHT TRUCK
TRANSPORT CASK ASSY
ANSTO FUEL

PROJECT 315-40		DRAWING 139	REV 1
SCALE 1/8	WEIGHT	SH 1 OF 1	8:28AM 7-29-2008

Figure Withheld Under 10 CFR 2.390

NAC INTERNATIONAL

WELDMENT,
7 CELL BASKET,
TOP MODULE,
ANSTO FUEL

PROJECT	DRAWING	REV
315-40	140	1
SCALE 1/2.5 WEIGHT NOTED	SH 1 OF 2	11:37AM

Figure Withheld Under 10 CFR 2.390

NAC INTERNATIONAL

WELDMENT,
7 CELL BASKET,
TOP MODULE,
ANSTO FUEL

PROJECT 315-40		DRAWING 140	REV 1
SCALE 1/2	WEIGHT N/A	SH 2 OF 2	11:41AM 7-30-2008

Figure Withheld Under 10 CFR 2.390

NAC INTERNATIONAL

WELDMENT,
7 CELL BASKET,
INTERMEDIATE MODULE,
ANSTO FUEL

PROJECT 315-40		DRAWING 141	REV 1
SCALE 1/2.5	WEIGHT NOTED	SH 1 OF 2	10:34AM 7-29-2008

Figure Withheld Under 10 CFR 2.390

NAC INTERNATIONAL

WELDMENT,
7 CELL BASKET,
INTERMEDIATE MODULE,
ANSTO FUEL

PROJECT 315-40		DRAWING 141	REV 1
SCALE 1/2	WEIGHT NOTED	SH 2 OF 2	10:34AM 7-29-2008

Figure Withheld Under 10 CFR 2.390

NAC INTERNATIONAL			
WELDMENT, 7 CELL BASKET, BASE MODULE, ANSTO FUEL			
PROJECT 315-40		DRAWING 142	REV 1
SCALE 1/2.5	WEIGHT NOTED	SH 1 OF 2	1:28PM 7-30-2008

Figure Withheld Under 10 CFR 2.390

Figure Withheld Under 10 CFR 2.390

NAC INTERNATIONAL

WELDMENT,
7 CELL BASKET,
BASE MODULE,
ANSTO FUEL

PROJECT 315-40		DRAWING 142	REV 1
SCALE 1/2	WEIGHT NOTED	SH 2 OF 2	1:30PM 7-30-2008

Figure Withheld Under 10 CFR 2.390

NAC INTERNATIONAL

IRRADIATED HARDWARE,
LID SPACER,
LWT CASK

PROJECT	DRAWING	REV
315-40	145	0
	SH 1 OF 1	8:51 AM 10-20-2006

Figure Withheld Under 10 CFR 2.390

NAC INTERNATIONAL

LEGAL WEIGHT TRUCK
TRANSPORT CASK ASSY
ANSTO–DIDO
COMBINATION BASKET

PROJECT		DRAWING	REV
315–40		148	0
1/8		SH 1 OF 1	11:23AM 8-5-2005

1.5 Unclassified DOE Reference Documents and Drawings

The unclassified DOE reference documents and drawings are contained in the following appendices.

- Appendix 1-A – TTQP-1-015, "Description of the Tritium-Producing Burnable Absorber Rod for the Commercial Light Water Reactor," Revision 14
- Appendix 1-B – TTQP-1-091, "Unclassified TPBAR Releases, Including Tritium," Revision 11
- Appendix 1-C – TTQP-1-111, "Unclassified Bounding Source Term, Radionuclide Concentrations, Decay Heat, and Dose Rates for the Production TPBAR," Revision 5
- Appendix 1-D – DOE Drawing H-3-307845, "Production TPBAR Reactor Interface Dimensions Watts Bar," Revision 10, Sheet 1 of 2
- Appendix 1-E – DOE Drawing H-3-308875, "Production TPBAR Reactor Interface Dimensions Sequoyah," Revision 5, Sheet 1 of 2
- Appendix 1-F – DOE Drawing H-3-310568, "Mark 8 Multi-Pencil TPBAR – Watts Bar Reactor Interface," Revision 0, Sheet 1 of 2
- Appendix 1-G – PNNL Letter, TTP-06-056, Subject: Exposure of Shipping Casks to Tritium, February 21, 2006

APPENDIX 1-A

TTQP-1-015, "Description of the Tritium-Producing Burnable Absorber Rod for the Commercial Light Water Reactor," Revision 14

LIMITED DISTRIBUTION
COPY NO. 00003

R-204392

TRITIUM TECHNOLOGY PROGRAM

DESCRIPTION OF THE TRITIUM-PRODUCING BURNABLE ABSORBER ROD FOR THE COMMERCIAL LIGHT WATER REACTOR

TTQP-1-015

Revision 14

Effective Date: 3/10/06

TRITIUM TECHNOLOGY PROGRAM

DESCRIPTION OF THE TRITIUM-PRODUCING BURNABLE ABSORBER ROD FOR THE COMMERCIAL LIGHT WATER REACTOR

Revision 14

Major formatting revision; no revision marks

Prepared By:	D.D. Lanning **D.D. Lanning, Author**	2/27/06 **Date**
Concurrence:	R.O. Gates **R.O. Gates, Independent Reviewer**	2/28/06 **Date**
Concurrence:	 **Authorized Derivative Classifier**	3/2/06 **Date**
Approved By:	T. M. Brewer **T. M. Brewer, Quality Engineer**	3-3-06 **Date**
Approved By:	B.D. Reid **B.D. Reid, Design Task Manager**	3/6/06 **Date**
Approved By:	C.K. Thornhill **C.K. Thornhill, TTP Project Manager**	3/8/06 **Date**

1.0 ABSTRACT

Tritium-producing burnable absorber rods (TPBARs) used in the U.S. Department of Energy's Tritium Readiness Program are designed to produce tritium when placed in a Westinghouse or Framatome 17x17 fuel assembly and irradiated in a pressurized water reactor (PWR). This document provides an unclassified description of the design baseline for the TPBARs. This design baseline is currently valid only for Watts Bar reactor production cores.

2.0 DESIGN BASIS DOCUMENTS

The TPBAR design basis for the Watts Bar reactor production cores consists of this unclassified design basis description plus a collection of design basis documents. The design basis documents include the design drawings, the design specifications, and the component acceptance test requirements. These documents are listed in Appendices A, B, and C, respectively.

3.0 GENERAL FUNCTIONS AND REQUIREMENTS

TPBARs are similar in size and nuclear characteristics to standard, commercial PWR, stainless-steel-clad burnable absorber rods. The exterior of the TPBAR is a stainless-steel tube, approximately 152 inches from tip to tip at room temperature. The nominal outer diameter of the stainless-steel cladding is 0.381 inches. The internal components have been designed and selected to produce and retain tritium.

Figure 1 illustrates the concentric, cylindrical, internal components of a TPBAR. Within the stainless-steel cladding is a metal getter tube that encircles a stack of annular, ceramic pellets of lithium aluminate. The pellets are enriched with the ^{6}Li isotope. When irradiated in a PWR, the ^{6}Li pellets absorb neutrons, simulating the nuclear characteristics of a burnable absorber rod, and produce tritium, a hydrogen isotope. The tritium chemically reacts with the metal getter, which captures the tritium as a metal hydride.

To meet design limitations on rod internal pressure and burn-up of the lithium pellets, the amount of tritium production per TPBAR is limited to a maximum of 1.2 grams over the full design life of the rod (approximately 550 equivalent full-power days). The potential release rate of tritium into the reactor coolant is subject to a design limit that is consistent with the plant tritium release limits from the plant licensing basis. This is achieved by the combined effects of the metal getter tube surrounding the lithium aluminate pellets and an aluminide barrier coating on the inner surface of the cladding.

4.0 TPBAR COMPONENTS

The TPBAR cladding is double-vacuum-melted, Type 316 stainless steel. To prevent hydrogen from diffusing inward from the coolant to the TPBAR getter and to prevent

tritium from diffusing outward from the TPBAR to the reactor coolant, an aluminide coating is on the inner surface of the cladding. This coating barrier must remain effective during fabrication, handling, and in-reactor operations.

The annular ceramic pellets are composed of sintered, high-density, lithium aluminate ($LiAlO_2$).

The metal getter tube located between the cladding and the lithium aluminate pellets is composed of nickel-plated Zircaloy-4. The getter absorbs the molecular tritium (T_2) generated during irradiation. Nickel plating is used on both sides of the getter to prevent oxidation of the Zircaloy-4 surfaces, which would reduce the tritium absorption rate. Consequently, this plating must remain effective during fabrication, handling, and in-reactor operations.

One or more unplated Zircaloy-4 tube(s) line the inside of the annular pellets. This component is called the "liner." (In the Mark 8 design these include the liner and the cracking flange). Because the tritium produced in the pellets is mainly released as oxidized molecules (T_2O), a reactive metal liner is needed to reduce these species to molecular tritium by reacting with the oxygen. The liner also provides mechanical support to prevent axial movement of pellet material in case any pellets crack during TPBAR handling or operation.

5.0 PREVIOUS PRODUCTION TPBAR DESIGNS

In this section, two previous TPBAR designs are described: the production TPBAR design, in which the pellet column and getter tubes are segmented into sections called "pencils"; and the production full-length getter TPBAR design, in which the getter tube runs the full length of the TPBAR. These designs are augmented by added features in the Mark 8 TPBAR design, described in Section 6.0.

5.1 Production TPBAR Design (Irradiated in Watts Bar Cycles 6 and 7)

The getter tube is cut and rolled over (coined) to capture the liner and pellets within an assembly called a "pencil." There are a total of 11 pencil assemblies stacked within the cladding tube of each TPBAR (see Figure 2.) The majority of the pencils are of standard length (approximately 12 inches). Two of the pencils are of variable length.

To minimize the impact of power peaking in adjacent fuel rods resulting from the axial gaps between the stacked pencils, there is more than one type of TPBAR. The types are differentiated by where the variable-length pencils are loaded within the pencil stack. The loading sequence of the pencils is tracked, and each TPBAR is identified by type so that the location of each TPBAR type within a TPBAR assembly can be specified.

5.2 Production Full-Length Getter TPBAR Design Option

The axial arrangement of components is altered for the production full-length getter TPBAR design option. In this design, a single getter tube runs the full length of the TPBAR, and surrounds both the pellet column and the upper and lower spacer tubes (see Figure 3). The spacer tubes at the top and bottom of the pellet column are nickel-plated Zircaloy getters. The Zircaloy liner tubes and lithium aluminate pellet stacks in the full-length getter design are longer than in the standard design: typically approximately 16 inches compared to approximately 12 inches in the standard design.

The use of the production full-length getter design eliminates the need for variable-length pencils and different TBPAR types to minimize the impact of power peaking in adjacent fuel rods resulting from axial gaps between pencils. The pellet column in the production full-length getter TPBAR design is essentially continuous, and there is no power peaking penalty from axial gaps in the absorber column.

5.3 Common TPBAR Design Features

For hermetic closure of the TPBARs, end plugs similar to those used in commercial PWR burnable absorber rods are welded to each end of the cladding tube. As shown in Figures 2 and 3, a gas plenum space is located above the top of the absorber column and below the top end plug. A spring clip in this plenum space holds the internals in place during pre-irradiation handling and shipping. Depending on the design, either a top plenum getter tube or a spacer tube is placed in the plenum space to getter additional tritium.

The length of the column of enriched lithium aluminate must be variable to provide optimal flexibility in reactor core design. Consequently, the column of enriched lithium aluminate pellets is approximately centered axially about the core mid-plane elevation, but ranges in total length from about 126 to 132 inches. A thick-walled, nickel-plated, Zircaloy-4 spacer tube is placed between the bottom of the absorber column and the bottom end plug both to support the absorber column and to getter tritium.

6.0 THE MARK 8 DESIGN

The Mark 8 multi-pencil design corresponds with the production TPBAR designs described in Section 5.0 above, with the following changes and additions:

- Each pencil contains an added short flanged Zircaloy tube, called a "cracking flange", which interfaces with the inner liner at the top of the pencil, as shown in Figure 4. In the multi-pencil design, the pencil getter tube is coined to capture the pellet column

and the inner liner, as in the production TPBAR design; and the flange on the cracking flange similarly lies below and is captured by the coined-over getter on the top of the pencil.

- The pellet stack within each standard length pencil will consist of 13 pellets each approximately 1 inches long, instead of 6 pellets each approximately 2 inches long as in previous designs. However, the overall pellet stack length remains unchanged. The pellets within variable length pencils will similarly be slightly less than 1 inch in length.
- The upper and lower plenums in the multi-pencil design each contain "spacer assemblies" consisting of an outer NPZ getter tube (the "plenum getter") and an NPZ spacer tube within this outer getter tube (the "spacer getter").
- The upper spacer assembly contains two sections of NPZ spacer getter tube. The upper portion of the assembly contains an NPZ spacer getter tube only. The lower portion of the assembly contains in addition a Zircaloy "spacer liner tube" inside the lower section of the spacer getter tube (Figure 4). The spacer liner tube is flanged at its top end, and this flange separates the upper and lower sections of the spacer getter tube.
- The bottom spacer assembly in the multi-pencil design includes an outer NPZ getter tube and within that an NPZ lower spacer getter tube. A flanged spacer liner tube is inserted into the top of the lower spacer assembly. The outer NPZ getter tube is coined to capture both the lower spacer getter tube and the spacer liner (Figure 4).
- The top end plug design has been altered to include a hex- shaped shank on the upper body, and the neck-down region of the end plug has been removed. In addition, the diameter of the bored out region has been reduced and the length of the end plug insert has been reduced.
- The bored out region in the bottom end plug is removed, the length of the end plug insert has been reduced, and an NPZ getter disk resides on the insert of the bottom end plug (Figure 4).

7.0 TPBAR ASSEMBLIES

A TPBAR assembly is shown in Figure 5. It should be noted, however, that a typical design used in a 17x17 fuel assembly would be 20 TPBARs, rather than the eight illustrated in Figure 5 Compatibility with alternate fuel assembly designs can be accommodated by changes to the TPBAR lengths and end plugs.

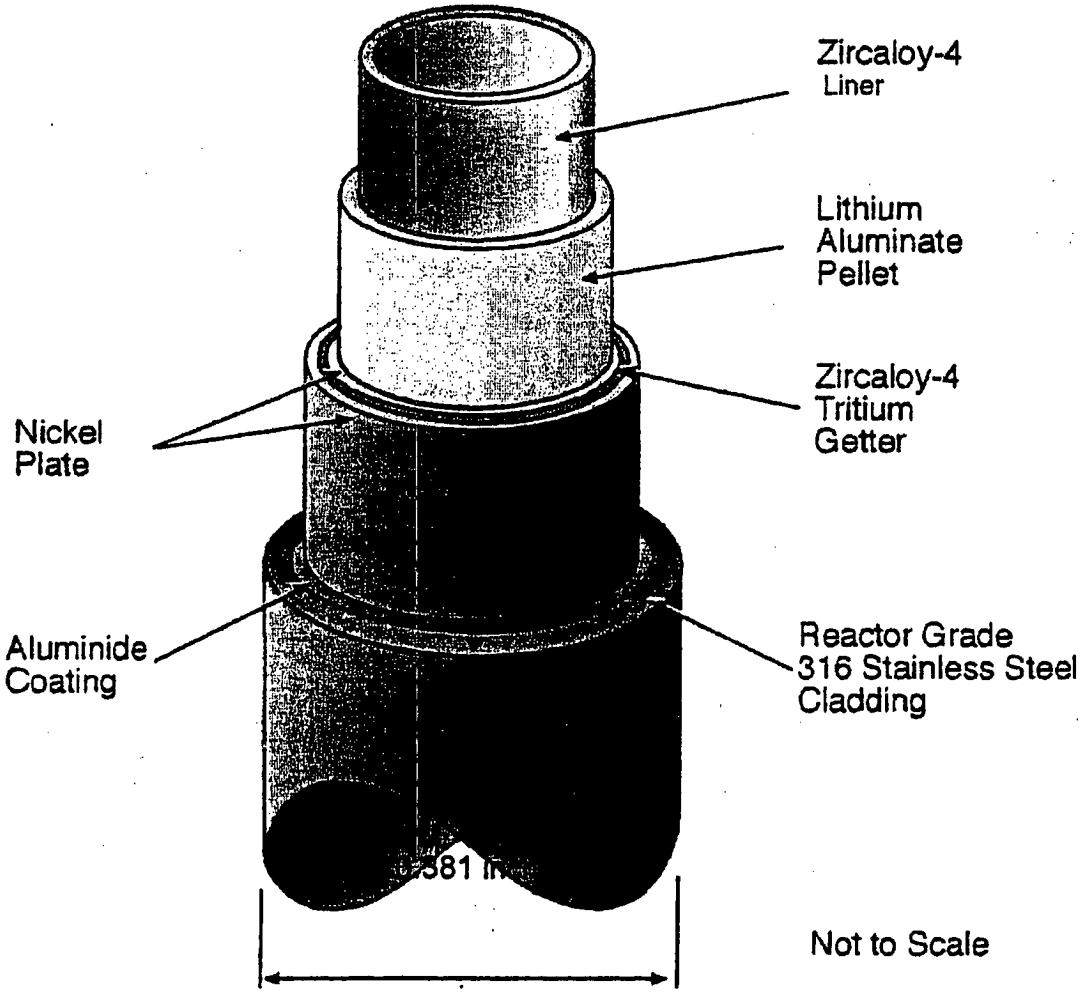

Figure 1. Isometric Section of a Tritium-Producing Burnable Absorber Rod

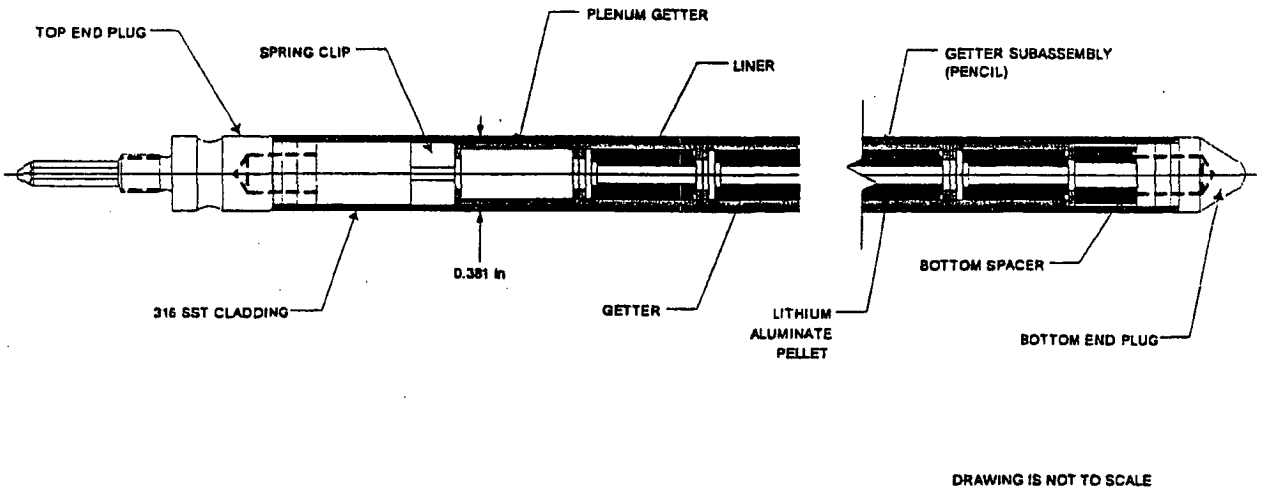

Figure 2. Axial Layout of TPBAR Internal Components –Production Standard Design

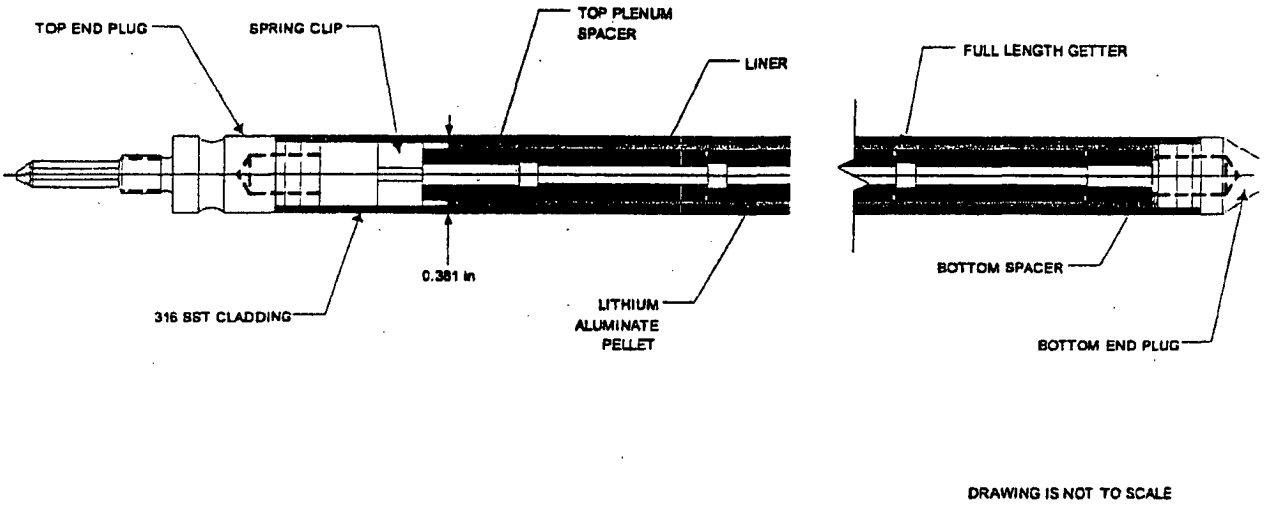

Figure 3. Axial Layout of TPBAR Internal Components –Production Full-Length Getter Design

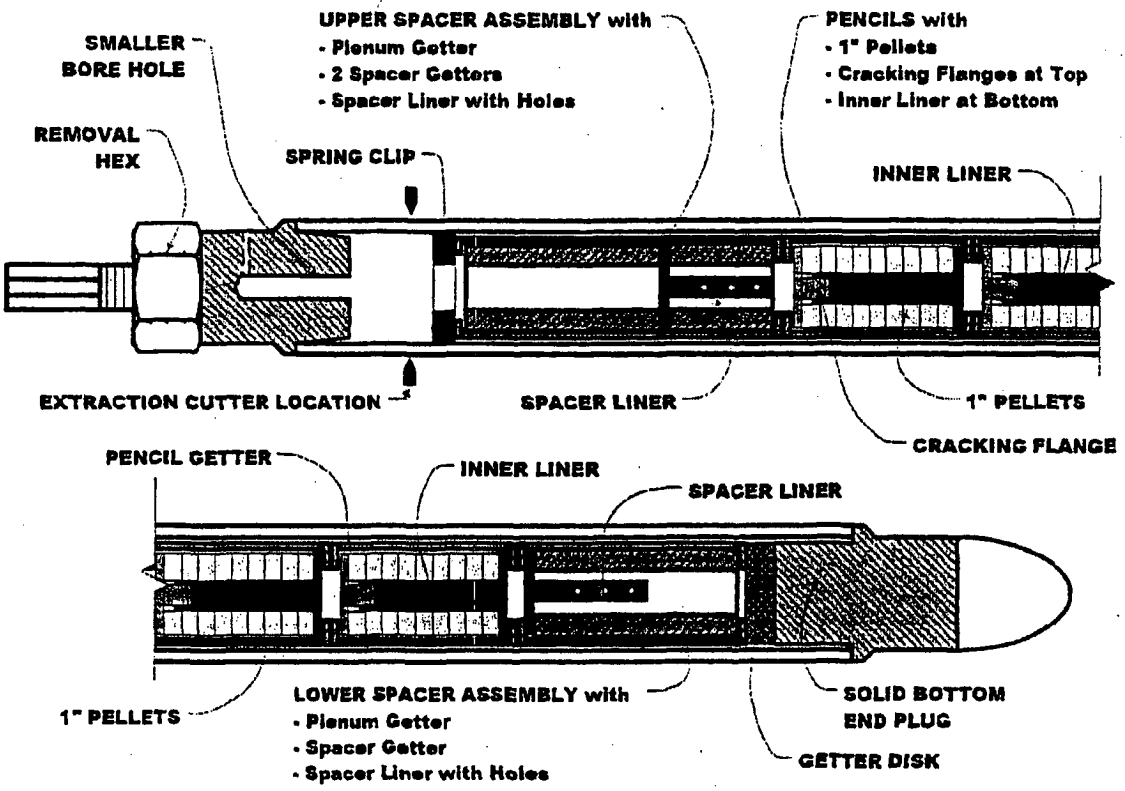

Figure 4 Axial Layout of Internal Components – Mark 8 Multi Pencil Design

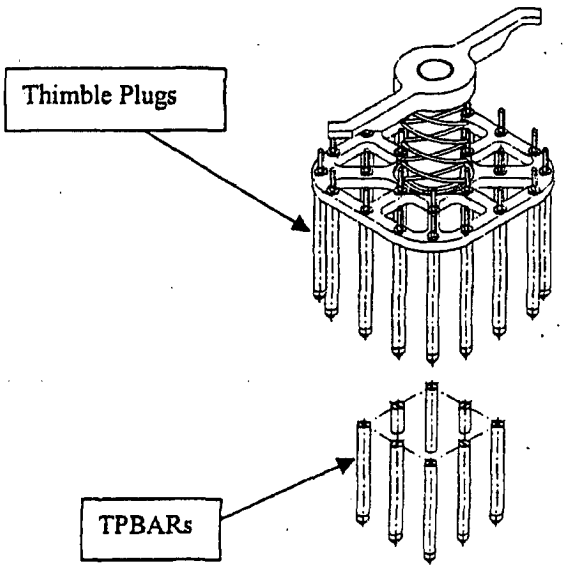

Figure 5 Typical TPBAR Assembly

APPENDIX A: LIST OF DESIGN DRAWINGS

Table A.1. List of Design Drawings for Standard Production TPBAR Design

Drawings are compiled in the latest revision of PNNL-TTQP-1-720, *Design Drawings for the Production TPBAR.*

Drawing	Title (Note: "U" designates an unclassified title.)	Classification
H-3-307843 Sheets 1 to 8	Production TPBAR Assembly Watts Bar (U)	Classified Sheet 2 is Unclassified
H-3-308874 Sheets 1 to 8	Production TPBAR Sequoyah (U)	Classified Sheet 2 is Unclassified
H-3-307844	Production Design Drawing List	Unclassified
H-3-307845 Sheets 1 and 2	Production TPBAR Interface Dimensions Watts Bar	Sheet 1 Unclassified Sheet 2 Classified
H-3-308875 Sheets 1 and 2	Production TPBAR Interface Dimensions Sequoyah	Sheet 1 Unclassified Sheet 2 Classified
H-3-307846	Production Cladding Tube	Unclassified
H-3-307847	Production Coated Cladding Tube (U)	Classified
H-3-307848 Sheets 1 and 2	Production Trimmed Coated Cladding Tube with End Prep (U)	Classified
H-3-307849	Production Standard Pencil Assembly (U)	Classified
H-3-307850	Production Variable Length Pencil Assembly (U)	Classified
H-3-307851 Sheets 1 and 2	Production Bottom Spacer (U)	Classified
H-3-307852	Production Top Plenum Spacer (U)	Classified
H-3-307853	Production Standard Pellet Stack	Unclassified
H-3-307854	Production Variable Length Pellet Stack	Unclassified
H-3-307855	Production Getter Tube Stock	Unclassified
H-3-307856 Sheets 1 and 2	Production Plated Getter Tube (U)	Classified
H-3-307857	Production Standard Inner Liner Tube	Unclassified
H-3-307858	Production Variable Length Inner Liner Tube	Unclassified
H-3-307859	Production Bottom Spacer Tube Stock	Unclassified
H-3-307860 Sheets 1 to 3	Production Top End Plug	Unclassified
H-3-307861 Sheets 1 and 2	Production Bottom End Plug	Unclassified
H-3-307862	Production Spring Clip	Unclassified
H-3-307325	Production Coated Cladding Bottom End Plug Assembly (U)	Classified
H-3-307326	Production Coated Cladding Bottom End Plug Assembly With End Prep (U)	Classified
H-3-309517	Activation Heat Treatment Profiles (U)	Classified
Full-Length Parts Needed FOR Multi-Pencil TPBAR Design (See PNNL-TTQP-1-769)		
H-3-307317	Spring Clip	Unclassified
H-3-310191 Sheets 1 to 3	Top End Plug	Unclassified
H-3-310192 Sheets 1 and 2	Bottom End Plug	Unclassified

Table A.2. List of Design Drawings for Production Full-Length Getter TPBAR Design

Drawings are compiled in the latest revision of PNNL-TTQP-1-769, *Production Full-Length Getter TPBAR Design Drawings (U)*

Drawing	Title (Note: "U" designates an unclassified title.)	Classification
H-3-307310 Sheets 1 to 6	Production Full-Length Getter TPBAR - Watts Bar (U)	Classified Sheet 2 is Unclassified
H-3-307311 Sheets 1 to 6	Production Full-Length Getter TPBAR - Sequoyah (U)	Classified Sheet 2 is Unclassified
H-3-307312 Sheets 1 to 4	Full-Length Getter TPBAR Interface Dimensions	Sheets 1 and 3 Unclassified Sheet 2 and 4 Classified
H-3-307313	Reserved for future use	
H-3-307314	Full-Length Getter Spacer Stock	Unclassified
H-3-307315	Full-Length Getter Plated Spacer (U)	Classified
H-3-307316	Full-Length Getter Finished Bottom Spacer (U)	Classified
H-3-307317	Spring Clip	Unclassified
H-3-307318	Reserved for future use	---
H-3-307319	Full-Length Getter Finished Top Plenum Spacer (U)	Classified
H-3-307320	Full-Length Getter Pellet Stack	Unclassified
H-3-307321	Full-Length Getter Inner Liner Tube	Unclassified
H-3-307322	Full-Length Getter Tube Stock	Unclassified
H-3-307323 Sheets 1 and 2	Full-Length Getter Plated Getter Tube (U)	Classified
H-3-307324	Production Full-Length Getter TPBAR Design Drawing List	Unclassified
H-3-307327	Activation Heat Treatment Profiles for Spacers (U)	Classified
H-3-310191 Sheets 1 to 3	Top End Plug	Unclassified
H-310192 Sheets 1 and 2	Bottom End Plug	Unclassified
Production Parts Needed for Full-Length Getter TPBAR Design (See PNNL-TTQP-1-720)		
H-3-307325	Production Coated Cladding Bottom End Plug Assembly (U)	Classified
H-3-307326	Production Coated Cladding Bottom End Plug Assembly With End Prep (U)	Classified
H-3-307846	Production Cladding Tube	Unclassified
H-3-307847	Production Coated Cladding Tube (U)	Classified
H-3-307848 Sheets 1 and 2	Production Trimmed Coated Cladding Tube with End Prep (U)	Classified
H-3-307853	Production Standard Pellet Stack	Unclassified
H-3-307854	Production Variable Length Pellet Stack	Unclassified
H-3-307857	Production Standard Inner Liner Tube	Unclassified
H-3-307858	Production Variable Length Inner Liner Tube	Unclassified
H-3-307860 Sheets 1 to 3	Production Top End Plug	Unclassified
H-3-307861 Sheets 1 and 2	Production Bottom End Plug	Unclassified

Table A.3. List of Design Drawings for Mark 8 Multi-Pencil TPBAR Design

Drawings are compiled in the latest revision of PNNL-TTQP-1-976, *Mark 8 TPBAR Design Drawings.*

Drawing	Title (Note: "U" designates an unclassified title.)	Classification
H-3-310566	Mark 8 TPBAR Drawing List	Unclassified
H-3-310567 Sheets 1 to 6	Mark 8 TPBAR Multi-Pencil Watts Bar (U)	Classified Sheet 2 is Unclassified
H-3-310568 Sheets 1 and 2	Mark 8 TPBAR Multi Pencil –Reactor Interface Mark 8 TPBAR Multi-Pencil –Extraction Interface	Sheet 1 Unclassified Sheet 2 Classified
H-3-310571 Sheets 1 to 3	Top End Plug	Unclassified
H-3-310572 Sheets 1 and 2	Trimmed Cladding Tube with End Prep (U)	Classified
H-3-310573	Coated Cladding Bottom End Plug Assembly (U)	Classified
H-3-310574	Coated Cladding Bottom End Plug Assembly with End Prep (U)	Classified
H-3-310575	Upper Spacer Assembly (U)	Classified
H-3-310576	Spacer Getters (U)	Classified
H-3-310580	Pencil Assemblies – Cracking Flange (U)	Classified
H-3-310583	Lower Spacer Assembly (U)	Classified
H-3-310584	Getter Disk (U)	Classified
H-3-310585	Getter Disk Stock	Unclassified
H-3-310586 Sheets 1 and 2	Bottom End Plug	Unclassified
H-3-310587	Cracking Flange	Unclassified
H-3-310591	Spacer Liner	Unclassified
H-3-310593	Mark 8 Variable Pellet Stack	Unclassified
H-3-310594	Mark 8 Standard Pellet Stack	Unclassified
H-3-310595 Sheets 1 to 5	Mark 8 EM TPBAR	Classified Sheet 2 Unclassified
H-3-310596	Mark 8 EM Pencil Assemblies (U)	Classified
H-3-310597	Mark 8 EM Beta Liner	Unclassified
H-3-310598	Mark 8 EM End Effect Pellet Stack	Unclassified

Table A.3. List of Design Drawings for Mark 8 Multi-Pencil TPBAR Design (continued)

Drawings listed below are reference drawings from PNNL-TTQP-1-720 and PNNL-1-769 (at the latest revision) for parts or items used in the Mark 8 design.

Drawing	Title (Note: "U" designates an unclassified title.)	Classification
H-3-307846	Production Cladding Tube	Unclassified
H-3-307847	Production Coated Cladding Tube (U)	Classified
H-3-307862	Production Spring Clip	Unclassified
H-3-307855	Production Getter Tube Stock	Unclassified
H-3-307856 Sheets 1 and 2	Production Plated Getter Tube (U)	Classified
H-3-307314	Full Length Getter Spacer Stock	Unclassified
H-3-307315	Full Length Getter Plated Spacer (U)	Classified
H-3-307853	Production Standard Pellet Stack	Unclassified
H-3-307854	Production Variable Length Pellet Stack	Unclassified
H-3-307857	Production Standard Inner Liner Tube	Unclassified
H-3-307858	Production Variable Length Inner Liner Tube	Unclassified
H-3-309517	Activation Heat Treatment Profiles (U)	Classified
H-3-307327	Activation Heat Treatment Profiles for Spacers (U)	Classified

APPENDIX B: LIST OF DESIGN SPECIFICATIONS (All at Latest Revision)

NOTE: "PNNL" prefix in the document number denotes a classified document, and "U" following the document title designates an unclassified title.

Document Number	Title
TTQP-1-072	*Production Specification for 316 Stainless Steel Seamless Cladding Tubes*
TTQP-1-073	*Manufacturing Specification for Production LWR Tritium Target Rod Getter Tube Stock*
TTQP-1-075	*Production Specification for LWR Tritium Target Rod Stainless Steel Bar Stock for Cladding*
TTQP-1-076	*Production Specification for Enriched Annular $LiAlO_2$ Pellets*
TTQP-1-077	*Production Specification for LWR Tritium Target Rod Bare Zircaloy Tube*
TTQP-1-079	*Production Specification for LWR Tritium Target Rod Top and Bottom End Plugs*
TTQP-1-080	*Production Specification for LWR Tritium Target Rod Top and Bottom End Plug Welding*
TTQP-1-083	*Production Specification for LWR Tritium Target Rod Stainless Steel Bar Stock for End Plugs*
TTQP-1-089	*Production Specification for LWR Tritium Target Rod Spring Clip*
TTQP-1-134	*Production Specification for Assembling TPBARs onto a Holddown Base Plate*
PNNL-TTQP-1-690	*Production Specification for LWR Tritium Target Rod Final Assembly (U)*
PNNL-TTP-1-1078	*Mark 8 Final Assembly Specification (U)*
PNNL-TTQP-1-692	*Specification for LWR Tritium Target Rod Inside Diameter Aluminide Barrier (U)*
PNNL-TTQP-1-826	*Final Product Specification for Production LWR Activated, Plated Getter Tubes (U)*
PNNL-TTQP-1-920	*Specification for Production LWR Full-Length Getter Tubes (U)*
PNNL-TTQP-1-941	*Production Specification for LWR Tritium Target Rod Final Assembly Using Full-Length Getters (U)*
PNNL-TTP-1-1073	*Specification for LWR TPBAR Getter Disks (U)*

APPENDIX C: COMPONENT ACCEPTANCE TEST REQUIREMENTS (ALL AT LATEST REVISION)

Note: "PNNL" prefix in the document number denotes a classified document, and "U" following the document title designates an unclassified title.

Document Number	Title
TTQP-1-081	*TPBAR Component Characteristics and Related Importance Factors*
TTQP-1-085	*Design Requirements for TTQP Weld Joint Burst Testing Matrix/Test Plan*
TTQP-1-129	*Qualification Requirements for Coated Cladding Bending*
PNNL-TTQP-1-829	*Standard Getter Rate Test Requirements (U)*
PNNL-TTQP-1-830	*Requirements for a Standard Cladding D_2 Permeation Test (U)*
PNNL-TTQP-1-867	*Test Plan for Target Rod Spring Clip (U)*

APPENDIX 1-B

TTQP-1-091, "Unclassified TPBAR Releases, Including Tritium," Revision 11

TRITIUM TECHNOLOGY PROGRAM

UNCLASSIFIED TPBAR RELEASES, INCLUDING TRITIUM

TTQP-1-091

Revision 11

Effective Date: 08/16/06

TRITIUM TECHNOLOGY PROGRAM

UNCLASSIFIED TPBAR RELEASES, INCLUDING TRITIUM

Revision 11

Prepared By:	D.D. Lanning **D.D. Lanning, Author**	8/15/06 **Date**
Reviewed By:	E.R. Gilbert **E.R. Gilbert, Independent Reviewer**	8/15/06 **Date**
Concurrence:	Ann Labahn **TTP Authorized Derivative Classifier**	8/16/06 **Date**
	VS Dukelow for TMB **T.M. Brewer, Quality Engineer**	4/15/06 **Date**
	Ann Labahn for BD Reid **B.D. Reid, Design Task Manager**	8/16/06 **Date**
Approval:	CK Thornhill **C.K. Thornhill, TTP Project Manager**	8/16/06 **Date**

1.0 INTRODUCTION

This document provides a complete listing of all unclassified tritium release values that should be assumed for unclassified analysis. Much of the information is brought forth from the related documents listed in Section 5.0 to provide a single-source listing of unclassified release values. Some information, however, is new or updated based on current design analysis and available experimental data.

This document provides unclassified information for a larger number of release scenarios than previously analyzed. This information is summarized in Tables 1, 2, and 3. In addition, a section is included to address lithium and aluminum release in the event of a 24-TPBAR breach in the spent fuel pool.

2.0 SUMMARY OF UNCLASSIFIED RELEASES, INCLUDING TRITIUM

All tritium-producing burnable absorber rod (TPBAR) analysis assumes a maximum of 1.2 grams of tritium per TPBAR will be generated during an 18-month operating cycle.

2.1 Intact TPBAR In-reactor Tritium Permeation

The in-reactor tritium permeation rate deduced from RCS tritium activity for the group of 240 TPBARs in Watts Bar Nuclear Cycle 6, averaged over a year extending to end-of-cycle, was 2.4 ± 1.8 Ci/TPBAR/year (95% confidence interval) (Lanning and Pagh, 2005). The 95% upper bound of 2.4 +1.8 = 4.2 Ci/TPBAR/year is recommended as the basis for assessing the tritium release from intact TPBARs.

2.2 In-reactor Tritium Release from a Failed TPBAR

The first scenario involves a TPBAR that may have a fabrication defect or may be damaged prior to insertion into the reactor for irradiation. In this case, 100 percent of the tritium generated in the TPBAR is assumed to be released to the reactor coolant as it is generated.

2.3 TPBAR Releases from Spent Fuel Pool Accidents

2.3.1 Spent Fuel Pool Tritium Concentration Limit

It has been determined that following the simultaneous breach of 24 TPBARs, the Tennessee Valley Authority take-action limit for tritium concentration in the spent fuel pool water will not be exceeded. The concentration limit is 60 microcuries per milliliter. The best estimate of total tritium release in this event is less than 25% of the TPBAR inventory. The release will not be instantaneous, but will occur

at a steady rate over a time period substantially greater than 8 hours. The rate will thus be less than 3% (of initial inventory) per hour.

2.3.2 Instantaneous Tritium Release per TPBAR

In particular, the instantaneous release of tritium from breached TPBARs in the spent fuel pool (as gas within the released gas from the TPBARs) will not exceed 0.001 Ci/TPBAR.

2.3.3 Lithium and Aluminum Release

In the event of a 24-TPBAR breach in the spent fuel, the following concentration limits for lithium and aluminum will not be exceeded:

- 400 ppb lithium
- 50 ppb aluminum.

2.4 Tritium Releases from TPBARs within Storage Canisters (<200°F)

The upper-bounding tritium partial pressure within storage canisters containing lead test assembly (LTA) TPBARs and sections is not expected to exceed 20 torr under nominal storage conditions (~86°F). The quoted bounding pressure for maximum temperatures (<200°F) is estimated by increasing this figure by the ratio of Kelvin temperatures, to 25 torr.

Tritium release from extracted TPBARs in storage will not exceed 1% of the declared post-extraction residual tritium (Clemmer et al. 1984; and Johnson et al. 1976).

In both cases, the form of the released tritium will be tritiated water vapor or condensate (HTO).

2.5 TPBAR Transportation Cask Event Releases

2.5.1 Intact TPBARs

2.5.1.1 For TPBAR temperatures ranging from ambient to less than 200°F, and for casks containing 1,200 or less TPBARs, the tritium release from the entire cask loading would be less than the regulatory requirement of 0.05 mCi per hour (10 CFR 71.51). The tritium would be released from the TPBARs in the form of molecular tritium gas (i.e., T_2 or HT).

2.5.1.2 For TPBAR temperatures ranging from 200°F to 650°F, the average tritium release would be less than 0.48 mCi per

TPBAR per hour based on the upper-bound in-reactor release rate of 4.2 Ci/TPBAR/year. The tritium would be released from the TPBARs in the form of tritium gas.

2.5.1.3 For TPBAR temperatures ranging from 650°F up to 1050°F (565°C), the tritium release should be considered to be an instantaneous release of less than 0.5 Ci per TPBAR per hour. Again, the tritium would be released from the TPBARs in the form of tritium gas.

The potential for TPBAR rupture was assessed at 1050°F because this is one of the temperature break-points in the Modal Study matrix cited earlier (Laity 1998). It was determined that the TPBARs are unlikely to rupture at temperatures less than 1050°F, but may rupture at higher temperatures.

2.5.1.4 Helium release from intact TPBARs is negligible.

2.5.2 Event-failed TPBARs

2.5.2.1 For TPBAR temperatures ranging from ambient to 200°F, the tritium release from a TPBAR whose cladding fails mechanically (e.g., due to impact forces) after cask loading should be considered to be less than 0.1 Ci per TPBAR per hour, not to exceed 1% of the tritium inventory in the lithium aluminate pellets. The release should be considered to be in the form of tritiated water and a very small fraction of methane.

2.5.2.2 For TPBAR temperatures ranging from 200°F to 650°F, the tritium release from a TPBAR whose cladding fails mechanically (e.g., due to impact forces) after cask loading should be considered to be less than 55 curies total due to desorption release. The release should be considered to be in the form of tritiated water and a very small fraction of methane.

2.5.2.3 For TPBAR temperatures ranging from 650°F to 1050°F, the tritium release should be considered to be up to 100% of the TPBAR tritium inventory, in the form of tritiated water and methane.

2.5.2.4 For TPBAR temperatures in excess of the T4 Modal Study break-point (1050°F), it should be assumed that 100 percent of

the tritium inventory of the TPBAR would be instantaneously released in the form of tritiated water and methane.

2.5.2.5 The helium inventory per TPBAR following shutdown and a 90-day cooling period is calculated to be 0.42 moles (total of He-4 from fill gas plus tritium production, plus residual He-3 and decay-generated He-3) [Pagh 2003]. The additional He-3 moles per TPBAR generated by tritium decay at any time "t" (years) following the cooldown can be calculated as:

$$\text{He-3(moles)} = 0.39\{1 - \exp[-\ln(2.0)t/12.33]\}.$$

It is recommended that 100% of all He-3 and He-4 be assumed to be released from event-failed TPBARs. This assumption may be significantly conservative for decay-generated He-3, since it is largely retained within the solid internal components of the TPBAR. However, a specific postirradiation temperature history for the TPBAR components would be required to calculate specific release fractions.

2.5.3 Pre-failed TPBARs

2.5.3.1 For pre-failed TPBARs at temperatures ranging from ambient to less than 200°F, the tritium release would be less than 0.1 Ci per TPBAR per hour. The release should be considered to be in the form of tritiated water and a very small quantity of methane. This rate applies to both rods breached in the dry condition and to rods which were breached in water (spent fuel pool drop) prior to cask loading, but which were dried after cask loading.

2.5.3.2 Without further definition of the cask environmental conditions and prefailed TPBAR conditions, it is assumed that the pre-failed TPBAR is waterlogged, and that consequently 100 percent of its tritium inventory would be released to the cask during transport when temperatures exceed 200°F. The tritium release will be in the form of tritiated water (i.e., T_2O and HTO) and, potentially, some tritiated methane. A further definition of the cask environment during transportation may permit a less-conservative tritium release estimate to be defined for some classes of pre-failed rods. To provide a more complete analysis of pre-failed rods, PNNL would need the following information: temperature range(s) for analysis; time period that TPBARs are in the temperature range(s)

(a time/temperature profile would be sufficient); and the maximum allowable quantity of tritium in the cask atmosphere.

3.0 FLAMMABLE GAS SOURCES

Because accident temperatures are not estimated to exceed 400°F, flammable gas generation for temperatures greater than that temperature are not considered here. The very limited tritium release from intact rods at temperatures <650°F have already been stated to be in the form of T_2 and HT.

Releases from event-failed rods at <200°F have been declared to be in the form of tritiated water and negligible methane fraction. Conversion of this water to T_2 or HT at such low temperatures is negligible.

Releases from event-failed rods at <650°F (i.e., 55Ci/TPBAR) have been declared to be in the form of T_2O and HTO. However, as a bounding estimate for flammable gas source, it will be assumed that 2% of this release will be converted to T_2 or HT from reaction with hot metal surfaces.

The pre-failed TPBARs are assumed to be waterlogged, for the purposes of estimating tritium release (Section 2.5.3.2 above). The potential for flammable hydrogen (H_2) gas formation from these rods is dependent upon actual conditions regarding water inventory, water release from the TPBARs, and water vapor reduction by hot metal surfaces. These conditions are not well defined. Hence, a bounding estimate of 0.15 moles per pre-failed TPBAR per year is made here, for temperatures between 200 and 400°F. This is calculated assuming 100% release of the potential 7.7 moles of water per TPBAR and a bounding conversion of 2% of this water to hydrogen gas (per year) from reaction with hot steel surfaces. Note that this is a very conservative (high) estimate, since anticipated cask internal temperatures are significantly less than 400°F. Below 200°F, hydrogen formation is considered negligible.

{These estimates do not include addition of hydrogen formed from radiolysis; however prior calculations indicate this would be less than 1% of available water per year, or less than 0.075 moles per pre-failed TPBAR per year.}

These bounding estimates for flammable gas formation are summarized in Table 4.

4.0 SHIPMENT OF TPBAR SEGMENTS AND FINES

Shipment of sectioned TPBARs plus cutting fines is planned. Such shipments will be bounded in content by up to 55 equivalent TPBAR lengths, with tritium content of the TPBARs less than the design limit of 1.2 grams tritium per TPBAR. The segments are expected to retain their internal components largely intact; however, impact loads during shipment could result in an undetermined extent of pellet cracking and further

fragmentation of pellet pieces. Conservatively, it is assumed that 100% of the tritium in the pellets is released during shipment. (It is noted that less than 40% of the tritium produced per TPBAR is contained in the pellets at the end of irradiation (Lanning et al. 2003.) This bounding assumption regarding tritium release from pellets is judged to include any in-shipment release of the residual tritium in the cutting fines.

The same declarations made in section 3.0 above apply to the shipment of TPBAR segments, regarding the expected form of the released tritium and the conversion to flammable species. That is, the expected forms of the released tritium are T_2O and HTO and the conversion to flammable species (T_2 and HT) is expected to be <2% per year, given cask temperatures less than 400°F.

Table 5 has been added to indicate the bounding quantities of released tritium and flammable gas generation for shipment of TPBAR segments as described above. As in Table 4, the flammable gas estimates do not include conversion due to radiolysis effects; but these are expected to be less than 1% of the available tritiated water vapor per year, or less than 0.044 moles per year.

5.0 RELATED DOCUMENTS

PNNL. 1997. *Report on the Evaluation of the Tritium Producing Burnable Absorber TPBAR Lead Test Assembly.* PNNL-11419, Revision 1, Pacific Northwest National Laboratory, Richland, Washington.

Letter. October 8, 1997. WW Laity (PNNL) to SM Sohinki (DOE), "CLWR: Tritium Permeation," Pacific Northwest National Laboratory, Richland, Washington.

Letter. June 3, 1998. WW Laity (PNNL) to SM Sohinki (DOE), "CLWR: Unclassified Tritium Releases for Transportation Casks," Pacific Northwest National Laboratory, Richland, Washington.

Letter. June 25, 1998. WW Laity (PNNL) to SM Sohinki (DOE), "CLWR: Unclassified Tritium Releases for Transportation Casks," Pacific Northwest National Laboratory, Richland, Washington.

Letter. November 30, 1998. WW Laity (PNNL) to SM Sohinki (DOE), "CLWR: Unclassified LTA TPBAR Tritium Releases for Transportation Casks," Pacific Northwest National Laboratory, Richland, Washington.

Letter. October 23, 2000. JS Chardos (Tennessee Valley Authority) to CK Thornhill (PNNL), "Verification of Design Inputs for Calculations of Breached TPBAR Leaching the Spent Fuel Pool," TVA Letter Number TVATP-00-068, Spring City, Tennessee.

Letter. July 1, 2002. CK Thornhill (PNNL) to D Duncan (ANL-W), *Tritium Pressure from Previously Breached TPBARs During Storage* (U), PNNL-TTQP-1-1937 (CRD), Pacific Northwest National Laboratory, Richland, Washington.

Clemmer, RG, PA Finn, RF Malecha, B Misra, MC Billone, DL Bowers, AK Fischer, LR Greenwood, RF Mattas, and SW Tam. 1984. *The TRIO Experiment*, ANL-84-55, Argonne National Laboratory, Argonne IL.

Johnson, AB, TJ Kabele, and WE Gurwell. 1976. *The Coproduct Program*, BNWL-2097, Pacific Northwest National Laboratory, Richland, Washington.

Lanning, DD. 2001. *Estimated Tritium Release from TPBARs in a Spent Fuel Storage Pool (U)*, PNNL-TTQP-1-722, Revision 6, Pacific Northwest National Laboratory, Richland, Washington.

Lanning, DD, ME Cunningham, DL Baldwin, and SE Marschman, 2003. *Results of Nondestructive and Destructive Examinations on the LTA TPBARs*, PNNL-TTQP-3-542, Revision 1, Pacific Northwest National Laboratory, Richland, Washington.

Lanning, DD. 2004. *TPBAR Tritium Releases* (U), PNNL-TTQP-1-735, Revision 7 (CRD), Pacific Northwest National Laboratory, Richland, Washington.

Lanning, DD, and RT Pagh, 2005. *Estimation of WBN Cycle 6 TPBAR Tritium Release from Analysis and Qualification of RCS Tritium Activity*, TTP-1-2064, Revision 0, Pacific Northwest National Laboratory, Richland, Washington.

Pagh, RT. 2003. *Release of Gas-Phase Components and Fines During Transportation Breach of Production TPBAR*, TTQP-1-2061, Revision 1, Pacific Northwest National Laboratory, Richland, Washington.

Table 1. Summary of Unclassified Tritium Release Assumptions for Non-Transportation Scenarios

In-Reactor Permeation	In-Reactor Release from Defective TPBARs	Spent Fuel Pool Accident Releases (<200°F)	Tritium Releases from TPBARs in Storage Canisters (<200°F)
Less than 0.48 mCi per TPBAR per hour	Released as it is generated	The Tennessee Valley Authority take-action limit of 60 microcuries per ml of spent fuel pool water will not be exceeded following the simultaneous breach of up to 24 TPBARs. The best estimate total tritium release in this event is less than 25% of the total TPBAR tritium inventory. The release rate will be < 3% (of initial inventory) per hour. The instantaneous release of tritium from breached TPBARs (as gas within the released gas from the TPBARs) will not exceed 0.001 Ci/TPBAR. The concentration of lithium and aluminum in the spent fuel pool following a 24-TPBAR breach will not exceed 400 ppb and 50 ppb, respectively.	Tritium partial pressure within storage canisters containing LTA TPBARs and sections will not exceed 25 torr. Tritium release from extracted TPBARs will not exceed 1% of the declared tritium residual.

Table 2. Summary of Unclassified Tritium Release Assumptions for Cask Transportation Scenarios

Intact TPBARs			Event-Failed TPBARs				TPBARs Pre-Failed In-Reactor	
<200°F	200°F to 650°F	650°F to 1050°F	Ambient to <200°F	200°F to 650°F	650°F to 1050°F	>1050°F	Ambient to <200°F	>200°F
< 0.05 mCi per hour for 1200 or less TPBARs	<0.48 mCi per TPBAR per hour (based on average TPBAR in the core)	<0.5 Ci per TPBAR per hour	<0.1 Ci per TPBAR per hour, not to exceed 1% of the pellet tritium inventory	<55 Ci total per TPBAR	<100% of inventory	100% of inventory	<0.1 Ci per TPBAR per hour	up to 100% of inventory

Table 3. Unclassified Helium Release Assumption for Cask Transportation Scenarios

TPBAR Condition	Helium Release to Cask
Intact	No release
Event-Failed	0.42 moles per TPBAR (following shutdown and 90-day cooling period), plus the decay-generated moles of He-3 at time t (years) following the cooldown, calculated as: $He\text{-}3(moles) = 0.39\{1 - \exp[-\ln(2.0)t/12.33]\}$

Table 4. Summary of Unclassified Bounding Flammable Gas Formation for Cask Transportation Scenarios (moles refer to moles H_2 equivalent)

Intact TPBARs		Event-Failed TPBARs		TPBARs Pre-Failed In-Reactor	
<200°F	200°F to 400°F	Ambient to <200°F	200°F to 400°F	Ambient to <200°F	200°F to 400°F
<7.1E-13 moles per TPBAR per hour	<<2.0E-9 moles per TPBAR per hour	Negligible moles per TPBAR	<1.9E-5 moles per TPBAR per year	Negligible moles total per TPBAR	<0.15 moles total per TPBAR per year

Table 5. Summary of Unclassified Bounding Tritium Release and Flammable Gas Formation for Cask Shipment of TPBAR Segments and Cutting Fines (up to 55 Equivalent TPBARs)

Tritium Releases		Flammable Gas Generation (moles refer to moles H_2 equivalent)	
<200°F	200°F to 400°F	Ambient to <200°F	200°F to 400°F
100% of Pellet inventory = < 26.4 grams	100% of Pellet inventory = < 26.4 grams	Negligible moles per TPBAR	< 0.088 moles per year

APPENDIX 1-C

TTQP-1-111, "Unclassified Bounding Source Term, Radionuclide Concentrations, Decay Heat, and Dose Rates for the Production TPBAR," Revision 5

VERIFIED DISTRIBUTION
COPY NO. 00009

R- 204306

TRITIUM TECHNOLOGY PROGRAM

UNCLASSIFIED BOUNDING SOURCE TERM, RADIONUCLIDE CONCENTRATIONS, DECAY HEAT, AND DOSE RATES FOR THE PRODUCTION TPBAR

TTQP-1-111

Revision 5

Effective Date: 12/14/05

TRITIUM TECHNOLOGY PROGRAM

UNCLASSIFIED BOUNDING SOURCE TERM, RADIONUCLIDE CONCENTRATIONS, DECAY HEAT, AND DOSE RATES FOR THE PRODUCTION TPBAR

Revision 5

Prepared By:	Richard J Pagh **R.T. Pagh, Senior Development Engineer**	12/13/05 **Date**
Reviewed By:	George H. Merrimethin **Technical Reviewer**	12/13/05 **Date**
	for T Brewer **Quality Engineer**	12/13/05 **Date**
	B D Reid **Authorized Derivative Classifier**	12/13/05 **Date**
Approved By:	B D Reid **B.D. Reid, Design Task Manager**	12/13/05 **Date**
	C K Thornhill **C.K. Thornhill, TTP Project Manager**	12/14/05 **Date**

TTP Design Analysis Report	EDP: D01398-EDP03 Rev. 12 TTQP-1-112, Rev. 12
Title: Unclassified Bounding Source Term, Radionuclide Concentrations, Decay Heat, and Dose Rates for the Production TPBAR (U)	Number: TTQP-1-111 Revision: 5

Purpose and Description of Design Analysis: The constituents of a TPBAR become radioactive during irradiation in a reactor. This analysis will determine the unclassified bounding source term, radionuclide concentrations, decay heat, and dose rates of an irradiated production TPBAR and the hold-down assembly.

Changes to Previous Proven Designs or the Analysis of Previous Proven Designs: Inclusion of Appendix D containing trace radionuclide concentrations in TPBAR.

Unverified Assumptions and/or Unverified Inputs (including source identification if available): None

Method of Analysis: Radionuclide concentrations, decay heat, and source terms are estimated using ORIGEN2. Dose rates are estimated using MCNP.

Computer Codes used including Version and Computer Processor(s) or Model(s) Used: ORIGEN2 Version 2.1b, MCNP 4C, and Excel 97 on a Dell OptiPlex Gx1, Pentium II processor. ORIGEN2 Version 2.2 on a Dell Precision 650, Pentium IV processor.

Summary of Results: The primary calculated values are given in the body of this report. Complete results for TPBAR radionuclide concentrations, decay heat, and source terms are presented in Tables 3 through 5, respectively, for various decay times. Similar results for the hold-down assembly are presented in Tables 6-8, results for the thimble plug are given in Tables 9-11. Complete results for the dose rates for a TPBAR and hold-down assembly are presented in Tables 12 and 13, respectively. Axial power profile is shown in Figure 2. Material constituents are given in Appendix A. ORIGEN2 input is given in Appendix B. MCNP input is given in Appendix C. Trace radionuclide concentrations for the TPBAR are provided in Appendix D.

	Signature	Date
Responsible Engineer(s)	RT Pagh Richard T Pagh	12/13/05
Design Verifier(s)	George H. Meriotti	12/13/05
TTP ADC	BDReid	12/13/05
Quality Engineer	JS Dukelow for T Brewer	12/13/05
Design Task Manager	BDReid	12/13/05
Design Database Administrator (N/A for Revision 0)	Neil Marco	12/13/05

1.0 INTRODUCTION

During the tritium-producing burnable absorber rod (TPBAR) irradiation, the components of the TPBAR will become radioactive as a result of neutron capture. The irradiated TPBAR will emit a spectrum of photons from the radioactive decay of these activation products. This radioactive decay also generates decay heat in the TPBAR.

Unclassified bounding estimates of radionuclide concentrations, photon source term, and decay heat have been made for an irradiated production TPBAR and are presented in this calculation. These results bound irradiation of the production TPBAR in any anticipated host reactor. This information is needed to address waste classification, waste disposal, and transportation. Additionally, the source term is needed for dose-rate calculations. Dose rate calculations are performed for several representative configurations and are included in this calculation.

These calculations are performed for both the TPBAR (absorber, getter, liner, cladding, plenum, spring clip, and end plugs) and the hold-down assembly. This calculation bounds all TPBAR designs including the full-length getter design.

2.0 METHODOLOGY

2.1 ORIGEN2 Methodology

The radionuclide concentrations, source term, and decay heat of an irradiated TPBAR and hold-down assembly were estimated using the ORIGEN2 code (RSIC 1996). The ORIGEN family of codes has been used extensively in the past to estimate radionuclide inventories when measurements were not available. Input to ORIGEN2 consists primarily of the total masses of the constituent elements (including trace elements), the power density of the fuel, and the irradiation time.

Reactor data is given in Table 1. A uranium-235 enrichment of 3% was assumed. A lower enrichment is more conservative than a higher enrichment because the neutron flux will be higher to maintain the desired power level. The specific power used for the ORIGEN2 input was calculated by dividing the assembly burnup by the irradiation time. The specific power represents a radial peaking factor of 1.5 for the reactor.

Masses for the elements present in a TPBAR and hold-down assembly are derived in Appendix A. Impurities, which are important for both source term and waste classification analysis, are included for the various components. The cobalt in the stainless steel is the primary contributor to the dose rate for both the TPBAR and hold-down assembly. Both SS-304 and SS-316 contain 500 ppm cobalt. It needs to be noted that the bounding mass derived in Appendix A is valid only for

radiological source calculations. For mechanical analysis or radiological shielding analysis, the bounding TPBAR mass of 2.3 lbs. listed in Lopez (2002) for the Sequoyah Units and Lopez (2003) for Watts Bar should be referenced.

Table 1. Reactor Data

Reactor Data from Lopez 2002, 2003	
Parameter	**Value**
Mass of U, kg/assembly	462
Number of assemblies	193
Reactor Power, MW	3,459
Irradiation Time, d	510
Maximum Assembly Burnup, MWd/MTU	29,700
Assumptions	
U-235 enrichment, wt%	3.000
U-234 content is small and can be treated as if it is U-238.	
Reactor is at full power throughout the cycle.	
Calculated Numbers	
Mass U-235, g/MTU	30000
Mass U-238, g/MTU	970000
Specific Power for Assembly, MW/MTU	58.24
Radial Assembly Peaking Factor	1.50

ORIGEN2 was executed for the following 3 cases:

- complete TPBAR
- hold-down assembly (without thimble plugs)
- single thimble plug (SS-304)

The hold-down assembly and the thimble plugs are located above the active core. Therefore, the results must be modified by conservative "scaling factors" to account for the fact that these components are located outside the active region of the core.

The various components, their masses determined for radiological source analysis, and appropriate scaling factors are summarized in Table 2. Note that the average scaling factor for a thimble plug is 0.2 for radionuclide concentrations and decay heat. Since the thimble plug will activate more at the end closer to the core, where the scaling factor is estimated to be 0.5 (Guenther et al. 1988), the scaling factor for the thimble plug photon source term is assumed to be 0.5 to be conservative.

The scaling factor for the hold-down assembly was applied to the output from the ORIGEN2 calculation. The calculation for the thimble plug was made as one gram of material. The output from each calculation was multiplied by the mass of the thimble plug (150 grams) and the appropriate scaling factors.

Table 2. Summary of ORIGEN2 Cases

Component	Material	Mass (g)	Scaling Factor
Complete TPBAR	SS-316, Lithium Aluminate, Nickel, Aluminum, Zircaloy	1245	1.0 (no scaling factor) Note: Mass is valid only for radiological source calculations. Bounding mechanical and shielding mass of 2.3 lbs. is listed in Lopez (2002) and Lopez (2003).
Hold-Down Assembly (no thimble plugs)	SS-304 and Inconel	2815	0.1 (Migliore et al. 1994)
Single Thimble Plug	SS-304	150	0.2 for radionuclide concentrations and decay heat (Luksic 1989, averaged over whole thimble plug) 0.5 for source terms (Guenther et al. 1988)

ORIGEN2 input for each of these cases is given in Appendix B.

ORIGEN2 output does not report a complete list of radionuclides generated by irradiation as this list would be quite long. Rather the code provides a threshold value below which concentrations are not reported. For the above cases the threshold is set at a value such that any radionuclide whose value is nine orders of magnitude below the total for the item is not reported. In most cases this is sufficient to identify important radionuclides of concern. However, parent-daughter products (such as Sr-90 and Y-90) may not both be displayed if one of the radionuclides does not meet the threshold. Appendix D provides a listing of radionuclide concentrations for the TPBAR where the threshold has been lowered to report any concentration greater than 1 picocurie.

2.2 MCNP Methodology

Dose rates were estimated for the unshielded TPBAR and hold-down assembly using the MCNP code (RSICC 2000). MCNP is a general-purpose particle transport code commonly used for shielding applications. MCNP allows the user to model the problem geometry in as much detail as the user demands. Input includes the problem geometry, materials, and source term.

TPBAR Geometry. The TPBAR was modeled in a simplified manner as a piece of bare cladding using smeared geometry (but not smeared compositions) as described in Love (2003). Smeared geometry was used because the source term was calculated for the entire TPBAR, not for individual TPBAR components. To add conservatism the source (Table 5) is uniformly distributed throughout the smeared cladding region (i.e., no source in the inner region of the TPBAR). This assumption was made because the largest contributor to the dose rate is from cobalt activation in the cladding. Even more conservatism could be added by using unsmeared cladding dimensions because this would concentrate the source closer to the surface, but this level of conservatism is unwarranted because there will be a contribution to the dose rate from the TPBAR internals, which is approximately modeled by using smeared cladding dimensions. The entire length of the TPBAR was modeled. No shielding material was used in the model and the TPBAR is detached from the hold-down assembly.

Hold-Down Assembly Geometry. The geometry of the hold-down assembly was modeled in a simplified manner. All dimensions used in the model are approximate and sufficient to describe the hold-down assembly for the purpose of dose rate analyses. Dimensions are assumed and were chosen based upon the approximate cross sectional area of a fuel assembly and from personal communication with Westinghouse.

The TPBARs will be removed from the hold-down assembly prior to extraction, leaving only the thimble plugs. It was assumed that a hold-down assembly would contain at least 4 TPBARs, leaving 20 thimble plugs on the hold-down assembly. Figure 1 shows the assumed loading pattern. Each thimble plug was modeled as a cylinder with a radius of 0.5 cm and a length of 16 cm. The hold-down assembly itself was modeled as a cylindrical plate 0.7 cm thick with a radius of 12 cm. (Note: The entire mass and source term of the hold-down assembly is modeled as a single plate.) The steel composition was modeled as pure iron with an assumed density of 8 g/cc (approximate density of steel from Livingston 2001). No shielding material was used in the model.

The source term for the hold-down assembly (Table 8) is distributed uniformly throughout the plate. The source term for a thimble plug (Table 11) is distributed uniformly throughout each thimble plug. Note that the average scaling factor for a thimble plug is 0.2 for radionuclide concentrations (see Table 2). Because the thimble plug will activate more at the end closer to the core, where the scaling factor is estimated to be 0.5, to be conservative the source strength for a thimble plus is assumed to be 0.5 in the MCNP calculations.

Flux-to-dose rate conversion factors are used by MCNP to estimate dose rates. The conversion factors used are the ANSI/ANS-6.1.1-1977 standard

(Battat 1977). A 1991 standard is also available, but the 1977 standard is still in wide use and gives more conservative results than the 1991 standard.

The dose rates for both the TPBAR and hold-down assembly are computed for decay times of 7 days, 90 days, 180 days, 1 year, and 5 years. For the TPBAR, dose rates are calculated at the surface and at a distance of lm along the entire length. Dose rates at lm (radial) are also given for the centermost lm (axial) and represent an average over this axial region. For the hold-down assembly, dose rates are calculated at the top of the assembly, bottom of the thimble plugs, and around the sides of the assembly (at a radial distance of 12 cm from the centerline). All dose rates are averaged over surface areas.

Select MCNP input files are included in Appendix C.

3.0 ORIGEN2 RESULTS FOR RADIONUCLIDE CONCENTRATIONS, DECAY HEAT, AND PHOTON SOURCE TERMS; MCNP RESULTS FOR DOSE RATES

Complete results for TPBAR radionuclide concentrations, decay heat, and source terms are presented in Tables 3 through 5, respectively, for various decay times. The tritium results for the complete TPBAR have been forced to match the functional requirement of 1.2 g tritium maximum per TPBAR (e.g., the ORIGEN2 results for tritium are not reported in Tables 3 and 4). Similar results for the hold-down assembly are presented in Tables 6 through 8 and results for the thimble plug are given in Tables 9 through 11.

Complete results for the dose rates for a TPBAR and hold-down assembly are presented in Tables 12 and 13, respectively.

The source term was axially distributed uniformly throughout the TPBAR, i.e., core axial peaking was ignored in both the source term and dose rate analyses. Sufficient conservatism exists in the calculation that treating the axial peaking explicitly was unwarranted. The components were also modeled as existing in a vacuum and having no air attenuation, back-scattering, or other buildup factors included in the dose rates.

The relative axial profile of power per unit length for the TPBAR (without the bottom end plug) is shown in Figure 2. The peak-to-average ratio for this profile is 1.15. The bottom end plug is not shown as it represents 6.8% of the total power of the TPBAR. The remainder of the power is distributed as shown in Figure 2. This axial power distribution accounts for axial distribution of neutron fluence as deduced from the end of life axial distribution of tritium production, and also accounts for the higher mass/unit length in the bottom spacer region, which is the cause of the rise at the bottom end. This profile is provided for reference but was not used in these calculations.

The calculations in this document are conservative based upon the input assumptions and the calculational approach. The major assumptions are:

- Cobalt-60 is the major contributor to the dose rates. 500 ppm of cobalt was assumed for the calculations, which is the highest allowed by the stainless steel specification. The actual cobalt concentration could be a factor of 2 lower, which would cause the actual dose rates to be a factor of 2 lower than those calculated.

- Experimental data shows that ORIGEN2 tends to calculate cobalt-60 approximately 50% higher than expected (Migliore et. al. 1994).

- The flux-to-dose-rate conversion factors used in MCNP are a conservative set. The dose rates would decrease if a less conservative set of factors were used.

- The hold-down assembly was modeled as a plate. The actual hold-down assembly extends above the bottom plate, which would spread the source over a larger volume. The dose rate at the top of the hold-down assembly should decrease if a more detailed model were employed.

Table 3. Radionuclide Concentrations in a TPBAR (Ci/TPBAR)

Nuclide	7 Days	30 Days	90 Days	180 Days	1 Year	5 Years	10 Years
H-3[1]	1.16E+04	1.15E+04	1.14E+04	1.13E+04	1.10E+04	8.76E+03	6.61E+03
C 14	1.42E-03	1.42E-03	1.42E-03	1.42E-03	1.42E-03	1.42E-03	1.42E-03
NA 24	1.98E-02	1.65E-13	0.00E+00	0.00E+00	0.00E+00	0.00E+00	0.00E+00
P 32	1.03E+00	3.38E-01	1.84E-02	2.35E-04	3.02E-08	5.78E-10	5.75E-10
S 35	1.37E-02	1.15E-02	7.15E-03	3.52E-03	8.18E-04	8.22E-09	4.65E-15
AR 37	3.79E-01	2.40E-01	7.32E-02	1.23E-02	3.15E-04	8.74E-17	1.76E-32
AR 39	9.49E-03	9.49E-03	9.48E-03	9.48E-03	9.46E-03	9.37E-03	9.25E-03
K 42	2.18E-04	8.34E-12	8.31E-12	8.27E-12	8.18E-12	7.52E-12	6.77E-12
CA 41	7.51E-05	7.51E-05	7.51E-05	7.51E-05	7.51E-05	7.51E-05	7.51E-05
CA 45	3.13E-01	2.84E-01	2.20E-01	1.50E-01	6.82E-02	1.37E-04	5.78E-08
CA 47	1.57E-04	4.66E-06	4.86E-10	5.17E-16	2.62E-28	0.00E+00	0.00E+00
SC 46	8.20E-03	6.78E-03	4.13E-03	1.96E-03	4.24E-04	2.39E-09	6.57E-16
SC 47	5.68E-04	1.76E-05	1.86E-09	1.98E-15	1.00E-27	0.00E+00	0.00E+00
CR 51	9.67E+02	5.44E+02	1.21E+02	1.28E+01	1.24E-01	1.66E-17	2.38E-37
MN 54	4.19E+01	3.98E+01	3.48E+01	2.85E+01	1.89E+01	7.41E-01	1.29E-02
FE 55	2.15E+02	2.12E+02	2.03E+02	1.90E+02	1.66E+02	5.71E+01	1.51E+01
FE 59	1.98E+01	1.39E+01	5.52E+00	1.38E+00	7.96E-02	1.34E-11	8.14E-24
CO 58	2.69E+02	2.15E+02	1.19E+02	4.95E+01	8.06E+00	4.92E-06	8.41E-14
CO 60	3.60E+01	3.57E+01	3.49E+01	3.38E+01	3.16E+01	1.87E+01	9.68E+00
NI 59	1.68E-01	1.68E-01	1.68E-01	1.68E-01	1.68E-01	1.68E-01	1.68E-01

1 The ORIGEN2 values for H-3 are not reported. The values given for H-3 are based on a maximum of 1.2 g of tritium per TPBAR at discharge, as specified in the Functional Requirements document (Lopez 2003). There is 9664 Ci per gram of tritium, and the half-life of tritium is 12.33 years. The value of 1.2 g at discharge is decayed appropriately for the various decay times.

Nuclide	7 Days	30 Days	90 Days	180 Days	1 Year	5 Years	10 Years
NI 63	2.29E+01	2.29E+01	2.28E+01	2.28E+01	2.27E+01	2.20E+01	2.12E+01
NI 66	1.52E-04	1.38E-07	1.59E-15	1.97E-27	0.00E+00	0.00E+00	0.00E+00
CU 64	1.27E-03	1.04E-16	0.00E+00	0.00E+00	0.00E+00	0.00E+00	0.00E+00
CU 66	1.52E-04	1.38E-07	1.59E-15	1.97E-27	0.00E+00	0.00E+00	0.00E+00
ZN 65	4.13E-03	3.87E-03	3.26E-03	2.52E-03	1.49E-03	2.34E-05	1.31E-07
AS 76	8.74E-01	4.25E-07	1.44E-23	0.00E+00	0.00E+00	0.00E+00	0.00E+00
SE 75	8.88E-01	7.77E-01	5.49E-01	3.26E-01	1.12E-01	2.38E-05	6.13E-10
BR 82	1.14E-03	2.25E-08	1.18E-20	0.00E+00	0.00E+00	0.00E+00	0.00E+00
SR 89	7.51E-02	5.48E-02	2.40E-02	6.99E-03	5.49E-04	1.07E-12	1.39E-23
Y 89M	5.48E-04	4.18E-06	1.24E-11	6.39E-20	0.00E+00	0.00E+00	0.00E+00
Y 90	5.14E-01	1.30E-03	1.38E-06	1.37E-06	1.36E-06	1.23E-06	1.09E-06
Y 91	1.92E-01	1.46E-01	7.19E-02	2.47E-02	2.76E-03	8.38E-11	3.36E-20
ZR 89	5.49E-04	4.18E-06	1.25E-11	6.40E-20	5.60E-37	0.00E+00	0.00E+00
ZR 93	1.13E-04	1.13E-04	1.13E-04	1.13E-04	1.13E-04	1.13E-04	1.13E-04
ZR 95	6.57E+01	5.12E+01	2.67E+01	1.01E+01	1.36E+00	1.81E-07	4.63E-16
ZR 97	1.12E-01	1.65E-11	0.00E+00	0.00E+00	0.00E+00	0.00E+00	0.00E+00
NB 92	3.04E-01	6.34E-02	1.06E-03	2.28E-06	7.41E-12	0.00E+00	0.00E+00
NB 93M	3.68E-06	4.02E-06	4.87E-06	6.15E-06	8.73E-06	2.69E-05	4.49E-05
NB 94	4.76E-04	4.76E-04	4.76E-04	4.76E-04	4.76E-04	4.76E-04	4.76E-04
NB 95	6.93E+01	6.50E+01	4.45E+01	1.99E+01	2.94E+00	4.02E-07	1.03E-15
NB 95M	4.80E-01	3.80E-01	1.98E-01	7.48E-02	1.01E-02	1.34E-09	3.44E-18
NB 96	1.20E-03	9.19E-11	2.51E-29	0.00E+00	0.00E+00	0.00E+00	0.00E+00
NB 97	1.13E-01	1.78E-11	0.00E+00	0.00E+00	0.00E+00	0.00E+00	0.00E+00
NB 97M	1.06E-01	1.57E-11	0.00E+00	0.00E+00	0.00E+00	0.00E+00	0.00E+00
MO 93	1.04E-03	1.04E-03	1.04E-03	1.04E-03	1.04E-03	1.04E-03	1.04E-03
MO 99	1.68E+01	5.11E-02	1.38E-08	1.94E-18	0.00E+00	0.00E+00	0.00E+00
TC 99	4.35E-05	4.36E-05	4.36E-05	4.36E-05	4.36E-05	4.36E-05	4.36E-05
RU103	3.21E-03	2.14E-03	7.41E-04	1.52E-04	5.76E-06	3.67E-17	3.71E-31
CD115	2.91E-04	2.27E-07	1.78E-15	1.23E-27	0.00E+00	0.00E+00	0.00E+00
CD115M	1.84E-04	1.28E-04	5.05E-05	1.25E-05	7.00E-07	9.62E-17	4.52E-29
IN113M	1.31E+00	1.14E+00	7.94E-01	4.62E-01	1.51E-01	2.28E-05	3.83E-10
IN114	1.26E-01	9.13E-02	3.94E-02	1.12E-02	8.36E-04	1.10E-12	8.64E-24
IN114M	1.32E-01	9.54E-02	4.12E-02	1.17E-02	8.73E-04	1.15E-12	9.03E-24
SN113	1.31E+00	1.14E+00	7.93E-01	4.61E-01	1.51E-01	2.28E-05	3.82E-10
SN117M	8.21E+00	2.63E+00	1.35E-01	1.57E-03	1.64E-07	0.00E+00	0.00E+00
SN119M	8.42E+00	7.89E+00	6.66E+00	5.16E+00	3.06E+00	4.90E-02	2.80E-04
SN121	7.39E-02	4.66E-08	3.12E-24	0.00E+00	0.00E+00	0.00E+00	0.00E+00
SN121M	5.54E-04	5.53E-04	5.52E-04	5.50E-04	5.46E-04	5.17E-04	4.82E-04
SN123	4.78E-01	4.22E-01	3.06E-01	1.89E-01	6.99E-02	2.75E-05	1.52E-09
SN125	2.20E+00	4.21E-01	5.63E-03	8.71E-06	1.43E-11	0.00E+00	0.00E+00
SB122	1.10E-01	2.99E-04	6.12E-11	5.66E-21	0.00E+00	0.00E+00	0.00E+00
SB124	1.86E-02	1.43E-02	7.16E-03	2.54E-03	3.01E-04	1.49E-11	1.10E-20
SB125	1.67E+00	1.66E+00	1.60E+00	1.50E+00	1.32E+00	4.87E-01	1.39E-01

Nuclide	7 Days	30 Days	90 Days	180 Days	1 Year	5 Years	10 Years
SB126	5.64E-02	1.56E-02	5.45E-04	3.55E-06	1.13E-10	0.00E+00	0.00E+00
TE123M	3.02E-03	2.65E-03	1.87E-03	1.11E-03	3.80E-04	8.02E-08	2.05E-12
TE 125M	3.26E-01	3.40E-01	3.58E-01	3.56E-01	3.22E-01	1.19E-01	3.40E-02
CS131	5.10E-02	2.34E-02	1.17E-03	7.33E-06	1.50E-10	0.00E+00	0.00E+00
BA131	3.68E-02	9.53E-03	2.81E-04	1.43E-06	2.69E-11	0.00E+00	0.00E+00
BA133	7.43E-04	7.40E-04	7.32E-04	7.20E-04	697E-04	5.38E-04	3.90E-04
BA133M	3.65E-05	1.95E-09	1.39E-20	2.26E-37	0.00E+00	0.00E+00	0.00E+00
BA135M	2.77E-04	4.49E-10	3.51E-25	0.00E+00	0.00E+00	0.00E+00	0.00E+00
LA140	3.92E-04	1.86E-07	6.07E-09	4.62E-11	2.02E-15	0.00E+00	0.00E+00
LU177	2.13E-03	1.99E-04	1.57E-06	7.79E-07	3.40E-07	4.95E-10	1.40E-13
HF175	3.25E-02	2.59E-02	1.43E-02	5.86E-03	9.37E-04	4.88E-10	6.84E-18
HF181	8.82E-01	6.06E-01	2.27E-01	5.22E-02	2.52E-03	1.07E-13	1.15E-26
TA182	1.07E+01	9.33E+00	6.50E+00	3.78E+00	1.24E+00	1.85E-04	3.84E-09
TA183	2.54E+01	1.12E+00	3.21E-04	1.56E-09	1.82E-20	0.00E+00	0.00E+00
W181	5.88E-03	5.16E-03	3.66E-03	2.19E-03	7.58E-04	1.78E-07	5.17E-12
W185	2.09E-01	1.69E-01	9.69E-02	4.22E-02	7.64E-03	1.06E-08	5.09E-16
W187	2.68E-02	2.99E-09	2.18E-27	0.00E+00	0.00E+00	0.00E+00	0.00E+00
W188	1.65E-02	1.31E-02	7.22E-03	2.94E-03	4.62E-04	2.12E-10	2.54E-18
RE186	3.18E-02	4.66E-04	7.70E-09	5.16E-16	8.85E-31	0.00E+00	0.00E+00
RE188	1.79E-02	1.33E-02	7.29E-03	2.97E-03	4.67E-04	2.15E-10	2.57E-18
OS191	4.87E-05	1.73E-05	1.16E-06	2.03E-08	4.86E-12	0.00E+00	0.00E+00
TOTAL	1.34E+04	1.28E+04	1.21E+04	1.17E+04	1.12E+04	8.86E+03	6.66E+03

Table 4. Decay Heat in a TPBAR (Watts/TPBAR)

Nuclide	7 Days	30 Days	90 Days	180 Days	1 Year	5 Years	10 Years
H-3[2]	3.90E-01	3.89E-01	3.85E-01	3.80E-01	3.69E-01	2.95E-01	2.23E-01
P 32	1.04E-02	3.42E-03	1.87E-04	2.38E-06	3.06E-10	5.86E-12	5.83E-12
CR 51	2.07E-01	1.17E-01	2.60E-02	2.74E-03	2.66E-05	3.57E-21	5.10E-41
MN 54	2.09E-01	1.98E-01	1.73E-01	1.42E-01	9.42E-02	3.69E-03	6.42E-05
FE 55	7.28E-03	7.15E-03	6.85E-03	6.41E-03	5.60E-03	1.93E-03	5.08E-04
FE 59	1.54E-01	1.08E-01	4.28E-02	1.07E-02	6.16E-04	1.04E-13	6.30E-26
CO 58	1.61E+00	1.29E+00	7.14E-01	2.96E-01	4.82E-02	2.94E-08	5.03E-16
CO 60	5.55E-01	5.50E-01	5.39E-01	5.21E-01	4.88E-01	2.88E-01	1.49E-01
NI 63	2.30E-03	2.30E-03	2.30E-03	2.30E-03	2.29E-03	2.22E-03	2.14E-03
AS 76	7.74E-03	3.76E-09	1.28E-25	0.00E+00	0.00E+00	0.00E+00	0.00E+00
ZR 95	3.33E-01	2.60E-01	1.36E-01	5.11E-02	6.87E-03	9.18E-10	2.35E-18
NB 95	3.32E-01	3.12E-01	2.13E-01	9.53E-02	1.41E-02	1.93E-09	4.93E-18

2 The ORIGEN2 values for H-3 are not reported. The values given for H-3 are based on a maximum of 1.2 g of tritium per TPBAR at discharge, as specified in the Functional Requirements document (Lopez 2003). There is 0.325 W per gram of tritium, and the half-life of tritium is 12.33 years. The value of 1.2 g at discharge is decayed appropriately for the various decay times.

MO 99	5.40E-02	1.64E-04	4.44E-11	6.24E-21	0.00E+00	0.00E+00	0.00E+00
SN117M	1.52E-02	4.88E-03	2.50E-04	2.91E-06	3.03E-10	0.00E+00	0.00E+00
SN119M	4.35E-03	4.08E-03	3.44E-03	2.67E-03	1.58E-03	2.53E-05	1.45E-07
SN125	1.46E-02	2.79E-03	3.73E-05	5.77E-08	9.47E-14	0.00E+00	0.00E+00
SB125	5.23E-03	5.20E-03	5.00E-03	4.70E-03	4.14E-03	1.52E-03	4.35E-04
TA182	9.55E-02	8.31E-02	5.79E-02	3.36E-02	1.10E-02	1.65E-06	3.42E-11
TA183	1.61E-01	7.08E-03	2.03E-06	9.91E-12	1.15E-22	0.00E+00	0.00E+00
Total	4.19E+00	3.35E+00	2.31E+00	1.55E+00	1.05E+00	5.92E-01	3.75E-01

Table 5. Source Term in a TPBAR (Photons/s/TPBAR)

Energy (MeV)	7 Days	30 Days	90 Days	180 Days	1 Year	5 Years	10 Years
1.00E-02	7.73E+12	5.07E+12	2.33E+12	1.14E+12	6.01E+11	3.17E+11	2.28E+11
2.50E-02	6.71E+11	4.15E+11	2.59E+11	1.76E+11	1.03E+11	1.95E+10	7.02E+09
3.75E-02	1.80E+11	1.08E+11	6.65E+10	3.72E+10	1.85E+10	6.83E+09	2.84E+09
5.75E-02	5.80E+11	4.44E+11	2.90E+11	1.60E+11	5.27E+10	4.20E+09	2.15E+09
8.50E-02	1.52E+11	9.81E+10	5.86E+10	2.93E+10	9.11E+09	1.66E+09	8.49E+08
1.25E-01	2.24E+11	1.41E+11	8.80E+10	4.66E+10	1.45E+10	7.08E+08	3.45E+08
2.25E-01	4.52E+11	2.38E+11	1.20E+11	6.46E+10	2.15E+10	1.30E+09	4.20E+08
3.75E-01	3.06E+12	1.73E+12	4.10E+11	6.55E+10	1.94E+10	6.57E+09	1.90E+09
5.75E-01	2.75E+12	2.17E+12	1.21E+12	5.16E+11	1.02E+11	8.36E+09	2.39E+09
8.50E-01	1.56E+13	1.29E+13	7.83E+12	3.77E+12	1.11E+12	2.70E+10	5.28E+08
1.25E+00	3.05E+12	2.96E+12	2.81E+12	2.63E+12	2.38E+12	1.38E+12	7.16E+11
1.75E+00	5.01E+10	3.96E+10	2.20E+10	9.10E+09	1.48E+09	9.09E+02	5.52E+00
2.25E+00	2.12E+09	3.75E+08	3.27E+07	1.84E+07	1.30E+07	7.33E+06	3.80E+06
2.75E+00	7.48E+08	6.48E+04	5.30E+04	4.48E+04	3.88E+04	2.27E+04	1.18E+04
3.50E+00	5.05E+05	1.88E+00	6.13E-02	4.70E-04	3.16E-06	2.87E-06	2.58E-06
5.00E+00	5.21E+03	5.25E-08	6.64E-09	4.23E-09	1.67E-09	1.11E-12	1.93E-15
7.00E+00	6.37E-10	5.81E-10	4.31E-10	2.75E-10	1.09E-10	7.23E-14	1.25E-16
9.50E+00	4.03E-11	3.68E-11	2.72E-11	1.74E-11	6.87E-12	4.57E-15	7.93E-18
TOTAL	3.45E+13	2.63E+13	1.55E+13	8.65E+12	4.44E+12	1.78E+12	9.63E+11

Table 6. Radionuclide Concentrations in a Hold-Down Assembly, no thimble plugs (Ci/HDA) (scaling factor of 0.1 applied)

Isotope	7 Days	30 Days	90 Days	180 Days	1 Year	5 Years	10 Years
H 3	8.61E-07	8.58E-07	8.50E-07	8.39E-07	8.15E-07	6.51E-07	4.92E-07
C 14	3.10E-08	3.10E-08	3.10E-08	3.10E-08	3.10E-08	3.10E-08	3.10E-08
NA 24	1.11E-05	9.27E-17	0.00E+00	0.00E+00	0.00E+00	0.00E+00	0.00E+00
P 32	6.41E-01	2.10E-01	1.15E-02	1.46E-04	1.87E-08	2.15E-10	2.14E-10
P 33	2.92E-05	1.54E-05	2.92E-06	2.41E-07	1.42E-09	3.63E-27	0.00E+00
S 35	1.88E-02	1.57E-02	9.77E-03	4.81E-03	1.12E-03	1.12E-08	6.36E-15
CA 45	4.18E-04	3.79E-04	2.94E-04	2.00E-04	9.11E-05	1.83E-07	7.73E-11
CA 47	1.94E-06	5.77E-08	6.01E-12	6.40E-18	3.25E-30	0.00E+00	0.00E+00
SC 46	5.68E-02	4.69E-02	2.86E-02	1.36E-02	2.93E-03	1.65E-08	4.55E-15
SC 47	2.39E-02	2.05E-04	8.57E-10	3.13E-17	1.24E-29	0.00E+00	0.00E+00
SC 48	6.64E-04	1.07E-07	1.36E-17	1.95E-32	0.00E+00	0.00E+00	0.00E+00
CR 51	5.23E+02	2.94E+02	6.56E+01	6.90E+00	6.71E-02	8.99E-18	1.30E-37

Isotope	7 Days	30 Days	90 Days	180 Days	1 Year	5 Years	10 Years
MN 54	1.96E+01	1.87E+01	1.63E+01	1.34E+01	8.87E+00	3.47E-01	6.04E-03
FE 55	9.65E+01	9.49E+01	9.08E+01	8.50E+01	7.43E+01	2.56E+01	6.74E+00
FE 59	9.09E+00	6.38E+00	2.53E+00	6.33E-01	3.65E-02	6.15E-12	3.73E-24
CO 58	4.10E+01	3.27E+01	1.82E+01	7.53E+00	1.23E+00	7.49E-07	1.28E-14
CO 60	5.41E+01	5.37E+01	5.25E+01	5.09E+01	4.76E+01	2.81E+01	1.46E+01
NI 59	2.56E-02	2.56E-02	2.56E-02	2.56E-02	2.56E-02	2.56E-02	2.56E-02
NI 63	3.48E+00	3.48E+00	3.48E+00	3.47E+00	3.46E+00	3.35E+00	3.23E+00
NI 66	2.31E-05	2.10E-08	2.42E-16	3.00E-28	0.00E+00	0.00E+00	0.00E+00
CU 64	9.68E-04	7.98E-17	0.00E+00	0.00E+00	0.00E+00	0.00E+00	0.00E+00
CU 66	2.32E-05	2.10E-08	2.43E-16	3.01E-28	0.00E+00	0.00E+00	0.00E+00
CU 67	1.03E-06	2.11E-09	2.08E-16	6.40E-27	0.00E+00	0.00E+00	0.00E+00
ZN65	3.18E-03	2.98E-03	2.51E-03	1.95E-03	1.15E-03	1.81E-05	1.01E-07
Y 89M	3.13E-05	2.38E-07	7.10E-13	3.65E-21	0.00E+00	0.00E+00	0.00E+00
Y 90	1.44E-04	3.64E-07	4.92E-11	4.88E-11	4.82E-11	4.38E-11	3.89E-11
ZR 89	3.13E-05	2.39E-07	7.11E-13	3.65E-21	3.36E-38	0.00E+00	0.00E+00
ZR 95	4.18E-04	3.26E-04	1.70E-04	6.41E-05	8.62E-06	1.15E-12	2.95E-21
NB 92	3.04E-02	6.32E-03	1.06E-04	2.27E-07	7.38E-13	0.00E+00	0.00E+00
NB 94	7.76E-04	7.76E-04	7.76E-04	7.76E-04	7.76E-04	7.76E-04	7.76E-04
NB 95	1.38E+00	8.78E-01	2.69E-01	4.57E-02	1.20E-03	2.56E-12	6.54E-21
NB 95M	3.05E-06	2.42E-06	1.26E-06	4.76E-07	6.40E-08	8.55E-15	2.19E-23
NB 96	3.16E-05	2.42E-12	6.60E-31	0.00E+00	0.00E+00	0.00E+00	0.00E+00
MO 93	5.92E-05	5.92E-05	5.92E-05	5.92E-05	5.91E-05	5.91E-05	5.90E-05
MO 99	9.60E-01	2.91E-03	7.87E-10	1.11E-19	0.00E+00	0.00E+00	0.00E+00
TC 99	2.48E-06	2.49E-06	2.49E-06	2.49E-06	2.49E-06	2.49E-06	2.49E-06
RU103	1.83E-04	1.22E-04	4.23E-05	8.64E-06	3.29E-07	2.09E-18	2.12E-32
TOTAL	7.50E+02	5.05E+02	2.50E+02	1.68E+02	1.36E+02	5.74E+01	2.46E+01

Table 7. Decay Heat in a Hold-Down Assembly, no thimble plugs (Watts/HDA)
(scaling factor of 0.1 applied)

Isotope	7 Days	30 Days	90 Days	180 Days	1 Year	5 Years	10 Years
P 32	6.50E-03	2.13E-03	1.16E-04	1.48E-06	1.89E-10	2.18E-12	2.17E-12
CR 51	1.12E-01	6.31E-02	1.41E-02	1.48E-03	1.44E-05	1.93E-21	2.78E-41
MN 54	9.77E-02	9.28E-02	8.13E-02	6.66E-02	4.41E-02	1.73E-03	3.01E-05
FE 55	3.26E-03	3.21E-03	3.07E-03	2.87E-03	2.51E-03	8.64E-04	2.28E-04
FE 59	7.04E-02	4.94E-02	1.96E-02	4.90E-03	2.83E-04	4.76E-14	2.89E-26
CO 58	2.45E-01	1.96E-01	1.09E-01	4.50E-02	7.34E-03	4.48E-09	7.65E-17
CO 60	8.35E-01	8.28E-01	8.10E-01	7.84E-01	7.34E-01	4.34E-01	2.25E-01
NI 63	3.51E-04	3.51E-04	3.50E-04	3.50E-04	3.48E-04	3.38E-04	3.25E-04
NB 95	6.63E-03	4.21E-03	1.29E-03	2.19E-04	5.76E-06	1.23E-14	3.14E-23
MO 99	3.08E-03	9.35E-06	2.53E-12	3.56E-22	0.00E+00	0.00E+00	0.00E+00
TOTAL	1.38E+00	1.24E+00	1.04E+00	9.06E-01	7.88E-01	4.36E-01	2.25E-01

Table 8. Source Term for Hold-Down Assembly, no thimble plugs (Photons/s/HDA) (scaling factor of 0.1 applied)

Energy (MeV)	7 Days	30 Days	90 Days	180 Days	1 Year	5 Years	10 Years
1.00E-02	2.76E+12	1.71E+12	6.17E+11	2.62E+11	1.50E+11	5.76E+10	2.93E+10
2.50E-02	4.42E+10	3.60E+10	2.69E+10	2.08E+10	1.67E+10	9.57E+09	4.98E+09
3.75E-02	2.73E+10	2.18E+10	1.60E+10	1.21E+10	9.57E+09	5.45E+09	2.83E+09
5.75E-02	3.48E+10	2.77E+10	1.97E+10	1.44E+10	1.09E+10	6.14E+09	3.18E+09
8.50E-02	1.80E+10	1.39E+10	9.34E+09	6.30E+09	4.39E+09	2.41E+09	1.25E+09
1.25E-01	1.21E+10	7.62E+09	4.79E+09	2.91E+09	1.77E+09	9.27E+08	4.80E+08
2.25E-01	1.31E+10	7.87E+09	4.41E+09	2.12E+09	7.69E+08	3.05E+08	1.58E+08
3.75E-01	1.62E+12	9.13E+11	2.04E+11	2.21E+10	4.49E+08	8.55E+07	4.43E+07
5.75E-01	4.05E+11	3.23E+11	1.80E+11	7.44E+10	1.21E+10	4.93E+06	2.54E+06
8.50E-01	2.21E+12	1.86E+12	1.25E+12	7.54E+11	3.66E+11	1.27E+10	3.13E+08
1.25E+00	4.01E+12	3.97E+12	3.89E+12	3.76E+12	3.52E+12	2.08E+12	1.08E+12
1.75E+00	7.50E+09	5.99E+09	3.33E+09	1.38E+09	2.25E+08	1.37E+02	2.00E-04
2.25E+00	2.12E+07	2.11E+07	2.06E+07	1.99E+07	1.87E+07	1.10E+07	5.71E+06
2.75E+00	4.76E+05	6.51E+04	6.37E+04	6.17E+04	5.77E+04	3.41E+04	1.77E+04
3.50E+00	2.81E+02	4.06E-09	1.53E-09	1.29E-09	9.14E-10	6.44E-11	7.67E-12
5.00E+00	2.92E+00	2.44E-11	0.00E+00	0.00E+00	0.00E+00	0.00E+00	0.00E+00
7.00E+00	0.00E+00	0.00E+00	0.00E+00	0.00E+00	0.00E+00	0.00E+00	0.00E+00
9.50E+00	0.00E+00	0.00E+00	0.00E+00	0.00E+00	0.00E+00	0.00E+00	0.00E+00
TOTAL	1.12E+13	8.91E+12	6.22E+12	4.94E+12	4.09E+12	2.18E+12	1.12E+12

Table 9. Radionuclide Concentrations for Single Thimble Plug (Ci/thimble plug) (scaling factor of 0.2 and mass of 150g applied)

Isotope	7 Days	30 Days	90 Days	180 Days	1 Year	5 Years	10 Years
H 3	9.18E-08	9.15E-08	9.07E-08	8.94E-08	8.69E-08	6.94E-08	5.24E-08
C 14	3.31E-09	3.31E-09	3.31E-09	3.31E-09	3.31E-09	3.31E-09	3.31E-09
P 32	7.69E-02	2.52E-02	1.38E-03	1.75E-05	2.23E-09	2.53E-11	2.51E-11
P 33	3.41E-06	1.80E-06	3.41E-07	2.81E-08	1.65E-10	4.23E-28	0.00E+00
S 35	2.19E-03	1.83E-03	1.14E-03	5.60E-04	1.30E-04	1.31E-09	7.41E-16
SC 47	3.40E-07	2.93E-09	1.34E-14	1.73E-21	8.28E-34	0.00E+00	0.00E+00
SC 48	1.11E-07	1.78E-11	2.26E-21	3.01E-36	0.00E+00	0.00E+00	0.00E+00
CR 51	5.69E+01	3.20E+01	7.13E+00	7.50E-01	7.29E-03	9.77E-19	0.00E+00
MN 54	2.35E+00	2.24E+00	1.96E+00	1.60E+00	1.06E+00	4.16E-02	7.25E-04
FE 55	1.15E+01	1.13E+01	1.08E+01	1.01E+01	8.82E+00	3.04E+00	8.01E-01
FE 59	1.09E+00	7.61E-01	3.02E-01	7.55E-02	4.36E-03	7.34E-13	4.46E-25
CO 58	2.65E+00	2.12E+00	1.18E+00	4.87E-01	7.94E-02	4.85E-08	8.28E-16
CO 60	1.69E+00	1.68E+00	1.64E+00	1.59E+00	1.49E+00	8.79E-01	4.55E-01
NI 59	1.65E-03	1.65E-03	1.65E-03	1.65E-03	1.65E-03	1.65E-03	1.65E-03
NI 63	2.25E-01	2.25E-01	2.25E-01	2.24E-01	2.24E-01	2.17E-01	2.09E-01
NI 66	1.49E-06	1.35E-09	1.56E-17	1.94E-29	0.00E+00	0.00E+00	0.00E+00

Isotope	7 Days	30 Days	90 Days	180 Days	1 Year	5 Years	10 Years
CU 64	1.45E-07	1.20E-20	0.00E+00	0.00E+00	0.00E+00	0.00E+00	0.00E+00
CU 66	1.50E-06	1.36E-09	1.57E-17	1.94E-29	0.00E+00	0.00E+00	0.00E+00
ZN 65	1.01E-07	9.44E-08	7.96E-08	6.16E-08	3.64E-08	5.72E-10	3.19E-12
Y 89M	3.83E-06	2.92E-08	8.69E-14	4.47E-22	0.00E+00	0.00E+00	0.00E+00
Y 90	9.39E-07	2.38E-09	1.21E-12	1.21E-12	1.19E-12	1.08E-12	9.61E-13
ZR 89	3.84E-06	2.92E-08	8.70E-14	4.47E-22	0.00E+00	0.00E+00	0.00E+00
ZR 95	5.12E-05	3.99E-05	2.08E-05	7.85E-06	1.06E-06	1.41E-13	3.61E-22
NB 92	2.16E-03	4.49E-04	7.49E-06	1.62E-08	5.25E-14	0.00E+00	0.00E+00
NB 94	5.04E-06	5.04E-06	5.04E-06	5.04E-06	5.04E-06	5.04E-06	5.04E-06
NB 95	9.08E-03	5.78E-03	1.79E-03	3.13E-04	1.00E-05	3.13E-13	8.01E-22
NB 95M	3.74E-07	2.96E-07	1.55E-07	5.83E-08	7.83E-09	1.05E-15	2.68E-24
NB 96	1.02E-06	7.79E-14	2.12E-32	0.00E+00	0.00E+00	0.00E+00	0.00E+00
MO 93	7.25E-06	7.25E-06	7.25E-06	7.25E-06	7.24E-06	7.24E-06	7.23E-06
MO 99	1.18E-01	3.57E-04	9.65E-11	1.36E-20	0.00E+00	0.00E+00	0.00E+00
TC 99	3.04E-07	3.05E-07	3.05E-07	3.05E-07	3.05E-07	3.05E-07	3.05E-07
RU103	2.24E-05	1.49E-05	5.18E-06	1.06E-06	4.03E-08	2.57E-19	2.60E-33
TOTAL	7.65E+01	5.03E+01	2.32E+01	1.48E+01	1.17E+01	4.18E+00	1.47E+00

Table 10. Decay Heat in a Single Thimble Plug (Watts/thimble plug)
(scaling factor of 0.2 and mass of 150g applied)

Isotope	7 Days	30 Days	90 Days	180 Days	1 Year	5 Years	10 Years
P 32	7.79E-04	2.56E-04	1.39E-05	1.78E-07	2.26E-11	2.56E-13	2.55E-13
CR 51	1.22E-02	6.86E-03	1.53E-03	1.61E-04	1.56E-06	2.10E-22	0.00E+00
MN 54	1.17E-02	1.11E-02	9.75E-03	7.99E-03	5.30E-03	2.07E-04	3.61E-06
FE 55	3.87E-04	3.81E-04	3.65E-04	3.41E-04	2.98E-04	1.03E-04	2.71E-05
FE 59	8.40E-03	5.90E-03	2.34E-03	5.85E-04	3.37E-05	5.68E-15	3.45E-27
CO 58	1.59E-02	1.27E-02	7.04E-03	2.91E-03	4.75E-04	2.90E-10	4.95E-18
CO 60	2.61E-02	2.59E-02	2.53E-02	2.45E-02	2.29E-02	1.36E-02	7.02E-03
NI 63	2.27E-05	2.27E-05	2.27E-05	2.26E-05	2.25E-05	2.19E-05	2.11E-05
MO 99	3.77E-04	1.15E-06	3.10E-13	4.36E-23	0.00E+00	0.00E+00	0.00E+00
TOTAL	7.59E-02	6.31E-02	4.64E-02	3.65E-02	2.91E-02	1.39E-02	7.07E-03

Table 11. Source Term for a Single Thimble Plug (Photons/s/thimble plug)
(scaling factor of 0.5 and mass of 150g applied)

Energy (Mev)	7 Days	30 Days	90 Days	180 Days	1 Year	5 Years	10 Years
1.00E-02	6.95E+11	4.18E+11	1.34E+11	4.68E+10	2.27E+10	4.95E+09	2.35E+09
2.50E-02	6.68E+09	4.76E+09	3.01E+09	1.96E+09	1.36E+09	7.52E+08	3.92E+08
3.75E-02	4.25E+09	2.93E+09	1.83E+09	1.16E+09	7.80E+08	4.27E+08	2.22E+08
5.75E-02	5.49E+09	3.85E+09	2.34E+09	1.42E+09	8.96E+08	4.80E+08	2.49E+08
8.50E-02	2.97E+09	2.03E+09	1.18E+09	6.66E+08	3.69E+08	1.89E+08	9.77E+07
1.25E-01	2.36E+09	1.17E+09	6.53E+08	3.36E+08	1.55E+08	7.24E+07	3.75E+07

Energy (Mev)	7 Days	30 Days	90 Days	180 Days	1 Year	5 Years	10 Years
2.25E-01	2.53E+09	1.30E+09	6.81E+08	3.00E+08	8.15E+07	2.38E+07	1.23E+07
3.75E-01	4.40E+11	2.48E+11	5.54E+10	5.91E+09	8.33E+07	6.68E+06	3.46E+06
5.75E-01	6.56E+10	5.23E+10	2.90E+10	1.20E+10	1.96E+09	3.85E+05	1.99E+05
8.50E-01	4.50E+11	3.91E+11	2.82E+11	1.89E+11	1.04E+11	3.79E+09	6.98E+07
1.25E+00	3.13E+11	3.11E+11	3.04E+11	2.94E+11	2.75E+11	1.63E+11	8.42E+10
1.75E+00	1.21E+09	9.69E+08	5.38E+08	2.23E+08	3.63E+07	2.22E+01	1.32E-05
2.25E+00	1.66E+06	1.65E+06	1.61E+06	1.56E+06	1.46E+06	8.62E+05	4.46E+05
2.75E+00	5.13E+03	5.09E+03	4.98E+03	4.82E+03	4.51E+03	2.67E+03	1.38E+03
3.50E+00	1.32E-05	5.11E-10	4.56E-10	3.86E-10	2.75E-10	1.75E-11	5.16E-13
5.00E+00	1.38E-07	1.15E-18	0.00E+00	0.00E+00	0.00E+00	0.00E+00	0.00E+00
7.00E+00	0.00E+00	0.00E+00	0.00E+00	0.00E+00	0.00E+00	0.00E+00	0.00E+00
9.50E+00	0.00E+00	0.00E+00	0.00E+00	0.00E+00	0.00E+00	0.00E+00	0.00E+00
TOTAL	1.99E+12	1.44E+12	8.14E+11	5.54E+11	4.07E+11	1.73E+11	8.77E+10

Table 12. Dose Rates for the TPBAR (rem/hr)[3]

	7 days	90 days	180 days	1 year	5 years
Surface, Entire Length	77, 000	42,000	25,000	14,000	6200
1m from TPBAR, Entire Length	160	86	52	29	13
1m from TPBAR, lm In Center (average)	180	97	59	33	14

Table 13. Surface Dose Rates for the Hold-Down Assembly (rem/hr) (including 20 thimble plugs)[3]

	7 days	90 days	180 days	1 year	5 years
Top of Assembly	51,000	38,000	32,000	27,000	15,000
Bottom of Assembly	34,000	22,000	18,000	14,000	6800
Side of Assembly	28,000	19,000	16,000	13,000	6400

4.0 REFERENCES

ASTM A 213-95. *Standard Specification for Seamless Ferritic and Austenitic Alloy-Steel Boiler, Superheater, and Heat-Exchanger Tubes*. American National Standards Institute.

Battat ME. 1977. *American National Standard Neutron and Gamma-Ray Flux-to-Dose Rate Factors*. ANSI/ANS-6.1.1-1977 (N666). American Nuclear Society, LaGrange Park, Illinois.

3 The dose rates are rounded to two significant figures. The MCNP statistical uncertainty in the results is less than 1%.

Gates RO. 2001. *Production Specification for Enriched, Annular $LiAlO_2$ Pellets.* TTQP-1-076, Rev. 4. Pacific Northwest National Laboratory, Richland, Washington.

Guenther, RJ, DE Blanik, TK Campbell, UP Jenquin, JE Mendel, LE Thomas, and CK Thornhill. 1988. *Characterization of Spent Fuel Approved Testing Material – ATM-103.* PNL-5109-103. Pacific Northwest Laboratory, Richland, Washington.

Livingston JV. 2001. *Materials Properties Handbook for the Tritium Target Qualification Project.* TTQP-7-008, Rev. 3. Pacific Northwest National Laboratory, Richland, Washington.

Lopez Jr. A. 2002. *Production TPBAR Design Inputs for Sequoyah Units 1 and 2 (U).* TTQP-1-118, Rev. 7. Pacific Northwest National Laboratory, Richland, Washington.

Lopez Jr. A. 2003. *Production TPBAR Design Inputs for Watts Bar (U).* PNNL-TTQP-1-702, Rev. 9. Pacific Northwest National Laboratory, Richland, Washington.

Love EF. 2003. *Homogenization of the Production and Full-Length Getter TPBARs (U).* PNNL-TTQP-1-718, Rev. 4. Pacific Northwest National Laboratory, Richland, Washington. (CRD)

Luksic AT. 1989. *Spent Fuel Assembly Hardware: Characterization and 10 CFR 61 Classification with Calculation for Spent Fuel Assembly Hardware.* PNL-6906. Pacific Northwest Laboratory, Richland, Washington.

Migliore RJ, BD Reid, SK Fadeff, KA Pauley, and UP Jenquin. 1994. *Non-Fuel Assembly Components: 10 CFR 61.55 Classification for Waste Disposal.* PNL-10103. Pacific Northwest Laboratory. Richland, Washington.

Migliore RJ. 1998a. *Waste Classification for the Mark 2 TPBAR.* TTQP-1-2011, Rev. 0. Pacific Northwest Laboratory. Richland, Washington.

Migliore RJ. 1998b. *Source Term and Dose Rates for the LTA Hold-Down Assembly.* TTQP-1-084, Rev. 1. Pacific Northwest National Laboratory, Richland, Washington.

Migliore RJ. 1998c. *TPBAR Source Term, Radionuclide Concentrations, and Decay Heat.* TTQP-1-050, Rev. 2. Pacific Northwest National Laboratory, Richland, Washington.

Migliore RJ. 2000. *Bending Limits for Watts Bar Production TPBAR (U).* PNNL-TTQP-1-707, Rev. 3. Pacific Northwest National Laboratory, Richland, Washington. (CRD).

Migliore RJ, and UP Jenquin. 1998. *Bounding TPBAR Source Term, Radionuclide Concentrations, and Decay Heat.* TTQP-1-2012, Rev. 1. Pacific Northwest National Laboratory, Richland, Washington.

Pagh RT. 2003. *Bounding Source Term, Radionuclide Concentrations, Decay Heat, and Dose Rates for Production TPBAR (U).* PNNL-TTQP-1-726, Rev. 3. Pacific Northwest National Laboratory, Richland, Washington. (CRD).

RSIC Computer Code Collection. 1996. *ORIGEN2.1: Isotope Generation and Depletion Code - Matrix Exponential Method.* CCC-371, Oak Ridge National Laboratory, Oak Ridge, Tennessee.

RSICC Computer Code Collection. 2000. *MCNP4C – Monte Carlo N-Particle Transport Code System.* CCC-700. Oak Ridge National Laboratory, Oak Ridge, Tennessee.

RSICC Computer Code Collection. 2002. *ORIGEN2.2: Isotope Generation and Depletion Code - Matrix Exponential Method.* CCC-371, Oak Ridge National Laboratory, Oak Ridge, Tennessee.

Special Metals. 2003. http://www.magellanmetals.com/inconel_X750.htm

Walker FW, JR Parrington, and F Feiner. 1989. *Chart of the Nuclides 14th Edition.* General Electric Co., San Jose, California.

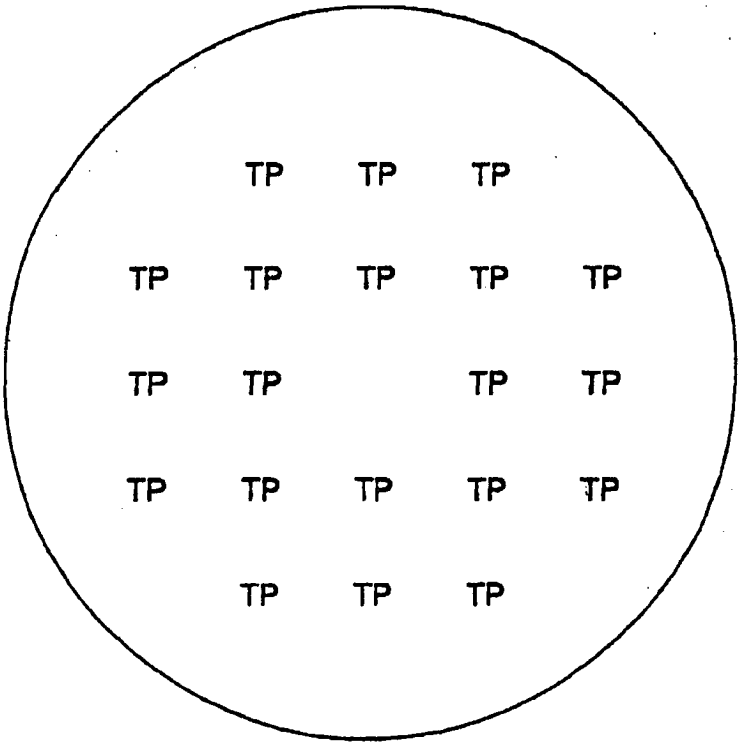

Figure 1. Assumed Hold-Down Assembly Thimble Plug (TP) Loading Pattern

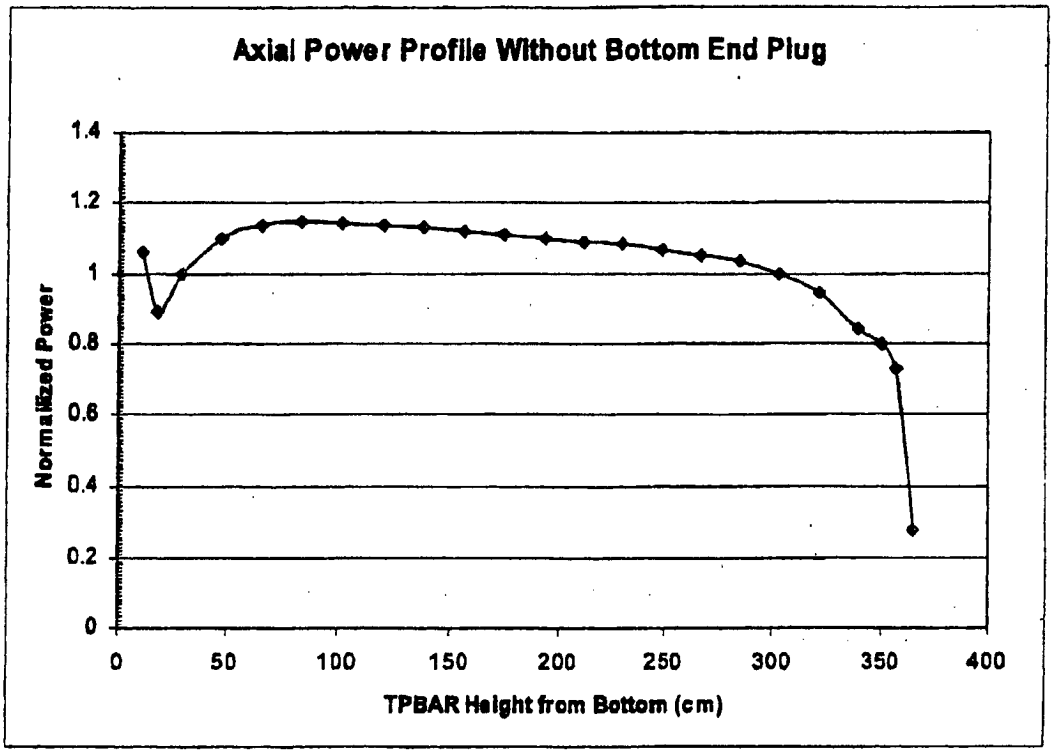

Figure 2. Axial Power Profile without Bottom End Plug

APPENDIX A

TPBAR Constituents

Masses for the elements present in a TPBAR were obtained from various sources as referenced on pages 20-22. All material in the TPBAR was accounted for including the aluminide barrier and the nickel plating on the getters. The bounding masses derived here are for radiological source assessment and not mechanical analysis or radiological shielding (self-shielding) analysis. Bounding mechanical and shielding masses are 2.3 lbs. from Lopez (2002) for the Sequoyah Units and Lopez (2003) for Watts Bar.

Compositions of the Zircaloy and SS-316 were taken from Livingston (2001).

Composition of the pellet was taken from Gates (2001).

Composition of the Inconel was taken from Special Metals (2003).

Composition of the SS-304 was taken primarily from ASTM A 213. Because this ASTM standard does not contain values for cobalt, niobium, and molybdenum, the weight percent of cobalt was assumed, while the weight percent of the molybdenum and niobium were taken from Migliore (1998b).

Table A-1. Data for Developing the TPBAR Constituents

Parameter	Value	Reference
Mass of hold-down assembly (SS304)	5.29 lb	PNNL-TTQP-1-702 R9
Mass of inconel in HDA	0.5 lb	PNNL-TTQP-1-702 R9
Mass of thimble plug (SS304)	0.3 lb	PNNL-TTQP-1-702 R9
Atomic Weight of Ni	58.69 g/mole	Chart of the Nuclides
Atomic Weight of Li-6	6.015 g/mole	Chart of the Nuclides
Atomic Weight of Li-7	7.016 g/mole	Chart of the Nuclides
Atomic Weight Al	26.9815 g/mole	Chart of the Nuclides
Atomic Weight of O	15.9994 g/mole	Chart of the Nuclides
Avogrado's No.	6.022E+23 a/mole	Chart of the Nuclides
Li Nominal Enrichment	33.7% atom%	PNNL-TTQP-1-702 R9
Assumptions		
Assumed Mass of Stainless Steel (total)	565 g	PNNL-TTQP-1-726 R3
Assumed Mass Zircaloy-4	215 g	PNNL-TTQP-1-726 R3
Assumed Mass LiA1O2	210 g	PNNL-TTQP-1-726 R3
Assumed Mass of Nickel Plating	255 g	PNNL-TTQP-1-726 R3
Cobalt Concentration	500 ppm	For SS-304
Add the pellet impurities to the given pellet mass. The resulting mass will be larger than the value given above, bringing the total to 217g.		
Fe+Cr+Ni impurity in the pellet is split equally.		
U in the Zircaloy-4 and F, Cl, I, & Br in the pellet have a negligible contribution and will not be included in the ORIGEN2 model.		
Calculated Values		
Mass of hold-down assembly (SS304)	2815 g	Bounding Value
Mass of inconel in HDA	365 g	Bounding Value
Mass of thimble plug (SS304)	150 g	Bounding Value
Atomic Weight of Enriched Li	6.679 g/mole	
Molecular Weight of LiA1O2	65.66 g/mole	
Mass of Li-6	6.48 g	
Mass of Li-7	14.88 g	
Mass of Al	86.30 g	
Mass of O	102.34 g	

Table A-2. Material Impurities, wt%

Element	Zircaloy-4	316-SS	Pellet	304-SS	Inconel X
	TTQP-7-008 R3	TTQP-7-008 R3	TTQP-1-076 R4	ASTM A 213	Special Metals
Fe	0.24	Remainder		Remainder	9.0
Cr	0.13	18.0		20	17.0
Ni	0.0070	14.0		11	Remainder
Zr	Remainder				
Fe+Cr+Ni			0.6		
F+Cl+I+Br			0.06		
Al	0.0075	0.05			1.0
As		0.03	0.05		
B	0.00005	0.002			
Ba			0.08		
C	0.027	0.06	0.15	0.08	0.08
Ca			0.4		
Cd	0.00005				
Co	0.0020	0.050		0.05[4]	1.0
Cu	0.0050	0.04			0.5
H	0.0025				
Hf	0.010				
K			0.5		
Mg	0.0020		0.2		
Mn	0.0050	2.00		2	1.0
Mo	0.0050	3.00		0.3965	
N	0.0080	0.01			
Na			0.5		
Nb		0.05		0.01[5]	1.2
P		0.04		0.04	
Pb			0.04		
S		0.01		0.03	0.01
Se			0.035		
Si	0.0120	0.75	1.0	0.75	0.5
Sn	1.70				
Ta		0.02			
Ti	0.0050				2.75
V		0.05			
W	0.010				
Zr					
U	0.00035				
Total	2.18	38.16	3.62	34.36	34.04
Calculated Numbers, wt%					
Fe		61.84		65.64	
Zr	97.82				
Ni					65.96

4 Assumed.
5 From Migliore 1998b

Table A-3. Nuclide Mass Values, g

							pounds	g
					SS in holddown		5.401	2450
ORIGEN2 Mass Input					Inconel in holddown		0.805	365
Mass(g) =		215.0	565.0	210.0		1.0	1.0	
Nuclide	ORIGEN2 ID	Zircaloy-4	316-SS	Pellet	TPBAR (with Ni)	304-SS	Inconel X	HDA
Li-6	30060			6.48E+00	6.48E+00			
Li-7	30070			1.49E+01	1.49E+01			
Fe	260000	5.16E-01	3.49E+02	4.20E-01	3.50E+02	6.56E-01	9.00E-02	1.64E+03
Cr	240000	2.80E-01	1.02E+02	4.20E-01	1.02E+02	2.00E-01	1.70E-01	5.52E+02
Ni[6]	280000	1.51E-02	7.91E+01	4.20E-01	3.35E+02	1.10E-01	6.60E-01	5.10E+02
O	80000			1.02E+02	1.02E+02			
Al	130000	1.61E-02	2.83E-01	8.63E+01	8.66E+01		1.00E-02	3.65E+00
As	330000		1.70E-01	1.05E-01	2.75E-01			
B	50000	1.08E-04	1.13E-02		1.14E-02			
Ba	560000			1.68E-01	1.68E-01			
C	60000	5.81E-02	3.39E-01	3.15E-01	7.12E-01	8.00E-04	8.00E-04	2.25E+00
Ca	200000			8.40E-01	8.40E-01			
Cd	480000	1.08E-04			1.08E-04			
Co	270000	4.30E-03	2.83E-01		2.87E-01	5.00E-04	1.00E-02	4.88E+00
Cu	290000	1.08E-02	2.26E-01		2.37E-01		5.00E-03	1.83E+00
H	10000	5.38E-03			5.38E-03			
Hf	720000	2.15E-02			2.15E-02			
K	190000			1.05E+00	1.05E+00			
Mg	120000	4.30E-03		4.20E-01	4.24E-01			
Mn	250000	1.08E-02	1.13E+01		1.13E+01	2.00E-02	1.00E-02	5.27E+01
Mo	420000	1.08E-02	1.70E+01		1.70E+01	3.96E-03		9.70E+00
N	70000	1.72E-02	5.65E-02		7.37E-02			
Na	110000			1.05E+00	1.05E+00			
Nb	410000		2.83E-01		2.83E-01	1.00E-04	1.20E-02	4.63E+00
P	150000		2.26E-01		2.26E-01	4.00E-04		9.80E-01
Pb	820000			8.40E-02	8.40E-02			
S	160000		5.65E-02		5.65E-02	3.00E-04	1.00E-04	7.72E-01
Se	340000			7.35E-02	7.35E-02			
Si	140000	2.58E-02	4.24E+00	2.10E+00	6.36E+00	7.50E-03	5.00E-03	2.02E+01
Sn	500000	3.66E+00			3.66E+00			
Ta	730000		1.13E-01		1.13E-01			
Ti	220000	1.08E-02			1.08E-02		2.75E-02	1.00E+01
V	230000		2.83E-01		2.83E-01			
W	740000	2.15E-02			2.15E-02			
Zr	400000	2.10E+02			2.10E+02			
U	920000	7.53E-04			7.53E-04			
Total		2.15E+02	5.65E+02	2.17E+02	1.25E+03	1.00E+00	1.00E+00	2.82E+03

6 The total value for nickel in column 6 includes the assumed 255g of nickel plating.

APPENDIX B

ORIGEN2 Input and Output

The ORIGEN2 input files are listed on the following pages. They are:

- TPBAR.INP- One TPBAR
- HDA.INP- One hold-down assembly (no thimble plugs)
- SS304.INP-One gram of SS304 (thimble plug)

The PWRU library was used for the calculations because its enrichment (3.1%) most closely matches the assumed assembly enrichment (3.0%).

ORIGEN2 was executed on a Dell OptiPlex Gx1 Pentium-II with Windows 98, which has been approved for Commercial Nuclear Related calculations.

TPBAR.INP

```
-1
-1
-1
TIT     Prod.  Reactor Target Rod Waste Eval.:  TPBAR
RDA     PD = 58.24 MW/MTU   E = 3.0
BAS     1 TPBAR
LIB     0 1 2 3 204 205 206 9 3 0 1 1
PHO     101 102 103 10
LIP     0 0 0
INP     1 1 -1 -1 1 1
BUP
IRP      50.  58.24    1  2  4  2
IRP     100.  58.24    2  3  4  0
IRP     150.  58.24    3  4  4  0
IRP     200.  58.24    4  5  4  0
IRP     250.  58.24    5  6  4  0
IRP     300.  58.24    6  7  4  0
IRP     350.  58.24    7  8  4  0
IRP     400.  58.24    8  9  4  0
IRP     450.  58.24    9 10  4  0
IRP     500.  58.24   10 11  4  0
IRP     510.  58.24   11  1  4  0
BUP
DEC      7.            1  2  4  2
DEC     30.            2  3  4  0
DEC     90.            3  4  4  0
DEC    180.            4  5  4  0
DEC      1.            5  6  5  0
DEC      5.            6  7  5  0
DEC     10.            7  8  5  0
HED    1   Discharge
HED    2    7 Days
HED    3   30 Days
HED    4   90 Days
HED    5  180 Days
HED    6    1 Year
HED    7    5 Years
HED    8   10 Years
OPTL   8 8 8 8 7 8 7 8 7 8 8 8 8 8 8 8 8 8 8 8 8 8 8 8 8
OPTA   8 8 8 8 7 8 8 8 8 8 8 8 8 8 8 8 8 8 8 8 8 8 8 8 8
OPTF   8 8 8 8 8 8 8 8 8 8 8 8 8 8 8 8 8 8 8 8 8 8 8 8 8
CUT    7 1.0E-9 -1
OUT    8  1  0  -1
STP    4
1       30060 6.48E+00    30070 1.49E+01        0      0.0
2      922350  30000.0   922380 970000.0        0      0.0
4      260000 3.50E+02   240000 1.02E+02   280000 3.35E+02    80000 1.02E+02
4      130000 8.66E+01   330000 2.75E-01    50000 1.14E-02   560000 1.68E-01
4       60000 7.12E-01   200000 8.40E-01   480000 1.08E-04   270000 2.87E-01
4      290000 2.37E-01    10000 5.38E-03   720000 2.15E-02   190000 1.05E+00
4      120000 4.24E-01   250000 1.13E+01   420000 1.70E+01    70000 7.37E-02
4      110000 1.05E+00   410000 2.83E-01   150000 2.26E-01   820000 8.40E-02
4      160000 5.65E-02   340000 7.35E-02   140000 6.36E+00   500000 3.66E+00
```

```
4       730000 1.13E-01   220000 1.08E-02   230000 2.83E-01   740000 2.15E-02
4       400000 2.10E+02        0      0.0
0
END
```

HDA.INP

```
-1
-1
-1
TIT     Prod.  Reactor Target Rod Waste Eval.:  HDA
RDA     PD = 58.24 MW/MTU   E = 3.0
BAS     1 hold-down assembly, no thimble plugs
LIB     0 1 2 3 204 205 206 9 3 0 1 1
PHO     101 102 103 10
LIP     0 0 0
INP     1 1 -1 -1 1 1
BUP
IRP      50.  58.24    1  2  4  2
IRP     100.  58.24    2  3  4  0
IRP     150.  58.24    3  4  4  0
IRP     200.  58.24    4  5  4  0
IRP     250.  58.24    5  6  4  0
IRP     300.  58.24    6  7  4  0
IRP     350.  58.24    7  8  4  0
IRP     400.  58.24    8  9  4  0
IRP     450.  58.24    9 10  4  0
IRP     500.  58.24   10 11  4  0
IRP     510.  58.24   11  1  4  0
BUP
DEC       7.           1  2  4  2
DEC      30.           2  3  4  0
DEC      90.           3  4  4  0
DEC     180.           4  5  4  0
DEC       1.           5  6  5  0
DEC       5.           6  7  5  0
DEC      10.           7  8  5  0
HED     1   Discharge
HED     2    7 Days
HED     3   30 Days
HED     4   90 Days
HED     5  180 Days
HED     6    1 Year
HED     7    5 Years
HED     8   10 Years
OPTL    8 8 8 8 7 8 7 8 7 8 8 8 8 8 8 8 8 8 8 8 8 8 8 8
OPTA    8 8 8 8 7 8 8 8 8 8 8 8 8 8 8 8 8 8 8 8 8 8 8 8
OPTF    8 8 8 8 8 8 8 8 8 8 8 8 8 8 8 8 8 8 8 8 8 8 8 8
CUT     7 1.0E-9 -1
OUT     8  1  0  -1
STP     4
1        30060 0.00E+00    30070 0.00E+00        0      0.0
2       922350  30000.0   922380 970000.0        0      0.0
4       260000 1.64E+03   240000 5.52E+02   280000 5.10E+02    80000 0.00E+00
```

```
4        130000 3.65E+00   330000 0.00E+00    50000 0.00E+00   560000 0.00E+00
4         60000 2.25E+00   200000 0.00E+00   480000 0.00E+00   270000 4.88E+00
4        290000 1.83E+00    10000 0.00E+00   720000 0.00E+00   190000 0.00E+00
4        120000 0.00E+00   250000 5.27E+01   420000 9.70E+00    70000 0.00E+00
4        110000 0.00E+00   410000 4.63E+00   150000 9.80E-01   820000 0.00E+00
4        160000 7.72E-01   340000 0.00E+00   140000 2.02E+01   500000 0.00E+00
4        730000 0.00E+00   220000 1.00E+01   230000 0.00E+00   740000 0.00E+00
4        400000 0.00E+00        0      0.0
0
END
```

SS304.INP

```
-1
-1
-1
TIT     Prod.  Reactor Target Rod Waste Eval.:  ss304
RDA     PD = 58.24 MW/MTU   E = 3.0
BAS     1g of ss304
LIB     0 1 2 3 204 205 206 9 3 0 1 1
PHO     101 102 103 10
LIP     0 0 0
INP     1 1 -1 -1 1 1
BUP
IRP      50.   58.24     1  2  4  2
IRP     100.   58.24     2  3  4  0
IRP     150.   58.24     3  4  4  0
IRP     200.   58.24     4  5  4  0
IRP     250.   58.24     5  6  4  0
IRP     300.   58.24     6  7  4  0
IRP     350.   58.24     7  8  4  0
IRP     400.   58.24     8  9  4  0
IRP     450.   58.24     9 10  4  0
IRP     500.   58.24    10 11  4  0
IRP     510    58.24    11  1  4  0
BUP
DEC       7.             1  2  4  2
DEC      30.             2  3  4  0
DEC      90.             3  4  4  0
DEC     180.             4  5  4  0
DEC       1.             5  6  5  0
DEC       5.             6  7  5  0
DEC      10.             7  8  5  0
HED     1   Discharge
HED     2    7 Days
HED     3   30 Days
HED     4   90 Days
HED     5  180 Days
HED     6    1 Year
HED     7    5 Years
HED     8   10 Years
OPTL    8 8 8 8 7 8 7 8 7 8 8 8 8 8 8 8 8 8 8 8 8 8 8 8
OPTA    8 8 8 8 7 8 8 8 8 8 8 8 8 8 8 8 8 8 8 8 8 8 8 8
```

```
OPTF     8 8 8 8 8 8 8 8 8 8 8 8 8 8 8 8 8 8 8 8 8 8 8 8
CUT      7 1.0E-9 -1
OUT      8  1  0  -1
STP      4
1         30060 0.00E+00    30070 0.00E+00        0      0.0
2        922350  30000.0   922380 970000.0        0      0.0
4        260000 6.56E-01   240000 2.00E-01   280000 1.10E-01    80000 0.00E+00
4        130000 0.00E+00   330000 0.00E+00    50000 0.00E+00   560000 0.00E+00
4         60000 8.00E-04   200000 0.00E+00   480000 0.00E+00   270000 5.00E-04
4        290000 0.00E+00    10000 0.00E+00   720000 0.00E+00   190000 0.00E+00
4        120000 0.00E+00   250000 2.00E-02   420000 3.96E-03    70000 0.00E+00
4        110000 0.00E+00   410000 1.00E-04   150000 4.00E-04   820000 0.00E+00
4        160000 3.00E-04   340000 0.00E+00   140000 7.50E-03   500000 0.00E+00
4        730000 0.00E+00   220000 0.00E+00   230000 0.00E+00   740000 0.00E+00
4        400000 0.00E+00      0.0         0
0
END
```

APPENDIX C

MCNP Input

The MCNP input files are:

TPBAR7.I	TPBAR dose rates, 7 day decay time
TPBAR90.I	TPBAR dose rates, 90 day decay time
TPBAR180.I	TPBAR dose rates, 180 day decay time
TPBAR1.I	TPBAR dose rates, 1 year decay time
TPBAR5.I	TPBAR dose rates, 5 year decay time
HDA7.I	HDA dose rates, 7 day decay time
HDA90.I	HDA dose rates, 90 day decay time
HDA180.I	HDA dose rates, 180 day decay time
HDA1.I	HDA dose rates, 1 year decay time
HAD5.I	HDA dose rates, 5 year decay time

Because many of these input files are similar, only the files TPBAR7.I and HDA7.I are presented.

TPBAR7.I

```
Dose rate, TPBAR, 7 day decay time
999    0        -14:13:12         imp:p=0
10     0         14 -13 -11       imp:p=1
11     1 -8.0    14 -13  11 -10   imp:p=1
12     0         14 -13  10 -12   imp:p=1

10     cz   0.4839    $ cladding OR
11     cz   0.3848    $ cladding IR
12     cz   100.4839  $ 1m tally surface
13     pz   193       $ top of TPBAR
14     pz  -193       $ bottom of TPBAR
20     pz   50        $ tally cutting surface
21     pz  -50        $ tally cutting surface

print     -85
c
c       tallies
c
fc12      Contact dose rate, entire length
f12:p     10
fs12      13 -14
sd12      1174 2r
c
fc22      Contact dose rate, middle 1m
f22:p     10
fs22      20 -21
sd22      304 2r
c
fc32      1m from side, entire length
f32:p     12
fs32      13 -14
sd32      2.437e5 2r
c
fc42      1m from side, middle 1m
f42:p     12
fs42      20 -21
sd42      63136  2r
c
mode     p
prdmp     j j 1 2
nps      1000000
sdef       cel=11 erg=d1 pos=0 0 0 rad=d2
           ext=d3 axs=0 0 1 wgt=3.45e13
si2        0.3848 0.4839
si3        193
c
m1       26000 1
c
c        Photon source
c
c          E, MeV     photons/s
#             si1     sp1
              1         d
```

```
                0.01     7.73E+12
               0.025     6.71E+11
              0.0375     1.80E+11
              0.0575     5.80E+11
               0.085     1.52E+11
               0.125     2.24E+11
               0.225     4.52E+11
               0.375     3.06E+12
               0.575     2.75E+12
                0.85     1.56E+13
                1.25     3.05E+12
                1.75     5.01E+10
                2.25     2.12E+09
                2.75     7.48E+08
                 3.5     5.05E+05
                 5.0     5.21E+03
                 7.0     6.37E-10
                 9.5     4.03E-11
c         TOTAL    3.45E+13
c
c         Flux to Dose conversion from MCNP Manual
c         ANSI/ANS-6.1.1-1977
c
c         E, MeV      (rem/hr)/(photons/cm2/s)
#           de0          df0
          0.01        3.96e-6
          0.03        5.82e-7
          0.05        2.90e-7
          0.07        2.58e-7
          0.1         2.83e-7
          0.15        3.79e-7
          0.2         5.01e-7
          0.25        6.31e-7
          0.3         7.59e-7
          0.35        8.78e-7
          0.4         9.85e-7
          0.45        1.08e-6
          0.5         1.17e-6
          0.55        1.27e-6
          0.6         1.36e-6
          0.65        1.44e-6
          0.7         1.52e-6
          0.8         1.68e-6
          1.0         1.98e-6
          1.4         2.51e-6
          1.8         2.99e-6
          2.2         3.42e-6
          2.6         3.82e-6
          2.8         4.01e-6
          3.25        4.41e-6
          3.75        4.83e-6
          4.25        5.23e-6
          4.75        5.60e-6
          5.0         5.80e-6
          5.25        6.01e-6
```

```
          5.75        6.37e-6
          6.25        6.74e-6
          6.75        7.11e-6
          7.5         7.66e-6
          9.0         8.77e-6
          11.0        1.03e-5
          13.0        1.18e-5
          15.0        1.33e-5
```

HDA7.I

```
Dose rate, entire hold-down assembly, 7 day decay time
999    0          -40:42:35     imp:p=0
10     1 -8.0     41 -42 -35    imp:p=1  $ plate
20     1 -8.0    -41  40 -10    imp:p=1  $ thimble plug
22     1 -8.0    -41  40 -11    imp:p=1  $ thimble plug
24     1 -8.0    -41  40 -12    imp:p=1  $ thimble plug
26     0          40 -41 -13    imp:p=1  $ void
27     0          40 -41 -14    imp:p=1  $ void
28     1 -8.0    -41  40 -15    imp:p=1  $ thimble plug
30     1 -8.0    -41  40 -16    imp:p=1  $ thimble plug
32     1 -8.0    -41  40 -17    imp:p=1  $ thimble plug
34     1 -8.0    -41  40 -18    imp:p=1  $ thimble plug
36     1 -8.0    -41  40 -19    imp:p=1  $ thimble plug
38     1 -8.0    -41  40 -20    imp:p=1  $ thimble plug
40     1 -8.0    -41  40 -21    imp:p=1  $ thimble plug
43     0          40 -41 -22    imp:p=1  $ center void
44     1 -8.0    -41  40 -23    imp:p=1  $ thimble plug
46     1 -8.0    -41  40 -24    imp:p=1  $ thimble plug
48     1 -8.0    -41  40 -25    imp:p=1  $ thimble plug
50     1 -8.0    -41  40 -26    imp:p=1  $ thimble plug
52     1 -8.0    -41  40 -27    imp:p=1  $ thimble plug
54     1 -8.0    -41  40 -28    imp:p=1  $ thimble plug
56     1 -8.0    -41  40 -29    imp:p=1  $ thimble plug
58     0          40 -41 -30    imp:p=1  $ void
59     0          40 -41 -31    imp:p=1  $ void
60     1 -8.0    -41  40 -32    imp:p=1  $ thimble plug
62     1 -8.0    -41  40 -33    imp:p=1  $ thimble plug
64     1 -8.0    -41  40 -34    imp:p=1  $ thimble plug
66     0          10 11 12 13 14 15 16 17  $ void between plugs
                  18 19 20 21 22 23 24 25
                  26 27 28 29 30 31 32 33
                  34
                 -35 40 -41 imp:p=1

c      20 thimble plugs, 4 TPBAR voids, 1 instrument tube void
10     c/z -3.78  7.56 0.5
11     c/z  0     7.56 0.5
12     c/z  3.78  7.56 0.5
13     c/z -6.3   6.3  0.5  $ TPBAR void
14     c/z  6.3   6.3  0.5  $ TPBAR void
15     c/z -7.56  3.78 0.5
16     c/z -3.78  3.78 0.5
17     c/z  0     3.78 0.5
18     c/z  3.78  3.78 0.5
```

```
19     c/z  7.56 -3.78 0.5
20     c/z -7.56  0    0.5
21     c/z -3.78  0    0.5
22     cz              0.5  $ instrument tube void
23     c/z  3.78  0    0.5
24     c/z  7.56  0    0.5
25     c/z -7.56 -3.78 0.5
26     c/z -3.78 -3.78 0.5
27     c/z  0    -3.78 0.5
28     c/z  3.78 -3.78 0.5
29     c/z  7.56 -3.78 0.5
30     c/z -6.3  -6.3  0.5  TPBAR void
31     c/z  6.3  -6.3  0.5  TPBAR void
32     c/z -3.78 -7.56 0.5
33     c/z  0    -7.56 0.5
34     c/z  3.78 -7.56 0.5
c      hold-down plate
35     cz    12
c
40     pz   -16   $ bottom of thimble plug
41     pz    0    $ bottom of plate
42     pz    0.7  $ top of plate

c
m1      26000  1
c
print    -85
c
c      tallies
c
fc12     Top of Plate
f12:p    42
fs12     -35
sd12     452.4 1r
c
fc22     Bottom of Assembly
f22:p    40
fs22     -35
sd22     452.4 1r
c
fc32     Side of Assembly
f32:p    35
fs32     42 -40
sd32     1259 2r
c
mode    p
prdmp    j j 1 2
nps     1000000
sdef      cel=d10 erg=fcel=d20 pos=fcel=d30 rad=fcel=d40
          ext=fcel=d50 axs=0 0 1  wgt=5.1e13
si10     1 10                        $ plate
           20 22 24 28 30 32 34 36   $ thimble plugs
           38 40 44 46 48 50 52 54
           56 60 62 64
sp10      1.13e13 1.99e12 19r
```

```
ds20      s 21 22 19r
ds30      l   0  0  0.35
             -3.78  7.56 -8      0  7.56 -8
              3.78  7.56 -8  -7.56  3.78 -8
             -3.78  3.78 -8      0  3.78 -8
              3.78  3.78 -8   7.56  3.78 -8
             -7.56     0 -8  -3.78     0 -8
              3.78     0 -8   7.56     0 -8
             -7.56 -3.78 -8  -3.78 -3.78 -8
                 0 -3.78 -8   3.78 -3.78 -8
              7.56 -3.78 -8  -3.78 -7.56 -8
                 0 -7.56 -8   3.78 -7.56 -8
ds40     s 41 42 19r
si41       12
si42       0.5
ds50     s 51 52 19r
si51       0.35
si52       8
c
c       Photon source
c         Plate                      Thimble Plugs
c         E, MeV    photons/s        E, MeV    photons/s
#            si21     sp21              si22      sp22
                1        d                 1         d
            0.01   2.76E+12          0.01   6.95E+11
           0.025   4.42E+10         0.025   6.68E+09
          0.0375   2.73E+10        0.0375   4.25E+09
          0.0575   3.48E+10        0.0575   5.49E+09
           0.085   1.80E+10         0.085   2.97E+09
           0.125   1.21E+10         0.125   2.36E+09
           0.225   1.31E+10         0.225   2.53E+09
           0.375   1.62E+12         0.375   4.40E+11
           0.575   4.05E+11         0.575   6.56E+10
            0.85   2.21E+12          0.85   4.50E+11
            1.25   4.01E+12          1.25   3.13E+11
            1.75   7.50E+09          1.75   1.21E+09
            2.25   2.12E+07          2.25   1.66E+06
            2.75   4.76E+05          2.75   5.13E+03
             3.5   2.81E+02           3.5   1.32E-05
               5   2.92E+00             5   1.38E-07
               7   0.00E+00             7   0.00E+00
             9.5   0.00E+00           9.5   0.00E+00
c       TOTAL      1.12E+13                 1.99E+12
c       Grand      5.10E+13
c        Flux to Dose conversion from MCNP Manual
c        ANSI/ANS-6.1.1-1977
c
c        E, MeV      (rem/hr)/(photons/cm2/s)
#          de0          df0
         0.01        3.96e-6
         0.03        5.82e-7
         0.05        2.90e-7
         0.07        2.58e-7
         0.1         2.83e-7
         0.15        3.79e-7
```

0.2	5.01e-7
0.25	6.31e-7
0.3	7.59e-7
0.35	8.78e-7
0.4	9.85e-7
0.45	1.08e-6
0.5	1.17e-6
0.55	1.27e-6
0.6	1.36e-6
0.65	1.44e-6
0.7	1.52e-6
0.8	1.68e-6
1.0	1.98e-6
1.4	2.51e-6
1.8	2.99e-6
2.2	3.42e-6
2.6	3.82e-6
2.8	4.01e-6
3.25	4.41e-6
3.75	4.83e-6
4.25	5.23e-6
4.75	5.60e-6
5.0	5.80e-6
5.25	6.01e-6
5.75	6.37e-6
6.25	6.74e-6
6.75	7.11e-6
7.5	7.66e-6
9.0	8.77e-6
11.0	1.03e-5
13.0	1.18e-5
15.0	1.33e-5

APPENDIX D

Trace Isotope Concentrations

ORIGEN2 output does not report a complete list of radionuclides generated by irradiation as this list would be quite long. Rather, the code provides a threshold value below which concentrations are not reported. For the standard cases, the threshold is set at a value such that any radionuclide whose value is nine orders of magnitude below the total for the TPBAR, Hold-Down Assembly, or Single Thimble Plug is not reported. In most cases this is sufficient to identify important radionuclides of concern. However, parent-daughter products (such as Sr-90 and Y-90) may not both be displayed if one of the radionuclides does not meet the threshold requirements.

Additionally, the calculated ORIGEN2 cases (described in Appendix B) use the power irradiation option to generate the irradiation profile of the components. Power irradiation assumes uranium isotopes to be contained in fuel pins, not trace uranium contained in the metal components of a TPBAR, Hold-Down Assembly, or Single Thimble Plug. Therefore, fission products generated in the ORIGEN2 output for these cases are for fuel pins. Based upon the threshold output value for these standard cases it would not be expected to see the fission products from uranium impurities in the TPBAR, Hold-Down Assembly, or Single Thimble Plug, so the absence from the standard calculations is of no concern.

There are applications, however, where it is necessary to know the concentrations of trace radionuclides generated either from irradiation or from fission of uranium in metal components. A trace radionuclide is defined for the purposes of this calculation as a concentration greater than one picocurie. Table D1 provides a list of these trace radionuclides for the TPBAR excluding tritium.

Table D1. Trace Radionuclide Concentrations in a TPBAR (Ci/TPBAR)

Nuclide	7 Days	30 Days	90 Days	180 Days	1 Year	5 Years	10 Years
BE 10	3.76E-09	3.76E-09	3.76E-09	3.76E-09	3.76E-09	3.76E-09	3.76E-09
C 14	1.42E-03	1.42E-03	1.42E-03	1.42E-03	1.42E-03	1.42E-03	1.42E-03
NA 24	1.71E-02	1.43E-13	0.00E+00	0.00E+00	0.00E+00	0.00E+00	0.00E+00
MG 28	1.53E-10	1.73E-18	0.00E+00	0.00E+00	0.00E+00	0.00E+00	0.00E+00
AL 28	1.53E-10	1.73E-18	0.00E+00	0.00E+00	0.00E+00	0.00E+00	0.00E+00
SI 32	5.76E-10	5.76E-10	5.76E-10	5.76E-10	5.76E-10	5.73E-10	5.70E-10
P 32	9.13E-01	2.99E-01	1.63E-02	2.08E-04	2.68E-08	5.73E-10	5.70E-10
P 33	1.90E-05	1.01E-05	1.90E-06	1.57E-07	9.23E-10	2.36E-27	0.00E+00
S 35	2.77E-01	2.31E-01	1.44E-01	7.08E-02	1.65E-02	1.65E-07	9.36E-14
CL 36	7.09E-05	7.09E-05	7.09E-05	7.09E-05	7.09E-05	7.09E-05	7.09E-05
AR 37	3.40E-01	2.15E-01	6.57E-02	1.11E-02	2.83E-04	7.84E-17	1.57E-32
AR 39	9.48E-03	9.48E-03	9.47E-03	9.47E-03	9.46E-03	9.36E-03	9.24E-03
AR 42	7.78E-12	7.77E-12	7.74E-12	7.70E-12	7.62E-12	7.01E-12	6.31E-12
K 40	3.03E-08	3.03E-08	3.03E-08	3.03E-08	3.03E-08	3.03E-08	3.03E-08
K 42	1.89E-04	7.77E-12	7.74E-12	7.70E-12	7.62E-12	7.01E-12	6.31E-12
K 43	1.37E-06	6.08E-14	4.01E-33	0.00E+00	0.00E+00	0.00E+00	0.00E+00

Nuclide	7 Days	30 Days	90 Days	180 Days	1 Year	5 Years	10 Years
CA 41	7.50E-05	7.50E-05	7.50E-05	7.50E-05	7.50E-05	7.50E-05	7.50E-05
CA 45	2.99E-01	2.71E-01	2.10E-01	1.43E-01	6.52E-02	1.30E-04	5.52E-08
CA 47	1.36E-04	4.05E-06	4.23E-10	4.50E-16	2.28E-28	0.00E+00	0.00E+00
SC 46	7.79E-03	6.44E-03	3.92E-03	1.86E-03	4.02E-04	2.27E-09	6.24E-16
SC 47	4.93E-04	1.53E-05	1.62E-09	1.72E-15	8.74E-28	0.00E+00	0.00E+00
SC 48	1.13E-05	1.83E-09	2.32E-19	3.33E-34	0.00E+00	0.00E+00	0.00E+00
CR 51	8.61E+02	4.84E+02	1.08E+02	1.14E+01	1.10E-01	1.48E-17	2.11E-37
MN 54	4.09E+01	3.88E+01	3.40E+01	2.78E+01	1.85E+01	7.22E-01	1.26E-02
FE 55	2.13E+02	2.10E+02	2.01E+02	1.88E+02	1.64E+02	5.65E+01	1.49E+01
FE 59	1.79E+01	1.26E+01	5.00E+00	1.25E+00	7.20E-02	1.21E-11	7.36E-24
CO 58	2.57E+02	2.05E+02	1.14E+02	4.73E+01	7.70E+00	4.70E-06	8.03E-14
CO 60	3.58E+01	3.55E+01	3.48E+01	3.37E+01	3.15E+01	1.86E+01	9.64E+00
NI 59	1.68E-01	1.68E-01	1.68E-01	1.68E-01	1.68E-01	1.68E-01	1.68E-01
NI 63	2.28E+01	2.28E+01	2.28E+01	2.27E+01	2.27E+01	2.20E+01	2.12E+01
NI 66	1.14E-04	1.03E-07	1.19E-15	1.48E-27	0.00E+00	0.00E+00	0.00E+00
CU 64	1.10E-03	9.03E-17	0.00E+00	0.00E+00	0.00E+00	0.00E+00	0.00E+00
CU 66	1.14E-04	1.03E-07	1.19E-15	1.48E-27	0.00E+00	0.00E+00	0.00E+00
CU 67	1.12E-06	2.30E-09	2.26E-16	6.98E-27	0.00E+00	0.00E+00	0.00E+00
ZN 65	4.00E-03	3.75E-03	3.16E-03	2.45E-03	1.45E-03	2.27E-05	1.27E-07
ZN 69	1.09E-12	9.19E-25	0.00E+00	0.00E+00	0.00E+00	0.00E+00	0.00E+00
ZN 69M	1.02E-12	8.56E-25	0.00E+00	0.00E+00	0.00E+00	0.00E+00	0.00E+00
ZN 72	5.87E-09	1.57E-12	7.46E-22	7.75E-36	0.00E+00	0.00E+00	0.00E+00
GA 72	8.45E-09	2.25E-12	1.07E-21	1.12E-35	0.00E+00	0.00E+00	0.00E+00
GA 73	5.74E-18	0.00E+00	0.00E+00	0.00E+00	0.00E+00	0.00E+00	0.00E+00
GE 73M	5.74E-18	0.00E+00	0.00E+00	0.00E+00	0.00E+00	0.00E+00	0.00E+00
GE 77	2.47E-11	4.88E-26	0.00E+00	0.00E+00	0.00E+00	0.00E+00	0.00E+00
AS 76	7.57E-01	3.68E-07	1.25E-23	0.00E+00	0.00E+00	0.00E+00	0.00E+00
AS 77	1.11E-07	5.82E-12	3.93E-23	0.00E+00	0.00E+00	0.00E+00	0.00E+00
SE 75	8.38E-01	7.33E-01	5.18E-01	3.08E-01	1.05E-01	2.25E-05	5.78E-10
SE 77M	2.76E-10	1.44E-14	9.75E-26	0.00E+00	0.00E+00	0.00E+00	0.00E+00
SE 79	8.52E-06	8.52E-06	8.52E-06	8.52E-06	8.52E-06	8.52E-06	8.52E-06
BR 80	6.00E-12	0.00E+00	0.00E+00	0.00E+00	0.00E+00	0.00E+00	0.00E+00
BR 80M	5.61E-12	0.00E+00	0.00E+00	0.00E+00	0.00E+00	0.00E+00	0.00E+00
BR 82	1.75E-01	3.43E-06	1.81E-18	7.47E-37	0.00E+00	0.00E+00	0.00E+00
KR 79	4.01E-07	6.94E-12	2.63E-24	0.00E+00	0.00E+00	0.00E+00	0.00E+00
KR 81	1.60E-06	1.60E-06	1.60E-06	1.60E-06	1.60E-06	1.60E-06	1.60E-06
KR 85	9.11E-06	9.07E-06	8.97E-06	8.83E-06	8.55E-06	6.60E-06	4.78E-06
KR 85M	7.87E-16	0.00E+00	0.00E+00	0.00E+00	0.00E+00	0.00E+00	0.00E+00
RB 86	7.35E-07	3.13E-07	3.37E-08	1.19E-09	1.22E-12	0.00E+00	0.00E+00
RB 87	6.12E-15	6.12E-15	6.12E-15	6.12E-15	6.12E-15	6.12E-15	6.12E-15
SR 89	6.86E-02	5.01E-02	2.20E-02	6.39E-03	5.02E-04	9.81E-13	1.27E-23
SR 90	2.22E-05	2.22E-05	2.21E-05	2.20E-05	2.17E-05	1.97E-05	1.75E-05
SR 91	7.17E-08	2.31E-25	0.00E+00	0.00E+00	0.00E+00	0.00E+00	0.00E+00
Y 89M	4.76E-04	3.62E-06	1.08E-11	5.55E-20	0.00E+00	0.00E+00	0.00E+00
Y 90	4.45E-01	1.15E-03	2.21E-05	2.20E-05	2.17E-05	1.98E-05	1.75E-05

Nuclide	7 Days	30 Days	90 Days	180 Days	1 Year	5 Years	10 Years
Y 91	1.76E-01	1.34E-01	6.59E-02	2.27E-02	2.53E-03	7.68E-11	3.08E-20
Y 91M	2.05E-09	6.61E-27	0.00E+00	0.00E+00	0.00E+00	0.00E+00	0.00E+00
Y 92	1.72E-17	0.00E+00	0.00E+00	0.00E+00	0.00E+00	0.00E+00	0.00E+00
Y 93	1.02E-08	3.61E-25	0.00E+00	0.00E+00	0.00E+00	0.00E+00	0.00E+00
ZR 89	4.77E-04	3.63E-06	1.08E-11	5.56E-20	5.04E-37	0.00E+00	0.00E+00
ZR 93	1.13E-04	1.13E-04	1.13E-04	1.13E-04	1.13E-04	1.13E-04	1.13E-04
ZR 95	6.03E+01	4.70E+01	2.45E+01	9.25E+00	1.24E+00	1.66E-07	4.25E-16
ZR 97	9.67E-02	1.42E-11	0.00E+00	0.00E+00	0.00E+00	0.00E+00	0.00E+00
NB 92	2.67E-01	5.56E-02	9.27E-04	2.00E-06	6.49E-12	0.00E+00	0.00E+00
NB 93M	3.83E-06	4.16E-06	5.02E-06	6.29E-06	8.85E-06	2.69E-05	4.49E-05
NB 94	4.75E-04	4.75E-04	4.75E-04	4.75E-04	4.75E-04	4.75E-04	4.75E-04
NB 95	6.51E+01	6.07E+01	4.11E+01	1.83E+01	2.70E+00	3.69E-07	9.43E-16
NB 95M	4.41E-01	3.49E-01	1.82E-01	6.86E-02	9.23E-03	1.23E-09	3.15E-18
NB 96	9.87E-04	7.55E-11	2.06E-29	0.00E+00	0.00E+00	0.00E+00	0.00E+00
NB 97	9.75E-02	1.53E-11	0.00E+00	0.00E+00	0.00E+00	0.00E+00	0.00E+00
NB 97M	9.19E-02	1.35E-11	0.00E+00	0.00E+00	0.00E+00	0.00E+00	0.00E+00
MO 93M	5.03E-09	0.00E+00	0.00E+00	0.00E+00	0.00E+00	0.00E+00	0.00E+00
MO 93	1.04E-03	1.04E-03	1.04E-03	1.04E-03	1.04E-03	1.03E-03	1.03E-03
MO 99	1.46E+01	4.43E-02	1.20E-08	1.68E-18	0.00E+00	0.00E+00	0.00E+00
TC 98	1.58E-11	1.58E-11	1.58E-11	1.58E-11	1.58E-11	1.58E-11	1.58E-11
TC 99	4.34E-05	4.35E-05	4.35E-05	4.35E-05	4.35E-05	4.35E-05	4.35E-05
TC 99M	2.36E-04	7.16E-07	1.94E-13	2.73E-23	0.00E+00	0.00E+00	0.00E+00
RU103	4.22E-03	2.81E-03	9.75E-04	1.99E-04	7.58E-06	4.83E-17	4.88E-31
RU105	4.83E-15	0.00E+00	0.00E+00	0.00E+00	0.00E+00	0.00E+00	0.00E+00
RU106	4.61E-04	4.41E-04	3.94E-04	3.33E-04	2.35E-04	1.50E-05	4.81E-07
RH102	5.31E-10	5.23E-10	5.03E-10	4.74E-10	4.20E-10	1.61E-10	4.89E-11
RH103M	1.16E-03	7.76E-04	2.69E-04	5.50E-05	2.09E-06	1.33E-17	1.35E-31
RH105	4.29E-05	8.58E-10	4.73E-22	0.00E+00	0.00E+00	0.00E+00	0.00E+00
RH105M	1.36E-15	0.00E+00	0.00E+00	0.00E+00	0.00E+00	0.00E+00	0.00E+00
RH106	4.61E-04	4.41E-04	3.94E-04	3.33E-04	2.35E-04	1.50E-05	4.81E-07
PD107	7.55E-11	7.55E-11	7.55E-11	7.55E-11	7.55E-11	7.55E-11	7.55E-11
PD109	6.72E-08	3.04E-20	0.00E+00	0.00E+00	0.00E+00	0.00E+00	0.00E+00
PD111	5.74E-16	0.00E+00	0.00E+00	0.00E+00	0.00E+00	0.00E+00	0.00E+00
PD111M	7.87E-16	0.00E+00	0.00E+00	0.00E+00	0.00E+00	0.00E+00	0.00E+00
PD112	1.28E-07	6.92E-16	2.19E-37	0.00E+00	0.00E+00	0.00E+00	0.00E+00
AG106	5.17E-11	7.92E-12	5.94E-14	3.86E-17	1.06E-23	0.00E+00	0.00E+00
AG108	3.03E-11	3.03E-11	3.02E-11	3.02E-11	3.01E-11	2.95E-11	2.87E-11
AG108M	3.40E-10	3.40E-10	3.40E-10	3.39E-10	3.38E-10	3.31E-10	3.22E-10
AG109M	5.98E-06	5.72E-06	5.23E-06	4.57E-06	3.47E-06	3.91E-07	2.55E-08
AG110	4.41E-08	4.14E-08	3.50E-08	2.73E-08	1.63E-08	2.84E-10	1.79E-12
AG110M	3.32E-06	3.11E-06	2.63E-06	2.05E-06	1.23E-06	2.13E-08	1.35E-10
AG111	4.30E-05	5.06E-06	1.90E-08	4.40E-12	1.44E-19	0.00E+00	0.00E+00
AG111M	8.24E-16	0.00E+00	0.00E+00	0.00E+00	0.00E+00	0.00E+00	0.00E+00
AG112	1.52E-07	8.20E-16	0.00E+00	0.00E+00	0.00E+00	0.00E+00	0.00E+00
AG113	8.48E-15	0.00E+00	0.00E+00	0.00E+00	0.00E+00	0.00E+00	0.00E+00

Nuclide	7 Days	30 Days	90 Days	180 Days	1 Year	5 Years	10 Years
CD109	5.92E-06	5.72E-06	5.23E-06	4.57E-06	3.47E-06	3.91E-07	2.55E-08
CD113M	3.55E-08	3.54E-08	3.51E-08	3.47E-08	3.39E-08	2.80E-08	2.21E-08
CD115	2.55E-04	1.99E-07	1.56E-15	1.08E-27	0.00E+00	0.00E+00	0.00E+00
CD115M	1.68E-04	1.18E-04	4.62E-05	1.14E-05	6.41E-07	8.81E-17	4.14E-29
IN113M	1.23E+00	1.07E+00	7.48E-01	4.35E-01	1.43E-01	2.15E-05	3.61E-10
IN114	1.17E-01	8.46E-02	3.65E-02	1.04E-02	7.75E-04	1.02E-12	8.01E-24
IN114M	1.22E-01	8.84E-02	3.82E-02	1.08E-02	8.09E-04	1.06E-12	8.37E-24
IN115	1.03E-20	1.04E-20	1.06E-20	1.07E-20	1.07E-20	1.07E-20	1.07E-20
IN115M	2.51E-06	2.04E-09	3.35E-11	8.27E-12	4.65E-13	6.38E-23	2.96E-35
SN113	1.23E+00	1.07E+00	7.48E-01	4.35E-01	1.43E-01	2.15E-05	3.60E-10
SN117M	7.22E+00	2.31E+00	1.19E-01	1.38E-03	1.44E-07	0.00E+00	0.00E+00
SN119M	8.16E+00	7.65E+00	6.45E+00	5.00E+00	2.96E+00	4.75E-02	2.71E-04
SN121	6.40E-02	4.03E-08	2.70E-24	0.00E+00	0.00E+00	0.00E+00	0.00E+00
SN121M	5.52E-04	5.52E-04	5.51E-04	5.49E-04	5.45E-04	5.15E-04	4.81E-04
SN123	4.53E-01	4.00E-01	2.90E-01	1.79E-01	6.62E-02	2.61E-05	1.44E-09
SN125	1.93E+00	3.69E-01	4.93E-03	7.65E-06	1.26E-11	0.00E+00	0.00E+00
SN126	4.33E-10	4.33E-10	4.33E-10	4.33E-10	4.33E-10	4.33E-10	4.33E-10
SB122	9.51E-02	2.59E-04	5.31E-11	4.91E-21	0.00E+00	0.00E+00	0.00E+00
SB124	1.75E-02	1.35E-02	6.74E-03	2.39E-03	2.83E-04	1.40E-11	1.03E-20
SB125	1.66E+00	1.65E+00	1.59E+00	1.49E+00	1.31E+00	4.82E-01	1.38E-01
SB126	4.95E-02	1.37E-02	4.78E-04	3.12E-06	1.59E-10	6.06E-11	6.06E-11
SB126M	4.33E-10	4.33E-10	4.33E-10	4.33E-10	4.33E-10	4.33E-10	4.33E-10
SB127	3.14E-05	5.00E-07	1.02E-11	9.31E-19	3.04E-33	0.00E+00	0.00E+00
SB128	3.80E-11	1.38E-29	0.00E+00	0.00E+00	0.00E+00	0.00E+00	0.00E+00
SB129	5.98E-16	0.00E+00	0.00E+00	0.00E+00	0.00E+00	0.00E+00	0.00E+00
TE123M	2.88E-03	2.52E-03	1.78E-03	1.06E-03	3.61E-04	7.64E-08	1.95E-12
TE125M	3.30E-01	3.42E-01	3.57E-01	3.53E-01	3.19E-01	1.18E-01	3.37E-02
TE127	6.64E-05	3.20E-05	2.15E-05	1.21E-05	3.74E-06	3.45E-10	3.12E-15
TE127M	3.71E-05	3.22E-05	2.20E-05	1.24E-05	3.82E-06	3.52E-10	3.19E-15
TE129	5.02E-05	3.13E-05	9.07E-06	1.42E-06	3.10E-08	2.52E-21	0.00E+00
TE129M	7.72E-05	4.80E-05	1.39E-05	2.18E-06	4.76E-08	3.88E-21	1.69E-37
TE131	5.95E-07	1.72E-12	6.11E-27	0.00E+00	0.00E+00	0.00E+00	0.00E+00
TE131M	2.64E-06	7.64E-12	2.71E-26	0.00E+00	0.00E+00	0.00E+00	0.00E+00
TE132	2.63E-04	1.97E-06	5.64E-12	2.73E-20	2.25E-37	0.00E+00	0.00E+00
I129	6.19E-11	6.21E-11	6.23E-11	6.23E-11	6.23E-11	6.23E-11	6.23E-11
I130	9.21E-09	3.32E-22	0.00E+00	0.00E+00	0.00E+00	0.00E+00	0.00E+00
I131	4.73E-04	6.52E-05	3.70E-07	1.58E-10	1.83E-17	0.00E+00	0.00E+00
I132	2.71E-04	2.03E-06	5.81E-12	2.81E-20	0.00E+00	0.00E+00	0.00E+00
I133	6.06E-06	6.22E-14	8.98E-35	0.00E+00	0.00E+00	0.00E+00	0.00E+00
I135	3.37E-11	0.00E+00	0.00E+00	0.00E+00	0.00E+00	0.00E+00	0.00E+00
XE127	7.86E-05	5.08E-05	1.62E-05	2.92E-06	8.59E-08	7.17E-20	5.72E-35
XE129M	5.31E-03	7.23E-04	4.00E-06	1.64E-09	1.76E-16	0.00E+00	0.00E+00
XE131M	1.21E-05	4.52E-06	1.74E-07	9.62E-10	1.99E-14	0.00E+00	0.00E+00
XE133	7.57E-04	3.66E-05	1.32E-08	9.01E-14	2.10E-24	0.00E+00	0.00E+00
XE133M	8.53E-06	5.96E-09	3.37E-17	1.43E-29	0.00E+00	0.00E+00	0.00E+00

Nuclide	7 Days	30 Days	90 Days	180 Days	1 Year	5 Years	10 Years
XE135	1.16E-08	6.10E-27	0.00E+00	0.00E+00	0.00E+00	0.00E+00	0.00E+00
XE135M	5.40E-12	0.00E+00	0.00E+00	0.00E+00	0.00E+00	0.00E+00	0.00E+00
CS131	4.51E-02	2.06E-02	1.02E-03	6.44E-06	1.32E-10	0.00E+00	0.00E+00
CS132	1.03E-07	8.78E-09	1.43E-11	9.32E-16	2.27E-24	0.00E+00	0.00E+00
CS134	6.66E-05	6.52E-05	6.17E-05	5.68E-05	4.79E-05	1.25E-05	2.32E-06
CS135	9.73E-11	9.73E-11	9.73E-11	9.73E-11	9.73E-11	9.73E-11	9.73E-11
CS136	2.01E-05	5.96E-06	2.49E-07	2.13E-09	1.18E-13	0.00E+00	0.00E+00
CS137	4.19E-05	4.19E-05	4.17E-05	4.15E-05	4.10E-05	3.74E-05	3.33E-05
BA131	3.23E-02	8.36E-03	2.47E-04	1.25E-06	2.37E-11	0.00E+00	0.00E+00
BA133	7.40E-04	7.37E-04	7.29E-04	7.18E-04	6.94E-04	5.36E-04	3.89E-04
BA133M	3.16E-05	1.69E-09	1.20E-20	2.26E-37	0.00E+00	0.00E+00	0.00E+00
BA135M	2.40E-04	3.88E-10	3.04E-25	0.00E+00	0.00E+00	0.00E+00	0.00E+00
BA136M	3.31E-06	9.82E-07	4.11E-08	3.51E-10	1.95E-14	0.00E+00	0.00E+00
BA137M	3.97E-05	3.96E-05	3.95E-05	3.92E-05	3.88E-05	3.53E-05	3.15E-05
BA140	9.03E-04	2.60E-04	1.01E-05	7.65E-08	3.34E-12	0.00E+00	0.00E+00
LA138	2.71E-20	2.71E-20	2.71E-20	2.71E-20	2.71E-20	2.71E-20	2.71E-20
LA140	1.37E-03	2.99E-04	1.16E-05	8.81E-08	3.84E-12	0.00E+00	0.00E+00
LA141	1.84E-16	0.00E+00	0.00E+00	0.00E+00	0.00E+00	0.00E+00	0.00E+00
CE141	1.08E-03	6.63E-04	1.84E-04	2.71E-05	5.21E-07	1.55E-20	1.91E-37
CE142	9.97E-15	9.97E-15	9.97E-15	9.97E-15	9.97E-15	9.97E-15	9.97E-15
CE143	3.24E-05	2.99E-10	2.18E-23	0.00E+00	0.00E+00	0.00E+00	0.00E+00
CE144	6.43E-04	6.08E-04	5.25E-04	4.22E-04	2.68E-04	7.61E-06	8.86E-08
PR142	9.80E-08	2.02E-16	0.00E+00	0.00E+00	0.00E+00	0.00E+00	0.00E+00
PR143	8.34E-04	2.59E-04	1.21E-05	1.21E-07	9.40E-12	0.00E+00	0.00E+00
PR144	6.43E-04	6.08E-04	5.25E-04	4.22E-04	2.68E-04	7.61E-06	8.86E-08
PR144M	7.72E-06	7.29E-06	6.30E-06	5.06E-06	3.22E-06	9.14E-08	1.06E-09
ND144	2.84E-19	2.97E-19	3.28E-19	3.66E-19	4.23E-19	5.20E-19	5.22E-19
PR145	2.70E-12	0.00E+00	0.00E+00	0.00E+00	0.00E+00	0.00E+00	0.00E+00
PM146	1.19E-09	1.18E-09	1.16E-09	1.12E-09	1.05E-09	6.35E-10	3.38E-10
SM146	2.82E-17	2.85E-17	2.92E-17	3.02E-17	3.22E-17	4.43E-17	5.30E-17
ND147	3.27E-04	7.73E-05	1.80E-06	6.39E-09	5.80E-14	0.00E+00	0.00E+00
PM147	6.65E-05	6.83E-05	6.62E-05	6.21E-05	5.43E-05	1.89E-05	5.04E-06
SM147	2.95E-16	3.23E-16	3.95E-16	4.97E-16	6.88E-16	1.56E-15	1.90E-15
PM148	7.20E-05	4.16E-06	1.85E-07	4.03E-08	1.80E-09	4.03E-20	1.96E-33
PM148M	1.31E-05	8.88E-06	3.24E-06	7.16E-07	3.20E-08	7.15E-19	3.48E-32
SM148	1.45E-20	1.46E-20	1.47E-20	1.48E-20	1.48E-20	1.48E-20	1.48E-20
PM149	5.60E-05	4.15E-08	2.83E-16	1.60E-28	0.00E+00	0.00E+00	0.00E+00
EU150	3.42E-15	3.41E-15	3.40E-15	3.39E-15	3.35E-15	3.10E-15	2.82E-15
PM151	3.06E-06	4.29E-12	2.31E-27	0.00E+00	0.00E+00	0.00E+00	0.00E+00
SM151	1.94E-07	1.94E-07	1.94E-07	1.94E-07	1.93E-07	1.87E-07	1.80E-07
EU152	1.88E-09	1.88E-09	1.86E-09	1.84E-09	1.79E-09	1.46E-09	1.13E-09
EU152M	2.02E-13	2.99E-31	0.00E+00	0.00E+00	0.00E+00	0.00E+00	0.00E+00
SM153	3.02E-05	8.35E-09	4.35E-18	5.17E-32	0.00E+00	0.00E+00	0.00E+00
GD153	1.46E-08	1.37E-08	1.16E-08	8.92E-09	5.25E-09	7.99E-11	4.28E-13
EU154	4.56E-06	4.53E-06	4.48E-06	4.39E-06	4.21E-06	3.05E-06	2.04E-06

Nuclide	7 Days	30 Days	90 Days	180 Days	1 Year	5 Years	10 Years
EU155	3.08E-06	3.05E-06	2.98E-06	2.88E-06	2.68E-06	1.53E-06	7.62E-07
SM156	1.14E-10	2.40E-28	0.00E+00	0.00E+00	0.00E+00	0.00E+00	0.00E+00
EU156	1.02E-04	3.58E-05	2.32E-06	3.81E-08	8.09E-12	0.00E+00	0.00E+00
EU157	1.38E-08	1.61E-19	0.00E+00	0.00E+00	0.00E+00	0.00E+00	0.00E+00
GD159	1.40E-08	1.63E-17	0.00E+00	0.00E+00	0.00E+00	0.00E+00	0.00E+00
TB160	7.71E-07	6.19E-07	3.48E-07	1.47E-07	2.49E-08	2.06E-14	5.12E-22
TB161	8.00E-07	7.99E-08	1.96E-10	2.39E-14	2.09E-22	0.00E+00	0.00E+00
DY166	8.97E-09	8.20E-11	3.94E-16	4.14E-24	0.00E+00	0.00E+00	0.00E+00
HO166	1.47E-08	1.22E-10	5.86E-16	6.17E-24	0.00E+00	0.00E+00	0.00E+00
HO166M	1.53E-12	1.53E-12	1.53E-12	1.53E-12	1.53E-12	1.52E-12	1.52E-12
ER169	1.58E-10	2.90E-11	3.48E-13	4.57E-16	5.34E-22	0.00E+00	0.00E+00
TM170	3.20E-11	2.82E-11	2.04E-11	1.26E-11	4.63E-12	1.76E-15	9.34E-20
TM171	5.22E-13	5.10E-13	4.81E-13	4.40E-13	3.66E-13	8.64E-14	1.42E-14
TM172	6.04E-10	1.47E-12	2.25E-19	1.34E-29	0.00E+00	0.00E+00	0.00E+00
YB175	4.08E-12	9.08E-14	4.44E-18	1.52E-24	8.74E-38	0.00E+00	0.00E+00
LU177	1.88E-03	1.76E-04	1.47E-06	7.45E-07	3.25E-07	4.73E-10	1.34E-13
LU177M	7.02E-06	6.33E-06	4.84E-06	3.24E-06	1.41E-06	2.06E-09	5.84E-13
HF175	2.98E-02	2.37E-02	1.31E-02	5.37E-03	8.58E-04	4.47E-10	6.26E-18
HF180M	3.08E-11	0.00E+00	0.00E+00	0.00E+00	0.00E+00	0.00E+00	0.00E+00
HF181	7.98E-01	5.48E-01	2.06E-01	4.72E-02	2.28E-03	9.65E-14	1.04E-26
HF182	7.65E-10	7.65E-10	7.65E-10	7.65E-10	7.65E-10	7.65E-10	7.65E-10
TA182	1.05E+01	9.16E+00	6.38E+00	3.71E+00	1.21E+00	1.82E-04	3.78E-09
TA183	2.17E+01	9.53E-01	2.74E-04	1.34E-09	1.55E-20	0.00E+00	0.00E+00
W181	5.56E-03	4.87E-03	3.46E-03	2.07E-03	7.16E-04	1.68E-07	4.88E-12
W185	1.94E-01	1.57E-01	9.00E-02	3.92E-02	7.09E-03	9.88E-09	4.72E-16
W187	2.33E-02	2.59E-09	1.89E-27	0.00E+00	0.00E+00	0.00E+00	0.00E+00
W188	1.40E-02	1.11E-02	6.12E-03	2.49E-03	3.91E-04	1.80E-10	2.16E-18
RE186	2.86E-02	4.19E-04	6.92E-09	4.64E-16	7.95E-31	0.00E+00	0.00E+00
RE187	6.01E-11	6.01E-11	6.01E-11	6.01E-11	6.01E-11	6.01E-11	6.01E-11
RE188	1.52E-02	1.13E-02	6.18E-03	2.52E-03	3.96E-04	1.82E-10	2.18E-18
RE189	5.96E-08	8.65E-15	1.25E-32	0.00E+00	0.00E+00	0.00E+00	0.00E+00
OS191	4.34E-05	1.54E-05	1.04E-06	1.81E-08	4.34E-12	0.00E+00	0.00E+00
OS191M	6.15E-09	1.02E-21	0.00E+00	0.00E+00	0.00E+00	0.00E+00	0.00E+00
OS193	1.23E-11	5.34E-17	5.55E-31	0.00E+00	0.00E+00	0.00E+00	0.00E+00
IR192	9.83E-06	7.92E-06	4.52E-06	1.95E-06	3.43E-07	8.05E-12	7.55E-12
IR192M	7.76E-12	7.76E-12	7.76E-12	7.75E-12	7.74E-12	7.65E-12	7.54E-12
IR194	1.52E-09	1.34E-13	1.31E-13	1.28E-13	1.20E-13	7.57E-14	4.25E-14
PT193	3.08E-11	3.09E-11	3.09E-11	3.09E-11	3.09E-11	3.07E-11	3.05E-11
PT193M	5.54E-09	1.36E-10	8.57E-15	4.29E-21	4.61E-34	0.00E+00	0.00E+00
PT195M	6.53E-12	4.07E-14	7.21E-20	1.70E-28	0.00E+00	0.00E+00	0.00E+00
TL207	1.08E-17	1.32E-17	1.78E-17	2.70E-17	4.38E-17	1.86E-16	3.83E-16
TL208	4.94E-14	5.77E-14	8.54E-14	1.31E-13	2.47E-13	1.40E-12	2.25E-12
TL209	6.95E-19	4.78E-19	1.62E-19	1.71E-19	1.62E-19	1.87E-19	2.35E-19
PB205	1.47E-10	1.47E-10	1.47E-10	1.47E-10	1.47E-10	1.47E-10	1.47E-10
PB209	3.22E-17	2.21E-17	7.50E-18	7.91E-18	7.48E-18	8.64E-18	1.09E-17

Nuclide	7 Days	30 Days	90 Days	180 Days	1 Year	5 Years	10 Years
PB210	2.15E-19	2.32E-19	2.47E-19	2.55E-19	2.74E-19	1.03E-18	4.77E-18
PB211	1.08E-17	1.32E-17	1.79E-17	2.70E-17	4.39E-17	1.86E-16	3.84E-16
PB212	1.38E-13	1.61E-13	2.38E-13	3.65E-13	6.86E-13	3.90E-12	6.27E-12
PB214	6.58E-19	6.58E-19	9.11E-19	1.18E-18	1.87E-18	1.33E-17	4.30E-17
BI210	2.90E-09	1.21E-10	3.00E-14	3.73E-19	2.74E-19	1.03E-18	4.77E-18
BI211	1.08E-17	1.32E-17	1.79E-17	2.70E-17	4.39E-17	1.86E-16	3.84E-16
BI212	1.38E-13	1.61E-13	2.38E-13	3.65E-13	6.86E-13	3.90E-12	6.27E-12
BI213	3.22E-17	2.21E-17	7.50E-18	7.91E-18	7.48E-18	8.64E-18	1.09E-17
BI214	6.58E-19	6.58E-19	9.11E-19	1.18E-18	1.87E-18	1.33E-17	4.30E-17
PO210	4.83E-09	4.40E-09	3.26E-09	2.08E-09	8.22E-10	5.47E-13	6.68E-17
PO211	3.02E-20	3.69E-20	5.00E-20	7.57E-20	1.23E-19	5.21E-19	1.08E-18
PO212	8.81E-14	1.03E-13	1.52E-13	2.34E-13	4.40E-13	2.50E-12	4.02E-12
PO213	3.15E-17	2.16E-17	7.34E-18	7.74E-18	7.32E-18	8.45E-18	1.07E-17
PO214	1.26E-17	6.05E-18	1.62E-18	1.20E-18	1.87E-18	1.33E-17	4.30E-17
PO215	1.08E-17	1.32E-17	1.79E-17	2.70E-17	4.39E-17	1.86E-16	3.84E-16
PO216	1.38E-13	1.61E-13	2.38E-13	3.65E-13	6.86E-13	3.90E-12	6.27E-12
PO218	6.58E-19	6.58E-19	9.11E-19	1.18E-18	1.87E-18	1.33E-17	4.30E-17
AT217	3.22E-17	2.21E-17	7.50E-18	7.91E-18	7.48E-18	8.64E-18	1.09E-17
RN218	1.20E-17	5.39E-18	7.10E-19	1.75E-20	0.00E+00	0.00E+00	0.00E+00
RN219	1.08E-17	1.32E-17	1.79E-17	2.70E-17	4.39E-17	1.86E-16	3.84E-16
RN220	1.38E-13	1.61E-13	2.38E-13	3.65E-13	6.86E-13	3.90E-12	6.27E-12
RN222	6.58E-19	6.58E-19	9.11E-19	1.18E-18	1.87E-18	1.33E-17	4.30E-17
FR221	3.22E-17	2.21E-17	7.50E-18	7.91E-18	7.48E-18	8.64E-18	1.09E-17
FR223	2.09E-19	2.36E-19	3.08E-19	4.16E-19	6.42E-19	2.57E-18	5.29E-18
RA222	1.20E-17	5.39E-18	7.10E-19	1.75E-20	0.00E+00	0.00E+00	0.00E+00
RA223	1.08E-17	1.32E-17	1.79E-17	2.70E-17	4.39E-17	1.86E-16	3.84E-16
RA224	1.38E-13	1.61E-13	2.38E-13	3.65E-13	6.86E-13	3.90E-12	6.27E-12
RA225	2.88E-17	1.48E-17	7.21E-18	7.21E-18	7.48E-18	8.64E-18	1.09E-17
RA226	6.95E-19	7.52E-19	9.11E-19	1.18E-18	1.87E-18	1.33E-17	4.30E-17
RA228	0.00E+00	0.00E+00	0.00E+00	0.00E+00	0.00E+00	0.00E+00	6.27E-21
AC225	3.22E-17	2.21E-17	7.50E-18	7.91E-18	7.48E-18	8.64E-18	1.09E-17
AC227	1.51E-17	1.71E-17	2.23E-17	3.01E-17	4.65E-17	1.86E-16	3.84E-16
AC228	1.98E-24	0.00E+00	0.00E+00	0.00E+00	0.00E+00	0.00E+00	6.27E-21
TH226	1.20E-17	5.39E-18	7.10E-19	1.75E-20	0.00E+00	0.00E+00	0.00E+00
TH227	1.23E-17	1.46E-17	1.97E-17	2.74E-17	4.32E-17	1.83E-16	3.79E-16
TH228	1.42E-13	1.66E-13	2.37E-13	3.63E-13	6.84E-13	3.89E-12	6.27E-12
TH229	7.28E-18	7.29E-18	7.32E-18	7.37E-18	7.48E-18	8.64E-18	1.09E-17
TH230	2.02E-15	2.12E-15	2.37E-15	2.74E-15	3.50E-15	9.71E-15	1.79E-14
TH231	4.18E-12	3.30E-12	3.30E-12	3.30E-12	3.30E-12	3.30E-12	3.30E-12
TH232	1.81E-21	1.94E-21	2.28E-21	2.79E-21	3.84E-21	1.21E-20	2.25E-20
TH234	2.46E-10	2.46E-10	2.46E-10	2.46E-10	2.46E-10	2.46E-10	2.46E-10
PA231	1.00E-15	1.01E-15	1.02E-15	1.03E-15	1.07E-15	1.35E-15	1.70E-15
PA232	1.25E-12	6.49E-18	1.06E-31	0.00E+00	0.00E+00	0.00E+00	0.00E+00
PA233	7.53E-11	7.89E-11	8.28E-11	8.38E-11	8.39E-11	8.45E-11	8.62E-11
PA234M	2.46E-10	2.46E-10	2.46E-10	2.46E-10	2.46E-10	2.46E-10	2.46E-10

Nuclide	7 Days	30 Days	90 Days	180 Days	1 Year	5 Years	10 Years
PA234	3.20E-13	3.20E-13	3.20E-13	3.20E-13	3.20E-13	3.20E-13	3.20E-13
U230	1.16E-17	5.24E-18	3.50E-19	0.00E+00	0.00E+00	0.00E+00	0.00E+00
U231	1.20E-15	2.55E-17	1.28E-21	4.53E-28	0.00E+00	0.00E+00	0.00E+00
U232	1.15E-12	1.26E-12	1.52E-12	1.90E-12	2.61E-12	5.86E-12	7.00E-12
U233	1.98E-15	2.00E-15	2.06E-15	2.15E-15	2.33E-15	3.81E-15	5.67E-15
U234	1.67E-10	1.67E-10	1.67E-10	1.68E-10	1.69E-10	1.77E-10	1.86E-10
U235	3.30E-12	3.30E-12	3.30E-12	3.30E-12	3.30E-12	3.30E-12	3.30E-12
U236	4.20E-11	4.20E-11	4.20E-11	4.20E-11	4.20E-11	4.20E-11	4.21E-11
U237	1.52E-04	1.43E-05	3.26E-08	2.39E-09	2.33E-09	1.92E-09	1.51E-09
U238	2.46E-10	2.46E-10	2.46E-10	2.46E-10	2.46E-10	2.46E-10	2.46E-10
U240	2.35E-11	3.66E-16	3.66E-16	3.66E-16	3.66E-16	3.66E-16	3.66E-16
NP235	1.77E-12	1.70E-12	1.53E-12	1.31E-12	9.46E-13	7.34E-14	3.00E-15
NP236M	1.83E-11	7.52E-19	0.00E+00	0.00E+00	0.00E+00	0.00E+00	0.00E+00
NP236	1.45E-15	1.45E-15	1.45E-15	1.45E-15	1.45E-15	1.45E-15	1.45E-15
NP237	8.25E-11	8.37E-11	8.39E-11	8.39E-11	8.39E-11	8.45E-11	8.62E-11
NP238	1.32E-05	7.10E-09	1.68E-11	1.67E-11	1.67E-11	1.64E-11	1.60E-11
NP239	2.96E-03	3.41E-06	1.24E-08	1.24E-08	1.24E-08	1.24E-08	1.24E-08
NP240M	2.37E-11	3.66E-16	3.66E-16	3.66E-16	3.66E-16	3.66E-16	3.66E-16
PU236	1.76E-10	1.73E-10	1.67E-10	1.57E-10	1.39E-10	5.25E-11	1.56E-11
PU237	2.01E-10	1.42E-10	5.69E-11	1.45E-11	8.68E-13	1.97E-22	1.73E-34
PU238	6.11E-07	6.23E-07	6.46E-07	6.71E-07	6.99E-07	7.03E-07	6.76E-07
PU239	2.33E-07	2.34E-07	2.34E-07	2.34E-07	2.34E-07	2.34E-07	2.34E-07
PU240	3.24E-07	3.24E-07	3.24E-07	3.24E-07	3.24E-07	3.24E-07	3.24E-07
PU241	9.95E-05	9.92E-05	9.84E-05	9.73E-05	9.49E-05	7.83E-05	6.16E-05
PU242	1.34E-09	1.34E-09	1.34E-09	1.34E-09	1.34E-09	1.34E-09	1.34E-09
PU243	2.42E-14	4.01E-17	4.01E-17	4.01E-17	4.01E-17	4.01E-17	4.01E-17
PU244	3.67E-16	3.67E-16	3.67E-16	3.67E-16	3.67E-16	3.67E-16	3.67E-16
PU245	1.44E-14	3.04E-30	0.00E+00	0.00E+00	0.00E+00	0.00E+00	0.00E+00
PU246	2.40E-13	5.52E-14	1.20E-15	3.21E-18	2.41E-23	8.12E-25	8.12E-25
AM239	4.75E-17	5.16E-31	0.00E+00	0.00E+00	0.00E+00	0.00E+00	0.00E+00
AM240	1.82E-11	9.73E-15	2.86E-23	4.58E-36	0.00E+00	0.00E+00	0.00E+00
AM241	5.71E-08	6.71E-08	9.31E-08	1.32E-07	2.10E-07	7.61E-07	1.31E-06
AM242M	3.35E-09	3.35E-09	3.35E-09	3.35E-09	3.34E-09	3.28E-09	3.21E-09
AM242	4.56E-08	3.34E-09	3.33E-09	3.33E-09	3.32E-09	3.26E-09	3.19E-09
AM243	1.24E-08	1.24E-08	1.24E-08	1.24E-08	1.24E-08	1.24E-08	1.24E-08
AM244	5.33E-11	1.88E-27	0.00E+00	0.00E+00	0.00E+00	0.00E+00	0.00E+00
AM245	1.79E-14	3.77E-18	3.31E-18	2.73E-18	1.83E-18	7.71E-20	1.48E-21
AM246	2.40E-13	5.53E-14	1.20E-15	3.81E-18	2.41E-23	8.12E-25	8.12E-25
CM241	9.17E-12	5.89E-12	1.85E-12	3.28E-13	9.26E-15	5.62E-27	0.00E+00
CM242	2.33E-05	2.11E-05	1.64E-05	1.12E-05	5.09E-06	1.30E-08	2.64E-09
CM243	8.85E-09	8.83E-09	8.80E-09	8.75E-09	8.64E-09	7.84E-09	6.94E-09
CM244	1.26E-06	1.26E-06	1.25E-06	1.24E-06	1.21E-06	1.04E-06	8.60E-07
CM245	8.80E-11	8.80E-11	8.80E-11	8.80E-11	8.80E-11	8.80E-11	8.80E-11
CM246	1.65E-11	1.65E-11	1.65E-11	1.65E-11	1.65E-11	1.65E-11	1.65E-11
CM247	4.01E-17	4.01E-17	4.01E-17	4.01E-17	4.01E-17	4.01E-17	4.01E-17

Nuclide	7 Days	30 Days	90 Days	180 Days	1 Year	5 Years	10 Years
CM248	8.05E-17	8.05E-17	8.05E-17	8.05E-17	8.05E-17	8.05E-17	8.05E-17
CM249	8.38E-19	3.42E-19	3.47E-20	1.69E-21	1.26E-24	0.00E+00	0.00E+00
BK249	2.74E-13	2.60E-13	2.29E-13	1.88E-13	1.26E-13	5.32E-15	1.02E-16
BK250	1.83E-18	1.73E-18	1.49E-18	1.17E-18	7.29E-19	4.14E-20	1.47E-20
CF249	6.32E-17	9.65E-17	1.76E-16	2.77E-16	4.32E-16	7.28E-16	7.34E-16
CF250	3.75E-15	3.74E-15	3.70E-15	3.66E-15	3.56E-15	2.88E-15	2.21E-15
CF251	1.99E-17	1.99E-17	1.99E-17	1.99E-17	1.99E-17	1.98E-17	1.97E-17
CF252	3.45E-15	3.39E-15	3.25E-15	3.05E-15	2.67E-15	9.32E-16	2.51E-16
CF253	2.70E-16	1.10E-16	1.12E-17	5.45E-19	4.04E-22	0.00E+00	0.00E+00
CF254	4.35E-18	3.21E-18	1.76E-18	5.59E-19	2.14E-19	1.15E-26	9.40E-36
ES253	2.06E-16	1.85E-16	5.00E-17	3.95E-18	4.73E-19	0.00E+00	0.00E+00
ES254M	5.27E-18	3.12E-22	2.91E-33	0.00E+00	0.00E+00	0.00E+00	0.00E+00
ES254	1.83E-18	1.73E-18	1.47E-18	1.13E-18	7.29E-19	4.14E-20	1.47E-20
TOTAL	1.65E+03	1.15E+03	6.03E+02	3.72E+02	2.55E+02	9.87E+01	4.61E+01

In order to provide the results in Table D1 it was necessary to convert the ORIGEN2 case from a power irradiation to a flux irradiation for the TPBAR. The output file from the input file shown in Appendix B provides an equivalent flux irradiation to the specified power irradiation in the input file. Using this information, it is possible to include the trace uranium in the metal components to generate a complete listing of radionuclides. Table D1 contains a summation of the activation products, the actinides and daughters, and the fission products. A listing of the input file is provided below.

Small_Origen.inp

```
-1
-1
-1
TIT     Prod.  Reactor Target Rod Waste Eval.:  TPBAR
RDA     FLUX=5.16435E14
BAS     1 TPBAR
LIB     0 1 2 3 204 205 206 9 3 0 1 1
PHO     101 102 103 10
LIP     0 0 0
INP     1 1 -1 -1 1 1
BUP
IRF      50.  5.16435E14  1  2  4  2
IRF     100.  5.16435E14  2  3  4  0
IRF     150.  5.16435E14  3  4  4  0
IRF     200.  5.16435E14  4  5  4  0
IRF     250.  5.16435E14  5  6  4  0
IRF     300.  5.16435E14  6  7  4  0
IRF     350.  5.16435E14  7  8  4  0
IRF     400.  5.16435E14  8  9  4  0
IRF     450.  5.16435E14  9 10  4  0
IRF     500.  5.16435E14 10 11  4  0
IRF     510.  5.16435E14 11  1  4  0
BUP
DEC      7.              1  2  4  2
```

```
DEC      30.            2  3  4  0
DEC      90.            3  4  4  0
DEC     180.            4  5  4  0
DEC       1.            5  6  5  0
DEC       5.            6  7  5  0
DEC      10.            7  8  5  0
HED     1   Discharge
HED     2     7 Days
HED     3    30 Days
HED     4    90 Days
HED     5   180 Days
HED     6     1 Year
HED     7     5 Years
HED     8    10 Years
OPTL    8 8 8 8 7 8 7 8 7 8 8 8 8 8 8 8 8 8 8 8 8 8 8 8
OPTA    8 8 8 8 7 8 7 8 8 8 8 8 8 8 8 8 8 8 8 8 8 8 8 8
OPTF    8 8 8 8 7 8 7 8 8 8 8 8 8 8 8 8 8 8 8 8 8 8 8 8
CUT     7 3.0E-17 -1
OUT     8  1  0  -1
STP     4
1        30060 6.48E+00    30070 1.49E+01        0      0.0
2       922340 4.14E-08   922350 5.42E-06   922380 7.48E-04        0      0.0
4       260000 3.50E+02   240000 1.02E+02   280000 3.35E+02    80000 1.02E+02
4       130000 8.66E+01   330000 2.75E-01    50000 1.14E-02   560000 1.68E-01
4        60000 7.12E-01   200000 8.40E-01   480000 1.08E-04   270000 2.87E-01
4       290000 2.37E-01    10000 5.38E-03   720000 2.15E-02   190000 1.05E+00
4       120000 4.24E-01   250000 1.13E+01   420000 1.70E+01    70000 7.37E-02
4       110000 1.05E+00   410000 2.83E-01   150000 2.26E-01   820000 8.40E-02
4       160000 5.65E-02   340000 7.35E-02   140000 6.36E+00   500000 3.66E+00
4       730000 1.13E-01   220000 1.08E-02   230000 2.83E-01   740000 2.15E-02
4       400000 2.10E+02    90000 3.15E-02   170000 3.15E-02   530000 3.15E-02
4       350000 3.15E-02        0      0.0
0
END
```

APPENDIX 1-D

DOE Drawing H-3-307845, "Production TPBAR Reactor Interface Dimensions Watts Bar," Revision 10, Sheet 1 of 2

Figure Withheld Under 10 CFR 2.390

U. S. DEPARTMENT OF ENERGY
HOLLAND OPERATIONS OFFICE
PACIFIC NORTHWEST NATIONAL LABORATORY
OPERATED BY BATTELLE MEMORIAL INSTITUTE

PRODUCTION TPBAR REACTOR
INTERFACE DIMENSIONS WATTS BAR

TRITIUM TECHNOLOGY PROGRAM

D	9803	338	H-3-307845	10
		SCALE 4" = 1"	SHEET 1 OF 2	

UNCLASSIFIED

APPENDIX 1-E

DOE Drawing H-3-308875, "Production TPBAR Reactor Interface Dimensions Sequoyah," Revision 5, Sheet 1 of 2

Figure Withheld Under 10 CFR 2.390

PRODUCTION TPBAR REACTOR
INTERFACE DIMENSIONS SEQUOYAH

TRITIUM TECHNOLOGY PROGRAM

D	5003	338	H-3-308875	5
		SCALE 4" = 1"	SHEET 1 OF 2	

UNCLASSIFIED

APPENDIX 1-F

DOE Drawing H-3-310568, "Mark 8 Multi-Pencil TPBAR – Watts Bar Reactor Interface," Revision 0, Sheet 1 of 2

Figure Withheld Under 10 CFR 2.390

MARK 8 MULTI PENCIL
TPBAR – WATTS BAR
REACTOR INTERFACE

TRITIUM TECHNOLOGY PROGRAM

SIZE	ORDER NO	BLDG NO	DWG NO	REV NO
D	5003	538	H-3-310568	0

SCALE 4" = 1" SHEET 1 OF 2

UNCLASSIFIED

APPENDIX 1-G

PNNL Letter, TTP-06-056, Subject: Exposure of Shipping Casks to Tritium, February 21, 2006

Pacific Northwest National Laboratory
Operated by Battelle for the U.S. Department of Energy

February 21, 2006 TTP-06-056

Ms. Nanette D. Founds
Tritium Readiness Subprogram
Office of Stockpile Technology (NA-123)
Department of Energy/NNSA
PO Box 5400
Albuquerque, NM 87185-5400

Dear Ms. Founds:

EXPOSURE OF SHIPPING CASKS TO TRITIUM

Pacific Northwest National Laboratory was assigned a Tritium Readiness Subprogram Action Item to "Draft position on NRC tritium cask exposure issue" (AI 43). Attached is a white paper summarizing the conclusions we presented during the teleconference with NAC International, Inc.; U.S. Nuclear Regulatory Commission; and National Nuclear Security Administration to complete this action.

If you have any questions regarding the information in this paper, please contact me or Bruce Reid at (509) 372-4135.

Sincerely,
Cheryl K. Thornhill
Cheryl K. Thornhill, Manager
Tritium Technology Program

/bjk
Enclosure

ecc: J. R. Chapman, SAIC
C. J. Rogers, SAIC
M. Holloway, SAIC
cc: J. Adam, NAC
B. G. McLeod, DOE-PNSO
NA-123 RMS/SS (05-10)

902 Battelle Boulevard • P.O. Box 999 • Richland, WA 99352

Telephone 509-375-2532 □ Email cheryl.thornhill@pnl.gov □ Fax 509-375-2610

Nuclear Regulatory Commission Concerns Regarding Shipping Tritium Producing Burnable Absorber Rods in the NAC-LWT Cask

Background

In conversations with NAC licensing personnel in preparation for their submittal of a license amendment request for the NAC-LWT cask to handle future shipments of tritium producing burnable absorber rods (TPBARs), staff from the U.S. Nuclear Regulatory Commission (NRC) expressed some concerns regarding the potential for residual tritium contamination in the crystalline structure of the stainless steel to be an issue for subsequent cask users. While the NRC had no firm calculations, some "back-of-the-envelope" calculations by an NRC materials expert indicated that residual tritium could be an issue of concern for the subsequent cask users who were not expecting tritium contamination.

A conference call was held on January 26, 2006 with representatives of NRC, NNSA, Westinghouse Savannah River Company (WSRC), NAC and Pacific Northwest National Laboratory (PNNL) participating. At the conclusion of the call, NRC was satisfied with the responses received and requested that NAC provide, in Chapter 7 of the NAC-LWT Safety Analysis Report, a discussion of the procedures to be followed when unloading TPBARs and before sending the empty cask back to NAC.

During the conference call, PNNL staff discussed the experience with shipping TPBARs to date and the potential for tritium to permeate from the irradiated TPBARs into the Stainless Steel cask wall.

Transportation Experience

The NRC has licensed the NAC-LWT cask to ship up to 300 TPBARs including 2 pre-failed TPBARs. To date, there have been 9 shipments of TPBARs to various locations as noted below:

- 4 shipments of 8 TPBARs each from Watts Bar Nuclear Plant (WBN) to Idaho National Laboratory (INL) (1999)
- 1 shipment of 3 sectioned TPBARs (12 sections) from INL to PNNL (2000)
- 1 shipment of 6 TPBARs from WBN to INL (2005)
- 1 shipment of 3 TPBARs from INL to PNNL (2005)
- 1 shipment of 215 TPBARs from WBN to the Savannah River Site Tritium Extraction Facility (TEF) (2005)
- 1 shipment of 19 TPBARs from WBN to TEF (2005)

The last two shipments will remain stored at TEF in the NAC-LWT shipping casks until the TEF is ready to process the tritium.

Nuclear Regulatory Commission Concerns Regarding Shipping Tritium Producing Burnable Absorber Rods in the NAC-LWT Cask

Discussion

Prior to opening the casks bearing TPBARs, both INL and PNNL have sampled the gas in the cask cavity to assure that there would not be a tritium release to the environment or to facility personnel. In all cases, the gas samples have tested at negligible levels for tritium (~1E-6 μCi/cc). Also, prior to sending the empty cask back to NAC for use by others, "swipes" of the internal surfaces have been taken to assure that contamination was not present. Samples taken on the consolidation container and the basket within the cask cavity showed tritium levels ranging from ~25 to ~1050 disintegrations per minute per 100 cm^2, well below any levels of concern for contamination. A similar procedure will be followed at TEF when they open and return the NAC-LWT casks. The TPBARs are contained in the stainless steel consolidation container and the basket holds the consolidation container. Both are between the TPBARs and the cask inner wall, thus if contamination is present, it would be noticed first on the consolidation container and basket before it would affect the cask wall.

When the TPBARs at INL were punctured, the gas pressure inside the rod was measured and the gas analyzed. The tritium partial pressure in the gas was below 5 $X10^{-3}$ Pa of T_2 which is ~5 X 10^{-8} atmospheres, i.e., equivalent to a very good vacuum with respect to tritium. Hence, there is little driving force for permeation of the tritium out of the unbreached TPBARs during storage and shipment. With no driving force, there is no mechanism for the tritium to permeate from the TPBARs into the cask inner wall. As noted above, there have been no shipments to date at the licensed limit (300) for TPBARs; however the number of TPBARs in the cask will not change the tritium partial pressure inside the individual TPBAR. The number of TPBARs in the shipment does affect the temperature in the cask cavity (at 30 days after discharge from the reactor, each TPBAR produces ~3.3 watts of decay heat). The temperature that will exist when shipping 300 TPBARs is well below the temperature required to drive the tritium out of the TPBARs to any significant degree within the time frame of expected residence in the cask.

With regard to the two (2) pre-failed TPBARs in a shipment, which is part of the licensing basis for the cask, it is assumed that the failure occurs near the end of the plant operating cycle when the TPBAR has generated the maximum amount of tritium. The isotopic exchange that takes place between the tritium in the TPBAR and the hydrogen in the reactor coolant system (and the spent fuel pool after the TPBARs are discharged from the reactor) is expected to remove essentially all of the tritium from the TPBAR, thus the tritium available to "leak" from the TPBAR to the cask wall is still expected to be negligible. The failed TPBARs will have no internal pressure and any residual tritium would first contact the consolidation container and basket before the cask inner wall is exposed. Another scenario would be damage to two TPBARs during handling in the spent fuel pool while removing the TPBAR base plate from the fuel assembly. In this case, TVA procedures will have the breached TPBAR placed in another tube which can be sealed to prevent further tritium contamination of the spent fuel pool. During the time

it will take to remove the TPBAR from the baseplate, get the secondary tube, and place the TPBAR in the tube, a significant amount of the tritium will have been released to the spent fuel pool through isotopic exchange. Because of the precautions to be taken and the low driving force to move tritium from the TPBAR, contamination of the cask cavity is not expected to be a significant issue. In this scenario, the TPBAR will be enclosed in a secondary tube contained in the consolidation container, so an additional barrier will exist between the TPBAR and the cask wall.

If the tritium partial pressure in the cask did rise to some higher level (we have not performed calculations to determine what pressure would be required) then tritium surface contamination would be expected. Experiments performed by Hirayabashi and Saeki (JNM 120 (1984) 309-315) examined stainless steel coupons after exposing the coupons to relatively high pressure tritium gas (13,300 Pa compared to the $<5X10^{-3}$ Pa found inside of TPBARs at INL). They did find subsurface tritium in the steel after exposure at this pressure. However, it is significant to note that they also found surface concentrations of tritium in the sample almost 2 orders of magnitude greater than the levels in the bulk (i.e. beneath the surface). Hence, extrapolation of these results to the NAC-LWT cask situation would indicate that highly contaminated surface smears would identify that subsurface tritium concentrations of lower levels (~2 orders of magnitude lower) existed. At some level of surface contamination, it is evident from the literature that the surface contamination would indicate there had been enough tritium permeate into the cask wall that subsequent leaching of tritium from the bulk could present a concern for subsequent users. No work has been done to determine what this level of surface contamination is. However, at the low tritium partial pressure in the TPBARs, the risk of achieving a high level of surface contamination is small and, as noted above, there are other stainless steel surfaces between the TPBARs and the cask wall. If an abnormally high level of surface contamination is found, this issue will need to be addressed.

Conclusion

Based on past experience and the above discussion, it is concluded that the potential for tritium contamination of the NAC-LWT cask inner wall is minimal. The steps that will be taken to monitor the cask gas prior to opening the cask and the taking of smears on the internal surfaces will provide assurance that residual tritium contamination is not an issue of concern for subsequent users.

Table of Contents

2 STRUCTURAL EVALUATION 2-1
2.1 Structural Design 2.1.1-1
2.1.1 Discussion 2.1.1-1
2.1.2 Basic Design Criteria 2.1.2-1
2.1.2.1 Containment Structures 2.1.2-1
2.1.2.2 Noncontainment Structures 2.1.2-1
2.1.3 Miscellaneous Structural Failure Modes 2.1.3-1
2.1.3.1 Brittle Fracture 2.1.3-1
2.1.3.2 Fatigue – Normal Operating Cycles 2.1.3-1
2.1.3.3 Extreme Total Stress Intensity Range 2.1.3-5
2.1.3.4 Buckling 2.1.3-5
2.2 Weights and Centers of Gravity 2.2.1-1
2.2.1 Major Component Statistics 2.2.1-1
2.3 Properties of Materials 2.3.1
2.3.1 Mechanical Properties of Materials 2.3.1-1
2.3.1.1 Cask Body Materials 2.3.1-1
2.3.1.2 Port Cover Materials 2.3.1-1
2.3.1.3 Fuel Basket Materials 2.3.1-1
2.3.1.4 Bolting Material 2.3.1-2
2.3.1.5 Shielding Material (Gamma Radiation) 2.3.1-2
2.4 General Standards for All Packages 2.4-1
2.4.1 Minimum Package Size 2.4.1-1
2.4.2 Tamperproof Feature 2.4.2-1
2.4.3 Positive Closure 2.4.3-1
2.4.4 Chemical and Galvanic Reactions 2.4.4-1
2.4.5 Cask Design 2.4.5-1
2.4.6 Continuous Venting 2.4.6-1
2.5 Lifting and Tiedown Standards 2.5.1-1
2.5.1 Lifting Devices 2.5.1-1
2.5.1.1 Lifting Trunnion 2.5.1-1
2.5.1.2 Lid Lifting Bolts 2.5.1-7
2.5.1.3 Can Assembly (315-40-98) 2.5.1-8
2.5.2 Tiedown Devices 2.5.2-1
2.5.2.1 Discussion and Loads 2.5.2-1
2.5.2.2 Rear Support 2.5.2-5
2.5.2.3 Front Support 2.5.2-11
2.6 Normal Conditions of Transport 2.6.1-1
2.6.1 Hot Case 2.6.1-1
2.6.1.1 Discussion 2.6.1-1
2.6.1.2 Analysis Description 2.6.1-1
2.6.1.3 Detailed Analysis 2.6.1-2
2.6.1.4 Conclusion 2.6.1-3
2.6.2 Cold Case 2.6.2-1

Table of Contents (continued)

2.6.2.1 Discussion 2.6.2-1
2.6.2.2 Analysis Description 2.6.2-1
2.6.2.3 Detailed Analysis 2.6.2-2
2.6.2.4 Conclusion 2.6.2-3
2.6.3 Reduced External Pressure 2.6.3-1
2.6.4 Increased External Pressure 2.6.4-1
2.6.5 Vibration 2.6.5-1
2.6.6 Water Spray 2.6.6-1
2.6.7 Free Drop (1 Foot) 2.6.7-1
2.6.7.1 End Drop (1 Foot) 2.6.7-1
2.6.7.2 Side Drop (1 Foot) 2.6.7-2
2.6.7.3 Corner Drop (1 Foot) 2.6.7-3
2.6.7.4 Impact Limiters 2.6.7-4
2.6.7.5 Closure Lid 2.6.7-22
2.6.7.6 Bolts – Closure Lid (Normal Conditions of Transport) 2.6.7-24
2.6.7.7 Neutron Shield Tank 2.6.7-26
2.6.7.8 Expansion Tank 2.6.7-41
2.6.7.9 Upper Ring/Outer Shell Intersection Analysis 2.6.7-44
2.6.7.10 PWR/BWR Rod Transport Canister Assembly Analysis 2.6.7-48
2.6.8 Corner Drop 2.6.8-1
2.6.9 Compression 2.6.9-1
2.6.10 Penetration 2.6.10-1
2.6.10.1 Impact Limiter – Penetration 2.6.10-1
2.6.10.2 Expansion Tank – Penetration 2.6.10-1
2.6.10.3 Neutron Shield Tank – Penetration 2.6.10-5
2.6.10.4 Port Cover – Penetration 2.6.10-6
2.6.10.5 Alternate Port Cover – Penetration 2.6.10-8
2.6.11 Fabrication Conditions 2.6.11-1
2.6.11.1 Lead Pour 2.6.11-1
2.6.11.2 Cooldown 2.6.11-3
2.6.11.3 Lead Creep 2.6.11-12
2.6.12 Fuel Basket Analysis 2.6.12-1
2.6.12.1 Discussion 2.6.12-1
2.6.12.2 PWR Basket Construction 2.6.12-1
2.6.12.3 PWR Basket Analysis 2.6.12-2
2.6.12.4 BWR Basket Construction 2.6.12-4
2.6.12.5 Metallic Fuel Basket Construction 2.6.12-5
2.6.12.6 MTR Fuel Basket Construction 2.6.12-7
2.6.12.7 TRIGA Fuel Basket One-Foot Drop Evaluation 2.6.12-26
2.6.12.8 DIDO Fuel Basket Construction 2.6.12-53
2.6.12.9 General Atomics IFM Basket Construction 2.6.12-62
2.6.12.10 TPBAR Basket Analysis 2.6.12-71
2.6.12.11 ANSTO Basket Analysis 2.6.12-85

Table of Contents (continued)

2.6.12.12 TPBAR Basket with the PWR/BWR Rod Transport Canister 2.6.12.92
2.6.12.13 Conclusion 2.6.12-95
2.7 Hypothetical Accident Conditions 2.7-1
2.7.1 Free Drop (30 Feet) 2.7.1-1
2.7.1.1 End Drop 2.7.1-2
2.7.1.2 Side Drop 2.7.1-5
2.7.1.3 Oblique Drops 2.7.1-10
2.7.1.4 Shielding for Lead Slump Accident 2.7.1-18
2.7.1.5 Bolts - Closure Lid (Hypothetical Accident - Free Drop) 2.7.1-19
2.7.1.6 Crush 2.7.1-20
2.7.1.7 Rod Shipment Can Assembly Analysis 2.7.1-21
2.7.2 Puncture 2.7.2-1
2.7.2.1 Puncture - Cask Side Midpoint 2.7.2-1
2.7.2.2 Puncture - Center of Cask Closure Lid 2.7.2-3
2.7.2.3 Puncture - Center of Cask Bottom 2.7.2-6
2.7.2.4 Puncture - Port Cover 2.7.2-9
2.7.2.5 Puncture Accident - Shielding Consequences 2.7.2-17
2.7.2.6 Puncture - Conclusion 2.7.2-17
2.7.3 Fire 2.7.3-1
2.7.3.1 Discussion 2.7.3-1
2.7.3.2 Thermal Stress Evaluation 2.7.3-1
2.7.3.3 Bolts - Closure Lid (Hypothetical Accident - Fire) 2.7.3-3
2.7.3.4 Inner Shell Evaluation 2.7.3-4
2.7.3.5 Conclusion 2.7.3-5
2.7.4 Immersion - Fissile Material 2.7.4-1
2.7.5 Immersion – Irradiated Nuclear Fuel Packages 2.7.5-1
2.7.5.1 Method of Analysis 2.7.5-1
2.7.5.2 Closure Lid Stresses 2.7.5-1
2.7.5.3 Outer Bottom Head Forging Stresses 2.7.5-2
2.7.5.4 Cask Cylindrical Shell Stresses 2.7.5-3
2.7.5.5 Containment Seal Evaluation 2.7.5-5
2.7.6 Damage Summary 2.7.6-1
2.7.7 Fuel Basket Accident Analysis 2.7.7-1
2.7.7.1 Discussion 2.7.7-1
2.7.7.2 PWR Basket Construction 2.7.7-1
2.7.7.3 PWR Basket Analysis 2.7.7-1
2.7.7.4 BWR Basket Construction 2.7.7-3
2.7.7.5 Metallic Fuel Basket Analysis 2.7.7-6
2.7.7.6 MTR Fuel Basket Construction 2.7.7-8
2.7.7.7 Conclusion 2.7.7-18
2.7.7.8 PWR Spacer 2.7.7-18
2.7.7.9 TRIGA Fuel Basket Thirty-Foot Drop Evaluation 2.7.7-24

Table of Contents (continued)

2.7.7.10 DIDO Fuel Basket Construction 2.7.7-48
2.7.7.11 General Atomics IFM Basket Construction 2.7.7-53
2.7.7.12 TPBAR Basket Analysis 2.7.7-56
2.7.7.13 ANSTO Basket Analysis 2.7.7-68
2.7.7.14 TPBAR Basket with the PWR/BWR Rod Transport Canister 2.7.7-72
2.8 Special Form 2.8-1
2.9 Spent Fuel Contents 2.9-1
2.9.1 PWR and BWR Fuel Rods 2.9-1
2.9.2 TRIGA Fuel Elements 2.9-1
2.9.2.1 End Drop 2.9-2
2.9.2.2 Side Drop 2.9-3
2.9.3 PULSTAR Intact Fuel Elements 2.9-5
2.9.4 ANSTO Fuels 2.9-6
2.9.4.1 MARK III Spiral Fuel Assemblies 2.9-6
2.9.4.2 MOATA Plate Bundles 2.9-10
2.9.4.3 DIDO Fuel Assemblies 2.9-14
2.10 Appendices 2.10.1-1
2.10.1 Computer Program Descriptions 2.10.1-1
2.10.1.1 ANSYS 2.10.1-1
2.10.1.2 RBCUBED - A Program to Calculate Impact Limiter Dynamics 2.10.1-2
2.10.2 Finite Element Model Description 2.10.2-1
2.10.2.1 Boundary and Loading Conditions Used in the 30-Foot Drop Finite Element Analysis 2.10.2-2
2.10.3 Finite Element Evaluations 2.10.3-1
2.10.3.1 Isothermal Plot - Hot Case 2.10.3-1
2.10.3.2 Isothermal Plot - Cold Case 2.10.3-1
2.10.3.3 Determination of Component Critical Stresses 2.10.3-1
2.10.4 Oblique Drop Slapdown 2.10.4-1
2.10.4.1 Discussion 2.10.4-1
2.10.4.2 Analysis 2.10.4-1
2.10.4.3 Energy Calculation 2.10.4-3
2.10.4.4 Rotational Velocity Change 2.10.4-4
2.10.5 Lead Slump - End Drop 2.10.5-1
2.10.6 Inner Shell Buckling Design Criteria and Evaluation 2.10.6-1
2.10.6.1 Code Case N-284 ..... 2.10.6-1
2.10.6.2 Theoretical Elastic Buckling Stresses 2.10.6-1
2.10.6.3 Capacity Reduction Factors 2.10.6-2
2.10.6.4 Plasticity Reduction Factors 2.10.6-3
2.10.6.5 Upper Bound Magnitudes for Compressive Stresses and In-Plane Shear Stresses 2.10.6-3
2.10.6.6 Interaction Equations 2.10.6-4
2.10.6.7 Detailed Buckling Evaluation - Sample Calculation 2.10.6-4

Table of Contents (continued)

2.10.6.8 Conclusion 2.10.6-7
2.10.7 Detailed Finite Element Stress Summary 2.10.7-1
2.10.7.1 Finite Element Stress Tables – Normal Operation Hot Condition 2.10.7-1
2.10.7.2 Finite Element Stress Tables - Normal Operation Cold Condition 2.10.7-1
2.10.7.3 Finite Element Stress Tables – 1-Foot End Drop 2.10.7-1
2.10.7.4 Finite Element Stress Tables – 1-Foot Side Drop 2.10.7-1
2.10.7.5 Finite Element Stress Tables – 1-Foot Corner Drop 2.10.7-1
2.10.7.6 Finite Element Stress Tables – 30-Foot End Drop 2.10.7-1
2.10.7.7 Finite Element Stress Tables – 30-Foot Side Drop 2.10.7-1
2.10.7.8 Finite Element Stress Tables – 30-Foot Oblique Drop 2.10.7-2
2.10.8 Quarter-Scale Model Drop Test Program for the NAC-LWT Cask 2.10.8-1
2.10.8.1 Introduction 2.10.8-1
2.10.8.2 Purpose 2.10.8-1
2.10.8.3 Summary 2.10.8-1
2.10.8.4 Description of Quarter-Scale LWT Cask Model 2.10.8-4
2.10.8.5 Description of Test Procedures and Instrumentation 2.10.8-5
2.10.8.6 Detailed Test Results 2.10.8-7
2.10.8.7 Metrology Results 2.10.8-14
2.10.8.8 Discussion of Test Results 2.10.8-15
2.10.8.9 Post-Test Revisions 2.10.8-17
2.10.9 Bolts – Closure Lid (Stress Evaluations) 2.10.9-1
2.10.9.1 Analysis Approach 2.10.9-1
2.10.9.2 Closure Bolt Analyses – Analytics and Assumptions 2.10.9-2
2.10.10 Finite Element Stress Results for the 30-Foot Drop Accident Conditions 2.10.10-1
2.10.10.1 Discussion 2.10.10-1
2.10.10.2 Procedures 2.10.10-1
2.10.10.3 Analysis and Results 2.10.10-3
2.10.10.4 Conclusion 2.10.10-6
2.10.11 Hand Calculation for the 30-Foot Drop Accident Conditions 2.10.11-1
2.10.11.1 Top End Drop 2.10.11-1
2.10.11.2 Side Drop 2.10.11-2
2.10.12 Impact Limiter Force-Deflection Curves and Data 2.10.12-1
2.10.12.1 Potential Energy and Cask Drop Motion 2.10.12-1
2.10.12.2 Potential to Kinetic Energy Conversion 2.10.12-3
2.10.12.3 Deceleration Forces and Energy Absorption Calculation 2.10.12-4
2.10.12.4 RBCUBED Calculated Force-Deflection Graphs 2.10.12-7
2.10.12.5 Quarter-Scale Model Quasi-Static Force-Deflection Tests 2.10.12-7

Table of Contents (continued)

2.10.13 Structural Evaluation of Failed Fuel Cans and Liners (Baskets) 2.10.13-1
2.10.13.1 Discussion 2.10.13-1
2.10.13.2 Method of Analysis 2.10.13-1
2.10.13.3 Input Geometry & Data 2.10.13-2
2.10.13.4 Mechanical Properties of Materials 2.10.13-3
2.10.13.5 Thermal Evaluation 2.10.13-3
2.10.13.6 Structural Evaluation 2.10.13-3
2.10.13.7 Results and Conclusion 2.10.13-11
2.10.13.8 Failed Fuel Shipment Component Drawings 2.10.13-12
2.10.14 Structural Evaluation of the NAC-LWT Cask Body with TPBAR Contents 2.10.14-1
2.10.14.1 Normal Conditions of Transport for Cask Body with TPBAR Contents 2.10.14-1
2.10.14.2 Hypothetical Accident Conditions for Cask Body with TPBAR Contents 2.10.14-3
2.10.14.3 Inner Shell Buckling 2.10.14-4
2.10.14.4 NAC-LWT Cask Closure Lid and Bolts 2.10.14-5
2.10.14.5 Conclusion 2.10.14-6
2.10.15 NAC-LWT Alternate B Port Cover 2.10.15-1
2.10.15.1 Alternate B Port Cover Bolt Analysis 2.10.15-1
2.10.16 Structural Evaluation of the NAC-LWT Cask Body with TPBARs in the PWR/BWR Rod Transport Canister 2.10.16-1
2.10.16.1 Normal Conditions of Transport for Cask Body and TPBARS in the PWR/BWR Rod Transport Canister 2.10.16-1
2.10.16.2 Hypothetical Accident Conditions for Cask Body with TPBARS and the PWR/BWR Rod Transport Canister 2.10.16-2
2.10.16.3 Inner Shell Buckling 2.10.16-3
2.10.16.4 NAC-LWT Cask Closure Lid and Bolts 2.10.16-4
2.10.16.5 Conclusion 2.10.16-5

List of Figures

Figure 2.1.3-1 Design Fatigue Curve for High Strength Steel Bolting 2.1.3-7
Figure 2.3.1-1 Static Stress-Strain Curve for Chemical Copper Lead 2.3.1-3
Figure 2.3.1-2 Dynamic Deformation Stress-Strain Curve for Chemical Copper Lead 2.3.1-4
Figure 2.5.1-1 Trunnion Cross-Section and Forging Shear Area 2.5.1-10
Figure 2.5.2-1 Front Support and Tiedown Geometry 2.5.2-13
Figure 2.5.2-2 Pressure Distribution of Horizontal Bearing Between Cask and Support Saddle 2.5.2-14
Figure 2.5.2-3 Free Body Diagram of Cask Subjected to Lateral Load 2.5.2-15
Figure 2.5.2-4 Rotation Trunnion Pocket 2.5.2-16
Figure 2.6.1-1 NAC-LWT Cask Critical Sections (Hot Case) 2.6.1-4
Figure 2.6.2-1 NAC-LWT Cask Critical Sections (Cold Case) 2.6.2-4
Figure 2.6.7-1 1-Foot Bottom End Drop with 130°F Ambient Temperature and Maximum Decay Heat Load 2.6.7-61
Figure 2.6.7-2 1-Foot Bottom End Drop with -40°F Ambient Temperature and Maximum Decay Heat Load 2.6.7-62
Figure 2.6.7-3 1-Foot Bottom End Drop with -40°F Ambient Temperature and No Decay Heat Load 2.6.7-63
Figure 2.6.7-4 1-Foot Top End Drop with 130°F Ambient Temperature and Maximum Decay Heat Load 2.6.7-64
Figure 2.6.7-5 1-Foot Top End Drop with -40°F Ambient Temperature and Maximum Decay Heat Load 2.6.7-65
Figure 2.6.7-6 NAC-LWT Cask Critical Sections (1-Foot Side Drop with 100°F Ambient Temperature) 2.6.7-66
Figure 2.6.7-7 1-Foot Top Corner Drop with 130°F Ambient Temperature and Maximum Decay Heat Load - Drop Orientation = 15.74 Degrees 2.6.7-67
Figure 2.6.7-8 1-Foot Bottom Corner Drop with 130°F Ambient Temperature and Maximum Decay Heat Load - Drop Orientation = 15.74 Degrees 2.6.7-68
Figure 2.6.7-9 1-Foot Top Corner Drop with -40°F Ambient Temperature and No Decay Heat Load - Drop Orientation = 15.74 Degrees 2.6.7-69
Figure 2.6.7-10 NAC-LWT Cask with Impact Limiters 2.6.7-70
Figure 2.6.7-11 Cross-Section of Top Impact Limiter 2.6.7-71
Figure 2.6.7-12 Load Versus Deflection Curve (Typical Aluminum Honeycomb) 2.6.7-72
Figure 2.6.7-13 Quarter-Scale Model Limiter End Drop Cross-Section 2.6.7-73
Figure 2.6.7-14 End Drop Impact Limiter Cross-Section 2.6.7-74
Figure 2.6.7-15 Impact Limiter Lug Detail 2.6.7-75
Figure 2.6.7-16 Cask Lug Detail 2.6.7-76
Figure 2.6.7-17 RBCUBED Output Summary – Center of Gravity Over Top Corner 2.6.7-77
Figure 2.6.7-18 Free Body Diagram - Top Impact Limiter - Center of Gravity Over Corner 2.6.7-78
Figure 2.6.7-19 Free Body Diagram - Top Impact Limiter - Cask Wedging Forces 2.6.7-79
Figure 2.6.7-20 Cask Lid Configuration 2.6.7-80
Figure 2.6.7-21 Closure Lid Free Body Diagram 2.6.7-81

List of Figures (continued)

Figure 2.6.7-22 NAC-LWT Cask Cross-Section 2.6.7-82
Figure 2.6.7-23 Component Parts of Shield Tank Structure 2.6.7-83
Figure 2.6.7-24 Shield Tank Cross-Section 2.6.7-84
Figure 2.6.7-25 Shield Tank Quarter-Section Geometry 2.6.7-85
Figure 2.6.7-26 Partial Bottom/Top End Plate Plan and Cross-Section 2.6.7-86
Figure 2.6.7-27 Shield Tank End Plate 2.6.7-87
Figure 2.6.7-28 Gusset Profile 2.6.7-88
Figure 2.6.7-29 End Plate Welds 2.6.7-89
Figure 2.6.7-30 Component Parts of the Expansion Tank Structure 2.6.7-90
Figure 2.6.7-31 Expansion Tank Top and Bottom End Plate 2.6.7-91
Figure 2.6.7-32 Expansion Tank Stiffener Load Geometry 2.6.7-92
Figure 2.6.7-33 Cask Upper Ring at Trunnion - ANSYS Model 2.6.7-93
Figure 2.6.7-34 Cask Upper Ring at Trunnion - Model Loads and Boundary Conditions 2.6.7-94
Figure 2.6.7-35 NACAC-LWT Cask Upper Ring at Trunnion - Critical Sections 2.6.7-95
Figure 2.6.10-1 Impact of Penetration Cylinder on Neutron Shield Tank and Expansion Tank – Points of Impact 2.6.10-12
Figure 2.6.10-2 Impact of Penetration Cylinder on Neutron Shield Tank and Expansion Tank – Details for Analysis 2.6.10-13
Figure 2.6.10-3 Impact of Penetration Cylinder on Port Cover 2.6.10-14
Figure 2.6.10-4 One-Sixth Model of the Alternate Port Cover – 60° Symmetry 2.6.10-15
Figure 2.6.12-1 Cask Side Drop Fuel Tube Loading – MTR Fuel Basket 2.6.12-24
Figure 2.6.12-2 Baseplate Supports for Cask End Drop Loads - MTR Fuel Basket 2.6.12-25
Figure 2.6.12-3 DIDO Fuel Basket Module Structural Model – Top View 2.6.12-57
Figure 2.6.12-4 DIDO Fuel Basket Module Structural Model – Bottom View 2.6.12-58
Figure 2.6.12-5 DIDO Fuel Basket Module Maximum Stress Locations for the Side Drop Orientation 2.6.12-59
Figure 2.6.12-6 DIDO Fuel Basket Module Maximum Stress Locations for the End Drop Orientation 2.6.12-60
Figure 2.6.12-7 Cross-Section of TPBAR Basket 2.6.12-83
Figure 2.6.12-8 TPBAR Spacer Schematic Triangular Top Plate and Tube 2.6.12-84
Figure 2.7.1-1 30-Foot Bottom End Drop with 130°F Ambient Temperature and Maximum Decay Heat Load 2.7.1-30
Figure 2.7.1-2 30-Foot Bottom End Drop with -40°F Ambient Temperature and Maximum Decay Heat Load 2.7.1-31
Figure 2.7.1-3 30-Foot Bottom End Drop with -40°F Ambient Temperature and No Decay Heat Load 2.7.1-32
Figure 2.7.1-4 30-Foot Top End Drop with 130°F Ambient Temperature and Maximum Decay Heat Load 2.7.1-33
Figure 2.7.1-5 30-Foot Top End Drop with -40°F Ambient Temperature and Maximum Decay Heat Load 2.7.1-34
Figure 2.7.1-6 Circumferential Load Distribution for Cask Side Drop Impact 2.7.1-35

List of Figures (continued)

Figure 2.7.1-7	Six Term Fourier Series Representation of Circumferential Load Distribution for Cask Side Drop Impact	2.7.1-36
Figure 2.7.1-8	NAC-LWT Cask Critical Sections (30-Foot Side Drop with 100°F Ambient Temperature)	2.7.1-37
Figure 2.7.1-9	Circumferential Load Distribution for Cask Oblique Drop Impact	2.7.1-38
Figure 2.7.1-10	30-Foot Top Corner Drop with 130°F Ambient Temperature - Drop Orientation = 15.74 Degrees	2.7.1-39
Figure 2.7.1-11	30-Foot Top Oblique Drop with 130°F Ambient Temperature - Drop Orientation = 30 Degrees	2.7.1-40
Figure 2.7.1-12	30-Foot Top Oblique Drop with 130°F Ambient Temperature - Drop Orientation = 45 Degrees	2.7.1-41
Figure 2.7.1-13	30-Foot Oblique Drop with 130°F Ambient Temperature - Drop Orientation = 60 Degrees	2.7.1-42
Figure 2.7.1-14	30-Foot Top Corner Drop with -40°F Ambient Temperature - Drop Orientation = 15.74 Degrees	2.7.1-43
Figure 2.7.1-15	30-Foot Top Oblique Drop with -40°F Ambient Temperature - Drop Orientation = 30 Degrees	2.7.1-44
Figure 2.7.1-16	30-Foot Top Oblique Drop with -40°F Ambient Temperature - Drop Orientation = 45 Degrees	2.7.1-45
Figure 2.7.1-17	30-Foot Top Oblique Drop with -40°F Ambient Temperature - Drop Orientation = 60 Degrees	2.7.1-46
Figure 2.7.1-18	30-Foot Bottom Oblique Drop with 130°F Ambient Temperature – Drop Orientation = 15.74 Degrees	2.7.1-47
Figure 2.7.1-19	30-Foot Bottom Oblique Drop with 130°F Ambient Temperature - Drop Orientation = 30 Degrees	2.7.1-48
Figure 2.7.1-20	30-Foot Bottom Oblique Drop with 130°F Ambient Temperature - Drop Orientation = 45 Degrees	2.7.1-49
Figure 2.7.1-21	30-Foot Bottom Oblique Drop with 130°F Ambient Temperature - Drop Orientation = 60 Degrees	2.7.1-50
Figure 2.7.1-22	Sectional Stress Plot - 30-Foot Bottom Oblique Drop with 130°F Ambient Temperature - Drop Orientation = 60 Degrees	2.7.1-51
Figure 2.7.1-23	Sectional Stress Plot (P_m) – 30-Foot Bottom Oblique Drop with 130°F Ambient Temperature - Drop Orientation = 60 Degrees	2.7.1-52
Figure 2.7.1-24	Sectional Stress Plot ($P_m + P_b$) - 30-Foot Bottom Oblique Drop with 130°F Ambient Temperature - Drop Orientation = 60 Degrees	2.7.1-53
Figure 2.7.1-25	Bottom Closure Plate - Section Cut Identification	2.7.1-54
Figure 2.7.1-26	Sectional Stress Plot - 30-Foot Bottom Oblique Drop with 130°F Ambient Temperature - Drop Orientation = 45 Degrees	2.7.1-55
Figure 2.7.1-27	Sectional Stress Plot - 30-Foot Bottom Oblique Drop with 130°F Ambient Temperature - Drop Orientation = 30 Degrees	2.7.1-56
Figure 2.7.2-1	NAC-LWT Cask Midpoint Section	2.7.2-18
Figure 2.7.2-2	Cask Lid Configuration	2.7.2-19
Figure 2.7.2-3	NAC-LWT Cask Bottom Design Configuration	2.7.2-20

List of Figures (continued)

Figure 2.7.2-4 Port Cover Geometry 2.7.2-21
Figure 2.7.2-5 Puncture of Cask at Valve Cover Region 2.7.2-22
Figure 2.7.2-6 Alternate Port Cover Thermal Analysis Geometry 2.7.2-23
Figure 2.7.7-1 PWR Spacer Geometry 2.7.7-23
Figure 2.9.4-1 DIDO Fuel Assembly Model and Boundary Conditions 2.9-19
Figure 2.9.4-2 DIDO Stress Intensities for 30-Foot Side Drop 2.9-20
Figure 2.10.2-1 ANSYS Finite Element Model – NAC-LWT Cask 2.10.2-5
Figure 2.10.2-2 Cask Bottom of Model 2.10.2-6
Figure 2.10.2-3 Inner, Lead and Outer Shells – Lower Region of Model 2.10.2-7
Figure 2.10.2-4 Inner, Lead and Outer Shells – Lower Middle Region of Model 2.10.2-8
Figure 2.10.2-5 Inner, Lead and Outer Shell – Upper Middle Region of Model 2.10.2-9
Figure 2.10.2-6 Inner, Lead and Outer Shells – Upper Region of Model 2.10.2-10
Figure 2.10.2-7 Upper Ring Forging on Model 2.10.2-11
Figure 2.10.2-8 Closure Lid on Model 2.10.2-12
Figure 2.10.2-9 ANSYS Finite Element Model – Component Identification 2.10.2-13
Figure 2.10.3-1 NAC-LWT Cask Isotherms (Hot Case) 2.10.3-3
Figure 2.10.3-2 NAC-LWT Cask Isotherms (Cold Case) 2.10.3-4
Figure 2.10.3-3 Stress Contour Plot – Hot Case 2.10.3-5
Figure 2.10.4-1 Cask Slapdown Geometry 2.10.4-6
Figure 2.10.4-2 Force Deflection Curve of Drop Tested Limiter – 0-Degree Impact 2.10.4-7
Figure 2.10.4-3 Force Deflection Curve of Drop Tested Limiter – 14-Degree Impact 2.10.4-8
Figure 2.10.4-4 Force Deflection Curve of Drop Tested Limiter – 90 Degree Impact 2.10.4-9
Figure 2.10.4-5 Oblique Drop 2.10.4-10
Figure 2.10.7-1 Representative Section Cut Diagram 2.10.7-3
Figure 2.10.8-1 Drawing of Quarter-Scale Model 2.10.8-19
Figure 2.10.8-2 Drawing of Model Body 2.10.8-20
Figure 2.10.8-3 Drawing of Model Lid 2.10.8-23
Figure 2.10.8-4 Drawing of Model Upper Impact Limiter 2.10.8-24
Figure 2.10.8-5 Drawing of Model Lower Impact Limiter 2.10.8-25
Figure 2.10.8-6 Drawing of Model Simulated Cask Contents 2.10.8-26
Figure 2.10.8-7 Quarter-Scale Model 2.10.8-27
Figure 2.10.8-8 Model Rigged for 30-Foot End Drop 2.10.8-28
Figure 2.10.8-9 Model Positioned for 30-Foot End Drop 2.10.8-29
Figure 2.10.8-10 Model Position Following 30-Foot End Drop 2.10.8-30
Figure 2.10.8-11 Top End Impact Limiter Following 30-Foot End Drop 2.10.8-31
Figure 2.10.8-12 Exterior of Top Impact Limiter Following 30-Foot End Drop 2.10.8-32
Figure 2.10.8-13 Model Rigged for 30-Foot Corner Drop 2.10.8-33
Figure 2.10.8-14 Model Positioned for 30-Foot Corner Drop 2.10.8-34
Figure 2.10.8-15 Model Following 30-Foot Corner Drop 2.10.8-35
Figure 2.10.8-16 Top Impact Limiter Following 30-Foot Corner Drop 2.10.8-36
Figure 2.10.8-17 Model Position Following 30-Foot Side Drop – View 1 ..... 2.10.8-37
Figure 2.10.8-18 Model Position Following 30-Foot Side Drop – View 2 ..... 2.10.8-38
Figure 2.10.8-19 Top Impact Limiter Following 30-Foot Side Drop 2.10.8-39

List of Figures (continued)

Figure 2.10.8-20 Bottom Impact Limiter Following 30-Foot Side Drop – View 1 ..... 2.10.8-40
Figure 2.10.8-21 Bottom Impact Limiter Following 30-Foot Side Drop – View 2 ..... 2.10.8-41
Figure 2.10.8-22 Model Rigged for 30-Foot Oblique Drop 2.10.8-42
Figure 2.10.8-23 Model Positioned for 30-Foot Oblique Drop 2.10.8-43
Figure 2.10.8-24 Model Position Following 30-Foot Oblique Drop 2.10.8-44
Figure 2.10.8-25 Bottom Impact Limiter Following 30-Foot Oblique Drop 2.10.8-45
Figure 2.10.8-26 Top Impact Limiter Following 30-Foot Oblique Drop 2.10.8-46
Figure 2.10.8-27 Model Rigged for Midpoint 40-Inch Pin Drop 2.10.8-47
Figure 2.10.8-28 Model Positioned for 40-Inch Pin Drop 2.10.8-48
Figure 2.10.8-29 Instant Before Midpoint 40-Inch Pin Drop 2.10.8-49
Figure 2.10.8-30 Model Position Following Midpoint 40-Inch Pin Drop 2.10.8-50
Figure 2.10.8-31 Impact Location – Midpoint 40-Inch Pin Drop 2.10.8-51
Figure 2.10.8-32 Angular Orientation of Instrumentation 2.10.8-52
Figure 2.10.8-33 Strain Gauge Time History for Channel 3 – End Drop 2.10.8-53
Figure 2.10.8-34 Strain Gauge Time History for Channel 4 – End Drop 2.10.8-54
Figure 2.10.8-35 Strain Gauge Time History for Channel 5 – End Drop 2.10.8-55
Figure 2.10.8-36 Strain Gauge Time History for Channel 3 – Side Drop 2.10.8-56
Figure 2.10.8-37 Strain Gauge Time History for Channel 4 – Side Drop 2.10.8-57
Figure 2.10.8-38 Strain Gauge Time History for Channel 5 – Side Drop 2.10.8-58
Figure 2.10.8-39 Location of Block Sets 2.10.8-59
Figure 2.10.10-1 Stress Point Locations 2.10.10-7
Figure 2.10.11-1 Mathmatical Model of NAC-LWT Cask (30-foot Top End Impact 2.10.11-8
Figure 2.10.12-1 Side Drop ($\theta = 90°$) 2.10.12-9
Figure 2.10.12-2 End Drop ($0° \leq \theta < 15°$) 2.10.12-10
Figure 2.10.12-3 Oblique Drop ($15° \leq \theta < 90°$) 2.10.12-11
Figure 2.10.12-4 Force Deflection Graph (0-Degree, Top End Drop) 2.10.12-12
Figure 2.10.12-5 Force-Deflection Graph (0-Degree, Bottom-End Drop) 2.10.12-13
Figure 2.10.12-6 Force-Deflection Graph (15.74-Degree, Top Corner Drop) 2.10.12-14
Figure 2.10.12-7 Force-Deflection Graph (14.5-Degree, Bottom Corner Drop) 2.10.12-15
Figure 2.10.12-8 Force-Deflection Graph (30-Degree, Top Oblique Drop) 2.10.12-16
Figure 2.10.12-9 Force-Deflection Graph (30-Degree, Bottom Oblique Drop) 2.10.12-17
Figure 2.10.12-10 Force-Deflection Graph (45-Degree, Top Oblique Drop) 2.10.12-18
Figure 2.10.12-11 Force-Deflection Graph (45-Degree, Bottom Oblique Drop) 2.10.12-19
Figure 2.10.12-12 Force-Deflection Graph (60-Degree, Top Oblique Drop) 2.10.12-20
Figure 2.10.12-13 Force-Deflection Graph (60-Degree, Bottom Oblique Drop) 2.10.12-21
Figure 2.10.12-14 Force-Deflection Graph (75-Degree, Top Oblique Drop) 2.10.12-22
Figure 2.10.12-15 Force-Deflection Graph (75-Degree, Bottom Oblique Drop) 2.10.12-23
Figure 2.10.12-16 Force-Deflection Graph (90-Degree, Top Side Drop) 2.10.12-24
Figure 2.10.12-17 Force-Deflection Graph (90-Degree, Bottom Side Drop) 2.10.12-25
Figure 2.10.12-18 Force-Deflection Curve (0-Degree Impact, Drop Tested Limiter) 2.10.12-26
Figure 2.10.12-19 Force-Deflection Curve (14-Degree Impact, Drop Tested Limiter) .. 2.10.12-27
Figure 2.10.12-20 Force-Deflection Curve (90-Degree Impact, Drop Tested Limiter) .. 2.10.12-28
Figure 2.10.12-21 End Drop Impact Limiter Cross Section 2.10.12-29

List of Figures (continued)

Figure 2.10.13-1 LWT Cask, Metal Fuel Basket Assembly Safety Analysis Report, NAC Drawing No. 315-40-12 ..... 2.10.13-13
Figure 2.10.13-2 Liner-Failed Fuel Can, 2.75 I.D., LWT Cask, Safety Analysis Report, NAC Drawing No. 315-040-43 ..... 2.10.13-14
Figure 2.10.13-3 Failed Fuel Rod Can – 4.00 I.D., Fuel Rod Containerization, NAC Drawing No. 340-108-D1 ..... 2.10.13-15
Figure 2.10.13-4 Failed Fuel Rod Can – 2.75 I.D., Fuel Rod Containerization, NAC Drawing No. 340-108-D2 ..... 2.10.13-16
Figure 2.10.13-5 Failed Fuel Filter, NAC Drawing No. 491-042 ..... 2.10.13-17
Figure 2.10.14-1 ANSYS Finite Element Model of the Cask Body 2.10.14-7
Figure 2.10.14-2 Detailed View of the Cask Body Finite Element Model Top 2.10.14-8
Figure 2.10.14-3 Detailed View of the Cask Body Finite Element Model Bottom 2.10.14-9
Figure 2.10.14-4 Location of Sections of the NAC-LWT Cask Body Model 2.10.14-10
Figure 2.10.15-1 Alternate B Port Cover Finite Element Model 2.10.15-10

List of Tables

Table 2.1.2-1 Allowable Stress Limits for Containment Structures 2.1.2-2
Table 2.1.2-2 Allowable Stress Limits for Noncontainment Structures 2.1.2-3
Table 2.1.3-1 Extreme Total Stress Intensities 2.1.3-8
Table 2.2.1-1 Weights of the NAC-LWT Cask Major Components 2.2.1-2
Table 2.2.1-2 Weights and Center of Gravity Locations for the NAC-LWT Cask Shipping Configurations 2.2.1-3
Table 2.3.1-1 Mechanical Properties of Type 304 Stainless Steel 2.3.1-5
Table 2.3.1-2 Mechanical Properties of Type XM-19 Stainless Steel 2.3.1-6
Table 2.3.1-3 Mechanical Properties of SA-705, Grade 630, Precipitation-Hardened Stainless Steel 2.3.1-7
Table 2.3.1-4 Mechanical Properties (6061-T6 and T651 per ASTM B-209) 2.3.1-8
Table 2.3.1-5 Mechanical Properties of SA-193, Grade B6 High Alloy, Steel Bolting Material 2.3.1-9
Table 2.3.1-6 Mechanical Properties of SA-453, Grade 660 High Alloy, Steel Bolting Material 2.3.1-10
Table 2.3.1-7 Static Mechanical Properties of Chemical Copper Lead 2.3.1-11
Table 2.3.1-8 Dynamic Mechanical Properties of Chemical Copper Lead 2.3.1-12
Table 2.3.1-9 Mechanical Properties of SB-637, Grade N07718, Nickel Alloy Steel Bolting Material 2.3.1-13
Table 2.5.1-1 Maximum Capacity of the Lifting Components 2.5.1-11
Table 2.5.2-1 Reactions Caused By Tiedown Devices 2.5.2-17
Table 2.6.1-1 Critical Stress Summary (Hot Case) - P_m 2.6.1-5
Table 2.6.1-2 Critical Stress Summary (Hot Case) - $P_m + P_b$ 2.6.1-6
Table 2.6.1-3 Critical Stress Summary (Hot Case) – Total Range 2.6.1-7
Table 2.6.2-1 Critical Stress Summary (Cold Case) - P_m 2.6.2-5
Table 2.6.2-2 Critical Stress Summary (Cold Case) - $P_m + P_b$ 2.6.2-6
Table 2.6.2-3 Critical Stress Summary (Cold Case) – Total Range 2.6.2-7
Table 2.6.7-1 Critical Stress Summary (1-Foot Bottom End Drop) – Loading Condition 1 – P_m 2.6.7-96
Table 2.6.7-2 Critical Stress Summary (1-Foot Bottom End Drop) – Loading Condition 1 - $P_m + P_b$ 2.6.7-97
Table 2.6.7-3 Critical Stress Summary (1-Foot Bottom End Drop) – Loading Condition 1 - Total Range 2.6.7-98
Table 2.6.7-4 Critical Stress Summary (1-Foot Bottom End Drop) – Loading Condition 2 – P_m 2.6.7-99
Table 2.6.7-5 Critical Stress Summary (1-Foot Bottom End Drop) – Loading Condition 2 - $P_m + P_b$ 2.6.7-100
Table 2.6.7-6 Critical Stress Summary (1-Foot Bottom End Drop) – Loading Condition 2 - Total Range 2.6.7-101
Table 2.6.7-7 Critical Stress Summary (1-Foot Bottom End Drop) – Loading Condition 3 – P_m 2.6.7-102
Table 2.6.7-8 Critical Stress Summary (1-Foot Bottom End Drop) – Loading Condition 3 - $P_m + P_b$ 2.6.7-103

List of Tables (continued)

Table 2.6.7-9 Critical Stress Summary (1-Foot Bottom End Drop) – Loading Condition 3 - Total Range 2.6.7-104
Table 2.6.7-10 Critical Stress Summary (1-Foot Top End Drop) – Loading Condition 1 – P_m 2.6.7-105
Table 2.6.7-11 Critical Stress Summary (1-Foot Top End Drop) – Loading Condition 1 - $P_m + P_b$ 2.6.7-106
Table 2.6.7-12 Critical Stress Summary (1-Foot Top End Drop) – Loading Condition 1 - Total Range 2.6.7-107
Table 2.6.7-13 Critical Stress Summary (1-Foot Top End Drop) – Loading Condition 2 – P_m 2.6.7-108
Table 2.6.7-14 Critical Stress Summary (1-Foot Top End Drop) – Loading Condition 2 - $P_m + P_b$ 2.6.7-109
Table 2.6.7-15 Critical Stress Summary (1-Foot Top End Drop) – Loading Condition 2 - Total Range 2.6.7-110
Table 2.6.7-16 Critical Stress Summary (1-Foot Side Drop) – Loading Condition 1 – P_m 2.6.7-111
Table 2.6.7-17 Critical Stress Summary (1-Foot Side Drop) – Loading Condition 1 - $P_m + P_b$ 2.6.7-112
Table 2.6.7-18 Critical Stress Summary (1-Foot Side Drop) – Loading Condition 1 - S_n 2.6.7-113
Table 2.6.7-19 Critical Stress Summary (1-Foot Side Drop) – Loading Condition 1 - Total Range 2.6.7-114
Table 2.6.7-20 Critical Stress Summary (1-Foot Top Corner Drop) – Loading Condition 1 – P_m – Drop Orientation = 15.74 Degrees 2.6.7-115
Table 2.6.7-21 Critical Stress Summary (1-Foot Top Corner Drop) – Loading Condition 1 - $P_m + P_b$ – Drop Orientation = 15.74 Degrees 2.6.7-116
Table 2.6.7-22 Critical Stress Summary (1-Foot Top Corner Drop) – Loading Condition 1 - S_n – Drop Orientation = 15.74 Degrees 2.6.7-117
Table 2.6.7-23 Critical Stress Summary (1-Foot Top Corner Drop) – Loading Condition 1 - Total Range – Drop Orientation = 15.74 Degrees 2.6.7-118
Table 2.6.7-24 Critical Stress Summary (1-Foot Bottom Corner Drop) – Loading Condition 1 – P_m – Drop Orientation = 15.74 Degrees 2.6.7-119
Table 2.6.7-25 Critical Stress Summary (1-Foot Bottom Corner Drop) – Loading Condition 1 - $P_m + P_b$ – Drop Orientation = 15.74 Degrees 2.6.7-120
Table 2.6.7-26 Critical Stress Summary (1-Foot Bottom Corner Drop) – Loading Condition 1 - S_n – Drop Orientation = 15.74 Degrees 2.6.7-121
Table 2.6.7-27 Critical Stress Summary (1-Foot Bottom Corner Drop) – Loading Condition 1 - Total Range – Drop Orientation = 15.74 Degrees 2.6.7-122
Table 2.6.7-28 Critical Stress Summary (1-Foot Top Corner Drop) – Loading Condition 3 – P_m – Drop Orientation = 15.74 Degrees 2.6.7-123
Table 2.6.7-29 Critical Stress Summary (1-Foot Top Corner Drop) – Loading Condition 3 - $P_m + P_b$ – Drop Orientation = 15.74 Degrees 2.6.7-124

List of Tables (continued)

Table 2.6.7-30	Critical Stress Summary (1-Foot Top Corner Drop) – Loading Condition 3 - S_n – Drop Orientation = 15.74 Degrees	2.6.7-125
Table 2.6.7-31	Critical Stress Summary (1-Foot Top Corner Drop) – Loading Condition 3 - Total Range – Drop Orientation = 15.74 Degrees	2.6.7-126
Table 2.6.7-32	Summary of Results - Impact Limiter Analysis for 1-Foot Free Drop	2.6.7-127
Table 2.6.7-33	Summary of Results - Impact Limiter Analysis for 30-Foot Free Drop Subsequent to a 1-Foot Fall	2.6.7-129
Table 2.6.7-34	Summary of Cask Drop Equivalent G Load Factors	2.6.7-131
Table 2.6.7-35	NAC-LWT Cask Hot Bolt Analysis – Normal Conditions	2.6.7-132
Table 2.6.7-36	NAC-LWT Cask Cold Bolt Analysis – Normal Conditions	2.6.7-133
Table 2.6.7-37	Summary of Neutron Shield Tank Analysis	2.6.7-134
Table 2.6.7-38	Normal Transport Shield Tank Temperatures	2.6.7-135
Table 2.6.7-39	Normal Transport Shield Tank Pressures	2.6.7-136
Table 2.6.7-40	Summary of Expansion Tank Analysis	2.6.7-136
Table 2.6.7-41	Upper Ring – Cross-Section Principal Stresses	2.6.7-137
Table 2.6.12-1	Maximum Primary Membrane Stress for the 1-Foot Drop (DIDO Basket)	2.6.12-61
Table 2.6.12-2	Maximum Primary Membrane Plus Bending Stress for the 1-Foot Drop (DIDO Basket)	2.6.12-61
Table 2.7.1-1	Critical Stress Summary (30-Foot Bottom End Drop) – Loading Condition 1 – P_m	2.7.1-57
Table 2.7.1-2	Critical Stress Summary (30-Foot Bottom End Drop) – Loading Condition 1 - $P_m + P_b$	2.7.1-58
Table 2.7.1-3	Critical Stress Summary (30-Foot Bottom End Drop) – Loading Condition 1 - Total Range	2.7.1-59
Table 2.7.1-4	Critical Stress Summary (30-Foot Bottom End Drop) – Loading Condition 2 – P_m	2.7.1-60
Table 2.7.1-5	Critical Stress Summary (30-Foot Bottom End Drop) – Loading Condition 2 - $P_m + P_b$	2.7.1-61
Table 2.7.1-6	Critical Stress Summary (30-Foot Bottom End Drop) – Loading Condition 2 - Total Range	2.7.1-62
Table 2.7.1-7	Critical Stress Summary (30-Foot Bottom End Drop) – Loading Condition 3 – P_m	2.7.1-63
Table 2.7.1-8	Critical Stress Summary (30-Foot Bottom End Drop) – Loading Condition 3 - $P_m + P_b$	2.7.1-64
Table 2.7.1-9	Critical Stress Summary (30-Foot Bottom End Drop) – Loading Condition 3 - Total Range	2.7.1-65
Table 2.7.1-10	Critical Stress Summary (30-Foot Top End Drop) – Loading Condition 1 – P_m	2.7.1-66
Table 2.7.1-11	Critical Stress Summary (30-Foot Top End Drop) – Loading Condition 1 - $P_m + P_b$	2.7.1-67

List of Tables (continued)

Table 2.7.1-12 Critical Stress Summary (30-Foot Top End Drop) – Loading Condition 1 - Total Range 2.7.1-68
Table 2.7.1-13 Critical Stress Summary (30-Foot Top End Drop) – Loading Condition 2 – P_m 2.7.1-69
Table 2.7.1-14 Critical Stress Summary (30-Foot Top End Drop) – Loading Condition 2 - $P_m + P_b$ 2.7.1-70
Table 2.7.1-15 Critical Stress Summary (30-Foot Top End Drop) – Loading Condition 2 - Total Range 2.7.1-71
Table 2.7.1-16 Side Drop Load Analysis Description 2.7.1-72
Table 2.7.1-17 Critical Stress Summary (30-Foot Side Drop) – Loading Condition 1 - P_m 2.7.1-73
Table 2.7.1-18 Critical Stress Summary (30-Foot Side Drop) – Loading Condition 1 - $P_m + P_b$ 2.7.1-74
Table 2.7.1-19 Critical Stress Summary (30-Foot Side Drop) – Loading Condition 1 - Total Range 2.7.1-75
Table 2.7.1-20 G Loads – Oblique Drop 2.7.1-76
Table 2.7.1-21 Impact and Contents Pressures – Oblique Drop 2.7.1-77
Table 2.7.1-22 Fourier Series Modal Coefficients – Oblique Drop 2.7.1-78
Table 2.7.1-23 Oblique Drop Load Analysis Description 2.7.1-79
Table 2.7.1-24 Critical Stress Summary (30-Foot Top Corner Drop) – Loading Condition 1 - P_m – Drop Orientation = 15.74 Degrees 2.7.1-80
Table 2.7.1-25 Critical Stress Summary (30-Foot Top Corner Drop) – Loading Condition 1 - $P_m + P_b$ – Drop Orientation = 15.74 Degrees 2.7.1-81
Table 2.7.1-26 Critical Stress Summary (30-Foot Top Corner Drop) – Loading Condition 1 – Total Range – Drop Orientation = 15.74 Degrees 2.7.1-82
Table 2.7.1-27 Critical Stress Summary (30-Foot Top Oblique Drop) – Loading Condition 1 - P_m – Drop Orientation = 30 Degrees 2.7.1-83
Table 2.7.1-28 Critical Stress Summary (30-Foot Top Oblique Drop) – Loading Condition 1 - $P_m + P_b$ – Drop Orientation = 30 Degrees 2.7.1-84
Table 2.7.1-29 Critical Stress Summary (30-Foot Top Oblique Drop) – Loading Condition 1 – Total Range – Drop Orientation = 30 Degrees 2.7.1-85
Table 2.7.1-30 Critical Stress Summary (30-Foot Top Oblique Drop) – Loading Condition 1 - P_m – Drop Orientation = 45 Degrees 2.7.1-86
Table 2.7.1-31 Critical Stress Summary (30-Foot Top Oblique Drop) – Loading Condition 1 - $P_m + P_b$ – Drop Orientation = 45 Degrees 2.7.1-87
Table 2.7.1-32 Critical Stress Summary (30-Foot Top Oblique Drop) – Loading Condition 1 – Total Range – Drop Orientation = 45 Degrees 2.7.1-88
Table 2.7.1-33 Critical Stress Summary (30-Foot Top Oblique Drop) – Loading Condition 1 - P_m – Drop Orientation = 60 Degrees 2.7.1-89
Table 2.7.1-34 Critical Stress Summary (30-Foot Top Oblique Drop) – Loading Condition 1 - $P_m + P_b$ – Drop Orientation = 60 Degrees 2.7.1-90
Table 2.7.1-35 Critical Stress Summary (30-Foot Top Oblique Drop) – Loading Condition 1 – Total Range – Drop Orientation = 60 Degrees 2.7.1-91

List of Tables (continued)

Table 2.7.1-36 Critical Stress Summary (30-Foot Top Corner Drop) – Loading Condition 3 - P_m – Drop Orientation = 15.74 Degrees 2.7.1-92
Table 2.7.1-37 Critical Stress Summary (30-Foot Top Corner Drop) – Loading Condition 3 - $P_m + P_b$ – Drop Orientation = 15.74 Degrees 2.7.1-93
Table 2.7.1-38 Critical Stress Summary (30-Foot Top Corner Drop) – Loading Condition 3 – Total Range – Drop Orientation = 15.74 Degrees 2.7.1-94
Table 2.7.1-39 Critical Stress Summary (30-Foot Top Oblique Drop) – Loading Condition 3 - P_m – Drop Orientation = 30 Degrees 2.7.1-95
Table 2.7.1-40 Critical Stress Summary (30-Foot Top Oblique Drop) – Loading Condition 3 - $P_m + P_b$ – Drop Orientation = 30 Degrees 2.7.1-96
Table 2.7.1-41 Critical Stress Summary (30-Foot Top Oblique Drop) – Loading Condition 3 – Total Range – Drop Orientation = 30 Degrees 2.7.1-97
Table 2.7.1-42 Critical Stress Summary (30-Foot Top Oblique Drop) – Loading Condition 3 - P_m – Drop Orientation = 45 Degrees 2.7.1-98
Table 2.7.1-43 Critical Stress Summary (30-Foot Top Oblique Drop) – Loading Condition 3 - $P_m + P_b$ – Drop Orientation = 45 Degrees 2.7.1-99
Table 2.7.1-44 Critical Stress Summary (30-Foot Top Oblique Drop) – Loading Condition 3 – Total Range – Drop Orientation = 45 Degrees 2.7.1-100
Table 2.7.1-45 Critical Stress Summary (30-Foot Top Oblique Drop) – Loading Condition 3 - P_m – Drop Orientation = 60 Degrees 2.7.1-101
Table 2.7.1-46 Critical Stress Summary (30-Foot Top Oblique Drop) – Loading Condition 3 - $P_m + P_b$ – Drop Orientation = 60 Degrees 2.7.1-102
Table 2.7.1-47 Critical Stress Summary (30-Foot Top Oblique Drop) – Loading Condition 3 – Total Range – Drop Orientation = 60 Degrees 2.7.1-103
Table 2.7.1-48 Critical Stress Summary (30-Foot Bottom Oblique Drop) – Loading Condition 1 - P_m – Drop Orientation = 15.74 Degrees 2.7.1-104
Table 2.7.1-49 Critical Stress Summary (30-Foot Bottom Oblique Drop) – Loading Condition 1 - $P_m + P_b$ – Drop Orientation = 15.74 Degrees 2.7.1-105
Table 2.7.1-50 Critical Stress Summary (30-Foot Bottom Oblique Drop) – Loading Condition 1 – Total Range – Drop Orientation = 15.74 Degrees 2.7.1-106
Table 2.7.1-51 Critical Stress Summary (30-Foot Bottom Oblique Drop) – Loading Condition 1 - P_m – Drop Orientation = 30 Degrees 2.7.1-107
Table 2.7.1-52 Critical Stress Summary (30-Foot Bottom Oblique Drop) – Loading Condition 1 - $P_m + P_b$ – Drop Orientation = 30 Degrees 2.7.1-108
Table 2.7.1-53 Critical Stress Summary (30-Foot Bottom Oblique Drop) – Loading Condition 1 – Total Range – Drop Orientation = 30 Degrees 2.7.1-109
Table 2.7.1-54 Critical Stress Summary (30-Foot Bottom Oblique Drop) – Loading Condition 1 - P_m – Drop Orientation = 45 Degrees 2.7.1-110
Table 2.7.1-55 Critical Stress Summary (30-Foot Bottom Oblique Drop) – Loading Condition 1 - $P_m + P_b$ – Drop Orientation = 45 Degrees 2.7.1-111
Table 2.7.1-56 Critical Stress Summary (30-Foot Bottom Oblique Drop) – Loading Condition 1 – Total Range – Drop Orientation = 45 Degrees 2.7.1-112

List of Tables (continued)

Table 2.7.1-57	Critical Stress Summary (30-Foot Bottom Oblique Drop) – Loading Condition 1 - P_m – Drop Orientation = 60 Degrees	2.7.1-113
Table 2.7.1-58	Critical Stress Summary (30-Foot Bottom Oblique Drop) – Loading Condition 1 - $P_m + P_b$ – Drop Orientation = 60 Degrees	2.7.1-114
Table 2.7.1-59	Critical Stress Summary (30-Foot Bottom Oblique Drop) – Loading Condition 1 – Total Range – Drop Orientation = 60 Degrees	2.7.1-115
Table 2.7.1-60	NAC-LWT Cask Hot Bolt Analysis Hypothetical Accident Conditions	2.7.1-116
Table 2.7.1-61	NAC-LWT Cask Cold Bolt Analysis Hypothetical Accident Conditions	2.7.1-117
Table 2.7.6-1	Summary of Maximum Calculated Stresses – 30-Foot Drop	2.7.6-2
Table 2.7.6-2	Summary of Maximum Calculated Stresses – 40-Inch Free Drop	2.7.6-3
Table 2.7.6-3	Summary of Maximum Calculated Stresses - Fire	2.7.6-4
Table 2.7.7-1	Maximum Primary Membrane Stress for the 30-Foot Drop	2.7.7-52
Table 2.7.7-2	Maximum Primary Membrane Plus Bending Stress for the 30-Foot Drop	2.7.7-52
Table 2.10.2-1	Node Definitions	2.10.2-14
Table 2.10.2-2	Applied Impact Pressure Loadings – 30-Foot Hypothetical Accident Conditions	2.10.2-48
Table 2.10.3-1	P_m Stress Summary – Upper Ring Critical Section	2.10.3-6
Table 2.10.3-2	$P_m + P_b$ Stress Summary – Upper Ring Critical Section	2.10.3-11
Table 2.10.4-1	Determination of Maximum Energy for Secondary Impact – Full-Scale Impact Limiter	2.10.4-11
Table 2.10.6-1	Inner Shell Geometry Parameters	2.10.6-8
Table 2.10.6-2	Material Properties of Type XM-19 Stainless Steel for Buckling Analysis Input (ASME, Section III, Appendix I)	2.10.6-9
Table 2.10.6-3	Theoretical Elastic Buckling Stress Values (Temperature Independent Form)	2.10.6-10
Table 2.10.6-4	Theoretical Elastic Buckling Stresses for Selected Temperatures	2.10.6-11
Table 2.10.6-5	Capacity Reduction Factors for the Type XM-19 Stainless Steel Inner Shell	2.10.6-12
Table 2.10.6-6	Fabrication Tolerances for the NAC-LWT Cask Inner Shell	2.10.6-13
Table 2.10.6-7	Upper Bound Buckling Stresses	2.10.6-14
Table 2.10.6-8	Calculated Maximum Compressive Stresses in the Inner Shell	2.10.6-15
Table 2.10.6-9	Calculated Stresses with ASME Factors of Safety	2.10.6-17
Table 2.10.6-10	Results – Interaction Equations	2.10.6-18
Table 2.10.7-1	Section Cut Identification	2.10.7-4
Table 2.10.7-2	P_m Stress Summary (Hot Case)	2.10.7-5
Table 2.10.7-3	$P_m + P_b$ Stress Summary (Hot Case)	2.10.7-6
Table 2.10.7-4	P_m Stress Summary (Cold Case)	2.10.7-7
Table 2.10.7-5	$P_m + P_b$ Stress Summary (Cold Case)	2.10.7-8
Table 2.10.7-6	P_m Stress Summary (1-Foot Bottom End Drop) – Loading Condition 1	2.10.7-9

List of Tables (continued)

Table 2.10.7-7 $P_m + P_b$ Stress Summary (1-Foot Bottom End Drop) – Loading Condition 1 ..... 2.10.7-10
Table 2.10.7-8 P_m Stress Summary (1-Foot Bottom End Drop) – Loading Condition 2 ..... 2.10.7-11
Table 2.10.7-9 $P_m + P_b$ Stress Summary (1-Foot Bottom End Drop) – Loading Condition 2 ..... 2.10.7-12
Table 2.10.7-10 P_m Stress Summary (1-Foot Bottom End Drop) – Loading Condition 3 ..... 2.10.7-13
Table 2.10.7-11 $P_m + P_b$ Stress Summary (1-Foot Bottom End Drop) – Loading Condition 3 ..... 2.10.7-14
Table 2.10.7-12 P_m Stress Summary (1-Foot Top End Drop) – Loading Condition 1 .. 2.10.7-15
Table 2.10.7-13 $P_m + P_b$ Stress Summary (1-Foot Top End Drop) – Loading Condition 1 ..... 2.10.7-16
Table 2.10.7-14 P_m Stress Summary (1-Foot Top End Drop) – Loading Condition 2 .. 2.10.7-17
Table 2.10.7-15 $P_m + P_b$ Stress Summary (1-Foot Top End Drop) – Loading Condition 2 ..... 2.10.7-18
Table 2.10.7-16 P_m Stress Summary (1-Foot Side Drop) – Loading Condition 1 ..... 2.10.7-19
Table 2.10.7-17 $P_m + P_b$ Stress Summary (1-Foot Side Drop) – Loading Condition 1 . 2.10.7-20
Table 2.10.7-18 S_n Stress Summary (1-Foot Side Drop) – Loading Condition 1 ..... 2.10.7-21
Table 2.10.7-19 P_m Stress Summary (1-Foot Top Corner Drop) – Loading Condition 1 – Drop Orientation = 15.74 Degrees 2.10.7-22
Table 2.10.7-20 $P_m + P_b$ Stress Summary (1-Foot Top Corner Drop) – Loading Condition 1 – Drop Orientation = 15.74 Degrees 2.10.7-23
Table 2.10.7-21 S_n Stress Summary (1-Foot Top Corner Drop) – Loading Condition 1 – Drop Orientation = 15.74 Degrees 2.10.7-24
Table 2.10.7-22 P_m Stress Summary (1-Foot Bottom Corner Drop) – Loading Condition 1 – Drop Orientation = 15.74 Degrees 2.10.7-25
Table 2.10.7-23 $P_m + P_b$ Stress Summary (1-Foot Bottom Corner Drop) – Loading Condition 1 – Drop Orientation = 15.74 Degrees 2.10.7-26
Table 2.10.7-24 S_n Stress Summary (1-Foot Bottom Corner Drop) – Loading Condition 1 – Drop Orientation = 15.74 Degrees 2.10.7-27
Table 2.10.7-25 P_m Stress Summary (1-Foot Top Corner Drop) – Loading Condition 3 – Drop Orientation = 15.74 Degrees 2.10.7-28
Table 2.10.7-26 $P_m + P_b$ Stress Summary (1-Foot Top Corner Drop) – Loading Condition 3 – Drop Orientation = 15.74 Degrees 2.10.7-29
Table 2.10.7-27 S_n Stress Summary (1-Foot Top Corner Drop) – Loading Condition 3 – Drop Orientation = 15.74 Degrees 2.10.7-30
Table 2.10.7-28 P_m Stress Summary (30-Foot Bottom End Drop) – Loading Condition 1 ..... 2.10.7-31
Table 2.10.7-29 $P_m + P_b$ Stress Summary (30-Foot Bottom End Drop) – Loading Condition 1 ..... 2.10.7-32
Table 2.10.7-30 P_m Stress Summary (30-Foot Bottom End Drop) – Loading Condition 2 ..... 2.10.7-33

List of Tables (continued)

Table 2.10.7-31 $P_m + P_b$ Stress Summary (30-Foot Bottom End Drop) – Loading Condition 2 ..... 2.10.7-34
Table 2.10.7-32 P_m Stress Summary (30-Foot Bottom End Drop) – Loading Condition 3 ..... 2.10.7-35
Table 2.10.7-33 $P_m + P_b$ Stress Summary (30-Foot Bottom End Drop) – Loading Condition 3 ..... 2.10.7-36
Table 2.10.7-34 P_m Stress Summary (30-Foot Top End Drop) – Loading Condition 1 ..... 2.10.7-37
Table 2.10.7-35 $P_m + P_b$ Stress Summary (30-Foot Top End Drop) – Loading Condition 1 ..... 2.10.7-38
Table 2.10.7-36 P_m Stress Summary (30-Foot Top End Drop) – Loading Condition 2 ..... 2.10.7-39
Table 2.10.7-37 $P_m + P_b$ Stress Summary (30-Foot Top End Drop) – Loading Condition 2 ..... 2.10.7-40
Table 2.10.7-38 P_m Stress Summary (30-Foot Side Drop) – Loading Condition 1 ..... 2.10.7-41
Table 2.10.7-39 $P_m + P_b$ Stress Summary (30-Foot Side Drop) – Loading Condition 1 ..... 2.10.7-42
Table 2.10.7-40 P_m Stress Summary (30-Foot Top Corner Drop) – Loading Condition 1 – Drop Orientation = 15.74 Degrees 2.10.7-43
Table 2.10.7-41 $P_m + P_b$ Stress Summary (30-Foot Top Corner Drop) – Loading Condition 1 – Drop Orientation = 15.74 Degrees 2.10.7-44
Table 2.10.7-42 P_m Stress Summary (30-Foot Top Oblique Drop) – Loading Condition 1 – Drop Orientation = 30 Degrees 2.10.7-45
Table 2.10.7-43 $P_m + P_b$ Stress Summary (30-Foot Top Oblique Drop) – Loading Condition 1 – Drop Orientation = 30 Degrees 2.10.7-46
Table 2.10.7-44 P_m Stress Summary (30-Foot Top Oblique Drop) – Loading Condition 1 – Drop Orientation = 45 Degrees 2.10.7-47
Table 2.10.7-45 $P_m + P_b$ Stress Summary (30-Foot Top Oblique Drop) – Loading Condition 1 – Drop Orientation = 45 Degrees 2.10.7-48
Table 2.10.7-46 P_m Stress Summary (30-Foot Top Oblique Drop) – Loading Condition 1 – Drop Orientation = 60 Degrees 2.10.7-49
Table 2.10.7-47 $P_m + P_b$ Stress Summary (30-Foot Top Oblique Drop) – Loading Condition 1 – Drop Orientation = 60 Degrees 2.10.7-50
Table 2.10.7-48 P_m Stress Summary (30-Foot Top Corner Drop) – Loading Condition 3 – Drop Orientation = 15.74 Degrees 2.10.7-51
Table 2.10.7-49 $P_m + P_b$ Stress Summary (30-Foot Top Corner Drop) – Loading Condition 3 – Drop Orientation = 15.74 Degrees 2.10.7-52
Table 2.10.7-50 P_m Stress Summary (30-Foot Top Oblique Drop) – Loading Condition 3 – Drop Orientation = 30 Degrees 2.10.7-53
Table 2.10.7-51 $P_m + P_b$ Stress Summary (30-Foot Top Oblique Drop) – Loading Condition 3 – Drop Orientation = 30 Degrees 2.10.7-54
Table 2.10.7-52 P_m Stress Summary (30-Foot Top Oblique Drop) – Loading Condition 3 – Drop Orientation = 45 Degrees 2.10.7-55

List of Tables (continued)

Table 2.10.7-53 $P_m + P_b$ Stress Summary (30-Foot Top Oblique Drop) – Loading Condition 3 – Drop Orientation = 45 Degrees 2.10.7-56
Table 2.10.7-54 P_m Stress Summary (30-Foot Top Oblique Drop) – Loading Condition 3 – Drop Orientation = 60 Degrees 2.10.7-57
Table 2.10.7-55 $P_m + P_b$ Stress Summary (30-Foot Top Oblique Drop) – Loading Condition 3 – Drop Orientation = 60 Degrees 2.10.7-58
Table 2.10.7-56 P_m Stress Summary (30-Foot Bottom Corner Drop) – Loading Condition 1 – Drop Orientation = 15.74 Degrees 2.10.7-59
Table 2.10.7-57 $P_m + P_b$ Stress Summary (30-Foot Bottom Corner Drop) – Loading Condition 1 – Drop Orientation = 15.74 Degrees 2.10.7-60
Table 2.10.7-58 P_m Stress Summary (30-Foot Bottom Oblique Drop) – Loading Condition 1 – Drop Orientation = 30 Degrees 2.10.7-61
Table 2.10.7-59 $P_m + P_b$ Stress Summary (30-Foot Bottom Oblique Drop) – Loading Condition 1 – Drop Orientation = 30 Degrees 2.10.7-62
Table 2.10.7-60 P_m Stress Summary (30-Foot Bottom Oblique Drop) – Loading Condition 1 – Drop Orientation = 45 Degrees 2.10.7-63
Table 2.10.7-61 $P_m + P_b$ Stress Summary (30-Foot Bottom Oblique Drop) – Loading Condition 1 – Drop Orientation = 45 Degrees 2.10.7-64
Table 2.10.7-62 P_m Stress Summary (30-Foot Bottom Oblique Drop) – Loading Condition 1 – Drop Orientation = 60 Degrees 2.10.7-65
Table 2.10.7-63 $P_m + P_b$ Stress Summary (30-Foot Bottom Oblique Drop) – Loading Condition 1 – Drop Orientation = 60 Degrees 2.10.7-66
Table 2.10.8-1 Scaling Relations 2.10.8-60
Table 2.10.8-2 Metrology Results of Inner Diameter Measurements Before Drop 2.10.8-62
Table 2.10.8-3 Metrology Results of Outer Diameter Measurements Before Drop 2.10.8-63
Table 2.10.8-4 Metrology Results of External Length Measurements Before Drop 2.10.8-64
Table 2.10.8-5 Metrology Results of Inner Diameter Measurements After Drop 2.10.8-65
Table 2.10.8-6 Metrology Results of Outer Diameter Measurements After Drop 2.10.8-66
Table 2.10.8-7 Metrology Results of External Length Measurements After Drop 2.10.8-67
Table 2.10.9-1 NAC-LWT Cask Hot Bolt Analysis Hypothetical Accident Conditions 2.10.9-9
Table 2.10.10-1 Stress Point Locations 2.10.10-8
Table 2.10.10-2 Constraint Forces for the 30-Foot Top End Drop Condition ($\phi = 0°$) 2.10.10-12
Table 2.10.10-3 Constraint Forces for the 30-Foot Top Corner Drop Condition ($\phi = 15.74°$) 2.10.10-13
Table 2.10.10-4 Constraint Forces for the 30-Foot Top Oblique Drop Condition ($\phi = 60°$) 2.10.10-13
Table 2.10.10-5 Constraint Forces for the 30-Foot Side Drop Condition ($\phi = 90°$) 2.10.10-13
Table 2.10.10-6 Stress Components – Thermal; 130°F; 1.12-Inch Outer Shell Thickness 2.10.10-14

List of Tables (continued)

Table 2.10.10-7 Stress Components – Internal Pressure; 50 psi; 1.12-Inch Outer Shell Thickness 2.10.10-18
Table 2.10.10-8 Stress Components – Bolt Preload; 1.12-Inch Outer Shell Thickness 2.10.10-22
Table 2.10.10-9 Stress Components – Impact and Inertial Loads; 30-Foot Top End Drop; $\phi = 0°$; 1.12-Inch Outer Shell Thickness 2.10.10-26
Table 2.10.10-10 Stress Components – Impact and Inertial Loads; 30-Foot Top Corner Drop; $\phi = 15.74°$; 1.12-Inch Outer Shell Thickness 2.10.10-30
Table 2.10.10-11 Impact and Inertial Loads; 30-Foot Top Oblique Drop; $\phi = 60°$; 1.12-Inch Outer Shell Thickness 2.10.10-34
Table 2.10.10-12 Stress Components – Impact and Inertial Loads; 30-Foot Side Drop; $\phi = 90°$; 1.20-Inch Outer Shell Thickness; Circumferential Location = 0° 2.10.10-38
Table 2.10.10-13 Stress Components – Thermal; 130°F; 1.20-Inch Outer Shell Thickness 2.10.10-42
Table 2.10.10-14 Stress Components – 50 psi Internal Pressure and Bolt Preload; 1.20-Inch Outer Shell Thickness 2.10.10-46
Table 2.10.10-15 Primary Stresses; 30-Foot Top End Drop; $\phi = 0°$; 1.12-Inch Outer Shell Thickness 2.10.10-50
Table 2.10.10-16 Primary Plus Secondary Stresses; 30-Foot Top End Drop; $\phi = 0°$; 1.12-Inch Outer Shell Thickness 2.10.10-54
Table 2.10.10-17 Primary Membrane (P_m) Stresses; 30-Foot Top End Drop; $\phi = 0°$; 1.12-Inch Outer Shell Thickness 2.10.10-58
Table 2.10.10-18 Primary Membrane Plus Primary Bending ($P_m + P_b$) Stresses; 30-Foot Top End Drop; $\phi = 0°$; 1.12-Inch Outer Shell Thickness 2.10.10-59
Table 2.10.10-19 Primary Membrane (P_m) and Primary Membrane Plus Primary Bending ($P_m + P_b$) Stress Qualification; 30-Foot Top End Drop; $\phi = 0°$; 1.12-Inch Outer Shell Thickness 2.10.10-60
Table 2.10.10-20 Primary Stresses; 30-Foot Top Corner Drop; $\phi = 15.74°$; 1.12-Inch Outer Shell Thickness 2.10.10-61
Table 2.10.10-21 Primary Plus Secondary Stresses; 30-Foot Top Corner Drop; $\phi = 15.74°$; 1.12-Inch Outer Shell Thickness 2.10.10-65
Table 2.10.10-22 Primary Membrane (Pm) Stresses; 30-Foot Top Corner Drop; $\phi = 15.74°$; 1.12-Inch Outer Shell Thickness 2.10.10-69
Table 2.10.10-23 Primary Membrane Plus Primary Bending ($P_m + P_b$) Stresses; 30-Foot Top Corner Drop; $\phi = 15.74°$; 1.12-Inch Outer Shell Thickness 2.10.10-70
Table 2.10.10-24 Primary Membrane (P_m) and Primary Membrane Plus Primary Bending ($P_m + P_b$) Stresses; 30-Foot Top Corner Drop; $\phi = 15.74°$; 1.12-Inch Outer Shell Thickness 2.10.10-71
Table 2.10.10-25 Primary Stresses; 30-Foot Top Oblique Drop; $\phi = 60°$; 1.12-Inch Outer Shell Thickness 2.10.10-72

List of Tables (continued)

Table 2.10.10-26 Primary Plus Secondary Stresses; 30-Foot Top Oblique Drop; ϕ = 60°; 1.12-Inch Outer Shell Thickness 2.10.10-76
Table 2.10.10-27 Primary Membrane (P_m) Stresses; 30-Foot Top Oblique Drop; ϕ = 60°; 1.12-Inch Outer Shell Thickness 2.10.10-80
Table 2.10.10-28 Primary Membrane Plus Primary Bending ($P_m + P_b$) Stresses; 30-Foot Top Oblique Drop; ϕ = 60°; 1.12-Inch Outer Shell Thickness . 2.10.10-81
Table 2.10.10-29 Primary Membrane (P_m) and Primary Membrane Plus Primary Bending ($P_m + P_b$) Stresses; 30-Foot Top Oblique Drop; ϕ = 60°; 1.12-Inch Outer Shell Thickness 2.10.10-82
Table 2.10.10-30 Primary Stresses; 30-Foot Side Drop; ϕ = 90°; 1.20-Inch Outer Shell Thickness; Circumferential Location = 0° 2.10.10-83
Table 2.10.10-31 Primary Plus Secondary Stresses; 30-Foot Side Drop; ϕ = 90°; 1.20-Inch Outer Shell Thickness; Circumferential Location = 0° 2.10.10-87
Table 2.10.10-32 Primary Membrane (P_m) Stresses; 30-Foot Side Drop; ϕ = 90°; 1.20-Inch Outer Shell Thickness; Circumferential Location = 0° 2.10.10-91
Table 2.10.10-33 Primary Membrane Plus Primary Bending ($P_m + P_b$) Stresses; 30-Foot Side Drop; ϕ = 90°; 1.20-Inch Outer Shell Thickness; Circumferential Location = 0° 2.10.10-92
Table 2.10.10-34 Primary Membrane (P_m) Stresses; 30-Foot Side Drop; ϕ = 90°; 1.20-Inch Outer Shell Thickness; Circumferential Location = 90° ... 2.10.10-93
Table 2.10.10-35 Primary Membrane Plus Primary Bending ($P_m + P_b$) Stresses; 30-Foot Side Drop; ϕ = 90°; 1.20-Inch Outer Shell Thickness; Circumferential Location = 90° 2.10.10-94
Table 2.10.10-36 Primary Membrane (P_m) Stresses; 30-Foot Side Drop; ϕ = 90°; 1.20-Inch Outer Shell Thickness; Circumferential Location = 180° . 2.10.10-95
Table 2.10.10-37 Primary Membrane Plus Primary Bending ($P_m + P_b$) Stresses; 30-Foot Side Drop; ϕ = 90°; 1.20-Inch Outer Shell Thickness; Circumferential Location = 180° 2.10.10-96
Table 2.10.10-38 Primary Membrane (P_m) and Primary Membrane Plus Primary Bending ($P_m + P_b$) Stress Qualification; 30-Foot Side Drop; ϕ = 90°; 1.20-Inch Outer Shell Thickness; Circumferential Location = 0° 2.10.10-97
Table 2.10.11-1 Geometric Dimensions of the Cask 2.10.11-9
Table 2.10.11-2 Comparison of the Hand-Calculated and Finite Element Results 2.10.11-10
Table 2.10.12-1 Determination of Maximum Energy Remaining for Secondary Impact – Full-Scale Impact Limiter 2.10.12-30
Table 2.10.12-2 Determination of Extreme Force During Cask Deceleration (First Limiter) – Quarter-Scale Impact Limiter 2.10.12-31
Table 2.10.14-1 Material Designations for Sections 2.10.14-11
Table 2.10.14-2 1-Foot Side Drop with Internal Pressure, P_m Stresses, ksi 2.10.14-12
Table 2.10.14-3 Side Drop with Internal Pressure, $P_m + P_b$ Stresses, ksi 2.10.14-13
Table 2.10.14-4 1-Foot Side Drop with Internal Pressure, P + Q Stresses, ksi 2.10.14-14

List of Tables (continued)

Table 2.10.14-5 1-Foot Top-End Drop with Normal Internal Pressure, P_m Stresses, ksi 2.10.14-15
Table 2.10.14-6 1-Foot Top-End Drop with Internal Pressure, $P_m + P_b$ Stresses, ksi .. 2.10.14-16
Table 2.10.14-7 1-Foot Top-End Drop with Internal Pressure, P + Q Stresses, ksi 2.10.14-17
Table 2.10.14-8 1-Foot Top-Corner Drop with Internal Pressure, P_m Stresses, ksi 2.10.14-18
Table 2.10.14-9 1-Foot Top-Corner Drop with Internal Pressure, $P_m + P_b$ Stresses, ksi 2.10.14-19
Table 2.10.14-10 1-Foot Top-Corner Drop with Internal Pressure, P + Q Stresses, ksi 2.10.14-20
Table 2.10.14-11 1-Foot Bottom-End Drop with Internal Pressure, P_m Stresses, ksi 2.10.14-21
Table 2.10.14-12 1-Foot Bottom-End Drop with Internal Pressure, $P_m + P_b$ Stresses, ksi 2.10.14-22
Table 2.10.14-13 1-Foot Bottom-End Drop with Internal Pressure, P + Q Stresses, ksi 2.10.14-23
Table 2.10.14-14 1-Foot Bottom-Corner Drop with Internal Pressure, P_m Stresses, ksi 2.10.14-24
Table 2.10.14-15 1-Foot Bottom-Corner Drop with Internal Pressure, $P_m + P_b$ Stresses, ksi 2.10.14-25
Table 2.10.14-16 1-Foot Bottom-Corner Drop with Internal Pressure, P + Q Stresses, ksi 2.10.14-26
Table 2.10.14-17 30-Foot Side Drop with Internal Pressure, P_m Stresses, ksi 2.10.14-27
Table 2.10.14-18 30-Foot Side Drop with Internal Pressure, $P_m + P_b$ Stresses, ksi 2.10.14-28
Table 2.10.14-19 30-Foot Top-End Drop with Internal Pressure, P_m Stresses, ksi 2.10.14-29
Table 2.10.14-20 30-Foot Top-End Drop with Internal Pressure, $P_m + P_b$ Stresses, ksi 2.10.14-30
Table 2.10.14-21 30-Foot Top-Corner Drop with Internal Pressure, P_m Stresses, ksi ... 2.10.14-31
Table 2.10.14-22 30-Foot Top-Corner Drop with Internal Pressure, $P_m + P_b$ Stresses, ksi 2.10.14-32
Table 2.10.14-23 30-Foot Bottom-End Drop with Internal Pressure, P_m Stresses, ksi .. 2.10.14-33
Table 2.10.14-24 30-Foot Bottom-End Drop with Internal Pressure, $P_m + P_b$ Stresses, ksi 2.10.14-34
Table 2.10.14-25 30-Foot Bottom-Corner Drop with Internal Pressure, P_m Stresses, ksi 2.10.14-35
Table 2.10.14-26 30-Foot Bottom-Corner Drop with Internal Pressure, $P_m + P_b$ Stresses, ksi 2.10.14-36
Table 2.10.14-27 Accident Internal Pressure with Inertia Load, P_m Stresses, ksi 2.10.14-37
Table 2.10.14-28 Accident Internal Pressure with Inertia Load , $P_m + P_b$ Stresses, ksi. 2.10.14-38

2 STRUCTURAL EVALUATION

The structural analysis of the NAC-LWT spent-fuel transportation cask demonstrates that the package satisfies the requirements of Part 71 of Title 10, Chapter 1 of the Code of Federal Regulations, specifically, Subpart E, "Package Approval Standards" and Subpart F, "Package and Special Form Tests." It is shown that containment is not breached under any of the normal operations or hypothetical accident conditions.

Analysis techniques that utilize the current state-of-the-art methods for the calculation of stresses in large structures subject to both steady state and transient loadings are used throughout these analyses. The evaluation of the structural characteristics of the containment boundary is based upon a conservative interpretation of the requirements of the American Society of Mechanical Engineers (ASME) Boiler and Pressure Vessel Code.

This section of the Safety Analysis Report demonstrates that the NAC-LWT cask design is capable of meeting the rigors of transport while carrying nuclear fuel; it documents the results of the analyses that are performed to provide assurance that the design also satisfies the statutory requirements for licensing.

2.1 Structural Design

2.1.1 Discussion

The NAC-LWT cask consists of six major components: (1) the cask body; (2) the closure lid and bolts; (3) the neutron shield/expansion tanks; (4) the trunnions; (5) the fuel basket; and (6) the energy absorbing impact limiters, which are located over the ends of the cask. The bottom plate, the inner shell, the upper ring and the closure lid, including seals and bolts, form the primary containment boundary.

The NAC-LWT cask body is constructed of Type 304 stainless steel with Type XM-19 stainless steel inner and outer shells and with lead shielding in the side wall and bottom end (Section 1.4, License Drawings). The cask bottom consists of a 3.5-inch thick, 20.75-inch diameter Type 304 stainless steel forging on the outside; a 3.0-inch thick, 20.75-inch diameter lead plate; and a 4.0-inch thick, 17.80-inch diameter Type 304 stainless steel forging on the inside; these components are enclosed by a 10.5-inch thick, 28.63-inch outside diameter, 17.80-inch inside diameter, Type 304 stainless steel forging. The cask bottom is welded directly to the Type XM-19 stainless steel inner shell (0.75-inch thick with 1.26-inch thick transition regions at each end; 13.375-inch inside diameter, 14.88-inch outside diameter) and the Type XM-19 stainless steel outer shell (1.20-inch thick with 1.87-inch thick transition regions at each end; 26.38-inch inside diameter, 28.78-inch outside diameter); the shells are 175.05 inches long. The annulus between the shells (26.38-inch outside diameter, 14.88-inch inside diameter) is filled with lead for gamma shielding. The Type 304 stainless steel top forging is welded directly to the inner and outer shells and has three stepped regions to accommodate the closure lid, the seals and the lid bolts. The total height of the top forging is 14.25 inches with an outside diameter of 28.63 inches and stepped inside diameters of 13.375 inches × 6.25 inches long, 20.6 inches × 4.9 inches long, and 22.63 inches × 3.1 inches long.

The stainless steel closure lid is 11.3 inches thick with stepped regions of length and diameters to match those of the top forging so that the closure lid is recessed in the top forging and flush with its top surface. The twelve 1-8 UNC closure lid bolts are SA-453, Grade 660 high alloy bolting material. The inner and outer seals on the closure lid are metallic and tetrafloroetheylene (TFE) O-rings, respectively.

There are three penetrations into the NAC-LWT cask cavity – the closure lid, a vent port and a drain port. There also is a penetration into the region between the two closure lid O-rings to test the containment seal. The vent and drain ports contain quick-disconnect valves and are located in the cask body upper ring region. There are two port cover designs—the alternate port cover and the Alternate B port cover.

The port cover designs are physically similar, but the O-ring designs and materials are different. The primary containment O-ring seal for the alternate port cover is provided by a Viton® O-ring located in a groove on the face (inner end) of the port barrel of the cover body. The secondary (test annulus) seal is a single Viton® O-ring located in a groove on the barrel of the port cover. The bolts for the alternate port cover are SA-193 (Type 410 stainless steel) socket-head cap screws.

The Alternate B port cover has the same basic geometry as the alternate port cover. With the exception of modifications made to the sealing surface and the material of construction, the Alternate B port cover is the same design as the alternate port cover. The Alternate B port cover has two face seals on the inner end of the port cover. The primary containment seal is provided by an inner metal face seal located in a groove on the inner end of the barrel of the port cover body. The metal face seal maintains the containment boundary meeting the leaktight definition of ANSI N14.5-1997. The secondary (test annulus) face seal is a Viton® O-ring located in a groove on the inner end towards the outer edge of the barrel of the port cover body. The Alternate B port cover is fabricated from Type XM-19 stainless steel to provide maximum thermal expansion compatibility with the Type 304 stainless steel cask body. The Alternate B port cover is fastened to the cask body using three high-strength SB-637 Grade N07718 bolts.

The neutron shield tank shell is 0.24-inch thick stainless steel, which is 164.0 inches long with an outside diameter of 39.28 inches and an inside diameter of 38.81 inches. The bottom plate of the neutron shield tank is 0.50-inch thick stainless steel. The expansion tank shell is 0.32-inch thick stainless steel, which is 46.0 inches long with an outside diameter of 44.24 inches and an inside diameter of 43.61 inches. The top end of the shield and expansion tanks is a single 0.50-inch thick stainless steel plate. A pressure relief valve is located in the neutron shield tank shell. The relief valve is selected to contain any shield/expansion tank pressure due to the 10 CFR 71 prescribed normal operations conditions, but will release at higher pressures (165 psig) before gross failure of either tank occurs.

Four stainless steel lifting trunnions, located at 90-degree intervals, are welded to the exterior of the upper ring. Two stainless steel socket pads are welded to the outer shell for support of the cask on a trailer or in a shipping container.

The fuel basket assembly locates and supports the fuel in the cask cavity.

The aluminum honeycomb impact limiters control the g loads acting on the cask during impact load conditions. The g loads acting upon the cask are controlled by the honeycomb material crush strength.

2.1.2 Basic Design Criteria

2.1.2.1 Containment Structures

Regulatory Guides 7.6 and 7.8 are used to establish the design criteria for analyses to evaluate the package containment boundaries for both the normal transport and the hypothetical accident conditions. Material data used in the evaluations correspond to the design stress values (S_m), yield strengths (S_y), and ultimate strengths (S_u) presented in Section 2.3. The containment cavity is described by the solid 4.0-inch thick bottom end forging, welded to a 13.375-inch inner diameter 0.75-inch thick stainless steel shell, which is welded at the upper end to the upper end ring. The 11.3-inch thick stainless steel lid and metal O-ring seal, when bolted in place to the upper ring, close the containment cavity at the top of the cask. The cavity shell has two penetrations located near the top of the cask body: 1) the vent port for venting and filling; and 2) the drain port for draining. These penetrations are closed by either alternate port covers or the Alternate B port covers with the respective O-ring seals. The containment boundary is further described in Section 4.1.

A summary of allowable stress criteria used for containment structures and bolting materials is presented in Table 2.1.2-1. This data is consistent with Regulatory Guide 7.6 and applicable parts of Subsection NB-3000 and Appendix F of the "ASME Boiler and Pressure Vessel Code."

2.1.2.2 Noncontainment Structures

Noncontainment structures include all structural members other than the primary containment boundary components, but excluding the impact limiters. Noncontainment structural members are shown to satisfy similar structural criteria as the containment structure, although Regulatory Guide 7.6 applies only to containment structures. Allowable stresses for the noncontainment structures and noncontainment bolting materials are presented in Table 2.1.2-2. In addition, noncontainment lifting and handling structures satisfy the requirements of NUREG-0612 for the lifting of heavy loads.

While performing their intended function during all free drop conditions, the impact limiters crush and absorb the energy of impact. Crushing of the impact limiter prevents any cask "peak load hard points" from occurring during the impact.

Table 2.1.2-1 Allowable Stress Limits for Containment Structures

	Allowable Stresses		Bolt Allowable Stresses*	
Stress Category	**Normal Conditions**	**Accident Conditions**	**Normal Conditions**	**Accident Conditions**
Primary Membrane	S_m	Lesser of: 2.4 S_m and: 0.7 S_u	S_y	S_y
Primary Membrane + Primary Bending	1.5 S_m	Lesser of: 3.6 S_m and: S_u	S_y	S_y
Range of Primary + Secondary	3.0 S_m	NA		
Bearing	S_y	S_y for containment boundary surfaces S_u elsewhere		
Pure Shear	0.5 S_y	0.5 S_u		
Peak	Per Section 2.6.5			
Buckling	Per Section 2.10.6			

* Not considering stress concentrations (Section 2.1.3-1).

Table 2.1.2-2 Allowable Stress Limits for Noncontainment Structures

	Allowable Stresses		Bolt Allowable Stresses*	
Stress Category	**Normal Conditions**	**Accident Conditions**	**Normal Conditions**	**Accident Conditions**
Primary Membrane	Greater of: S_m and: S_y	0.7 S_u	Greater of: 2.0 S_m and: S_y	Greater of: S_y and: 0.7 S_u
Primary Membrane + Primary Bending	Greater of: 1.5 S_m and: S_y	S_u	Greater of: 3.0 S_m and: S_y	S_u
Range of Primary + Secondary	Greater of: 3.0 S_m and: S_y	NA		
Bearing	S_y	S_u		
Pure Shear	Greater of: 0.6 S_m and: 0.6 S_y	0.5 S_u		
Peak	Per Section 2.6.5			
Buckling	Per Section 2.10.6			

* Not considering stress concentrations (Section 2.1.3.2).

2.1.3 Miscellaneous Structural Failure Modes

2.1.3.1 Brittle Fracture

The materials used to fabricate the NAC-LWT cask body meet all appropriate brittle fracture requirements. The cask structure consists of Type XM-19 stainless steel inner and outer shells with the remainder of the cask body being Type 304 stainless steel. The neutron shield/ expansion tank system is also fabricated of Type 304 stainless steel. The Type XM-19 and Type 304 austenitic stainless steels do not undergo a ductile to brittle transition in the temperature range of interest.

The closure lid bolts are SA-453, Grade 660 high alloy bolting material. The port covers are SA-705, Grade 630 stainless steel. The port cover bolts are SA-193, Grade B6 alloy steel bolting material. All of these materials meet the impact energy absorption requirements of ASTM A370 and A20-77 (Annual Book of ASTM Standards, 1986).

The impact limiters and the fuel basket are fabricated from aluminum. Since the aluminum does not undergo a ductile to brittle transition in the cask structure temperature range, brittle fracture is not a concern.

2.1.3.2 Fatigue - Normal Operating Cycles

2.1.3.2.1 Cask Structure

A normal operating cycle is defined as the sequence of loading an empty cask at ambient temperature with contents of maximum heat load, transporting the contents to a destination, unloading the contents and letting the cask return to ambient temperature. The expected number of operating cycles for the NAC-LWT cask is approximately 480 (24 cycles/year $\times$ 20 years). For the purpose of performing a fatigue stress evaluation, the LWT cask is assumed to be subjected to 2,000 cycles. From the "ASME Boiler and Pressure Vessel Code," Appendix I, Figure I-9.2.1, the fatigue allowable stress intensity amplitude (S_a) for austenitic stainless steels for 2,000 cycles is 98,000 psi (one-half of the alternating stress range). This value, when multiplied by the ratio of elastic moduli at 70°F to that at 300°F ($27.0 \times 10^6 / 28.3 \times 10^6$), and multiplied by two, gives a fatigue allowable alternating stress intensity range of 187,000 psi. However, the allowable primary plus secondary (S_n) stress intensity range, from "ASME Boiler and Pressure Vessel Code," Subsection NB-3222.2, is 60,000 psi (3.0 S_m) for Type 304 stainless steel. No stress concentration factor is greater than 3.0 for the Type 304 stainless steel cask body components. The fatigue allowable alternating stress intensity range, 187,000 psi, is greater than three times the maximum allowable S_n stress intensity range for Type 304 stainless steel.

Similarly, for Type XM-19 stainless steel, the allowable S_n stress intensity range is 100,000 psi (3.0 S_m). No stress concentration factor for the inner and outer shells is greater than 1.5; the fatigue allowable alternating stress intensity range, 187,000 psi, is greater than 1.5 times the maximum allowable S_n stress intensity range for Type XM-19 stainless steel. Therefore, the S_n allowable stress intensity governs.

2.1.3.2.2 Bolts - Closure Lid (Fatigue)

Lid closure bolts indirectly complete containment by holding the lid in place on the upper forging. The maximum cyclic stress in the lid bolts results from preloading the bolts to the 260 foot-pounds torque (3120 inch-pounds) specified for installation. The actual required bolt preload torque (T), is given by:

$$T = \left[\frac{d_m}{2d}\left(\frac{\tan\psi + \mu\sec\alpha}{1 - \mu\tan\psi\sec\alpha}\right) + 0.625\mu\right](F)(d)$$

$$= 2862 \text{ in-lb } (238.5 \text{ ft-lb})$$

where:

F = preload force, lb

d = 1.0 in (bolt diameter)

ψ = 2.494° (helix angle)

α = 30° (one-half the thread angle)

μ = 0.060 (coefficient of friction)

d_m = 0.9134 in (mean diameter of threads)

The required bolt preload force is calculated for the top corner drop as follows:

1. Inertial Weight of Lid

$$F_I = \frac{W_t}{g}(a) = \frac{941}{32.2}(60 \text{ x } 32.2)$$

$$= 56{,}460 \text{ lbs}$$

where:

W_t = 941 lbs (Table 2.2.0-1)

a = 60 g (Table 2.6.7-34)

2. Inertial Weight of Cask Contents

$$F_2 = \frac{W_c}{g}(a) = \frac{4000}{32.2}(60 \times 32.2)$$

$$= 240{,}000 \text{ lbs}$$

where:

W_c = 4000 lbs (Table 2.2.0-1)

a = 60 g (Table 2.6.7-34)

3. Force Resulting From Internal Pressure

$F_{ip} = P_{ip}(A) = 30(171.36)$

$= 5141$ lbs

where:

$P_{ip} = 30$ psig

$$A = \frac{\pi}{4}(14.771^2)$$

$= 171.36 \text{ in}^2$

4. Force Resulting From Compression of TFE O-Ring

The TFE material used in the NAC-LWT cask lid O-ring (outer) (Shamban, Part No. S11214-460) has a nominal diameter of 0.275 inch and is compressed to a height of 0.242 inch, yielding a compression of 12 percent. The rated load on the O-ring using a shore hardness of 90 and 12 percent compression is 50 pounds per linear inch. The total compressive force on the O-ring is calculated as:

$F_{tr} = 50(\pi \times 15.75)$

$= 2{,}474$ lbs

5. Force Resulting From Compression of Metallic O-Ring

The rated load on the 14.75-inch diameter metal O-ring, Inconel X-750 material, with an 0.188-inch outside diameter and 0.032-inch wall thickness is 1.4(1225) pounds per linear inch. The compressive force on the O-ring is calculated as:

$F_{mr} = (1.4 \times 1225)(\pi \times 14.75)$

$= 79{,}470$ lbs

The total required bolt preload force (12 bolts) is:

$$F_T = F_1 + F_2 + F_{ip} + F_{tr} + F_{mr}$$

$$= 383,545 \text{ lbs}$$

For each of the twelve 1 - 8 UNC bolts in the lid, the required maximum bolt preload force is:

$$F = 383,545 / 12$$

$$= 31,962 \text{ lbs}$$

Conservatively, an installed bolt preload of 34,843 pounds is specified.

From Table 6-2, page 230, of Shigley, the tensile stress area (A_t) of each lid bolt is 0.606 square inches. Bolt stress resulting from the specified preload is:

$$S = F/At = 34,843 \text{ lb}/0.606 \text{ in}^2$$

$$= 57,497 \text{ psi}$$

According to Juvinall, page 251, it is assumed that the stress concentration factor is approximately 3.8 for unified and American standard threads. The modulus of elasticity of the bolting material at 300°F is 26.7×10^6 psi. The extreme temperature, normal transport condition, which the bolting material may experience, is actually calculated to be 230°F, adding a level of conservatism to this analysis. Figure 2.1.3-1 ("ASME Boiler and Pressure Vessel Code," Figure I-9.4, page 199) is based on a modulus of elasticity of 30.0×10^6 psi; therefore, by ratioing the moduli, the equivalent stress range is given by:

$$S_{range} = (57,497 \text{ psi}) (3.8) [(30.0/26.7)]$$

$$= 245,492 \text{ psi}$$

The equivalent stress range defines the endpoints of the stress cycle; thus, the alternating component would be half the range or 122,746 psi. From Figure 2.1.3-1, using the 3.0 S_m curve, the allowable number of operating cycles is greater than 550. Conservatively assuming that the bolts are torqued twice each month, the bolts would be cycled 24 times in one year. Then, 550 cycles represent a minimum service life of 22.9 years. The lid bolts will be replaced after 20 years of operational service to ensure that the fatigue limit is satisfied.

2.1.3.2.3 Containment Vessel

Fatigue concerns associated with normal over-the-road vibration are addressed in Section 2.6.5.

2.1.3.3 Extreme Total Stress Intensity Range

Regulatory Guide 7.6, paragraph C.7 requires that the extreme total stress intensity range (including stress concentrations) between the initial state, the fabrication state, the normal operations condition, and the accident condition be less than twice the adjusted value (adjusted to account for the modulus of elasticity at the highest temperature) of S_a at 10 cycles given by the appropriate design fatigue curves. Table 2.1.3-1 (constructed from the finite element analysis results of the normal operations and accident conditions) shows a maximum total stress intensity range of 1311 ksi in component 7. This stress intensity range is based on an unrealistic finite element analysis calculated stress intensity value, which results from the applied boundary condition in the ANSYS program (refer to Section 2.7.1.3 for the explanation of this singularity condition). From the Type 304 stainless steel material property summary Table 2.3.1-1, the allowable stress for 10 cycles at 230°F is 686.0 ksi. The allowable stress range is then 1372 ksi (2 × 686.0 ksi). For Type 304 stainless steel, this allowable stress at 10 cycles (1372 ksi) is greater than the unrealistically high limiting stress range for low cycle fatigue (1311 ksi). Based on the significantly higher strength of Type XM-19 stainless steel, when compared to Type 304 stainless steel, no further evaluation of the extreme total stress intensity range is necessary. The low cycle fatigue limits for the containment material are not exceeded for the highly conservative value of stress intensity range considered in this analysis.

2.1.3.4 Buckling

Regulatory Guide 7.6, paragraph C.5, states that buckling of a shipping cask containment vessel must not occur under any circumstances. Precluding large deformations assures that the assumptions of elastic analyses and quasi-linear stress allowances remain valid as stated in paragraph C.6 of the above reference.

Two concentric stainless steel shells, both welded to a large ring at each end, define the primary cask structure. The annulus between the shells is filled with lead. The inner shell is considered to be the only load bearing member, taking no credit for the outer shell or the elastic support of the lead in the analyses. The analyses demonstrate that the inner shell will not buckle for normal transport or hypothetical accident conditions. For reference, the nominal dimensions of the cask shells follow.

Shell	Mean Diameter (D_m)(in)	Thickness (T)(in)	Length (L)(in)	D_m /T**	L/D_m***
Outer Shell	27.58	1.20	181.25*	23.0	6.6
Inner Shell	14.12	0.75	181.25	18.8	12.8

* Assumed shell length, no credit taken for the end forgings.

** Mean diameter divided by thickness.

*** Length divided by mean diameter.

The NAC-LWT cask inner shell is analyzed for structural stability (buckling) using Code Case N-284 (Metal Containment Shell Buckling Design Methods) of the "ASME Boiler and Pressure Vessel Code." The details of these analyses are presented in Section 2.10.6; however, the basic methodology used is as follows:

1. Calculate the theoretical elastic hoop, axial compression, and inplane shear loading using classical methodology.
2. Calculate shell geometry-dependent capacity reduction factors and shell ovality coefficients. These factors and coefficients account for differences between classical and predicted instability stresses for fabricated shells and for geometric variances from perfect cylinders.
3. Calculate plasticity reduction factors, which are used if the calculated buckling stress exceeds a material's proportional limit.
4. Identify the factors of safety (FS) to be used in the buckling evaluation. Article-1400, Code Case N-284, "ASME Boiler and Pressure Vessel Code," defines the factors of safety to be applied to compressive buckling stresses: (1) FS = 2.0 for Design Conditions and Level A and B Service Limits, which correspond to the normal transport conditions of Regulatory Guide 7.6; and (2) FS = 1.34 for Level D Service Limits, which correspond to the hypothetical accident conditions of Regulatory Guide 7.6. These factors of safety are used in the buckling evaluations of the NAC-LWT cask inner shell.
5. Using the appropriate interaction equations and the factors identified in 2, 3 and 4, calculate the worst case applied compressive stresses and in-plane shear stresses.
6. Compare worst case stresses to the classically determined buckling allowables and determine the margins of safety for the critical locations on the inner shell.

Figure 2.1.3-1 Design Fatigue Curve for High Strength Steel Bolting

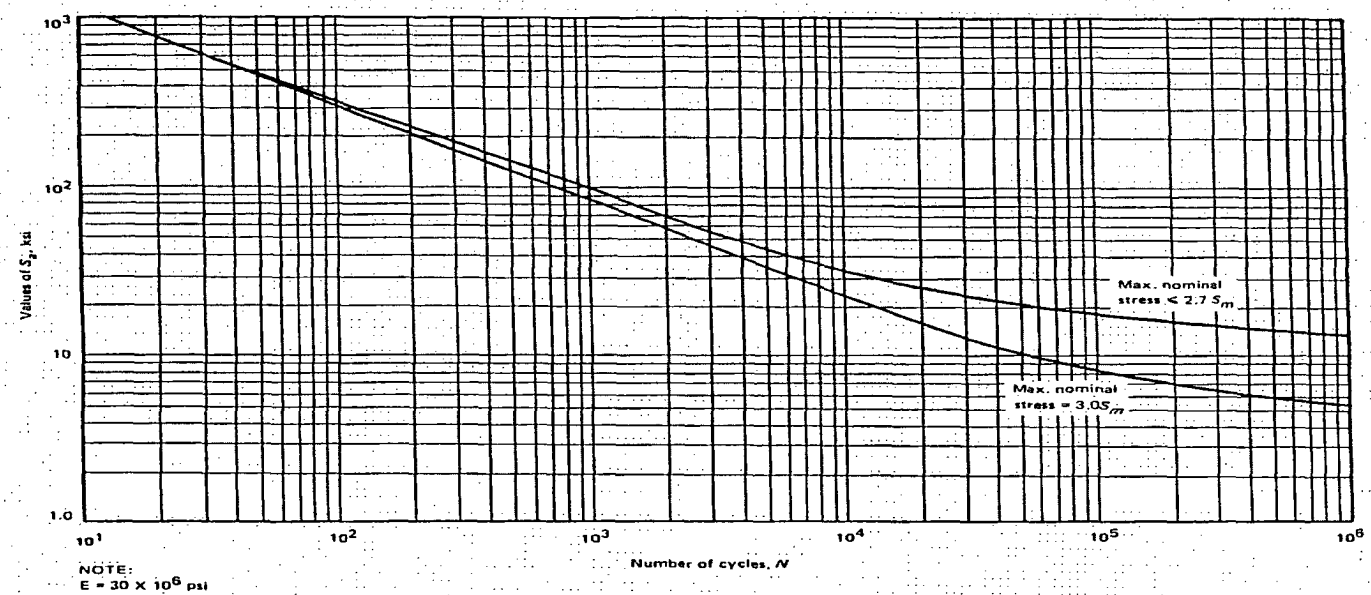

FIG. I-9.4 DESIGN FATIGUE CURVE FOR HIGH STRENGTH STEEL BOLTING
FOR TEMPERATURES NOT EXCEEDING 700°F
Table I-9.1 Contains Tabulated Values and a Formula for Accurate
Interpolation of These Curves

Table 2.1.3-1 Extreme Total Stress Intensities

Component	Algebraic Maximum and Minimum Stress Intensities (ksi)	Total Stress Intensity Range (ksi)
Closure Lid (1)	-1310.41[1], 0.0	1310.41[1]
Top Ring (3)	-62.23, 0.0	62.23
Inner Shell (4)	-39.98, 0.0	39.98
Outer Shell (6)	-77.65[1], 0.0	77.65[1]
Bottom (7)	-1311.20[1], 0.0	1311.20
Bottom Cover Plate (8)	-81.86[1], 0.0	81.86[1]

[1] Refer to Section 2.7.1.3 for discussion of these values, which are unrealistic due to finite element model boundary conditions.

2.2 Weights and Centers of Gravity

2.2.1 Major Component Statistics

The weights of the major components of the NAC-LWT cask and their respective centers of gravity are presented in Table 2.2.1-1. The axial location of the center of gravity is measured from the bottom surface of the cask body. The center of gravity is always on the longitudinal centerline of the cask because the cask is essentially axisymmetric about that axis. The center of gravity location of the fuel is representative of typical fuel configurations.

The weights and centers of gravity of the cask package in eight different shipping configurations are presented in Table 2.2.1-2. In each case, the center of gravity is measured from the bottom surface of the cask body. The term "loaded" refers to the presence of fuel or other radioactive materials in the cask cavity; the term "empty" implies the absence of any fuel or other radioactive materials in the cask cavity. However, the fuel basket does remain in the cask cavity for the "empty" configuration. The weight of a lifting yoke is not included in the tabulated package weights.

All of the values tabulated in Table 2.2.1-1 and Table 2.2.1-2 are calculated to the nearest pound to obtain an accurate cask weight and center of gravity. The cask package weight and center of gravity used in the analyses of this report are the design values - 52,000 pounds and 98.93 inches. A design value of 4,000 pounds is conservatively used for the total weight of the cask contents (including the appropriate basket).

Table 2.2.1-1 Weights of the NAC-LWT Cask Major Components

Component	Weight (pounds)	Axial Center of Gravity Location (inches)
Cask Body	39,906	96.46
Closure Lid and Bolts	941	195.11
Impact Limiters		
Top	1,535	202.98
Bottom	1,320	-3.18
Shield Tank Fluid	3,506	96.26
PWR Fuel Basket and Spacer	874	100.98
PWR High Burnup Rod Payload	1,620	95.33
PWR Fuel Payload (Maximum)	3,126	96.63
BWR Fuel Basket	1,124	97.88
BWR Fuel Payload	1,500	97.88
Metallic Fuel Basket	128	96.40
Metallic Fuel Payload	2,080	96.40
MTR Four Unit Basket	982	96.20
MTR Four Unit Fuel Payload	840[1]	96.20
MTR Four Unit PULSTAR Fuel Payload	2,240[2]	96.20
MTR Five Unit Basket	1,015	96.20
MTR Five Unit Fuel Payload	1,050[1]	96.20
MTR Six Unit Basket	1,002	96.20
MTR Six Unit Fuel Payload	1,260[1]	96.20
GA IFM Basket and Spacer	818	98.06
GA IFM Fuel Payload	148	167.34
TPBAR Basket and Spacer	675	110.40
TPBAR Payload	978[3]	96.00
ANSTO Basket	911	100.95
ANSTO Payload	756	100.95
TPBAR Basket	575	97.43
TPBAR with Rod Transport Canister Payload	1,326[4]	102.26

[1] For conservatism, a design basis MTR fuel weight of 30 lbs/assy is used in the structural analysis. The maximum MTR element weight is 13.2 lbs for an intact element and 9.7 lbs for the cut elements in the 42-element configuration.

[2] For conservatism, a bounding weight of 80 pounds is considered for each of the 28 fuel cells for PULSTAR fuel

[3] TPBAR payload represents the combined weight of the TPBAR and consolidation canister. A conservative 1,000 lb weight is applied in the structural analysis.

[4] TPBAR with Rod Transport Canister payload represents the combined weight of the 25 TPBARs, the PWR /BWR Rod Transport Canister and the PWR insert.

Table 2.2.1-2 Weights and Center of Gravity Locations for the NAC-LWT Cask Shipping Configurations

Component	Weight (pounds)	Axial Center of Gravity Location (inches)
Package -Loaded for Shipment (PWR) Maximum Payload	51,208	98.96
Package – Loaded for Shipment PWR High Burnup Rods	49,702	99.0
Package - Empty for Shipment (PWR)	48,082	99.12
Package - Loaded for Shipment (BWR)	49,832	99.00
Package - Empty for Shipment (BWR)	48,332	99.07
Package - Loaded for Shipment* (Metallic Fuel)	45,910	98.88
Package - Empty for Shipment* (Metallic Fuel)	43,830	99.09
Package - Loaded for Shipment (PULSTAR Fuel, MTR Four Unit Basket)	50,430	99.1
Package - Loaded for Shipment (MTR Fuel, Four Unit Basket)	49,030	99.1
Package - Empty for Shipment (MTR Fuel, Four Unit Basket)	48,190	98.9
Package - Loaded for Shipment (MTR Fuel, Five Unit Basket)	49,273	99.1
Package - Empty for Shipment (MTR Fuel, Five Unit Basket)	48,223	98.9
Package - Loaded for Shipment (MTR Fuel, Six Unit Basket)	49,470	99.1
Package - Empty for Shipment (MTR Fuel, Six Unit Basket)	48,210	98.9
Package - Loaded for Shipment (GA IFM Fuel and Basket)	48,147	99.3
Package - Empty for Shipment (GA IFM Basket)	48,026	99.3
Package – Loaded for Shipment (TPBARs and Basket)	48,861	99.2
Package – Empty for Shipment (TPBAR Basket)	47, 883	99.2
Package - Loaded for Shipment (ANSTO Fuel and Basket)	48,875	99.2
Package - Empty for Shipment (ANSTO Basket)	48,119	99.1

* Neutron Shield Tank is empty.

Table 2.2.1-2 Weights and Center of Gravity Locations for the NAC-LWT Cask Shipping Configurations (cont'd)

Component	Weight (pounds)	Axial Center of Gravity Location (inches)
Package - Loaded for Shipment TPBARs in the PWR/BWR Rod Transport Canister	49,109	99.2
Package - Empty for Shipment (TPBAR Basket for PWR/BWR Rod Transport Canister)	47,783	99.1
Package - Design for Shipment	52,000	98.93

2.3 Properties of Materials

The NAC-LWT cask body consists of six materials: (1) the inner and outer shells are Type XM-19 stainless steel; (2) the remainder of the cask body, the closure lid and the lifting trunnions are Type 304 stainless steel; (3) the annulus between the cask shells and the cavity in the bottom is filled with chemical copper lead for gamma radiation shielding; (4) the port covers are fabricated from SA-705, Grade 630 (Type 17-4PH) precipitation-hardened stainless steel; (5) the port cover bolts are made from SA-193, Grade B6 (Type 410) stainless steel; and (6) the closure lid bolts are fabricated from SA-453, Grade 660 high alloy steel bolting material.

The PWR and BWR fuel baskets are fabricated from Type 304 stainless steel and 6061-T6 aluminum alloy. The metallic fuel basket is fabricated from 6061-T6 aluminum alloy. The MTR, TRIGA, DIDO and GA IFM fuel baskets are fabricated from Type 304 stainless steel.

2.3.1 Mechanical Properties of Materials

The structural analyses of the NAC-LWT cask for normal operations and accident load conditions utilize the mechanical properties of the component materials. These properties are also used in calculating the allowable stresses for each component under each load condition.

The American Society of Mechanical Engineers is the source for the mechanical properties of Type 304 stainless steel, Type XM-19 stainless steel, SA-705, Grade 630 precipitation-hardened stainless steel, SA-193, Grade B6 (Type 410) stainless steel, and SA-453, Grade 660 high alloy steel bolting material ("ASME Boiler and Pressure Vessel Code," Appendix I). The effects of temperature on the material properties are included. The coefficient of thermal expansion presented in the tables represents the mean value for a temperature range from 70°F to the indicated temperature.

MIL-HDBK-5C is the source for the material properties of the aluminum alloys and for the equations used to evaluate the relationships of their material properties at elevated temperatures.

2.3.1.1 Cask Body Materials

The material of the inner and outer shells is Type XM-19 stainless steel. The remainder of the cask body and the closure lid are Type 304 stainless steel. These materials are selected because they are strong, ductile and highly resistant to corrosion and brittle fracture. The mechanical properties of Type 304 and Type XM-19 stainless steel are listed in Table 2.3.1-1 and Table 2.3.1-2, respectively.

2.3.1.2 Port Cover Materials

The alternate port covers are manufactured from SA-705, 17-4 PH Grade 630 precipitation-hardened stainless steel. The mechanical properties for this material are given in Table 2.3.1-3. The Alternate B port covers are manufactured from SA-479 XM-19 stainless steel. The mechanical properties for this material are given in Table 2.3.1-2.

2.3.1.3 Fuel Basket Materials

The materials used for the fuel basket are 6061-T6 aluminum and Type 304 stainless steel sheet, plate and bar. The mechanical properties of Type 304 stainless steel and 6061-T6 aluminum alloys are listed in Table 2.3.1-1 and Table 2.3.1-4, respectively.

2.3.1.4 Bolting Material

The port cover bolts for the alternate port cover are SA-193, Grade B6 (Type 410) stainless steel as described in Table 2.3.1-5. The bolts for Alternate B port covers are SB-637, Grade N07718, and nickel alloy steel as described in Table 2.3.1-9.

2.3.1.5 Shielding Material (Gamma Radiation)

Chemical copper lead fills the cylindrical region of the cask between the inner and outer cask shells and bottom plates. This lead core provides the required gamma radiation shielding. The presence of copper slightly increases the strength of lead at elevated temperatures. There is no concern that the lead will fail during normal transport conditions because it is completely enclosed inside the cask walls and bottom plates. Its shielding function requires no strength.

The finite element structural analysis program (ANSYS), used in the structural analysis of the cask, requires that the stress versus strain curve for this material be bilinear in the elastic to plastic transition region.

2.3.1.5.1 Static Mechanical Properties of Lead

The static mechanical properties of chemical copper lead are used in the NAC-LWT cask thermal stress analyses. The coefficient of thermal expansion for lead is of particular significance, because it is approximately twice that of stainless steel. The mechanical properties are obtained from testing reports (Tietz, Gallagher, Baumeister, NUREG/CR-0481). The properties are tabulated in Table 2.3.1-7 for the range of temperatures considered in the structural analysis. The bilinearized static stress-strain curve used in the finite element (ANSYS) analysis is shown in Figure 2.3.1-1; it is based on NUREG/CR-0481, Figure 24, and Table 2.3.1-7 of this report.

2.3.1.5.2 Dynamic Mechanical Properties of Lead

The dynamic mechanical properties of chemical copper lead are important for use in the NAC-LWT cask impact analyses. These properties are obtained from the "Cask Designer's Guide" (Shappert), which provides conservative values for dynamic yield strength. This property is used for calculating the shield deformation and for calculation of the maximum deceleration loading. These dynamic mechanical properties are listed in Table 2.3.1-8 for the range of temperatures considered in the structural analysis. The bilinearized dynamic deformation stress-strain curve used in the finite element (ANSYS) structural analysis is shown in Figure 2.3.1-2; it is based on NUREG/CR-0481, Figure 24, and Table 2.3.1-8 of this report.

Figure 2.3.1-1 Static Stress-Strain Curve for Chemical Copper Lead

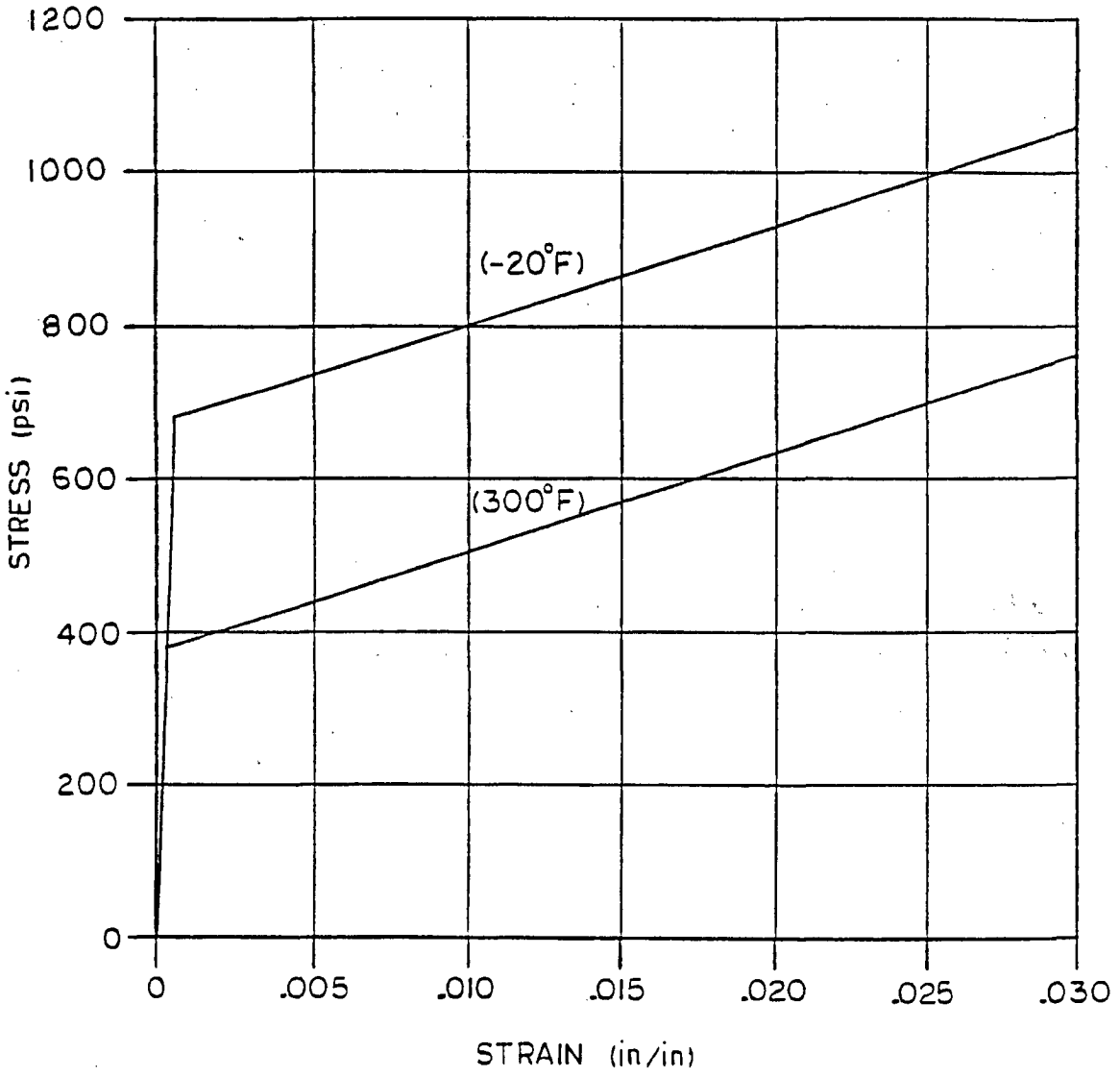

Figure 2.3.1-2 Dynamic Deformation Stress-Strain Curve for Chemical Copper Lead

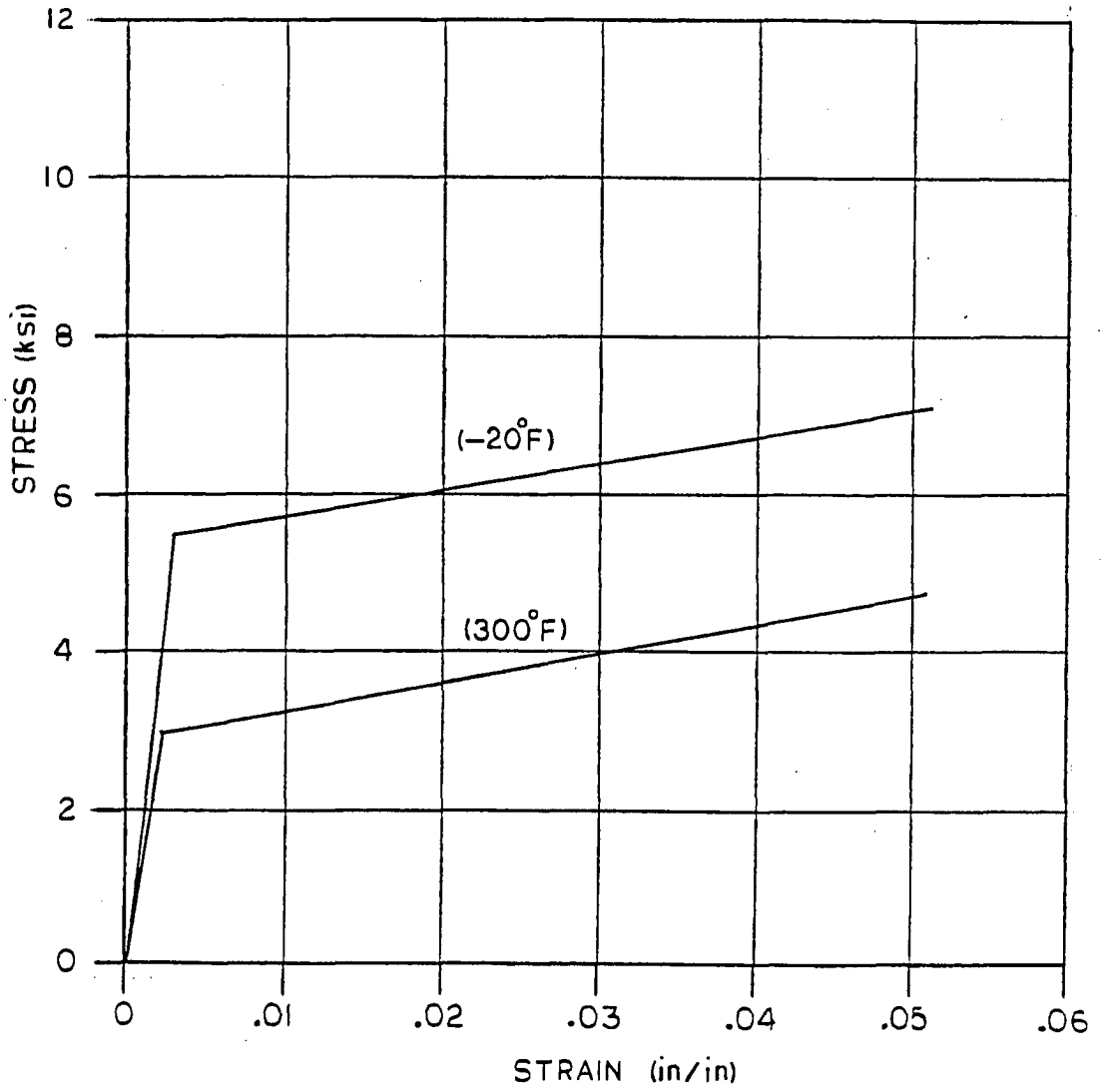

Table 2.3.1-1 Mechanical Properties of Type 304 Stainless Steel

Property (units)/Temperature (°F)	-40	-20	+70	+150	+200	+300	+600	+750
Ultimate Strength (ksi)	79.4	78.8	76.0	73.0	71.0	66.0	63.5	63.1
Yield Strength (ksi)	36.0	35.4	31.4	27.5	25.0	22.5	18.2	17.3
Design Stress Intensity	> 20.0	> 20.0	20.0	20.0	20.0	20.0	16.4	15.6
Modulus of Elasticity (ksi)	28.8E+3	28.7E+3	28.3E+3	27.9E+3	27.6E+3	27.0E+3	25.3E+3	24.4E+3
Alternating Stress @10 Cycles	720.5	718.0	708.0	698.0	690.5	675.5	632.9	610.4
Alternating Stress @10^6 Cycles	28.8	28.7	28.3	27.9	27.6	27.0	25.3	24.4
Strain at Yield (in/in)	0.00125	0.00123	0.00111	0.00099	0.00091	0.00083	0.00072	0.00071
Coefficient of Thermal Expansion (in/in/°F)	8.16E-6	8.23E-6	8.46E-6	8.67E-6	8.79E-6	9.00E-6	9.53E-6	9.76E-6
Poisson's Ratio	0.275							
Density	497 lbm/ft^3 (0.288 lbm/in^3)							

Reference:
ASME Boiler and Pressure Vessel Code, Section III, Division I, Appendix I.

Table 2.3.1-2 Mechanical Properties of Type XM-19 Stainless Steel

Property (units)/Temperature (°F)	-40	-20	+70	+150	+200	+300	+600	+750
Ultimate Strength (ksi)	104.5	103.7	100.0	99.8	99.5	94.3	87.8	85.7
Yield Strength (ksi)	63.0	62.0	55.0	51.0	47.0	43.4	37.3	35.8
Design Stress Intensity (ksi)	> 33.3	> 33.3	33.3	33.2	33.2	31.4	29.2	28.5
Modulus of Elasticity (ksi)	28.8E+3	28.7E+3	28.3E+3	27.9E+3	27.6E+3	27.0E+3	25.3E+3	24.4E+3
Alternating Stress @10 Cycles	720.5	718.0	708.0	698.0	690.5	675.5	632.9	610.4
Alternating Stress @10^6 Cycles	28.8	28.7	28.3	27.9	27.6	27.0	25.3	24.4
Coefficient of Thermal Expansion (in/in/°F)	8.16E-6	8.19E-6	8.27E-6	8.40E-6	8.48E-6	8.65E-6	9.03E-6	9.20E-6
Poisson's Ratio	0.275							
Density	497 lbm/ft^3 (0.288 lbm/in^3)							

Reference:
ASME Boiler and Pressure Vessel Code, Section III, Division I, Appendix I.

Table 2.3.1-3 Mechanical Properties of SA-705, Grade 630, Precipitation-Hardened Stainless Steel

Property (units)/Temperature (°F)	-40	-20	+70	+150	+200	+300	+600	+750
Ultimate Strength (ksi)	> 135.0	> 135.0	135.0	135.0	135.0	135.0	126.7	125.2
Yield Strength (ksi)	> 105.0	> 105.0	105.0	101.1	97.1	93.0	84.7	81.3
Design Stress Intensity	> 45.0	> 45.0	45.0	45.0	45.0	45.0	42.1	41.3
Modulus of Elasticity (ksi)	28.8E+3	28.7E+3	28.3E+3	27.9E+3	27.6E+3	27.0E+3	25.3E+3	24.4E+3
Alternating Stress @10 Cycles	720.5	718.0	708.0	698.0	690.5	675.5	632.9	610.4
Alternating Stress @10^6 Cycles	28.8	28.7	28.3	27.9	27.6	27.0	25.3	24.4
Strain at Yield (in/in)	0.00365	0.00366	0.00371	0.00362	0.00352	0.00344	0.00335	0.00333
Coefficient of Thermal Expansion (in/in/°F)	5.88E-6	5.88E-6	5.89E-6	5.89E-6	5.90E-6	5.90E-6	5.93E-6	5.95E-6
Poisson's Ratio	0.287							
Density	487 lbm/ft^3 (0.282 lbm/in^3)							

References:

1. ASME Boiler and Pressure Vessel Code, Section III, Division I, Appendix I.
2. MIL-HDBK-5C, Section 2.7.4.
3. Baumeister, pages 5 – 6.

Table 2.3.1-4 Mechanical Properties (6061-T6 and T651 per ASTM B-209)

Property (units)/Temperature (°F)	+70	+360[1]	+500[1]
Ultimate Strength (ksi)	42.0	30.2	17.2
Yield Strength (ksi)	35.0	26.6	15.8
Comp. Yield Strength (ksi)	35.0	26.6	15.8
Ultimate Shear Strength (ksi)	27.0	19.4	11.1
Yield Shear Strength (ksi)	20.0	15.2	9.0
Modulus of Elasticity (E), (ksi)	9,900	9,100	8,000
Coefficient of Thermal Expansion (in/in/°F)	12.6×10^{-6}	13.5×10^{-6}	13.9×10^{-6}

1. Strength at elevated temperatures calculated using the following relationships from MIL-HDBK-5A, pages 325, 326, and 328.

   @360°F: $(S_u)_{360} = 0.72(S_u)_{70}$; $(S_y)_{360} = 0.76(S_{70})$; $(E)_{360} = 0.92(E)_{70}$
   @500°F: $(S_u)_{500} = 0.41(S_u)_{70}$; $(S_y)_{500} = 0.45(S_{70})$; $(E)_{500} = 0.81(E)_{70}$

   Reference:
   MIL-HDBK-5C, pages 3–208 and 3-214.

Property (units)/Temperature (°F)	70	100	200	300	400
Design Stress Intensity[2] (ksi)	10.5	10.5	10.5	8.4	4.4

2. ASME Code, Section II-D, Table 1-B

Table 2.3.1-5 Mechanical Properties of SA-193, Grade B6 High Alloy, Steel Bolting Material

Property (units)/Temperature (°F)	-40	-20	+70	+150	+200	+300	+600	+750
Ultimate Strength (ksi)	> 110.0	> 110.0	110.0	108.2	106.6	104.3	96.8	90.0
Yield Strength (ksi)	> 85.0	> 85.0	85.0	83.5	82.3	80.5	74.8	69.5
Modulus of Elasticity (ksi)	30.3E+3	30.1E+3	29.2E+3	28.8E+3	28.5E+3	27.9E+3	26.1E+3	25.1E+3
Alternating Stress @10^6 Cycles	20.2	20.1	19.8	19.5	19.3	19.0	17.9	17.3
Poisson's Ratio	0.32							
Density	489 lbm/ft^3 (0.283 lbm/in^3)							

References:

1. ASME Boiler and Pressure Vessel Code, Section III, Division I, Appendix I.
2. MIL-HDBK-5C, Section 2.3.1.

Table 2.3.1-6 Mechanical Properties of SA-453, Grade 660 High Alloy, Steel Bolting Material

Property (units)/Temperature (°F)	-40	-20	+70	+150	+200	+300	+600	+750
Ultimate Strength (ksi)	> 130.0	> 130.0	130.0	130.0	130.0	130.0	122.0	120.6
Yield Strength (ksi)	> 85.0	> 85.0	85.0	83.9	82.8	81.9	81.0	80.1
Modulus of Elasticity (ksi)	28.3E+3	28.2E+3	27.8E+3	27.3E+3	27.1E+3	26.7E+3	25.2E+3	23.8E+3
Coefficient of Thermal Expansion (in/in/°F)	7.93E-6	8.00E-6	8.22E-6	8.31E-6	8.39E-6	8.54E-6	8.94E-6	9.11E-6
Poisson's Ratio	0.32							
Density	489 lbm/ft^3 (0.283 lbm/in^3)							

References:

1. ASME Boiler and Pressure Vessel Code, Section III, Division I, Appendix I.
2. MIL-HDBK-5C, Section 2.3.1.

Table 2.3.1-7 Static Mechanical Properties of Chemical Copper Lead

Property (units)/Temperature (°F)	-40	-20	+70	+150	+200	+300	+600
Ultimate Strength (psi)	700	680	640	550	490	380	20
Modulus of Elasticity (ksi)	2.45E+3	2.42E+3	2.28E+3	2.16E+3	2.06E+3	1.94E+3	1.5E+3
Strain at Yield (in/in)	0.000286	0.000281	0.000291	0.000255	0.000238	0.000196	0.000133
Coefficent of Thermal Expansion (in/in/°F)	15.6E-6	15.7E-6	16.1E-6	16.4E-6	16.6E-6	17.2E-6	20.2E-6
Poisson's Ratio	0.40						
Density	708 lbm/ft^3 (0.41 lbm/in^3)						

References:

1. Tietz.
2. Gallagher.
3. NUREG/CR-0481.
4. Baumeister, pages 6-10.

Table 2.3.1-8 Dynamic Mechanical Properties of Chemical Copper Lead

Property (units)/Temperature (°F)	-40	-20	+70	+150	+200	+300	+600
Deformation Yield Strength (psi)	5620	5510	5000	4440	3960	3100	150
Deceleration Loading Yield Strength (ksi)	11,200	11,000	10,320	8870	7800	6100	300
Modulus of Elasticity (ksi)	2.45E+3	2.42E+3	2.28E+3	2.16E+3	2.06E+3	1.94E+3	0.15E+3
Strain at Yield (Deformation) (in/in)	0.00229	0.00228	0.00219	0.00206	0.00192	0.00160	0.00100

References:

1. Shappert.
2. NUREG/CR-0481.

Table 2.3.1-9 Mechanical Properties of SB-637, Grade N07718, Nickel Alloy Steel Bolting Material

Property (units)/Temperature (°F)	-40	-20	+70	+200	+300	+400	+500	+750
Ultimate Strength (ksi)	> 185.0	> 185.0	185.0	177.6	173.5	170.6	168.7	165.0
Yield Strength (ksi)	> 150.0	> 150.0	150.0	144.0	140.7	138.3	136.8	133.8
Modulus of Elasticity (ksi)	29.6E+3	29.5E+3	29.0E+3	28.3E+3	27.8E+3	27.6E+3	27.1E+3	26.1E+3
Coefficient of Thermal Expansion (in/in/°F)			7.05E-6	7.22E-6	7.33E-6	7.45E-6	7.57E-6	7.82E-6
Poisson's Ratio	0.31							
Density	503 lbm/ft^3 (0.291 lbm/in^3)							

Reference:
1. ASME Boiler and Pressure Vessel Code, Section III, Division I.

2.4 General Standards for All Packages

This section demonstrates that general requirements found in 10 CFR 71.43 are addressed in the design and analysis of the NAC-LWT cask, a spent-fuel shipping package. A package is defined as the assembly of components necessary to ensure compliance with 10 CFR 71 for the transportation of radioactive contents. The package includes the radioactive contents.

2.4.1 Minimum Package Size

The minimum transverse dimension of the NAC-LWT package is 44.24 inches (112 cm), and the minimum longitudinal dimension is 199.8 inches (507 cm). Both dimensions are greater than 10 centimeters; therefore, the requirements of 10 CFR 71.43(a) are satisfied.

2.4.2 Tamperproof Feature

One railroad car type seal is looped through a hole near the end of one ball-lock pin, which attaches the impact limiter attachment lugs to the mating cask lugs.

To tamper with the closure lid or port cover bolts, it is necessary to remove the upper impact limiter; thus, a severed seal will indicate purposeful tampering. This satisfies the tamperproof requirement of 10 CFR 71.43(b). This vent port and the drain port are protected by port covers. Both port covers are covered by the upper impact limiter; therefore, they cannot be operated by unauthorized personnel. This satisfies the requirements of 10 CFR 71.43(e).

2.4.3 Positive Closure

Inadvertent opening of the cask closure lid or the port covers from the combined effects of shock, vibration, thermal expansion, internal loads and/or external loads, cannot occur because of the large preload applied to the lid bolts. Loosening of these bolts is resisted by friction from the large clamping forces produced by the applied bolt preload torque. A cask operations procedure is followed, ensuring that each bolt is torqued. It is necessary to deliberately loosen the bolts with a wrench to facilitate inadvertent opening. The cover bolts cannot be loosened/removed while the upper impact limiter is attached with tamper-indicating seals in place. Therefore, the NAC-LWT cask containment system cannot be opened unintentionally and is protected against unauthorized operation; the requirements of 10 CFR 71.43(c) and (e) are satisfied.

2.4.4 Chemical and Galvanic Reactions

The structural materials of this package, which are in direct contact with each other, will not produce significant chemical or galvanic reaction in an electrically conductive environment. An inert stainless steel material is used to separate anodic from cathodic materials. The lead shielding material is completely encapsulated by the stainless steel shells; thereby, being separated from the aluminum basket. The aluminum honeycomb used for impact limiters is sealed inside an aluminum shell. The material of the miscellaneous cask components is stainless steel, which is compatible with all adjacent materials. Therefore, the materials do not have chemical or galvanic reactions in accordance with 10 CFR 71.43(d).

2.4.5 Cask Design

The cask is designed to meet the applicable sections of 10 CFR 71. Criticality, shielding, thermal, radiological and structural requirements of 10 CFR 71 are analytically shown to be satisfied. Conclusions drawn from the structural analyses are supported by quarter scale model drop tests. The NAC-LWT cask is an exclusive use package designed for transport in a 130°F environment such that personnel barrier temperatures do not exceed 180°F; thus, meeting the requirements of 10 CFR 71.43(g).

2.4.6 Continuous Venting

The neutron shield/expansion tank is the only vented system of the NAC-LWT cask. The shield/expansion tank contains a solution of ethylene glycol and water. No venting of the shield/expansion tank occurs during normal operations conditions; thus, meeting the requirements of 10 CFR 71.43(h).

2.5 Lifting and Tiedown Standards

2.5.1 Lifting Devices

The NAC-LWT cask has three types of lifting devices: (1) four lifting trunnions; (2) four lid lifting bolts; and (3) two rotation trunnions. These lifting devices are designed to meet the requirements of NUREG-0612, "Control of Heavy Loads at Nuclear Power Plants."

Lifting of the cask is accomplished by utilizing the lifting trunnions near the top of the cask. Two lifting yokes are used to provide redundancy. Each lifting yoke is attached to two diametrically opposite lifting trunnions. An overhead crane lifts the cask by these yokes. No impact limiter is attached to the cask during lifting and handling. The bottom impact limiter could be attached for protection during handing, but the top impact limiter cannot be used while the lifting yoke is in place.

The lid lifting bolts are used to attach cables for lifting the lid during installation or removal.

The rotation trunnions are used to rotate the cask from the horizontal to the vertical position. The rotation trunnions also support the cask in the transportation cradle.

2.5.1.1 Lifting Trunnion

The NAC-LWT cask is equipped with four lifting trunnions located on the upper ring near the top of the cask and spaced at 90-degree intervals; thus, either a nonredundant, two-arm yoke or a redundant, four-arm yoke system may be used to lift and handle the cask.

2.5.1.1.1 Loads

The lifting trunnions were analyzed for the most severe load, a single, nonredundant load path lift. Using the requirements of 10 CFR 71.45(a), the applied load factor is 3.0 on the yield strength. The yield strength of the material at 200°F is used. Any dynamic load effects are negligible when considered in combination with the large applied load factor.

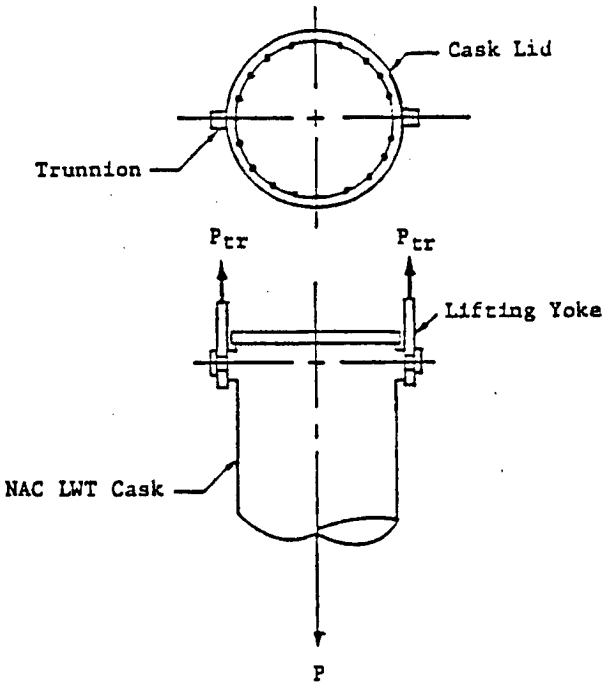

Lifting Trunnion Loads and Reactions

$P = LF \times W$

Fully Loaded Cask Weight (W) = 52,000 lbs

Load Factor on Yield $(LF)_y = 3.0$

$P_y = 3.0\ (52{,}000) = 156{,}000$ lbs

$(P_{tr})_y = 0.5\ (P_y) = 78{,}000$ lbs

2.5.1.1.2 Material Properties at 200°F

Trunnion and Cask Upper Ring (Base Metal)

ASME SA-240, Type 304

$S_y = 25{,}000$ psi

The shear strength is half the tensile strength if the compressive and tensile strengths are equal (Timoshenko, 1976, p. 449), which is conservative for stainless steel.

$$F_{sy} = \frac{S_y}{2} = 12{,}500 \text{ psi}$$

Weld Metal

The weld metal properties exceed those of the base metal, which is a standard welding code practice; therefore, the base metal properties are used for the weld analysis.

2.5.1.1.3 Stress Analysis

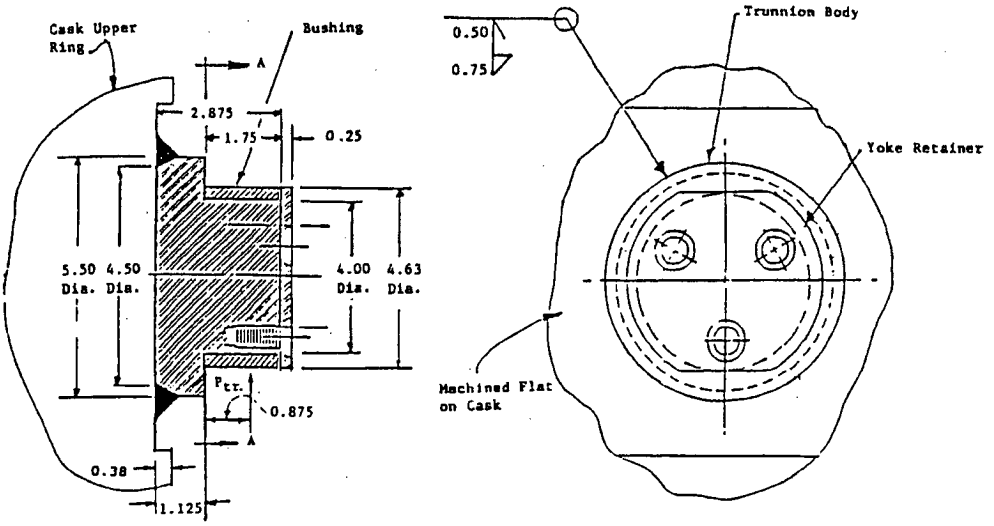

Typical Lifting Trunnion

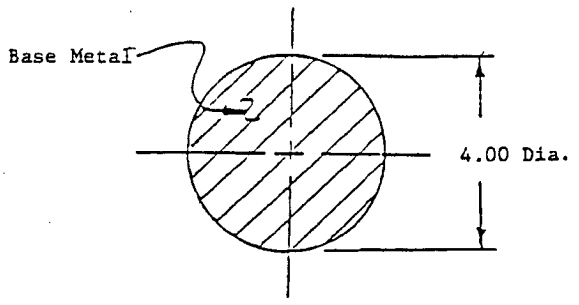

Section A-A

Shear Stress in Base Metal at Section A-A

$$(S_s)_y = \frac{(P_{tr})_y}{A_{aa}} = \frac{78{,}000}{\pi\,(2.00)^2} = 6{,}207 \text{ psi}$$

Margin of Safety at Section A-A

$$(M.S.)_y = \frac{F_{sy}}{(S_s)_y} - 1 = \frac{12{,}500}{6207} - 1 = \underline{+1.01}$$

Critical Weld Section

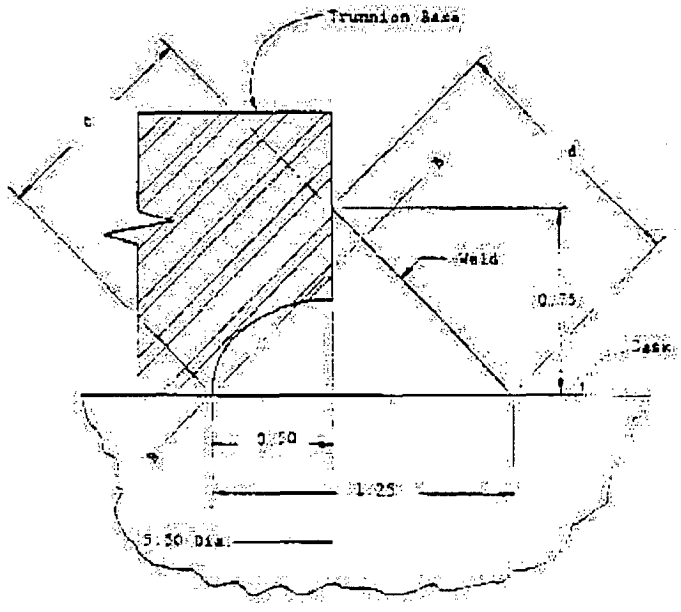

Effective Weld Throat

The most critical section of the weld shown in the above sketch is Section B-B. Its length is:

$$L_{bb} = 0.707\,(1.25) = 0.884 \text{ in}$$

The mean diameter of the center of gravity of Section B-B is:

$$d_{bb} = 5.50 - 2\,(0.50) + 2\,(\frac{1.25}{4}) = 5.125 \text{ inches}$$

Vertical Shear Force/Inch in Welds at Section B-B

$$(f_v)_y = \frac{(P_{tr})_y}{(d)_{bb}} = \frac{78{,}000}{\pi(5.125)} = 4{,}845 \text{ pounds / inch}$$

Horizontal Shear Force/Inch in Welds at Section B-B

$$(f_h)_y = \frac{(M_{bb})_y}{(Z_w)_{bb}} = \frac{78{,}000\ (1.125 + 1.75/2)}{\pi\ (5.125)^2/4} = 7{,}562 \text{ pounds/inch}$$

Combined Shear Force/Inch in Welds at Section B-B

$$(f_r)_y = \sqrt{[(f_v)_y]^2 + [(f_h)_y]^2} = \sqrt{(4845)^2 + (7562)^2}$$

$$= 8{,}981 \text{ pounds/inch}$$

Shear Stress in Weld at Section B-B

$$(f_w)_y = \frac{(f_r)_y}{L_{bb}} = \frac{8981}{0.884} = 10{,}159 \text{ psi}$$

Margin of Safety (MS) in Weld at Section B-B

$$(M.S.)_y = \frac{F_{sy}}{(f_w)_y} - 1 = \frac{12{,}500}{10{,}159} - 1 = \underline{+0.23}$$

2.5.1.1.4 Sequence of Lifting Component Failure

In addition to the load factor requirements in 10 CFR 71.45(a), lifting components must be designed such that, if the component fails under excessive load, the package will continue to meet other 10 CFR 71 requirements. To establish that the package continues to meet other 10 CFR 71 requirements, it is shown below that the trunnions will fail before the containment boundary fails. Trunnion failure enables other cask features (for example, impact limiters, cask body, etc.) to perform their function and bring the cask and contents to rest without breaching containment.

The maximum load carrying capacity of the trunnions, the trunnion welds, and the upper forging are calculated in this section.

Trunnions

The trunnions are manufactured from Type 304 stainless steel. To conservatively evaluate the maximum load carrying capacity of the trunnions, bending is neglected and the trunnion is considered in pure shear failure. The maximum load carrying capacity is calculated by multiplying the ultimate shear strength of Type 304 stainless steel by the cross-sectional area of the trunnion. The ultimate shear strength is calculated by multiplying the ultimate tensile strength (UTS) by 0.50 (Section 2.1.2.2).

$$P_u = (S_{su})(A_t)$$
$$= 446{,}235 \text{ lbs}$$

where:

P_u = maximum load capacity (lb)

S_{su} = (UTS) (0.50), Type 304 stainless steel @ 200°F (psi)

= 35,500 psi

D_t = 4.00 in.

A_t = shear area of trunnion (in^2) = $(\pi/4)\ (D_t)^2$

= 12.57 in^2

Trunnion Weld Interface

The width of the interface between the trunnion and the weld is $(0.50^2 + 0.75^2)^{0.5} = 0.901$ inch with an effective diameter of 5.0 inches. The ultimate shear capacity of the trunnion at the weld interface is:

$$P_u = (5.0)(\pi\pi(0.901)(35{,}500)$$
$$= 502{,}427 \text{ lbs}$$

Trunnion Weld

Figure 2.5.1-1 shows the lifting component (trunnion and trunnion weld) attached to the upper forging. The applied load, W, acts 2.125 inches from the weld and outer shell. The effects of bending are conservatively ignored because the line of action of the load is less than one diameter from the trunnion weld.

The effective weld area for the fillet/groove weld is the circular ring described by the minimum throat area as described in Section 2.5.1.1.3. The weld area is calculated as:

$$A_w = (L_w)(\pi)(D_m)$$
$$= 14.23 \text{ in}^2$$

where:

A_w = effective weld area (in^2)

L_w = minimum throat length = 0.884 in

D_m = mean diameter = 5.125 inches

The ultimate shear stress, S_{su}, for AWS E308 electrodes, which are used to weld Type 304 stainless steel, is (0.5)(80,000) = 40,000 psi. The maximum load that the trunnion weld can withstand is:

$$P_u = (A_w)(S_{su})$$
$$= 569{,}200 \text{ lbs}$$

Cask Upper Forging

The lifting components are attached to the upper forging of the NAC-LWT cask. Since the upper end casting is a solid piece of Type 304 stainless steel, this calculation considers the 1.25-inch wide ring of parent material beneath the trunnions (shown as a cross-hatched area in Figure 2.5.1-1). The maximum load that the outer shell can withstand is:

$$P_u = (A_p)(S_{su})$$
$$= 801{,}590 \text{ lbs}$$

where:

$$A_p = (\pi/4)(D_o^2 - D_i^2)$$
$$= (\pi/4)(7.00 - 4.50^2)$$
$$= 22.58 \text{ in}^2$$
$$S_{su} = 35{,}500 \text{ psi}$$

Conclusion

The maximum load carrying capacity of the trunnion, the trunnion/weld interface, the trunnion weld, and the upper forging are summarized in Table 2.5.1-1. The trunnion has a minimum load carrying capacity; its failure under excessive load will not impair the ability of the package to meet the other requirements of 10 CFR 71, Subpart E.

2.5.1.2 Lid Lifting Bolts

The top of the NAC-LWT cask lid is equipped with four 1 - 8 UNC threaded holes on a 9.0-inch square pattern to accommodate bolts to be used to lift the lid. These holes are threaded 1.5 inches deep.

A load factor of 3.0 for yield strength analysis is applied to the load for handling safety. The weight of the lid without attachment bolts is 919 pounds; thus, the tensile force on each bolt is (3.0)(919)/4 = 689 pounds. For conservatism, it is assumed that the bolt and the lid are of the same material, Type 304 stainless steel, which has a yield strength (S_y) equal to 27,500 psi at

150°F. Any dynamic load effects are negligible when considered in combination with the large applied load factors.

The tensile stress area (A_t) for a 1 - 8 UNC bolt, according to Table III.3 of "Screw-Thread Standards for Federal Services," is 0.606 square inches. Therefore, the stress in the bolt is 689/0.606 = 1044 psi and the margin of safety is (27,500/1044) - 1 = +LARGE.

The minimum length of thread engagement (L_e) required to fully develop the tensile strength of the bolt is calculated from "Screw-Thread Standards for Federal Services," Section II, Article 23, which gives the equation:

$$L_e = \frac{2A_t}{\pi n K_{n_{max}} + \left[0.5n + 0.57735\left(E_{s_{min}} - K_{n_{max}}\right)\right]}$$

where ("Screw-Thread Standards for Federal Services," Table III.10):

n = number of threads per inch = 8

$K_{n_{max}}$ = maximum minor diameter of threaded hole = 0.890 in

$E_{s_{min}}$ = minimum pitch diameter of bolt threads = 0.910 in

$$L_e = \frac{2(0.606)}{\pi(8)(0.890)\left[1/2(8) + 0.57735(0.910 - 0.890)\right]} = 0.7318 \text{ in}$$

This length is less than the 1.25-inch actual depth of threads, assuming the first and last threads are inactive; therefore, the internal threads of the tapped hole possess enough strength to cause the bolt to fail before the threads shear.

2.5.1.3 Can Assembly (315-40-98)

The LWT can assembly lifting is accomplish by lifting the assembly at the handle on the can lid. A factor of safety on yield strength of 3 is required for handling safety. The weight lifted by the handle (considering a 10% dynamic load factor) is:

$$W = (350 + 310 + 240 + 75) \times 1.1 = 1{,}072 \text{ lbs}$$

During lifting, the tensile stress at the minimum cross section of the handle is:

$$\sigma_t = \frac{W}{A} = \frac{1{,}072 \text{ lb}}{0.78 \text{ in.}^2} \cong 1{,}374 \text{ psi}$$

where:

$A = (4.25 - 3.0) \times 5/8 = 0.78 \text{ in}^2$

Because the factor of safety, $FS = \frac{17{,}300}{1{,}326} = 13.0 > 3$, the design condition lifting stresses have a factor of safety of 3 on the basis of yield strength is met.

The maximum shear occurs at the center of the handle and is computed as:

$$\tau = \frac{W}{A} = \frac{1{,}072 \text{ lbs}}{(3.23 - 1.5 - 0.23 - 0.88)(0.625) \text{ in.}} \cong 2{,}766 \text{ psi}$$

The factor of safety (FS) is conservatively calculated using a shear allowable of $0.6S_m$ at 750°F.

$$FS = \frac{0.6(17{,}300 \text{ psi})}{2{,}766 \text{ psi}} = 3.38 > 3$$

Therefore, the design condition that lifting stresses have a factor of safety of 3 on the basis of yield strength is met.

Figure 2.5.1-1 Trunnion Cross-Section and Forging Shear Area

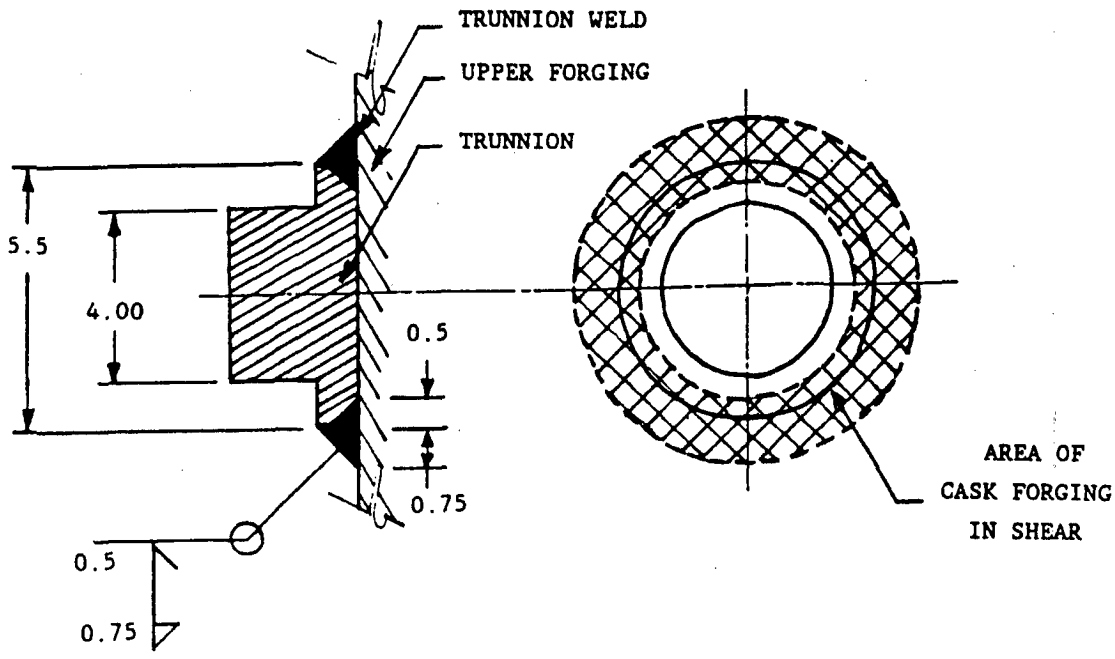

Table 2.5.1-1 Maximum Capacity of the Lifting Components

Lifting Trunnion	446,235 lbs
Trunnion/Weld Interface	502,427 lbs
Trunnion Weld	569,200 lbs
Cask - Upper Forging	801,590 lbs

2.5.2 Tiedown Devices

The NAC-LWT cask is tied down to the shipping skid using the following: (a) rotation trunnions near the bottom at point i (Figure 2.5.2-1); and (b) a 90-degree saddle support, hold-down straps and a shear ring near the top end at point j (Figure 2.5.2-1). Longitudinal force towards the bottom of the cask is resisted by the supports at the rotation trunnions; a shear ring welded to the outer shell resists the longitudinal force towards the top end of the cask. A 0.50-inch gap is provided between the shear ring and the saddle support to accommodate the thermal expansion of the cask.

In accordance with 10 CFR 71.45(b), the tiedown components of the cask are designed for static forces having a vertical component of two times the weight of the package, a longitudinal component of ten times the weight of the package, and a lateral component of five times the weight of the package. The design weight of the NAC-LWT cask with its contents and impact limiters is 52,000 pounds.

2.5.2.1 Discussion and Loads

The resultant force on the shear ring is assumed to act at the centroid of the contact area between the shear ring and the saddle support. Referring to Figure 2.5.2-1, the distance of the centroid from the center of the cask is determined:

$$\bar{y} = (A_o \bar{y}_o - A_i \bar{y}_i)/(A_o - A_i)$$

$$\bar{y} = \left|(2 \sin\theta\, (R_o^3 - R_i^3)\right|/\left|3\theta(R_o^2 - R_i^2)\right|$$

$$= 13.90 \text{ inches}$$

where:

$A = \theta R^2$

$\bar{y} = (2R \sin\theta / 3\theta$

$\theta = 45° = \pi/4$ radians

$R_o = 15.81$ inches

$R_i = 15.06$ inches

There are three loading cases for the tiedown components - vertical, longitudinal, and lateral loads. The reaction forces for each loading case are determined by the equations of equilibrium.

2.5.2.1.1 Vertical Load

Downward Direction Case

$F_y = -2W = -2(52,000) = -104,000$ lbs

Summing moments M_z about point j:

$\Sigma M_z = -104,000(82.22) + 2R_{iy}(165.63) = 0$

$R_{iy} = +25,813$ lbs

Summing vertical forces:

$2R_{iy} + R_{jy} - 104,000 = 0$

$R_{jy} = 52,374$ lbs

Note: $R_{ix} = R_{jx} = 0$ because of the gap provided at the shear ring.

Upward Direction Case

$F_y = +2W = +2(52,000) = +104,000$ lbs

similarly (Section 2.5.2.1.1),

$R_{iy} = -25,813$ lbs

$R_{jy} = -52,374$ lbs

Note that the support saddle cannot carry any upward load. Hence, the negative R_{jy} is resisted by tiedown straps.

2.5.2.1.2 Longitudinal Load

Load Toward the Top End of the Cask

$F_x = +10W = +10(52,000) = +520,000$ lbs

Summing horizontal forces:

$520,000 + R_{jx} = 0$

$R_{jx} = -520,000$ lbs

Summing moments about j:

$520,000(13.90) + 2R_{iy}(165.63) = 0$

$R_{iy} = -21,820$ lbs

Summing vertical forces:

R_{jy} - 2(21,820) = 0

R_{jy} - 43,640 lbs

Load Toward the Bottom of the Cask

F_x = -10W = -10(52,000) = -520,000 lbs

Summing horizontal forces:

-520,000 + $2R_{ix}$ = 0

R_{ix} = +260,000 lbs

Summing moments about j:

-520,000(13.90) + 2(260,000)(13.90 + 3) + $2R_{iy}$ (165.63) = 0

R_{iy} = -4,709 lbs

Summing vertical forces:

R_{jy} – 2(4709) = 0

R_{jy} = 9,418 lbs

2.5.2.1.3 Lateral Load

F_z = 5W = 5(52,000) = 260,000 lbs

To find the reactions resisting the above load, it is necessary to find the location of the bearing pressure between the support saddle and the cask surface. The contact surface is one-half of the saddle, as shown in Figure 2.5.2-2. Assume that the horizontal bearing pressure at any point is proportional to the sine function of the angular distance of the point from the lowest point in the saddle.

Referring to Figure 2.5.2-2, take a unit radius:

$dA = \sin\theta[\cos\theta - \cos(\theta + d\theta)]$

$= \sin\theta[\cos\theta - (\cos\theta\cos d\theta - \sin\theta\sin d\theta)]$

For small angle $d\theta$, $\cos d\theta \approx 1$, $\sin d\theta \approx d\theta$

hence,

$dA = \sin^2\theta d\theta$

$$A = \int_0^{\pi/4} \sin^2\theta d\theta$$

$$= \frac{1}{2}\theta - \frac{1}{4}\sin 2\theta$$

$$= (\pi - 2)/8 = 0.1427$$

The first moment of area about the horizontal line through the center is:

$$dM = ydA$$

$$= \cos\theta \sin^2\theta d\theta$$

$$M = \int_0^{\pi/4} \cos\theta os\theta^2 \theta d\theta$$

$$= (\sin^3\theta)/3$$

$$= 0.17785$$

$$\bar{y} = \frac{M}{A} = 0.8259$$

where:

$R = 14.31$ inches

$\bar{y} = 11.82$ inches

Call the location of this centroid: point k.

The horizontal distance from the center of the cask to the support point i is 16.87 inches.

Summing moments about the vertical line through k (Figure 2.5.2-3):

$$260{,}000(82.22) + R'_{iz}(165.63) = 0$$

$$R'_{iz} = -129{,}066 \text{ lbs}$$

Summing forces along the Z-axis:

$$260{,}000 - 129{,}066 + R_{jz} = 0$$

$$R_{jz} = -130{,}934 \text{ lbs}$$

Summing forces along the Y-axis:

$$R_{iy} = -R'_{iy}$$

Summing moments about the longitudinal axis of the cask:

$$130{,}934(11.82) - 129{,}066(3) - R'_{ig}\,(16.87 + 16.87) = 0$$

$$R'_{iy} = 34{,}394 \text{ lbs}$$

$$R_{iy} = -34{,}394 \text{ lbs}$$

(Opposite Lateral Load)

$$F_z = -5W = -5(52{,}000) = -260{,}000 \text{ lbs}$$

The reactions for this case are opposite to the previous case.

2.5.2.1.4 Loads Summary

The results of all the loading cases are summarized in Table 2.5.2-1.

2.5.2.2 Rear Support

The NAC-LWT cask rear tiedown attachment is at the rotation trunnions. There are two rotation trunnions, which are slots located 16 inches above the bottom of the cask and spaced at approximately 180-degree positions in line with two of the lifting trunnions. Each slot is a machined part, which is welded all around to the cask outer shell. The neutron shield tank shell is cut out to provide access to the slots. The geometry details of the shield tank cut-outs and the rotation trunnion slots are shown in Figure 2.5.2-4.

2.5.2.2.1 Loads

The rotation trunnions are analyzed for the cask tiedown load condition defined in 10 CFR 71.45(b). The condition used for this analysis assumes that the cask is supported horizontally on a trailer and is subjected to a 10 g longitudinal shock load simultaneously with a 2 g vertical shock load and a 5 g lateral shock load. The direct lateral load is transferred to the cask through bearing on the large trunnion slot base. Any dynamic load effects are negligible when considered in combination with the large applied load factors. The critical loads on the rotation trunnions are derived in Section 2.5.2.1.

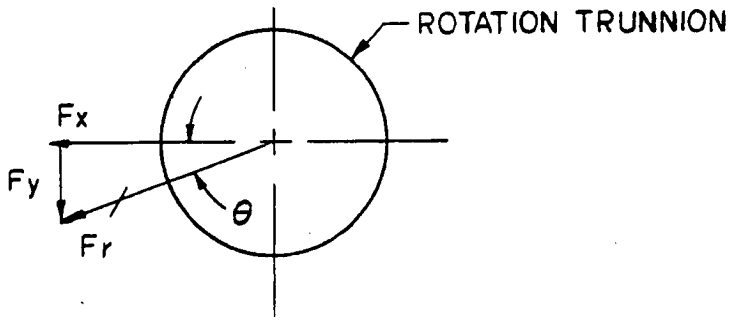

Resultant Load Determination

$$F_r = \sqrt{(F_x)^2 + (F_y)^2}$$

$$= 272{,}632 \text{ lbs}$$

where:

$F_x = 260{,}000$ lbs

$F_y = 82{,}027$ lbs (Table 2.5.2-1; Section 2.5.2.1)

then

$\theta = \arctan(82{,}027/260{,}000)$

$= 17.5$ degrees

2.5.2.2.2 Material Properties at 200°F

The yield strength of each material at 200°F is the allowable stress:

Type 304 stainless steel

$S_y = 25{,}000$ psi

Cask and Trunnion Slot (Base Metal)

The bearing stress ratio is taken from MIL-HDBK-5A where the bearing yield stress for the austenitic stainless steels at ambient temperature is specified as 50,000 psi and the yield strength as 30,000 psi. It is assumed that the ratio of bearing stress to yield stress remains constant up to 200°F:

$S_{bry} = 1.67(25{,}000) = 41{,}750$ psi

The shear strength is (0.6) (yield strength):

$S_{sy} = 0.6S_y = 15{,}000$ psi

Weld Metal

The weld metal properties exceed those of the base metal, based on standard welding code practice; therefore, the base metal properties will be used for the weld analysis:

$(S_{sy})_w = 15{,}000$ psi

2.5.2.2.3 Stress Analysis

Bearing Stress in Trunnion Slot (Figure 2.5.2-4)

$F_y = 272{,}632$ lbs

Length of engagement for 4.00-in diameter pin = 3.25 inches

$A_{br} = 4.00(3.25) = 13.00$ in^2

$$S_{br} = \frac{F_r}{A_{br}}$$

$= 20{,}972$ psi

$$MS = \frac{S_{bry}}{S_{br}} - 1 = \underline{+0.99}$$

Stress in Weld Connecting Trunnion to Cask (Figure 2.5.2-4)

Assume the entire load transferred to the cask outer shell through the weld at the base of the trunnion.

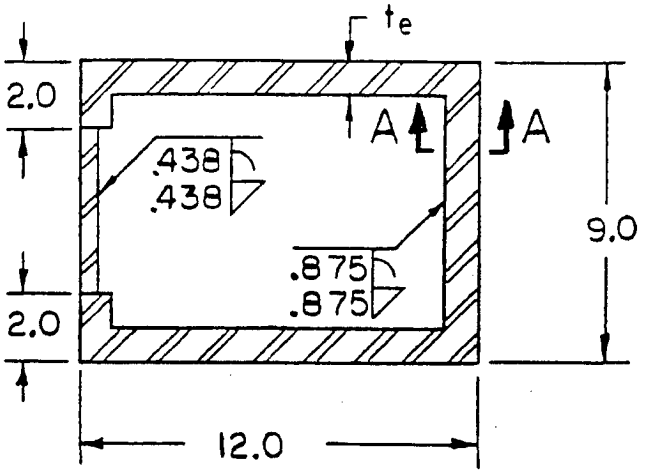

Section Through Weld at Base of Pocket

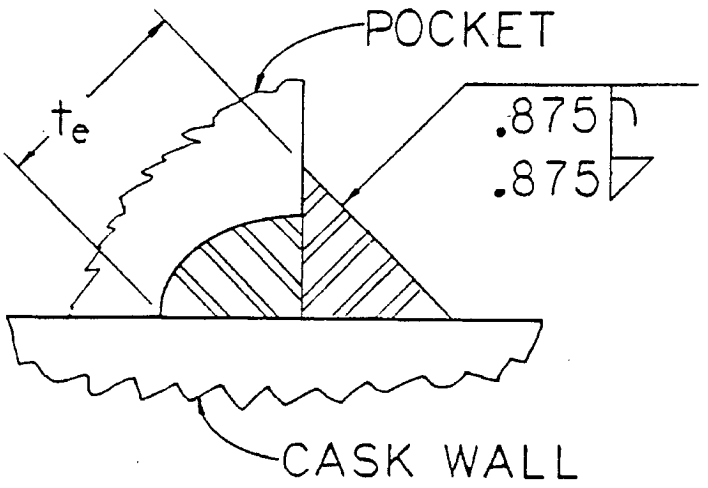

Section A-A

Effective thickness of weld (t_e) = ($\sqrt{2}$) (t_w)

for:

t_w = 0.875 in; t_e = 1.237 in

t_w = 0.438 in; t_e =0.619 in

Section Properties of Weld Group

Area (A_w) = 42.741 in^2

$\bar{y}$ = 4.500 inches

$\bar{x}$ = 6.412 inches

I_{xx} = 501.924 in^4

I_{yy} = 718.398 in^4

$J_{xy} = I_{xx} + I_{yy}$ = 1220.322 in^4

Loads on Weld Group

F_x = 260,000 lbs

F_y = 82,027 lbs

e_x = 6.412 – 4.000 = 2.412 inches

e_z = 19.08 – 14.00 – 3.25/2 = 3.455 inches

$M_x = F_y (e_z) = 82,027 (3.455) = 283,403$ in-lbs

$M_y = F_x (e_z) = 260,000 (3.455) = 898,300$ in-lbs

$M_z = F_y (e_x) = 82,027 (2.412) = 197,849$ in-lbs

Maximum Stresses on Effective Thickness of Weld Group

$$S_X = \frac{F_X}{A_W} + \frac{M_Z C_y}{J_{xy}} = \frac{260,000}{42.741} + \frac{(197,849)(4.50)}{1220.322}$$

$= 6813$ psi

$$S_y = \frac{F_y}{A_w} + \frac{M_z C_x}{J_{xy}} = \frac{82,027}{42.741} + \frac{(197,849)(6.412)}{1220.322}$$

$= 2959$ psi

$$S_z = \frac{M_x C_y}{I_{xx}} + \frac{M_y C_x}{I_{yy}} = \frac{(283,403)(4.5)}{(501.924)} + \frac{(898,300)(6.412)}{(718.398)}$$

$= 10,559$ psi

$$S_{smax} = (S_X^2 + S_y^2 + S_z^2)^{0.5}$$

$= 12,910$ psi

$$\text{M.S.} = \frac{(S_{sy})_w}{S_{smax}} - 1 = \underline{+0.16}$$

The positive margins of safety show that the rotation trunnion meets the requirements of 10 CFR 71.45(b).

2.5.2.2.4 Overload - Tiedowns

According to 10 CFR 71.45(b)(3), each tiedown device that is a structural part of a package must be designed so that failure of the device under excessive load would not impair the ability of the package to meet the other requirements of 10 CFR 71. For this reason, the shear capacity of the rotation trunnions, weld and outer shell are compared.

The weld attaching the rotation trunnion to the outer shell and the lower forging is shown in Section 2.5.2.2.3. The shear capacities of the rotation trunnions, weld and outer shell are calculated below (see sketch of Section A-A on page 2.5.2-8 for geometry details).

Rotation Trunnion

The width of the interface between the rotation trunnion base metal and the weld is:

$b_{rt} = \pi(0.875)/2$

$= 1.374$ in

The ultimate shear capacity of the rotation trunnion base metal per inch of length along the weld is:

$F_{rt} = 1.374(0.50\ S_{tu})$

$= 1.374(0.50 \times 71{,}000)$

$= 48{,}777$ lbs/in

Weld

The effective throat of the weld is:

$t_e = 1.414(0.875)$

$= 1.237$ in

The welding electrode used to weld Type 304 stainless steel is AWS E308 with a tensile strength of 80,000 psi. The ultimate shear capacity per inch of length of weld is:

$F_w = 1.237(0.50 \times 80{,}000)$

$= 49{,}480$ lbs/in

Outer Shell

The width of the interface between the weld and the outer shell base metal is:

$b_{os} = 2(0.875)$

$= 1.75$ in

The ultimate shear capacity of the outer shell base metal per inch of length along the weld is:

$F_{os} = 1.75(0.50 \times 71{,}000)$

$= 62{,}125$ lbs/in

The maximum shear capacities per inch of length along the weld interface are summarized as follows:

Rotation trunnion = 48,777 lbs/in
Weld = 49,480 lbs/in
Outer shell = 62,125 lbs/in

Thus, the rotation trunnions and the weld will fail in shear before the outer shell, assuring that failure caused by excessive overload on the rotation trunnions will not impair the ability of the package to meet the other requirements of 10 CFR 71.

2.5.2.3 Front Support

2.5.2.3.1 Discussion

The longitudinal force toward the top end of the cask is resisted by a shear ring welded to the cask outer shell. The shear ring is located at the juncture of the neutron shield shell top plate with the outer shell.

2.5.2.3.2 Shear Ring

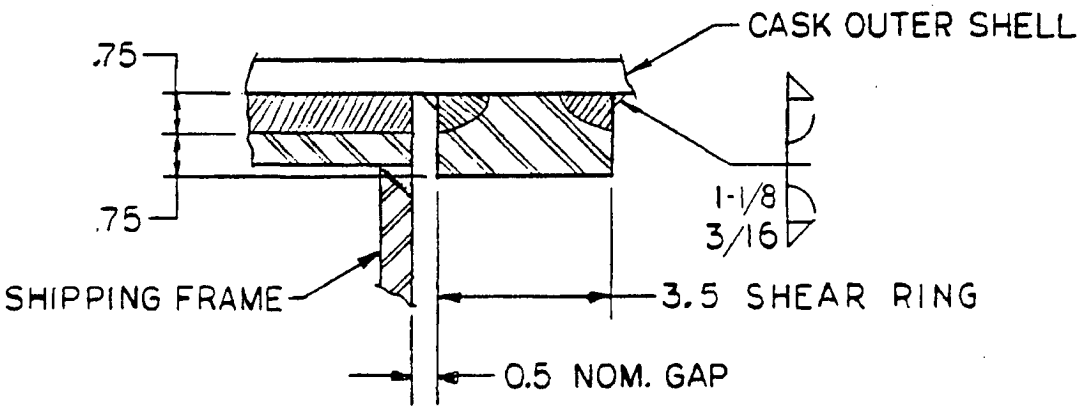

Shear Ring Geometry

The shear ring geometry bears on the shipping frame along a 90-degree arc (Figure 2.5.2-1). The load on the shear ring is:

R_{jx} = 520,000 lbs (Section 2.5.2)

Assuming that 0.75 inch of the ring thickness is in direct bearing against the side of the support frame, the bearing pressure is:

S_{brg} = 520,000/(0.5)(π)(15.06)(0.75)

= 29,309 psi

The allowable bearing on the surface of Type 304 stainless steel is:

$(S_{brg})_{ALL}$ = 41,750 psi at 200°F

The margin of safety for bearing is:

MS = (41,750/29,309) - 1= +0.42

The shear stress across the weld is:

$$S_s = (29{,}309)(0.75)/(1.12)(2) = 9{,}813 \text{ psi/in}$$

In addition, the bar is subject to flexure:

$$M = (29{,}309)(0.75)(0.75 + 0.375)$$

$$= 24{,}729 \text{ in-lb/in}$$

The moment of inertia of the welded area is:

$$I = (1)(3.5)^3/12 - (1)(1.25)^3/12$$

$$= 3.410 \text{ in}^4$$

The flexural stress is:

$$S_b = (24{,}729)(1.75)/3.410$$

$$= 12{,}690 \text{ psi}$$

The equivalent stress is:

$$S_{eq} = \left(S_b^{\,2} + 3S_s^{\,2}\right)^{0.5}$$

$$= 21{,}211 \text{ psi}$$

The margin of safety at 200°F is:

$$MS = (25{,}000/21{,}211) - 1 = +0.18$$

where:

$S_y = 25{,}000$ psi at 200°F.

Figure 2.5.2-1 Front Support and Tiedown Geometry

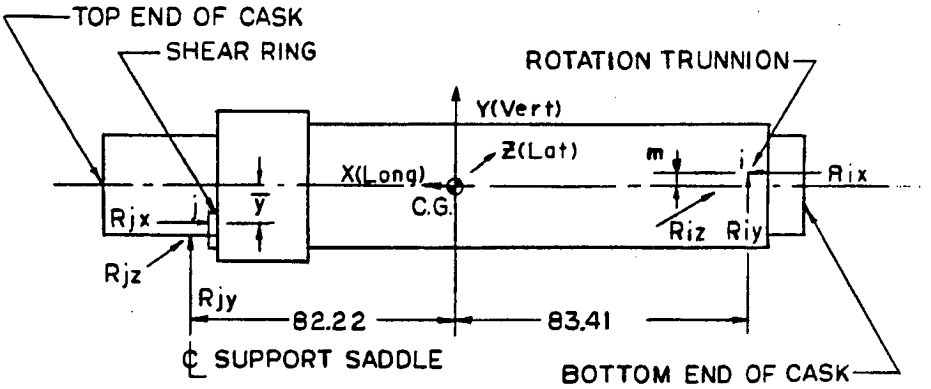

Free Body Diagram

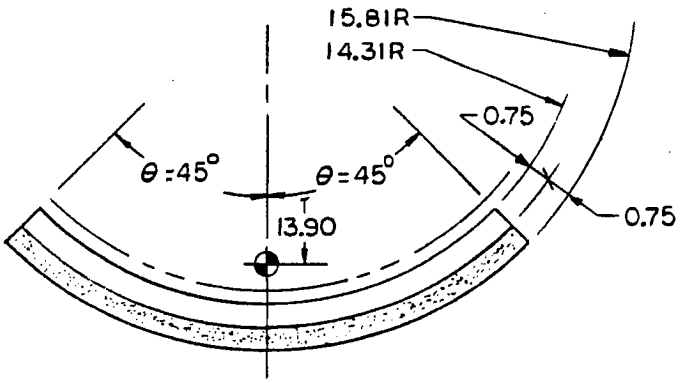

Shear Ring Geometry

Figure 2.5.2-2 Pressure Distribution of Horizontal Bearing Between Cask and Support Saddle

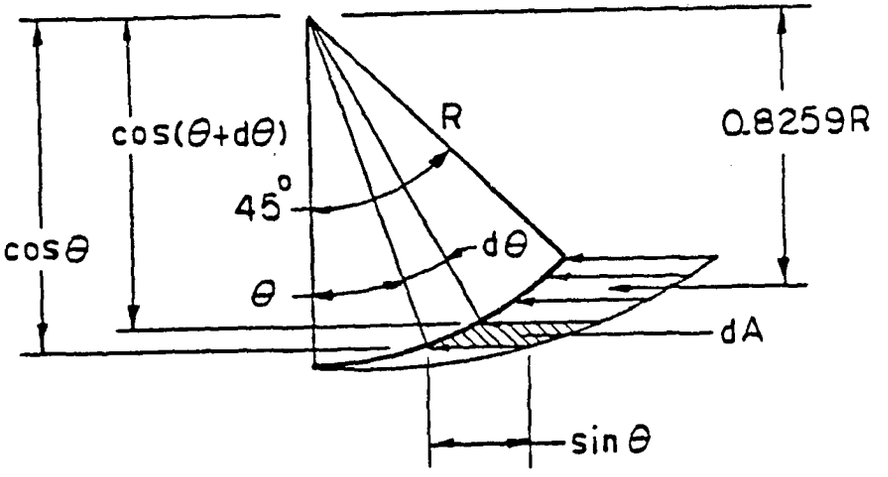

Figure 2.5.2-3 Free Body Diagram of Cask Subjected to Lateral Load

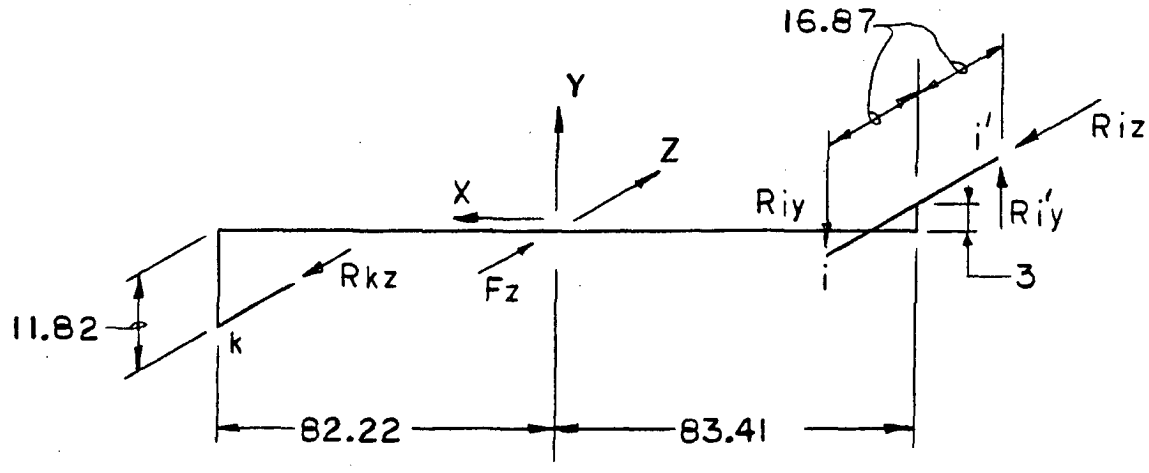

Figure 2.5.2-4 Rotation Trunnion Pocket

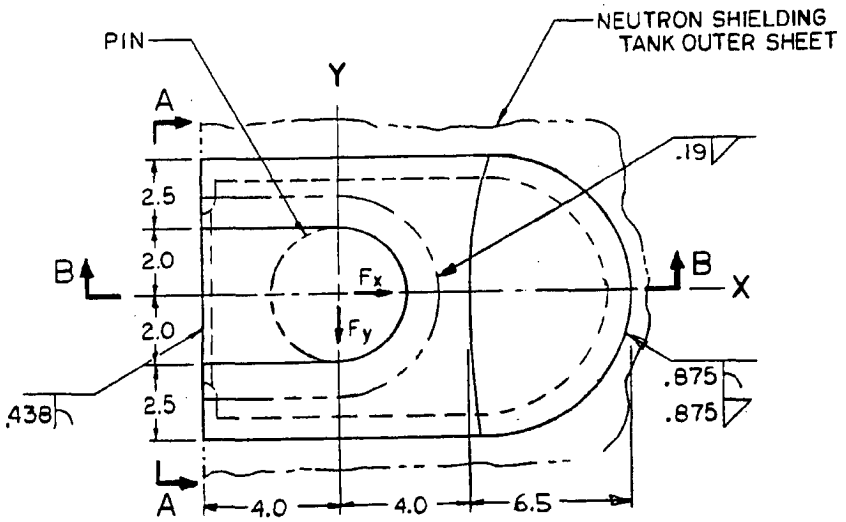

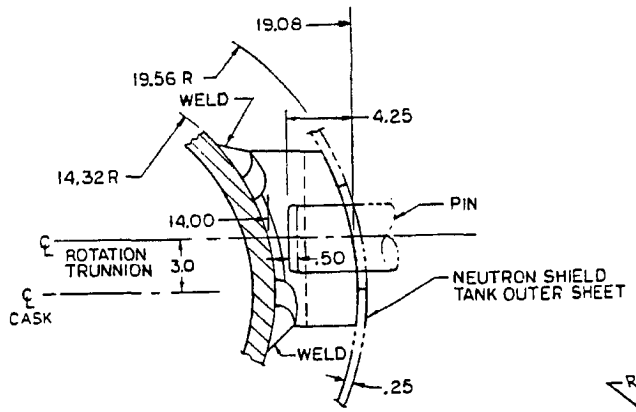

View A-A

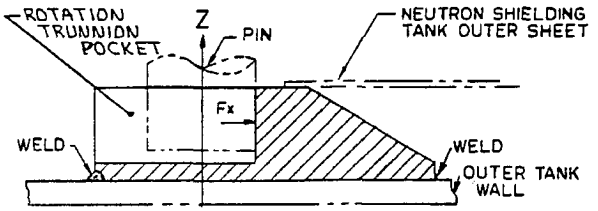

Section B-B

Table 2.5.2-1 Reactions Caused By Tiedown Devices

		Reactions (lb)					
Load Case	Load (lb)	R_{jx}	R_{jy}	R_{jz}	R_{ix}	R_{iy}	R_{iz}
A1	F_y = -104,000	0	52,374	0	0	25,813	0
A2	F_y = 104,000	0	-52,374	0	0	-25,813	0
B1	F_x = 520,000	-520,000	43,640	0	0	-21,820	0
B2	F_x = -520,000	0	9418	0	260,000	-4709	0
C1	F_z = 260,000	0	0	-130,934	0	-34,394	-129,066
C2	F_z = -260,000	0	0	130,934	0	34,394	-129,066
Maximum combined reactions		0	96,014	130,934	260,000	60,207	129,066
(A + B + C)		-520,000	-52,374	-130,934	0	-82,027	0

2.6 Normal Conditions of Transport

2.6.1 Hot Case

2.6.1.1 Discussion

The NAC-LWT cask body and lid are analyzed for structural adequacy in accordance with the requirements of 10 CFR 71.71(l) Heat (normal transport conditions). The cask is assumed to be loaded and ready for shipment in the horizontal position with an ambient temperature of 130°F.

The stress analysis of the cask is performed by the finite element method using the ANSYS computer program (See Sections 2.10.1 and 2.10.2 for model and computer program descriptions).

2.6.1.2 Analysis Description

2.6.1.2.1 Geometry

The finite element model is described in Section 2.10.2. The temperature-dependent material properties presented in Section 2.3 are used in the analysis.

2.6.1.2.2 Loadings

An internal pressure of 50 psig is applied on the cask cavity and lid interior surfaces in the outward normal direction. The pressure loading region includes the lid and upper body forging mating surfaces outward to the inner cask lid seal centerline.

The total cask lid bolt torque, as calculated in Section 2.1.3.2.2, is applied to the bolt, which is modeled as a beam element with a preload force of 39,788.74 pounds/radian (This is equivalent to an initial strain of 0.0021361 in/in-radian).

Cask temperatures as determined in Section 3.4.2 (based on 130°F ambient temperature) are imposed on the model. See Section 2.10.3.1 for the resulting isothermal temperature plot.

Mechanical loads resulting from the total weight of the cask structure and contents are imposed on the model. The total weight of the finite element model is 37,519 pounds, which is less than the design weight of 52,000 pounds (The design weight includes the total weight of the cask and its contents). Therefore, an acceleration of 1.387 g (535.94 in/sec^2) is uniformly applied to the finite element model in the positive global x-direction (The model is defined in the positive x-y plane).

Fabrication stresses are considered negligible as demonstrated in Section 2.6.11.

2.6.1.2.3 Displacement Boundary Conditions

The finite element model is restrained radially at all centerline nodes and longitudinally at the node located on the centerline at the cask model global origin; i.e., at the bottom of the cask model.

2.6.1.3 Detailed Analysis

Stresses throughout the finite element model of the cask body and closure lid are calculated for the combined pressure, bolt preload, thermal and mechanical load conditions as previously described. In accordance with the design criteria presented in Section 2.1.2, the calculated stresses are evaluated as primary membrane (P_m), primary membrane plus primary bending ($P_m + P_b$), S_n and total stress categories. The secondary stresses (thermal) are conservatively included in the primary stress categories and margin of safety calculations; therefore, the 3 S_m limit on the S_n stress intensity range is satisfied because it is enveloped by the 1.0 S_m limit on primary stress intensity.

To satisfy this criteria, procedures have been implemented (as demonstrated in Section 2.10.3) to determine the following:

1. The critical P_m and $P_m + P_b$ section stresses for each cask component.
2. The critical total stress for each cask component.

The most critical sections for each cask component are shown in Figure 2.6.1-1. The maximum P_m and $P_m + P_b$ stresses for each component are reported in Table 2.6.1-1 and Table 2.6.1-2, respectively. Both tables consider the allowable stress for a component with a temperature of 300°F. Additionally, the stresses at representative sections throughout the cask are presented in the tables in Section 2.10.7. These tables document the maximum stress locations tabulated for each component. The critical total stress for each cask component is reported in Table 2.6.1-3. For the fatigue evaluation, refer to Section 2.1.3.2.

The minimum margin of safety is shown to be +0.30, which occurs in component 7 (the Type 304 stainless steel cask bottom) for the condition of $P_m + P_b$ stress. This section is located 5.50 inches axially from the bottom of the cask body at the region where the bottom lead shielding is located.

2.6.1.4 Conclusion

Using conservatively applied loadings and stress categorization, it is demonstrated that the minimum margin of safety for the NAC-LWT cask for the heat condition is +0.30. Therefore, the NAC-LWT cask satisfies the requirements of 10 CFR 71 for consideration of the heat load condition.

Figure 2.6.1-1 NAC-LWT Cask Critical Sections (Hot Case)

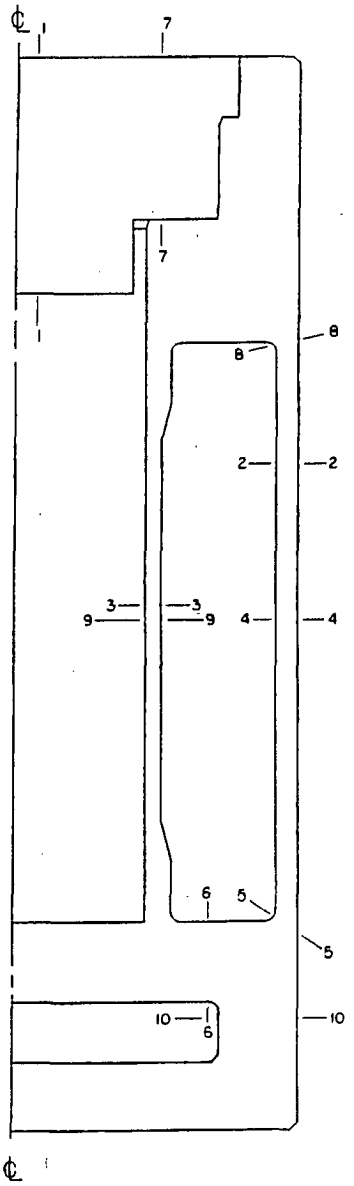

Table 2.6.1-1 Critical Stress Summary (Hot Case) - P_m

		P_m Stresses (ksi)				Principal Stresses					
Comp. No.[1]	Cut Node to Node	S_x	S_y	S_z	S_{xy}	S_1	S_2	S_3	S.I.	Allow. Stress 1.0 S_m	Margin of Safety
	1-1										
1	2302 to 2562	0.67	0.16	-0.44	0.51	0.99	-0.15	-0.44	1.43	20.0	Large
	2-2										
3	1595 to 1598	0.00	10.20	0.27	-0.06	10.20	0.27	0.00	10.20	20.0	+1.0
	3-3										
4	1121 to 1124	-0.03	3.38	0.45	0.00	3.38	0.45	-0.03	3.41	31.4	+8.2
	4-4										
6	1115 to 1118	-0.01	11.18	0.05	0.00	11.18	0.05	-0.01	11.19	31.4	+1.8
	5-5										
7	375 to 300	1.80	6.23	3.47	-4.98	9.46	3.47	-1.43	10.90	20.0	+0.8
	6-6										
8	192 to 342	-5.61	1.21	-0.75	3.56	2.73	-0.75	-7.13	9.85	20.0	+1.0

[1] Refer to Figure 2.10.2-9 for component identification.

Table 2.6.1-2 Critical Stress Summary (Hot Case) - $P_m + P_b$

		$P_m + P_b$ Stresses (ksi)				Principal Stresses					
Comp. No.[1]	Section Cut Node to Node	S_x	S_y	S_z	S_{xy}	S_1	S_2	S_3	S.I.	Allow. Stress 1.5 S_m	Margin of Safety
	7-7										
1	2371 to 2571	-3.06	-0.26	0.10	0.18	0.10	-0.25	-3.08	3.17	30.0	+8.5
	8-8										
3	1852 to 1856	-0.30	13.09	3.90	-0.56	13.11	3.90	-0.32	13.43	30.0	+1.2
	9-9										
4	1101 to 1104	0.00	3.68	0.68	0.00	3.68	0.68	0.00	3.68	47.1	Large
	2-2										
6	1595 to 1598	-0.01	11.59	0.48	-0.06	11.59	0.48	-0.01	11.60	47.1	+3.0
	10-10										
7	168 to 175	-13.48	9.78	1.46	-1.09	9.83	1.46	-13.53	23.36	30.0	+0.3
	6-6										
8	192 to 342	-16.04	1.21	-0.75	3.56	1.91	-0.75	-16.74	18.66	30.0	+0.6

[1] Refer to Figure 2.10.2-9 for component identification.

Table 2.6.1-3 Critical Stress Summary (Hot Case) – Total Range

		Total Stress Range (ksi)				Principal Stresses			Stress Differences		
Comp. No.[1]	Node	S_x	S_y	S_z	S_{xy}	S_1	S_2	S_3	S_1-S_2	S_2-S_3	S_3-S_1
1	2561	1.05	0.01	1.05	-18.80	19.34	1.05	-18.28	18.29	19.33	-37.62
3	1856	-0.30	12.04	3.33	0.18	12.04	3.33	-0.30	8.71	3.63	-12.34
4	1584	0.23	4.07	1.37	0.25	4.09	1.37	0.21	2.72	1.16	-3.88
6	1118	0.00	11.50	0.30	0.00	11.50	0.30	0.00	11.20	0.30	-11.50
7	1	4.81	0.03	4.81	23.99	26.53	4.81	-21.69	21.72	26.50	-48.22
8	192	1.59	-18.05	-7.95	2.20	1.83	-7.95	-18.29	9.78	10.34	-20.12

[1] Refer to Figure 2.10.2-9 for component identification.

2.6.2 Cold Case

2.6.2.1 Discussion

The NAC-LWT cask body and lid are analyzed for structural adequacy in accordance with the requirements of 10 CFR 71.71(c)(2) Cold (normal transport conditions). The cask is assumed to be loaded and ready for shipment in a horizontal position in an ambient steady-state environmental air temperature of -40°F.

The stress analysis of the cask is performed by the finite element method using the ANSYS computer program. See Sections 2.10.1 and 2.10.2 for model and computer program descriptions.

2.6.2.2 Analysis Description

2.6.2.2.1 Geometry

The finite element model is described in Section 2.10.2. The temperature-dependent material properties presented in Section 2.3 are used in this analysis.

2.6.2.2.2 Loadings

An internal pressure of 50 psig is applied on the cask cavity and lid interior surfaces in the outward normal direction. The pressure loading region includes the lid and upper body forging mating surfaces outward to the inner cask lid seal centerline.

The total cask lid bolt torque, as calculated in Section 2.1.3.2.2, is applied to the bolt that is modeled as a beam element with a preload force of 39,788.74 pounds/radian, which is equivalent to an initial strain of 0.0021361 in/in-radian. Cask temperatures as determined in Section 3.4.3 (based on -40°F ambient temperature) are imposed on the model. See Section 2.10.3.2 for the resulting isothermal temperature plot.

Mechanical loads due to the total weight of the cask structure and contents are imposed on the model. Since the total weight of the finite element model is 37,519 pounds, it is less than the design weight (52,000 pounds), which includes the total weight of the cask and its contents. Therefore, an acceleration of 1.387 g (535.94 in/sec^2) is uniformly applied to the finite element model in the positive global x-direction (The model is defined in the positive x-y plane).

Fabrication stresses are considered negligible as demonstrated in Section 2.6.11.

2.6.2.2.3 Displacement Boundary Conditions

The finite element model is restrained radially at all centerline nodes and longitudinally at the node located on the center line at the cask model global origin, i.e., at the bottom of the cask model.

2.6.2.3 Detailed Analysis

Stresses throughout the finite element model of the cask body and closure lid are calculated for the combined pressure, bolt preload, thermal and mechanical load conditions as previously described.

In accordance with the design criteria presented in Section 2.1.2, the calculated stresses are evaluated as P_m, $P_m + P_b$, S_n and total stress categories. The secondary stresses (thermal) are conservatively included in the primary stress categories and margin of safety calculations; therefore, the 3 S_m limit on S_n stress intensity range is satisfied because it is enveloped by the 1.0 S_m limit on primary stress intensity.

To satisfy this criteria, procedures have been implemented (as demonstrated in Section 2.10.3) to determine the following:

1. The critical P_m and $P_m + P_b$ section stresses for each cask component
2. The critical total stress for each cask component.

The most critical sections for each cask component are shown in Figure 2.6.2-1. The maximum P_m and $P_m + P_b$ stresses for each component are reported in Table 2.6.2-1 and Table 2.6.2-2, respectively. Both tables consider the allowable stress for a component with a temperature of 300°F. Additionally, the stresses at representative sections throughout the cask are presented in the tables in Section 2.10.7. These tables document the maximum stress locations tabulated for each component. The critical total stress for each cask component is reported in Table 2.6.2-3. For the fatigue evaluation, refer to Section 2.1.3.2.

The minimum margin of safety is shown to be +1.50, which occurs in component 7 (the Type 304 stainless steel cask bottom) for the condition of $P_m + P_b$ stress. This section is located 10.50 inches axially from the bottom of the cask body at the intersection of the outer shell with the bottom.

2.6.2.4 Conclusion

Using conservatively applied loadings and stress categorization, it is demonstrated that the minimum margin of safety for the NAC-LWT cask for the cold condition is +1.50. Therefore, the NAC-LWT cask satisfies the requirements of 10 CFR 71 for consideration of the cold load condition.

Figure 2.6.2-1 NAC-LWT Cask Critical Sections (Cold Case)

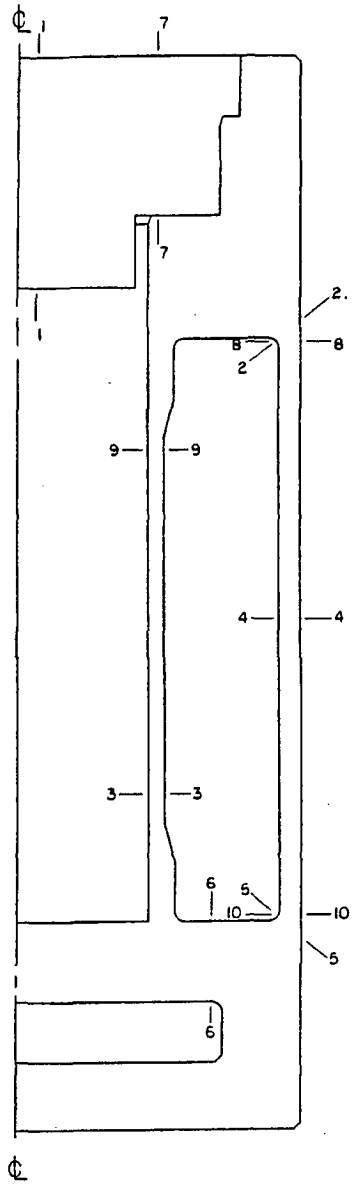

Table 2.6.2-1 Critical Stress Summary (Cold Case) - P_m

		P_m Stresses (ksi)				Principal Stresses					
Comp. No.[1]	Section Cut Node to Node	S_x	S_y	S_z	S_{xy}	S_1	S_2	S_3	S.I.	Allow. Stress 1.0 S_m	Margin of Safety
	1-1										
1	2302 to 2562	0.75	0.07	-0.53	0.51	1.02	-0.20	-0.53	1.55	20.0	Large
	2-2										
3	1835 to 1856	-0.28	6.08	2.12	1.66	6.49	2.12	-0.69	7.18	20.0	+1.8
	3-3										
4	701 to 704	-0.01	-2.59	0.13	-0.01	0.13	-0.01	-2.59	2.72	31.4	Large
	4-4										
6	1115 to 1118	-0.01	7.82	0.06	0.00	7.82	0.06	-0.01	7.83	31.4	+3.0
	5-5										
7	375 to 325	0.24	5.24	3.42	-3.08	6.71	3.42	-1.23	7.93	20.0	+1.5
	6-6										
8	192 to 342	-2.72	-0.74	-0.38	0.82	-0.38	-0.45	-3.01	2.64	20.0	+6.6

[1] Refer to Figure 2.10.2-9 for component identification.

Table 2.6.2-2 Critical Stress Summary (Cold Case) - $P_m + P_b$

		$P_m + P_b$ Stresses (ksi)				Principal Stresses					
Comp. No.[1]	Section Cut Node to Node	S_x	S_y	S_z	S_{xy}	S_1	S_2	S_3	S.I.	Allow. Stress 1.5 S_m	Margin of Safety
	7-7										
1	2371 to 2571	-3.81	-0.39	0.06	0.19	0.06	-0.38	-3.82	3.88	30.0	+6.7
	8-8										
3	1852 to 1856	-0.26	10.30	3.87	-0.19	10.30	3.87	-0.26	10.57	30.0	+1.8
	9-9										
4	1521 to 1524	0.00	-3.08	-0.25	-0.01	0.00	-0.25	-3.08	3.08	47.1	Large
	4-4										
6	1115 to 1118	0.00	8.30	0.48	0.00	8.30	0.48	0.00	8.30	47.1	+4.7
	10-10										
7	346 to 350	-0.23	11.86	5.77	-0.29	11.87	5.77	-0.24	12.10	30.0	+1.5
	6-6										
8	192 to 342	-6.67	-0.74	-0.38	0.82	-0.38	-0.63	-6.78	6.41	30.0	+3.7

[1] Refer to Figure 2.10.2-9 for component identification.

Table 2.6.2-3 Critical Stress Summary (Cold Case) – Total Range

		Total Stress Range (ksi)				Principal Stresses			Stress Differences		
Comp. No.[1]	Node	S_x	S_y	S_z	S_{xy}	S_1	S_2	S_3	S_1-S_2	S_2-S_3	S_3-S_1
1	2561	0.28	0.01	0.27	-18.80	18.95	0.27	-18.66	18.68	18.93	-37.61
3	1856	-0.26	10.18	3.50	-0.01	10.18	3.50	-0.26	6.68	3.76	-10.44
4	1261	0.00	-2.66	-0.39	0.00	0.00	-0.39	-2.66	0.39	2.27	-2.66
6	1278	-0.03	8.16	0.20	0.00	8.16	0.20	-0.03	7.96	0.23	-8.19
7	1	4.64	0.02	4.64	23.99	26.43	4.64	-21.77	21.79	26.41	-48.20
8	192	-0.97	-7.36	-2.70	1.45	-0.66	-2.70	-7.67	2.04	4.97	-7.01

[1] Refer to Figure 2.10.2-9 for component identification.

2.6.3 Reduced External Pressure

The drop in atmospheric pressure to 3.5 psia, as specified in 10 CFR 71.71(c)(3), effectively results in an additional internal pressure in the cask of 11.2 psig. This additional pressure has a negligible effect on the NAC-LWT cask because the cask is conservatively analyzed for a normal operations conditions internal pressure of 50.0 psig in Section 2.6.1.2.

2.6.4 Increased External Pressure

An increased external pressure of 20 psia (5.3 psig external pressure), as specified in 10 CFR 71.71(c)(4), has a negligible effect on the NAC-LWT cask because of the thick outer shell and end closures of the cask. Conservatively, applying a 20-psi external pressure to the expansion tank shell and to the neutron shield tank shell produces hoop stresses of only 1373 psi and 1627 psi, respectively. These stresses are negligible. Additionally, Section 2.6.7 addresses many different loading cases, which exceed these prescribed external pressure requirements.

2.6.5 Vibration

The effect of vibrations normally incident to transportation is considered to be negligible for the NAC-LWT cask. This conclusion is based on the fact that the calculated stresses for vibrations normally incident to transportation are much smaller than the calculated stresses for the normal transport 1-foot side drop event. The following analysis documents this fact.

The normal transport 1-foot side drop, discussed in Section 2.6.7.3, results in an impact deceleration equal to 24.3 g. This impact force produces a 17,420 psi stress intensity in the inner shell and a 23,590 psi stress intensity in the outer shell of the NAC-LWT cask.

As a conservative worst case, it is assumed that the normal transport vibration acceleration is equal to the equivalent acceleration which will produce the normal vertical loading imposed on the tiedown devices by 10 CFR 71.45(b)(1). This regulation specifies a load factor of 2.0 to be applied to the package weight; therefore, it is assumed that the tiedown devices and the cask must resist an imposed 2.0 g vibration acceleration.

The maximum stress intensity range for normal transport vibration is obtained by multiplying the stress from the 1-foot side drop impact by the ratio of acceleration values from vibration to those for the drop impact. Thus the stress intensities in the outer shell (the critical component) are S_{max} = (2/24.3)(23,590) = 1942 psi and S_{min} = -(2/24.3)(23,590) = -1942 psi, and the maximum stress intensity range is S_n = 3884 psi. The allowable alternating stress intensity for austenitic stainless steel is determined as the 10^{11} cycle value from the "ASME Boiler and Pressure Vessel Code," Table I-9.2.2 ratioed for the effect of the 300°F temperature. This value is S_e = 12,975 psi; therefore, the margin of safety for the critical component of the NAC-LWT cask for normal transport vibration is:

$$MS = (Se / Salt) - 1 = (12{,}295/1942) - 1 = +\underline{Large}$$

where:

$$Salt = 0.5\ Sn$$

The rotation trunnions serve as the rear tiedown for the NAC-LWT cask during normal transport. The rotation trunnion is the critical tiedown component for all three load axes; the front of the cask is supported in a cradle and restrained vertically by a band attached to the trailer. From Section 2.5.2.2, the critical component on the rotation trunnion is the attachment weld between the trunnion and the cask outer shell, which has an applied shear stress of 11,500 psi. This applied shear stress is produced by the 10.2 g resultant from the combined longitudinal and vertical shock (10.0 g longitudinal and 2 g vertical) tiedown load components.

The same method is used to determine the maximum stress intensity range as is used for the cask, except that the ratio of the normal transport vibration acceleration to the resultant acceleration for the combined longitudinal and vertical shock was used. The allowable alternating stress for the weld is the same as that for the cask. The alternating shear stresses are S_{max} = (2/10.2)(11,500) = 2255 psi and S_{min} = -(2/10.2)(11,500) = -2255 psi, and the maximum stress intensity range is S_n = 4510 psi. The margin of safety for the rotation trunnion as a rear tiedown device for normal transport vibration is:

$$MS = (S_e / S_{alt}) = 1\ (12{,}975/2255) - 1 = +\underline{Large}$$

where:

$$S_{alt} = 0.5\ S_n$$

The NAC-LWT cask satisfies the requirements for normal vibration incident to transportation as required by 10 CFR 71.71(c)(5).

2.6.6 Water Spray

Water causes negligible corrosion of the stainless steel materials used to fabricate the NAC-LWT cask; the cask contents are protected in the sealed cavity. A water spray as specified in 10 CFR 71.71(c)(6) has no adverse effect on this package.

2.6.7 Free Drop (1 Foot)

The free drop scenario outlined by Subpart F of 10 CFR 71 requires the NAC-LWT cask to be structurally adequate for a 1-foot drop (normal transport conditions) onto a flat, essentially unyielding, horizontal surface in the orientation that inflicts the maximum damage to the cask. The following subsections evaluate the cask body; the impact limiters; the closure lid and bolts; the neutron shield shell; the expansion tank shell; and the upper ring components; for the end, side, and corner drop orientations.

2.6.7.1 End Drop (1 Foot)

2.6.7.1.1 Discussion

The NAC-LWT cask is analyzed for the effects of a normal operations end drop impact condition. The event scenario is that the NAC-LWT cask, equipped with an impact limiter, drops 1 foot onto a flat, unyielding, horizontal surface. The cask strikes the surface in a vertical position on either its bottom or its top end.

The 1-foot end drop analysis can be carried out in an identical fashion as was used in the 30-foot accident end drop analysis, Section 2.7.1.1. The general comments, analysis descriptions and the analysis method described in Section 2.7.1.1 also apply to this section.

The only difference between the 30-foot end drop analysis (Section 2.7.1.1) and this 1-foot end drop analysis is the magnitude of the impact force, i.e., impact load, which is expressed in terms of a g factor. The magnitude of the impact force varies with the different drop heights. As calculated in Section 2.6.7-4, the g loads for the 1-foot end drop condition and for the 30-foot end drop condition are 15.8 g and 60 g, respectively. These g loads are conservatively based on a maximum crush strength of 3850 psi for the aluminum honeycomb impact limiters, although the design maximum crush strength is 3675 psi. Also, these analyses conservatively use a 1.12-inch thick outer shell, although the actual outer shell thickness is 1.20 inches. Using the analysis results obtained in Section 2.7.1.1 to represent the structural response of the NAC-LWT cask for the 1-foot end drop condition is conservative and acceptable. Therefore, Tables 2.7-1 through 2.7-15 were used to compose Table 2.6.7-1 through Table 2.6.7-16, for the 1-foot drop analyses. The most critical sections for each component during a particular loading condition are shown in Figure 2.6.7-1 through Figure 2.6.7-5. The critical P_m, $P_m + P_b$, and total stresses for each component are documented in Table 2.6.7-1 through Table 2.6.7-16. The allowable stresses are those defined in Section 2.1.2 for the normal operations conditions based on 300°F. Note that the maximum cask component temperatures are below 300°F for all of the conditions that are considered. Additionally, the stresses at representative sections throughout the cask are

presented in the tables in Section 2.10.7. These tables document the maximum stress locations tabulated for each component.

The secondary stresses (thermal) are conservatively included in the primary stress categories and margin of safety calculations; therefore, the 3 S_m limit on the S_n stress intensity range is satisfied. This is because it is enveloped by the 1.5 S_m limit on $P_m + P_b$ stress intensity.

2.6.7.1.2 Results and Conclusions

Since the margins of safety are positive for all of the cask components, the NAC-LWT cask maintains its containment capability and satisfies the 10 CFR 71 requirements for the 1-foot normal operations end drop condition.

2.6.7.2 Side Drop (1 Foot)

2.6.7.2.1 Discussion

This section presents the evaluation of the structural adequacy of the NAC-LWT cask for the 1-foot side drop impact condition. In this event, the NAC-LWT cask with impact limiters attached over each end experiences a free drop through a distance of 1 foot onto a flat, unyielding surface, and strikes the surface in a horizontal position.

The 1-foot side drop analysis is performed in the same manner as was done for the 30-foot side drop analysis in Section 2.7.1.2. The general comments, analysis descriptions, and the analysis methods described in Section 2.7.1.2 also apply to this section.

The difference between the 30-foot side drop analysis and the 1-foot side drop analysis is the magnitude of the impact force, which varies because of the different drop heights. As determined in Section 2.6.7.4, the g loads for the 1-foot side drop condition and for the 30-foot side drop accident condition are 24.3 g and 49.7 g, respectively.

Analysis of the NAC-LWT cask for the normal operations conditions side drop follows the same methodology as used for the accident side drop analysis. Because all calculations for the accident side drop analysis are performed on a basis of linear elastic behavior, the stress components for the 1-foot side drop condition are calculated by multiplying the 30-foot side drop stress components (resulting from the effects of inertial and impact loads) by the ratio of the 1-foot side drop g load to the 30-foot side drop g load. These stress components are then combined with those induced by the thermal effects, internal pressure, and bolt preload.

2.6.7.2.2 Results and Conclusions

Since the material properties of the cask structure are temperature-dependent, varying environmental temperatures will produce changes in the calculated stresses in the cask for the thermal load cases. Environmental temperatures will not change the calculated stresses in the

cask produced by other types of loads. This is verified by comparing the finite element results for the NAC-LWT cask subjected to a gravity load for different temperature conditions. Also, the stress levels produced by the following thermal loading conditions were evaluated: (1) 100°F ambient temperature with maximum decay heat load, (2) -40°F ambient temperature with maximum decay heat load, and (3) -40°F ambient temperature with no decay heat load. The combination effect of the thermal loads with other load types (e.g., inertial body load) has also been studied. It is determined that the side drop event with 100°F ambient temperature represents the worst case for the normal operations 1-foot side drop condition. Therefore, only the stress results produced by a 1-foot side drop with 100°F ambient temperature are reported.

Stress components and stress intensities are calculated throughout the finite element model for the combined loads due to internal pressure, bolt preload, thermal, inertia, and impact. Table 2.6.7-16 through Table 2.6.7-19 report the P_m stress intensities, the $P_m + P_b$ stress intensities, the S_n stress intensities, and the total stress intensities for each cask component, which are obtained from the finite element side drop analysis. Additionally, the stresses at representative sections throughout the cask are presented in the tables in Section 2.10.7. These tables document the maximum stress locations tabulated for each component.

As mentioned previously, the finite element cask model conservatively ignores the effect of the neutron shield shell on the overall bending of the cask structure.

The margins of safety reported in Table 2.6.7-16 through Table 2.6.7-18 are positive for all cask components. It has been demonstrated that all margins of safety are positive for the normal operations 1-foot side drop condition.

The NAC-LWT cask maintains its containment capability and satisfies the 10 CFR 71 requirements for the normal operations 1-foot side drop condition.

2.6.7.3 Corner Drop (1 Foot)

2.6.7.3.1 Discussion

The analysis of the NAC-LWT cask for a 1-foot corner drop condition uses the same methods as those used for the hypothetical accident oblique drop analyses. The general comments, analysis descriptions, and analysis methods discussed in Section 2.7.1.3 also apply to this section. The difference between the hypothetical accident analysis and the normal operations conditions analysis in this section is the drop height. Refer to Section 2.6.7.4 for the calculation of the g loads induced by a normal operations conditions 1-foot corner drop and by an accident condition 30-foot corner drop. These g loads are conservatively based on a maximum crush strength of 3850 psi for the aluminum honeycomb impact limiters, although the design maximum crush strength is 3675 psi. The stress components for the 1-foot corner drop are calculated by multiplying the accident condition stress components (resulting from the effects of inertial and

impact loads) by the ratio of the 1-foot corner drop g load to the 30-foot corner drop g load. These stress components, then, are combined with those resulting from internal pressure, bolt preload, and thermal effects. These analyses conservatively use a 1.12-inch thick outer shell, although the actual outer shell thickness is 1.20 inches.

2.6.7.3.2 Results and Conclusions

The most critical sections for each component during a particular loading condition are shown in Figure 2.6.7-7 through Figure 2.6.7-9. Table 2.6.7-20 through Table 2.6.7-23 report the maximum P_m stress intensities, the maximum $P_m + P_b$ stress intensities, the maximum S_n stress intensities, and the maximum total stress intensities for each component resulting from the 1-foot top corner drop condition with a 130°F ambient temperature and maximum decay heat load. Similarly, Table 2.6.7-24 through Table 2.6.7-27 report those stress intensities resulting from the 1-foot bottom corner drop condition with a 130°F ambient temperature and maximum decay heat load. Also, Table 2.6.7-28 through Table 2.6.7-31 report the stress intensities for each component resulting from the 1-foot top corner drop condition with a -40°F ambient temperature. Additionally, the stresses at representative sections throughout the cask are presented in the tables in Section 2.10.7. These tables document the maximum stress locations for each component.

It has been demonstrated that all margins of safety are positive for the normal operations 1-foot corner drop condition. The NAC-LWT cask maintains its containment capability and satisfies the 10 CFR 71 requirements for the normal operations 1-foot corner drop condition.

2.6.7.4 Impact Limiters

2.6.7.4.1 Introduction

Removable impact limiters are supplied with the NAC-LWT cask to ensure that the design impact loads on the cask are not exceeded for any of the defined impact conditions. These defined conditions are:

1. The cask falls 1 foot and lands on: (a) its side, impacting both limiters simultaneously; (b) flat on one limiter at either end; or (c) oblique on either corner (the center of gravity is directly above the corner of the impact limiter).
2. The cask, having experienced a normal operating conditions 1-foot drop, is dropped through a distance of 30 feet and lands on its end, its side, or at any oblique angle. The impact limiter analysis considers a 31-foot drop (1 foot + 30 feet). This provides conservative impact loads, which are used in the cask analyses.

2.6.7.4.2 Assumptions

The following assumptions form the basis for the impact limiter analysis:

1. The cask impacts on an unyielding surface.
2. The impact limiter remains in position on the cask during all impact events. (The qualification of the impact limiter attachment is presented in Section 2.6.7.4.7.)

2.6.7.4.3 Load Conditions

The impact limiters described and analyzed in the following paragraphs decelerate the cask by applying a force in the direction opposite the motion of the cask. The deceleration force is generated by crushing the aluminum honeycomb material of the limiter between the cask and the unyielding surface. The energy absorbed during crushing is the net force, the vector sum of the cask weight (downward) and the deceleration force (upward), multiplied by the distance crushed. The amount of energy an impact limiter can absorb is calculated for various cask impact orientations, from vertical (0°) to horizontal (90°).

The specific loading conditions for the impact limiters are defined by 10 CFR 71.71(c)(7), 10 CFR 71.73(c)(1) and Regulatory Guide 7.8, as follows:

1. A 1-foot fall of the cask on one limiter, impacted at any angle from vertical (flat end) to corner (cask center of gravity is directly above the point of impact).
2. A 1-foot fall of the cask horizontally, so that the side surfaces of both limiters impact the unyielding surface simultaneously.
3. Any of the 1-foot falls can be followed by a 30-foot fall at an end, a side, or an oblique orientation.

Based on these loading conditions, the NAC-LWT cask impact limiters are designed for a 31-foot fall. Either of the first two conditions plus the third condition is equivalent to a single drop at the combined heights, as explained in Section 2.6.7.4.5. The maximum impact force and the maximum crush depth for the 1-foot falls are obtained from the computer output for the 31-foot fall analyses at the value of the energy dissipated in a 1-foot fall. This method is explained in Section 2.6.7.4.5.

2.6.7.4.4 Descriptions - Impact Limiters

Figure 2.6.7-10 shows the location on the cask and the primary dimensions of the impact limiters. A different impact limiter is used on the bottom of the cask to reduce weight. The top impact limiter diameter is larger because it is required to clear the cask lifting trunnions and to be of sufficient depth over the trunnions to prevent the limiter from behaving as a solid in the event of a side impact. The larger diameter provides greater distance from the point of impact to the cask body; however, the effective depth of the limiter is maintained at the trunnions and the same corner impact absorption capability is retained. Figure 2.6.7-11 shows a cross-section of the top impact limiter.

The bottom impact limiter does not have the cut-outs for the trunnions. It has a smaller outside diameter and larger bottom depth than the top impact limiter.

Each impact limiter consists of two different layers of aluminum honeycomb, which are enclosed in a thin outer aluminum shell. The layers of aluminum honeycomb are separated by a thin aluminum sheet. The honeycomb material absorbs the impact energy as it is crushed. A typical load versus deflection curve for aluminum honeycomb is presented in Figure 2.6.7-12. The force deflection curves and test data for the NAC-LWT cask impact limiters at the various drop angles are provided in Appendix 2.10.12. The nominal crush strength of the bottom layer of aluminum honeycomb is 250 psi axially, and is negligible radially. The nominal crush strength of the second layer is 3500 psi in both the axial and the radial directions. The tolerance on the crush strength is +5, -10 percent. The bottom, 250-psi crush strength, single-directional layer of honeycomb material absorbs the majority of the energy in a 1-foot flat impact on the end, and limits the impact force to a value acceptable for normal operations. The lower crush strength is necessary because the impact area is considerably greater in a flat bottom impact than in any other orientation. The second, 3500-psi crush strength, multi-directional layer of honeycomb material absorbs the majority of the energy in an impact on the corner of the impact limiter, and all of the energy in an impact on the side of the impact limiter. Both crushable aluminum honeycomb materials behave as a solid when compressed to 30 percent of their original depth.

The outside diameters of the impact limiters are 65.25 inches and 60.25 inches for the top and bottom impact limiters, respectively. The depth of the bottom aluminum honeycomb layer is 1.5 inches on each limiter. The second aluminum honeycomb layer is 14.0 inches deep for the top impact limiter and 14.5 inches for the bottom impact limiter. The top impact limiter has four recesses to provide clearance around the trunnions. This clearance is closed during the impact for a 30-foot side drop. Therefore, the trunnion provides a rigid foundation for the impact limiter in the region near the trunnion.

The impact limiter shells are positioned against the cask lid and bottom surfaces; the impact limiters overlap the cask cylinder by a length of 12 inches. The shells are mechanically attached to the cask as described in Section 2.6.7.4.7.

For each of the impact load conditions considered in this analysis, the impact limiters remain in position on the cask and absorb the energy of the impact; thus, they limit the impact load to the values calculated in this section.

2.6.7.4.5 Method of Analysis

The primary areas of analytical evaluation that are required in an impact limiter analysis are: (1) crush depth; (2) maximum crush force; and (3) attachment to the cask. The crush depth and

maximum crush force are dependent on the crush strength of the crushable material, the area engaged in crushing, the geometry of the impact limiter, and the energy to be dissipated.

Deceleration forces for constant crush strength aluminum honeycomb impact limiters are directly related to the area crushing. The area engaged in crushing can be best explained by examining the experimental results of a top end drop impact test. Figure 2.6.7-13 shows a quarter-scale model impact limiter just before crushing begins. The cask and the unyielding surface are rigid and undeformable compared to the honeycomb material. The 3.9 inches of honeycomb material are trapped in place between the cask and the impacted surface.

The 250-psi crush strength honeycomb is designed to absorb the potential energy of the cask in a 1-foot drop. The area of the 250-psi honeycomb covering the entire bottom of the impact limiter is 208.7 square inches. The higher crush strength honeycomb structurally supports or "backs" the lower crush strength honeycomb, even if just the cask backs the higher crush strength honeycomb. The force necessary to begin crushing the 250 psi crush strength material is 52,168 pounds. The quarter-scale model weighs approximately 800 pounds; therefore, the 52,168 pounds of force is equivalent to 65 g for the model (The normal operation g-load for the full-size cask is calculated to be 16.3 g).

The 3500-psi crush strength honeycomb absorbs the kinetic energy of the cask in a 30-foot drop. The area of the bottom of the scale model cask is 40.7 square inches. The force necessary to crush the 3500-psi crush strength honeycomb trapped between the model cask and the impacted surface is 142,500 pounds, or 178 g, based on the model weight of 800 pounds.

A force imbalance is immediately established between the lower and higher strength honeycombs at the onset of crushing. It requires 52,168 pounds to crush the lower strength honeycomb, which is 2.7 times smaller than the force required to crush the higher strength honeycomb. The lower strength honeycomb of constant crush strength will crush until lock-up occurs. When lock-up occurs, the crush strength of the lower strength honeycomb increases and exceeds that of the higher strength honeycomb. Crushing now begins beneath the cask because the force to crush the 16.3-inch diameter of the locked-up, lower strength honeycomb exceeds the 142,500 pounds necessary to crush the backed-up higher strength honeycomb.

The cask has kinetic energy gained while falling prior to the impact limiter contacting the unyielding surface. (Section 2.10.12 gives a more complete description of the kinetic energy gain.) Some kinetic energy was dissipated in crushing the lower strength honeycomb. The remaining energy will be absorbed by crushing the higher strength honeycomb between the cask and the impacted surface. The cask "backs" the higher crush strength honeycomb; therefore, the maximum force is easily compared with the average maximum force from the quasi-static test as adjusted to reflect the dynamic crush strength of the honeycomb (For an explanation of the term "dynamic" as applied to quasi-static tests, refer to Appendix 2.10.12).

Figure 2.6.7-14 is a photograph of a section of an end impact tested quarter-scale limiter. The average maximum force from the end drop quasi-static crush test is 158,400 pounds. If the backed and unbacked area were to crush, the required force would be 3500 psi x $\pi/4$ $(16.3)^2$ = 730,400 pounds of force. This is a factor of 4.6 times more than the actual measured force and shows that the unbacked area did not contribute to the limiter force. The calculated maximum force using the backed-up area of the limiter is approximately 11 percent lower than the test results. The scale model limiter crush test, therefore, demonstrates that the unbacked area did not crush and generate a force. One reason for the difference is the shearing of the high crush strength honeycomb, which is clearly visible in Figure 2.6.7-14. Shearing acts in a plane, surrounding the shear area. In an end impact crush, the plane is a thin ring with a diameter equal to the diameter of the cask. Since the crush force is proportional to the backed area, which depends on the square of the cask diameter, for the full-scale impact limiters, shearing becomes a much less significant part of the maximum force.

Figure 2.6.7-14 shows the sequence of crushing and the backed area as described above. The lower crush strength honeycomb is crushed to stack height completely to the outer edge of the cask. Higher crush strength honeycomb beneath the cask is crushed, while material on the "other side" of the shear plane is uncrushed.

The combination of the accurate prediction of measured impact limiter crush forces and the visual evidence in the sectioned limiter after the test shows that only the backed-up area crushes for aluminum honeycomb with a 3500-psi, multi-directional, dynamic crush strength.

The cask orientation for a corner impact is defined by the angle from vertical of the cask's longitudinal axis when the cask center of gravity is vertically aligned with the impact point on the limiter. This angle is 15.74 degrees for the top limiter and 14.52 degrees for the bottom limiter.

A proprietary computer program, RBCUBED, is used to analyze an impact limiter for an impact event, to determine the dynamics of the event, to determine the forces generated during that event, and to determine the depth of crush (Section 2.10.1.2).

The computer program, RBCUBED, is run for many combinations of crushable material strength until satisfactory results are obtained. Two runs are made for each impact orientation. One run is made using the maximum value of the aluminum honeycomb crush strength, 105 percent of the nominal crush strength, to determine the maximum force on the cask. A second run, using the minimum value for the aluminum honeycomb crush strength, 90 percent of the nominal crush strength, is also made to find the maximum crush depth of the crushable material.

A single RBCUBED run is necessary to determine the reaction force for a 1-foot fall and a subsequent 30-foot fall. The 1-foot fall crushes the limiter a distance (δ_1), and absorbs

12 inches × 52,000 lbs = 0.624×10^6 inch-pounds of energy. Then, the impact limiter must absorb the additional energy of 360 inches × 52,000 lbs = 18.72×10^6 inch-pounds by crushing an additional distance (δ_2) from a 30-foot drop. The total displacement is $\delta_1 + \delta_2$ and the total energy is $(18.72 + 0.624) \times 10^6 = 19.344 \times 10^6$ inch-pounds. Dividing this energy by the cask weight gives 372 inches (31 feet), which demonstrates that a 1-foot fall followed by a 30-foot fall can be evaluated from data for a 31-foot fall. The maximum impact force and the maximum crush depth for the 1-foot fall can be obtained from the RBCUBED output for the 31-foot fall analysis at the value of the energy dissipated in a 1-foot fall.

2.6.7.4.6 Results

The data in Table 2.6.7-32 and Table 2.6.7-33 give the results of the impact limiter design analyses for a 1-foot fall and a subsequent 30-foot fall, respectively. The calculated g loads for the 30-foot fall side impact are based on the 3675-psi design maximum crush strength of the multidirectional aluminum honeycomb. The calculated g loads for all of the other 1-foot and 30-foot fall impacts are conservatively based on an aluminum honeycomb maximum crush strength of 3850 psi. A design cask weight of 52,000 lbs is used.

The calculated (RBCUBED) and measured (quasi-static, adjusted for dynamic crush strength) force-deflection curves for the NAC-LWT cask impact limiters for all drop orientations are presented in Appendix 2.10.12. To verify the results, the area under the curves is calculated by the trapezoidal method. This area represents the energy dissipated for each of the cases, i.e., $E_{max} = 19.344 \times 10^6$ inch-pounds for the top limiter at maximum strength, and $E_{min} = 19.206 \times 10^6$ inch-pounds for the bottom limiter at minimum strength. The potential energy to be dissipated consists of the cask weight (52,000 lbs) multiplied by the distance the cask falls (372 inches), i.e., $E_p = 372 \times 52{,}000 = 19.344 \times 10^6$ inch-pounds. The calculated and actual values compare within 0.71 percent, which indicates that the proper amount of potential energy is dissipated in the RBCUBED analysis. Another check is to multiply the total crush area (the maximum area backed by the cask) by the crush strength of the impact limiters to determine the reacting force. This hand-calculated value of the reaction force for maximum impact limiter crush strength compares within 0.38 percent of the RBCUBED calculated value for the bottom impact limiter and within 1.88 percent for the top impact limiter. The hand-calculated value of the reaction force for minimum impact limiter crush strength compares within 0.46 percent of the RBCUBED calculated value for the bottom impact limiter and within 1.83 percent for the top impact limiter. These results verify both the energy absorption and the reaction force calculations of RBCUBED for the impact limiters.

A study of a side drop shows that the cask will come to rest at an angle of 0.76 degrees with the horizontal because the radius of the top limiter is 2.5 inches larger than that of the bottom limiter.

The RBCUBED analysis, analyzing the side drop as horizontal, is not affected by this small angle because the horizontal component of the forces is negligible.

With both impact limiters at their minimum allowable crush strength (maximum crush depth case), clearance is maintained between the neutron shield/expansion tank and the unyielding surface for the 1-foot side impact.

An evaluation of the displacements obtained from the RBCUBED runs is as follows:

1. The RBCUBED run for the 31-foot side drop assumes the cask is a rigid element and does not include the trunnions; therefore, the displacement from the 31-foot drop must be analyzed, by referring to Figure 2.6.7-11, as follows:

   The free distance of crushable material between the impact limiter and the trunnion equals 14.995 inches. The aluminum honeycomb compresses to 70 percent of its free height before exhibiting behavior as a solid (10.497 inches). The RBCUBED run for the 31-foot side drop with the crushable material at minimum strength calculates a crush depth of 10.00 inches; thus, 0.497 inch of crushable material remains before solid height occurs. Therefore, an impact directly on a trunnion does not change the energy absorbing characteristics of the impact limiter for this condition.

   The impact from a 31-foot side drop on the bottom impact limiter with the crushable material at minimum strength exhibits solid behavior at a displacement of 10.73 inches, which leaves 0.43 inch displacement before solid height occurs (crush depth = 10.30 inches).

2. The impact from a 31-foot flat end drop onto the top impact limiter with the crushable material at minimum strength exhibits solid behavior at a displacement of 10.85 inches, which leaves 0.61 inch displacement before solid height occurs. Similarly, for the bottom impact limiter, solid behavior occurs at 11.20 inches, which leaves 0.90 inch displacement before solid height occurs.

3. For a 31-foot corner drop on the top impact limiter with the crushable material at minimum crush strength, the crush distance of 12.72 inches is much less than the solid height displacement of 16.86 inches. Similarly, for the bottom impact limiter, the 12.70-inch crush distance is much less than the 15.83-inch solid height displacement.

The cask analysis for these impact conditions is based on the maximum deceleration (g) derived from the RBCUBED results. The critical condition for maximum lateral deceleration from both a 1-foot and a 31-foot drop is the side drop with the crushable material at its maximum strength. The critical condition for maximum longitudinal deceleration from a 1-foot drop is the flat bottom drop with the crushable material at its maximum strength, and from a 31-foot drop is the corner drop. The longitudinal component of the deceleration from the 31-foot corner drop was used as the longitudinal criteria; that is, 60.4 cos 15.74 degrees equals 58.1 g. Nevertheless, a 60.0 g (deceleration) is conservatively used as the maximum longitudinal deceleration. The design g load factors (deceleration values) for the NAC-LWT cask analyses are summarized in Table 2.6.7-34. The design g load for the 31-foot side drop is based on the 3675-psi design

maximum crush strength of the aluminum honeycomb impact limiters. The design g loads for all of the other 1-foot and 31-foot drops are conservatively based on an aluminum honeycomb maximum crush strength of 3850 psi.

2.6.7.4.7 Impact Limiter Attachment Analysis

A three-part design criteria applies to the method of attachment of the impact limiters to the cask body. These three criteria are as follows:

1. The impact limiters must remain attached to the cask body during normal handling and transport. Satisfaction of this criterion ensures that the limiters will be in a proper position to perform their impact limiting function in the event of a free drop (normal or accident).
2. In a free drop (normal or accident), the limiter(s) making initial contact with the unyielding surface must remain in position on the end(s) of the cask for the full duration of the initial impact. Satisfaction of this criterion ensures that the limiter(s) will be able to properly perform their impact limiting function.
3. In a free drop (normal or accident) involving an initial impact on a single impact limiter, the limiter on the opposite end of the cask must remain attached to the cask during the initial impact. Satisfaction of this criterion ensures that the limiter will be in a proper position to perform its impact limiting function in a subsequent secondary impact following the initial impact.

Section 2.6.7.4.7 demonstrates that each of the above criterion are satisfied.

Impact Limiter Attachment During Normal Handling and Transport

Attachment of the impact limiters to the cask body during normal handling and transport is ensured by demonstrating that the attachment hardware (pins, lugs and associated welds) does not yield under normal handling and transport conditions. The worst case loading associated with normal handling and transport is taken to be a 10-g axial loading associated with rail transport [10 CFR 71.45 (b)]. This bounds the 2.0-g load corresponding to the peak shock loading expected as the result of truck transport (per ANSI N14.23 for air ride suspensions). For this normal condition evaluation, it will be assumed that only two of the four attachment points for each limiter are effective. The load, P, per attachment point therefore becomes:

$$P = 10.0(1535)/2$$
$$= 7{,}675 \text{ lbs}$$

where 1,535 lbs is the weight of the heaviest (top) impact limiter.

Analysis of Impact Limiter Lug

The geometry of the impact limiter lug is as shown in Figure 2.6.7-15. As shown, the lug has an outer width of 2.0 inches, a hole diameter of 0.53 inch and an edge distance of 1.7 inches. The

lug is made of 6061-T651 aluminum and is 0.5 inch thick. According to Table 2.3.1-4, the yield strength of the aluminum at 150°F is 32,700 psi. Potential failure modes of tension across the net section and 40-degree shearout are considered as follows:

Tension Across the Net Section

$P = 7{,}675$ lbs

$A = 0.5(2.0 - 0.53)$

$= 0.735$ in^2

$S_t = 7{,}675/0.735 = 10{,}442$ psi ($S_y = 32{,}700$ psi)

$MS = 32{,}700/10{,}442 - 1$

$= +2.13$

40-Degree Shearout

$P = 7{,}675$ lbs

$e = 1.7 - (0.53/2) \cos 40°$

$= 1.497$ inches

$A_s = 2(0.5)(e)$

$= 1.497$ in^2

$S_s = 7{,}675/1.497$

$= 5{,}127$ psi ($0.6\ S_y = 19{,}620$ psi)

$MS = 19{,}620/5{,}127 - 1$

$= +2.83$

An optional impact limiter lug configuration permits the gusset plate impact limiter attachment tab to be an assembly of the tab and gusset plate using a full-penetration weld. The structural strength of the weld using a mock-up test confirms that the minimum weld yield strength is equal to or greater than 10 ksi. The only stress applicable to the weld is the tension across the entire section of the weld. Using the bounding load of 7,675 pounds, the margin of safety for the weld region is:

$MS = 10{,}000/7{,}675 - 1$

$= +0.30$

Both the 6061-T651 continuous tab gusset configuration and the optional full-penetration weld assembly configuration are confirmed to maintain the attachment of the impact limiters to the cask body for truck or rail transport.

Analysis of Cask Lug

The geometry of the cask lug is a shown in Figure 2.6.7-16. As shown, the lug actually consists of two, 0.5-inch thick lugs, which are integral to a common base plate (the lugs and base plate are machined from one piece). Each of these two lugs is 2.0 inches wide, has a hole diameter of 0.53 inch and has a minimum edge distance of 0.72 inch. The base plate is 1.6 inches wide and 2.0 inches long. The material used is Type 304 stainless steel, which exhibits a yield strength at 150°F of 27,500 psi. Potential failure modes of 40-degree shearout and failure of the weld (3/8-inch bevel plus 3/8-inch fillet), which attaches the base plate to the cask body, are considered as follows:

40-Degree Shearout

$F = P/2 = 1535/2$

$= 768$ lbs

$e = 0.72 - (0.53/2) \cos 40°$

$= 0.517$ in

$A_s = 2(0.5)(e)$

$= 0.517$ in^2

$S_s = 768/0.517$

$= 1485$ psi ($0.6\ S_y = 16{,}500$ psi)

MS = 16,500/1485 - 1 = +Large

Weld Stresses

The analysis of the weld will conservatively ignore the 3/8-inch bevel weld and only consider the 3/8-inch fillet weld around the perimeter of the base plate. Stresses in this weld resulting from the imposed bending moment and the imposed direct shear load will both be treated as shear stresses, combined using a square root sum of squares approach and compared against a shear allowable limit. The stress in the weld due to the applied moment is as follows:

$s_1 = 4.24M/(h[b^2 + 3L(b + h)])$

$= 2006$ psi

where:

$M = 1.78(P) = 2732$ in-lb

$P = 1{,}535$ lbs

$h = 3/8 = 0.375$ in

$b = 2.0$ inches

$L = 1.6$ inches

The stress in the weld due to the applied shear load is:

$s_2 = P/A_s$

$= 804$ psi

where:

$P = 1{,}535$ lbs

$A_s = 2(1.6 + 2.0)(0.707)(0.375)$

$= 1.909$ in^2

The combined stress is therefore:

$s = (s_1^2 + s_2^2)^{0.5}$

$= 2161$ psi ($0.6\ S_y = 16{,}500$ psi)

$MS = 16{,}500/2161 - 1$

$= +$Large

Analysis of Ball-Lock Pin

The 1/2-inch, AVIBANK 57459-1 ball-lock pins have a 36,800-pound capacity in double shear. With an applied load of 1,535 lbs, the margin of safety is very large.

Response of Impact Limiter(s) During Initial Impact of Package with Ground

The second criterion applicable to the impact limiters requires that the limiter(s) making initial contact with the unyielding surface must remain in position on the end(s) of the cask for the full duration of the initial impact. To satisfy this criterion, attachment hardware (pins, lugs and/or associated welds) may fail during an impact event as long as the limiter(s) being crushed remains in position on the end of the cask and does not separate from the cask. The ability of the limiter to remain in position during an impact is demonstrated with reference to a series of dynamic, free drop tests (end, center of gravity over corner, side and oblique), during which some attachment hardware failure occurred, and to several static crush tests, during which the only attachment mechanism was a strip of duct tape. All of the tests were performed using quarter-scale models of the limiters. Analytic evaluations are also presented to further justify that the limiters will remain in position during the impact.

Dynamic Free Drop Test Results

As presented in Appendix 2.10.8, a series of 30-foot free drop tests were performed on a quarter-scale model of the NAC-LWT cask. Drop orientations included an end drop, a center of gravity over struck corner drop, a side drop and an oblique drop with a subsequent secondary impact. A study of the drop test photographs presented in Appendix 2.10.8 indicates that although attachment hardware failed in some of the dynamic free drop tests, the limiters did not physically

separate from the cask body and did completely perform their intended impact limiting function. In fact, the limiters wedged themselves even more securely onto the cask body.

At all times during the testing, the limiters remained in position on the ends of the cask. Notably, rebound from the drop pad due to the whipping action of the restraint cables, did not result in the limiters separating from the cask even though some attachment hardware failure had occurred. This observation demonstrates a tendency for the limiters to become wedged onto the cask body as the result of an impact.

Based on the above test observations, the conclusion reached is that the limiters will remain in position on the cask body during the full duration of the free drop impact event.

Static Crush Test Results

A series of quasi-static crush tests have been performed on quarter-scale models of the bottom impact limiter for the NAC-LWT cask. The limiter orientations tested were end (axial), side and center of gravity over corner (15.7 degrees from axial). The purpose of the quasi-static crush tests was to document the force-deflection and energy absorption characteristics of the honeycomb material used in the impact limiter. Additionally, the tests demonstrated that the limiters need not be mechanically attached to the cask body in order to remain in position to absorb the energy of crushing. No attachment between the model limiter and the test fixture was used for the end (axial) test. A strip of duct tape was adequate to retain the model limiters in position on the side (90-degree) and center of gravity over corner (15.7-degree) fixtures. Once crushing of the limiter is initiated, its cup-shaped geometry causes it to maintain its position on the fixture, which is identical to a quarter-scale model cask body. Thus, attachment of the impact limiter to the cask body is not necessary for maintaining proper position and energy absorption capability.

Analytic Evaluations

Although the results from the above discussed test programs are considered to be the primary proof that the limiters will remain in position during the impact event and properly perform their impact limiting function, analytic studies can also be used to confirm the test observations. Analytic assessments presented in this evaluation indicate that failure of the attachment hardware can be expected to occur for some drop orientations, but subsequent to such failure, the cask tends to wedge into the limiter and separation of the limiter from the cask does not occur. As shown, a significant resistance to the applied separation moment exists due to a combination of crushing of the limiter at the cask interface and due to frictional resistance that exists there. This total resistance is shown to be greater than the applied separation moment and is approximately 7.9 times greater than that provided by the attachment hardware alone.

Additionally, it is noted that the maximum applied separation moment occurs early in the impact when crush depths are small. As crush depths increase, the moment arm and the separation moment decrease to zero. The maximum separation moments occur early in the impact event when the package still possesses a significant downward velocity (87 percent of the initial impact velocity). Additionally, the duration of the impact is very short (approximately 0.04 to 0.06 seconds) and minimal rotation (approximately 1 degree) of the package occurs during the impact. Thus, the cask "drives" into the limiter and physically "traps" the limiter between the cask body and the ground.

The remainder of this section presents a detailed analytic study of the center of gravity over top corner impact event. This near vertical orientation, coupled with the fact that little energy will be converted into rotational energy of the entire package (that is, the center of gravity is over the impacted corner), makes this particular orientation a representative worst case regarding the development of significant separation moments. The available impact limiter analysis program results associated with the corner drop are summarized in Figure 2.6.7-17. The crush depths, crush forces and package velocities presented in the summary figure are directly available from the impact limiter analysis program, RBCUBED, and the separation moment is calculated based on the geometry (that is, the crush footprint) existing at the particular position of interest. Of note, the velocity of the package is still 466.2 inches/second (87 percent of the initial impact velocity) when the maximum separation moment of 7.67×10^6 inch-pounds has developed.

Capability of Attachment Hardware

Figure 2.6.7-18 presents a free body diagram for the top impact limiter during a top down center of gravity over corner impact. With point "A" being the pivot point of the impact limiter on the cask, taking moments about point "A" yields the following:

$$F_i x_i = 14.45\ F_2 + (14.45 + 16.1)\ F_1$$
$$= 14.45\ F_1 + 30.55\ F_1$$
$$= 45.0\ F_1 = \text{separation moment}$$

where:

F_1 = maximum force on a lug

$F_2 = 2(F_1/2) = F_1$

$F_3 = 0.0$ (approximately)

F_i = impact force at limiter to ground interface

x_i = moment arm for force F_i

According to the section titled "Response of Secondary Impact Limiter During Initial Impact of Package," the failure mode for the attachment hardware is tension on the net section of the

impact limiter lug. Failure will occur at a load of 28,445 pounds, which corresponds to a stress equal to the ultimate strength of the aluminum lug. Substitution into the above separation moment equation indicates that a moment of 1.28×10^6 inch-pounds can be expected to fail the attachment hardware. As seen from Figure 2.6.7-17, this moment is exceeded prior to 2 inches of crush occurring for the limiter. Attachments may, therefore, fail in the center of gravity over top corner drop.

Resistance to Separation Following Attachment Hardware Failure

If attachments do fail, the cask tends to wedge itself into the limiter as shown in the free body diagram presented as Figure 2.6.7-19. From that figure:

f_{max} = force required to crush limiter honeycomb

= 28.9 S_c (projected area x crush strength) = 28.9(3850)

= 111,265 lb/in

where:

S_c = crush strength of honeycomb used in limiter

= 3850 psi (conservative upper bound crush strength, which was the case selected for Figure 2.6.7-17; the design upper bound crush strength is 3675 psi)

From moment equilibrium:

$F_i x_i = (6\ f_{max}) = 36\ f_{max}$

$= 4.006 \times 10^6$ in-lb

A significant frictional resistance to separation of the limiter also exists. Selecting a coefficient of friction of approximately 0.5 for aluminum on steel (Baumeister, pages 3-26), the frictional resistance to the separation moment is:

$M_f = F_f d$

$= 6.145 \times 10^6$ in-lb

where:

F_f = friction force

$0.5(6\ f_{max}) = 3\ f_{max} = 333{,}795$ lbs

and with the centroid of a 180-degree arc (that is, the arc over which f_{max} acts) being located at 63.7 percent of its radius:

$d = 0.637(28.9)$

= 18.41 inches

The total resistance to separation, therefore, becomes:

$$M_t = 4.006 \times 10^6 + 6.145 \times 10^6$$
$$= 10.151 \times 10^6 \text{ in-lb}$$

This total resistance to separation exceeds the maximum applied separation moment of 7.67×10^6 inch-pounds (Figure 2.6.7-17). Separation of the limiter from the cask body will not occur. As discussed in the section titled "Dynamic Free Drop Test Results," this particular center of gravity over corner case was tested. Test results are consistent with the preceding analysis in that attachment hardware did fail, that the cask did tend to wedge itself into the impact limiter, and that physical separation did not occur (Appendix 2.10.8, Figures 2.10.8-15 and 2.10.8-16).

Response of Secondary Impact Limiter During Initial Impact of Package

The final criterion to be satisfied is for a free drop (normal or accident) involving an initial impact on a single impact limiter, that the limiter on the opposite end of the cask (secondary limiter) must remain attached to the cask during the initial impact. This ensures that the secondary limiter will be in position to absorb the secondary impact and, as discussed in the section titled "Response of Impact Limiter(s) During Initial Impact of Package with Ground," it remains in position for the full duration of the secondary impact and performs its impact limiting function. Attachment is ensured by demonstrating that the attachment hardware (pins, lugs and associated welds) does not fail during the initial impact while the far end of the transport cask is rotating about the end that is in contact with the ground. For this evaluation, the worst case loading on the secondary impact limiter to separate it from the cask is bounded by the condition that all of the kinetic energy at the time of impact is converted to angular rotation. The angular rotation speed (ω) results in a radial angular acceleration (A_r) of the far end of the cask (a radius of r) that is computed by $r\omega^2$. The angular speed is determined by using conservation of energy,

$$\omega = \sqrt{\frac{2WH}{I}}$$

where:

The moment of inertia of the cask (I) about the point of rotation is computed for a 199.8-in long, 39.23-in diameter, right circular cylinder about the edge in conjunction with the impact limiter (M_L) (see page 34 of "Formulas for Natural Frequency and Mode Shape," Robert D. Blevins, Ph.D, Krieger Publishing Co., Inc., 1984):

$$I = (M) \times \left[\frac{1}{12} \left(3 \times (R)^2 + (L)^2 \right) + (R)^2 \right] + M_L \times L^2$$

$$= (118.2\ \text{lb}\cdot\text{sec}^2/\text{in}) \times \left[\frac{1}{12} \left(3 \times \left(\frac{39.23\ \text{in}}{2} \right)^2 + (199.8\ \text{in})^2 \right) + \left(\frac{39.23\ \text{in}}{2} \right)^2 \right] + 3.97 \times 199.8^2$$

$$= 6.09 \times 10^5\ \text{lb}\cdot\text{sec}^2\cdot\text{in}$$

where,

M = mass of the empty cask, less the weight of one impact limiter =

$$\frac{45{,}673\ \text{lbs}}{386.4\ \text{in}/\text{sec}^2} = 118.2\ \text{lb}\cdot\text{sec}^2/\text{in}$$

M_L = mass of the impact limiter = $\dfrac{1{,}535\ \text{lbs}}{386.4\ \text{in}/\text{sec}^2} = 3.97\ \text{lb}\cdot\text{sec}^2/\text{in}$

The bounding angular velocity is therefore:

$$\varpi = \sqrt{\frac{2 \times W \times H}{I}} = \sqrt{\frac{2 \times 47{,}208\ \text{lbs} \times 360\ \text{in}}{6.09 \times 10^5\ \text{lb}\cdot\text{sec}^2\cdot\text{in}}} = 7.47\ \text{rad}/\text{sec}$$

The radial acceleration (A_r) (g) using a radius of 200 inches from the bottom to the top end of the cask is:

$$A_r(g) = \frac{200\ \text{in} \times \left(7.47\ \text{rad}/\text{sec}\right)^2}{386.4} = 28.9\ \text{g's}$$

The calculations for the stress conservatively use the maximum acceleration of 30 g's. With four attachment points, the load, P, per attachment point therefore becomes:

P = 30 × 1,535/4

= 11,513 lbs

where 1,535 pounds is the weight of the heaviest (top) impact limiter.

Analysis of Impact Limiter Lug

The impact limiter lug is evaluated using the same approach as was used in the section titled "Analysis of Impact Limiter Lug," but the allowable limit is based on ultimate strength rather than yield strength. As shown in Table 2.3.1-4, the ultimate strength of 6061-T651 aluminum at 150°F is 38,700 psi. Potential failure modes of tension across the net section and 40-degree shearout are considered as follows:

Tension Across the Net Section

$P = 11,513$ lbs

$A = 0.5(2.0 - 0.53)$

$= 0.735$ in^2

$S_t = 11,513/0.735$

$= 15,664$ psi ($S_u = 38,700$ psi)

$MS = 38,700/15,664 - 1$

$= +1.47$

40-Degree Shearout

$P = 11,513$ lbs

$e = 1.7 - (0.53/2) \cos 40°$

$= 1.497$ inches

$A_s = 2(0.5)(e)$

$= 1.497$ in^2

$S_s = 11,513/1.497$

$= 7,691$ psi ($0.6\ S_u = 23,220$ psi)

$MS = 23,220/7,691 - 1$

$= +2.02$

An optional impact limiter lug configuration permits the gusset plate impact limiter attachment tab to be an assembly of the tab and gusset plate using a full-penetration weld, as described in Section 8.2.1.1, Impact Limiter Attachment Lug Repairs. Structural strength of the weld using a mock-up test confirms that the minimum weld tensile strength is equal to or greater than 20 ksi. The only stress applicable to the weld is the tension across the entire section of the weld. Using the bounding load of 11,513 pounds, the tensile stress is 11,513 (2×1/2) or 11,513 psi and the margin of safety for the weld region is:

$MS = 20,000/11,513-1$

$= +0.74$

Both the 6061-T651 continuous tab gusset configuration and the optional full-penetration weld assembly configuration are confirmed to maintain the attachment of the impact limiters during the bounding condition of the accident side drop condition.

Analysis of Cask Lug

The cask lug is evaluated using the same approach as was used in the section titled "Analysis of Impact Limiter Lug," but the allowable limit is based on ultimate strength rather than yield strength. The ultimate strength of Type 304 stainless steel at 150°F is 73,000 psi. Potential failure modes of 40-degree shearout and failure of the weld (3/8-inch bevel plus 3/8-inch fillet), which attaches the base plate to the cask body, are considered as follows:

40-Degree Shearout

$F = P/2 = 23,179/2$

$= 11,590$ lbs

$e = 0.72 - (0.53/2) \cos 40°$

$= 0.517$ in

$A_s = 2(0.5)(e)$

$= 0.517$ in^2

$S_s = 11,590/0.517$

$= 22,418$ psi ($0.6\ S_u = 43,800$ psi)

$MS = 43,800/22,418 - 1$

$= +0.95$

Weld Stresses

The analysis will again conservatively ignore the 3/8-inch bevel weld and only consider the 3/8-inch fillet weld around the perimeter of the base plate.

The stress in the weld due to the applied moment is:

$s_1 = 4.24\ M/(h[b^2 + 3\ L(b + h)])$

$= 30,292$ psi

where:

$M = 1.78(P) = 41,259$ in-lb

$P = 23,179$ lbs

$h = 3/8 = 0.375$ in

$b = 2.0$ in

$L = 1.6$ in

The stress in the weld due to the applied shear load is:

$$s_2 = P/A_s$$
$$= 12,142 \text{ psi}$$

where:

$$P = 23,179 \text{ lbs}$$
$$A_s = 2(1.6 + 2.0)(0.707)(0.375)$$
$$= 1.909 \text{ in}^2$$

The combined stress is therefore:

$$s = (s_1^2 + s_2^2)^{0.5}$$
$$= 32,635 \text{ psi } (0.6\ S_u = 43,800 \text{ psi})$$
$$MS = 43,800/32,635 - 1$$
$$= +0.34$$

Analysis of Ball-Lock Pin

The 1/2-inch, AVIBANK 57459-1 ball-lock pins have a 36,800-pound capacity in double shear. With an applied load of 23,179 pounds, the margin of safety becomes:

$$MS = 36,800/23,179 - 1$$
$$= +0.59$$

2.6.7.5 Closure Lid

2.6.7.5.1 Discussion

The NAC-LWT cask closure lid is analyzed for structural adequacy in accordance with the requirements of 10 CFR 71.73(c)(1) free drop (hypothetical accident condition). The cask is assumed to be inverted, with the lid downward, when dropped through a distance of 30 feet onto a flat, unyielding, horizontal surface. The structural evaluation is performed by classical elastic analysis methods.

2.6.7.5.2 Analysis Description

Geometry

The closure lid geometry is shown in Figure 2.6.7-20. The lid is bolted in position on the upper end of the cask. The lid material is Type 304 stainless steel. The temperature-dependent material properties for Type 304 stainless steel, which are presented in Section 2.3, are used in this analysis.

Loadings

During impact, the cask cavity contents are considered to apply an internal inertia pressure on the interior surface of the lid in the outward normal direction. The impact limiter applies an external inertia pressure on the exterior lid surface in the inward normal direction; however, this pressure is conservatively ignored in this analysis. Each bolt is torqued to a preload force of 21,000 pounds. The lid is also loaded with an assumed 50-psig internal pressure for the 130°F ambient temperature hot case.

Displacement Boundary Conditions

The closure lid is restrained from vertical and rotational deformation at the 17.875-inch bolt circle diameter by the preloaded lid bolts.

Detailed Analysis

For the loading and boundary conditions described, the structural behavior of the closure lid may be assessed by superposition of maximum stresses from Section 2.6.1, which includes consideration of thermal effects, bolt preload, and internal pressure, with the maximum stresses produced by the inertia loading. The maximum $P_m + P_b$ component stresses from Section 2.6.1 (Table 2.6.1-2) are:

$$S_x = -3060 \text{ psi};\ S_y = -260 \text{ psi};\ S_z = 100 \text{ psi};\ S_{xy} = 180 \text{ psi}$$

The free body diagram of Figure 2.6.7-21 can be evaluated by applying formulas from Case 6 (Roark, page 217) for a uniformly loaded circular plate.

The total deceleration force of the contents, $F_D = 4000 \text{ lbf} \times 60 \text{ g deceleration} = 240{,}000 \text{ lbf}$, creates a pressure, W, on the lid interior surface:

$$W = \frac{240{,}000}{\pi(8.938)^2} = 956 \text{ psi}$$

The maximum radial, tangential, and vertical stresses on the lid are:

$$S_r = \frac{3Wa^2}{4t^2}$$

$$= 895 \text{ psi}$$

$$S_t = \frac{3Wa^2\gamma}{4t^2}$$

$$= 246 \text{ psi}$$

$$S_v = -W$$

$$= -956 \text{ psi}$$

where:

a = 8.938 inches

γ = 0.275

t = 8.0 inches

Conservatively combining these stresses with $P_m + P_b$ stresses from Section 2.6.1 (Table 2.6.1-2), the total $P_m + P_b$ component stresses on the lid are:

S_x = -3955 psi; S_y = - 1216 psi; S_z = 346 psi; S_{xy} = 180 psi

For small S_{xy}, the stress intensity becomes S.I. = $S_z - S_x$ = 4301 psi. Since the maximum cask lid temperature is less than 300°F for the 130°F ambient temperature hot case (Section 3.4.2), the closure lid allowable $P_m + P_b$ stress is 72,000 psi (3.6 S_m). Therefore, the minimum margin of safety is +Large; thus, containment is maintained.

2.6.7.5.3 Conclusion

It is demonstrated by use of a conservative loading that the minimum margin of safety is +4.23 and containment is maintained. Therefore, the NAC-LWT cask lid satisfies the requirements of 10 CFR 71 for consideration of the closure lid impact in the 30-foot free drop accident.

2.6.7.6 Bolts - Closure Lid (Normal Conditions of Transport)

The NAC-LWT cask closure lid is bolted to the cask body top forging with twelve 1 - 8 UNC bolts fabricated from SA-453, Grade 660 high alloy steel. The threaded portion of the bolt engages the cask body a minimum of 1.875 inches. In accordance with the free drop provisions of the normal conditions of transport, 10 CFR 71.71(c)(7), this bolted closure has been carefully

evaluated for structural adequacy and found to satisfy all regulatory requirements and design criteria. Details of this analytic evaluation follow.

The simultaneous loads that may be imposed upon the cask closure bolts include: pressure loads, thermal differential expansion loads, pre-loads and inertial loads arising from impact responses. For a given set of initial conditions, the pressure loads, thermal loads and pre-loads all remain constant. Inertial impact loads, however, vary with impact orientation and bolt location. Lateral impact loads acting upon the lid are directly related to the mass of the lid and the lateral impact acceleration. Longitudinal impact loads acting on the lid are proportional to the longitudinal impact acceleration, as well as, the mass of the lid and the payload within the containment cavity.

In general, these lid impact loads impose unequal individual forces, or loadings, in the closure bolts. This NAC-LWT cask evaluation conservatively assumes a set of impact forces that induce maximum containment closure separation forces and bolt loadings. With this conservative assumption, the external impact force is presumed to be located at a point where it cannot restrain those forces that tend to separate the cask lid from the cask body. This assumption locates the external impact force at the lower corner of the lid-body interface. With this assumption the lower corner of the lid is assumed to be pinned (by the impact forces), and bolt tension forces are assumed to vary linearly from zero at this pinned lower corner to a maximum value at the opposite, or upper, corner of the lid.

A complete range of impact orientations is evaluated, from an end impact at 0 degrees to a flat side impact at 90 degrees, and at 5-degree increments in between. Loads are derived from the normal impact accelerations summarized within Table 2.6.7-34. Where necessary, impact accelerations have been interpolated at 5-degree increments from those values given in Table 2.6.7-34.

The details of this analytic evaluation are described and performed within Section 2.10.9 for both normal conditions of transport and hypothetical accident conditions. Normal conditions of transport results are summarized in Table 2.6.7-35 and Table 2.6.7-36, corresponding to a "hot" initial condition and a "cold" initial condition, respectively. The hot initial condition bolt temperature is taken at 227°F, as summarized in Table 3.4-2. The cold initial condition bolt temperature is assumed to be -20°F, per regulatory requirements. Physical properties for the SA-453, Grade 660 bolts are conservatively taken at 300°F and at room temperature (70°F) for hot and cold conditions, respectively. As defined within Table 2.1.2-1, the allowable bolt stress is taken as S_y, leading to allowable direct tension stresses of 81.9 and 85.0 ksi, at 300°F and 70°F, respectively. Based on this thorough evaluation, the closure bolts incur a maximum stress intensity of 61,012 psi, which results in a minimum margin of safety of 34 percent. See Table 2.6.7-35 (at 5°):

MS = 81.9/61.042 - 1

= +0.34

Bolt engagement may be evaluated by computing shear stresses within the SA-336, Type 304, end forging material. At 300°F, the allowable shear stress is 0.5 S_y, or 11.25 ksi, according to Tables 2.1.2-1 and 2.3.1-1. The maximum tensile load is found as the product of the maximum bolt stress intensity, noted above, and the bolt stress area; that is, (61,042 psi)(0.6051) = 36,937 pounds. The shear area per inch of engagement for a 1 - 8 UNC internal thread is 2.325 in^2/in ("Table Speeds Calculation of Strength of Threads," pp. 41-49). The resultant shear stress and margin of safety within the top body forging is:

$\tau = P/A = (36,937)/[(2.325)(1.875)]$

= 8473 psi

MS = 11.25/8.473 - 1

= +0.33

Using consistently conservative assumptions, the NAC-LWT cask lid bolted closure can be shown to satisfy the performance and structural integrity requirements of 10 CFR 71.71(c)(7) for normal conditions of transport.

2.6.7.7 Neutron Shield Tank

2.6.7.7.1 Introduction

The neutron shield tank is welded to, and concentric with, the NAC-LWT cask outer shell. The tank consists of eight cells. The neutron shield fluid flows freely through holes in the longitudinal stiffeners between these cells. During thermal expansion or contraction, fluid passes through the valve assembly into or out of the expansion tank, which is external to and concentric with, the shield tank. Table 2.6.7-37 summarizes the results of the structural analyses described below. The table shows positive margins of safety, demonstrating that each component of the neutron shield tank satisfies the requirements of the normal operations conditions 1-foot free drop as described in 10 CFR 71.71. Classical analysis techniques are used to demonstrate that each tank component withstands the hydrodynamic loads from a 1-foot side or end drop in combination with internal tank pressure. Similarly, classical analyses show that the shield/expansion tank does not rupture, nor does the check valve sustain damage during the penetration test.

The shield tank wall has a mean diameter of 39.04 inches, is located approximately 23 inches below the top edge of the upper end casting, and extends 164 inches longitudinally. Constructed entirely of Type 304 stainless steel, the tank external shell and eight longitudinal stiffeners are 0.24-inch thick plate. Each end of the tank is a 0.50-inch thick end plate. Equally spaced

between stiffeners are eight 0.24-inch thick gusset plates, which provide additional support to the end plates.

A 56 percent by volume ethylene glycol and water solution provides the neutron shielding. The shield tank fluid volume (excluding stiffeners) is 84,742 cubic inches or approximately 370 gallons (3,280 pounds) of fluid. At the upper end, concentric with the shield tank, is the expansion tank. The expansion tank is 46 inches long and is constructed from 0.32-inch thick stainless steel plate; there are eight cells divided by equally spaced plate stiffeners with holes in them, which enables the fluid to flow from chamber to chamber. The expansion tank empty volume is 13,245 cubic inches. It is filled with 11.5 gallons (103 pounds) of solution initially, leaving an expansion volume of 10,589 cubic inches. At the bottom of the expansion tank is a siphon tube, which goes around the shield tank and exits at its top. Volumetric expansion forces fluid through the siphon tube. During heating, the solution in the shield tank expands into the expansion tank avoiding uncontrolled pressurization of the shield/expansion tank. A pressure relief valve in the shield tank assures that the tank structure is protected against over pressurization. The pressure relief valve is set to begin relieving pressure at 165 psig. Initially, the expansion tank is filled with 11.5 gallons of fluid to assure that the shield tank remains filled at -40°F. A cross section of the upper end of the cask with pertinent dimensions is shown in Figure 2.6.7-22.

2.6.7.7.2 Structural Criteria

The neutron shield tank and expansion tank analyses use 10 CFR 71 and Regulatory Guide 7.8 to determine load/ambient conditions to bound other load conditions. In this way, the shield/expansion tank components are conservatively analyzed for the most severe structural loads at maximum temperatures; thus, the material properties and allowable stresses have minimum values.

The 10 CFR 71 requires that all transport packages weighing more than 30,000 pounds be evaluated to determine the consequences of a free fall through a distance of 1-foot onto a horizontal, unyielding surface for normal operation; cask orientation during the fall shall be such that maximum damage is inflicted upon the cask. End and side drop g loads are the most severe normal operating loads that the cask sustains; analyses of the shield and expansion tanks are based on the end and side drop loads. All other cask drop orientations produce less severe g loads.

Table 2 in Regulatory Guide 7.8 defines three initial ambient states that guide the analyses. The two extreme cases used to envelope analyses are:

1. 100°F ambient temperature, with maximum insolation, decay heat, internal pressure, weight, and minimum external pressure

2. 20°F ambient temperature, with no insolation or decay heat, minimum internal pressure, weight, and external pressure.

These conditions are used to evaluate the shield tank fluid temperatures (Actually, Sections 3.4.2 and 3.4.3 results, which are based on the more limiting ambient temperatures of 130°F and -40°F are used). With the fluid temperatures established, it is then possible to calculate the shield/expansion tank pressures for the extreme cases and the resulting amount of fluid flowing between the shield tank and the expansion tank (for expansion tank sizing). Table 2.6.7-38 summarizes the calculated shield tank fluid temperatures used in analyzing the shield tank structure.

Since the functional and structural adequacy of the neutron shield and expansion tanks depend on linear elastic evaluations, the allowable stress criteria is selected as the material yield strength. All calculated stresses are less than this criteria. From Table 2.6.7-38, the highest average fluid temperature is 227°F; therefore, material properties for 250°F are used in the analyses. The evaluation of the shield/expansion tank and the resulting conclusions are conservative.

2.6.7.7.3 Neutron Shield and Expansion Tank Loads

Structural, hydrostatic/hydraulic pressure and expansion pressure are the three components of shield tank loads. Structural loads result from decelerating the cask structure. Hydrostatic and hydraulic loads (water hammer) result from the shield tank fluid decelerating against the shield tank structure. Expansion pressure loads are generated when the fluid expands during heating. An explanation of how each type of load is calculated follows.

Structural loads are loads imposed on the structure by the weight of the structure itself. The stainless steel materials from which the cask is fabricated all have mass and are acted upon by gravity and the normal operations conditions 1-foot drop deceleration. Shield tank structural components weigh approximately 2,116 pounds. Expansion tank components weigh approximately 610 pounds. These loads are included in the analysis of the tanks.

Hydrostatic pressure is the pressure at a given depth within a fluid caused by the mass of the fluid being accelerated by gravity. Hydraulic pressure is the hydrostatic pressure acted upon by accelerations other than gravity. To determine the hydrostatic pressure of fluid acting on the plate, the following formula is used:

$$p = \rho g h$$

where:

ρ = mass density of fluid (lbm/in^3)

g = acceleration due to gravity (in/sec/sec)

h = height of fluid above point considered (in)

When the cask is vertical, the maximum fluid height in the shield tank is 164 inches, which is equivalent to 6.3 psig under the acceleration of gravity (1 g). When the cask is in the horizontal position, there is a 39-inch maximum fluid height (diameter of shield tank) or 1.56 psig (1 g). The presence of the expansion tank around the shield tank is conservatively neglected, because the fluid pressure acting on the exterior of the shield tank reduces the forces acting on the shield tank components. During a 1-foot end drop (normal operations conditions), the cask undergoes a 15.8 g deceleration (Section 2.6.7.4). This results in a hydraulic pressure of 100 psig (6.3 psig × 15.8 g) at the bottom of the shield tank. Similarly, during the side drop, the pressure at the lowest point on the shield tank is 38 psig (1.56 psig × 24.3 g). The maximum hydrostatic and hydraulic pressures for the end and side drops and the location of the maximum pressure for the shield tank analyses are shown in the following sketches.

1-Foot End Drop (15.8 g)

Maximum Hydrostatic Pressure	Maximum Hydraulic Pressure
6.3 psig	100 psig

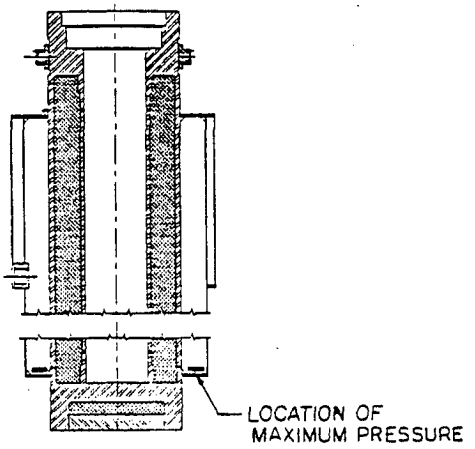

Vertical Orientation

1-Foot Side Drop (24.3 g)

Maximum Hydrostatic Pressure	Maximum Hydraulic Pressure
1.56 psig	38 psig

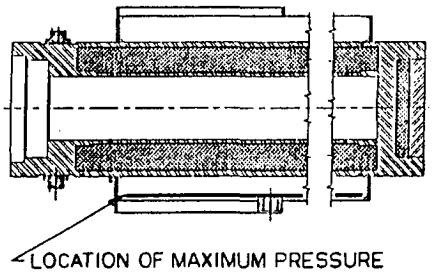

Horizontal Orientation

The g loads for various drop orientations and how they were calculated are explained in Section 2.6.7.4.

Once the shield/expansion tank is filled, it is a sealed compartment, which will not permanently deform under normal transport conditions. The neutron shield tank solution expands or contracts when heated or cooled. During heating the liquid expansion causes fluid to flow into the expansion tank, compressing the air in the expansion tank and causing the pressure to increase. Similarly, as the cask fluid temperatures reach 40°F, there is sufficient fluid in the expansion tank to always keep the neutron shield tank completely filled.

The neutron shield tank is completely filled in the upright configuration, when the fluid and ambient conditions are at 68°F. The 56 percent by volume ethylene glycol and water solution has a density of 67.07 lbs/ft^3 at 68°F. After the neutron shield tank is filled, 11.5 gallons of solution are poured into the expansion tank. Both tanks are then sealed.

The normal transport condition of maximum decay heat load, 100°F ambient temperature and maximum insolation results in an average (natural and forced mixing of fluid is assumed) shield tank fluid temperature of 227°F. The volume of fluid that enters the expansion tank as the temperature increases from 68°F to 227°F is:

$$\Delta V = V_1\left[\frac{\rho_1}{\rho_2} - 1\right] = 5539 \text{ in}^3$$

where:

ρ_1 = 67.07 lb/ft^3 = density of 56 percent ethylene glycol and water solution at 68°F

ρ_2 = 63.07 lb/ft^3 = density of 56 percent ethylene glycol and water solution at 230°F

V_1 = 87,398 lb/in^3 = volume of fluid in the expansion and shield tank at 68°F

ΔV = volume of fluid entering the expansion tank

Then the increased uniform air pressure in the expansion tank at 230°F is:

$$P_2 = P_1\left[\frac{V_1 T_2}{T_1 V_2}\right] = 40.3 \text{ psia (25.6 psig)}$$

where:

P_1 = 14.7 psia

V_1 = 10,589 in^3 (expansion tank air volume at 68°F)

T_1 = 528°R = 68°F

T_2 = 690°R = 230°F

$V_2 = 10{,}589\ in^3 - 5539\ in^3 - 5050\ in^3$ (expansion tank air volume at 230°F)

The same analysis procedure was used to calculate the pressures at other significant normal operating states; these pressures are presented in Table 2.6.7-39. Properties for the 56 percent by volume ethylene glycol and water solution are presented in Table 3.2-5. Two normal operating conditions are presented in Table 2.6.7-39, and are helpful in understanding how the cask operates, but are all bounded by the pressure relief valve release pressure (PRVR) shown in Table 2.6.7-39. The PRVR pressure is used to establish the structural loads for shield and expansion tank analyses.

Thus, the magnitude of the expansion pressure is determined as discussed previously by the volume of fluid added to the expansion tank during the initial filling. It is assumed that 11.5 gallons of fluid are added to the expansion tank, 0.5 gallons more than specified. This results in a maximum expansion pressure of 26 psig.

In addition to the expansion pressure acting radially outward, 10 CFR 71, Subpart F, requires that the cask be able to sustain a reduced external pressure. The cask is initially filled and pressurized at atmospheric pressure (14.7 psia). When the external pressure is reduced to 3.5 psia, there is a relative increase in internal pressure of 11.5 psig (rounded to 12 psig). The reduced external pressure load has been included in the analysis as an increase in internal pressure.

The calculated pressures for the end drop load condition are as follows:

Reduced external pressure	12 psig
Hydraulic pressure	100 psig
Expansion pressure	26 psig
TOTAL	138 psig

The calculated pressures for the side drop load condition are as follows:

Reduced external pressure	12 psig
Hydraulic pressure	38 psig
Expansion pressure	26 psig
TOTAL	76 psig

These pressures are conservatively assumed to add algebraically and represent the highest pressure expected at a point on the shield/expansion tank structure. All other pressures within the shield/expansion tank are less because the hydraulic pressure is a function of fluid depth.

2.6.7.7.4 Neutron Shield Tank Structural Analyses

To simplify analysis of the shield tank structure, the use of symmetry, superposition and analysis of worst case loads are employed to reduce the number of calculations to be performed. Major shield tank structural components are shown in Figure 2.6.7-23. Analyses performed and resulting conclusions for one location of the shield tank are directly applicable to the same relative location elsewhere on the shield tank structure. For reasons stated earlier, the normal operating conditions 1-foot end drop loads envelope all other normal operations conditions drop orientations, and is the only loading condition that is considered in the following analyses. Moreover, the bottom end drop g load is more severe than the top end drop, and is used in both the top and bottom end drop analyses. The shield tank analysis is performed with the shield tank pressure equal to 180 psig, a pressure 42 psig higher than the calculated 138 psig for the end drop (which envelops the side drop condition).

The bottom end plate, shield tank shell, gussets, top end plate, and welds are the major components of interest in the shield tank evaluation for normal transport conditions.

To ensure a conservative analysis of the neutron shield and expansion tank structure, several simplifying assumptions are made for all analyses performed (other assumptions are stated with each analysis). The allowable stress is taken as the yield strength of Type 304 stainless steel at 250°F, which is 23,750 psi. This is conservative since the maximum calculated shield/expansion tank normal operating temperature is 227°F.

Finally, the edge restraint of the structural components analyzed is considered to be simply supported. The smallest welds are considered in the analyses; a larger weld assures a conservative analysis.

Weld Allowable Stresses

The shield and expansion tanks are constructed primarily from 0.24-inch thick Type 304 stainless steel plate. The plates are welded together using 0.188-inch fillet welds, using Type 308 weld material. From the Metals Handbook, 9th Edition, Volume 3, page 20, the ultimate tensile strength is 75.0 ksi. The allowable strength for shield tank fillet welds is:

$$S_{ALL} = (0.3)(75{,}000)$$
$$= 22{,}500 \text{ psi}$$

or:

$$f_{ALL} = (0.707)(22{,}500)\omega$$
$$= 15{,}900\omega \text{ lb/in}$$

where:

f_{ALL} = fillet allowable (lb/in)

ω = fillet weld size (in)

The only size fillet weld considered in the shield tank analysis is a 0.188-inch fillet. Therefore, the 0.188-inch fillet weld has an allowable strength of:

f_{ALL} = (15,900)(0.188 in)

= 2980 lb/in

Structural Loads

Shield tank and end plate loads are considered in the neutron shield tank analysis. The weight of a unit depth of the 0.24-inch thick shield tank plate material is considered to be located at the mass centroid of the plate assembly. The mass centroid is 6.13 inches from the outer shell, as shown in the following analysis:

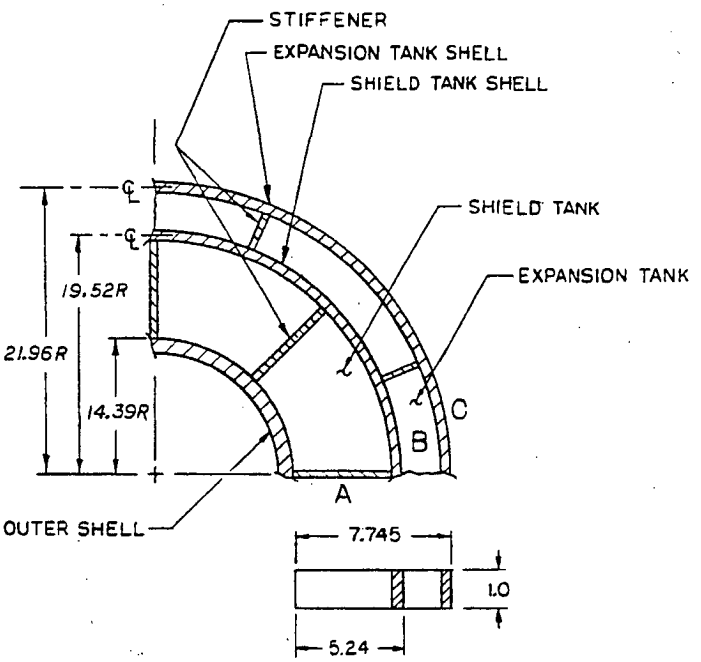

Quarter Section - NAC LWT Cask

Two "A" plates weigh 1.051 pounds with a mass centroid at 3.87 inches from the outer shell.
Two "B" plates weigh 2.005 pounds with a mass centroid at 5.12 inches from the outer shell.
Two "C" plates weigh 3.032 pounds with a mass centroid at 7.59 inches from the outer shell.
The total weight of the plates is 6.09 pounds.

The mass centroid is located at:

$$\bar{x} = \frac{(1.051\ lb)(3.873\ in) + (2.005\ lb)(5.12\ in) + (3.032\ lb)(7.59\ in)}{5.643\ lb}$$

$$= 6.134\ in$$

The weight of the neutron shield tank structural plates is considered to act at 6.09 inches from the outer shell. The weight of one stiffener and shield/expansion tank shell section is 3.54 pounds.

The shield tank end plates are 0.5-inch thick stainless steel plate. To determine the structural load, the weight of the plate was divided by its area. The resulting structural load is 3 pounds/square inch.

Shield Tank Shell

The shield tank shell is analyzed as a thin-walled tube, taking no credit for the eight radial stiffeners, which run the length of the tank. Using Case 1 (Roark, page 298), the meridional and hoop stresses are calculated:

$$S_1 = \frac{pR}{2t} = 7414\ psi$$

where:

p = 180 psig

R = 19.44 inches

t = 0.24 in

and

$$S_2 = \frac{pR}{t} = 14,827\ psi$$

Von Mises yield criterion is used to calculate an equivalent stress, S_e, which is compared to the yield strength of stainless steel.

$$S_e = \frac{1}{\sqrt{2}}\left[(S_1 - S_2)^2 + (S_2 - S_3)^2 + (S_3 - S_1)^2\right]^{0.5}$$

$$= 12,841\ psi$$

where:

S_1 = 7414 psi

$S_2 = 14{,}827$ psi

$S_3 = 0$ psi

then

$$M.S. = \frac{S_{ALL}}{S_e} - 1 = \underline{+0.07}$$

where:

$S_{ALL} = (0.577)(23{,}750 \text{ psi})$
$= 13{,}700$ psi

Stiffener

A 1-inch longitudinal section of the neutron shield tank is analyzed. The total pressure load (180 psi) acts equally between stiffeners as shown in Figure 2.6.7-24. No credit is taken for support from the end plates or the expansion tank end plate. The load acting on the stiffener (L = 2772 pounds) is the area of the tank shell 15.4 square inches (15.4 inches × 1 inch) multiplied by the total end drop pressure, 180 psi. The cross sectional area, A_p, of a 1-inch section of the stiffener plate is 0.24 square inches (0.24 inch × 1.0 inch). The tensile stress acting on the stiffener is calculated:

$$S_T = \frac{L}{A_p} = 11{,}746 \text{ psi}$$

then

$$M.S. = \frac{S_{ALL}}{S_T} - 1 = \underline{+0.17}$$

where:

$S_{ALL} = 13{,}700$ psi (Section 2.6.7.7.4)

The stiffeners are the structural members locating the shield tank shell and providing support for the end plates (similar to the gussets) during end drops. This analysis demonstrates that the stiffeners have adequate strength to withstand the maximum pressure in the shield tank. The analysis in Section 2.6.7.7.4 shows that the shield tank shell has adequate strength to withstand the maximum pressure in the shield tank. All other drop orientations offer less severe structural loads on both the stiffeners and tank shell. Lightening holes in each stiffener do not affect the structural integrity of the shield tank and stiffeners. Lightening holes are located away from the ends of the stiffeners where the hydraulic component of the pressure load is less severe.

Stiffener Weld

A unit section (1 inch longitudinal) of stiffener weld is analyzed. Two loads act on the weld attaching the stiffener to the cask outer shell. The drop pressure load acting on the stiffener is L = 2772 pounds (see section titled "Stiffener"). In addition to the pressure load, the structural load (L_s) is calculated concentrating the mass of the tank (stiffeners and shell) unit section (see section titled Structural Loads). The structural pressure loads and welds being examined are shown in Figure 2.6.7-25. Treating the two 1-inch welds as lines and determining the weld loading using methodology found in Design of Welded Structures (Blodgett, Section 7.4):

Tensile Load

f_t = 2772/2

= 1,386 lb/in

where:

L = 2,772 lbs

Shear Load

f_s = 55.9/2

= 28.0 lb/in

where:

L_s = 3.54 lb x 15.8 g

= 55.9 lbs

15.8 g = end drop g load
(Section 2.6.7.4)

The end drop structural load produces a bending moment on the weld group (Figure 2.6.7-25). The bending moment (M) is 343 inch-pounds (6.13 inches × 55.9 pounds). The section properties of the weld group are calculated from Blodgett, Table 5, page 7.4-7,

$$S_\omega = \frac{d^2}{3}$$

$$= 0.33 \text{ in}^2$$

where:

d = 1 in

Bending Load

$$f_b = \frac{M}{S_\omega}$$

$$= 343/0.33$$

$$= 1038 \text{ lb/in}$$

The resultant load on the weld group is calculated:

$$f_r = \sqrt{f_1^2 + f_2^2}$$

$$= 2424 \text{ lb/in}$$

where:

$f_1 = f_s = 28.0$ lb/in

$f_2 = f_t + f_b$

$= 2{,}424$ lb/in

The allowable weld load is $f_{ALL} = 2{,}980$ lb/in; therefore, the margin of safety is:

$$M.S. = \frac{f_{ALL}}{f_r} - 1 = \underline{+0.23}$$

Gusset Weld

It is assumed that the end drop load on the end plate is shared equally between the stiffeners and gussets (Figure 2.6.7-26). The fillet weld attaching the gusset to the cask outer shell and end plate is 0.188 inch and is on both sides of the gusset. Bending and shear stresses on the weld group A are calculated in the following analyses. Since the gussets and stiffeners share the end drop load, the end plate area, which the gusset must support, is calculated:

$$A = [\pi(R_o^2 - R_i^2) - (16)(T_{PLT})(R_o - R_i)]/16$$

$$= 33.95 \text{ in}^2$$

where:

$R_o = 19.6$ inches

$R_i = 14.3$ inches

$T_{PLT} = 0.25$ in

The distributed load is composed of the end drop pressure load (180 psig) and a structural load (3 psig) equivalent to the end plate weight. The concentrated load (L) is calculated by multiplying the area (A) by the sum of the distributed loads (183 psig): L = 6,213 pounds. Therefore, the moment acting on weld group A is:

$$M = L\left[\frac{5.1}{2}\right]$$

$$= 15{,}843 \text{ in-lb}$$

The section properties of the weld group are calculated from Blodgett, Table 5, page 7.4-7:

$$S_\omega = \frac{d^2}{3}$$

$$= 12 \text{ in}^2$$

where:

d = 6 inches

Bending Load

$$f_b = \frac{M}{S_\omega}$$

$$= 1320 \text{ lb/in}$$

Shear Load

$$f_s = \frac{L}{W_{LEN}}$$

$$= 518 \text{ lb/in}$$

where:

L = 6,213 lbs

W_{LEN} = 2 × 6 inches

= 12 inches

The resultant load on the weld group is calculated by:

$$f_r = \sqrt{f_1^2 + f_2^2}$$

$$= 1418 \text{ lb/in}$$

where:

$f_1 = f_s = 518$ lb/in

$f_2 = f_b = 1320$ lb/in

The allowable weld load is $f_{ALL} = 2980$ lb/in; therefore, the margin of safety is:

$$M.S. = \frac{f_{ALL}}{f_r} - 1 = \underline{+1.10}$$

Bottom End Plate

It is assumed that the portions of the end plate between a gusset and the adjacent stiffener can be modeled by a rectangular plate of the appropriate dimensions. The width (b) of the plate is the difference between radii of the cask outer shell and the shield tank shell as shown in Figure 2.6.7-27. The length (a) of the plate is the average of the inner and outer arc lengths, 6.7 inches ((7.7 inches + 5.6 inches)/2). Using Case 36 (Roark, page 225), the maximum bending stress on the 0.5-inch thick end plate is:

$$S_b = \beta \frac{wb^2}{t^2}$$

$$= 8{,}525 \text{ psi}$$

where:

$\beta = 0.4146$

$w = 183$ psi (see section titled "Gusset Weld")

$b = 5.3$ inches

$t = 0.5$-in thick

The margin of safety is:

$$M.S. = \frac{S_{ALL}}{S_B} - 1 = \underline{+1.79}$$

where:

$S_{ALL} = S_{y_{250°F}}$

$= 23{,}750$ psi

Gusset Plate Cross-Section

The plate was modeled as a large weld, with the throat in tension during an end drop. The end drop load (L) acting on the gusset is the load acting on the end plate between the gusset and adjacent stiffener. The gusset root cross-section (R) is considered to be in tension (Figure 2.6.7-28). From the section titled "Gusset Weld," the load on the gusset root is L = 6213 pounds. The gusset root cross-sectional area is calculated:

$A_R = 0.707(h)(T_{PLT})$

$= 0.865 \text{ in}^2$

where:

h = 5.1 in (shortest leg)

T_{PLT} = 0.24 in (thickness)

Calculating the tensile load:

$$S_T = \frac{L}{A_R}$$

$$= 7180 \text{ psi}$$

The margin of safety is:

$$M.S. = \frac{S_{ALL}}{S_T} - 1 = \underline{+LARGE}$$

where:

S_{ALL} = 23,750 psi

End Plate Welds

Peripheral weld group B (Figure 2.6.7-29) is considered to be in shear during an end drop. The end plate load is 6213 pounds, from the section titled "Gusset Weld." The area of weld material is:

$$A_W = 0.707\left(\frac{3}{16}[2(19.6 - 14.3) + 7.7] + \frac{3}{8}(5.6)\right)$$

$$= 3.9 \text{ in}^2$$

The tensile stress on weld group B is:

$$S_T = \frac{L}{A_W}$$

$$= 1593 \text{ psi}$$

The margin of safety is:

$$M.S. = \frac{S_{ALL}}{S_T} - 1 = \underline{+LARGE}$$

where:

S_{ALL} = 23,750 psi

Top End Plate - Normal Operations Conditions

In the analyses of the section titled "Bottom End Plate" and Section 2.6.7.8.2, the 0.5-inch thick bottom end plates are shown to be structurally adequate. This analysis shows that the top end plate, which is in effect equivalent to both bottom end plates welded together at the shield tank shell, is structurally adequate. Two bounding conditions are considered. The first condition considers the shield tank top end plate loaded with a pressure of 180 psig and the expansion tank top end plate unloaded. Using Case 38 (Roark, page 113), considering a unit strip of top end plate, where the two end points are considered pinned, the maximum bending stress is 10,272 psi, and the margin of safety equals +0.33. The second condition considers both the shield and expansion tank end plates loaded at 180 psig. Again using Case 38, the bending stress equals 11,172 psi, resulting in a margin of safety of +0.23. The maximum normal operations conditions pressure in the expansion tank is 162 psig; therefore, the top end plate is adequate for the normal operations conditions.

2.6.7.8 Expansion Tank

The expansion tank is located at the upper end of the cask and is concentric with the shield tank. As its name implies, the expansion tank provides a location for fluid to expand into during fluid heating; thus, protecting both the neutron shield tank and the expansion tank from over-pressurization during normal operations conditions. A description of the expansion tank, structural criteria, and structural loads is presented in Sections 2.6.7.7.1 through 2.6.7.7.3. Table 2.6.7-40 summarizes the results of the structural analyses described in the following sections. The table shows adequate margins of safety for each component of the expansion tank examined. Therefore, the normal operations conditions requirements of 10 CFR 71 are satisfied.

To simplify analysis of the expansion tank structure, the use of symmetry, superposition, and worst case loads are employed to reduce the number of calculations to be performed and yet provide a thorough analysis. Major expansion tank structural components are shown in Figure 2.6.7-30. Analysis of the expansion tank uses the same format and simplifying assumptions as were used in the neutron shield tank structural analysis.

2.6.7.8.1 Expansion Tank Shell

The expansion tank shell is analyzed as a thin-walled tube, taking no credit for the eight radial stiffeners, which run the length of the tank. Using Case 1 (Roark, page 298), the meridional and hoop stresses are calculated:

$$S_1 = \frac{pR}{2t}$$

$$= 6269 \text{ psi}$$

$$S_2 = \frac{pR}{t}$$

$$= 12,537 \text{ psi}$$

where:

p = 180 psig

R = 21.94 inches

t = 0.32 in

Von Mises yield criterion is used to calculate an equivalent stress (S_e), which is compared to the yield strength of Type 304 stainless steel.

$$S_e = \frac{1}{\sqrt{2}} \left[(S_1 - S_2)^2 + (S_2 - S_3)^2 + (S_3 - S_1)^2 \right]^{0.5}$$

$$= 10,857 \text{ psi}$$

where:

S_3 = 0 psi

then

$$M.S. = \frac{S_{ALL}}{S_e} - 1 = \underline{+0.26}$$

where:

S_{ALL} = 0.577 (23,750 psi)

= 13,700 psi

2.6.7.8.2 Bottom End Plate

It is assumed that the sections of end plate between stiffeners can be represented by a rectangular plate of appropriate dimensions. The width (b) of the plate is the difference between radii of the neutron shield tank and expansion tank shells, as shown in Figure 2.6.7-31. The length (a) of the plate is the average of the inner and outer arch lengths, a = 16.4 inches ((17.3 + 15.4)/2). Using Case 36 (Roark, page 225), the maximum bending stress on the 0.5-inch thick end plate is:

$$S_{max} = \beta \frac{wb^2}{t^2}$$

$$= 3375 \text{ psi}$$

where:

β = 0.75

w = 180 psig

b = 2.5 inches

t = 0.5 in

then

$$M.S. = \frac{S_{ALL}}{S_{max}} - 1 = \underline{+LARGE}$$

where:

S_{ALL} = 23,750 psi (S_y at 250°F)

2.6.7.8.3 Stiffener

The drop load is assumed to be distributed over all stiffeners equally. It is further assumed that the stiffener examined is in tension resulting from the drop load, as shown in Figure 2.6.7-32. The analysis shown below is for a 1-inch section (longitudinal) without credit for end plate welds. The drop pressure load is L = 3,114 pounds (17.3 in^2 x 180 psi). Additionally, the stiffener must support itself and the expansion tank shell during a drop, which adds an additional 45 pounds of structural load, bringing the total load (L) on the stiffener to 3,159 pounds. The cross sectional area of the 1-inch section analyzed is 132 in^2.

$$S_T = \frac{L}{A}$$

$$= 10,029 \text{ psi}$$

The margin of safety is:

$$M.S. = \frac{S_{ALL}}{S_T} - 1 = \underline{+0.37}$$

where:

S_{ALL} = 0.577(23,750) psi

= 13,700 psi

2.6.7.8.4 Stiffener Weld

This analysis of a unit section (1-inch longitudinal) of expansion tank shell assumes that the drop load is equally distributed among all stiffeners. The load acting on the weld attaching the stiffener to the adjacent shield tank stiffener equals the load acting on the stiffener, L = 3,114 pounds (Section 2.6.7.8.3). The weld is a 0.188-inch fillet, both sides with a total throat area, A_w = 0.265 in^2. The tensile stress acting on the weld is:

$$S_T = \frac{L}{A_w}$$

$$= 11,750 \text{ psi}$$

The resulting margin of safety is:

$$M.S. = \frac{S_y}{S_T} - 1 = \underline{+0.17}$$

where:

$S_y = 0.577(23,750)$ psi

$= 13,700$ psi

2.6.7.9 Upper Ring/Outer Shell Intersection Analysis

Membrane and bending stresses are induced in the upper ring/outer shell intersection region of the cask body. These stresses are calculated using a detailed finite element model (Figure 2.6.7-33) and the ANSYS PC-Linear computer program.

The upper ring/outer shell intersection region is conservatively analyzed utilizing an axisymmetric model, axisymmetric loading and minimum ring cross section properties. The actual loading occurs only at the two lifting trunnions, and the minimum ring cross section occurs only at four 90-degree locations around the ring circumference. The model is restrained in the longitudinal direction by roller boundary conditions on the inner and outer shells (Figure 2.6.7-34) located 10 inches below the upper ring/outer shell intersection (attenuation length = $2.5 (Rt)^{0.5} = 9.81$ inches). A fine mesh grid is used in the model in regions where peak stresses caused by concentration effects are expected. The following assumptions are made in this analysis:

1. The stiffness and support of the lead shell are not included.
2. The support/restraint of the upper ring provided by the closure lid and bolts is not included.
3. A uniform average temperature of 300°F is used in the analysis.
4. ANSYS STIF42 isoparametric quadrilateral elements adequately represent the cask geometry.

The sections analyzed as critical are shown in Figure 2.6.7-35. Section c-c is critical for P_m stress, and section a-a is critical for $P_m + P_b$ stress.

Applied Loads

The normal operations lifting trunnion loads used in this analysis are:

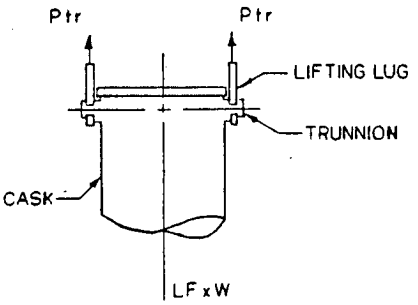

Lifting Load On Trunnions

Load Factor (LF) = 1.15

Cask Weight (W) = 52,000 lbs

P_{tr} = (LF)(W/2) = (1.15)(52,000/2) = 29,900 lbs

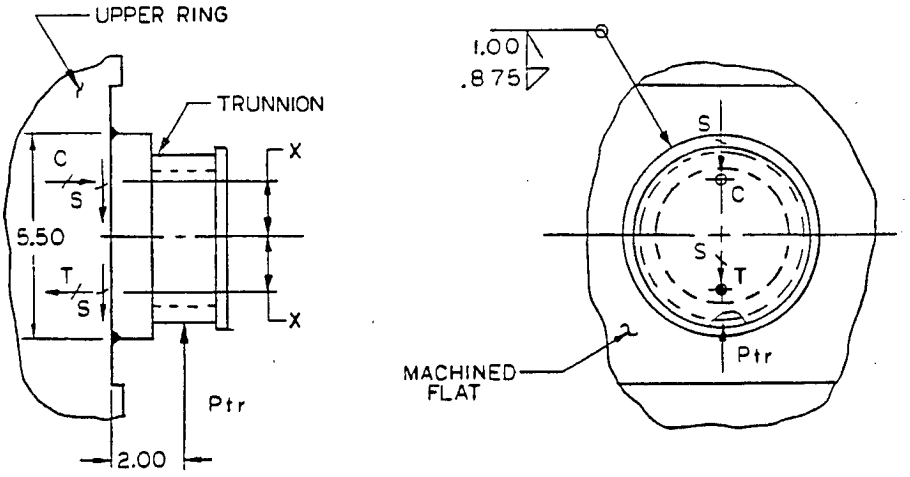

Lifting Trunnion Load Geometry

The concentrated loads were used to represent the distributed loads in the trunnion weld.

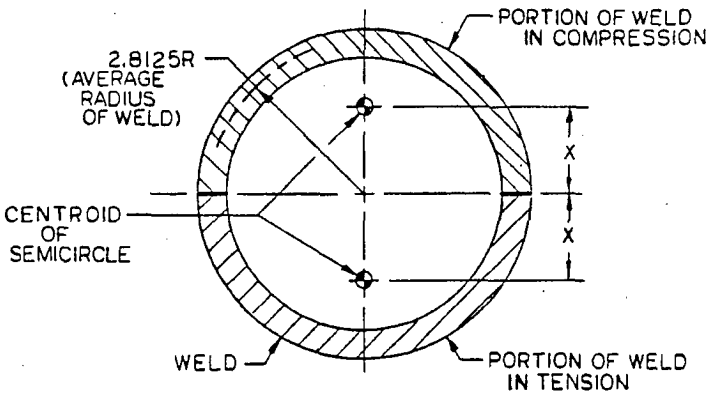

Trunnion Weld Group Centroid

To determine the trunnion weld group centroid:

$x = 0.6366\ R_{avg}$

$= 0.6366\ (2.8125)$

$= 1.790$ inches

$T = C = y\ (P_{tr}/2x)$

$= 2.00\ (29{,}900) / 2\ (2.8125)$

$= 16{,}704$ lbs

$S = P_{tr}/2$

$= 29{,}900/2$

$= 14{,}950$ lbs

Assume these loads are uniform over the trunnion weld diameter:

$T_u = C_u = 16{,}704/2(2.8125)$

$= 2969.6$ lb/in

$S_u = 14{,}950/2(2.8125)$

$= 2657.8$ lb/in

The ANSYS program requires that the loads for an axisymmetric model be input as load/radian:

Radians enclosed in 1 inch of circumference = 1/radius = 11/13.94 = 0.0717

$T_r = C_r = (2969.6)/0.0717$

= 41,396.22 lb/rad

S = 2657.8/0.0717
= 37,049.73 lb/rad

Calculated Stress Summary - Normal Operations Conditions

As anticipated, the maximum stresses occur at the upper ring/outer shell intersection, in the region of the machined flat and the internal radius of the outer shell. This analysis conservatively considers an outer shell thickness of 1.12 inches (actual shell thickness is 1.20 inches).

Stress peaking is present at the intersection of the outside surface of the outer shell with the upper ring because of stress concentration effects. The three sections through this region were investigated to determine the maximum stress intensity.

Section	Node	ANSYS Output Stress Summary			
		Radial S_x (ksi)	Axial S_y (ksi)	Hoop S_z (ksi)	Shear S_{xy} (ksi)
	66	1.6	7.3	2.9	-0.6
a-a	65	-0.1	4.9	1.9	-0.4
	64	-2.6	-0.4	-0.2	0.8
	66	1.6	7.3	2.9	-0.6
b-b	61	-0.7	5.1	1.6	0.5
	56	1.1	1.8	0.6	0.6
	66	1.6	7.3	2.9	-0.6
c-c	61	-0.7	5.1	1.6	0.5
	56	-0.2	4.5	0.6	0.6

The P_m and the $P_m + P_b$ stress components are determined by linearization of the ANSYS output stress components across sections a-a, b-b, and c-c. The principal stresses are calculated using the classical stress transformation law (Table 2.6.7-41).

The total normal operations lifting condition component stresses, principal stresses, and stress intensities at the critical section are calculated by combining the principal stresses from lifting, section b-b, with the internal pressure hot case (Table 2.6.1-1 and Table 2.6.2-2).

The P_m principal stress summary is:

	Principal Stresses (ksi)		
Load Condition	S_1	S_2	S_3
Lifting	5.5	-0.3	2.0
Internal Pressure	2.9	0.4	-0.4
Total	8.4	0.1	1.6

P_m stress differences are: S_{12} = 8.3 ksi, S_{23} = -1.5 ksi, and S_{31} = -6.8 ksi.

P_m stress intensity is S_i = 8.3 ksi.

Allowable stress intensity is S_a = 1.0 S_m = 20.0 ksi (Table 2.3.1-1).

$$M.S. = \frac{S_a}{S_i} - 1 = +1.41$$

The $P_m + P_b$ principal stress summary is:

	Principal Stresses (ksi)		
Load Condition	S_1	S_2	S_3
Lifting	9.1	-2.7	4.0
Internal Pressure	4.2	1.5	0.2
Total	13.3	-1.2	4.2

The $P_m + P_b$ stress differences are: S_{12} = 14.5 ksi, S_{23} = -5.4 ksi, and S_{31} = -9.1 ksi.

The $P_m + P_b$ stress intensity is S_i = 14.5 ksi.

Allowable stress intensity is S_a = 1.5 S_m = 30.0 ksi.

$$M.S. = \frac{S_a}{S_i} - 1 = +1.07.$$

The maximum peak stress, S_y = 7.3 ksi, is less than 1.5 S_m; therefore, a fatigue evaluation is not required.

2.6.7.10 PWR/BWR Rod Transport Canister Assembly Analysis

2.6.7.10.1 Discussion

The NAC-LWT PWR/BWR Rod Transport Canister is analyzed for structural adequacy in accordance with the requirements of 10 CFR 71 for a 1-foot drop (normal transport condition). The structural evaluation is performed by classical elastic analysis methods. The components

evaluated include the can weldment, internal spacer, 4 × 4 and 5 × 5 inserts (rod holder), PWR insert, BWR fuel assembly lattice spacer and can weldment spacer. In the 5×5 insert configuration, four of the tubes comprising the insert may be replaced with a single larger tube to accommodate an oversize nonfuel-bearing component (e.g., a single BWR water rod or a CE guide tube). Evaluations are performed for the inserts being comprised of 16 or 25 tubes to accommodate the fuel rods and these evaluations are considered to bound the insert configuration containing a single BWR water rod. The presence of the BWR water rod reduces the inertial loading due to contents, as well as employs a larger cross-section for the BWR water rod as compared to four smaller tubes containing fuel rods.

2.6.7.10.2 Analysis Description

Geometry

The geometry of the can assembly is shown in Drawing 315-40-098. Note that the tube component of the can assembly is fabricated from a 6-in.×6-in.×0.5-in.-thick tube that is machined to the final dimensions of 5.5-in.×5.5-in.×0.25-in.-thick. The can assembly is positioned within the basket during transport of the cask. If the cask is equipped with a PWR basket, the PWR insert is required to provide correct positioning within the basket. The can assembly is constructed of Type 304 stainless steel with the exception of the PWR insert, which is constructed of 6061 Aluminum.

Loadings

The magnitude of the impact force varies according to the drop height and drop orientation. As calculated in Section 2.6.7.4, the g-loads for the 1-foot end and side drops are 15.8 and 24.3g, respectively.

Detailed Analysis

The maximum temperatures of the components are shown below. For the can weldment and components outside the can weldment, the temperatures are significantly below 700°F, which are within the 800°F design limits. For the tubes supporting the fuel pins, the maximum temperatures are determined to be 925°F. The tubes, which are only used with the insert for the high burnup pins, are shown to be acceptable using ASME Code, Section III, Division I, Subsection NH, which specifies allowable stresses above 800°F. The remaining components are shown to be acceptable using the stress allowable in ASME Code, Section III, Subsection NB.

Thermal Stresses

To evaluate effects of the calculated temperatures within the can assembly, the nominal dimensions of the can are used to calculate the resulting thermal expansions. The coefficient of thermal expansion for ASME SA 240 Type 304 stainless steel is 9.0×10^{-6} in./in.-°F. All

components of the can assembly are constructed of Type 304 stainless steel, except for the PWR insert. The PWR insert is made of 6061 Aluminum with a coefficient of thermal expansion of 13.5E-6 in/in-°F. The following temperatures are used in the thermal expansion calculation and material property definitions.

Component Name	Maximum Operating Temperature (°F)	Temperature Used for Calculation (°F)
Aluminum PWR Insert	394	400
Can Weldment	538	575
5 × 5 Insert	885	925

Since the 5 × 5 insert is larger than the 4 × 4 insert, it is bounding for the thermal expansion calculations. The nominal gap between the insert and internal spacer is 3.56 – 3.44 = 0.12 inch. The growth of the insert is 3.44 × 9.0 E-6 in/in-°F × (925-70)°F = 0.027 inch. Since the growth of the insert is less than the nominal gap, no interference will occur.

The nominal gap between the internal spacer and can shell is 5.0 – 4.94 = 0.06 inch. The growth of the internal spacer is 4.94 × 9.0 E-6 in/in-°F × (575-70)°F = 0.023 inch. Since the growth of the internal spacer is less than the nominal gap, no interference will occur.

The nominal gap between the can shell and PWR insert is 5.75 – 5.5 = 0.25 inch. The growth of the can shell is 5.5 × 9.0 E-6 in/in-°F × (575-70)°F = 0.025 inch. Since the growth of the can shell is less than the nominal gap, no interference will occur.

Because the differential thermal expansion causes no interference or binding, no further thermal stress evaluation is required.

Can Weldment

The can weldment is contained within the basket assembly and not subjected to bending stresses in the side-drop case.

For the end drop, the can weldment is loaded by its own weight. The can contents bear against the bottom or top of the can assembly, depending on drop orientation.

LWT Can Body Compressive Stress

Under normal operating conditions the tube is evaluated for a 15.8 g acceleration for the end drop. The compressive load (P) on the tube is the combined weight of the lid and tube times the appropriate g factor.

The compressive stress (S_c) in the tube body is:

$$S_c = \frac{P}{A} = \frac{4{,}898 \text{ lb}}{4.98 \text{ in}^2} \cong 984 \text{ psi}$$

where:

$A = \pi (0.75^2 - 0.5^2) + 4 \times 4.0 \times 0.25 = 4.98 \text{ in}^2$

P = 310 × 15.8 = 4,898 lbs (conservatively, the weigh of the tube, lid, and bottom plate is used)

The margin of safety (MS) is then:

$$MS = \frac{S_m}{S_c} - 1 = \frac{17{,}300 \text{ psi}}{984 \text{ psi}} - 1 = +16.6.$$

LWT Can Body Bearing Stress

For the bottom end drop, the can base feet are subjected to a bearing stress. The compressive load (P) on the base is the combined weight of the can assembly, fuel and insert, and the internal spacer times the appropriate g factor.

P = [310 (can weldment) + 350 (fuel) + 75 (tube insert) + 240 (internal spacer)] × 15.8 = 15,405 lbs

The compressive stress (S_c) in the feet is:

$$S_c = \frac{P}{A} = \frac{15{,}405}{2.8} \cong 5{,}502 \text{ psi}$$

where:

$A = 4 \text{ x } 0.5 \text{ x } (2.0 - 0.6) = 2.8 \text{ in}^2$

The margin of safety (MS) for bearing is then:

$$MS = \frac{S_m}{S_c} - 1 = \frac{17{,}300 \text{ psi}}{5{,}502 \text{ psi}} - 1 = +2.14$$

Can Internal Pressure

Can weldment internal pressure is considered insignificant in the end-drop and side-drop cases because it will tend to reduce the compressive loads on the can tube sides.

The effect of internal pressure is evaluated for the bending stress that the pressure imposes on the can weldment sides. Conservatively, a one-inch-wide section of the tube wall, equal in length to the outside dimension of the tube (L = 5.5 in.) is analyzed as a cantilevered beam with a uniform load.

The maximum moment (M) is determined by the following relation:

$$M = \frac{wL^2}{12} = \frac{(85 - 14.7)(5.5^2)}{12} \cong 177.2 \text{ in.-lb}$$

where w is the maximum differential pressure across the can wall due to the maximum normal temperature (assumes that the cask internal pressure is atmospheric). The 85 psia envelopes the pressure reported in Section 3.4.4.2.

The combined stress (σ) in the 0.25-inch thick tube wall is:

$$\sigma = \frac{Mc}{I} + \frac{wL}{t}$$

$$= \frac{(177.2)(0.125)}{0.0013} + \frac{(85 - 14.7)(5.5)}{0.25} \cong 18{,}600 \text{ psi}$$

The margin of safety (MS) is:

$$MS = \frac{1.5 S_m}{\sigma} - 1 = \frac{25.35 \text{ ksi}}{18.6 \text{ ksi}} - 1 = +0.36 \text{ for the normal condition}$$

Can Lid Bolt Analysis

The tensile force (F_p) on each lid bolt due to internal pressure is:

$$F_p = \frac{PA}{n} = \frac{(85 - 14.7)(3.75^2)}{8} \cong 123.6 \text{ lbs}$$

where

P = the pressure differential across the can wall at maximum normal temperature (assumes cask internal pressure is atmospheric)

A = 3.75 in × 3.75 in, the area of the can lid exposed to pressure

n = 8, number of bolts

The total tensile force on each lid bolt is F_p + the initial preload force, F_i = 635 lbs

The lid bolt tensile stress (σ) is:

$$\sigma = \frac{F_p + F_i}{A_t} = \frac{758.6}{0.049} = 15{,}480 \text{ psi}$$

where

A_t = 0.049 in.^{2}, the bolt tensile stress area $\frac{\pi}{4}(0.25^2)$

The margin of safety (MS) for the normal condition is:

$$MS = \frac{S_y}{\sigma} - 1 = \frac{18.8 \text{ ksi}}{15.48 \text{ ksi}} - 1 = +0.21$$

Can Tube Buckling

The tube is evaluated, using the Euler formula, to determine the critical buckling load (P_{cr}):

$$P_{cr} = \frac{K\pi^2 EI}{L^2} = \frac{3.26\pi^2(24.4\times10^6)(24.2)}{(165.5)^2} = 0.698 \times 10^6 \text{ lbs}$$

where:

E = 24.4×10^6 psi at 750°F

$$I = \frac{5.5^4 - 5.0^4}{12} = 24.2 \text{ in}^4$$

L = tube body length (165.5 inches)

Because the maximum compressive load ($310 \times 15.8 = 4{,}898$ lbs) is much less than the critical buckling load (698×10^3 lbs), the tube has adequate resistance to buckling.

Internal Spacer

The internal spacer body is contained within the can assembly and not subjected to bending in the side drop condition.

The compressive stress in the internal spacer rails during the side drop is determined as follows:

$$\sigma_b = \frac{Wg}{A} = \frac{665 \text{ x } 24.3}{123.7} \cong 130.6 \text{ psi}$$

where:

W = total load = 350 (fuel) + 240 (internal spacer) + 75 (4x4 insert) = 665 lbs

g = 24.3 (normal condition side drop)

A = 123.7 in^2 cross-sectional area of spacer rails, $4 \times 0.188 \times (165.25 - 2 \times 0.38)$

The resulting margin of safety is large.

Internal Spacer Compressive Stress

For the end drop, the internal spacer shell is loaded by its own weight. The insert rail stiffness is conservatively neglected in the strength.

Under normal operating conditions, the spacer is evaluated for a 15.8 g acceleration. The compressive load (P) on the shell is due to the weight of the internal spacer. The entire weight of the internal spacer times the appropriate g factor will be used to calculate the compressive load.

$P = 240 \times 15.8 = 3{,}792$ lbs

The compressive stress (S_c) in the internal spacer body is:

$$S_c = \frac{P}{A} = \frac{3,792}{1.69} \cong 2,244 \text{ psi}$$

where:

$$A = (3.936^2 - 3.56^2) - 12 \times 0.5 \times 0.188 = 1.69 \text{ in}^2$$

The margin of safety (MS) is then:

$$MS = \frac{S_m}{S_c} - 1 = \frac{17,300}{2,244} - 1 = +6.71$$

Internal Spacer Buckling

The shell is evaluated, using the Euler formula for an axially distributed load, to determine the critical buckling load (P_{cr}):

$$P_{cr} = \frac{K\pi^2 EI}{L^2} = \frac{3.26\pi^2 (24.4\times10^6)(6.615)}{(165.25)^2} = 0.19 \times 10^6 \text{ lbs}$$

where:

$E = 24.4 \times 10^6$ psi at 750°F

$$I = \frac{3.936^4 - 3.56^4}{12} = 6.615 \text{ in}^4$$

L = spacer body length (165.25 inches)

Because the maximum compressive load (240×15.8 = 3,792 lbs) is much less than the critical buckling load (190×10^3 lbs), the internal spacer has adequate resistance to buckling.

4×4 and 5×5 Inserts

The 4×4 and 5×5 inserts are contained within the internal spacer. The 4×4 inserts are supported by straps on 10-inch spacing. These straps provide a clearance of 0.31 inches and will allow bending of the tubes to occur. The 5×5 insert tubes are evaluated for a diametrically opposed load due to the weight of the adjacent tubes during the side drop.

The 4×4 insert lower tube will be evaluated as a fixed-fixed beam over a 10-inch span. The weight of the 3 tubes above (as well as lower tube self-weight) will be considered in the analysis. The stiffness of the tubes above the lower tube will conservatively be neglected. The combined weight (P) of the fuel pins and insert tubes are considered as a uniformly distributed load over the 10-inch span. In addition, the weights are scaled by the appropriate deceleration factor depending on the drop orientation and condition being evaluated.

The maximum bending stress (f_b) is determined as follows:

$$f_b = \frac{Wlg}{12Z} = \frac{5.8(10.0)24.3}{12x0.0092} \cong 12{,}766 \text{ psi}$$

where:

W = load on 10-inch section = (14 + 9.5) x 4 x 10/163.0 = 5.8 lbs

l = 10 inches (span of tube)

g = 24.3 (normal condition side drop)

Z = $\pi/32\ (0.6875^4-0.6315^4) / 0.6875 = 0.0092\ in^3$ (section modulus of the tube)

The margin of safety (MS) is:

$$MS = \frac{1.5S_m}{\sigma_{max}} - 1 = \frac{1.5(12{,}050)}{12{,}766} - 1 = +0.42$$

The bending moment due to the diametrically opposed line load on the 5×5 insert is calculated by the following:

$$M_b = \frac{WRg}{\pi} = \frac{70/163.0 \text{ x } 0.344 \text{ x } 24.3}{\pi} \cong 1.143 \text{ lb} - \text{in}$$

where:

W = total load = 14 × 4 + 70/5 = 70 lbs

g = 24.3 (normal condition side drop)

R = 0.6875/2 = 0.344 in (radius of insert tube)

The resulting bending stress is:

$$f_b = \frac{6M_b}{t^2} = \frac{6x1.143}{0.028^2} \cong 8{,}745 \text{ psi}$$

The margin of safety (MS) is:

$$MS = \frac{1.5\ S_m}{\sigma_{max}} - 1 = \frac{1.5(12{,}050)}{8{,}745} - 1 = +1.07$$

4×4 and 5×5 Insert Tube Compressive Stress

Under normal operating conditions, the tube is evaluated for a 15.8 g acceleration. The compressive load (P) on the shell is due to the weight of the tube. The entire weight of the tube is calculated as:

P = $\pi/4\ (0.6875^2-0.6315^2)$ x 163.0 x 0.288 = 2.72 lbs

The compressive stress (S_c) in the tube body is:

$$S_c = \frac{P}{A} = \frac{2.72 \text{ x}15.8}{0.058} \cong 741 \text{ psi}$$

where:

$$A = \pi/4 \, (0.6875^2 - 0.6315^2) = 0.058 \text{ in}^2$$

The margin of safety (MS) is then:

$$MS = \frac{S_m}{S_c} - 1 = \frac{14{,}100}{741} - 1 = +18.0$$

PWR Insert

The PWR insert contains the can assembly for insertion into the PWR basket. The PWR insert comprises a square box section with smooth sides. Therefore, no bending stresses will be introduced in the side drop condition.

PWR Insert Bearing Stress

The bearing load (P) on the PWR insert is due to the weight of the loaded can assembly. The entire weight of the assembly times the appropriate g factor will conservatively be used to calculate the bearing load.

W = bearing load = [350 (fuel) + 310 (can) + 240 (internal spacer) + 75 (4x4 insert)] x 24.3 = 23,693 lbs

The compressive stress (S_c) in the tube body is:

$$S_c = \frac{P}{A} = \frac{23{,}693}{921.3} \cong 26 \text{ psi}$$

where:

$$A = 5.5 \times 167.5 = 921.3 \text{ in}^2$$

The margin of safety (MS) is then:

$$MS = \frac{S_y}{S_c} - 1 = \frac{23{,}500}{26} - 1 = +\text{Large}$$

PWR Insert Body Compressive Stress

Under normal operating conditions, the tube is evaluated for a 15.8 g acceleration. The compressive load (P) on the body is due to the weight of the PWR insert. The entire weight of the PWR insert, times the appropriate g factor, will conservatively be used to calculate the compressive load.

P = 650 lb × 15.8 = 10,270 lbs

The compressive stress (S_c) in the tube body is:

$$S_c = \frac{P}{A} = \frac{10{,}270}{39.2} \cong 262 \text{ psi}$$

where:

$$A = (8.5^2 - 5.75^2) = 39.2 \text{ in}^2$$

The margin of safety (MS) is then:

$$MS = \frac{S_y}{S_c} - 1 = \frac{23{,}500}{262} - 1 = +\text{Large}$$

PWR Insert Tube Buckling

The tube is evaluated, using the Euler formula, to determine the critical buckling load (P_{cr}):

$$P_{cr} = \frac{K\pi^2 EI}{L^2} = \frac{3.26\pi^2 \left(8.8\text{x}10^6\right)(343.9)}{(167.0)^2} = 3.86\times10^6 \text{ lbs}$$

where:

$E = 8.8\times10^6$ psi at 400°F

$$I = \frac{8.5^4 - 5.75^4}{12} = 343.9 \text{ in}^4$$

L = tube body length (167.0 inches)

Because the maximum compressive load (650 x 15.8 = 10,270 lbs) is much less than the critical buckling load (3.86×10^6 lbs), the PWR insert has adequate resistance to buckling.

PWR Insert Assembly Bolts

The PWR insert is comprised of four short and four long aluminum plates joined with ½-13 UNC × 1.5-in. long socket head cap screws to form a hollow box. Each plate is secured to each adjacent plate using three screws.

The screws joining the plates are loaded in shear when the two lift tabs are used to lift the PWR insert and its payload. The controlling load path is through the lift tab attached to the shorter side plate and the three screws connecting the shorter side plate to the adjacent long plate. The distance from the line of load application (centerline of the lift tab) to the centerline of the 3-screw pattern is approximately 3.6 inches. Any internal moment created by this eccentricity is reacted by the strong-direction section modulus of the side plates and is effectively countered by the stiffness inherent in the overall symmetry of the box section. The screw shear stress (τ) in each of the 3 screws is:

$$\tau = \frac{P/2}{A} = \frac{900}{3(0.130)} = 2{,}308 \text{ psi}$$

where:

P = [310 (can weldment)+350 (fuel rods)+240 (internal spacer)+70 (5×5 insert)+650 (PWR insert)]×1.1 = 1,782 lbs, use 1,800 lbs for analysis. (Total lift weight with 10% dynamic load factor.)

A = screw cross-sectional area = $(0.4069^2 \times \pi)/4 = 0.130$ in^2 (Thread minor diameter)

The safety factor (FS) is calculated using a shear allowable of $0.6S_m$ at 750°F.

$$FS = \frac{0.6(15{,}600)}{2{,}308} = 4.06 > 3$$

where

S_m = 15,600 psi for commercial austenitic stainless steel.

Therefore the design condition that lifting stresses have a load factor of 3 on the basis of yield strength is met.

Can Weldment Spacer

The can weldment spacer prevents the PWR basket, PWR insert, fuel, and can weldment from shifting during transport. The spacer (Drawing 315-40-125, Item 10) is placed on the top of the can weldment. The spacer is bolted to the bottom side of the lid and the cruciform stiffener functions as the spacer between the lid and can weldment. The maximum load applied to the spacer occurs during the top end drop. To bound both normal and accident conditions, stresses are compared using accident load conditions and are compared to allowable stresses for normal operating conditions. The stress in the spacer is:

$$\sigma = \frac{P \times g}{A} = \frac{1{,}945 \times 60}{8.4} = 13{,}893 \text{ psi}$$

where:

P= Conservative weight of the PWR basket, PWR insert, fuel, and can weldment
= 1,945 lbs

g= Top end drop acceleration (60g)

A= Cross-sectional area of cruciform
= $2 \times 7 \times 0.63 - 0.63^2 = 8.4$ in^2

The margin of safety (MS) is:

$$MS = \frac{1.0 \times S_m}{\sigma} - 1 = \frac{17{,}500 \text{ psi}}{13{,}893 \text{ psi}} - 1 = +0.26$$

where:

S_m = The stress intensity of 304 stainless steel at 500°F

Because the height-to-diameter ratio (4.5/6.0 = 0.75) is less than one, the spacer has adequate resistance to buckling.

Using a bounding weight of 50.0 lbs for the spacer, the maximum shear stress on the 1/8-inch fillet weld corresponds to the hypothetical accident bottom end drop condition of 60g. The shear stress in the weld is computed as:

$$\tau = \frac{60 \times 50}{28.0 \times 0.707 \times 0.125} = 1{,}212 \text{psi}$$

where:

the perimeter of cruciform is 28.0 in [(7-0.625) × 4 + 0.625 × 4]

The margin of safety, based on the normal condition of transport allowable stress, is:

$$MS = \frac{0.6S_m}{\tau} - 1 = \frac{0.6 \times 17{,}500}{1{,}212} - 1 = +7.66$$

The can weldment spacer is, therefore, determined to be structurally adequate for normal and accident conditions for the NAC-LWT cask.

Fuel Assembly Lattice Spacer

The BWR fuel assembly lattice fits into the PWR insert in place of the can assembly. The fuel assembly lattice holds up to 25 intact BWR fuel rods. To accommodate the fuel assembly lattice, the bottom plate of the PWR insert is removed. This allows the fuel assembly lattice to rest on the bottom of the cask. To prevent the PWR basket from shifting during transport, a spacer (Drawing 315-40-125, Item 12) is placed at the top of the fuel assembly lattice. The spacer is bolted to the bottom side of the lid and eight 1-inch diameter posts function as the spacer between the lid and PWR basket. The maximum load applied to the spacer occurs during the top end drop. To bound both normal and accident conditions, accident stresses are compared to the normal allowable stress. The stress in the spacer is:

$$\sigma = \frac{P \times g}{A \times Np} = \frac{400 \times 60}{0.785 \times 8} = 3{,}822 \text{ psi}$$

where:

P= Conservative weight of the PWR basket

g= Top end drop acceleration (Table 2.6.7-34)

A= Cross-sectional area of a post

Np = Number of posts

The margin of safety is:

$$MS = \frac{1.0 \times S_m}{\sigma} - 1 = \frac{17{,}500 \text{ psi}}{3{,}822 \text{ psi}} - 1 = +3.58$$

where:

S_m = The stress intensity of 304 stainless steel at 500°F

Buckling of the post is evaluated using the Euler formula. The critical buckling load (P_{cr}) is:

$$P_{cr} = \frac{K\pi^2 EI}{L^2} = \frac{0.25\pi^2 (25.8 \times 10^6)(0.0491)}{(13.4)^2} = 17{,}407 \text{ lbs}$$

where:

E = Modulus of elasticity = 25.8×10^6 psi at 500°F

I = Moment of inertia = $\frac{\pi \times d^4}{64} = 0.0491 \text{ in}^4$

d = Post diameter = 1 in

L = Post length = 13.38 inches

K = Euler buckling coefficient for fixed-free column = 0.25 (Marks, 9th Ed., p. 5-42)

Because the maximum compressive load ($400/8 \times 60 = 3{,}000$ lbs) is less than the critical buckling load (17,407 lbs), the spacer has adequate resistance to buckling.

Figure 2.6.7-1 1-Foot Bottom End Drop with 130°F Ambient Temperature and Maximum Decay Heat Load

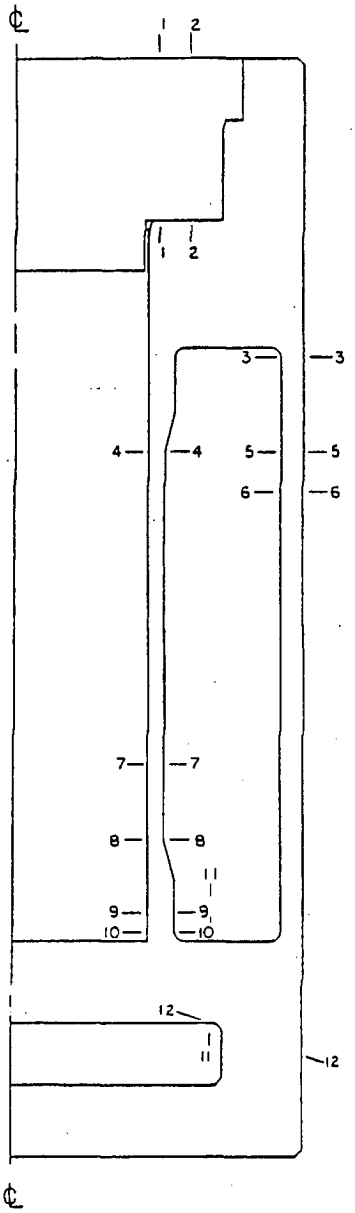

Figure 2.6.7-2 1-Foot Bottom End Drop with -40°F Ambient Temperature and Maximum Decay Heat Load

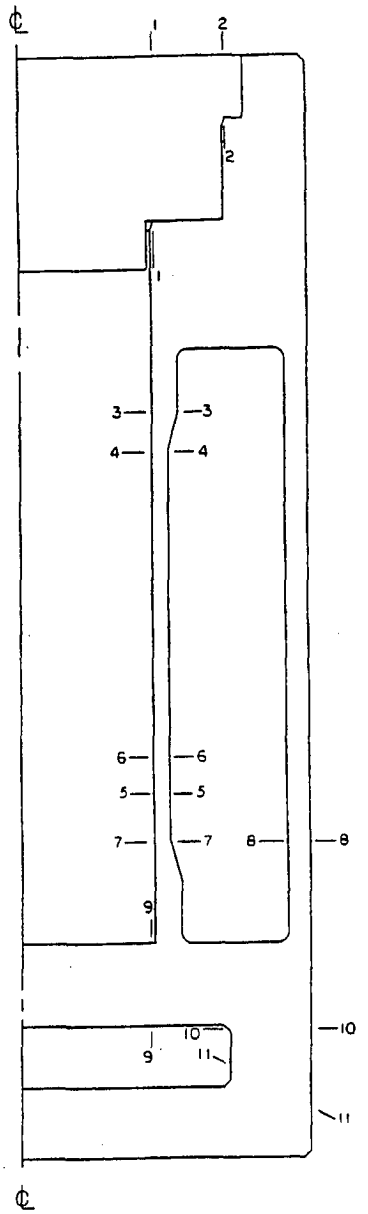

Figure 2.6.7-3 1-Foot Bottom End Drop with -40°F Ambient Temperature and No Decay Heat Load

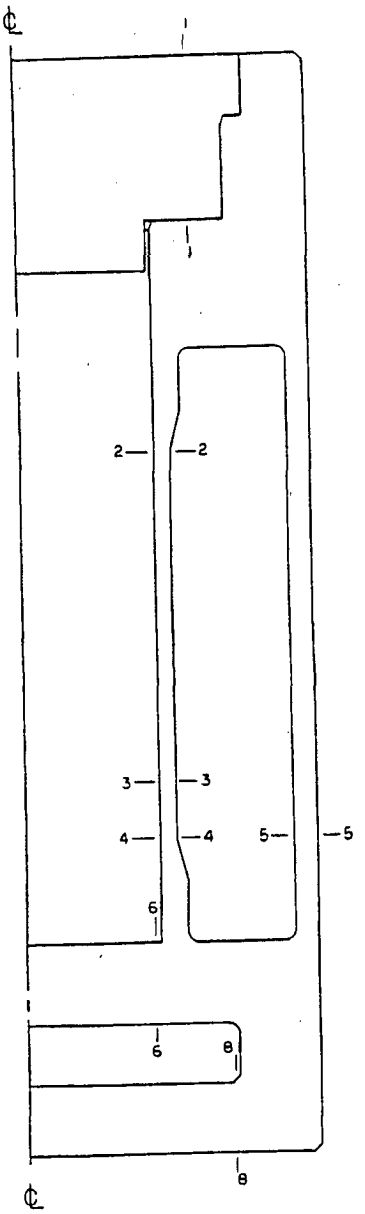

Figure 2.6.7-4 1-Foot Top End Drop with 130°F Ambient Temperature and Maximum Decay Heat Load

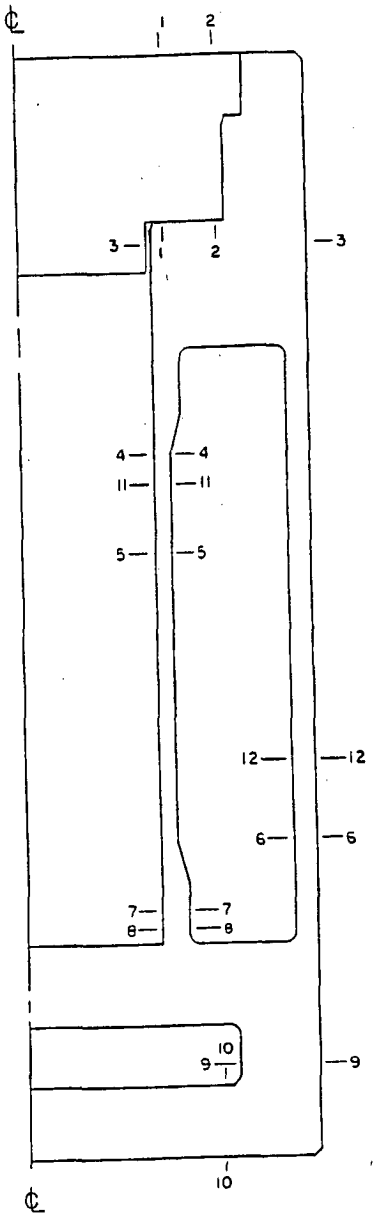

Figure 2.6.7-5 1-Foot Top End Drop with -40°F Ambient Temperature and Maximum Decay Heat Load

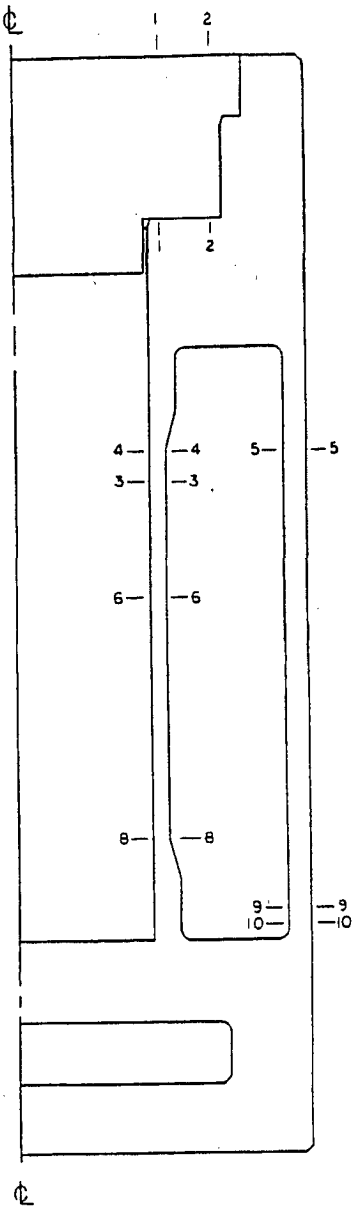

Figure 2.6.7-6 NAC-LWT Cask Critical Sections (1-Foot Side Drop with 100°F Ambient Temperature)

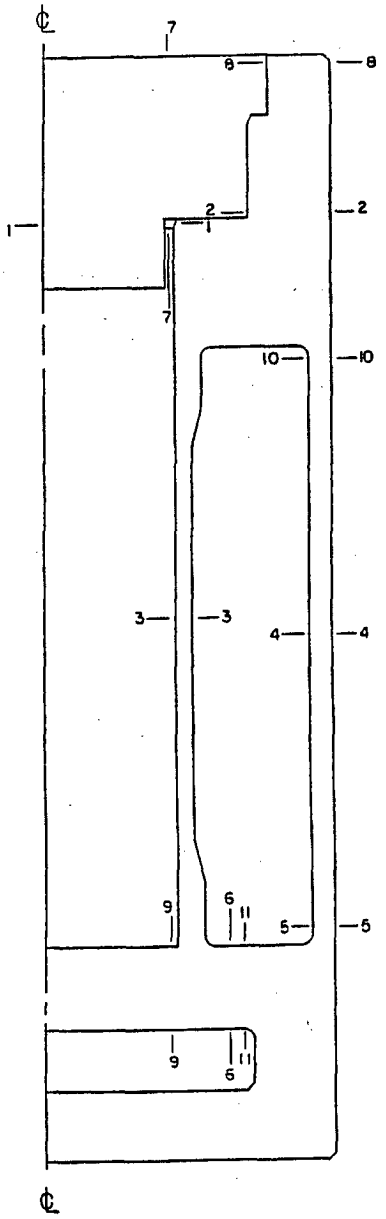

Figure 2.6.7-7 1-Foot Top Corner Drop with 130°F Ambient Temperature and Maximum Decay Heat Load - Drop Orientation = 15.74 Degrees

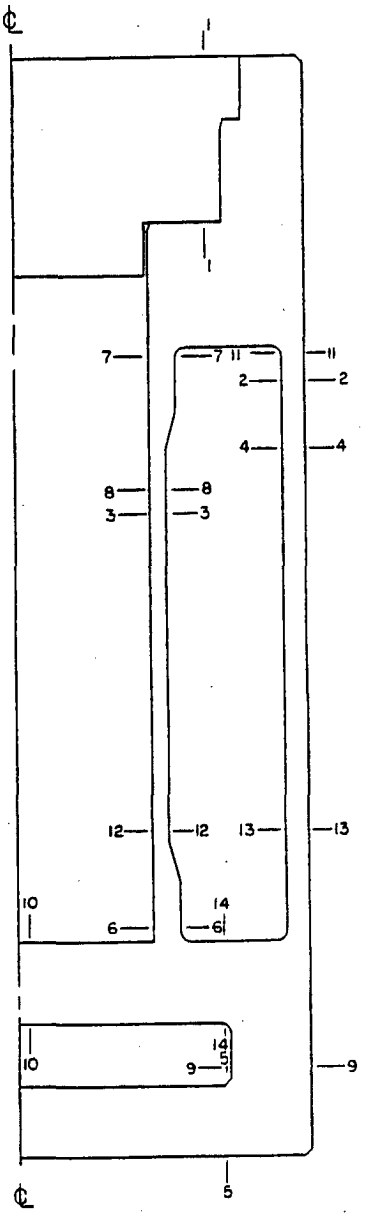

Figure 2.6.7-8 1-Foot Bottom Corner Drop with 130°F Ambient Temperature and Maximum Decay Heat Load - Drop Orientation = 15.74 Degrees

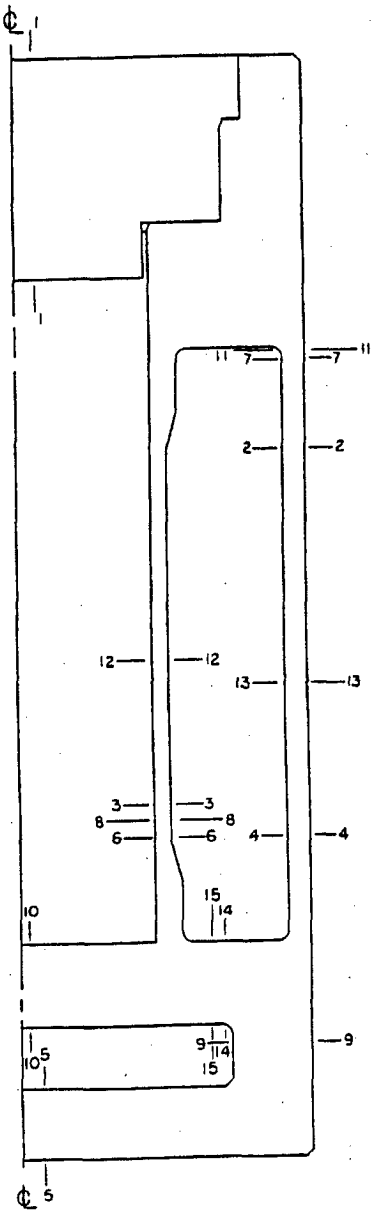

Figure 2.6.7-9 1-Foot Top Corner Drop with -40°F Ambient Temperature and No Decay Heat Load - Drop Orientation = 15.74 Degrees

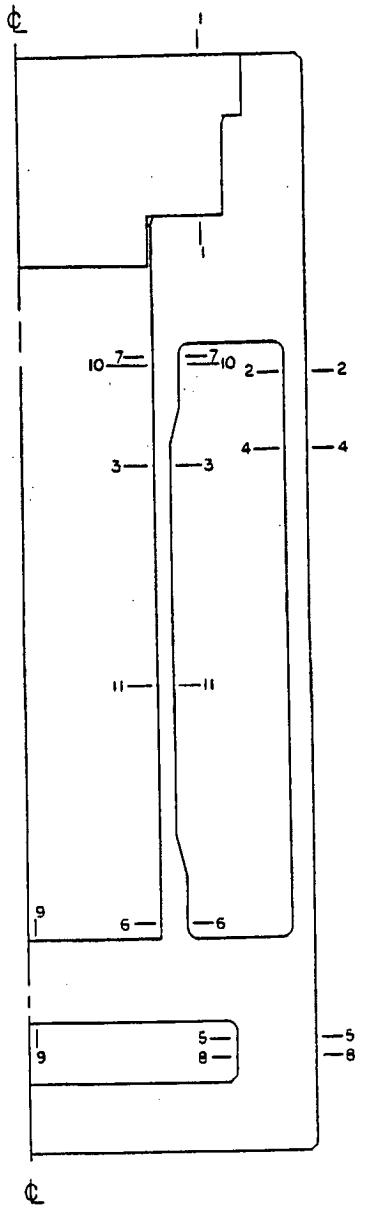

Figure 2.6.7-10 NAC-LWT Cask with Impact Limiters

Figure 2.6.7-11 Cross-Section of Top Impact Limiter

Figure 2.6.7-12 Load Versus Deflection Curve (Typical Aluminum Honeycomb)

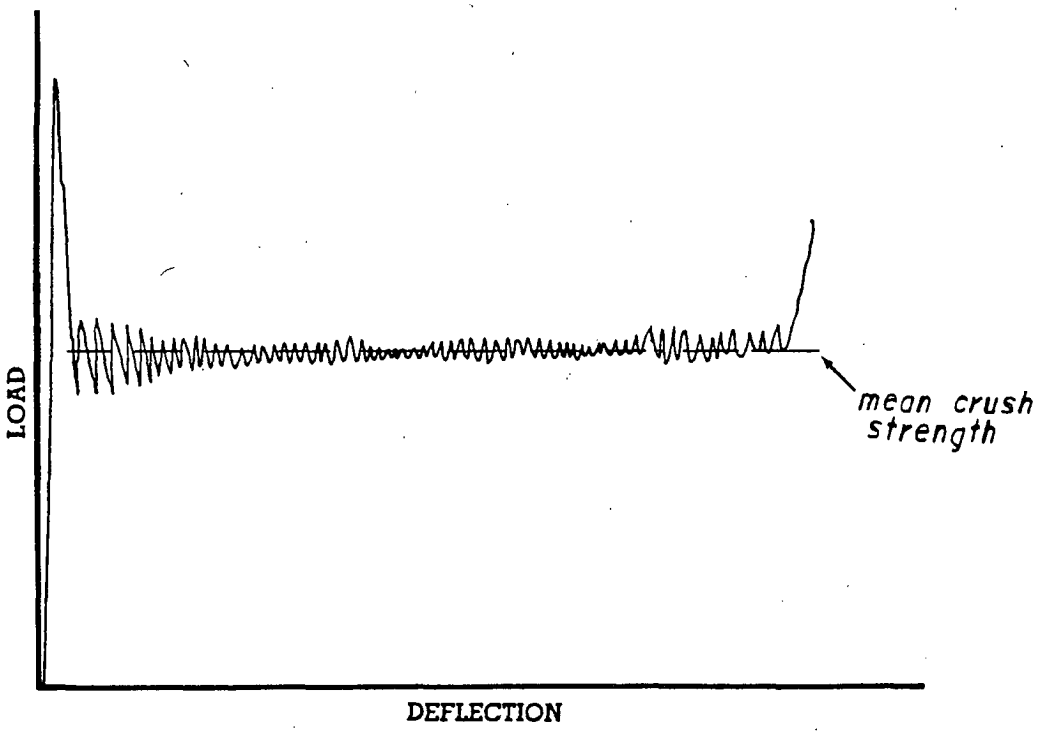

Figure 2.6.7-13 Quarter-Scale Model Limiter End Drop Cross-Section

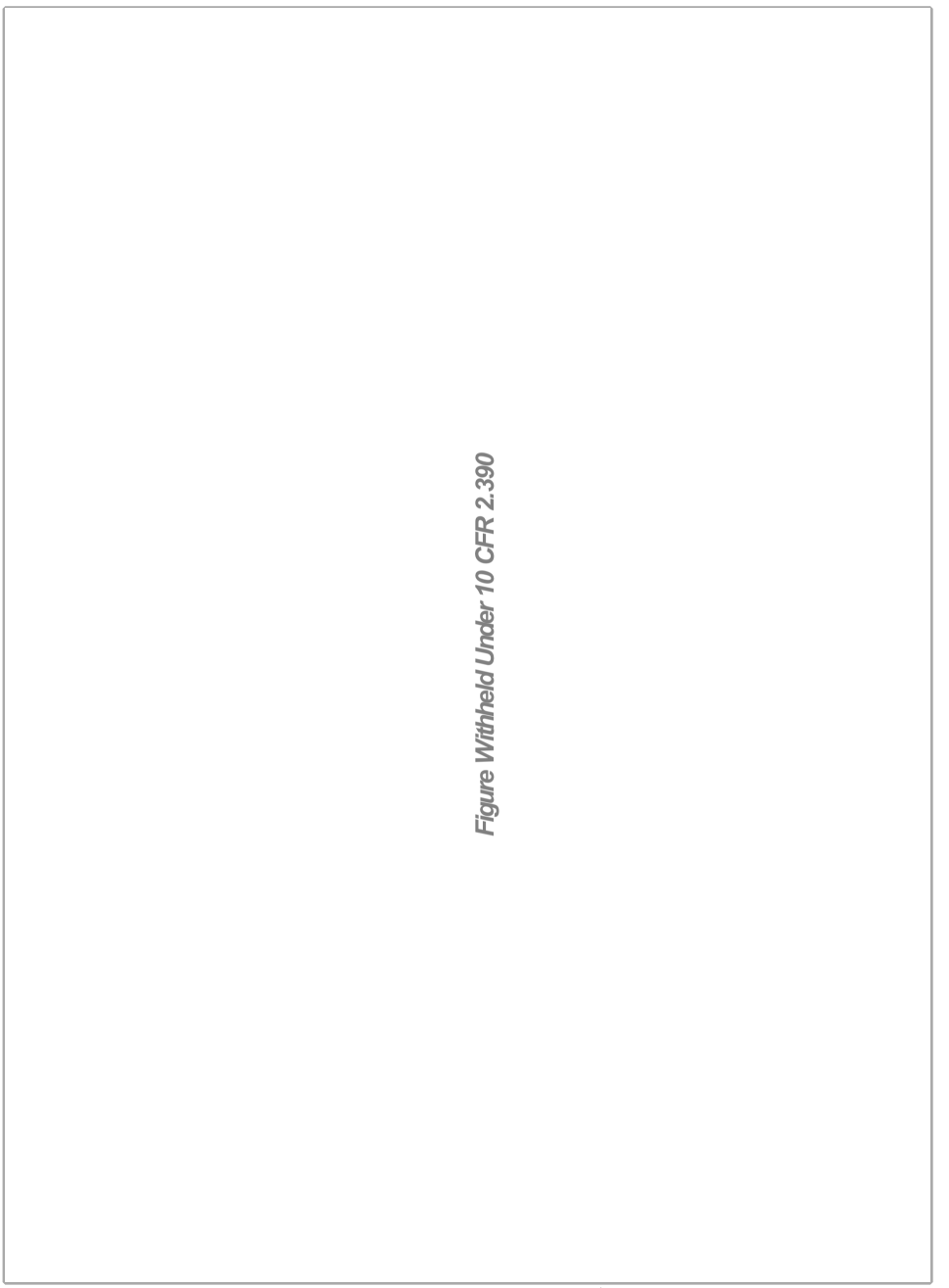

Figure 2.6.7-14 End Drop Impact Limiter Cross-Section

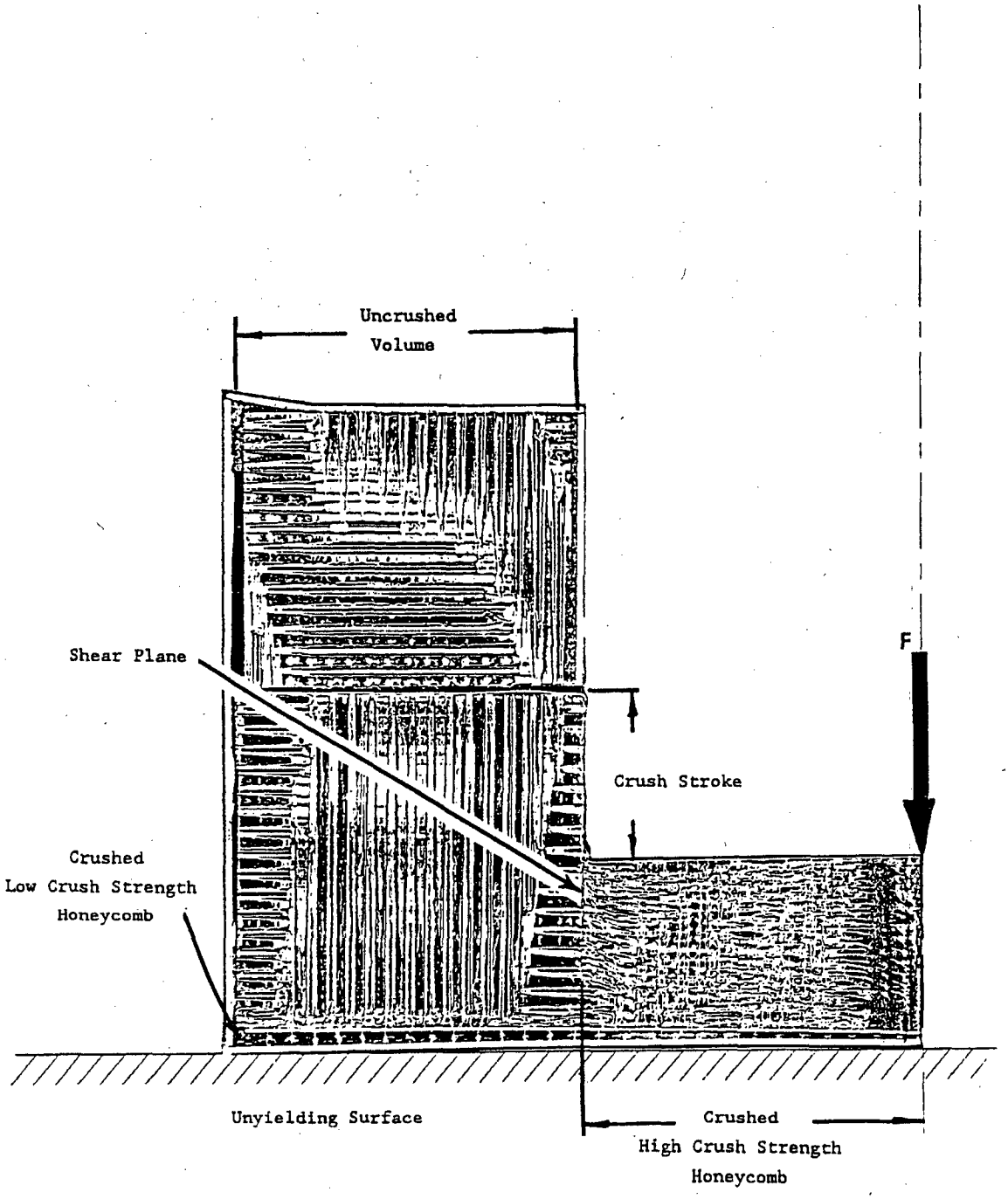

Figure 2.6.7-15 Impact Limiter Lug Detail

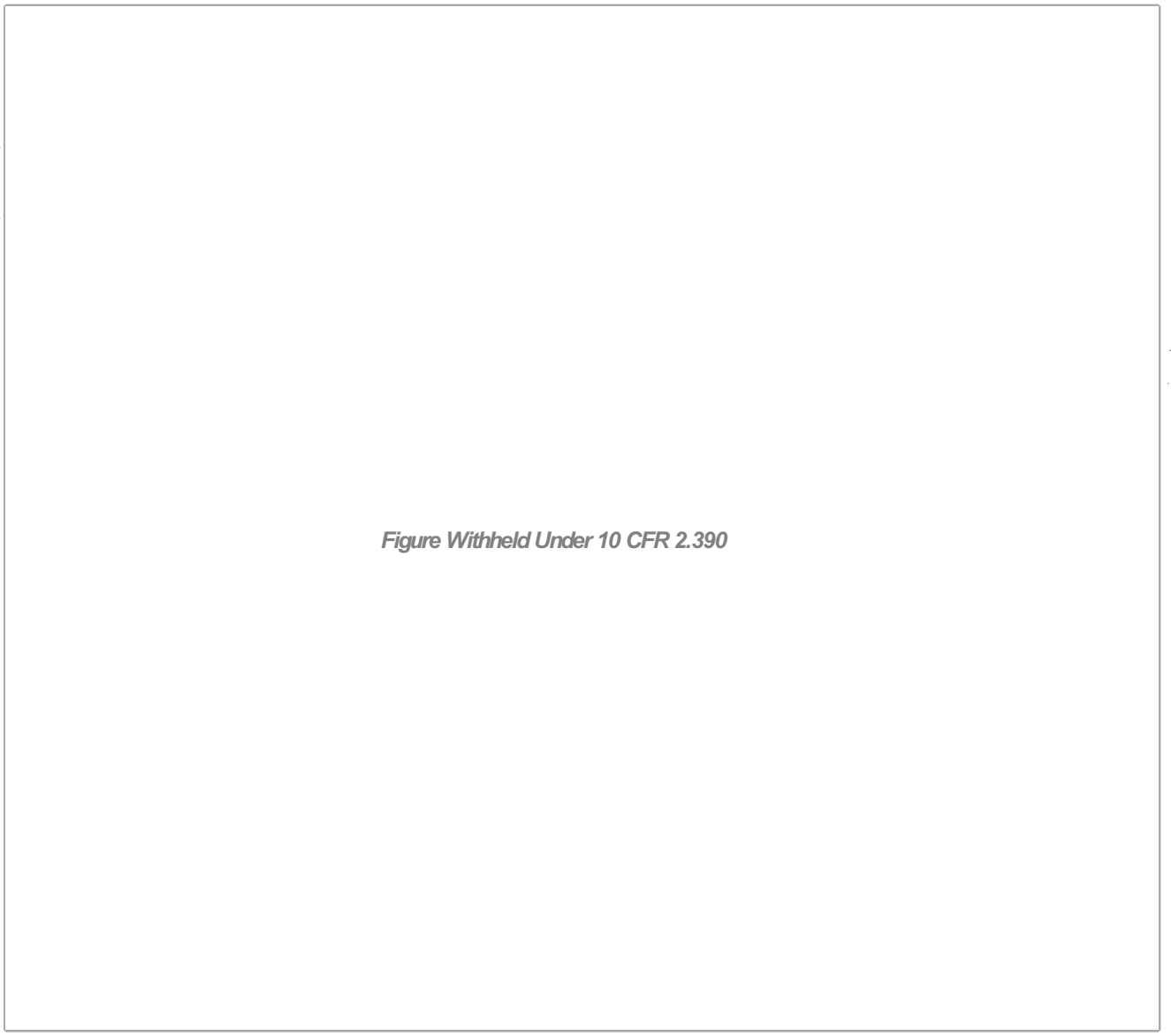

Figure 2.6.7-16 Cask Lug Detail

Figure 2.6.7-17 RBCUBED Output Summary – Center of Gravity Over Top Corner

Position	Crush Depth (in)	Crush Force, Fi (lb)	Package Velocity (in/sec)	Approximate Separation Moment (in-lb)
①	2	2.30×10^5	543.4	2.25×10^6
②	4	9.74×10^5	514.8	6.63×10^6
③	6	1.83×10^6	466.2	7.67×10^6
④	8	2.63×10^6	381.2	5.75×10^6

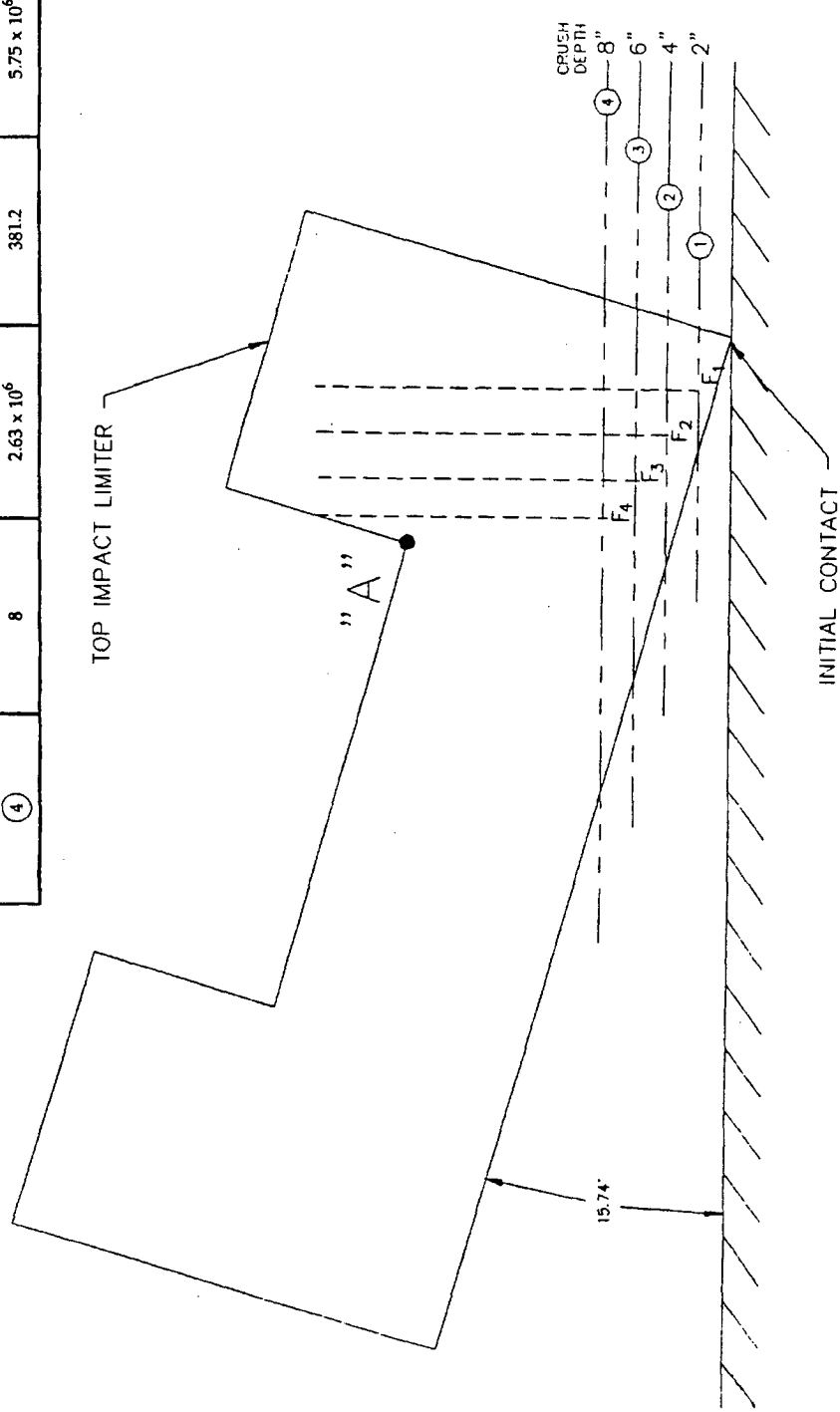

Figure 2.6.7-18 Free Body Diagram - Top Impact Limiter - Center of Gravity Over Corner

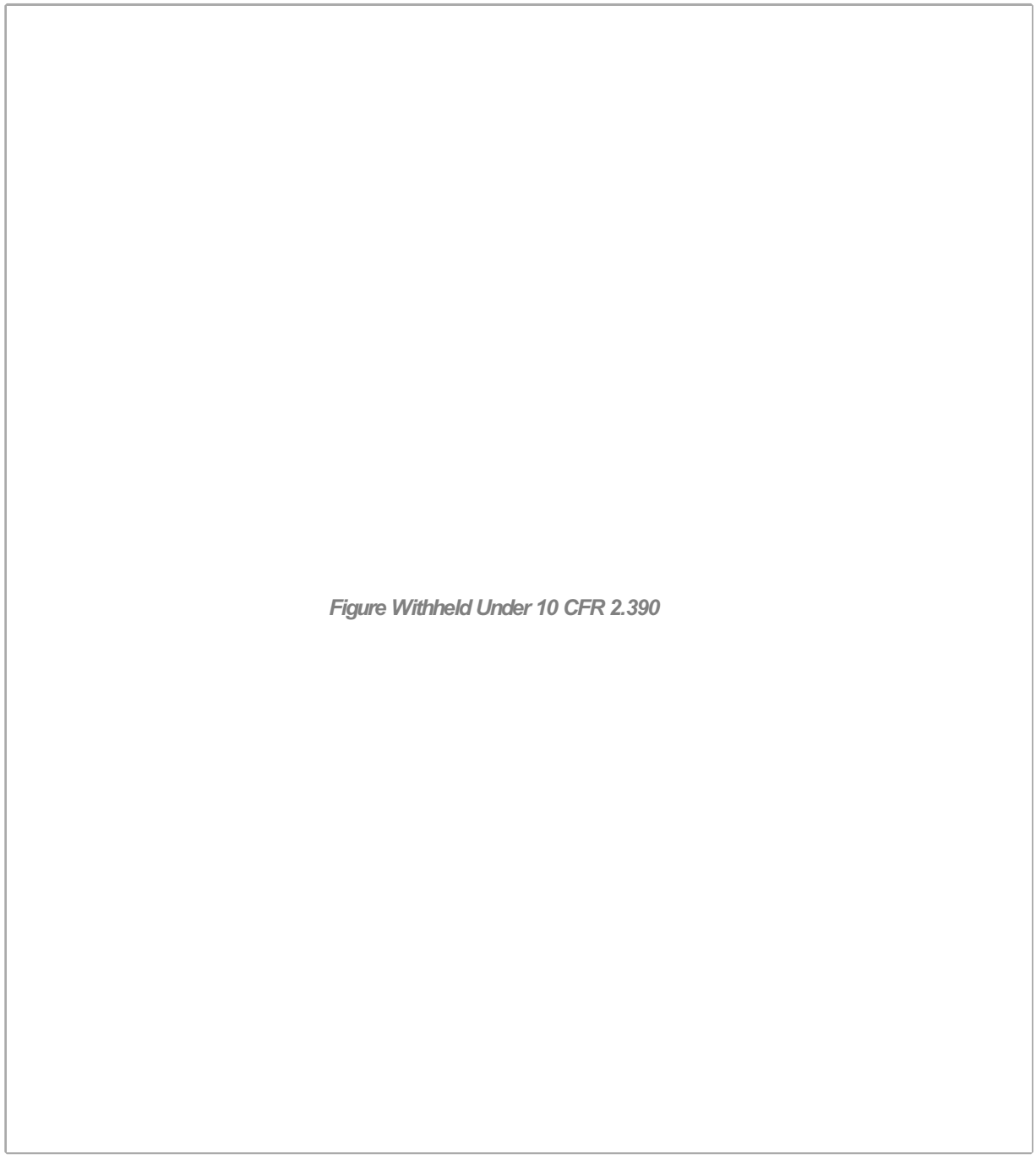

Figure 2.6.7-19 Free Body Diagram - Top Impact Limiter - Cask Wedging Forces

Figure 2.6.7-20 Cask Lid Configuration

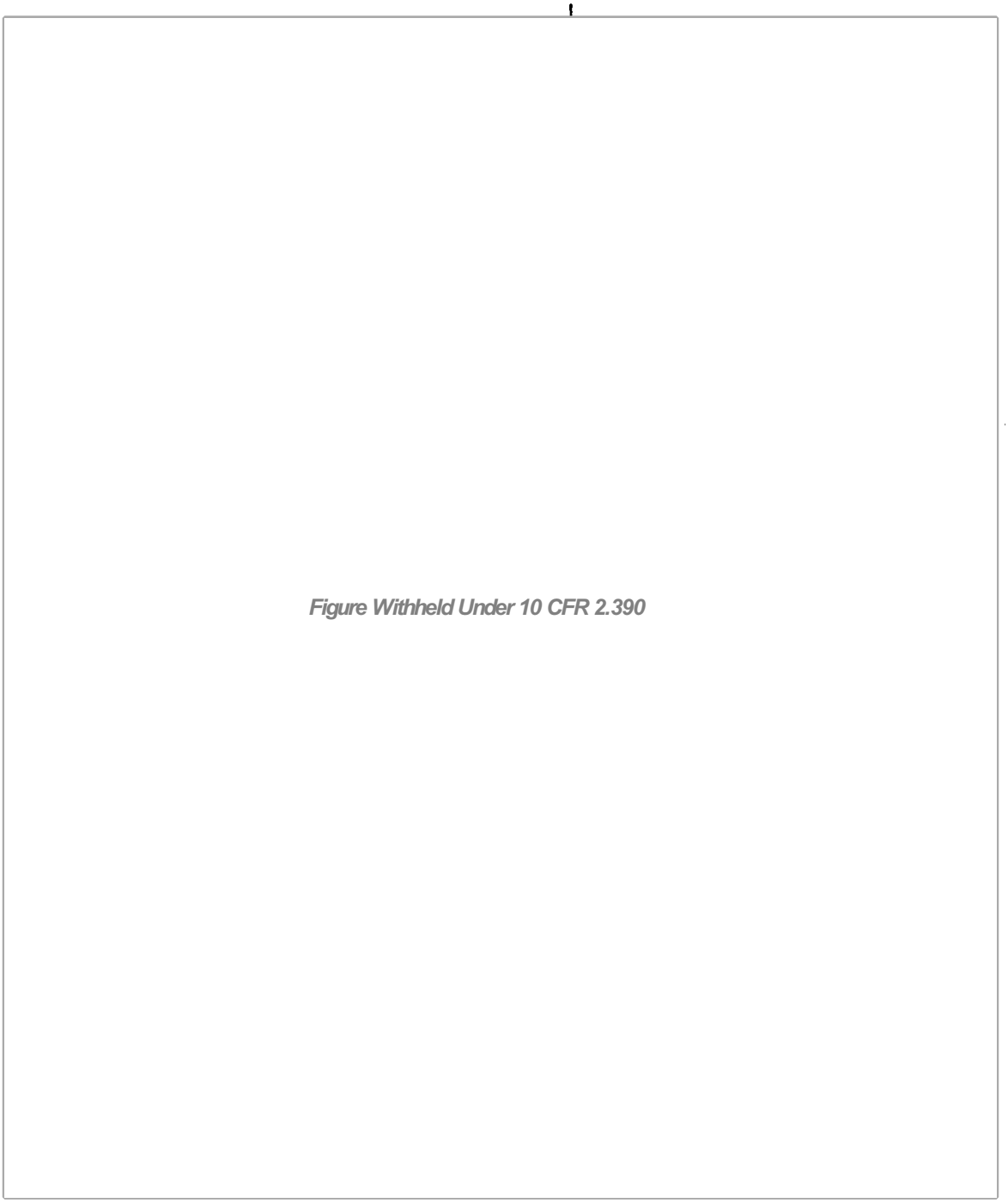

Figure 2.6.7-21 Closure Lid Free Body Diagram

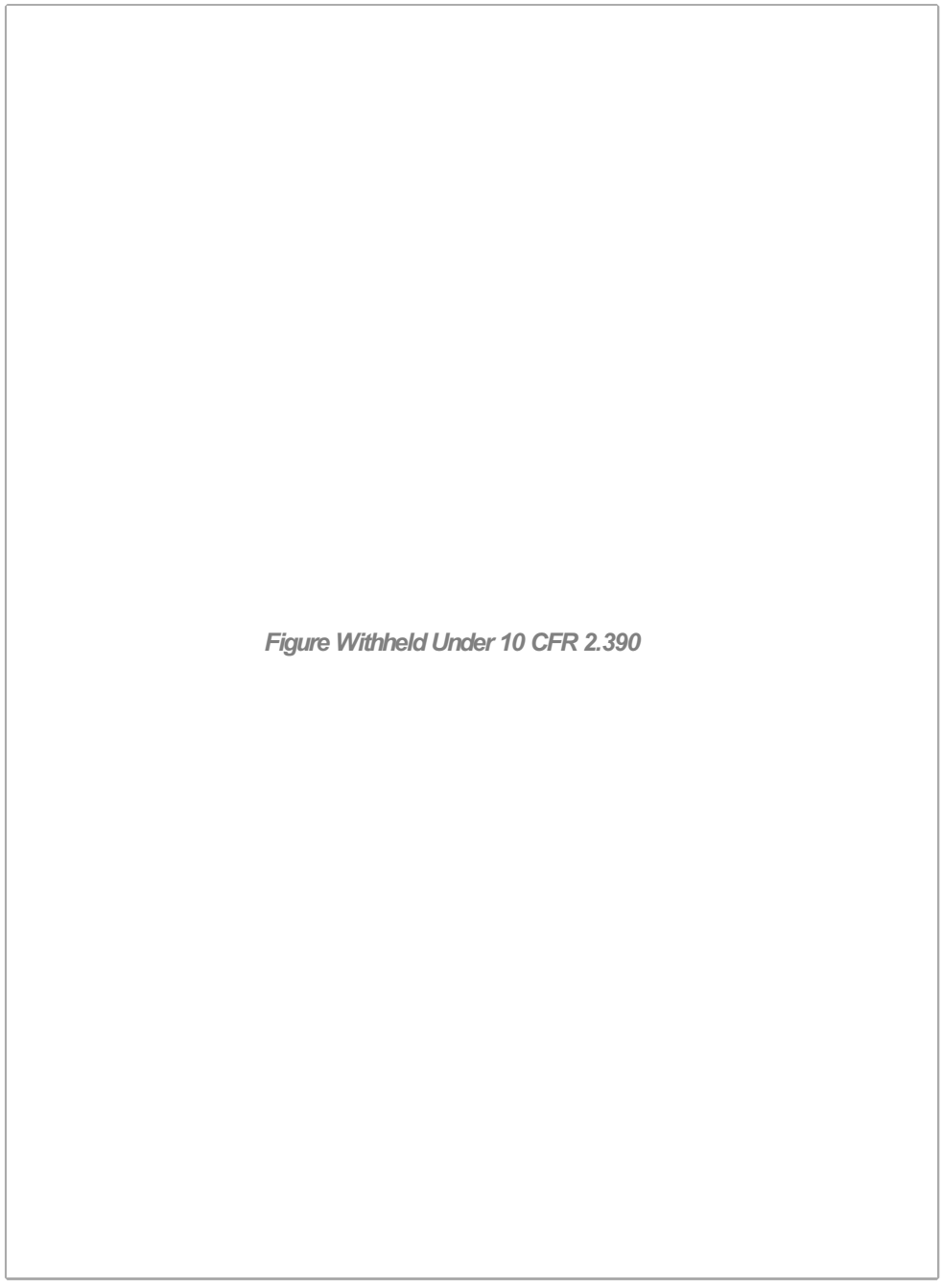

Figure 2.6.7-22 NAC-LWT Cask Cross-Section

Figure 2.6.7-23 Component Parts of Shield Tank Structure

Figure 2.6.7-24 Shield Tank Cross-Section

Figure 2.6.7-25 Shield Tank Quarter-Section Geometry

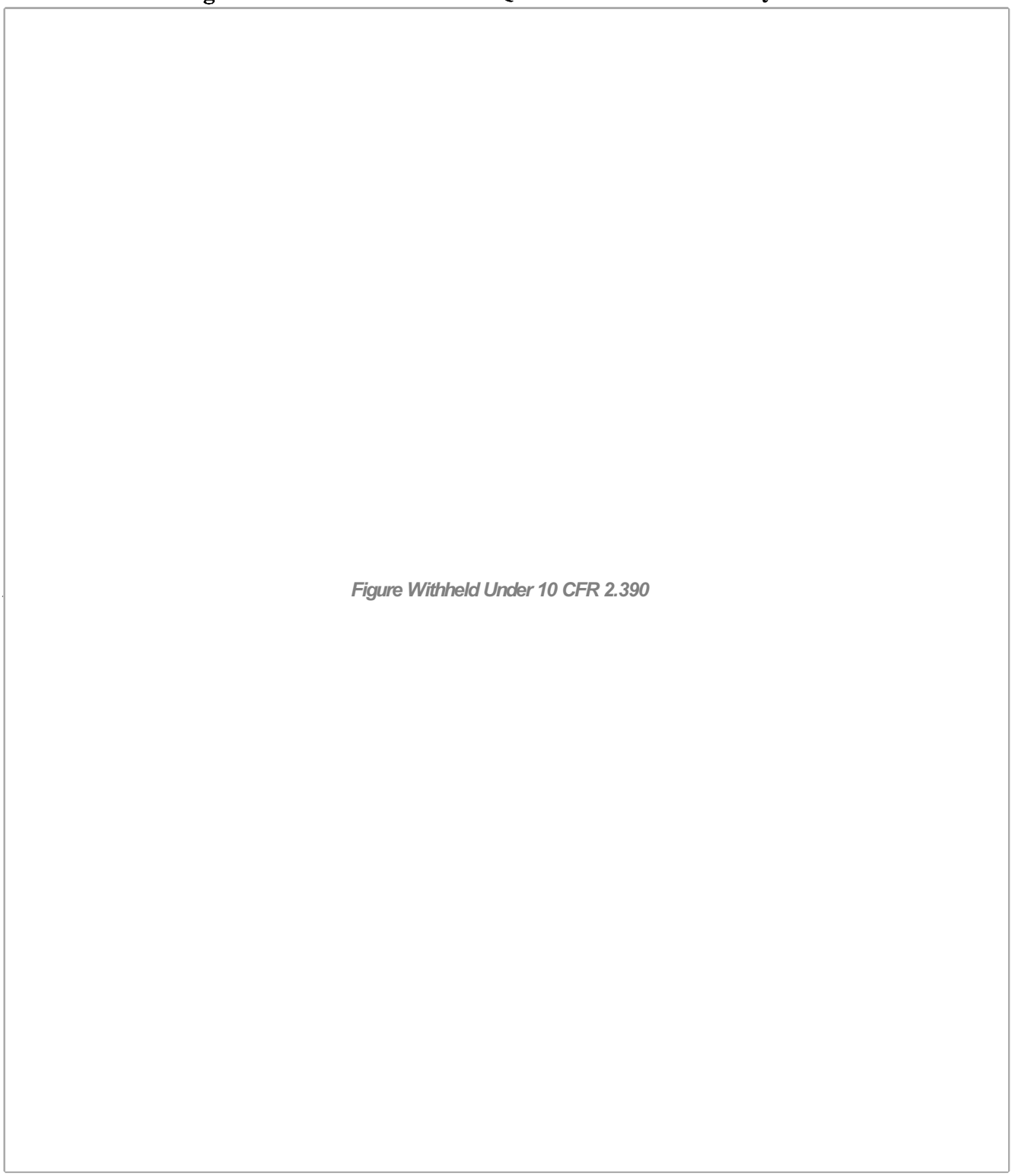

Figure 2.6.7-26 Partial Bottom/Top End Plate Plan and Cross-Section

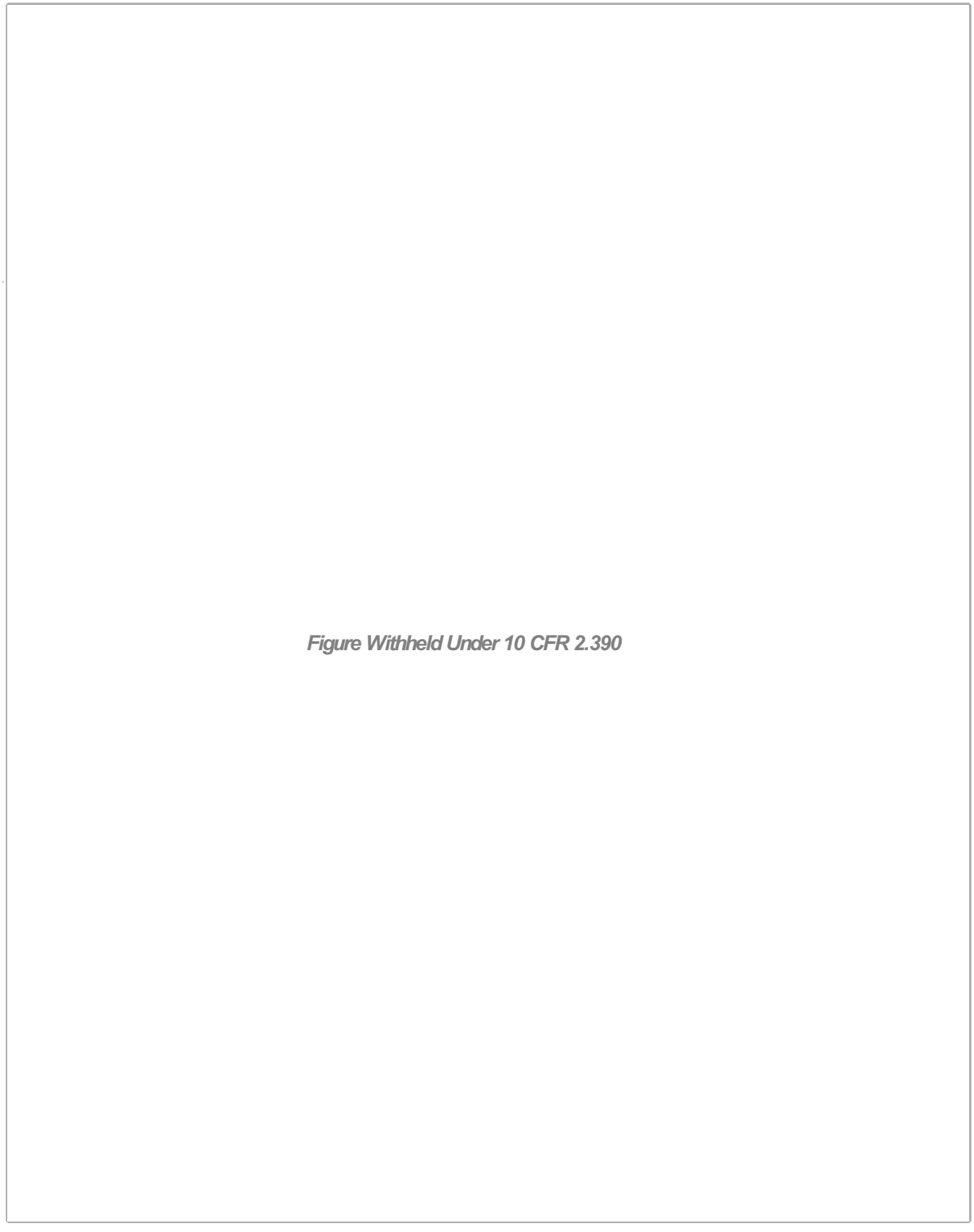

Figure 2.6.7-27 Shield Tank End Plate

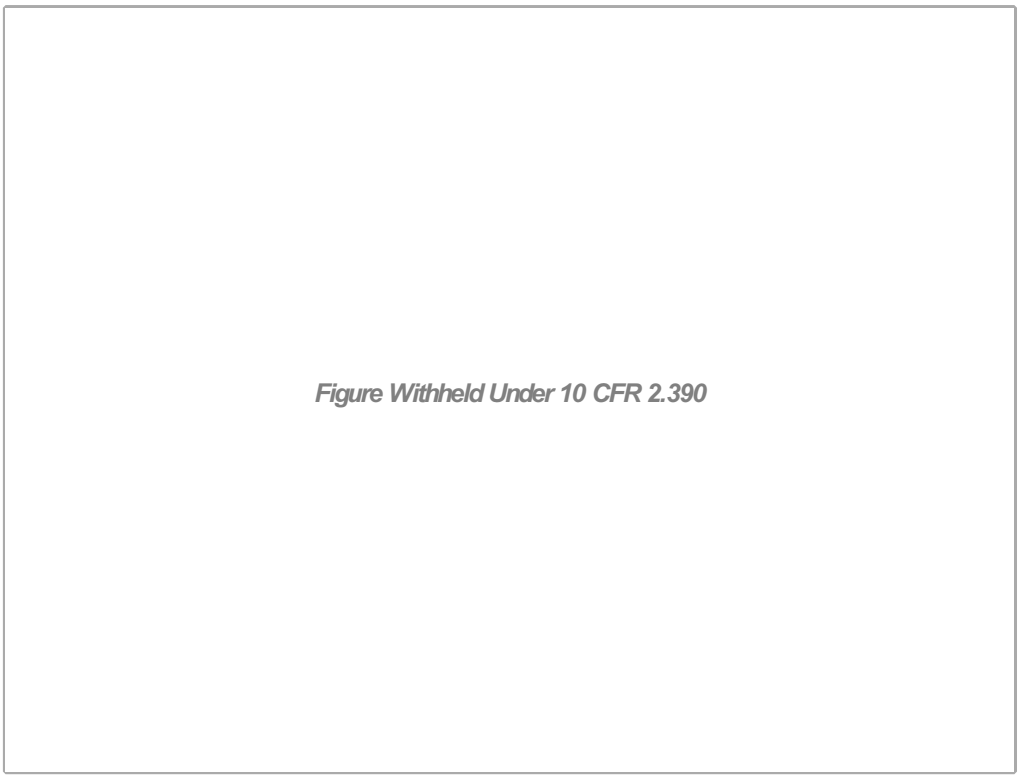

Figure 2.6.7-28 Gusset Profile

Figure 2.6.7-29 End Plate Welds

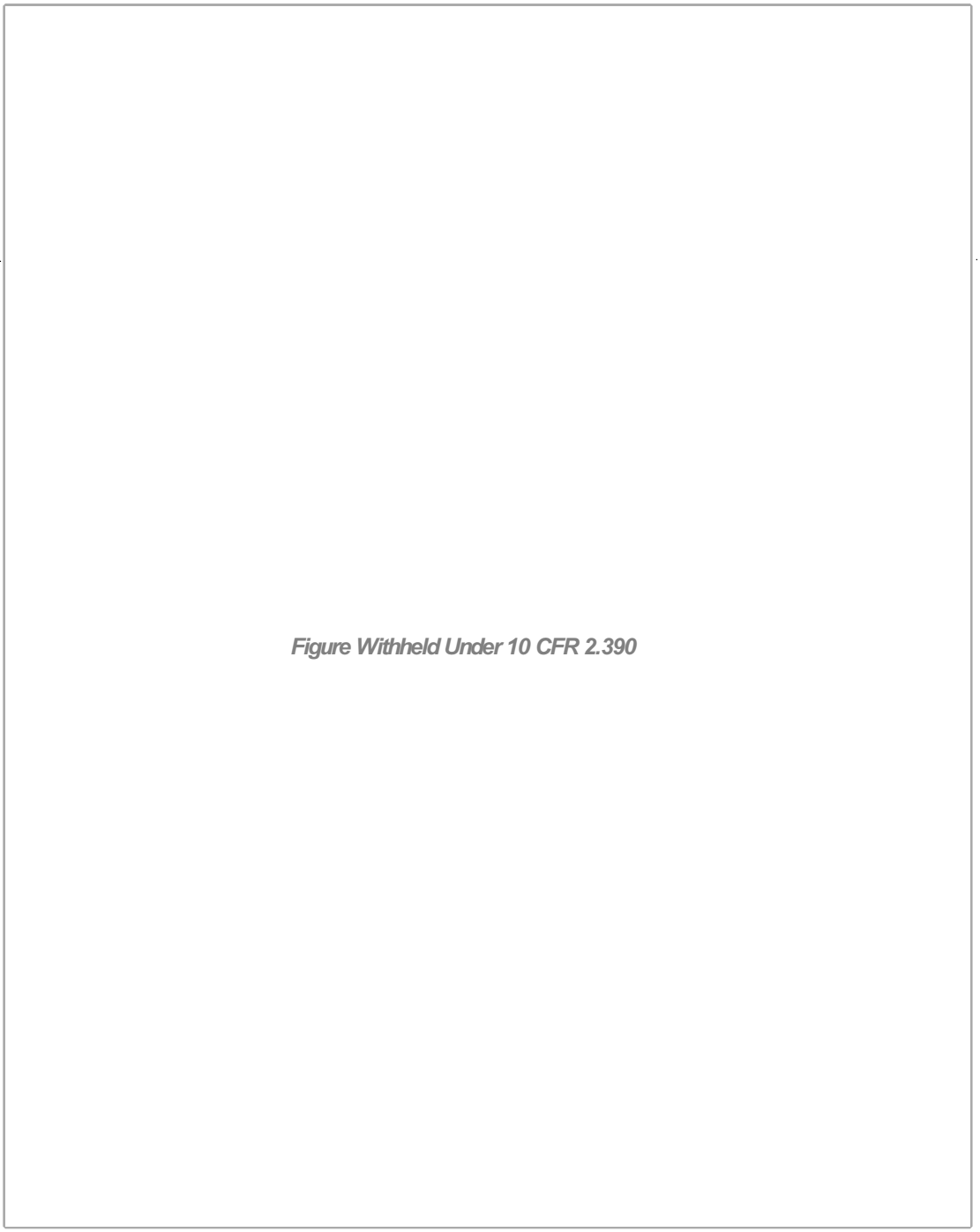

Figure 2.6.7-30 Component Parts of the Expansion Tank Structure

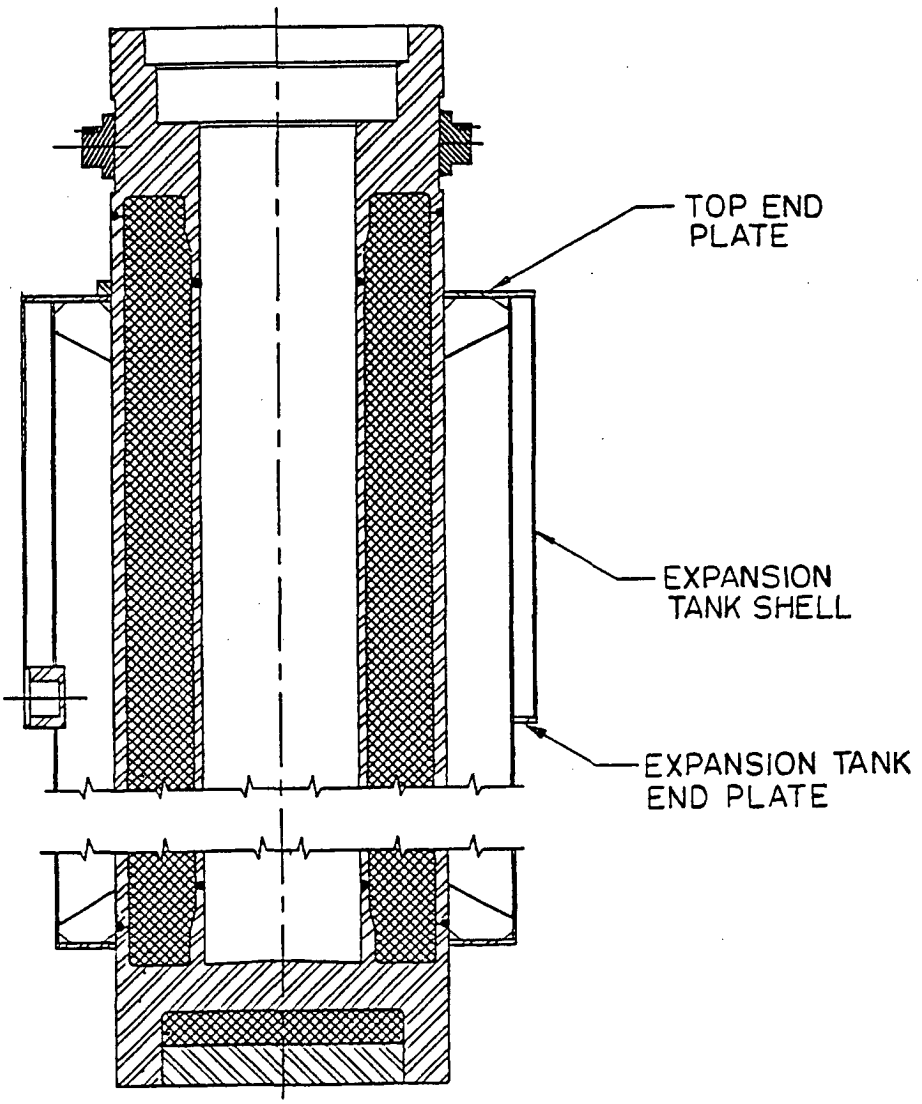

Figure 2.6.7-31 Expansion Tank Top and Bottom End Plate

Figure 2.6.7-32 Expansion Tank Stiffener Load Geometry

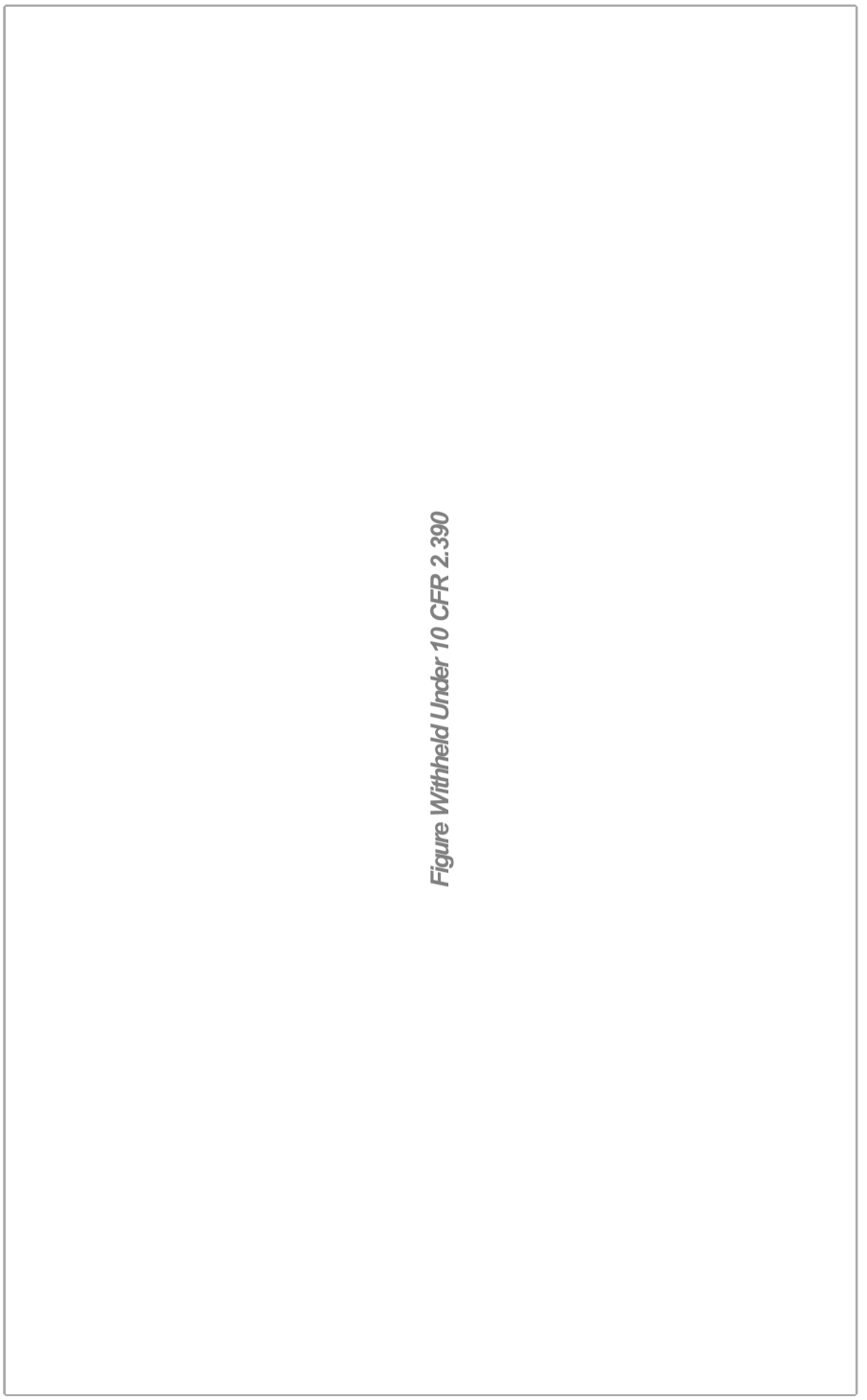

Figure 2.6.7-33 Cask Upper Ring at Trunnion - ANSYS Model

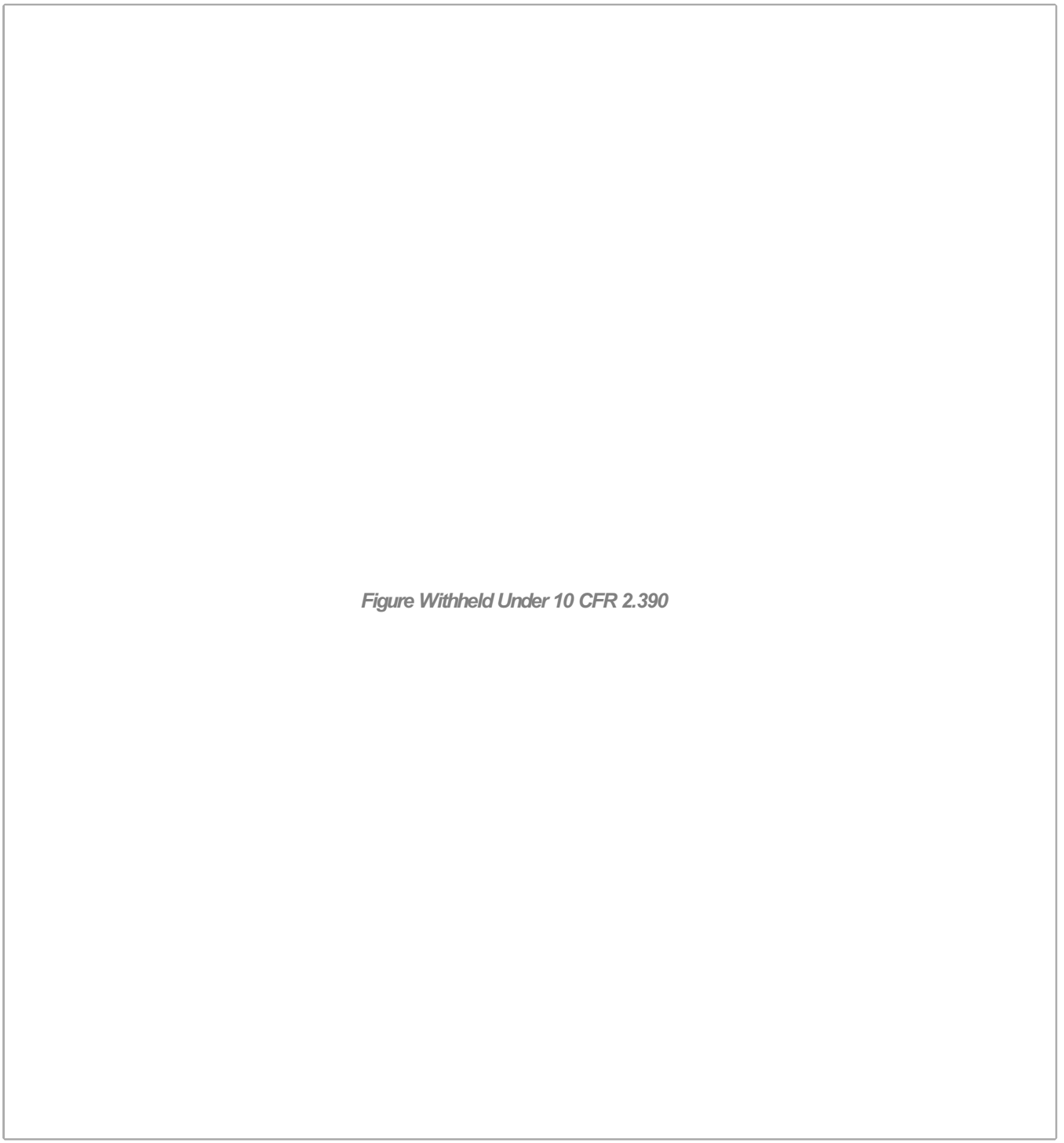

Figure 2.6.7-34 Cask Upper Ring at Trunnion - Model Loads and Boundary Conditions

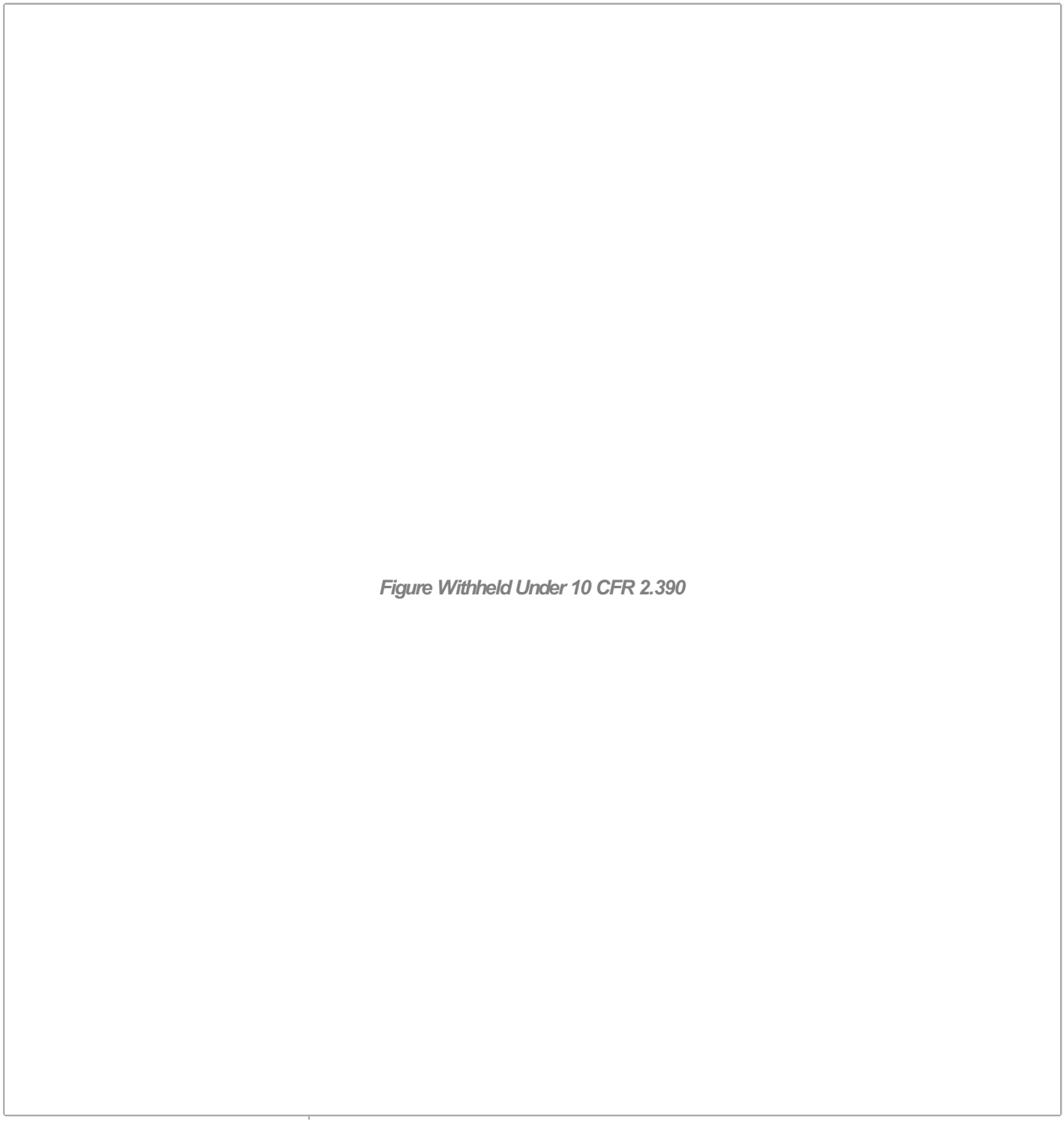

Figure 2.6.7-35 NAC-LWT Cask Upper Ring at Trunnion - Critical Sections

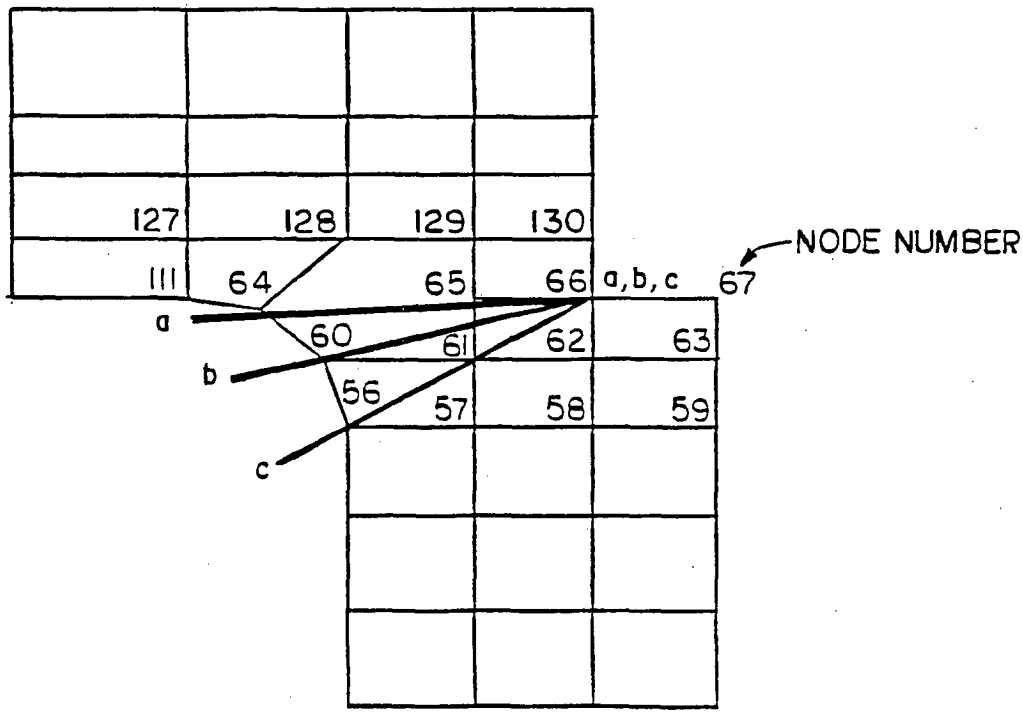

Table 2.6.7-1 Critical Stress Summary (1-Foot Bottom End Drop) – Loading Condition 1 – P_m

Loading Condition 1: 130°F Ambient Temperature and Maximum Decay Heat Load

		P_m Stresses[1] (ksi)				Principal Stresses					
Comp. No.[2]	Section Cut Node to Node	S_x	S_y	S_z	S_{xy}	S_1	S_2	S_3	S.I.	Allow. Stress 1.0 S_m	Margin of Safety
	2-2										
1	2375 to 2575	-0.17	-0.23	0.62	0.40	0.62	0.2	-0.6	1.22	20.0	Large
	4-4										
3	1581 to 1584	-0.1	-4.54	-0.16	-0.14	-0.1	-0.16	-4.55	4.45	20.0	+3.49
	7-7										
4	701 to 704	-0.03	-8.44	0.51	-0.02	0.51	-0.03	-8.44	8.94	31.4	+2.51
	6-6										
6	1515 to 1518	0.00	1.98	-0.16	-0.04	1.98	0.00	-0.16	2.14	31.4	Large
	11-11										
7	192 to 342	-6.50	1.18	1.28	1.69	1.54	1.28	-6.85	8.39	20.0	+1.38
	10-10										
8	361 to 365	0.77	-5.40	3.89	-0.99	3.89	0.92	-5.55	9.44	20.0	+1.19

[1] Conservatively based on a 1.12-inch thick outer shell and on a 3850-psi crush strength aluminum honeycomb impact limiter (Section 2.6.7.1.1).

[2] Refer to Figure 2.10.2-9 for component identification.

Table 2.6.7-2 Critical Stress Summary (1-Foot Bottom End Drop) – Loading Condition 1 - $P_m + P_b$

Loading Condition 1: 130°F Ambient Temperature and Maximum Decay Heat Load

		$P_m + P_b$ Stresses[1] (ksi)				Principal Stresses					
Comp. No.[2]	Section Cut Node to Node	S_x	S_y	S_z	S_{xy}	S_1	S_2	S_3	S.I.	Allow. Stress 1.5 S_m	Margin of Safety
	1-1										
1	2371 to 2571	-3.91	-0.35	0.11	0.00	0.11	-0.35	-3.91	4.01	30.0	+6.48
	3-3										
3	1835 to 1838	-0.1	4.66	2.25	0.29	4.68	2.25	-0.1	4.76	30.0	+5.30
	8-8										
4	621 to 624	0.15	-10.37	-1.16	0.28	0.16	-1.16	-10.38	10.54	47.1	+3.47
	5-5										
6	1595 to 1598	-0.01	3.03	0.57	0.00	3.03	0.57	-0.01	3.04	47.1	Large
	12-12										
7	150 to 193	9.25	-5.21	2.76	0.63	9.27	2.76	-5.24	14.51	30.0	+1.06
	9-9										
8	381 to 385	-0.21	-13.14	2.03	-1.07	2.03	-0.12	-13.23	15.26	30.0	+0.97

[1] Conservatively based on a 1.12-inch thick outer shell and on a 3850-psi crush strength aluminum honeycomb impact limiter (Section 2.6.7.1.1).

[2] Refer to Figure 2.10.2-9 for component identification.

Table 2.6.7-3 Critical Stress Summary (1-Foot Bottom End Drop) – Loading Condition 1 - Total Range

Loading Condition 1: 130°F Ambient Temperature and Maximum Decay Heat Load

		Total Stress Range[1] (ksi)				Principal Stresses			Stress Differences		
Comp. No.[2]	Node	S_x	S_y	S_z	S_{xy}	S_1	S_2	S_3	S_1-S_2	S_2-S_3	S_3-S_1
1	2376	0.80	-4.48	-0.22	-0.31	0.82	-0.22	-4.50	1.04	4.28	-5.32
3	1805	-0.19	-5.27	-2.19	-0.78	-0.07	-2.19	-5.39	2.12	3.20	-5.32
4	604	-0.69	-12.07	-1.65	0.61	-0.66	-1.65	-12.10	0.99	10.45	-11.44
6	1595	-0.02	2.93	0.48	0.00	2.93	0.48	-0.02	2.45	0.50	-2.95
7	192	12.54	-7.35	3.46	-3.90	13.28	3.46	-8.09	9.82	11.55	-21.37
8	361	-0.03	-16.44	0.82	-1.40	0.82	0.09	-16.57	0.73	16.65	-17.38

1 Conservatively based on a 1.12-inch thick outer shell and on a 3850-psi crush strength aluminum honeycomb impact limiter (Section 2.6.7.1.1).

2 Refer to Figure 2.10.2-9 for component identification.

Table 2.6.7-4 Critical Stress Summary (1-Foot Bottom End Drop) – Loading Condition 2 – P_m

Loading Condition 2: -40°F Ambient Temperature and Maximum Decay Heat Load

Comp. No.[2]	Section Cut Node to Node	P_m Stresses[1] (ksi)				Principal Stresses			S.I.	Allow. Stress 1.0 S_m	Margin of Safety
		S_x	S_y	S_z	S_{xy}	S_1	S_2	S_3			
	2-2										
1	2478 to 2578	0.03	-0.11	1.28	0.02	1.28	0.03	-0.11	1.39	20.0	Large
	4-4										
3	1581 to 1584	-0.15	-7.90	-0.93	-0.26	-0.14	-0.93	-7.91	7.77	20.0	+1.57
	6-6										
4	701 to 704	-0.02	-12.08	0.20	-0.03	0.20	-0.02	-12.08	12.28	31.4	+1.56
	8-8										
6	615 to 618	0.00	-2.85	0.80	0.00	0.80	0.00	-2.85	3.65	31.4	+7.60
	11-11										
7	100 to 143	-3.18	-4.19	2.15	2.18	2.15	-1.45	-5.93	8.07	20.0	+1.50
	7-7										
8	601 to 604	-0.23	-11.12	-1.21	0.46	-0.21	-1.21	-11.13	10.93	20.0	+0.83

[1] Conservatively based on a 1.12-inch thick outer shell and on a 3850-psi crush strength aluminum honeycomb impact limiter (Section 2.6.7.1.1).

[2] Refer to Figure 2.10.2-9 for component identification.

Table 2.6.7-5 Critical Stress Summary (1-Foot Bottom End Drop) – Loading Condition 2 - $P_m + P_b$

Loading Condition 2: -40°F Ambient Temperature and Maximum Decay Heat Load

		$P_m + P_b$ Stresses[1] (ksi)				Principal Stresses					
Comp. No.[2]	Section Cut Node to Node	S_x	S_y	S_z	S_{xy}	S_1	S_2	S_3	S.I.	Allow. Stress 1.5 S_m	Margin of Safety
	1-1										
1	2371 to 2571	-4.10	-0.43	0.14	0.00	0.14	-0.43	-4.10	4.24	30.0	+6.08
	3-3										
3	1701 to 1705	0.04	-8.08	-1.59	-0.34	0.05	-1.59	-8.10	8.15	30.0	+2.68
	5-5										
4	621 to 624	0.18	-13.91	-1.67	0.32	0.19	-1.67	-13.91	14.10	47.1	+2.34
	8-8										
6	615 to 618	0.03	-4.12	0.63	0.00	0.63	0.03	-4.12	4.75	47.1	+8.92
	10-10										
7	193 to 200	3.76	-9.04	1.83	-0.76	3.81	1.83	-9.09	12.89	30.0	+1.32
	9-9										
8	185 to 335	-12.66	-0.38	-0.11	1.93	-0.09	-0.11	-12.96	12.87	30.0	+1.33

1 Conservatively based on a 1.12-inch thick outer shell and on a 3850-psi crush strength aluminum honeycomb impact limiter (Section 2.6.7.1.1).

2 Refer to Figure 2.10.2-9 for component identification.

Table 2.6.7-6 Critical Stress Summary (1-Foot Bottom End Drop) – Loading Condition 2 - Total Range

Loading Condition 2: -40°F Ambient Temperature and Maximum Decay Heat Load

		Total Stress Range[1] (ksi)				Principal Stresses			Stress Differences		
Comp. No.[2]	Node	S_x	S_y	S_z	S_{xy}	S_1	S_2	S_3	S_1-S_2	S_2-S_3	S_3-S_1
1	2376	0.67	-4.03	0.05	-0.35	0.70	0.05	-4.06	0.65	4.11	-4.75
3	1805	-0.32	-9.36	-3.82	-1.34	-0.12	-3.82	-9.56	3.70	5.74	-9.44
4	604	-0.90	-15.99	-2.51	0.80	-0.86	-2.51	-16.03	1.65	13.52	-15.17
6	618	0.03	-4.20	0.57	0.00	0.57	0.03	-4.20	0.54	4.23	-4.77
7	143	-5.58	-14.56	-1.04	0.55	-1.04	-5.55	-14.59	4.51	9.05	-13.55
8	361	0.01	-14.97	-0.81	-1.62	0.18	-0.81	-15.14	0.99	14.33	-15.33

1 Conservatively based on a 1.12-inch thick outer shell and on a 3850-psi crush strength aluminum honeycomb impact limiter (Section 2.6.7.1.1).
2 Refer to Figure 2.10.2-9 for component identification.

Table 2.6.7-7 Critical Stress Summary (1-Foot Bottom End Drop) – Loading Condition 3 – P_m

Loading Condition 3: -40°F Ambient Temperature and No Decay Heat Load

Comp. No.[2]	Section Cut Node to Node	P_m Stresses[1] (ksi)				Principal Stresses					
		S_x	S_y	S_z	S_{xy}	S_1	S_2	S_3	S.I.	Allow. Stress 1.0 S_m	Margin of Safety
	1-1										
1	2375 to 2575	-0.21	0.00	-0.03	0.18	0.1	-0.03	-0.31	0.41	20.0	Large
	2-2										
3	1581 to 1584	-0.22	-3.78	-5.48	-0.28	-0.19	-3.80	-5.48	5.29	20.0	+2.78
	3-3										
4	621 to 624	0.04	-7.76	-1.05	0.24	0.04	-1.05	-7.77	7.81	31.4	+3.02
	5-5										
6	615 to 618	0.00	-6.85	-0.13	0.00	0.00	-0.13	-6.85	6.85	31.4	+3.58
	8-8										
7	18 to 118	-10.02	-0.60	-2.86	2.62	0.08	-2.86	-10.70	10.78	20.0	+0.86
	4-4										
8	601 to 604	-0.16	-7.07	-0.78	0.34	-0.14	-0.78	-7.09	6.95	20.0	+1.88

1 Conservatively based on a 1.12-inch thick outer shell and on a 3850-psi crush strength aluminum honeycomb impact limiter (Section 2.6.7.1.1).

2 Refer to Figure 2.10.2-9 for component identification.

Table 2.6.7-8 Critical Stress Summary (1-Foot Bottom End Drop) – Loading Condition 3 - $P_m + P_b$

Loading Condition 3: -40°F Ambient Temperature and No Decay Heat Load

		$P_m + P_b$ Stresses[1] (ksi)				Principal Stresses					
Comp. No.[2]	Section Cut Node to Node	S_x	S_y	S_z	S_{xy}	S_1	S_2	S_3	S.I.	Allow. Stress 1.5 S_m	Margin of Safety
	1-1										
1	2375 to 2575	-1.99	0.00	-0.03	0.18	0.01	-0.03	-2.01	2.02	30.0	Large
	2-2										
3	1581 to 1584	0.01	-3.30	-5.65	-0.28	0.03	-3.33	-5.65	5.68	30.0	+4.28
	3-3										
4	621 to 624	0.12	-8.99	-1.30	0.24	0.13	-1.30	-9.00	9.13	47.1	+4.16
	5-5										
6	615 to 618	0.00	-7.06	-0.19	0.00	0.00	-0.19	-7.06	7.06	47.1	+5.67
	8-8										
7	18 to 118	-20.14	-0.6	-2.86	2.62	-0.25	-2.86	-20.49	20.23	30.0	+0.48
	6-6										
8	185 to 335	-8.83	1.55	1.16	2.22	2.0	1.16	-9.29	11.29	30.0	+1.66

[1] Conservatively based on a 1.12-inch thick outer shell and on a 3850-psi crush strength aluminum honeycomb impact limiter (Section 2.6.7.1.1).

[2] Refer to Figure 2.10.2-9 for component identification.

Table 2.6.7-9 Critical Stress Summary (1-Foot Bottom End Drop) – Loading Condition 3 - Total Range

Loading Condition 3: -40°F Ambient Temperature and No Decay Heat Load

		Total Stress Range[1] (ksi)				Principal Stresses			Stress Differences		
Comp. No.[2]	Node	S_x	S_y	S_z	S_{xy}	S_1	S_2	S_3	S_1-S_2	S_2-S_3	S_3-S_1
1	2376	0.96	-3.75	-0.64	-0.11	0.96	-0.64	-3.75	1.60	3.11	-4.71
3	2176	3.74	-17.36	-1.84	-2.41	4.01	-1.84	-17.90	5.85	16.06	-21.91
4	604	-0.58	-10.47	-1.81	0.56	-0.55	-1.81	-10.50	1.26	8.69	-9.95
6	615	0.01	-7.05	-0.19	0.00	0.01	-0.19	-7.05	0.20	6.86	-7.06
7	143	0.08	-23.96	-3.03	-2.73	0.39	-3.03	-24.27	3.42	21.24	-24.66
8	361	-0.02	-10.55	0.26	-1.38	0.26	-0.16	-10.73	0.10	10.89	-10.99

1 Conservatively based on a 1.12-inch thick outer shell and on a 3850-psi crush strength aluminum honeycomb impact limiter (Section 2.6.7.1.1).

2 Refer to Figure 2.10.2-9 for component identification.

Table 2.6.7-10 Critical Stress Summary (1-Foot Top End Drop) – Loading Condition 1 – P_m

Loading Condition 1: 130°F Ambient Temperature and Maximum Decay Heat Load

		P_m Stresses[1] (ksi)				Principal Stresses					
Comp. No.[2]	Section Cut Node to Node	S_x	S_y	S_z	S_{xy}	S_1	S_2	S_3	S.I.	Allow. Stress 1.0 S_m	Margin of Safety
	2-2										
1	2377 to 2577	-7.46	-0.06	0.09	0.15	0.09	-0.05	-7.46	7.55	20.0	+1.65
	4-4										
3	1581 to 1584	-0.20	-7.58	-0.57	-0.33	-0.18	-0.57	-7.60	7.42	20.0	+1.70
	5-5										
4	1481 to 1484	-0.03	-8.19	0.52	0.02	0.52	-0.03	-8.19	8.71	31.4	+2.60
	12-12										
6	695 to 698	0.00	2.39	-0.10	0.04	2.40	0.00	-0.10	2.50	31.4	Large
	10-10										
7	17 to 117	-1.04	1.54	2.36	-2.84	3.37	2.36	-2.87	6.23	20.0	+2.21
	7-7										
8	401 to 405	-0.03	-2.63	1.89	-0.39	1.89	0.03	-2.69	4.58	20.0	+3.37

1 Conservatively based on a 1.12-inch thick outer shell and on a 3850-psi crush strength aluminum honeycomb impact limiter (Section 2.6.7.1.1).

2 Refer to Figure 2.10.2-9 for component identification.

Table 2.6.7-11 Critical Stress Summary (1-Foot Top End Drop) – Loading Condition 1 - $P_m + P_b$

Loading Condition 1: 130°F Ambient Temperature and Maximum Decay Heat Load

		$P_m + P_b$ Stresses[1] (ksi)				Principal Stresses					
Comp. No.[2]	Section Cut Node to Node	S_x	S_y	S_z	S_{xy}	S_1	S_2	S_3	S.I.	Allow. Stress 1.5 S_m	Margin of Safety
	1-1										
1	2371 to 2571	-12.69	-0.13	-0.22	-1.01	-0.05	-0.22	-12.77	12.72	30.0	+1.36
	3-3										
3	1941 to 1956	0.84	-10.28	-3.31	0.03	0.84	-3.31	-10.28	11.12	30.0	+1.70
	11-11										
4	1561 to 1564	0.12	-9.50	-0.89	-0.22	0.13	-0.89	-9.51	9.64	47.1	+3.89
	6-6										
6	615 to 618	-0.02	3.50	0.78	0.00	3.50	0.78	-0.02	3.52	47.1	Large
	9-9										
7	143 to 150	-7.68	6.60	1.37	1.33	6.72	1.37	-7.80	14.52	30.0	+1.07
	8-8										
8	381 to 385	-0.15	-6.77	0.67	-0.49	0.67	-0.12	-6.81	7.47	30.0	+3.02

1 Conservatively based on a 1.12-inch thick outer shell and on a 3850-psi crush strength aluminum honeycomb impact limiter (Section 2.6.7.1.1).

2 Refer to Figure 2.10.2-9 for component identification.

Table 2.6.7-12 Critical Stress Summary (1-Foot Top End Drop) – Loading Condition 1 - Total Range

Loading Condition 1: 130°F Ambient Temperature and Maximum Decay Heat Load

		Total Stress Range[1] (ksi)				Principal Stresses			Stress Differences		
Comp. No.[2]	Node	S_x	S_y	S_z	S_{xy}	S_1	S_2	S_3	S_1-S_2	S_2-S_3	S_3-S_1
1	2371	2.76	-10.30	0.04	3.56	3.67	0.04	-11.21	3.63	11.25	-14.88
3	1962	-1.54	-12.69	-5.46	-1.00	-1.45	-5.46	-12.78	4.01	7.32	-11.33
4	1584	-0.62	-10.96	-1.54	-0.54	-0.59	-1.54	-10.98	0.95	9.44	-10.39
6	615	-0.01	3.43	0.72	-0.01	3.43	0.72	-0.01	2.71	0.73	-3.44
7	143	-7.68	6.79	1.34	2.96	7.37	1.34	-8.26	6.03	9.60	-15.63
8	361	-0.07	-8.76	-0.09	-0.78	0.00	-0.09	-8.83	0.09	8.74	-8.83

1 Conservatively based on a 1.12-inch thick outer shell and on a 3850-psi crush strength aluminum honeycomb impact limiter (Section 2.6.7.1.1).

2 Refer to Figure 2.10.2-9 for component identification.

Table 2.6.7-13 Critical Stress Summary (1-Foot Top End Drop) – Loading Condition 2 – P_m

Loading Condition 2: -40°F Ambient Temperature and Maximum Decay Heat Load

		P_m Stresses[1] (ksi)				Principal Stresses					
Comp. No.[2]	Section Cut Node to Node	S_x	S_y	S_z	S_{xy}	S_1	S_2	S_3	S.I.	Allow. Stress 1.0 S_m	Margin of Safety
	2-2										
1	2377 to 2577	-7.42	-0.08	0.30	0.18	0.30	-0.08	-7.42	7.72	20.0	+1.59
	4-4										
3	1581 to 1584	-0.24	-10.89	-1.33	-0.44	-0.22	-1.33	-10.91	10.69	20.0	+0.87
	6-6										
4	1481 to 1484	-0.02	-11.77	0.24	0.04	0.24	-0.02	-11.77	12.01	31.4	+1.61
	5-5										
6	1595 to 1598	0.01	-2.37	1.0	0.02	1.0	0.01	-2.37	3.37	31.4	+8.32
	10-10										
7	375 to 378	-1.35	1.92	2.97	-0.61	2.97	2.03	-1.45	4.42	20.0	+3.52
	8-8										
8	601 to 604	-0.13	-7.55	-0.80	0.27	-0.12	-0.80	-7.56	7.44	20.0	+1.69

1 Conservatively based on a 1.12-inch thick outer shell and on a 3850-psi crush strength aluminum honeycomb impact limiter (Section 2.6.7.1.1).

2 Refer to Figure 2.10.2-9 for component identification.

Table 2.6.7-14 Critical Stress Summary (1-Foot Top End Drop) – Loading Condition 2 - $P_m + P_b$

Loading Condition 2: -40°F Ambient Temperature and Maximum Decay Heat Load

		$P_m + P_b$ Stresses[1] (ksi)				Principal Stresses					
Comp. No.[2]	Section Cut Node to Node	S_x	S_y	S_z	S_{xy}	S_1	S_2	S_3	S.I.	Allow. Stress 1.5 S_m	Margin of Safety
	1-1										
1	2371 to 2571	-12.88	-0.21	-0.19	-1.02	-0.13	-0.19	-12.96	12.84	30.0	+1.34
	4-4										
3	1581 to 1584	-0.52	-12.05	-1.44	-0.45	-0.51	-1.44	-12.07	11.56	30.0	+1.60
	3-3										
4	1561 to 1564	0.17	-13.22	-1.52	-0.30	0.17	-1.52	-13.23	13.40	47.1	+2.51
	5-5										
6	1595 to 1598	0.04	-3.78	0.86	0.02	0.86	0.04	-3.78	4.64	47.1	+9.15
	9-9										
7	395 to 398	-0.18	7.35	4.97	-0.78	7.42	4.97	-0.26	7.69	30.0	+2.90
	8-8										
8	601 to 604	-0.18	-7.94	-0.67	0.27	-0.18	-0.67	-7.95	7.78	30.0	+2.86

1 Conservatively based on a 1.12-inch thick outer shell and on a 3850-psi crush strength aluminum honeycomb impact limiter (Section 2.6.7.1.1).

2 Refer to Figure 2.10.2-9 for component identification.

Table 2.6.7-15 Critical Stress Summary (1-Foot Top End Drop) – Loading Condition 2 - Total Range

Loading Condition 2: -40°F Ambient Temperature and Maximum Decay Heat Load

		Total Stress Range[1] (ksi)				Principal Stresses			Stress Differences		
Comp. No.[2]	Node	S_x	S_y	S_z	S_{xy}	S_1	S_2	S_3	S_1-S_2	S_2-S_3	S_3-S_1
1	2371	2.56	-10.43	0.01	3.61	3.50	0.01	-11.37	3.49	11.38	-14.87
3	1962	-1.54	-12.88	-5.92	-1.05	-1.44	-5.92	-12.98	4.48	7.06	-11.54
4	1584	-0.85	-15.19	-2.48	-0.76	-0.81	-2.48	-15.23	1.67	12.75	-14.42
6	1598	0.02	-3.94	0.76	0.02	0.76	0.02	-3.94	0.74	3.96	-4.70
7	378	-0.19	7.42	4.95	-0.07	7.42	4.95	-0.19	2.47	5.14	-7.61
8	361	-0.02	-7.21	-1.70	-1.00	0.16	-1.70	-7.38	1.86	5.68	-7.54

1 Conservatively based on a 1.12-inch thick outer shell and on a 3850-psi crush strength aluminum honeycomb impact limiter (Section 2.6.7.1.1).

2 Refer to Figure 2.10.2-9 for component identification.

Table 2.6.7-16 Critical Stress Summary (1-Foot Side Drop) – Loading Condition 1 – P_m

Loading Condition 1: 100°F Ambient Temperature and Maximum Decay Heat Load

		P_m Stresses (ksi)				Principal Stresses					
Comp. No.[1]	Section Cut Node to Node	S_x	S_y	S_z	S_{xy}	S_1	S_2	S_3	S.I.	Allow. Stress 1.0 S_m	Margin of Safety
	1-1										
1	2361 to 2370	-3.39	-0.30	0.06	-0.26	0.06	-0.28	-3.42	3.48	20.0	+4.74
	2-2										
3	1969 to 1976	-10.14	1.89	-4.53	-1.65	2.11	-4.53	-10.37	12.47	20.0	+0.60
	3-3										
4	1141 to 1144	-0.11	15.43	0.25	0.00	15.43	0.25	-0.11	15.54	31.4	+1.02
	4-4										
6	1115 to 1118	-0.05	31.36	1.31	0.00	31.36	1.31	-0.05	31.4	31.4	+0.00
	5-5										
7	395 to 398	-2.17	4.06	-5.51	0.78	4.15	-2.27	-5.51	9.66	20.0	+1.07
	6-6										
8	192 to 342	-5.47	-0.35	-3.06	0.18	-0.35	-3.06	-5.48	5.13	20.0	+2.89

[1] Refer to Figure 2.10.2-9 for component identification.

Table 2.6.7-17 Critical Stress Summary (1-Foot Side Drop) – Loading Condition 1 - $P_m + P_b$

Loading Condition 1: 100°F Ambient Temperature and Maximum Decay Heat Load

		$P_m + P_b$ Stresses (ksi)				Principal Stresses					
Comp. No.[1]	Section Cut Node to Node	S_x	S_y	S_z	S_{xy}	S_1	S_2	S_3	S.I.	Allow. Stress 1.5 S_m	Margin of Safety
	7-7										
1	2301 to 2561	-0.78	0.06	0.82	3.96	3.62	0.82	-4.34	7.96	30.0	+2.77
	8-8										
3	2150 to 2156	-4.40	-0.08	-20.16	0.01	-0.08	-4.40	-20.16	20.08	30.0	+0.49
	3-3										
4	1141 to 1144	-0.07	16.41	0.86	0.00	16.41	0.86	-0.07	16.48	47.1	+1.86
	4-4										
6	1115 to 1118	0.01	33.37	1.50	0.00	33.37	1.50	0.01	33.36	47.1	+0.41
	5-5										
7	395 to 398	-1.11	16.09	-0.89	0.78	16.12	-0.89	-1.14	17.26	30.0	+0.74
	9-9										
8	177 to 327	-8.25	-1.80	0.27	-1.47	0.27	-1.48	-8.58	8.85	30.0	+2.39

[1] Refer to Figure 2.10.2-9 for component identification.

Table 2.6.7-18 Critical Stress Summary (1-Foot Side Drop) – Loading Condition 1 - S_n

Loading Condition 1: 100°F Ambient Temperature and Maximum Decay Heat Load

		S_n Stresses (ksi)				Principal Stresses					
Comp. No.[1]	Section Cut Node to Node	S_x	S_y	S_z	S_{xy}	S_1	S_2	S_3	S.I.	Allow. Stress 3.0 S_m	Margin of Safety
	1-1										
1	2361 to 2370	-9.54	-1.04	-1.24	-0.19	-1.04	-1.24	-9.55	8.51	60.0	+6.05
	10-10										
3	1815 to 1818	-0.09	22.64	2.62	-1.58	22.75	2.62	-0.20	22.95	60.0	+1.61
	3-3										
4	1141 to 1144	-0.07	17.55	0.98	0.00	17.55	0.98	-0.07	17.62	94.2	+4.34
	4-4										
6	1115 to 1118	0.01	38.01	1.65	0.00	38.01	1.65	0.01	38.00	94.2	+1.48
	11-11										
7	395 to 398	-1.10	19.46	0.52	0.51	19.47	0.52	-1.12	20.59	60.0	+1.91
	6-6										
8	177 to 327	-12.34	-1.86	-3.80	-1.48	-1.66	-3.80	-12.55	10.89	60.0	+4.51

[1] Refer to Figure 2.10.2-9 for component identification.

Table 2.6.7-19 Critical Stress Summary (1-Foot Side Drop) – Loading Condition 1 - Total Range

Loading Condition 1: 100°F Ambient Temperature and Maximum Decay Heat Load

		Total Stress Range (ksi)				Principal Stresses			Stress Differences		
Comp. No.[1]	Node	S_x	S_y	S_z	S_{xy}	S_1	S_2	S_3	S_1-S_2	S_2-S_3	S_3-S_1
1	2561	0.06	0.02	1.33	15.24	15.28	1.33	-15.19	13.95	16.52	-30.47
3	1815	1.72	24.87	3.61	7.38	27.05	3.61	-0.46	23.44	4.07	-27.51
4	1144	-0.07	17.55	0.96	0.00	17.55	0.96	-0.07	16.59	1.03	-17.62
6	1118	0.01	37.98	1.61	0.00	37.98	1.61	0.01	36.37	1.60	-37.97
7	395	-1.10	22.68	1.30	1.50	22.78	1.30	-1.20	21.48	2.50	-23.98
8	192	-22.96	-1.15	-9.18	-0.81	-1.10	-9.18	-23.00	8.08	13.82	-21.90

[1] Refer to Figure 2.10.2-9 for component identification.

Table 2.6.7-20 Critical Stress Summary (1-Foot Top Corner Drop) – Loading Condition 1 – P_m – Drop Orientation = 15.74 Degrees

Loading Condition 1: 130°F Ambient Temperature and Maximum Decay Heat Load

		P_m Stresses[1] (ksi)				Principal Stresses					
Comp. No.[2]	Section Cut Node to Node	S_x	S_y	S_z	S_{xy}	S_1	S_2	S_3	S.I.	Allow. Stress 1.0 S_m	Margin of Safety
	1-1										
1	2377 to 2577	-5.07	-0.37	-0.71	-0.29	-0.35	-0.71	-5.09	4.74	20.0	+3.22
	2-2										
3	1775 to 1778	-0.05	-4.39	0.55	0.01	0.55	-0.05	-4.39	4.95	20.0	+3.04
	3-3										
4	1501 to 1504	-0.03	-3.11	0.36	0.01	0.36	-0.03	-3.11	3.47	31.4	+8.05
	4-4										
6	1595 to 1598	-0.01	-3.94	0.52	0.03	0.52	-0.01	-3.94	4.46	31.4	+6.04
	5-5										
7	18 to 118	-1.72	2.83	0.47	-2.50	3.94	0.47	-2.83	6.76	20.0	+1.96
	6-6										
8	381 to 385	-1.83	-2.67	0.82	-0.32	0.82	-1.73	-2.77	3.60	20.0	+4.56

[1] Conservatively based on a 1.12-inch thick outer shell and on a 3850-psi crush strength aluminum honeycomb impact limiter (Section 2.6.7.3.1).

[2] Refer to Figure 2.10.2-9 for component identification.

Table 2.6.7-21 Critical Stress Summary (1-Foot Top Corner Drop) – Loading Condition 1 - $P_m + P_b$ – Drop Orientation = 15.74 Degrees

Loading Condition 1: 130°F Ambient Temperature and Maximum Decay Heat Load

		$P_m + P_b$ Stresses[1] (ksi)				Principal Stresses					
Comp. No.[2]	Section Cut Node to Node	S_x	S_y	S_z	S_{xy}	S_1	S_2	S_3	S.I.	Allow. Stress 1.5 S_m	Margin of Safety
	1-1										
1	2377 to 2577	-6.69	-0.37	-0.71	-0.29	-0.35	-0.71	-6.70	6.34	30.0	+3.73
	7-7										
3	1821 to 1825	-0.02	-4.40	1.73	0.32	1.73	0.00	-4.43	6.16	30.0	+3.87
	8-8										
4	1561 to 1564	0.06	-4.51	-0.67	-0.13	0.06	-0.67	-4.52	4.58	47.1	+9.28
	4-4										
6	1595 to 1598	0.01	-4.03	0.45	0.03	0.45	0.01	-4.03	4.47	47.1	+9.54
	9-9										
7	143 to 150	-7.82	11.71	1.04	1.55	11.83	1.04	-7.94	19.77	30.0	+0.52
	10-10										
8	176 to 326	-2.87	7.16	0.74	-0.96	0.74	-2.66	-7.37	8.10	30.0	+2.70

1 Conservatively based on a 1.12-inch thick outer shell and on a 3850-psi crush strength aluminum honeycomb impact limiter (Section 2.6.7.3.1).

2 Refer to Figure 2.10.2-9 for component identification.

Table 2.6.7-22 Critical Stress Summary (1-Foot Top Corner Drop) – Loading Condition 1 - S_n – Drop Orientation = 15.74 Degrees

Loading Condition 1: 130°F Ambient Temperature and Maximum Decay Heat Load

		S_n Stresses[1] (ksi)				Principal Stresses					
Comp. No.[2]	Section Cut Node to Node	S_x	S_y	S_z	S_{xy}	S_1	S_2	S_3	S.I.	Allow. Stress 3.0 S_m	Margin of Safety
	1-1										
1	2377 to 2577	-6.82	-0.40	0.32	-0.13	0.32	-0.40	-6.82	7.14	60.0	+7.40
	11-11										
3	1852 to 1856	-0.19	7.89	4.10	-0.42	7.91	4.10	-0.21	8.12	60.0	+6.39
	12-12										
4	601 to 604	0.09	-3.42	-0.54	-0.21	0.11	-0.54	-3.44	3.54	94.2	Large
	13-13										
6	615 to 618	-0.02	15.94	1.30	0.00	15.94	1.30	-0.02	15.95	94.2	+4.90
	14-14										
7	193 to 343	-7.81	12.82	1.50	1.46	12.93	1.50	-7.92	20.84	60.0	+1.88
	6-6										
8	381 to 385	-4.22	-7.18	-0.60	-0.96	-0.60	-3.93	-7.47	6.86	60.0	+7.74

1 Conservatively based on a 1.12-inch thick outer shell and on a 3850-psi crush strength aluminum honeycomb impact limiter (Section 2.6.7.3.1).

2 Refer to Figure 2.10.2-9 for component identification.

Table 2.6.7-23 Critical Stress Summary (1-Foot Top Corner Drop) – Loading Condition 1 - Total Range – Drop Orientation = 15.74 Degrees

Loading Condition 1: 130°F Ambient Temperature and Maximum Decay Heat Load

		Total Stress Range[1] (ksi)				Principal Stresses			Stress Differences		
Comp. No.[2]	Node	S_x	S_y	S_z	S_{xy}	S_1	S_2	S_3	S_1-S_2	S_2-S_3	S_3-S_1
1	2561	1.48	-1.26	0.20	43.95	44.08	0.20	-43.86	43.88	44.06	-87.94
3	1856	-0.19	7.24	3.70	0.08	7.24	3.70	-0.19	3.54	3.89	-7.43
4	1584	-0.13	-2.05	0.02	-0.11	0.02	0.12	-2.06	0.14	1.93	-2.08
6	1595	-0.05	7.09	0.97	0.01	7.09	0.97	-0.05	6.12	1.02	-7.14
7	192	-7.81	14.07	1.73	3.37	14.58	1.73	-8.32	12.85	10.05	-22.90
8	385	-7.64	-8.88	-3.12	-1.02	-3.12	-7.07	-9.46	3.95	2.39	-6.34

1 Conservatively based on a 1.12-inch thick outer shell and on a 3850-psi crush strength aluminum honeycomb impact limiter (Section 2.6.7.3.1).

2 Refer to Figure 2.10.2-9 for component identification.

Table 2.6.7-24 Critical Stress Summary (1-Foot Bottom Corner Drop) – Loading Condition 1 – P_m – Drop Orientation = 15.74 Degrees

Loading Condition 1: 130°F Ambient Temperature and Maximum Decay Heat Load

		P_m Stresses[1] (ksi)				Principal Stresses					
Comp. No.[2]	Section Cut Node to Node	S_x	S_y	S_z	S_{xy}	S_1	S_2	S_3	S.I.	Allow. Stress 1.0 S_m	Margin of Safety
	1-1										
1	2301 to 2561	-1.28	-0.32	0.62	0.30	0.62	-0.24	-1.37	1.99	20.0	Large
	2-2										
3	1595 to 1598	-3.44	-3.78	-1.65	-0.68	-1.65	-2.91	-4.31	2.66	20.0	+6.51
	3-3										
4	661 to 664	-0.04	-2.98	0.28	0.02	0.28	-0.04	-2.98	3.26	31.4	+8.63
	4-4										
6	615 to 618	-0.01	-4.93	0.28	-0.03	0.28	-0.01	-4.93	5.21	31.4	+5.03
	5-5										
7	2 to 102	-5.98	-3.63	-0.03	2.73	-0.03	-1.83	-7.78	7.76	20.0	+1.58
	6-6										
8	601 to 604	-0.10	-2.94	0.09	0.13	0.09	-0.09	-2.95	3.04	20.0	+5.58

[1] Conservatively based on a 1.12-inch thick outer shell and on a 3850-psi crush strength aluminum honeycomb impact limiter (Section 2.6.7.3.1).

[2] Refer to Figure 2.10.2-9 for component identification.

Table 2.6.7-25 Critical Stress Summary (1-Foot Bottom Corner Drop) – Loading Condition 1 - $P_m + P_b$ – Drop Orientation = 15.74 Degrees

Loading Condition 1: 130°F Ambient Temperature and Maximum Decay Heat Load

		$P_m + P_b$ Stresses[1] (ksi)				Principal Stresses					
Comp. No.[2]	Section Cut Node to Node	S_x	S_y	S_z	S_{xy}	S_1	S_2	S_3	S.I.	Allow. Stress 1.5 S_m	Margin of Safety
	1-1										
1	2301 to 2561	-4.05	-0.32	0.38	1.31	0.38	0.09	-4.46	4.84	30.0	+5.20
	7-7										
3	1815 to 1818	-1.55	4.49	-4.47	0.28	4.51	-1.56	-4.47	8.98	30.0	+2.34
	8-8										
4	621 to 624	0.04	-4.09	-0.52	0.09	0.04	-0.52	-4.10	4.14	47.1	Large
	4-4										
6	615 to 618	-0.02	-5.20	0.30	-0.03	0.30	-0.02	-5.20	5.49	47.1	+7.58
	9-9										
7	168 to 175	9.21	-3.47	-0.15	-0.29	9.22	-0.15	-3.48	12.70	30.0	+1.36
	10-10										
8	176 to 326	-6.65	0.00	-0.82	0.00	0.00	-0.82	-6.65	6.65	30.0	+3.51

1 Conservatively based on a 1.12-inch thick outer shell and on a 3850-psi crush strength aluminum honeycomb impact limiter (Section 2.6.7.3.1).

2 Refer to Figure 2.10.2-9 for component identification.

Table 2.6.7-26 Critical Stress Summary (1-Foot Bottom Corner Drop) – Loading Condition 1 - S_n – Drop Orientation = 15.74 Degrees

Loading Condition 1: 130°F Ambient Temperature and Maximum Decay Heat Load

		S_n Stresses[1] (ksi)				Principal Stresses					
Comp. No.[2]	Section Cut Node to Node	S_x	S_y	S_z	S_{xy}	S_1	S_2	S_3	S.I.	Allow. Stress 3.0 S_m	Margin of Safety
	1-1										
1	2301 to 2561	-6.94	-0.68	-0.30	-0.06	-0.30	-0.68	-6.94	6.64	60.0	+8.04
	11-11										
3	1852 to 1856	-0.13	11.99	3.05	-0.24	12.00	3.05	-0.13	12.13	60.0	+3.95
	12-12										
4	1301 to 1304	0.00	4.74	0.69	0.00	4.74	0.69	0.00	4.74	94.2	Large
	13-13										
6	1275 to 1278	-0.01	12.83	0.30	0.00	12.83	0.30	-0.01	12.84	94.2	+6.34
	14-14										
7	193 to 343	17.94	-0.43	1.20	2.27	18.22	1.20	-0.71	18.93	60.0	+2.17
	15-15										
8	192 to 342	-16.86	-0.12	-1.41	3.03	0.41	-1.41	-17.40	17.81	60.0	+2.37

1 Conservatively based on a 1.12-inch thick outer shell and on a 3850-psi crush strength aluminum honeycomb impact limiter (Section 2.6.7.3.1).

2. Refer to Figure 2.10.2-9 for component identification.

Table 2.6.7-27 Critical Stress Summary (1-Foot Bottom Corner Drop) – Loading Condition 1 - Total Range – Drop Orientation = 15.74 Degrees

Loading Condition 1: 130°F Ambient Temperature and Maximum Decay Heat Load

		Total Stress Range[1] (ksi)				Principal Stresses			Stress Differences		
Comp. No.[2]	Node	S_x	S_y	S_z	S_{xy}	S_1	S_2	S_3	S_1-S_2	S_2-S_3	S_3-S_1
1	2561	0.80	-4.34	0.23	4.73	3.61	0.23	-7.15	3.38	7.38	-10.76
3	1815	0.38	3.10	-0.93	1.68	3.90	-0.42	-0.93	4.32	0.51	-4.83
4	604	-0.19	-2.77	0.11	0.15	0.11	-0.18	-2.78	0.29	2.60	-2.89
6	615	-0.03	5.78	0.94	-0.03	5.78	0.94	-0.03	4.84	0.97	-5.81
7	1	3.73	-1.26	1.97	-43.45	44.76	1.97	-42.29	42.79	44.26	-87.04
8	192	0.11	-18.73	-9.11	2.58	0.46	-9.11	-19.08	9.57	9.97	-19.53

1 Conservatively based on a 1.12-inch thick outer shell and on a 3850-psi crush strength aluminum honeycomb impact limiter (Section 2.6.7.3.1).

2 Refer to Figure 2.10.2-9 for component identification.

Table 2.6.7-28 Critical Stress Summary (1-Foot Top Corner Drop) – Loading Condition 3 – P_m – Drop Orientation = 15.74 Degrees

Loading Condition 3: -40°F Ambient Temperature and No Decay Heat Load

		P_m Stresses[1] (ksi)				Principal Stresses					
Comp. No.[2]	Section Cut Node to Node	S_x	S_y	S_z	S_{xy}	S_1	S_2	S_3	S.I.	Allow. Stress 1.0 S_m	Margin of Safety
	1-1										
1	2377 to 2577	-4.89	-0.34	-0.78	-0.34	-0.32	-0.78	-4.91	4.59	20.0	+3.36
	2-2										
3	1775 to 1778	-0.06	-4.13	0.62	0.01	0.62	-0.06	-4.13	4.75	20.0	+3.21
	3-3										
4	1561 to 1564	0.02	-2.72	-0.33	-0.11	0.03	-0.33	-2.73	2.75	31.4	Large
	4-4										
6	1595 to 1598	-0.01	-3.71	0.53	0.03	0.53	-0.01	-3.71	4.23	31.4	+6.42
	5-5										
7	168 to 175	-2.03	3.20	1.06	-0.33	3.22	1.06	-2.05	5.27	20.0	+2.79
	6-6										
8	381 to 385	-1.93	-7.44	-1.79	0.32	-1.79	-1.91	-7.46	5.67	20.0	+2.53

1 Conservatively based on a 1.12-inch thick outer shell and on a 3850-psi crush strength aluminum honeycomb impact limiter (Section 2.6.7.3.1).

2 Refer to Figure 2.10.2-9 for component identification.

Table 2.6.7-29 Critical Stress Summary (1-Foot Top Corner Drop) – Loading Condition 3 - $P_m + P_b$ – Drop Orientation = 15.74 Degrees

Loading Condition 3: -40°F Ambient Temperature and No Decay Heat Load

		$P_m + P_b$ Stresses[1] (ksi)				Principal Stresses					
Comp. No.[2]	Section Cut Node to Node	S_x	S_y	S_z	S_{xy}	S_1	S_2	S_3	S.I.	Allow. Stress 1.5 S_m	Margin of Safety
	1-1										
1	2377 to 2577	-6.71	-0.34	-0.78	-0.34	-0.33	-0.78	-6.72	6.40	30.0	+3.69
	7-7										
3	1821 to 1825	0.03	-4.61	1.68	0.43	1.68	0.07	-4.65	6.33	30.0	+3.74
	3-3										
4	1561 to 1564	0.06	-3.75	-0.84	-0.11	0.06	-0.84	-3.75	3.81	94.2	Large
	4-4										
6	1595 to 1598	0.01	-3.81	0.45	0.03	0.45	0.01	-3.81	4.26	94.2	Large
	8-8										
7	143 to 150	-0.54	12.44	4.53	-0.50	12.46	4.53	-0.56	13.02	30.0	+1.30
	9-9										
8	176 to 326	-2.90	-8.30	-0.56	-0.22	-0.56	-2.89	-8.31	7.74	30.0	+2.87

1 Conservatively based on a 1.12-inch thick outer shell and on a 3850-psi crush strength aluminum honeycomb impact limiter (Section 2.6.7.3.1).

2 Refer to Figure 2.10.2-9 for component identification.

Table 2.6.7-30 Critical Stress Summary (1-Foot Top Corner Drop) – Loading Condition 3 - S_n – Drop Orientation = 15.74 Degrees

Loading Condition 3: -40°F Ambient Temperature and No Decay Heat Load

		S_n Stresses[1] (ksi)				Principal Stresses					
Comp. No.[2]	Section Cut Node to Node	S_x	S_y	S_z	S_{xy}	S_1	S_2	S_3	S.I.	Allow. Stress 3.0 S_m	Margin of Safety
	1-1										
1	2377 to 2577	-6.95	-0.47	-1.07	-0.53	-0.43	-1.07	-6.99	6.56	60.0	+8.15
	10-10										
3	1801 to 1805	0.47	14.21	7.54	1.89	14.46	7.54	0.22	14.25	60.0	+3.21
	11-11										
4	661 to 664	0.14	-7.03	-1.15	-0.29	0.15	-1.15	-7.04	7.20	94.2	Large
	4-4										
6	1595 to 1598	0.02	-7.43	0.70	0.05	0.70	0.02	-7.43	8.13	94.2	Large
	8-8										
7	143 to 150	-0.54	13.55	4.99	-0.59	13.58	4.99	-0.56	14.14	60.0	+3.24
	6-6										
8	381 to 385	-4.25	-8.32	-1.90	-0.23	-1.90	-4.23	-8.33	6.42	60.0	+8.34

1 Conservatively based on a 1.12-inch thick outer shell and on a 3850-psi crush strength aluminum honeycomb impact limiter (Section 2.6.7.3.1).

2 Refer to Figure 2.10.2-9 for component identification.

Table 2.6.7-31 Critical Stress Summary (1-Foot Top Corner Drop) – Loading Condition 3 - Total Range – Drop Orientation = 15.74 Degrees

Loading Condition 3: -40°F Ambient Temperature and Maximum Decay Heat Load

		Total Stress Range[1] (ksi)				Principal Stresses			Stress Differences		
Comp. No.[2]	Node	S_x	S_y	S_z	S_{xy}	S_1	S_2	S_3	S_1-S_2	S_2-S_3	S_3-S_1
1	2561	0.05	-1.17	-1.15	40.01	39.49	-1.15	-40.61	40.64	39.46	-80.10
3	1805	0.47	16.81	8.08	2.75	17.26	8.08	0.02	9.18	8.06	-17.24
4	1584	-0.04	4.04	-3.61	-0.44	4.09	-0.09	-3.61	4.17	3.52	-7.70
6	1598	-0.02	-7.58	0.65	0.03	0.65	-0.02	-7.58	0.67	7.56	-8.23
7	2	-0.55	14.68	5.23	0.43	14.69	5.23	-0.56	9.46	5.79	-15.25
8	385	-7.60	-7.37	-4.68	-1.24	-4.68	-6.24	-8.73	1.56	2.48	-4.05

1 Conservatively based on a 1.12-inch thick outer shell and on a 3850-psi crush strength aluminum honeycomb impact limiter (Section 2.6.7.3.1).

2 Refer to Figure 2.10.2-9 for component identification.

Table 2.6.7-32 Summary of Results - Impact Limiter Analysis for 1-Foot Free Drop

Analysis Description	Displacement (in)	Force (lb)	Equivalent[1] G Load Factor
Flat End Impact			
Bottom Limiter with Max Crush Strength	0.76	8.22×10^5	15.8
Bottom Limiter with Min Crush Strength	0.94	6.60×10^5	12.7
Top Limiter with Max Crush Strength	0.82	8.22×10^5	15.8
Top Limiter with Min Crush Strength	0.96	6.71×10^5	12.9
Corner Impact			
Bottom Limiter with Max Crush Strength	3.16	6.29×10^5	12.1
Bottom Limiter with Min Crush Strength	3.40	6.29×10^5	12.1
Top Limiter with Max Crush Strength	3.18	6.40×10^5	12.3
Top Limiter with Min Crush Strength	3.42	5.98×10^5	11.5

[1] Equivalent g load factor = Force/52,000.

Table 2.6.7-32 Summary of Results - Impact Limiter Analysis for 1-Foot Free Drop (continued)

Analysis Description	Displacement (in)	Force (lb)	Equivalent[1] G Load Factor
Flat Side Impact			
Bottom Limiter with Max Crush Strength	0.83	1.21×10^6	23.3
Bottom Limiter with Min Crush Strength	0.95	1.03×10^6	19.8
Top Limiter with Max Crush Strength	0.83	1.26×10^6	24.3
Top Limiter with Min Crush Strength	0.94	1.07×10^6	20.6

[1] Equivalent g load factor = Force/52,000.

Table 2.6.7-33 Summary of Results - Impact Limiter Analysis for 30-Foot Free Drop Subsequent to a 1-Foot Fall

Analysis Description	Displacement (in)	Force (lb)	Equivalent[1] G Load Factor
Flat End Impact			
Bottom Limiter with Max Crush Strength	8.50	2.50×10^6	48.1
Bottom Limiter with Min Crush Strength	10.30	2.03×10^6	39.0
Top Limiter with Max Crush Strength	8.47	2.51×10^6	48.3
Top Limiter with Min Crush Strength	10.24	2.04×10^6	39.2
Corner Impact			
Bottom Limiter with Max Crush Strength	11.30	3.08×10^6	59.2
Bottom Limiter with Min Crush Strength	12.70	2.58×10^6	49.6
Top Limiter with Max Crush Strength	11.38	3.14×10^6	60.4
Top Limiter with Min Crush Strength	12.72	2.98×10^6	57.3

[1] Equivalent g load factor = Force/52,000.

Table 2.6.7-33 Summary of Results - Impact Limiter Analysis for 30-Foot Free Drop Subsequent to a 1-Foot Fall (continued)

Analysis Description	Displacement (in)	Force (lb)	Equivalent[1] G Load Factor
Flat Side Impact			
Bottom Limiter with Max Crush Strength	8.60	2.65×10^6	48.7
Bottom Limiter with Min Crush Strength	10.30	2.17×10^6	41.8
Top Limiter with Max Crush Strength	8.42	2.71×10^6	49.7
Top Limiter with Min Crush Strength	10.00	2.22×10^6	42.7

[1] Equivalent g load factor = Force/52,000.

Table 2.6.7-34 Summary of Cask Drop Equivalent G Load Factors

Direction	Equivalent G Load Factor[1]			
	1-Foot Drop	31-Foot Drop		
		Total	Axial[2] Comp.	Lateral[3] Comp.
Lateral (Side)	24.3	49.7	—	49.7
Longitudinal	15.8	60.0	60.0	—
Corner (15.74°)	12.3	60.4	58.2	16.4
Oblique (30°)	—	54.4	47.1	27.2
Oblique (45°)	—	43.8	31.0	31.0
Oblique (60°)	—	44.4	22.2	38.5

[1] Equivalent g load factor = Force/52,000.
[2] Axial Component = total x cosθ where θ = 15.74°, 30°, 45°, or 60°
[3] Lateral Component = total x sinθ where θ = 15.74°, 30°, 45°, or 60°

Table 2.6.7-35 NAC-LWT Cask Hot Bolt Analysis – Normal Conditions

Nominal Diameter (in):	1.00		
Number of Bolts:	12		
Service Stress, Sy (ksi):	81.9	} at a 300	
Bolt Expansion (in/in):	9E-06	} degree-F	
Bolt Modulus (ksi):	26700	} Service	
Lid Expansion (in/in):	9E-06	} Temperature	
Lid Modulus (ksi):	27000	}	
Stress Area (in2):	0.6051		
Grip Length (in):	7.99		
Maximum Pressure (psi):	50		
Seal Diameter (in):	15.750		
Preload Torque (ft-lbs):	260	at RT	
Nominal Room Temp, RT:	70	deg-F	
Bolt Circle Diameter (in):	17.88		
Lid Diameter (in):	22.50		

(a) Longitudinal Weight (lbs):	4941
(b) Lateral Weight (lbs):	941
Service DT (degrees):	157
[default value =]	230
CALCULATED LOADS & STIFFNESS	
(c) Bolt Thermal Load (lbs):	1423
(d) Bolt Preload (lbs):	34770
(e) Bolt Pressure Load (lbs):	812
(f) Bolt Stiffness (lbs/in):	1.9E+06
(g) Lid Stiffness (lbs/in):	2.1E+07

Angle wrt Vert. (Deg)	Impact Accel. (g)	<**** LOADS (lbs.) Impact Tension	Impact Shear	Bolt Tension Applied	Bolt Tension Net ****	<**** STRESSES (psi) Direct Tension	Direct Shear	Principal Sig-1	Principal Sig-2	Stress Intens. ****	Margin of Safety
	(h)		(k)	(l)	(m)	(n)	(o)		(p)	(q)	(r)
0 End	60.00	24705[i]	0	25517	38292	63282	0	0	63282	63282	0.29
5 (+)	60.13	33641[j]	411	34453	39027	64497	679	-7	64504	64511	0.27
10 (+)	60.25	33327	820	34138	39001	64454	1356	-29	64483	64511	0.27
15.7 Corner	60.40	32657	1282	33469	38946	64363	2118	-70	64433	64503	0.27
20 (+)	58.60	30924	1572	31736	38804	64128	2597	-105	64233	64338	0.27
25 (+)	56.50	28758	1872	29570	38626	63833	3094	-150	63983	64133	0.28
30 (calc)	54.40	26459	2133	27271	38436	63521	3525	-195	63716	63911	0.28
35 (+)	50.87	23402	2288	24213	38185	63105	3781	-226	63331	63557	0.29
40 (+)	47.33	20364	2386	21176	37935	62692	3943	-247	62939	63186	0.30
45 (calc)	43.80	17394	2429	18206	37691	62289	4014	-258	62546	62804	0.30
50 (+)	44.00	15884	2643	16696	37567	62083	4368	-306	62389	62695	0.31
55 (+)	44.20	14238	2839	15050	37431	61860	4692	-354	62213	62567	0.31
60 (calc)	44.40	12468	3015	13280	37286	61619	4983	-400	62019	62420	0.31
65 (+)	45.68	10843	3247	11655	37152	61398	5366	-465	61863	62329	0.31
70 (+)	46.97	9022	3461	9834	37002	61150	5719	-530	61681	62211	0.32
75 (+)	48.25	7014	3655	7825	36837	60877	6040	-593	61471	62064	0.32
80 (+)	49.53	4831	3825	5643	36657	60581	6322	-653	61233	61886	0.32
85 (+)	50.82	2487	3970	3299	36465	60262	6560	-706	60968	61674	0.33
90 Side	52.10	0	4086	812	36260	59924	6752	-751	60675	61427	0.33

Minimum Margin of Safety: 0.27

Table 2.6.7-36 NAC-LWT Cask Cold Bolt Analysis – Normal Conditions

Nominal Diameter (in):	1.00	
Number of Bolts:	12	
Service Stress, Sy (ksi):	85	at a 70
Bolt Expansion (in/in):	8E-06	degree-F
Bolt Modulus (ksi):	27800	Service
Lid Expansion (in/in):	8E-06	Temperature
Lid Modulus (ksi):	28300	
Stress Area (in2):	0.6051	
Grip Length (in):	7.99	
Maximum Pressure (psi):	50	
Seal Diameter (in):	15.750	
Preload Torque (ft-lbs):	260	at RT
Nominal Room Temp, RT:	70	deg-F
Bolt Circle Diameter (in):	17.88	
Lid Diameter (in):	22.50	

Longitudinal Weight (lbs):	4941
Lateral Weight (lbs):	941
Service DT (degrees):	-90
[default value =]	0

CALCULATED LOADS & STIFFNESS

Bolt Thermal Load (lbs):	-594
Bolt Preload (lbs):	34770
Bolt Pressure Load (lbs):	812
Bolt Stiffness (lbs/in):	2.0E+06
Lid Stiffness (lbs/in):	2.2E+07

Angle wrt Vert. (Deg)	Impact Accel. (g)	<**** LOADS (lbs.) Impact Tension	Impact Shear	Bolt Tension Applied	Bolt Tension Net ****	<**** STRESSES (psi) Direct Tension	Principal Shear	Sig-1	Sig-2	Stress Intens. ****	Margin of Safety
0 End	60.00	24705	0	25517	36262	59928	0	0	59928	59928	0.42
5 (+)	60.13	33641	411	34453	36993	61135	679	-8	61143	61150	0.39
10 (+)	60.25	33327	820	34138	36967	61093	1356	-30	61123	61153	0.39
15.7 Corner	60.40	32657	1282	33469	36912	61002	2118	-73	61076	61149	0.39
20 (+)	58.60	30924	1572	31736	36771	60768	2597	-111	60879	60990	0.39
25 (+)	56.50	28758	1872	29570	36594	60475	3094	-158	60633	60791	0.40
30 (calc)	54.40	26459	2133	27271	36406	60165	3525	-206	60371	60577	0.40
35 (+)	50.87	23402	2288	24213	36156	59752	3781	-238	59990	60228	0.41
40 (+)	47.33	20364	2386	21176	35908	59341	3943	-261	59602	59863	0.42
45 (calc)	43.80	17394	2429	18206	35665	58940	4014	-272	59212	59484	0.43
50 (+)	44.00	15884	2643	16696	35541	58736	4368	-323	59059	59382	0.43
55 (+)	44.20	14238	2839	15050	35407	58514	4692	-374	58888	59262	0.43
60 (calc)	44.40	12468	3015	13280	35262	58275	4983	-423	58698	59121	0.44
65 (+)	45.68	10843	3247	11655	35129	58055	5366	-492	58547	59039	0.44
70 (+)	46.97	9022	3461	9834	34980	57809	5719	-560	58369	58930	0.44
75 (+)	48.25	7014	3655	7825	34816	57538	6040	-627	58165	58792	0.45
80 (+)	49.53	4831	3825	5643	34638	57243	6322	-690	57933	58622	0.45
85 (+)	50.82	2487	3970	3299	34446	56926	6560	-746	57672	58419	0.46
90 Side	52.10	0	4086	812	34243	56590	6752	-794	57384	58179	0.46

Minimum Margin of Safety: 0.39

Table 2.6.7-37 Summary of Neutron Shield Tank Analysis

Load Condition: 1-Foot End Drop and 1-Foot Side Drop

Description	Stress Magnitude (psi)	Margin of Safety[1]
Tank Shell	12,841	+0.07
Stiffener	11,746	+0.17
Stiffener Weld	2,424 lb/in	+0.23
Gusset Weld	1,418 lb/in	+1.10
Bottom End Plate	8,525	+1.79
Gusset Plate Cross Section	7,180	+LARGE
End Plate Welds	1,593	+LARGE
Top End Plate	11,172	+0.23

This table summarizes the stresses and margins for a design condition of 180 psig (Section 2.6.7.7.4), which envelops both the end drop and side drop conditions.

[1] Based on an allowable stress equal to the yield strength of Type 304 stainless steel at 250°F.

Table 2.6.7-38 Normal Transport Shield Tank Temperatures

Transport Condition	Average Fluid Temperature
100°F/Full Heat Load	227°F
68°F/No Heat Load	68°F
-20°F/Full Heat Load	99°F
-20°F/No Heat Load	-20°F

Table 2.6.7-39 Normal Transport Shield Tank Pressures

Transport Condition	Calculated Tank Pressure
PRVR	165 psig
100°F/Full Heat Load	25.6 psig
68°F/No Heat Load	0 psig

Table 2.6.7-40 Summary of Expansion Tank Analysis

Load Condition: 1-Foot End Drop and 1-Foot Side Drop

Description	Stress Magnitude (psi)	Margin of Safety[1]
Bottom/Top End Plate	3,375	+LARGE
Tank Shell	10,857	+0.26
Tank Stiffener	9,997	+0.37
Shell Weld	11,750	+0.17

This table summarizes the stresses and margins for a design condition of 180 psig (Sections 2.6.7.8 and 2.6.7.7.4), which envelops both the end drop and side drop conditions.

[1] Based on an allowable stress equal to the yield strength of Type 304 stainless steel at 250°F.

Table 2.6.7-41 Upper Ring – Cross-Section Principal Stresses

Section	P_m Stresses							$P_m + P_b$ Stresses						
	Component (ksi)				Principal (ksi)			Component (ksi)				Principal (ksi)		
	S_x	S_y	S_z	S_{xy}	S_1	S_2	S_3	S_x	S_y	S_z	S_{xy}	S_1	S_2	S_3
a-a	-0.8	4.7	1.9	-0.1	4.7	-0.8	1.9	-2.6	9.0	4.0	-1.0	9.1	-2.7	4.0
b-b	0.1	4.9	1.9	-0.2	4.9	0.1	1.9	1.2	8.0	2.9	-1.0	8.1	1.1	2.9
c-c	-0.1	5.5	2.0	0.5	5.5	-0.3	2.0	-0.2	6.5	2.6	1.0	6.6	-0.3	2.6

2.6.8 Corner Drop

According to 10 CFR 71.71(c)(8), this test is not applicable to the NAC-LWT cask because the cask is composed of materials other than fiberboard or wood.

2.6.9 Compression

According to 10 CFR 71.71(c)(9), this test is not applicable to the NAC-LWT cask because the package weight is greater than 5,000 kilograms (11,023 pounds).

2.6.10 Penetration

This condition is defined in 10 CFR 71.71(c)(10) as a 40-inch drop of a 13-pound, 1.25-inch diameter penetration cylinder with a hemispherical end, onto any exposed surface of the cask. The acceptance criteria is that there will be no adverse effects on either the ability of the cask to maintain containment of the contents or to survive a hypothetical accident. The following package components could potentially be damaged by this penetration impact: (1) the impact limiter, (2) the expansion tank, (3) the neutron shield tank, and (4) the port cover. An evaluation of a penetration impact on each of these components follows.

2.6.10.1 Impact Limiter - Penetration

The outer shell of the impact limiter resists puncture of the aluminum honeycomb by the penetration cylinder; however, this resistance is conservatively not considered in the analysis. The 13.0-pound penetration cylinder drops 40.0 inches producing 13.0 x 40.0 = 520 inch-pounds of energy, which is absorbed by the limiter. The minimum crush strength of the limiter is 3150 psi (Section 2.6.7.4.6), and the area of the penetration cylinder is 1.227 square inches. Therefore, using the minimum honeycomb crush strength and the average impact area in the conservation of energy equation, the penetration cylinder will compress the aluminum honeycomb to a depth of 520/[(3150)(1.227)/2] = 0.270 inch. This shallow depression does not adversely affect the performance of the impact limiter.

2.6.10.2 Expansion Tank - Penetration

The expansion tank shell is vulnerable to the penetration cylinder. This analysis documents the expansion tank shell structural adequacy to resist the penetration event.

The expansion tank shell is supported radially every 45 degrees by radial stiffeners. Assume the penetration cylinder impacts the shell at the center of the unsupported region as shown in Figure 2.6.10-1.

Chapter 12-5 of Strength of Materials (Singer) analyzes the problem of a falling object on an elastic member, and derives the following equation for the dynamic impact stress (S_{dyn}) in terms of the static displacement (δ_{st}) and the static stress (S_{st}), where the static values are for the weight (W) resting on the elastic member:

$$S_{dyn} = S_{st}\left[1 + \left[1 + \frac{2h}{\delta_{st}}\right]^{0.5}\right]$$

where:

h = height of drop = 40.0 inches

The static displacement is evaluated by assuming an arched plate with built-in edges (a stiffer plate provides a more conservative analysis), which is centrally loaded by the static weight (W) of the penetration cylinder. The dimensions of the arched plate representing the expansion tank are identified in Figure 2.6.12-2:

t = 0.315 in

r = 22.00 inches

a = 2πr x 45°/360° = 2π(22.0)(0.125) = 17.28 inches

b = 46.00 inches

Because the aspect ratio is small (2.66:1) the effect of the short edge fixity is considered. The effective width of the plate tangential to the radius is calculated by using Article 36 on page 133 of Formulas for Stress and Strain (Roark). Assume the circular area of the load is half the maximum; therefore, the radius c = $[(0.625)^2/2]^{0.5}$ = 0.442 inch, or 0.026(a). The table in the reference does not give a/b values of aspect ratios beyond 2:1; therefore, a/b = 2.0 is assumed.

Interpolation of the table in the reference for c = 0.026(a) yields e/b = 0.59; then, w_e = (0.59)(2)(17.28) = 20.39 inches. The effective width of the plate in the longitudinal direction is the (a) dimension. The amount of load transferred to each edge is calculated by assuming two fixed plates, free on two opposite edges and built-in on the other two, and solving for compatible deflections at the edge common to both plates. The equation for the percent of load taken by each plate is derived as follows:

The terms δ_a and δ_b, P_a and P_b, and k_a and k_b are deflections, loads, and spring constants for plates fixed on the (a) and (b) edges, respectively.

$$\delta_a = \delta_b;\ P_a/k_a = P_b/k_b;\ P_a = P_b(k_a/k_b)$$

$$P_a + P_b = W;\ P_b[(k_a/k_b) + 1] = W$$

$$P_b/W = k_b/(k_a + k_b);\ P_a/W = 1 - P_b/W$$

The spring constant (k_b) for edges fixed at (b) is evaluated as follows:

$k_b = P / \delta_b$

where:

P = any load

δ_b = the deflection due to P

"Charts Simplify Calculations for Moments and Deflections of Circular Arches" (Blake) gives the following equation for the static displacement (δ_b) of the arch with built-in edges:

$$\delta_b = (Pr^3/EI)K_b$$

where:

$E = 27 \times 10^6$ psi (300°F)

$r = 22.00$ in

$I = w_e t^3/12 = (20.39)(0.32)^3/12$
$= 0.0531$ in^3

$K_b = 0.00025$ (Blake, Figure 3, $\beta = 45°$)

thus

$$\delta_b = \frac{P(0.00025)(22.00)^3}{(27.0 \times 10^6)(0.0531)}$$

$$= P(1.857 \times 10^{-6}) \text{ in}$$

$$k_b = P/\delta_b = 5.385 \times 10^5 \text{ lb/in}$$

The spring constant (k_a) for edges fixed at (a) is evaluated as follows:

$k_a = P / \delta_a$

where:

P = any load

δ_a = the deflection due to P

The plate with the edges fixed at (a) is treated as a flat plate with a curvature, which increases the moment of inertia. The equation for the deflection at the center of the plate for a central load (P) is:

$\delta_a = P_b^3 / 192\ EI$
$= P(1.379 \times 10^{-5})$

where:

$I = r^3 t\ [a + \sin\alpha \cos\alpha - (2\sin^2\alpha)/\alpha]$ ("Research and Advanced Development Applied Mechanics," page 8)

$= 1.362 \text{ in}^4$

$\alpha = \pi/8$ radians

then

$k_a = P/\delta_a = 7.252 \times 10^4$ lb/in

and

$P_b/W = (5.385 \times 10^5)/[(7.252 \times 10^4) + (5.385 \times 10^5)]$

$= 0.881$, or P_b is 88.1 percent of W

$P_a/W = 1 - 0.881 = 0.119$, or P_a is 11.9 percent of W

The static deflection is calculated using the load, P_a, and the spring constant for the curved plate as a longitudinal beam:

$\delta_{st} = 0.881 \text{ W}/k_a = 0.881(13.00)/(5.385 \times 10^5)$

$= 2.128 \times 10^{-5}$ in

The static stress is calculated using the formulas from "Charts Simplify Calculations for Moments and Deflections of Circular Arches" (Blake) for an arched plate with a central load (P_a) as follows:

The static bending moment (M_{st}) at the load for the arched plate with built-in edges resulting from the central load P_b is:

$M_{st} = H_b r(\sin\theta - \sin\alpha) - Rr(\cos\alpha - \cos\theta) + M_o$

where:

$M_o = - P \text{ r } K_m = -0.881 \text{ W r } K_m$

$H_b = P \, K_{hb} = 0.881 \text{ W } K_{hb}$

$\theta = 90.0°$

$\alpha = 67.5°$

$R = 0.5 \, (0.881W) = 0.441W$

$K_m = 0.0225$

$K_{hb} = 2.375$ (Blake, Figure 3, $\beta = 45°$)

then

$H_b = (0.881)(13.0)(2.375) = 27.20$ lbs

$R = 0.441(13.0) = 5.73$ lbs

$M_o/r = -0.881(13.0)(0.0225) = -0.258$ in-lb

M_{st} = 22.00[27.20(sin 90.0° - sin 67.5°) - 5.73 (cos 67.5° - cos 90.0°) + (-0.258)]
= -8.37 in-lb

The static stress, determined from the elastic plate formula, is:

$$S_{st} = \frac{6M_{st}}{w_e t^2} + \frac{H_b}{w_e t}$$

$$= 29.06 \text{ psi}$$

Substitution of S_{st} and δ_{st} into the equation for the dynamic impact stress produces:

$$S_{dyn} = 29.06 \left[1 + \left[1 + \frac{(40.0)}{2.128 \times 10^{-5}}\right]^{0.5}\right]$$

$$= 56,374 \text{ psi}$$

This stress exceeds the 22,500 psi yield strength of Type 304 stainless steel at 300°F, but not the 66,000 psi ultimate strength; therefore, it is concluded that an impact by the penetration cylinder would produce a permanent deformation, but it would not rupture the expansion tank shell.

The expansion tank meets the requirements for penetration resistance per 10 CFR 71.71(c)(10).

2.6.10.3 Neutron Shield Tank - Penetration

The neutron shield tank shell is vulnerable to the penetration cylinder. This analysis documents the neutron shield tank shell structural adequacy to resist the penetration event.

The neutron shield tank shell is supported radially every 45 degrees by rigid stiffeners. Assume the penetration cylinder impacts the shell at the center of the unsupported region as shown in Figure 2.6.10-1.

The static displacements and stresses resulting from the impact of a 13-pound penetration cylinder are evaluated by the use of the ANSYS finite element method. The neutron shield tank shell is modeled as a complete circle, represented by 80 two-dimensional elastic beam (STIF3) elements, each spanning a 4.5-degree arc. Each stiffener is represented by four STIF3 elements. One edge of each stiffener is rigidly attached to the outer shell of the cask.

The dimensions of the arched plate representing the shield tank are identified in Figure 2.6.10-2:

t = 0.24 in

r = 19.345 inches

$a = 2\pi r \times 45°/360°$

$= 2\pi(19.345)(0.125)$

$= 15.12$ inches

$= 164.00$ inches

Because the aspect ratio is large (10.7:1), the effect of the short edge fixity is ignored. The effective width of the plate tangential to the radius is calculated by using Article 36 on page 133 of Formulas for Stress and Strain (Roark). As derived in Section 2.6.10.2, the radius of the load is 0.442 inch, or 0.0292(a). The maximum tabular value in the reference for b/a = 2 is conservatively assumed. Interpolation for c = 0.0292(a) gives e/b = 0.598; then, w_e = (0.598)(2)(15.12) = 18.084 inches.

The properties of the beam elements are as follows:

$E = 27 \times 10^6$ psi at 200°F

$A = 18.084 \times 0.24$

$= 4.268$ in^2

$I = 18.084 \times (0.24)^3/12$

$= 0.0198$ in^4

From the results of the ANSYS finite element analysis, the static deflection and stress at the point of load application are 0.0003451 inch and 116.18 psi, respectively. Substitution of S_{st} and δ_{st} into the equation for the dynamic impact stress (Section 2.6.10.2) produces:

$$S_{dyn} = 116.18 \left[1 + \left(1 + \frac{2(40)}{0.0003451}\right)^{0.5}\right]$$

$$= 56{,}054 \text{ psi}$$

The margin of safety for the noncontainment structure during an accident event is:

$$M.S. = \frac{S_{tu}}{S_{dyn}} - 1 = \frac{66{,}000}{56{,}054} - 1 = \underline{+0.18}$$

Impact by the penetration cylinder may produce a permanent deformation, but it will not rupture the neutron shield tank; therefore, the neutron shield tank meets the requirements for penetration resistance as specified in 10 CFR 71.71(c)(10).

2.6.10.4 Port Cover - Penetration

The port covers are analyzed for impact by the penetration cylinder. This analysis documents the structural adequacy of the port cover to resist the penetration event.

During normal operations, particularly during fuel loading, it is possible that a hand tool could drop onto the NAC-LWT cask. The following analysis is performed to demonstrate that such an occurrence (presumed to be a 13-pound, 1.25-inch diameter projectile dropped through a distance of 40 inches) will not cause loss of the cask containment capability as a result of damage to the port cover. The port cover is shown in Figure 2.6.10-3.

The static displacement and stress is evaluated by assuming the port cover is loaded at the center by the static weight (W) of the penetration cylinder. The port cover is stiffened by the attached cylinder wall and is clamped by the bolts. This geometry requires that the displacement be evaluated in two steps - (1) from the bolt circle to the outside diameter of the cylinder, and (2) from the inside diameter of the cylinder to the center of the plate.

The first step in the calculation is made by using equation (92) from Theory of Plates and Shells (Timoshenko, 1940) and treating the whole plate as being clamped at the bolt circle and finding the displacement at the outside diameter of the cylinder, $a_1 = 1.875$, $r_1 = 1.436$, as follows:

$$\delta_{st} = -\frac{Wr^2}{8\pi D}\ln\frac{r}{a} + \frac{W(a^2 - r^2)}{16\pi D}$$

$$D = \frac{Et^3}{12(1 - \nu^2)}$$

where:

ν = Poisson's ratio = 0.30

$$\delta_{st_1} = -\frac{0.75W(1 - \nu^2)}{\pi Et^3}\left[(a_1^2 - r_1^2) + 2\ln\frac{r_1}{a_1}\right]$$

$$= -9.3505 \times 10^{-8} \text{ in}$$

The second step in the calculation is to treat the portion of the plate from the inside diameter of the cylinder to the center of the plate as clamped, $a_2 = 0.8125$ and $r_2 = 0$, using the same equation, which reduces as follows:

$$\delta_{st_2} = -\frac{0.75Wa_2^2(1 - \nu^2)}{\pi Et^3}$$

$$= -6.7022 \times 10^{-8} \text{ in}$$

The total static displacement of the plate is:

$$\delta_{st} = \delta_{st_1} + \delta_{st_2} = -1.6043 \times 10^{-7} \text{ in}$$

The static stress at the point of impact is calculated using equation (97) from Theory of Plates and Shells (Timoshenko, 1940) using the portion of the plate inside the cylinder as a plate with clamped edges as follows:

$$S_{st} = \frac{W(1 - \nu)}{t^2}\left[0.485 \ln\left(\frac{a_2}{t}\right) + 0.52\right]$$

$$= 3.6974 \text{ psi}$$

Substitution of S_{st} and δ_{st} into the equation for dynamic impact stress referenced in Section 2.6.10.2 produces:

$$S_{dyn} = 3.6974\left[1 + \left(1 + \frac{2(40.0)}{1.6043 \times 10^{-7}}\right)^{0.5}\right]$$

$$= 82{,}570 \text{ psi}$$

The margin of safety against yield strength of the SA-705, Grade 630, Type H1150 stainless steel port cover at 300°F is:

MS = 93,000/82,570 - 1 = +0.23

The port cover meets the requirements for penetration resistance according to 10 CFR 71.71(c)(10).

2.6.10.5 Alternate Port Cover – Penetration

This analysis documents the adequacy of the alternate port cover design to resist a postulated normal condition of transport penetration event. Analyses presented evaluate the consequences of the penetration event on the port cover, attachment bolt stresses and inertial loads acting on the port cover to reduce the compressive load on the primary O-ring. A bounding analysis evaluating the consequences of differential thermal expansion on the attachment bolt stresses and the compressive load applied to the port cover primary O-ring is presented in Section 2.7.2.4.3.

The alternate port cover design is shown in Figure 2.6.10-3. The alternate port cover design includes the primary O-ring between the inner face of the port cover barrel and the sealing surface located in the cask top forging. The secondary (test) O-ring is located in a groove on the barrel of the port cover body. Both O-rings are manufactured from Viton®. The alternate port cover body is fabricated from Type 630, 17-4 PH precipitation-hardened stainless steel. The alternate port cover bolts are SA-193 GR B6 (Type 410 stainless steel) socket-head cap screws.

Normal operating condition requirements postulate a penetration event intended to represent a hand tool that inadvertently drops and strikes the port cover installed on the cask. A steel bar of

1-1/4 inch diameter with a hemispherical head and weighing 13 pounds simulates a tool for analysis purposes. The steel bar is assumed to be dropped from a height of 40 inches. This analysis shows that there is no loss of containment capability, even if the tool strikes the alternate port cover in its most vulnerable location.

The bolt preload applies the required compressive force on the face O-ring to maintain a seal between the port cover and the top forging. The O-ring compressive force required to maintain a seal is 120 pounds per linear inch of O-ring, according to the manufacturer. Using the average radius of the O-ring cavity to determine the length of the O-ring, the force to maintain a seal is 861 pounds. The force applied by the bolt preload torque is calculated as:

$$F = T / 0.2 (d)$$

where:

F = tensile load generated due to bolt torque, pounds

T = installation torque, 100 inch-pounds

d = minimum cross-sectional diameter, 0.281 inch

The calculated force applied by torquing one port cover bolt is 1,780 pounds, approximately twice the compressive load necessary to maintain a seal. There are three bolts for each port cover.

The tensile force applied by the port cover bolts to maintain the load on the O-ring is evaluated. ANSYS is used to model the reaction of the port cover structure to the compressive applied loads. The port cover bolt load acts against the load needed to load the O-ring through the port cover body. Two load cases for normal conditions of transport penetration loading and two load cases for hypothetical accident conditions pin puncture (presented in Section 2.7.2.4.3) are evaluated.

Finite element analysis is used to determine the dynamic impact load resulting from the penetrating loading event. Then the port cover bolt torque preload and pressure loads are evaluated and are combined with the dynamic impact load to determine the total compression load on the inner face O-ring.

A three-dimensional model of the port cover is used to determine the static deflection when a 13-pound load is applied at the center of the port cover exterior. The port cover is a hollow barrel, with a flat thick plate at the outer end of the barrel. The plate and barrel slide into a stepped cylindrical bore in the upper end forging. The only exposed port cover surface is the outer face of the 1-inch thick port cover bolting flange. Deflection of the port cover due to the static load is calculated and used to determine the equivalent dynamic load, resulting from the 40-inch free-fall of the steel bar.

A one-sixth (1/6) section, three-dimensional finite element model of the alternate port cover, shown in Figure 2.6.10-4, was constructed using ANSYS Version 5.5. The model is a 60° wedge section of the port cover body. The body is constructed using SOLID45 3-D structural solid elements, CONTAC52 node-to-node contact elements, and BEAM4 three-dimensional two node beam elements. The node-to-node contact elements are used at the inner end surface, where the O-ring is located, to evaluate the sealing force. An initial strain is specified in the BEAM4 elements to simulate the initial bolt torque preload force. Since the port cover bolt is positioned on a model symmetry plane, the calculated bolt preload force applied to the port cover is half (1/2) of the total preload force. A force of 120 lbs. per linear inch of O-ring is required to maintain a seal. Using the average radius of O-ring cavity, the total required sealing force is calculated to be 861 pounds. Since the model is 1/6 of the actual port cover, this corresponds to a force of 861/6 = 143.5 lbs. required in the model to maintain sealing.

Symmetry boundary conditions are applied to the model at 0° and 60° surfaces. Model nodal coordinate systems have been rotated in the cylindrical coordinate system to facilitate the application of the symmetry boundary conditions. To prevent axial motion of the port cover, the port cover bolt is restrained axially at the bottom. The node-to-node contact elements on the inner end surface, the "ground" node of the contact elements, is fixed in all degrees-of-freedom.

Two simplifying assumptions were made in the ANSYS analysis consistent with accepted engineering practice. First, it is assumed for small deflections that materials behave elastically, and second, nominal dimensions are the basis for the ANSYS model geometry.

The equivalent dynamic loading, from Ugural and Fenster, is calculated using the following relation:

$$P_{dyn} = W\,(1+ (1 + 2h / \delta_{st})^{1/2})$$

where:

P_{dyn} = dynamic load resulting from weight (W) free falling a height (h), lbs

W = weight, 13 lbs

h = drop height, 40 inches

δ_{st} = static deflection resulting from weight (W) on plate, inches

The dynamic penetration load was calculated to be 11,334 pounds, resulting from the 13-pound steel pin dropping a distance of 40 inches on to the port cover. The sealing surface bearing stress is calculated to be 4,027 psi, which results in a margin of safety of +4.9 compared with yield strength of the upper forging. The dynamic load on the port cover is applied as a bearing load, which will pass through the alternate port cover body, to the top forging. Also, the dynamic load

increases the compressive force on the inner end O-ring, trapped in an O-ring groove at the bottom of the port cover body. Thus, the primary seal is not affected.

Bolt preload alone and preload combined with the normal operating pressure are the two load cases evaluated for normal conditions of transport. The normal condition cavity pressure calculated in Section 3.4.4 is 28.3 psia. The allowable bolt stress of 2 S_m or 50,600 psi is conservatively evaluated at 400°F. The normal condition analysis results are:

Load Case	Preload	Preload + Normal Pressure
Evaluation Temperature (°F)	400	400
Calculated Seal Force (lbs)	891	883
Percent O-ring compression (20-30% compression to maintain seal)	25.2[1]	25.2[1]
Bolt Tensile Force (lbs)	1781	1782
Bolt Stress (based on Tensile Stress Area) (psi)	28,720	28,728
Bolt Margin of Safety	0.76	0.76

[1] Maximum compression possible due to metal to metal contact with O-ring fully compressed in O-ring groove.

Figure 2.6.10-1 Impact of Penetration Cylinder on Neutron Shield Tank and Expansion Tank – Points of Impact

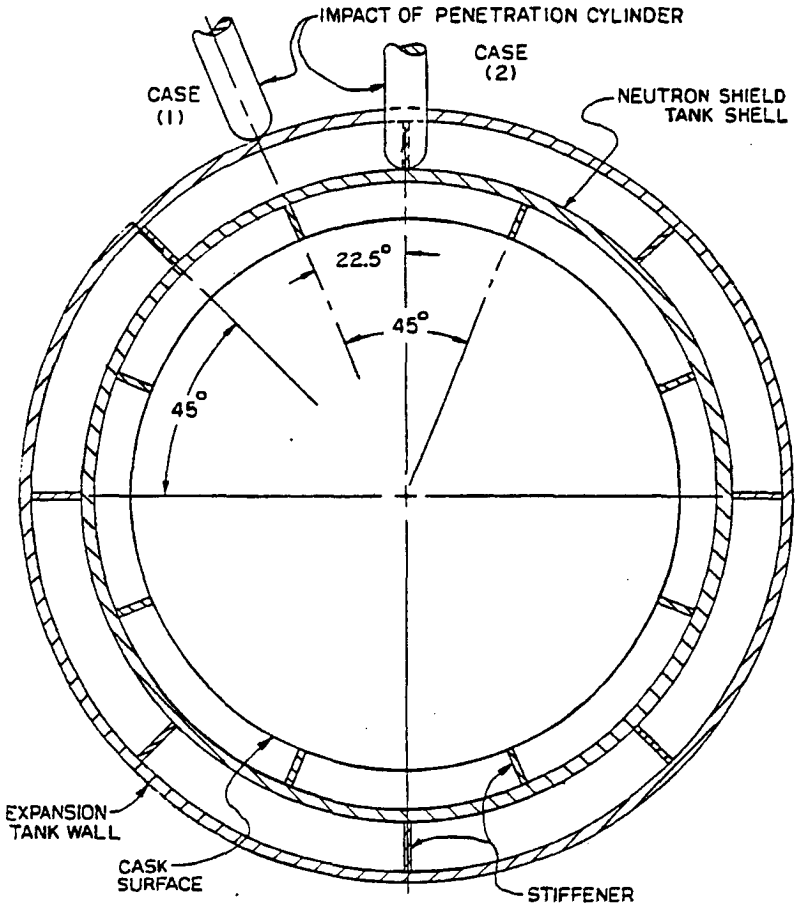

Figure 2.6.10-2 Impact of Penetration Cylinder on Neutron Shield Tank and Expansion Tank – Details for Analysis

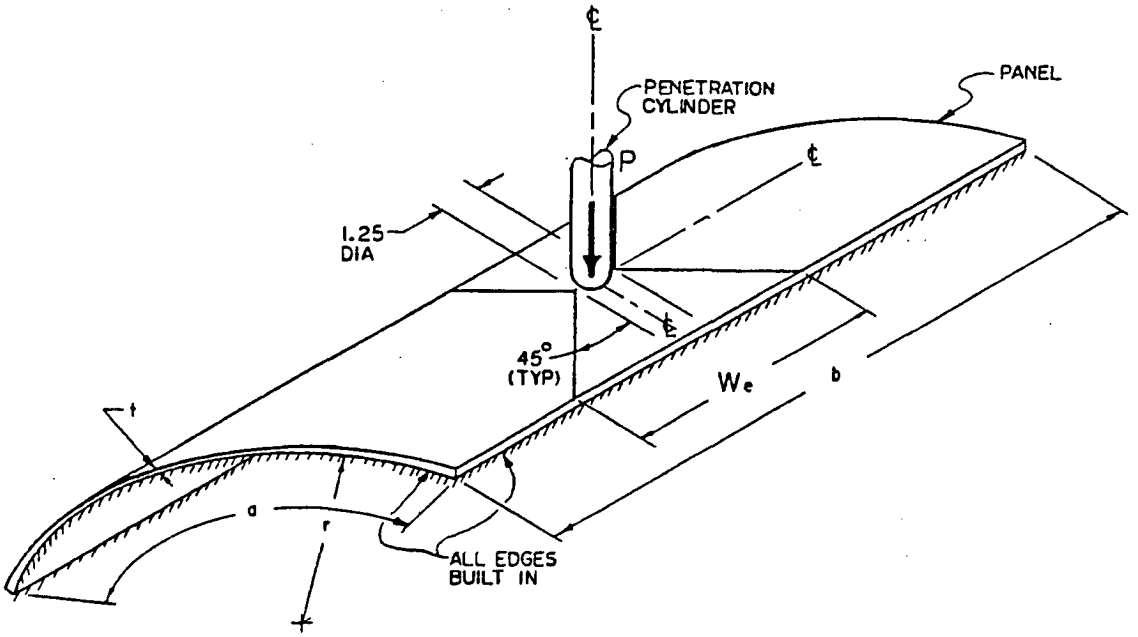

Figure 2.6.10-3 Impact of Penetration Cylinder on Port Cover

Figure 2.6.10-4 One-Sixth Model of the Alternate Port Cover – 60° Symmetry

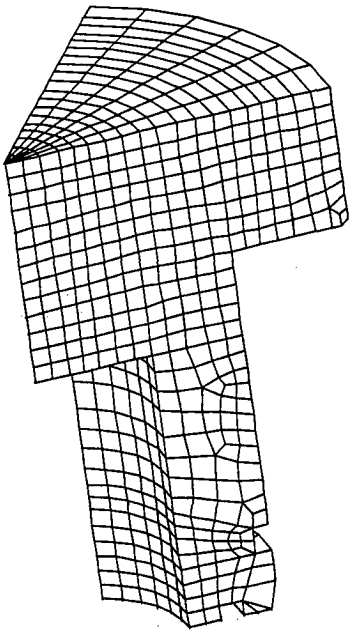

2.6.11 Fabrication Conditions

The process of manufacturing the NAC-LWT cask can introduce thermal stresses in the inner and outer shells as a result of pouring molten lead between them. These thermal stresses are evaluated to provide assurance that the manufacturing process does not adversely affect the normal operation of the cask or its ability to survive an accident. Residual stresses in the containment vessel and the outer shell induced by shrinkage of the lead shielding after the lead pouring operation are relieved early in the life of the cask because of the low yield strength of lead. Any residual stresses in the containment vessel shell due to inelastic strain associated with the secondary local bending stresses, which result from the lead pour thermal gradient, are considered in the total stress range for normal and accident load conditions according to Regulatory Position 7 of Regulatory Guide 7.6.

For the lead pouring process (Appendix 8.3), the temperature of the cask shells is controlled between 550°F (288°C) and 650°F (343°C), and the lead temperature before pouring is between 698°F (370°C) and 790°F (421°C). Heating of the cask is performed using heaters inside the inner shell and heating rings around the outer shell. Heat up is time controlled; consistent with maintaining shell temperatures uniformly. The shell temperatures are measured by thermocouples attached to the shell surfaces. A portable thermometer is also used to measure temperature at any location. Heating is carried out after all the preparations have been completed including melting of the lead in order to minimize the time that the cask is heated.

The lead is poured after the cask reaches the specified temperatures. Prior to lead pouring, the cask flange area is heated with hand-held burners to approximately 572°F (300°C). Pouring is carried out continuously using a filling tube with its open end maintained under the lead surface. The pouring time is kept as short as possible. During pouring, the interior heaters and exterior heating rings are continuously energized.

The cooling process consists of sequentially turning the heating rings and interior heaters off, starting from the lowest point, and of spraying the cask with water from the outside. Molten lead is maintained until the upper surface starts to solidify. This process allows the molten lead to fill the space created by the lead shrinkage as it cools.

2.6.11.1 Lead Pour

2.6.11.1.1 Cask Shell Geometry

At 70°F, the Type XM-19 stainless steel shell geometry is as follows:

Inner Shell		
Inside Diameter	d_i	13.375 inches
Outside Diameter	d_o	14.875 inches
Shell Thickness	t_i	0.75 in
Outer Shell		
Inside Diameter	D_i	26.375 inches
Outside Diameter	D_o	28.620 inches
Shell Thickness	T_o	1.12 inches

2.6.11.1.2 Stresses Due to Lead Pour

The melting point of lead is 620°F. Assuming that the lead and the inner and outer shells are uniformly at this temperature, the hydrostatic pressure produced by the column of lead is:

$$p = \rho h$$
$$= 72 \text{ psi}$$

where:

$\rho = 0.41$ lb/in^3 (lead density)

$h = 175$ inches (height of lead column)

At 620°F, the shell geometric dimensions are:

$$d'_o = d_o (1 + \alpha \Delta T)$$
$$D'_i = D_i (1 + \alpha \Delta T)$$
$$t' = t (1 + \alpha \Delta T)$$

where:

$$\alpha = 9.05 \times 10^{-6} \text{ in/in/°F at 620°F}$$

$$\Delta T = 620 - 70 = 550°F$$

$$d'_o = 14.875 \left[1 + 9.05 \times 10^{-6}(550)\right] = 14.9490 \text{ in}$$

$$D'_i = 26.375 \left[1 + 9.05 \times 10^{-6}(550)\right] = 26.5063 \text{ in}$$

$$t'_i = 0.75 \left[1 + 9.05 \times 10^{-6}(550)\right] = 0.7537 \text{ in}$$

$$t'_o = 1.12 \left[1 + 9.05 \times 10^{-6}(550)\right] = 1.1256 \text{ in}$$

The inner shell is subjected to an external hydrostatic pressure and the outer shell to an internal hydrostatic pressure, of 72 psi. This causes the inner shell to decrease in diameter and the outer shell to increase in diameter.

The inner shell decreases in size radially (Roark and Young, Case 1b, page 448):

$$\Delta r_o = \frac{q(r_o')^2}{Et_i'} = \frac{-72(14.9490/2)^2}{25.2 \times 10^6(0.7537)} = -0.0002 \text{ in}$$

where:

$E = 25.2 \times 10^6$ psi at 620°F.

The outer shell increases in size radially:

$$\Delta R_i = \frac{q(R_i')^2}{Et_o'} = \frac{72(26.5063/2)^2}{25.2 \times 10^6(1.1256)} = 0.0004 \text{ in}$$

The shell geometries at 620°F and 72 psi hydrostatic pressure are:

$d''_o = 14.9490 - 2(0.0002) = 14.9486$

$D''_i = 26.5063 + 2(0.0004) = 26.5055$

The hoop stresses in the inner and outer shells at 620°F are:

$$S_{hi} = \frac{Pd_o''}{2t_i'}$$

$$= \frac{-72(14.9486)}{2(0.7537)} = -714 \text{ psi (inner shell)}$$

$$S_{ho} = \frac{PD_i''}{2t_o'}$$

$$= \frac{72(26.5055)}{2(1.1256)} = 847 \text{ psi (outer shell)}$$

2.6.11.2 Cooldown

2.6.11.2.1 Hoop Stresses

Lead decreases in volume during solidification. As the lower lead region solidifies, the molten lead above fills the shrinkage void between the solidifying lead and the inner and outer shells, thus, maintaining the 72 psi pressure on the shells.

The stress-free inner and outer radii of the solidified lead can be calculated (Roark and Young, Case 1a and 1c, page 504) as:

$$\Delta a = \frac{q}{E}\left[\frac{2ab^2}{a^2 - b^2}\right] - \frac{qa}{E}\left[\frac{a^2 + b^2}{a^2 - b^2} - \nu\right]$$

$$= 0.0004 \text{ in}$$

$$\Delta b = \frac{qb}{E}\left[\frac{a^2 + b^2}{a^2 - b^2} + \nu\right] - \frac{q}{E}\left[\frac{2a^2b}{a^2 - b^2}\right]$$

$$= 0.0002 \text{ in}$$

where:

q = -72 psi pressure

E = 1.47 x 10^6 psi

ν = 0.4 Poisson's ratio

a = 26.5055/2 = 13.2527 inches

b = 14.9486/2 = 7.4743 inches

then

$$R_{o\ell} = 13.2527 + 0.0004 = 13.2531 \text{ in}$$

$$R_{i\ell} = 7.4743 + 0.0002 = 7.4745 \text{ in}$$

When cooled to 70°F, the inside radius of the lead is such that:

$$R'_{i\ell}\,(1 + \alpha\Delta T) = R_{i\ell}$$

where:

$R'_{i\ell}$ = inside radius of the stress-free lead at 70°

α = 20.4 x 10^{-6} in/in/°F

ΔT = 550°F (620-70)

then

$$R'_{i\ell} = 7.3936 \text{ in}$$

likewise

$$R'_{o\ell} = R_{o\ell}/(1 + \alpha\Delta T) = 13.1105 \text{ in}$$

The outside radius of the stress-free inner shell is 14.875/2 = 7.4375 inches, which is larger than the stress-free inner radius of the lead shell. Therefore, there exists an interface pressure between the lead and the inner shell after cooling to 70°F. The interface pressure, when acting on the lead cylinder and inner shell, is such that the inner radius of the lead cylinder is the same as the outer radius of the inner shell (Roark and Young, Case 1a, page 504).

$$R''_{i\ell} = b + \Delta b$$

$$= b + \frac{qb}{E}\left[\frac{a^2 + b^2}{a^2 - b^2} + \nu\right]$$

where:

$R''_{i\ell}$ = inside radius of lead cylinder at 70°F

$\nu = 0.4$

$E = 2.28 \times 10^6$ psi

$a = 13.1105$ inches

$b = 7.3936$ inches

then

$$R''_{i\ell} = 7.3936 + \left[\frac{7.3936q}{2.28 \times 10^6}\right]\left[\frac{13.1105^2 + 7.3936^2}{13.1105^2 - 7.3936^2} + 0.4\right]$$

The outside radius of the inner shell at 70°F under the interface pressure q (Roark and Young, Case 1c, page 504) is:

$$r_o = a_s - \Delta a_s$$

$$= a_s - \frac{qa_s}{E}\left[\frac{a_s^2 + b_s^2}{a_s^2 - b_s^2} - \nu\right]$$

where:

r_o = outside radius of inner shell at 70°F

$a_s = 14.875/2 = 7.4375$ inches

$b_s = 13.375/2 = 6.6875$ inches

$E = 28.3 \times 10^6$ psi

$\nu = 0.275$

then

$$r_o = 7.4375 - \left(\frac{7.4375q}{28.3 \times 10^6}\right)\left(\frac{7.4375^2 + 6.6875^2}{7.4375^2 - 6.6875^2} - 0.275\right)$$

Equating $R''_{i\ell}$ and r_o and solving for q:

q = 4401 psi interface +pressure

The lead shell geometry is:

$$R''_{i\ell} = 7.3936 + \left(\frac{7.3936(4401)}{2.28 \times 10^6}\right)\left(\frac{13.1105^2 + 7.3936^2}{13.1105^2 - 7.3936^2} + 0.4\right)$$

$$= 7.4269 \text{ in}$$

$$R''_{o\ell} = R'_{o\ell} + \frac{q}{E}\left(\frac{2R'_{o\ell}\, R'^{2}_{i\ell}}{R'^{2}_{o\ell} - R'^{2}_{i\ell}}\right)$$

$$= 13.1105 + \left(\frac{4401}{2.28 \times 10^6}\right)\left(\frac{2 \times 13.1105 \times 7.3936^2}{13.1105^2 - 7.3936^2}\right)$$

$$= 13.1341 \text{ in}$$

The corresponding maximum lead shell hoop stress is:

$$S_{hPb} = (4401)\left(\frac{13.1341^2 + 7.4269^2}{13.1341^2 - 7.4269^2}\right)$$

$$= 8538 \text{ psi}$$

Obviously, the lead cannot sustain the above stress. The interference between the lead shell and the inner shell is 0.0439 inches (7.4375 - 7.3936). To fully accommodate this interference, the lead must undergo a strain of 0.0439/7.3936 = 0.0059 or 0.59 percent. From Figure 21 of NUREG/CR-0481, the lead stress for the above strain is 850 psi. The corresponding interface pressure for this stress in the lead shell is:

$$q = (S)\left[\frac{R''^{2}_{o\ell} - R''^{2}_{i\ell}}{R''^{2}_{o\ell} + R''^{2}_{i\ell}}\right]$$

$$= (850)\left[\frac{13.1341^2 - 7.4269^2}{13.1341^2 + 7.4269^2}\right]$$

$$= 438 \text{ psi interface pressure}$$

The change in geometry of the inner shell for this interface pressure is:

$$\Delta a = \left[\frac{-438}{28.3 \times 10^6}\right]\left[\frac{2(7.4375)(6.6875^2)}{7.4375^2 - 6.6875^2}\right]$$

$$= 0.0010 \text{ in}$$

This can conservatively be neglected in the analysis. The inner shell hoop stress is:

$$S_{his} = (-438)\left[\frac{7.4375^2 + 6.6875^2}{7.4375^2 - 6.6875^2}\right]$$

$$= -4136 \text{ psi}$$

2.6.11.2.2 Axial Stresses

Axial stresses also develop in the lead shell and inner shell during fabrication as a result of the unequal shrinkage of the lead and steel shells. Assume bonding of the lead shell to the inner shell during the cooldown process after completion of lead pouring. The strain in the lead, when cooled to 70°F, is:

$$\epsilon = (\alpha_\ell - \alpha_s)\Delta T$$

$$= 0.0062 \text{ in/in or } 0.62 \text{ percent}$$

where:

$\alpha_\ell = 20.4 \times 10^{-6}$ in/in/°F

$\alpha_s = 9.05 \times 10^{-6}$ in/in/°F

$\Delta T = 620 - 70 = 550$°F

Extrapolating from Figure 2.3.1-1, for this strain, an axial stress of approximately 850 psi exists in the lead shell. The total force in the lead caused by assuming non-deformability of the inner shell is:

$$P_{sPb} = p_{\ell} A_{\ell}$$

$$= 850\pi(13.1875^2 - 7.4375^2)$$

$$= 316,687 \text{ lb tensile force}$$

The corresponding compression stress in the inner shell to maintain equilibrium is:

$$P_{SST} = \frac{P_s}{A_s}$$

$$= \frac{-316,687}{\pi[(7.4375)^2 - (6.6875)^2]}$$

$$= -9515 \text{ psi}$$

This is a highly conservative estimate of the compressive stress that can develop in the inner shell for the following reasons:

1. It assumes axial non-deformability of the inner shell and no load development in the outer shell. Any pre-strain in the inner shell reduces the total strain, thus reducing the lead stress and axial force.
2. Creep in the lead is neglected. This also reduces the stress and force in the lead (Section 2.6.11.3).
3. It assumes the strain is uniform through the thickness of the lead shell. A particle away from the inner shell develops less strain, consequently lower stress, than a particle adjacent to the inner shell; this also reduces the total force in the lead shell.

2.6.11.2.3 Effects of Temperature Differential During Cooldown

The preceding analyses assume that the inner and outer shells and the lead are always at the same temperature at any time during the cooldown process. This assumption may not be true under actual conditions. However, because of the high thermal conductivity of the stainless steel and the lead and the time-controlled cooldown process, the temperature differential between any two of the above shells is kept to a minimum. For the effect of temperature differential on the stresses in the shells, a temperature differential of 300°F is conservatively assumed. A temperature differential of this magnitude is very unlikely during the actual lead pour.

When the inner shell is cooler than the lead, the interference between them, as well as the corresponding interface pressure and hoop stresses are less than for the case of equal temperatures. Hence, the preceding analysis is conservative.

When the inner shell is hotter than the lead shell, an analysis is required. Assume the temperature of the inner shell to be 370°F and that of the lead to be 70°F. The inner radius of the stress-free lead shell at 70°F is 7.3936 inches (R'_{il}); the outer radius of the inner shell at 370°F is:

$$R = 7.4375\ [1 + 8.74(10^{-6})(300)]$$
$$= 7.4570 \text{ inches}$$

The interference between the inner shell and the lead is 0.0634 inches. To fully accommodate this interference, the lead has to undergo a strain of 0.0634/7.3936 = 0.0086 inch/inch or 0.86 percent. From Figure 21 of NUREG/CR-0481, the hoop stress in the lead is approximately 900 psi for a 0.0086 inch/inch strain. The interface pressure is:

$$q = (900)\left[\frac{13.1105^2 - 7.3936^2}{13.1105^2 + 7.3936^2}\right]$$

$$= 466 \text{ psi}$$

The hoop stress in the inner shell becomes:

$$S_{his} = (-466)\left[\frac{7.4375^2 + 6.6875^2}{7.4375^2 - 6.6875^2}\right]$$

$$= -4400 \text{ psi}$$

Note that the thermal expansion or contraction of a shell subjected to a constant pressure does not affect the hoop stress; i.e.,

$$S_h = q\left[\frac{(ka)^2 + (kb)^2}{(ka)^2 - (kb)^2}\right] = q\left[\frac{a^2 + b^2}{a^2 - b^2}\right]$$

where:

$$k = 1 + \alpha\Delta T$$

This -4400 psi hoop stress (the inner shell is 300°F hotter than the lead shell) reduces to the previously calculated hoop stress of -4136 psi as both the inner shell and lead reach an ambient temperature of 70°F. This, of course, does not take into account the beneficial effect of the creep properties of the lead.

The axial stress in the inner shell also increases when the inner shell is 300°F hotter than the lead shell. The axial stress of -9515 psi calculated when both the inner shell and lead shell are at 70°F is recalculated for the inner shell temperature of 370°F, $\alpha = 8.74 \times 10^{-6}$:

$$\epsilon_{\ell} = (20.38 - 9.05)(10^{-6})(620 - 70) + (8.74 \times 10^{-6})(370 - 70)$$

$$= 0.0085 \text{ in/in or } 0.85 \text{ percent}$$

Referring to Figure 21 of NUREG/CR-0481, the axial stress in the lead is approximately 900 psi. The corresponding axial stress in the inner shell is -10,300 psi. As before, cooling of the inner shell reduces this stress. The previous assumptions apply in arriving at this inner shell compressive stress.

Temperature differentials between the inner and outer shells are of no consequence, since the axial restraint between them is placed after cooldown when the cask is at a uniform ambient temperature. Welding of the outer shell and the cask bottom to the bottom ring after cooldown is, therefore, a necessary fabrication step.

The question of buckling of the inner shell due to the combined effect of external pressure and fabrication inaccuracies must also be addressed. According to the "ASME Boiler and Pressure Vessel Code," Article NE-4221.1, the difference between the maximum and minimum inside diameters at any cross section shall not exceed 1 percent of the nominal diameter at the cross section under consideration. This amounts to (0.01)(13.375) or 0.13375 inch. The relation between the initial radial deviation, ω_i, and the maximum and minimum diameter (Timoshenko, 1976, Figure 7-10) is:

$$D_{max} = D_{nom} + 2\omega_1$$

$$D_{min} = D_{nom} - 2\omega_1$$

thus

$$D_{max} - D_{min} = 4\omega_1$$

or

$$\Delta D = 4\omega_1$$

Hence, the maximum initial radial deviation allowed is:

$$\omega_{max} = \Delta D/4 = 0.13375/4 = 0.0334 \text{ in}$$

From Timoshenko, 1976, equation (7-16), page 293:

$$S_{cr} = \left[\frac{E_t}{1 - \nu^2}\right]\left[\frac{h}{2R}\right]^2$$

$$= 81,435 \text{ psi}$$

where:

$E_t = 26.7 \times 10^6$ psi at 370°F

$\nu = 0.275$

h = shell thickness = 0.75 in

R = shell radius = 7.0625 inches

This critical buckling stress is well beyond the yield point of the shell material and, thus, cannot exist. Per Timoshenko, 1976, page 294, $S_{cr} = S_{Yp} = 42,000$ psi at 370°F can be used. Then from Timoshenko, 1976, equation (7-12), page 294:

$$q_{cr} = \left[\frac{E}{4(1 - \nu^2)}\right]\left[\frac{h}{R}\right]^3$$

$$= S_{cr}\left[\frac{h}{R}\right]$$

$$= 4460.16 \text{ psi}$$

When the cylinder has fabrication inaccuracies, the external pressure, q_{YP}, required to produce yielding in the extreme fibers can be solved in the following equation (Timoshenko, 1976, equation (e), page 296):

$$q_{YP}^2 - \left[\frac{S_{YP}}{m} + (1 + 6mn)\, q_{cr}\right] q_{YP} + \frac{S_{YP}}{m}\, q_{cr} = 0$$

where:

$S_{YP} = 42,000$ psi at 370°F

$m = R/h = 7.0625/0.75 = 9.4167$

$n = \omega_1/R = \omega_1/7.0625$

then

$$q^2_{YP} - [4460.16 + (1 + 8\omega_1)\, 4460.16]\, q_{YP} + 19,893,211 = 0$$

The value of ω_1 can vary from 0.0 inches (perfect cylinder) up to 0.0334 inch maximum allowed according to the "ASME Boiler and Pressure Vessel Code." Solving q_{YP} for varying values of ω_1, gives the following:

Initial Radial Deviation ω_1 (in)	Yield Pressure q_{YP} (psi)
0.001	4079
0.01	3365
0.02	2998
0.0334	2675

Thus, the margin of safety against yielding for the inner shell with maximum allowed radial deviation subjected to 466 psi lead pressure (inner shell temperature is 300°F higher than lead temperature) is:

$$M.S. = \frac{2675}{466} - 1 = \underline{+4.74}$$

Since the margin of safety for this conservative load case exceeds zero, the inner shell does not buckle when subjected to the lead pressure produced during the cooling of the cask.

2.6.11.3 Lead Creep

As shown in Sections 2.6.11.2.1 and 2.6.11.2.2, cooling of the lead shell and inner shell introduces a hoop stress of -4136 psi and an axial stress of -9515 psi in the inner shell. However, the high rate of creep of lead at room or elevated temperatures causes the stresses to be relieved early in the life of the cask. From Figure 21 of NUREG/CR-0481, it can be seen that maintaining a constant strain of 0.59 percent at 325°F for only five hours reduces the lead pressure to approximately 200 psi. For this stress in the lead, the corresponding hoop and axial stresses in the inner shell are:

$$\sigma_h = \frac{200}{850}(-4136) = -973 \text{ psi}$$

$$\sigma_a = \frac{200}{850}(-9515) = -2239 \text{ psi}$$

During fabrication following the lead pour, the lead creep relieves the stresses in the lead shell and the stresses in the inner shell to a point that they become negligible.

2.6.12 Fuel Basket Analysis

2.6.12.1 Discussion

To assure that the cask contents are retained in a subcritical and safe configuration, a fuel basket supports the contents both laterally and longitudinally. During normal transport, the cask may sustain a 1-foot free fall to either the side, corner or end drop orientations. Fuel basket designs examined under normal operations conditions are: the PWR basket (Section 2.6.12.2); the BWR basket (Section 2.6.12.4); the metallic fuel basket (Section 2.6.12.5); the MTR basket (Section 2.6.12.6); the TRIGA fuel basket (Section 2.6.12.7); the DIDO fuel basket (Section 2.6.12.8); the GA IFM basket (Section 2.6.12.9); the TPBAR basket and spacer (Section 2.6.12.10); and the ANSTO fuel basket (Section 2.6.12.11). The transport configuration can also accommodate a combination of an ANSTO top basket module and five DIDO basket modules. Within the top ANSTO module of the ANSTO-DIDO combination basket assembly, a total of up to seven aluminum damaged fuel cans (DFCs) can be placed. The total additional weight of the seven DFCs is less than 35 pounds. The increased weight is bounded by the analysis weight of 1,770 lbs, per Section 2.6.12.11.2, which exceeds the calculated weight of the ANSTO baskets in Table 2.2.1-1 of 1,667 lbs (911 + 756 = 1,667) by 103 pounds. The analyses demonstrate that each of the basket designs is supported by the inner shell in bearing during a side drop, and that none of the basket designs will buckle during an end drop. The effects of a corner drop are bounded by the side and end drops.

2.6.12.2 PWR Basket Construction

The cylindrical basket body is fabricated from 6061-T6 aluminum alloy extrusions. An open, square, central core extends the length of the basket and provides lateral support for the cask contents. A 13.25-inch outside diameter, 0.125-inch thick aluminum tube that is 4.38 inches long, is bolted to the top of the basket body. This top tube protects the cask inner shell from damage during fuel loading operations and provides lifting points, which are used when the basket is removed from the cask. An aluminum spacer plate assembly is bolted to the bottom of the basket body. The spacer plate assembly supports the fuel basket and contents longitudinally, providing their movement within the cask. Additional spacer fixtures are either bolted to the cask lid or to the base of the fuel basket, if the cask contents do not fill the basket. The maximum spacer loads occur for the 30-foot drop hypothetical accident load conditions. The spacer analysis is presented in Section 2.7.7.8. A groove on the outside of the basket body is provided for the cask drain tube. The drain tube is connected to a fitting on the cask body, and is used to drain or fill the cask during cask loading or unloading operations.

For the shipment of up to 25 PWR or BWR rods, or up to 16 PWR MOX rods (or mixed MOX and UO_2 rods), a canister with insert will be utilized to position the fuel rod contents within the PWR basket. The canister for the fuel rods will be fabricated from Type 304 stainless steel (minimum thickness 0.12 inch) and will be designed to allow positive handling of the canister during loading and unloading operations. The size, shape, closure design and capacity of the canister will vary depending on the requirements of the shipping and/or receiving facilities. A spacer fabricated from stainless steel will be utilized, as required, to position the PWR/BWR rod canister longitudinally within the NAC-LWT cask cavity. A PWR insert fabricated from 6061-T651 aluminum is used to laterally position the rod canister within the PWR basket. The total weight of the fuel rods, canister and basket insert will be less than the maximum PWR fuel assembly payload weight of 1,650 pounds. Therefore, the up to 25 fuel rods content condition is bounded by the current PWR basket analyses.

2.6.12.3 PWR Basket Analysis

The minimum ambient temperature during normal transport, -40°F, combined with the maximum decay heat load produces an average inner wall temperature of 151°F. The 6061-T6 aluminum alloy expands approximately 1.5 times more per degree Fahrenheit than stainless steel. Assuming that both the cask and basket respond linearly, the maximum as-designed gap between the basket and the cavity, when the basket is centered in the cavity, is 0.094 in. Since aluminum expands faster than stainless steel, any increase in temperature will serve to decrease the basket-cavity gap. Since the gap is small, it is assumed that there is no relative motion between the basket and cask, and that the basket is in contact bearing on the inner shell during a side drop. The basket bearing loads are transmitted to the inner shell and cask structure.

2.6.12.3.1 Bearing Stress Calculation

The bearing stress is calculated using Case 6 (Roark, page 320), which models the cylindrical basket in a circular groove. The maximum compressive stress is calculated using:

$$S_{c_{max}} = 0.798 \left[\frac{\frac{P(D_1 - D_2)}{D_1 D_2}}{\frac{1 - \nu_1^2}{E_1} + \frac{1 - \nu_2^2}{E_2}} \right]^{0.5}$$

$$= 1570 \text{ psi}$$

where the material properties at 250°F are:

Stainless Steel

$D_1 = 13.405$ inches

$E_1 = 27.3 \times 10^6$ psi

$\nu_1 = 0.275$

Aluminum (6061-T6)

$D_2 = 13.25$ inches

$E_2 = 9.4 \times 10^6$ psi

$\nu_2 = 0.334$

contents + basket weight = 4,000 lbs

$P_{1g} = 4{,}000$ lb/178 in = 22.5 lb/in

$P_{24.3g} = (22.5 \text{ lb/in})(24.3 \text{ g}) = 547$ lb/in

(The 24.3 g side drop load is obtained from Table Table 2.6.7-34.)

The allowable compressive stress is selected to be the yield strength $(S_y)_{250°F}$ of Type 304 stainless steel, 23,800 psi. The margin of safety is calculated as:

$$M.S. = \frac{S_y}{S_{c_{max}}} - 1 = \underline{+Large}$$

2.6.12.3.2 Compressive Stress Calculation

The PWR basket and inner cavity length are designed to ensure that there is very limited longitudinal movement of the basket relative to the cask when the cask is carrying fuel. Additional spacers are attached to the cask or added in the PWR basket, if the fuel contents do not fill the basket cavity. The fuel contents are not attached to the PWR basket, and do not impart any longitudinal structural load on the basket body. However, the PWR basket must support itself during an end drop accident. To determine if the PWR basket is self-supporting, it is analyzed as a column, acted upon by a structural (weight) compressive load.

The PWR basket weighs 840 pounds, which, during a normal operations 1-foot fall, is decelerated at 15.8 g. The g loads are completely described for all cask drop orientations in Section 2.6.7.4. The total compressive load acting over the basket body cross section, 59.2 square inches, is $P_{max} = 840 \times 15.8 = 13{,}272$ pounds. The compressive stress (S_c), conservatively considered to act on the basket body, is 13,272/59.2 = 224 psi.

An Euler column analysis is used to determine the critical buckling stress of the PWR basket body. Assuming that the impacting end is fixed and the other is free, the critical buckling stress (Shigley, page 116) is calculated as:

$$P_{cr} = \frac{n\pi^2 EI}{L^2}$$

$$= 670,700 \text{ psi}$$

where:

n = 0.25, end fixity coefficient

$E_{Al_{250°F}} = 9.4 \times 10^6$ psi

$I_{basket\ body} = 870\ in^4$ (Roark, Case 10, page 75)

L = 178 inches, inner cavity length

$$M.S. = \frac{P_{cr}}{P_{max}} - 1 = \underline{+Large}$$

2.6.12.4 BWR Basket Construction

The BWR basket is fabricated from 6061-T6 aluminum alloy extrusions. Two open, square cores, located in the center of the basket body, extend the length of the basket, providing lateral support for the cask contents. A 13.25-inch outside diameter, 0.25-inch thick stainless steel tube that is 5.4 inches long is welded to a 0.62-inch thick plate and the top cover assembly is bolted to the basket body. The top cover protects the cask inner shell from damage during fuel loading operations and provides lifting points, which are used when the basket is removed from the cask. A stainless steel spacer plate assembly is bolted to the bottom of the basket body. The spacer plate assembly supports the fuel basket and contents longitudinally, preventing their movement within the cask. Additional spacer fixtures are either bolted to the cask lid or the base of the fuel basket if the cask contents do not fill the basket. A groove on the outside of the basket body is provided for the cask drain tube.

2.6.12.4.1 BWR Basket Analysis

The BWR basket body is fabricated from the same material as the PWR basket body. Moreover, the outer diameter and its tolerance are exactly the same for both basket designs. Therefore, the BWR basket is also considered to be in contact bearing for similar reasons to those stated in Section 2.6.12.3, and all basket bearing loads are transmitted to the cask inner shell.

2.6.12.4.2 Bearing Stress Calculation

The BWR basket and its contents weigh 2,624 pounds. The normal operations conditions 1-foot side drop g load is 24.3, resulting in a total bearing load of 63,760 pounds (2,624 lb x 24.3 g). The bearing load per unit length ($P_{24.3g}$) is 358 pounds/inch (63,760 lb/178 in). Using Case 6 (Roark, page 320) and the same material properties as described in Section 2.6.12.3.1, the

$S_{c_{max}}$ = 1383 psi. The allowable compressive stress is selected to be the yield strength $(S_y)_{250°F}$ of Type 304 stainless steel, 23,800 psi. The margin of safety is calculated as:

$$M.S. = \frac{S_y}{S_{c_{max}}} - 1 = \underline{+LARGE}$$

2.6.12.4.3 Compressive Stress Calculation

For the same reasons that are stated in Section 2.6.12.3.2, the BWR basket needs only to be self-supporting. The BWR basket weighs 1124 pounds, which during a normal operations 1-foot fall, is decelerated at 15.8 g. The total compressive load acting over the basket body cross-section (72.5 in^2), is P_c = 1124 lb × 15.8 g = 17,759 pounds. The compressive stress (S_c) conservatively considered to act on the basket body is 17,759 lb/72.5 in^2 = 245 psi, which is negligible.

An Euler column analysis is used to determine the critical buckling stress of the BWR basket body. Assuming that the impacting end is fixed and the other end is free, the critical buckling stress (Shigley, page 116) is calculated as:

$$P_{cr} = \frac{n\pi^2 EI}{L^2}$$

$$= 1.0 \times 10^6 \text{ psi}$$

where:

n = 0.25, end fixity coefficient

$E_{Al_{250°F}} = 9.4 \times 10^6$ psi

$I_{basket\ body}$ = 1,298 in^4 (Roark, Case 10, page 75)

L = 178 in, inner cavity length

$$M.S. = \frac{P_{cr}}{P_c} - 1 = \underline{+LARGE}$$

2.6.12.5 Metallic Fuel Basket Construction

The metallic fuel basket is fabricated from three 5.625-inch outer diameter 6061-T6 aluminum tubes, laterally restrained by five 13.0-inch diameter 0.25-inch thick, 6061-T6 aluminum bulkheads welded along the length of the tubes. Each tube provides lateral support for the cask contents. The uppermost bulkhead has three attachment points, which are lifting points used when the basket is removed from the cask. Welded to the bottom bulkhead is a 9.0-inch outer diameter, 0.25-inch thick, 6061-T6 aluminum spacer tube, 29.5 inches long, which supports the

fuel basket and contents longitudinally, preventing their movement within the cask. A groove on the outside of the basket body is provided for the cask drain tube.

2.6.12.5.1 Metallic Fuel Basket Analysis

The metallic fuel basket body is fabricated from similar material to the PWR basket body. Moreover, the outer diameter of the bulkheads and its tolerance are exactly the same for both basket designs. Therefore, the metallic fuel basket bulkheads are also considered in contact bearing for the same reasons stated in Section 2.6.12.3, and all basket bearing loads are transmitted to the inner shell and cask structure.

2.6.12.5.2 Bearing Stress Calculation

The metallic fuel basket and its contents weigh 2,208 pounds. The normal operations conditions 1-foot side drop g load is 24.3, resulting in a total bearing load of 53,654 pounds (2,208 lb × 24.3 g). It is assumed that the entire bearing load is distributed over the five 0.25-inch thick bulkheads. The bearing load per unit length ($P_{24.3g}$) is 42,924 pounds/inch (53,654 lb/1.25 in). From Case 6 (Roark, page 320) the maximum compressive stress is calculated using:

$$S_{c_{max}} = 0.798 \left[\frac{\frac{P(D_1 - D_2)}{D_1 D_2}}{\frac{1 - \nu_1^2}{E_1} + \frac{1 - \nu_2^2}{E_2}} \right]^{0.5}$$

$$= 36{,}530 \text{ psi}$$

where the material properties at 250°F are:

Stainless Steel

$D_1 = 13.405$ inches

$E_1 = 27.3 \times 10^6$ psi

$\nu_1 = 0.275$

Aluminum (6061-T6)

$D_2 = 13.0$ inches

$E_2 = 9.4 \times 10^6$ psi

$\nu_2 = 0.334$

The allowable compressive stress is selected to be $(1.5)(S_y)_{250°F}$ of 6061-T6 aluminum, 44,685 psi. The margin of safety is calculated as:

$$M.S. = \frac{S_y}{S_{c_{max}}} - 1 = \underline{+0.22}$$

2.6.12.5.3 Compressive Stress Calculation

For the same reasons that are stated in Section 2.6.12.3.2, the metallic fuel basket needs only to be self-supporting. The metallic fuel basket weighs 128 pounds, which during a normal operating conditions 1-foot fall, is decelerated at 15.8 g. The total compressive load acting over the three fuel tubes is P_F = 2,022 pounds (128 lb × 15.8 g). The total cross sectional area of the three aluminum fuel tubes is 6.48 square inches, resulting in a normal operating conditions compressive stress ($S_{c_{fuel}}$) of 312 psi (2,022 lb/6.48 in^2). The spacer tube must support the basket and its contents during a bottom end drop. The total weight that the spacer tube supports is 2,208 pounds, resulting in a normal operating conditions 1-foot bottom end drop compressive load of P_c = 34,886 pounds. The cross sectional area of the 9.0-inch outer diameter aluminum spacer tube is 6.87 square inches, resulting in a compressive stress ($S_{c_{spacer}}$) of 5078 psi. Assuming that the impacting end is fixed and the other end is free, the critical buckling stresses for each tube column (Shigley, page 116) is calculated:

Fuel Tubes (3)

$$P_{cr} = \frac{n\pi^2 EI}{L^2}$$

$$= 33,550 \text{ psi}$$

Spacer Tube

$$P_{cr} = \frac{n\pi^2 EI}{L^2}$$

$$= 1,754,000 \text{ psi}$$

where:

n = 0.25, end fixity coefficient
$E_{Al250°F} = 9 \times 4\ 10^6$ psi
$I_{basket\ body}$ = 46 in^4
L = 145.25 in, fuel tube length
MS = $\underline{P_{cr}}$ / P_F - 1 = $\underline{+Large}$

n = 0.25, end fixity coefficient
$E_{Al250°F} = 9.4 \times 10^6$ psi
$I_{spacer\ tube}$ = 66 in^4
L = 29.5 in, spacer tube length
MS = $\underline{P_{cr}}$ / P_c - 1 = $\underline{+Large}$

2.6.12.6 MTR Fuel Basket Construction

The MTR modular basket assembly has four configurations. One configuration is for 28 uncut (intact) MTR fuel assemblies (28 MTR – 4 unit basket); the second is for 35 partially cut MTR elements that have had portions of the upper and lower end fittings removed (35 MTR – 5 unit basket). The third configuration is for 42 MTR fuel assemblies (42 MTR – 6 unit basket) with

the upper and lower end fittings removed; and the fourth configuration is for up to 700 PULSTAR fuel elements loaded in the 28 MTR basket. The PULSTAR fuel may be intact fuel assemblies, intact fuel elements (rods) loaded in a fuel rod insert or in fuel cans, or damaged fuel elements, fuel debris, and nonfuel components of fuel assemblies loaded in fuel cans. Each MTR basket configuration consists of one base module, one top module, and two, three or four intermediate modules for the 28, 35 and 42 element configurations, respectively. Each MTR basket module is designed to hold up to seven MTR or PULSTAR fuel assemblies. The modules are not interchangeable between basket configurations. The structural analysis is not affected by the specific fuel element design or enrichment as long as the fuel characteristics are in compliance with the fuel characteristics listed in Table 1.2-4.

Axial fuel and plate spacers may be used to axially position the MTR fuel assemblies in the basket modules. Cell block spacers are used to prevent the loading of fuel assemblies in basket module positions 1, 2 and 3 when LEU MTR fuel elements having >470 g ^{235}U per element (>22 g ^{235}U per plate) are loaded. The presence and/or use of spacers, fuel plate canisters or fuel cans does not affect the structural integrity of the MTR fuel baskets as the total weight of fuel element, spacer and fuel plate canister or fuel can is limited to the evaluated load of 80 pounds/cell. The axial fuel and cell block spacers perform no safety function and are considered dunnage. Plate spacers are used, if required, to ensure that the criticality evaluation required minimum nonfuel hardware is provided.

Each module, fabricated from Type 304 stainless steel, is a weldment made up of two 1/2-inch thick, 13.265-inch diameter, circular plates at each end of the longitudinal divider plates creating seven MTR fuel assembly cavities. The outside wall of the four symmetric outermost fuel compartments is fabricated from 11-gage Type 304 stainless steel sheet. The 1/2-inch thick plate at the top end of the MTR fuel basket module is welded to the exterior surfaces of the fuel tube weldment with a 1/8-inch continuous weld on the under side of the top plate and with a continuous fillet seal weld on the top side. The 1/2-inch thick baseplate is continuously welded to the 1/4-inch thick divider plates and the 5/16-inch thick web plates. The 11-gage sheet metal and the 5/16-inch intermediate webs are discontinued at 1/4 inch from the surface of the baseplate to provide for compartment drainage. The 5/16-inch plate material may be machined to a minimum thickness of 0.28 inch. In addition to the drainage path at the base of each assembly cavity, a 1-inch diameter hole is located at the center of each of the compartments in the module. Each MTR basket base module sits on a 1.5-inch long, 10-inch schedule 80S pipe welded to the 1/2-inch thick baseplate. The 10-inch schedule 80S pipe carries the total weight of the MTR basket assembly and bears directly on the bottom forging of the cask.

The MTR fuel basket base module and intermediate modules have guide pins fixed to the surface of the top support plate. The guide pins fit into holes in the base plate of the top and intermediate modules and provide controlled alignment of the basket assembly. A groove slot on the outside of

each basket unit support plate is provided for the clearance of cask drain tube and for circumferential alignment of the MTR basket assembly.

The MTR Plate Canister (canister) is an all-aluminum rectangular canister that is suitable for transport in the NAC-LWT MTR 42 element basket. The canister may be transported in the 28 or 35 element basket if appropriate dunnage is used. The canister is fabricated from ASTM B209 or ASTM B221 6061 aluminum. The canister body comprises two thick walls and two thin walls that are welded together into a rectangular tube to contain up to 23 MTR fuel plates. Each end of the canister body is closed by identical aluminum lids milled from a solid piece to incorporate a lifting bail. The lids are fastened securely to the thick wall plates using aluminum socket head cap screws that are captive in the lid to facilitate closing the canister.

2.6.12.6.1 MTR Fuel Basket Analysis

The MTR basket assembly and the inner shell are both fabricated from Type 304 stainless steel material. The nominal radial gap between the MTR basket assembly and the cask inner shell is 0.055 inch. The nominal radial gap between the basket and the inner shell is 0.0531 inch at the design basis fuel normal operation steady-state temperature. As defined for other NAC-LWT fuel specific basket designs, since the gap between the basket and cask inner shell wall is small, it is assumed that there is no relative motion between the basket and the cask, and that the basket is in contact bearing on the inner shell during a side drop. The basket bearing loads are transmitted to the inner shell and cask structure.

The analysis of the MTR plate canister is presented in Section 2.6.12.6.6.

2.6.12.6.2 MTR Fuel Basket Normal Conditions 1-foot Side Drop

This section evaluates the MTR fuel basket for the normal conditions of transport 1-foot side drop.

Bearing Stress Calculation—Inner Shell (Cask 1-foot Side Drop)

The bearing stress is calculated using Roark's, Table 33, Case 2 (Roark's, 6th Edition), which models the cylindrical basket in a circular groove. The 28 MTR fuel assembly base module is the heaviest module when loaded with 25 PULSTAR fuel elements. The maximum compressive stress, for two elastic bodies with similar elastic modulus, is:

$$\sigma_c = 0.798\sqrt{\frac{\frac{gP(D_1 - D_2)}{D_1 D_2}}{\frac{2(1-\nu^2)}{E}}} = 16{,}679 \text{ psi}$$

where:

g = 1-foot side drop acceleration = 24.3

E = Elastic modulus = 28.3×10^6 psi (conservatively use E @ 70°F)

ν = Poisson's ratio for steel material = 0.275

D_1 = Cask cavity diameter = 13.405 inches

D_2 = Basket diameter = 13.265 inches

t = Thickness of stiffener at mid section of base module (less chamfers)

= $0.5 - 2 \times 0.13 = 0.24$ in

W = Maximum weight of MTR basket with contents (PULSTAR fuel elements)

= 3,222 lbs

W_r = Load supported by 28-assembly basket base module middle ring

= W/9 = 358 lbs

P = W_r/t = 358 lb/0.24 in = 1,491 lb/in

The allowable compressive stress, S_y, of Type 304 stainless steel at a conservative maximum operating temperature envelope of 600°F is 18,200 psi. The margin of safety is calculated as:

$$MS = \frac{S_y}{\sigma_c} - 1 = +0.09$$

Fuel Tube Stresses (Cask 1-foot Side Drop)

The maximum stress in the fuel tubes occurs in the 0.12-inch thick, 11-gage sheet metal tubes which support the entire length of the MTR fuel elements or PULSTAR fuel elements. There are two cases to consider. In the first case, the weight of the fuel assembly is transmitted to the tube through the two aluminum plates at the sides of the fuel assembly. As shown in Figure 2.6.12-1, this load path creates a uniform line load along the length of the tube located about 0.315 inch from the corners. The tube is analyzed as a simple beam, 1-inch wide, 0.12-inch thick, and 3.44-inches long with a concentrated load at 0.315 inch from the ends. The maximum bending moment, M_1, is:

$$M_1 = \frac{(8Pa + WL^2) \times g}{8} = 14.0 \text{ in-lb/in}$$

where:

W = Unit tube body weight = $0.288 \times t = 0.0346$ lb/in^2

L = Length = 3.44 inches

P = Bounding fuel load = $P_f / (2 \times L_f) = 1.67$ lb/in

P_f = Fuel weight = 80.0 lbs

L_f = Shortest length over which fuel load is applied = 24 inches

a = Distance from applied load, P to support = 0.315 in

g = 1-foot side drop acceleration = 24.3

In the second case, the weight of the fuel assembly is transmitted to the tube as a uniform load. The load path is shown in Figure 2.6.12-1. The maximum bending moment for this case, M_{II}, is:

$$M_{II} = \frac{(2PL^2 + WL^3)\times g}{8L} = 36.1 \text{ in-lb/in}$$

The maximum bending stress, σ, is:

$$\sigma = \frac{6M_{II}}{t^2} = 15{,}042 \text{ psi}$$

where:

t = Fuel tube thickness = 0.12 in

The stress allowable, $1.5S_m$, is 24,600 psi for Type 304 stainless steel at a conservative temperature of 600°F. The margin of safety is:

$$MS = \frac{24{,}600}{15{,}042} - 1 = +0.64$$

The 11-gage sheet metal tube is continuously welded to the adjacent divider plates with a 1/8-inch fillet weld. This weld resists shear developed in the simple beam analyzed above.

$$V = \frac{(2P + WL)\times g}{L} = 24.4 \text{ lb/in}$$

The shear stress, τ, is:

$$\tau = \frac{V}{t} = 203 \text{ psi}$$

The "throat" thickness of the weld is 0.088 in. The ratio of the plate thickness (0.12 in) to the weld "throat" thickness (0.088 in) is 1.36. The maximum stress of 203 psi calculated above is adjusted by a factor of 1.36 to obtain the maximum stress in the weld for the 1-foot side drop (24.3g). Maximum stress in the weld, S_w, is:

$$S_w = 1.36 \times \tau = 276 \text{ psi}$$

The ASME Code, Subsection NG-3352 recommends that the allowable stress be determined for a fillet weld with PT or MT surface examination by implementing a quality factor, n, of 0.4. The

stress allowable, S_y, of the base metal, Type 304 stainless steel, is 18,200 psi at a conservative operating temperature envelope of 600°F. The margin of safety for the fillet weld is:

$$MS = \frac{S_y \times n}{S_w} - 1 = \underline{+Large}$$

2.6.12.6.3 MTR Fuel Basket Normal Conditions 1-foot End Drop

This section evaluates the MTR fuel basket for the normal conditions of transport 1-foot end drop.

Bearing Stress Calculation—Bottom Forging (Cask 1-foot End Drop)

When in the vertical position a 0.5-inch thick, 10-inch nominal diameter schedule 80S pipe supports the MTR basket assembly. The 1.5-inch long pipe is welded to the baseplate of the base module. The compressive stress is:

$$\sigma_c = \frac{g \times W}{A} = 3{,}162 \text{ psi}$$

where:

W = Maximum weight of MTR basket with contents (PULSTAR fuel elements) = 3,222 lbs

A = Cross-sectional area of base pipe support = 16.1 in^2

g = 1-foot end drop acceleration = 15.8

The allowable stress, S_y, of Type 304 stainless steel at a conservative maximum operating temperature of 600°F is 18,200 psi. The margin of safety is:

$$MS = \frac{S_y}{\sigma_c} - 1 = +4.76$$

Compressive Stress Calculation—Fuel Tubes (Cask 1-foot End Drop)

The MTR basket assembly and the inner cavity length are designed to ensure that there is minimal longitudinal movement of the basket relative to the cask. The base module of the MTR basket assembly supports itself and the weight of the other basket modules, including fuel content during a 1-foot end drop. The normal operation load compressive stress developed in the basket tube wall is:

$$\sigma_c = \frac{g \times W}{A} = 6{,}208 \text{ psi}$$

where:

W = Maximum weight of MTR basket with contents (PULSTAR fuel elements)

= 3,222 lbs

g = 1-foot end drop acceleration = 15.8

A = Total compartment cross-sectional area at baseplate (Figure 2.6.12-2)

= 8.20 in^2

The allowable compressive stress, S_m, is 16,400 psi conservatively evaluated for Type 304 stainless steel at a conservative maximum operating temperature of 600°F. The margin of safety is:

$$MS = \frac{S_m}{\sigma_c} - 1 = +1.64$$

The Euler elastic buckling load formulation is used to determine the critical buckling load of the MTR basket base module. The base module is treated as simply supported, which results in an effective length that is twice the actual length, thus reducing the critical buckling load by a factor of 4.0. The basket base module buckling load is:

$$P_{cr} = \frac{\pi^2 EI_i}{(L_e)^2} = 1.55 \times 10^6 \text{ lb}$$

The margin of safety is:

$$MS = \frac{P_{cr}}{P_c} - 1 = \underline{+Large}$$

where:

P_c = Compressive load = 15.8g × 3,222 lbs = 50,908 lbs

I_i = Basket inertia moment = 47.92 in^4

E = Elastic modulus (@ 600°F) = 25.3×10^6 psi

L_e = Effective length of 28 assembly basket = 2 × 44.0 inches = 88 inches

Baseplate Stresses (Cask 1-foot End Drop)

The support plate at the top end of the basket modules is continuously welded to the outside periphery of the fuel compartment tubes. The baseplate of a typical basket module is continuously welded to the two 11.57-inch wide, 5/16-inch (min. 0.28-inch considering machining tolerance) thick web plates, and to the two 3.44-inch wide, 1/4-inch thick divider plates as shown in Figure 2.6.12-2. The ½-inch thick baseplate supports seven MTR or seven DIDO fuel assemblies or 25 PULSTAR fuel elements and is conservatively assumed to be supported by the main longitudinal webs mentioned above during a cask end drop. Two separate

load cases are examined. The maximum stress for each case is then combined to obtain the total stress on the baseplate. Figure 2.6.12-2 details the baseplate support.

The first case, Case I, examines a 3.44-inch square plate with two adjacent sides fixed and the other two sides free. The applied pressure over the entire plate is uniform (Roark's, 6th edition, Table 26, Case 11a). The bending stress is:

$$\sigma_I = \frac{-g\beta_I Pb^2}{at^2} = -8{,}947 \text{ psi}$$

where:

P = Fuel weight = 80.0 lbs

g = 1-foot end drop acceleration = 15.8

a = Area of plate = $(3.44 \text{ in})^2 = 11.83 \text{ in}^2$

t = Plate thickness = 0.5 inch

b = Plate width = 3.44 inches

β_I = Boundary condition stress factor = 1.769

The second case, Case II, examines a rectangular plate, 11.57 inches by 3.44 inches, fixed along the long edges, free along the short edges and uniformly loaded (Roark's, 6th edition, Table 26, Case 6a). The bending stress is:

$$\sigma_{II} = \frac{-g\beta_{II} Pb^2}{at^2} = -747 \text{ psi}$$

where:

a = Area of plate = $11.57 \times 3.44 \text{ in} = 39.8 \text{ in}^2$

β_{II} = Boundary condition stress factor = 0.497

The total bending stress is conservatively obtained by adding the individual stresses:

$\sigma = \sigma_I + \sigma_{II} = -9{,}694$ psi

The allowable stress, 1.5 S_m, is 24,600 psi for Type 304 stainless steel at the conservative maximum temperature envelope of 600°F. The margin of safety is:

$$MS = \frac{24{,}600}{9{,}694} - 1 = +1.54$$

2.6.12.6.4 Fuel Tube Stresses (Cask 1-foot Oblique Drop)

Table 2.6.7-34 summarizes the cask drop g-load factors for six drop orientations: the cask end drop (0 degrees), the cask corner drop (15.74 degrees), the cask oblique drops (30, 45 and, 60

degrees) and the cask side drop (90 degrees). To conservatively envelope the maximum stresses expected for all the 1-foot oblique drops, the calculated stresses of 6,208 psi in Section 2.6.12.6.3 for the end drop and 15,042 psi in Section 2.6.12.6.2 for the side drop are added as absolute values. The maximum stress in the MTR basket that envelops the maximum stresses expected for any 1-foot oblique drop is 21,250 psi. The margin of safety, against stress allowable, 1.5 S_m, of 24,600 psi, at 600°F, is:

$$MS = \frac{24,600}{21,250} - 1 = +0.16$$

2.6.12.6.5 Fuel Cans in a MTR Basket (Damaged PULSTAR Elements)

PULSTAR Damaged Fuel Can

The PULSTAR can is a modification of the existing damaged fuel can for TRIGA fuel, which has two different design lengths. The PULSTAR fuel can has the same cross-section (can width and wall thickness) as the TRIGA fuel can and is approximately four inches longer than the shorter TRIGA fuel can design. Identical materials of fabrication are used for both TRIGA and PULSTAR fuel cans. As shown in Section 2.6.12.7.6, the TRIGA fuel can is evaluated for a maximum weight of 59.6 lb, which includes a can weight of 20 lbs and a payload of 39.6 lbs. The weights of the PULSTAR fuel can and its maximum payload are approximately 15 lbs and 35 lbs, respectively, for a maximum total weight of 50 lbs. Therefore, the stress evaluation for inertia loads for the PULSTAR can is bounded by the evaluation for the TRIGA can.

The maximum internal pressure for the PULSTAR can is 3.4 atm (gage). The calculation for the TRIGA can in the section titled "Sealed Failed Fuel Can Bolt Evaluation" used a value of 3 atm (gage). In the evaluation of the bolt stresses and loads, the calculation in this section conservatively used a linear load of 700 lb/inch, which bounds the increased internal pressure of 3.4 atm (gage) for the PULSTAR can.

For the e valuation of the failed fuel can tube, the minimum margin of safety is +0.77 (actual stress is 9,241 psi) in the section titled "Sealed Failed Fuel Can Plate Stress Due to Side Drop" for the 1-foot side drop. Considering the damaged fuel can as a thin wall cylinder with a bounding internal pressure of 60 psig, the stresses in circumferential, radial, and longitudinal directions are:

$$\sigma_\theta = \frac{P \times r}{t} = 1,500 \text{ psi}$$

$$\sigma_r = -P = -60 \text{psi}$$

$$\sigma_Z = \frac{P \times r}{2 \times t} = 750 \text{ psi}$$

where:

P = 60 psig

r = 3.25/2 in., the radius of the can

t = 0.065 in., the thickness of the can

Combining the stresses caused by can contents (1-ft side drop) and the internal pressure, the bounding stress intensity is:

$$S_{int} = (1{,}500 + 9{,}241) - (-60) = 10{,}801 \text{ psi}$$

The minimum margin of safety for the one-foot side drop and internal pressure is:

$$\text{M.S.} = \frac{1.5\ S_m}{S_{int}} - 1 = +1.28$$

It is concluded that the PULSTAR fuel can is structurally adequate for normal conditions of transport. No additional analysis is required.

PULSTAR Screened Fuel Can

The PULSTAR screened can is a modification of the existing screened fuel can for TRIGA fuel, which has two different design lengths. The PULSTAR screened fuel can has the same cross-section (can width and wall thickness) as the TRIGA screened fuel can and is approximately four inches longer than the shorter TRIGA screened fuel can design. Identical materials of fabrication are used for both TRIGA and PULSTAR fuel cans. As shown in Section 2.6.12.7.5, the TRIGA fuel can is evaluated for a maximum weight of 71 lbs, which includes a maximum can weight of 17 lbs and a payload of 54 lbs. The weights of the PULSTAR screened fuel can and its maximum payload are 12 lbs and 54 lbs, respectively, for a maximum total weight of 66 lbs. Therefore, the evaluation presented in Section 2.6.12.7.5 for the TRIGA screened fuel can bounds the evaluation for the PULSTAR screened fuel can and it may be concluded that the PULSTAR screened fuel can is structurally adequate for normal conditions of transport. No additional analysis is required.

PULSTAR Fuel Rod Insert and Spacer

Intact PULSTAR fuel elements can be placed into the TRIGA fuel rod insert (Dwg. 315-40-096). This insert is identical to the TRIGA fuel rod insert evaluated in Section 2.6.12.7.9. The weight of the individual PULSTAR fuel element is 1.31 lbs, which is bounded by the weight of an individual TRIGA rod of 1.44 lbs reported in Section 2.6.12.7.9. Therefore no additional evaluation for PULSTAR fuel elements contained in the TRIGA fuel rod insert is required.

For an end drop, the maximum stress is computed using the accelerations for the accident condition, but is compared to the stress allowables for the normal condition. The stress in the aluminum spacer is:

$$\sigma = \frac{Pg}{A} = 0.5 \text{ ksi}$$

where:

P = 65 lbs Bounding load

g = End drop g-load for the 30-foot end drop= 60.0g

A = $\pi r^2 = 8.3$ in^2

r = Radius of cylinder = 3.25/2 = 1.625 inches

t = Wall thickness = 0.125 in

The margin of safety is

$$MS = \frac{0.7S_u}{\sigma} - 1 = \frac{0.7 \times 30.2}{0.5} - 1 = \underline{+Large}$$

Using NUREG / CR-6322, a buckling evaluation of the spacer is performed for the accident condition which corresponds to an acceleration of 60g. The critical buckling stress for the spacer is:

$$\sigma_c = \frac{\pi^2 E}{\left(\frac{KL}{r}\right)^2} = 99.7 \text{ ksi}$$

where:

K = Effective length factor for fixed-free end conditions = 2.0

L = spacer length = 16.5 inches, which bounds 12-inch length

r = Radius of gyration = $\sqrt{I/A}$ =1.1 in

A = Cross-sectional area of spacer = πDt = 1.28 in^2

I = Moment of inertia = $\frac{\pi D^3 t}{8}$ = 1.69 in^4

D = Spacer diameter = 3.25 inches

t = Spacer thickness = 0.125 in

E = Modulus of elasticity of aluminum = 9.1×10^6 psi

The margin of safety against buckling is:

$$MS = \frac{\sigma_c}{\sigma} - 1 = \frac{99.7}{0.5} - 1 = \underline{+Large}$$

2.6.12.6.6 MTR Plate Canister Analysis

The MTR Plate Canister (canister) is a handling fixture designed to assist loading MTR fuel plates into the removable modules of the NAC-LWT MTR fuel basket. The fuel basket modules are used to load and unload fuel from the NAC-LWT cask and are the analyzed support structure for the fuel and canister. Therefore, the canister is not a required operational feature for loading or unloading fuel from the cask and serves only as a spacer (dunnage) once inserted into a basket module.

In this section, the canister is evaluated and found to be structurally adequate for all normal conditions of handling and transport. Stresses developed during the normal (one-foot drop) conditions meet all appropriate allowable criteria with positive margins. Classical hand calculations are used to determine the stresses in the canister. Calculated stresses are compared to allowable stresses for non-containment structures shown in Table 2.1.2-2, "Allowable Stress Limits for Noncontainment Structures."

Design deceleration (g) factors used in the canister analysis are shown in Table 2.6.7-34, "Summary of Cask Drop Equivalent G Load Factors." A temperature of 295°F bounds the highest calculated canister temperature and is used for both normal and accident conditions analyses. Stresses for corner and oblique drops are considered to be enveloped by the stresses produced by the end and side drops based on the cask drop acceleration component loads summarized in Table 2.6.7-34.

Maximum Canister Temperature

The maximum heat load allowed in an MTR basket cell is 120 W (409.8 Btu/hr), which is assumed to be transmitted only through one plate of the canister, resulting in a conservative estimate of the ΔT through the thickness of the canister shell. The maximum basket temperature is listed in Table 3.4-6 as 292°F.

The change in temperature through the thickness of the shell is calculated using the following formula:

$$\Delta T = Q\,t / kA = 409.8 \text{ Btu/hr} \times 0.24 \text{ inch} / (6.23 \text{ Btu/hr-in-F} \times 76.26 \text{ in}^2) = 0.21°F$$

where:

$k = 6.77 - 0.0025 \times (292 - 77) = 6.23$ Btu/hr-in-F at 292°F

$A = 25.85(3.2 - 0.125 \times 2) = 76.26$ in^2 is the cross-sectional area of the plate

The peak canister shell temperature is then 292°F + 0.21°F = 292.21°F. A temperature of 295°F is conservatively used for the temperature of the canister.

MTR Plate Canister Weight

The canister component weights are determined by conservatively calculating the volume of each component and multiplying by the density of 6061 aluminum, 0.098 lb/in^3 ("ASME Boiler and Pressure Vessel Code, Section II, Part D – Properties," 1995 with 1995 Addendum).

Can Weldment

$$W_{canister} = W_1 + W_2 + W_3 + W_4 = 6.8 \text{ lbs (use 10 lbs for analysis)}$$

where:

Item/Description	Calculation of Weight
1 Plate-A (2)	$W_1 = 25.85 \times 3.20 \times 0.24 \times 0.098 \times 2 = 3.9$ lbs
2 Plate-B (2)	$W_2 = 25.85 \times 2.95 \times 0.125 \times 0.098 \times 2 = 1.9$ lbs
3 Lid (2)	$W_3 = 3.30 \times 3.20 \times 0.25 \times 0.098 \times 2 = 0.5$ lb
4 Bail (2)	$W_4 = [(0.46(4) + 2.94(2)) \times 0.125) + 1.04 \times 0.25] \times 0.098 \times 2 = 0.5$ lb

This weight calculation conservatively neglects holes in the lids.

NAC-LWT MTR Plate Canister Stress Analysis

The canister is evaluated for stresses developed during the normal (one-foot drop) conditions. The empty canister weight is assumed to be 10 pounds and the loaded canister weight is assumed to be 30 lbs throughout the calculations.

Side Drop

The canister is contained within the NAC-LWT MTR 42-element basket assembly in the side-drop case. Because of the support provided by the basket, only the uppermost canister plate is subjected to bending. Bending of the plate is analyzed by considering a 1-inch section as a fixed-fixed beam equal in length to the width of the plate and uniformly loaded by the plate weight times the appropriate acceleration (g).

Normal Operating Condition (1-foot drop)

With the 0.125-in. thick plate uppermost:

The maximum moment (M_{max}) is:

$$M_{max} = \frac{wL^2}{12} = \frac{(0.30)(3.3^2)}{12} = 0.272 \text{ in-lb}$$

$$S_b = \frac{Mc}{I} = \frac{(0.272)(0.0625)}{1.63 \times 10^{-4}} = 104 \text{ psi for the normal operating condition}$$

where:

$$w = 0.125 \times 1.0 \times 1.0 \times 0.098 \times 24.3g = 0.30 \text{ lb/in}$$

$$I = \frac{bh^3}{12} = \frac{(1.0)(0.125^3)}{12} = 1.63\times10^{-4} \text{ in}^4$$

With the 0.24-in. thick plate uppermost:

The maximum moment (M_{max}) is:

$$M_{max} = \frac{wL^2}{12} = \frac{(0.57)(3.3^2)}{12} = 0.517 \text{ in-lb}$$

$$S_b = \frac{Mc}{I} = \frac{(0.517)(0.125)}{1.15\times10^{-3}} = 56 \text{ psi for the normal operating condition}$$

where:

$$w = 0.24 \times 1.0 \times 1.0 \times 0.098 \times 24.3g = 0.57 \text{ lb/in}$$

$$I = \frac{bh^3}{12} = \frac{(1.0)(0.24^3)}{12} = 1.15\times10^{-3} \text{ in}^4$$

The minimum margin of safety (MS) for bending is:

$$MS = \frac{1.5S_m}{S_b} - 1 = \frac{(1.5)(11{,}500)}{104} - 1 = \underline{+\text{Large}}$$

Side Plate Buckling

The 0.125-inch-thick side plates are evaluated as axially loaded compression members. Buckling of the 0.24-inch thick plates is based on this analysis. Considering a 1-inch section of the plate, the slenderness ratio (C_c) is:

$$C_c = \sqrt{\frac{2\pi^2 E}{S_y}} = \sqrt{\frac{2\pi^2 9.6\times10^6}{27{,}900}} = 82.4$$

The radius of gyration (r) is:

$$r = \sqrt{\frac{I}{A}} = 0.036 \text{ in}^4$$

where:

$$I = \frac{bh^3}{12} = \frac{1.0(0.125)^3}{12} = 1.628\times10^{-4} \text{ in}^4$$

$$A = 0.125\times1.0 = 0.125 \text{ in}^2$$

For K = 1,

$$\frac{KL}{r} = \frac{1(3.3)}{0.036} = 91.67$$

For KL/r = 91.67 > C_c = 82.4, the allowable stress (S_a) is:

$$S_a = \frac{12\pi^2 E}{23\left(\frac{KL}{r}\right)^2} = \frac{12\pi^2\left(9.6\times10^6\right)}{23\left(91.67^2\right)} = 5{,}882 \text{ psi}$$

The allowable load (P_a) is:

$$P_a = S_a \times A = 5{,}882 \text{ psi} \times 0.125 \text{ in}^2 = 735 \text{ lbs}$$

The load (P) imposed upon the 0.125-inch-thick side plate by the 0.24-inch-thick side plate in the normal condition, one-foot side drop is:

$$P = 0.24 \times 1.0 \times 3.3 \times 0.098 \times 24.3g \cong 2 \text{ lbs}$$

This 2-pound load is conservative because the load from the thicker plate is actually shared between the two thinner plates.

The margin of safety (MS) is:

$$MS = \frac{P_a}{P} - 1 = \frac{735}{2} - 1 = +\underline{\text{Large}}$$

End Drop

For the end drop, the can weldment is loaded by its own weight. The canister contents bear against the bottom or top of the canister, depending on drop orientation.

Under normal operating conditions the canister body weldment is evaluated for a 15.8g end drop acceleration. The compressive load (P) on the tube is the combined weight of the lid and body plates times the appropriate g factor.

The compressive stress (S_c) in the canister body weldment is:

$$S_c = \frac{P}{A} = \frac{158 \text{ lb}}{2.24 \text{ in.}^2} \cong 70.5 \text{ psi}$$

where:

$$A = (3.2\times0.24 + 2.82\times0.125)(2) = 2.24 \text{ in}^2$$

P = 10 lb × 15.8g = 158 lb (Conservatively, the entire weight of the canister is used)

The margin of safety (MS) is then:

$$MS = \frac{S_m}{S_c} - 1 = \frac{11{,}500 \text{ psi}}{70.5 \text{ psi}} - 1 = \underline{+\text{Large}}$$

Lifting Bail Compressive Stress

Under normal operating conditions, the lifting bail is evaluated for a 1-foot end drop (15.8g acceleration). The compressive load (P) on the lifting bail is the combined weight of the canister and its contents (30 lbs) times the appropriate g factor.

The compressive stress (S_c) in the canister body weldment is:

$$S_c = \frac{P}{A} = \frac{474 \text{ lb}}{0.965 \text{ in}^2} = 491 \text{ psi}$$

where:

$$A = (0.46 \times 4 + 2.94 \times 2)(0.125) = 0.965 \text{ in}^2$$

$$P = 30 \text{ lb} \times 15.8g = 474 \text{ lbs}$$

The margin of safety (MS) is then:

$$MS = \frac{S_m}{S_c} - 1 = \frac{11{,}500 \text{ psi}}{491 \text{ psi}} - 1 = \underline{+\text{Large}}$$

Canister Body Buckling

The canister body is evaluated for buckling during the end drop by using the Euler formula to determine the critical buckling load (P_{cr}):

$$P_{cr} = \frac{K\pi^2 EI}{L^2} = \frac{0.722\pi^2 (9.6 \times 10^6)(2.98)}{(25.85)^2} =$$

305,073 lbs, assuming lower end fixed, upper end free

where:

$E = 9.6 \times 10^6$ psi

$K = 0.722$ (Reference Roark's Table 34, Case 3a)

$$I = \left(\frac{3.3 \text{ x } 3.2^3 - 2.82 \text{ x } 2.95^3}{12} \right) = 2.98^4, \text{ minimum moment of inertia}$$

L = tube body length (25.85 in.)

Because the maximum compressive load (10 lbs × 60g = 600 lbs under the accident condition) is much less than the critical buckling load (305,073 lbs), the canister body has adequate resistance to buckling.

As noted in the first paragraph of this section, the plate canister is only a handling fixture (not a structural component) and only serves as a spacer once inserted into the basket. Thus, retempering of the aluminum plates after welding is not required. The criticality evaluation presented in Section 6.4.3.10 includes the hypothetical separation of the canister fixture.

Figure 2.6.12-1 Cask Side Drop Fuel Tube Loading – MTR Fuel Basket

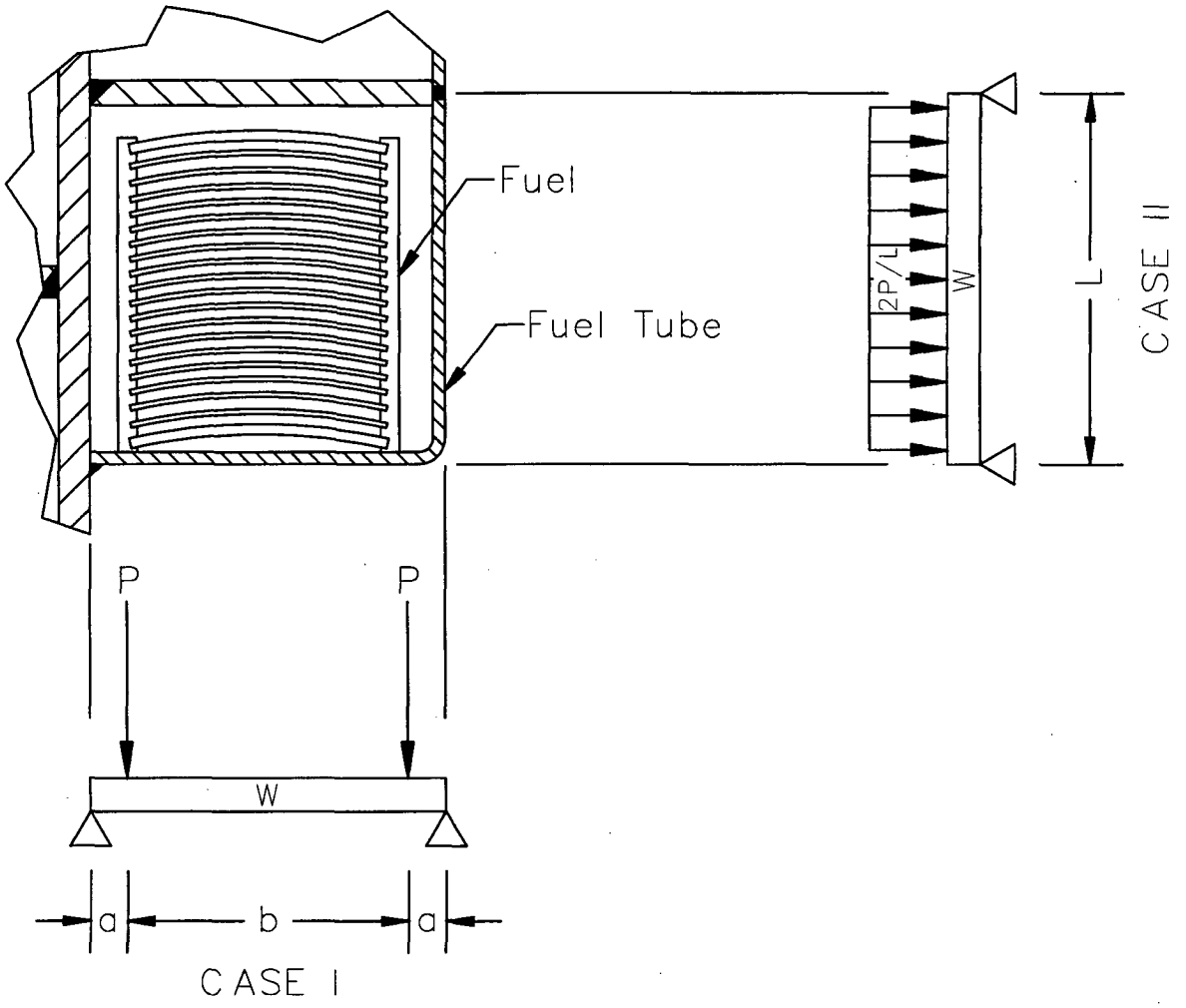

Figure 2.6.12-2 Baseplate Supports for Cask End Drop Loads - MTR Fuel Basket

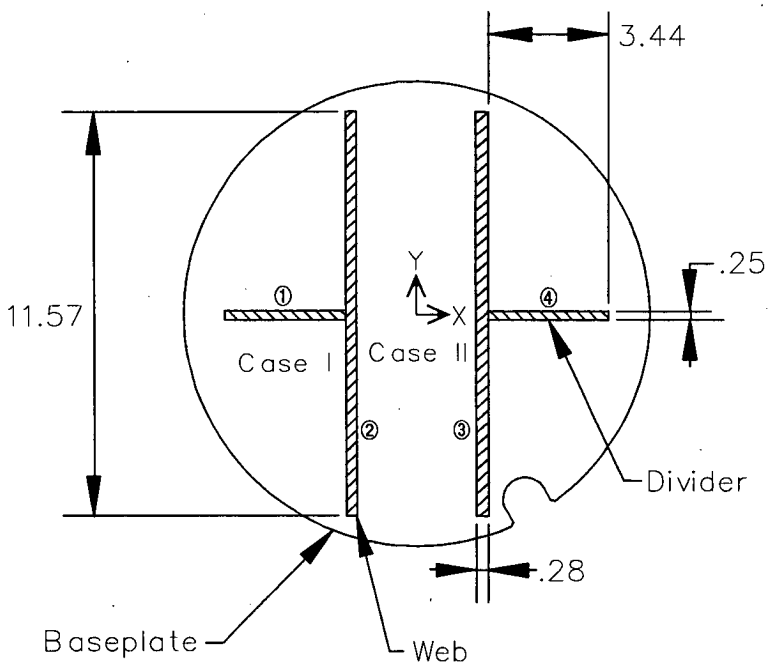

Notes:
Area of shaded portion = 8.20 in^2

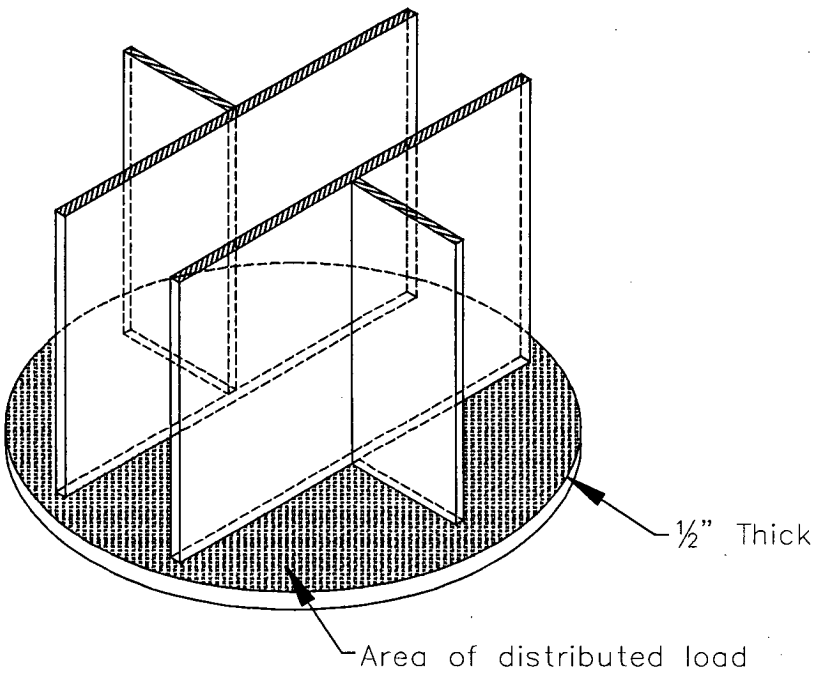

2.6.12.7 TRIGA Fuel Basket One-Foot Drop Evaluation

This section evaluates the stresses in TRIGA fuel baskets as a result of the normal condition one-foot drop. The basket assembly consists of 5 basket modules - a base module, a top module and 3 intermediate modules. During transport all 5 modules must be installed in the cask. The 3 intermediate modules are interchangeable, but the base and top modules are not. The top module is sized to accept TRIGA Fuel Follower elements, which are longer than the typical element. Two basket configurations are available, "nonpoisoned" and "poisoned," where the poisoned basket configuration utilizes borated steel plates for additional criticality control. Each module has up to 7 cells and each open cell holds up to 4 TRIGA fuel elements or up to 16 TRIGA fuel cluster rods. The center cell of each module of the nonpoisoned basket configuration is blocked by a solid 11-gage stainless steel plate that precludes fuel loading in the center cell. The structural evaluation is based on the poisoned TRIGA basket configuration, so that the structural evaluation bounds transportation of the nonpoisoned configuration with the center cell blocked. Intact fuel elements are loaded directly into the module cells, while intact fuel cluster rods are loaded into fuel rod inserts that are placed into the basket cells prior to fuel loading. For the poisoned basket design, an alternative is provided that utilizes one base module and four intermediate modules, along with a spacer to fill the space differential resulting from the use of an additional intermediate module, rather than a top module.

The top and bottom modules are designed to hold up to 4 intact TRIGA fuel elements in screened cans, or failed or damaged TRIGA fuel elements or fuel cluster rods in screened or sealed cans in each of the open cells. Up to four intact fuel elements may be confined within a screened failed fuel can. The screened can is a square tube of 14-gage Type 304 stainless steel, closed on its bottom end with a screen to allow water draining. It is closed with a lid.

Up to two failed TRIGA fuel elements or up to 6 failed TRIGA fuel cluster rods may be transported in a sealed failed fuel can. The sealed can has a circular cross-section and is fabricated from Type 304 stainless steel tubing with a 0.065-inch thick wall. The bottom end includes a check valve and drain plug to facilitate draining. The top end is closed with a metal seal and a lid that is bolted in place.

Each basket module is a Type 304 stainless steel weldment made up of two 1/2-inch thick, 13.27-inch diameter, circular plates at each end of longitudinal divider plates. The divider plates create seven compartments or cells. The outside wall of the four symmetric outermost fuel cells is fabricated from 11- gage Type 304 stainless steel sheet. The 1/2-inch plate at the top end of the module is welded to the exterior surfaces of the divider plates using a continuous 1/8-inch weld on the under side of the top plate and a continuous fillet weld on the top side. The 1/2-inch thick baseplate is continuously welded to the 1/2-inch thick divider plates and the 5/16-inch thick

web plates. The top module has an additional 1-inch thick support plate midway between the top and bottom circular plates that has a continuous fillet weld on the bottom side and a continuous seal weld on the top side. The 11-gage sheet metal, and the 5/16-inch thick (0.28-inches, min) intermediate webs, end 1/2-inch above the top surface of the baseplate to provide for module drainage. In addition, a 1-inch diameter hole is located in the module base plate, at the center of each of the cells. The bottom module sits on a 1.5-inch section of 10-inch diameter, schedule 80S, pipe welded to the baseplate. The pipe carries the total weight of the TRIGA basket assembly, and bears directly on the cask bottom forging. As previously noted, the center cell of each nonpoisoned basket module is blocked with an 11 gage plate welded to the cell walls. This plate prevents loading fuel elements in the center cell. The center cell is open at the bottom to ensure water draining.

Four of the seven cells in each poisoned basket module have a plate of borated stainless steel neutron absorber material on one side to ensure criticality control in transport. The borated plate extends over the active length of the TRIGA fuel assemblies, and covers the width and length of the cell face within the limits of the attachment welds. The configuration of the borated plate is shown in the license drawings in Section 1.4.

The bottom and intermediate modules have guide pins fixed to the surface of the top support plate. The pins fit into holes in the baseplate provided for that purpose to achieve alignment. A cutout in the baseplate and top plate is provided for clearance of the cask drain tube, and for circumferential alignment of the TRIGA basket assembly.

The weights of the TRIGA basket assembly and modules are shown below. The weight includes the heaviest fuel element that could be installed in the module, and failed fuel containers in the top and bottom modules. The calculated weight of each top and bottom module is increased by 70 lbs to account for the poison plates and to conservatively bound the structural analysis. Similarly, the calculated weight of the intermediate module is increased by 140 lbs.

Component	Weight of Fuel (lb) 140 Elements	Weight of Module(s)[1] (lb)	Total Weight (lb)	Length of Module(s) (in)
Bottom Module	247[2]	356	603	34.70
3 Intermediate Modules	741[2]	957	1,698	31.50
Top Module	370[3]	460	830	48.30
Weight of Empty Basket		1,773		
Loaded Weight of Basket			3,131	

Notes:

1. Includes the weight of failed fuel cans plus additional weight added for conservative design evaluation.
2. TRIGA fuel element design-basis weight is 8.82 pounds.
3. TRIGA fuel element design-basis weight is 13.2 pounds for top module.

The weight of TRIGA fuel cluster rods in a basket cell, including the weight of the fuel rod insert, is bounded by that of the TRIGA fuel elements. As reported in Section 1.2.3.1, the design basis weight of a TRIGA fuel element is 8.8 lbs, while the design basis weight of a TRIGA fuel cluster rod is 1.4 lbs and the weight of the insert is 11.2 lbs. Thus, four fuel elements in a cell weigh 35.2 lbs, while 16 fuel cluster rods and an insert in a cell weigh 33.6 lbs. Additionally, the active fuel cluster rod length is slightly longer than the length of the fuel elements, producing a smaller bearing load along the length of the fuel cluster rod and insert.

Therefore, the analyses of TRIGA basket modules and payload presented in the following sections are bounding for both nonpoisoned and poisoned basket configurations, and for all TRIGA fuel types.

2.6.12.7.1 NAC-LWT Inner Shell Bearing Stress Analysis

The nominal radial gap between the TRIGA fuel basket and the cask inner shell is 0.0531 inch at the calculated, steady state, normal conditions fuel temperature. As defined for other NAC-LWT fuel specific basket designs, it is assumed that there is no relative motion between the basket and the cask, and that the basket is in bearing contact with the cask cavity inner shell in the side drop. Bearing loads of the intact fuel, and the screened and sealed failed fuel cans, are thus transmitted directly to the inner shell and cask structure.

Bearing stress is calculated using Case 2C (Young) which models the cylindrical basket in a circular groove. The maximum compressive stress, for two elastic bodies with a similar elastic modulus, is:

$$S_c = 0.798\left\{\frac{\frac{gp(D_1 - D_2)}{D_1 D_2}}{\frac{2(1-\nu^2)}{E}}\right\}^{1/2} = 15{,}305 \quad \text{psi}$$

where:

g = 24.3, Dynamic load factor for the one-foot side drop

p = 1,256 lb/in., 1 g bearing load

D_1 = 13.405 inches, Cask cavity diameter

D_2 = 13.265 inches, Basket outside diameter.

ν = 0.275, Poisson's ratio for SS 304

E = 28.3 x 10^6 psi, Elastic modulus (conservatively use E at 70°F)

The bounding bearing load, p, is determined using the weight of the bottom module bearing on the inner shell of the cask at the top and bottom circular plates. The bearing surface considers the chamfer at the edge of the circular plates.

The allowable stress S_y = 18,200 psi at 600°F. Therefore:

$$MS = \frac{18,200}{15,305} - 1 = +0.19$$

2.6.12.7.2 NAC-LWT Bottom Forging Bearing Stress

The TRIGA basket assembly, when in the vertical position, is supported by a 0.5-inch thick, 10-inch nominal diameter schedule 80S pipe. The 1.5-inch long pipe is welded to the baseplate of the base unit. The compressive stress is:

$$S_c = \frac{g \times W}{A} = 3,073 \quad \text{psi}$$

where:

g = 15.8 Dynamic load factor for the one-foot end drop

W = 3,131 lbs, Total weight of the basket

A = 16.1 in^2, Area of 10-inch diameter Schedule 80S pipe

The allowable stress, S_y = 18,200 psi at 600 °F.

Therefore:

$$MS = \frac{18,200}{3,073} - 1 = +\underline{\text{Large}}$$

2.6.12.7.3 TRIGA Basket Compressive Stress Analysis

The TRIGA fuel basket is designed to ensure that the longitudinal movement of the basket relative to the cask inner cavity is limited. The fuel, and screened or sealed can contents are not attached to the basket, and do not impart any longitudinal structural load on the basket body. However, the basket must support itself during an end drop accident. The basket is analyzed as a column, acted upon by a structural (weight) compressive load.

The compressive stress developed in the basket compartment wall is:

$$S_c = \frac{g \times W}{A} = 6,033 \quad \text{psi}$$

where:

g = 15.8 Dynamic load factor for the one-foot end drop

W = 3,131 lbs, Total weight of the basket

A = 8.20 in^2, Total compartment cross-section area at base plate.

The allowable stress, S_m = 16,400 psi at 600°F.

Therefore:

$$MS = \frac{16,400}{6,033} - 1 = +\underline{1.72}$$

The Euler elastic buckling load formulation is used to determine the critical buckling load (P_{cr}) of the 10-inch diameter Schedule 80S pipe and the base module. The pipe and base module are conservatively treated as simply supported, which results in an effective length that is twice the actual length, reducing the critical buckling load by a factor of 4.0. For the 10-inch pipe, the critical buckling load is:

$$P_{cr} = \frac{\pi^2 EI}{L_e^{\ 2}} = 5.88 \times 10^9 \text{ lbs}$$

where:

E = 25.3 x 10^6 psi at 600°F

I = 212 in^4, inertia moment

L_e = 2 x 1.5 = 3.0 in., effective length (2L)

The calculated compressive load is:

P_c = W x g = 3,131 x 15.8 = 49,470 lbs

where:

g = 15.8 Dynamic load factor for the one-foot end drop

W = 3,131 lbs, Total weight of the basket

Therefore:

$$M.S. = \frac{P_{cr}}{P_c} - 1 = \frac{5.88 \times 10^9}{49,470} - 1 = +\underline{\text{Large}}$$

The critical buckling load for the base module is calculated using the same equation as above, by applying the moment of inertia of the fuel support structure. The fuel web and divider support structure is shown in the figure in the section titled "Baseplate Stress Due to End Drop."

The moment of inertia for the support structure is:

Item	$(I_o)_{yy}$	A	h	Ah^2	$(I_o)_{xx}$
2-11.57" x 0.28" web plate	0.0	6.48	1.86	22.42	72.28
2-3.44" x 0.25" divider plate	1.7	1.72	3.72	23.80	0.0
Total	1.7			46.22	72.28

$(I_o)_{yy} = I_o + \Sigma\, Ah^2 = 1.7 + 46.22 = 47.92\ in^4$

$(I_o)_{xx} = \Sigma\, I_o = 72.28\ in^4$

Choosing the smaller moment of inertia, $(I_o)_{yy}$, as I:

$I = 47.92\ in^4$

$$P_{cr} = \frac{\pi^2 EI}{L_e^{\,2}} = \frac{\pi^2 \times 25.3\times10^6 \times 47.92}{(2\times33.2)^2} = 2.11\times10^6 \text{ lbs}$$

where:

$L_e = 2 \times 33.2$ inches

$P_c = W \times g = 3{,}131 \times 15.8 = 49{,}470$ lbs

where:

g = 15.8, Dynamic load factor for 1 foot end drop

W = 3,131 lbs, Total weight of the basket

$$M.S. = \frac{P_{cr}}{P_c} - 1 = \frac{2.11\times10^6}{49{,}470} - 1 = +\underline{\text{Large}}$$

2.6.12.7.4 TRIGA Basket Lateral Stress Analysis

The base plate at the end of a typical TRIGA basket module supports the weight of up to 28 TRIGA fuel elements, or the loaded screened or sealed failed fuel cans, when the cask is in the vertical orientation (0 degree drop). With the cask in the horizontal orientation (90 degree drop), the fuel cell divider plates support the entire length of the TRIGA fuel. The base plate and the divider plates share in the support of the TRIGA fuel at drop orientations between 0 and 90 degrees.

Baseplate Stress Due to End Drop

The support plate at the top end of the modules is continuously welded to the outside periphery of the plates, including the support plates that form the fuel cells. The baseplate of the basket module is continuously welded to the two 11.57-inches wide, 5/16-inch thick (0.28-inch min)

web plates, and to the two 3.44-inches wide, 1/4-inch thick divider plates as shown in the following sketch.

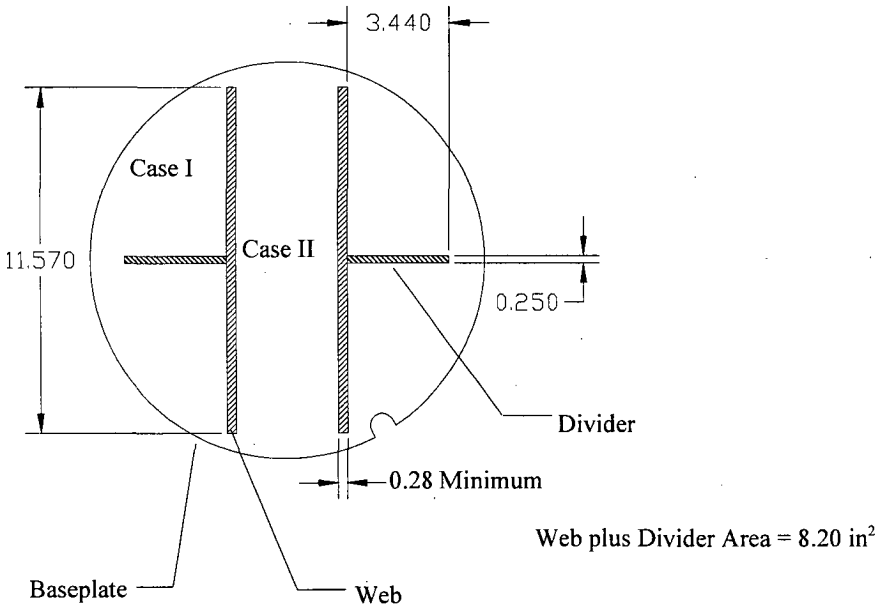

The baseplate supports 28 TRIGA fuel elements and is conservatively assumed to be supported by the main longitudinal support plates during a cask end drop. Two separate load cases are evaluated. The maximum stress for each case is combined to obtain the total stress on the baseplate.

The first case (Case I), evaluates a 3.44-inches square plate with adjacent sides fixed and the other sides free. The applied pressure over the entire plate is uniform (Young, page 471, case 11). The second case, Case II, examines a rectangular plate, 11.57 inches by 3.44 inches, fixed along the long edges, free along the short edges and uniform pressure (Young, page 462, case 6).

For Case I, the 3.44-inches square plate is analyzed as a cantilevered plate supported at two adjacent sides with the other two sides free. Load is assumed uniform over the area of the plate. The bounding fuel weight is applied. The maximum stress is expressed as (Young, page 471, case 11):

$$S_1 = \frac{-g \times B_1 \times P \times b^2}{A \times t^2} = -8{,}944 \text{ psi}$$

where:

g = 15.8, Dynamic load factor for the one-foot end drop

B_I = 1.769, Boundary condition stress factor

P = 80 lbs, Bounding module fuel weight

b = 3.44 inches, Width of plate

A = $(3.44)^2$ sq. in., Plate area

t = 0.5 in, Plate thickness

Case II, evaluates a plate 3.44-inches by 3.44-inches (width x length), fixed on two opposite sides, with the other two sides free. The maximum stress is expressed as (Young, page 462, case 6):

$$S_{II} = \frac{-g \times B_{II} \times P \times b^2}{A \times t^2} = -2{,}528 \text{ psi}$$

where:

g = 15.8, Dynamic load factor for the one-foot end drop

B_{II} = 0.5, Boundary condition stress factor

P = 80 lbs, Bounding module fuel weight

b = 3.44 inches, Width of plate

A = $(3.44)^2$ sq. in., Plate area

t = 0.5 in., Plate thickness

The total bending stress from Case I and Case II is:

$S_{total} = S_I + S_{II} = -11{,}472$ psi $< 1.5\ S_m = 24{,}600$ psi

Therefore:

$$MS = \frac{24{,}600}{11{,}472} - 1 = +\underline{1.14}$$

Support Plate Stress Due to Side Drop With Intact Fuel or the Screened Failed Fuel Can

The maximum stress in the support plates that form the fuel cells occurs in the 0.12-inch thick 11 gage sheet metal tubes which support the entire length of the TRIGA fuel elements, or the length of the loaded screened failed fuel can. The weight of the TRIGA fuel element is transmitted through the can walls to the support plates that form the fuel cell. This load path creates a uniform pressure load over the entire area as shown in the following sketch.

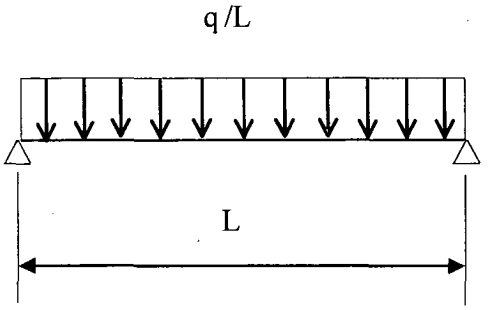

As stated in Section 2.6.12.7, the loading of TRIGA fuel cluster rods is bounded by the TRIGA fuel elements. The fuel weight per unit length for the bounding TRIGA fuel elements is:

Fuel Type	Max. Weight, W (lb)	Max. Length, L (in)	W/L (lb/in)
Aluminum Clad	6.4	28.53"	0.22
Stainless Steel Clad	8.82	29.88"	0.30
Fuel Follower Control Element	13.2	45"	0.29

The intact fuel bounding load, q_i, along the length of the tube is:

$$q_i = \frac{W_i}{L_s} = 1.850 \text{ lb / in}$$

The uniform pressure load for the shorter (L_s) failed fuel in the screened can is:

$$q_f = \frac{W_f}{L_s} = 1.950 \text{ lb/in}$$

The uniform pressure load of the longer (L_L) failed fuel in the screened can is:

$$q_f = \frac{W_f}{L_L} = 1.778 \text{ lb/in}$$

where:

L_s = 29.88 inches, length of short fuel element

L_L = 45 inches, length of long fuel element

Weight of long failed fuel can = 17 lbs

Weight of short failed fuel can = 13 lbs

Added weight for fuel can calculation = 10 lbs

The weight calculation below includes 4 fuel elements, added weight, plus fuel can.

W_f = 58.28 lbs for fuel can with fuel elements having a length of 29.88 inches (L_s)

W_f = 80 lbs for fuel can with fuel elements having a length of 45 inches (L_L)

W_i = 55.28 lbs for fuel can with intact fuel

The bounding load for TRIGA fuel is 1.950 lb/in.

The maximum bending moment is:

$$M_{max} = \frac{(q_f + w) \times gL}{8} = 21.6 \text{ in} - \text{lb}$$

where:

q_f = 1.950 lb/in

g = 24.3, dynamic load factor for one foot side drop

t = 0.12-inches (11 gage)

L = 3.44 = width of side support plate (11 gage)

w = 0.288 x 3.44 x t = 0.1185 lb/in, steel beam weight

$$S = \frac{6 \times M_{max}}{t^2} = 9{,}065 \text{ psi}$$

Therefore,

$$MS = \frac{24{,}600}{9{,}065} - 1 = +\underline{1.71}$$

The 11 gage sheet metal is continuously welded to the adjacent divider plates with a 1/8-inch fillet weld. This weld resists the shear developed in the simple beam analysis above.

$$V = \frac{(W_f + wL_s) \times g}{2 \text{ x } L_s} = 25.14 \text{ lbs}$$

where:

W_f = 58.28 lbs

L_s = 29.88 inches

$$S_v = \frac{V}{t \times 1} = 210 \text{ psi}$$

The throat thickness of 1/8-inch fillet weld is 0.707 x 0.125 = 0.088-inches. The square of the ratio of the plate thickness (0.12-inch) to the weld throat thickness (0.088-inches) is 1.86. ASME Code Subsection NG-3352 recommends that the calculated stress in a fillet weld be increased by a factor of 1/0.35 = 2.86. The maximum weld stress is:

$$S_w = S_v\,(1.86)\,(2.86) = 1{,}117 \text{ psi}$$

The allowable stress is $0.6S_m = 9{,}840$ psi at 600°F.

Therefore:

$$MS = \frac{9{,}840}{1{,}117} - 1 = +\underline{\text{Large}}$$

Support Plate Stress Due To Side Drop For the Sealed Failed Fuel Can

The total bounding weight of the long sealed can is 59.6 lbs, which includes 20 lbs for the can and a bounding weight of 39.6 lbs for the follower control elements.

The maximum stress in the support plates occurs in the 0.12-inch thick (11 gage) sheet metal tubes which supports the entire length of the sealed can. Since the sealed can is cylindrical, its weight is transmitted as a line load over the length to the supporting plate. For a unit cross-section of the supporting plate, the line load is treated as a concentrated load over the supporting plate as shown in the following loading diagram.

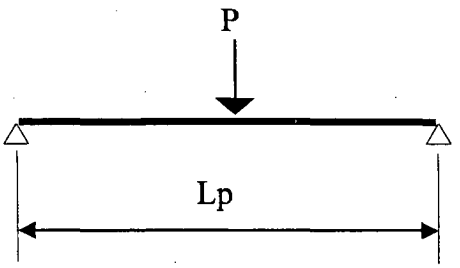

The load of the sealed can and its contents is represented by a uniformly distributed line load along the basket length that is in contact with the sealed can. For a unit length, the concentrated load due to the longer can is:

$$P = \frac{W_f \times g}{L} = 37.71 \text{ lb/in}$$

where:

W_f = 59.6 lbs, weight of the long sealed can (20 lbs) and the follower control elements (39.6 lbs)

g = 24.3, dynamic load factor for one-foot side drop

L = 38.41 inches, length of the longer body sealed can tube

For the shorter can:

$$P = \frac{W_f \times g}{L} = 45.24 \text{ lb / in.}$$

where:

W_f = 43.4 lbs, weight of the shorter sealed can (17 lbs) and bounding fuel element (26.4 lbs)

g = 24.3, dynamic load factor for one-foot side drop

L = 23.31 inches, length of the shorter body sealed can tube

The concentrated load from the shorter can, P = 45.24 lb/in., enveloping both the longer can and short can, is used to calculate the maximum bending moment. The unit length of the basket support plate with the 45.24 lbs concentrated force in the middle is treated as a simply supported beam. The maximum bending moment is:

$$M_{max} = \frac{P \times L_p}{4} = 38.91 \text{ in-lb}$$

where:

P = 45.24 lbs, concentrated load

L_p = 3.44 inches, width of the 11 gage support plate

The maximum bending stress is:

$$S = \frac{6 \times M_{max}}{t^2} = 16{,}321 \text{ psi}$$

where:

M_{max} = 38.91 in-lb, maximum bending moment

t= 0.12 in., thickness of the 11-gage support plate

The margin of safety is:

$$M.S. = \frac{1.5S_m}{S} - 1 = \frac{24{,}600}{16{,}321} - 1 = +\underline{0.51}$$

The 11 gage sheet metal is continuously welded to the adjacent divider plates with a 1/8-inch fillet weld. This weld resists shear developed in the simple beam analyzed above.

$$S_v = \frac{P}{t \times 1} = 378 \text{ psi}$$

where:

P = 45.24 lbs, load of unit length

t = 0.12 in, thickness of the 11 gage support plate

The throat thickness of 1/8-inch fillet weld is 0.707 × 0.125 = 0.088 in. The square of the ratio of the plate thickness (0.12 in) to the weld throat thickness (0.088 in) is 1.86. ASME Code Subsection NG-3352 recommends that the calculated stress in a fillet weld be increased by a factor of 1/0.35 = 2.86.

Maximum weld stress is the calculated stress in the material times the above factors.

$S_w = S_v\ (1.86)\ (2.86) = 378 \times 1.86 \times 2.86 = 2{,}011$ psi

The allowable stress is:

$0.6S_m = 9{,}840$ psi @ 600°F,

The margin of safety is:

$$MS = \frac{9{,}840}{2{,}011} - 1 = +\underline{3.9}$$

Maximum Basket Stress Due To Oblique Drop

As shown in the previous sections, the sealed can imposes the largest stress in the basket support plate due to its cylindrical cross-section. Therefore, the maximum stress in the basket is bounded by the stress induced by the sealed failed fuel can.

The maximum stress in the basket during oblique drop is found by combining the absolute value of the maximum stresses found in the basket during side drop and end drop determined in the previous sections. Although the stresses in the two different drop configurations do not occur in the same location, the stress combination method conservatively envelopes the maximum possible stress states during the oblique drop.

The maximum calculated stresses for the 1-foot end drop and the 1-foot side drop are:

Maximum stress = 6,033 psi for end drop

Maximum stress = 16,321 psi for side drop

Adding the two stress values to obtain the total oblique drop stress = 6,033 + 16,321 = 22,354 psi.

Allowable stress = 1.5 S_m = 1.5 x 16,400 = 24,600 psi @ 600°F,

$$MS = \frac{24{,}600}{22{,}354} - 1 = +\underline{0.10}$$

2.6.12.7.5 Screened Failed Fuel Can

This section evaluates the stresses in the screened failed fuel can as a result of the normal condition one-foot drop. The screened failed fuel can is described in Section 2.6.12.7. The screened failed fuel can is analyzed for side and end drops during transportation.

Screened Failed Fuel Can Compressive Stress Analysis

The fuel contents are not attached to the screened can and do not impart any longitudinal structural load on the can. The screened can must support itself during an end drop accident. The can is analyzed as a column acted upon by a structural (weight) compressive load consisting of the weight of the can and its contents. The screened can for fuel follower control rods is used since it is heavier, carries a heavier load and has the same properties as the screened can for the fuel rods.

The compressive stress developed in the screened can wall is:

$S_c = Wg/A = 1{,}145$ psi

where:

W = 71 lbs, weight of screened can and contents

g = 15.8, dynamic load factor for one foot end drop (normal condition)

A = 0.98 in^2, cross-section area of screened can

The allowable stress,

S_m=16,400 psi at 600°F.

Therefore:

MS = (16,400/1,145) - 1 = +Large

Buckling of the screened failed fuel can is evaluated using hypothetical accident loading conditions in Section 2.7.7.9.4. The loading conditions presented in that section bound normal condition loads.

Screened Failed Fuel Can Plate Stress Due to Side Drop

The plate making up the sides of the screened failed fuel can is analyzed for bending as a result of loads applied during a side drop. To bound the analysis, the weight of the longer failed fuel can is used and this load is distributed over the length of the shorter fuel can to determine the load acting on a one-inch wide strip (along the axial length of the can) of the fuel can cross section. This total load on a one-inch strip is conservatively applied to the area between fuel elements (1.5 inches), resting inside of the can. This is the longest span of plate subject to

bending from a side drop and the 1.5-inch long plate section (which is one-inch wide) is considered to be simply supported.

The bending moment in the plate due to a uniform load is:

$M = gPL/8 = 10.3$ in-lb

where:

g = 24.3, dynamic load factor for one foot side drop

P = 2.26 lbs., Total load on one inch wide strip

L = 1.5inches, spacing between fuel elements

The section modulus, s, of the cross-section resisting the bending moment is:

$s = t^2/6 = 0.00093$ in.^{3}

where:

t = 0.0747 in, thickness of plate making up the screened failed fuel can

The bending stress is:

$S_b = M/s = 11{,}075$ psi

The allowable stress is: $1.5S_m = 24{,}600$ psi

Therefore:

MS = (24,600/11,075) - 1 = +1.22

2.6.12.7.6 Sealed Failed Fuel Can

This section evaluates the stresses in the sealed failed fuel can as a result of the normal condition one-foot side and end drops. The sealed can is described in Section 2.6.12.7.

Sealed Failed Fuel Can Compressive Stress Analyses Due to End Drop

This section analyzes the compressive stress and buckling load in the fuel tube, bottom tube and lifting lugs. The bounding weight of the sealed can used in this analysis is 59.6 lbs, which includes 20 lbs for the can and conservatively 39.6 lbs for the follower control elements. Actual operational capacity is controlled to the weight of two fuel elements.

Fuel Tube

The fuel elements are not attached to the round tube that forms the wall of the can. However, it is conservatively assumed that the shell of the sealed can carries the entire weight of the can and contents. The compressive stress is:

$$\sigma_C = \frac{W \times g}{A} = 1{,}448 \text{ psi}$$

where:

W = 59.6 lbs, conservative weight of the can and contents

g = 15.8, dynamic load factor for one foot end drop

A = $\pi(1.625^2 - 1.56^2)$ = 0.6504 in.^{2} cross section area of the can

The margin of safety is:

$$MS = \frac{S_m}{\sigma_C} - 1 = \frac{16{,}400}{1{,}448} - 1 = +\underline{\text{Large}}$$

Bottom Tube

The compressive stress for the bottom tube is:

$$\sigma_C = \frac{W \times g}{A} = 1{,}010 \text{ psi}$$

where:

W = 59.6 lbs, conservative weight of the can and contents

g = 15.8, dynamic load factor for one foot end drop

A = $\pi(1.25^2 - 1.125^2)$ = 0.9327 in.^{2} cross section area of bottom tube

The margin of safety is:

$$MS = \frac{S_m}{\sigma_C} - 1 = \frac{16{,}400}{1{,}010} - 1 = +\underline{\text{Large}}$$

Lifting Lug

The sealed can lifting lugs may be subject to compressive or buckling loads in drop accident events. The load is considered evenly distributed to both lugs.

The compressive stress for two lift lugs is:

$$\sigma_C = \frac{W \times g}{A} = 3{,}657 \text{ psi}$$

where:

W = 59.6 lbs, conservative weight of the can and contents

g = 15.8, dynamic load factor for one foot end drop

A = 2 x 0.515 x 0.25 = 0.2575 in.^{2} smallest cross section area of the two lift lugs

The margin of safety is:

$$MS = \frac{S_m}{\sigma_C} - 1 = \frac{16,400}{3,657} - 1 = +\underline{3.48}$$

Considering the lifting lug as a cantilever beam with a fixed end, the load is carried by an equivalent moment, M:

$M = (P/2) \times d \times g = 114.2$ in-lbs

where:

g = 15.8, g load factor for the one foot end drop

P = 59.6 lbs, conservative weight of can and contents

d = 0.2425 in, the length of moment arm, measured from the center of the section to the point of load application (.5 - .515/2)

The total stress acting on the neck section is:

$$\sigma = \frac{(M \times c)}{I} + \sigma_C = 13,975 \text{ psi}$$

where:

σ_c = compressive stress, 3,657 psi

W = 114.2 in-lbs, equivalent moment

c = 0.515/2 inches, distance from center of neck section to the edge

$I = 0.25 \times (0.515)^3/12 = 2.85 \times 10^{-3}$ in^4, moment of inertia of the cross section

The margin of safety is:

$$MS = \frac{1.5S_m}{\sigma_c} - 1 = \frac{24,600}{13,975} - 1 = +\underline{0.76}$$

Buckling of the Sealed Failed Fuel Can

Buckling of the sealed failed fuel can, the bottom tube and the lifting lug is evaluated in Section 2.7.7.9.5. The loading conditions presented in that section bound the normal condition loads.

Sealed Failed Fuel Can Plate Stress Due to Side Drop

In the one-foot side drop, the sealed can supports the load applied by its contents.

The load applied to the can is considered as a linearly distributed load over the bottom 120° arc. The radial pressure w_x varies linearly from 0 at the beginning, to w at the bottom point of the can, as shown in the following sketch.

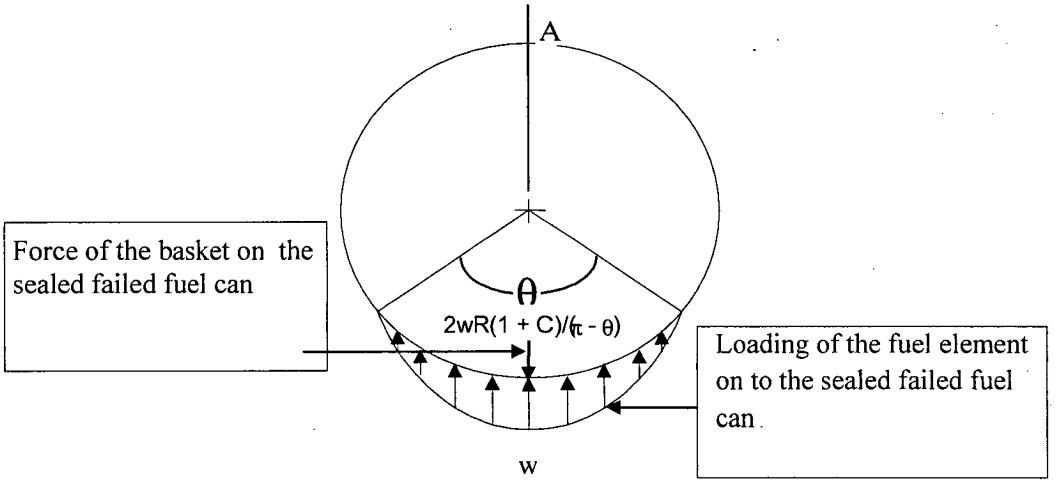

The load is uniformly distributed along the length of the can. For a unit length it is calculated as:

For the longer can:

$$p = \frac{W_f \times g}{L} = 25.05 \text{ lb / in.}$$

where:

W_f = 39.6 lbs, conservative fuel weight of three fuel follower control elements

g = 24.3, dynamic load factor for a one-foot side drop

L = 38.41 inches, length of the longer tube body

For the shorter can:

$$p = \frac{W_f \times g}{L} = 27.52 \text{ lb / in.}$$

where:

W_f = 24.4 lbs, conservative fuel weight of three fuel elements

g = 24.3, dynamic load factor for a one-foot side drop

L = 23.31 inches, length of the shorter tube body

To bound both the longer can and short can, p = 27.52 lb/in. is used to calculate the maximum distributed load.

Since (Young, 6th Edition, Table 17, Case 13):

$$p = 2wR(1+C) / (\pi - \theta)$$

$$w = \frac{p \times (\pi - \theta)}{2R \times (1 + C)} = 17.73 \text{ lb/in}$$

where:

p = 27.52 lbs, load on this unit length of the can tube

θ = 120° = 2π/3, angle

C = cos (θ) = -0.5

R = 3.25/2, radius of the can

The bending moment occurring at location A and C are respectively (Young, 6th Edition, Table 17, Case 13):

$$M_A = \frac{-wR^2}{\pi(\pi - \theta)} \left\{ 2 + 2C - s(\pi - \theta) + k_2 \left[1 + C - \frac{(\pi - \theta)^2}{2} \right] \right\} = -1.273 \text{ in-lb}$$

$$M_C = \frac{-wR^2}{\pi(\pi - \theta)} \left\{ \pi(\pi - \theta) - 2 - 2C - s\theta + k_2 \left[1 + C - \frac{(\pi - \theta)^2}{2} \right] \right\} = -6.507 \text{ in-lb}$$

where:

w = 17.73 lb/in, maximum distributed load

R = 3.25/2 - 0.625/2, curvature

θ = 120° = 2π/3, angle

C = cos (θ) = -0.5

s = sin(θ) = 0.866

$k_2 = 1 - \alpha = 1$ and $\alpha = \frac{I}{AR^2} = \frac{2.289e-5}{0.6504 \times 1.593^2} = 1.388 \times 10^{-5}$

$I = \frac{1 \times 0.065^3}{12} = 2.289 \times 10^{-5}$ in^4, moment of inertia of ring cross section

$A = \pi(1.625^2 - 1.56^2) = 0.6504$ in^2

The bending stress at location C, for unit length, is:

$$\sigma_c = \frac{M_C}{t^2/6} = 9{,}241 \text{ psi}$$

where:

M_C = 6.507 lb-in., bending moment at location C

t= 0.065 in., thickness of the can

Margin of safety is:

$$MS = \frac{S_m}{\sigma_C} - 1 = \frac{16{,}400}{9{,}241} - 1 = +\underline{0.77}$$

Sealed Failed Fuel Can Bolt Evaluation

The sealed failed fuel can bolts are evaluated using the worst case loading conditions. For analysis purposes, the maximum differential thermal expansion (from accident conditions), lifting loads, and bolt preload are combined to calculate the maximum bolt stresses.

Bolt Thread Stress

The shear stress caused by lifting is:

$$\tau_L = \frac{1.1 \times W}{A_S} = 170 \text{ psi}$$

where:

1.1 = dynamic load factor for lifting

W = total weight of the canister and contents, 59.6 lbs

A_s = shear area of the external thread, 0.3859 $in.^2$

The load caused by pre-load on each bolt is:

$F_T = (\pi \text{ x } D \text{ x } P)/4 = 1{,}721$ lbs

where:

P = 700 lb/in., conservative linear load required to crush the seal

D = 3.131 inches, diameter of the seal

The linear load, P, considers both the load to seat the metal seal as well as the internal pressure of the gas in the failed fuel canister. The contribution of the pressure to the linear load is:

$$\frac{P_{gas} D}{4} = \frac{(3\,\text{atm})(14.7\,\text{psi / atm})(3.131\,\text{in.})}{4} = 34.5 \text{ lb / in.}$$

Three (3) atm is conservatively used for the internal gas pressure during the fire. The linear load to seat the metal seal is 514 lbs. Combining the linear loads due to the pressure and seal gives a total value of 548.5 lb/inch. For analysis purposes, a conservative value of 700 lb/in. is used.

The shear stress caused by pre-loads in the bolts is:

$$\tau_t = \frac{F_t}{A_s} = 4{,}460 \text{ psi}$$

where:

F_t = 1,721 lbs, bolt pre-load

A_s = shear area for 3/8 -16 UNC 2A thread = 0.3859 sq. inch

Total shear caused by lifting and pre-load is obtained by conservatively adding the shear stresses:

$$\tau = \tau_L + \tau_t = 4{,}630 \text{ psi}$$

The margin of safety is:

$$MS = \frac{0.6S_m}{\tau} - 1 = \frac{0.6 \times 45{,}200}{4{,}630} - 1 = +\underline{4.86}$$

The average tensile stress due to pre-load in the bolts is:

$$S_t = \frac{F_t}{A_t} = 23{,}039 \text{ psi}$$

where:

F_t = 1,721 lbs, bolt pre-load

A_t = tensile stress area for 3/8-14 UNC 2A thread = 0.0747 in^2

The tensile stress due to the differential expansion of the bolt and the top plate is:

$$S_{dt} = \Delta T(\alpha_L - \alpha_{637})E_{637} = 26{,}912 \text{ psi}$$

where:

ΔT = (600 - 70)°F = 530°F (The actual maximum temperature of the can during the fire accident is 551°F.)

α_L = 9.53 x 10^{-6} (in/in/°F), coefficient of thermal expansion of top plate (S.S.304) at 600°F

α_{637} = 7.67 x 10^{-6} (in/in/°F), coefficient of thermal expansion of bolt (SB - 637) at 600°F

E_{637} = 27.3 x 10^6 psi at 600°F, bolt material elastic modulus at 600°F

The total stress due to pre-load and differential expansion of the bolt and the top plate is:

$$S = S_{dt} + S_t = 49{,}951 \text{ psi}$$

The margin of safety is:

$$M.S = \frac{2S_m}{S} - 1 = \frac{2 \times 45{,}200}{49{,}951} - 1 = +\underline{0.81}$$

The relation between the torque value and tensile force is:

$$T = \left[\left(\frac{d_m}{2d}\right)\left(\frac{\tan\lambda + \mu \sec\alpha}{1 - \mu \tan\lambda \sec\alpha}\right) + 0.625\mu\right](F_T)(d) \qquad \text{(Machinery's)}$$

$$T = (0.2096) \times F_T \times d = 135 \text{ in-lb}$$

where:

T = applied torque in inch-pounds

F_T = pre-load force in pounds

d = 3/8 in, bolt diameter

$\tan\lambda = L/(\pi d_m)$

L = 1/16 in

d_m = 0.3911 in, mean diameter of threads

α = 30°, one-half the thread angle

μ = 0.15, coefficient of friction

The torque required to engage the bolt is 135 in-lb. However, the maximum torque is 160 in-lb. The torsional stress due to this torque value is:

$$\tau_t = \frac{T \times r}{J} = \frac{160 \times 0.1875}{1.94 \times 10^{-3}} \text{ psi} = 15{,}464 \text{ psi}$$

where:

T = 160 in-lb, the torque on a bolt

r = (3/8)/2 = 0.1875 in, radius of bolt

J = $(\pi r^4)/2 = (\pi \times 0.1875^4)/2 = 1.94 \times 10^{-3}$ in^4, polar moment of inertia

The margin of safety is:

$$MS = \frac{0.8S_m}{\tau_t} - 1 = \frac{0.8 \times 45{,}200}{15{,}464} - 1 = +\underline{1.34}$$

Top Plate Thread Stress

The effect of Heli-Coil is conservatively ignored. The shear stress consists of two parts; one is caused by the lifting load; the other is caused by the combination of pre-load P (700 lbs/in.) and differential thermal expansion. The shear stress due to the lifting load is:

$$t_L = \frac{1.1 \times W}{A_n} = 118 \text{ psi}$$

where:

1.1 = the dynamic load factor for lifting

W = 59.6 lbs, total weight of the canister and contents

A_n = 0.5548 in^2, shear area of the inner thread

The shear stress due to pre-load and differential thermal expansion in the top plate is:

$$S = \frac{F_t}{A_n} = 6{,}725 \text{ psi}$$

where:

F_t = 1,721+26,912 x 0.0747 = 3,731 lbs, bolt pre-load

A_n = 0.5548 in^2, shear area for 3/8 -16 UNC 2A thread

Total shear caused by lifting, pre-load and differential expansion is obtained by conservatively adding the separate shear stresses:

$$\tau = \tau_L + S = 6{,}843 \text{ psi}$$

The margin of safety is:

$$MS = \frac{0.6S_m}{\tau} - 1 = \frac{0.6 \times 16{,}400}{6843} - 1 = +\underline{0.44}$$

Top Plate Bearing Stress

Top plate bearing stress is developed from the combination of pre-load and the differential thermal expansion of the bolt and the top plate. The pre-load is 1,721 lbs on one bolt and thermal load is 2,010 lbs (0.0747 in^2 × 26,912 psi). The total bearing is 3,731 lbs. Then, the bearing stress on the top plate is:

$$S_b = \frac{P_b}{A_b} = \frac{3731}{0.2311} = 16{,}145 \text{ psi}$$

where:

P_b = 3,731 lbs, total bearing force

$A_b = \pi(0.68^2-0.41^2)/4 = 0.2311$ in^2, bearing area

The margin of safety for top plate is:

$$MS = \frac{1.0S_y}{S_b} - 1 = \frac{18{,}200}{16{,}145} - 1 = +\underline{0.13}$$

2.6.12.7.7 Borated Stainless Steel Plate Weld Stress

The borated stainless steel plate utilized in the poisoned TRIGA baskets is assumed to be welded on two sides to the divider plates using a 1/16-inch fillet weld. This assumption is conservative since the borated plate is welded completely around its periphery. For the end drop condition, the only load applied on the weld is the self weight of the plate, which results in a shear stress. For side drop, the load applied on the weld is the self weight of plate, which also results in shear stress. The plate also carries the weight of the fuel, which results in compressive stress.

The welded area for one stainless steel plate is:

Parameter	Base Module	Intermediate Module	Top Module
Weight of Plate (lb)*	14.44	13.64	21.61
Length of Plate (in)	30.45	28.75	45.55
Cross Section Area (in^2)	99.27	93.73	148.49
Weld Area (in^2)	3.81	3.59	5.69

Using the smallest area, 3.59 in^2 and largest weight, 21.61 lbs, the end drop shear stress is:

$$S_{se} = \frac{g \times W}{A} = \frac{15.8 \times 21.61}{3.59} = 95.11 \text{ psi}$$

where:

g = 15.8 one-foot end drop load factor

W = 21.61 lbs bounding poison plate weight

A = 3.59 in^2 bounding weld area

The allowable shear stress for normal condition is 0.6 S_m = 9840 psi. The margin of safety is:

$$\text{Margin of Safety} = \frac{0.6S_m}{S_{se}} - 1 = \frac{9840}{95.11} - 1 = +\underline{\text{Large}}$$

Using the smallest area, 3.59 in^2 and largest weight, 21.61 lbs, the side drop shear stress is:

$$S_{ss} = \frac{g \times W}{A} = \frac{24.3 \times 21.61}{3.59} = 146.27 \text{ psi}$$

where:

g = 24.3 one-foot side drop load factor

W =21.61 lbs bounding poison plate weight

A = 3.59 in^2 bounding weld area

The allowable shear stress for normal condition is 0.6 S_m = 9840 psi. The margin of safety is:

$$\text{Margin of Safety} = \frac{0.6S_m}{S_{ss}} - 1 = \frac{9840}{146.27} - 1 = +\underline{\text{Large}}$$

The compressive stress is evaluated using a bounding fuel cell weight of 80 lbs. The minimum cross section area is 93.73 in^2.

$$S_c = \frac{g \times W}{A} = \frac{24.3 \times 80}{93.73} = 20.74 \text{ psi}$$

where:

g = 24.3 one-foot side drop load factor

W = 80 lbs bounding fuel cell weight

A = 93.73 in^2 bounding cross section area

The allowable stress is 1.0S_m = 16,400 psi. The margin of safety is:

$$\text{Margin of Safety} = \frac{1.0S_m}{S_c} - 1 = \frac{16{,}400}{20.74} - 1 = +\underline{\text{Large}}$$

This evaluation shows that the weld has large margins of safety for the stresses that could occur in normal conditions.

2.6.12.7.8 TRIGA Fuel Spacer Evaluation

A spacer fabricated from Type 304 stainless steel is used in poisoned TRIGA basket Configuration 2 (base module and 4 intermediate modules). The spacer consists of 8-inch diameter pipe with a 1-inch thick plate welded to the bottom, and a 0.5-inch thick plate welded to the top. The top plate is attached to the underside of the NAC-LWT cask lid using four 1/2-inch diameter SA-193, Grade B6, bolts. It has a calculated weight of 85 lbs.

The spacer and bolts are analyzed for the effects of a normal condition 1-foot side and end drop. The material temperatures and properties are the same as those imposed on the fuel baskets. The compression load is calculated as 50,813 lbs, which results in a calculated stress of 6,049 psi

(Margin of Safety = +1.71). The stress on the bolts in combined shear and tension is 11,881 psi. All margins of safety are positive with a minimum Margin of Safety of +0.21 for the bolts in shear and tension as a result of the side drop condition.

2.6.12.7.9 TRIGA Fuel Cluster Rods Basket One Foot Drop Evaluation

The fuel cluster rod is restrained from motion by the aluminum tube, which has a 0.75-inch outer diameter and a 0.62-inch inner diameter. An array of four by four is inserted into an aluminum shell of 0.125-inch thickness, which is loaded into the stainless steel basket.

The bearing stress between the aluminum tubes is required to be less than the yield stress of the 6061-T6 aluminum. The yield stress is evaluated at the maximum aluminum temperature of 300°F, corresponding to a yield stress of 27.5 ksi. The maximum bearing load would occur between the aluminum tube and the 0.125 aluminum shell (Point 2 in the following sketch), but the maximum bearing stress would occur between two adjacent cylinders (Point 1 in the following sketch).

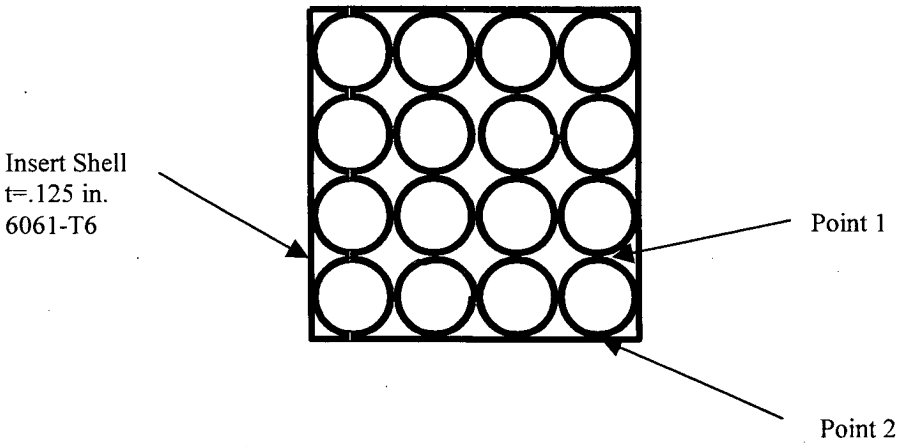

Using Roark, 6th edition, Table 33, Case 2a, which is the bearing stress between two adjacent cylinders, the bearing stress (S_{brg}) is:

$$S_{brg} = .789 \times \sqrt{\frac{P}{K_D C_E}}$$

$$P = \text{the line load} = (3 \text{ tubes}) \left(\frac{1.44}{27.5} + \frac{\pi}{4}(0.75^2 - 0.62^2)(0.098) \right)$$

$P = 0.198$ lbs/in (for dead weight only)

where:

TRIGA fuel cluster rod weight = 1.44 lbs

rod length = 27.5 inches

aluminum density = 0.098 lb/in^3

aluminum tube OD = 0.75 in

aluminum tube ID = 0.62 in

$$C_E = \frac{1-\upsilon_1^2}{E_1} + \frac{1-\upsilon_2^2}{E_2} = 1.937e-7$$

where for 6061-T6 Aluminum at 300°F:

E = 9.2 x 10^6 psi

V = 0.33 and the subscripts 1 and 2 refer to each of the cylinders

where:

$$K_D = \frac{D_1 D_2}{D_1 + D_2} = .375$$

where D is the outer diameter of the tube, .75 in (the subscripts 1 and 2 refer to the individual tubes). The bearing stress corresponding to 24.3 g is:

$$S_{brg} = .798 \times \sqrt{\frac{24.3 \times 0.198}{0.375 \times 1.937e-7}} = 6495 \text{ psi}$$

$$MS = \frac{27400}{6495} - 1 = +\underline{3.21}$$

The bending stress in the aluminum insert tube is evaluated as a curved beam using the diametrical point forces, as contained in Roark's, 6th Edition, Table 17, Case 1.

Conservatively using 400°F to evaluate the aluminum properties, and the weight of four tubes (which results in a line load of 1.33 × 0.198 = 0.263 lbs/in), the maximum bending stress in the aluminum tube is:

$$S_b = \frac{6M}{bt^2}$$

Where b = 1.0 in, which is the axial length for the purpose of the calculation.

$$M = 0.3183 \cdot P \cdot R \cdot k_2$$

$$k_2 = 1 - \alpha$$

$$\alpha = \frac{I}{AR^2}$$

$$t_{ring} = \frac{.75 - .62}{2} = 0.065\text{in} \qquad I = \frac{0.065^3 \times 1}{12} = 2.29\text{e-}5\,\text{in}^4 \qquad A = .065 \times 1 = 0.065\,\text{in}^2$$

$$R = \frac{0.62}{2} + \frac{0.065}{2} = 0.343\text{in} \qquad \alpha = \frac{2.29\text{e-}5}{0.065 \times 0.343^2} = 0.003 \qquad k_2 = 1 - 0.003 = 0.997$$

$$M = 0.3183 \times (4 \times 0.263) \times 0.343 \times 0.997 = 0.115 \text{ in-lb/in}$$

$$S_b = \frac{6 \times 0.115 \times 24.3}{1 \times 0.065^2} = 3969 \text{ psi}$$

$$MS = \frac{1.5S_m}{S_b} - 1 = \frac{8250}{3969} - 1 = +\underline{1.07}$$

Where 24.3 g corresponds to the side drop accelerations.

This verifies that the aluminum insert tube is acceptable for the normal operational conditions.

2.6.12.8 DIDO Fuel Basket Construction

The DIDO modular basket assembly consists of a top module, four intermediate modules, and a base module. The top module is 29.8 inches long and the intermediate modules are each 29.3 inches long and all have an outer diameter of 13.27 inches. The base module has a length of 29.8 inches and an outer diameter of 13.27 inches. Each module is capable of holding seven DIDO fuel assemblies. Each module is a weldment made up of a 13.27 inch diameter 1/2-inch thick base plate and two 13.27 inch diameter 1/2-inch thick support plates scalloped on the inner diameter to fit around six peripheral fuel tubes. The weldment structure, fuel tubes and base and support plates are fabricated from Type 304 stainless steel. Each fuel tube has an inner diameter of 4.01 inches and a wall thickness of 0.12 inches. The bottom of each fuel tube is welded to the 1/2-inch thick base plate. At the bottom of each fuel tube, where it is welded to the base plate, there is a 0.3-inch slot to permit water to drain from the tube. The base plate supports the fuel in the end drop orientation. The base module sits on a 0.5-inch long, 10-inch diameter schedule 80S pipe that is welded to the base plate. The total weight of the DIDO basket assembly bears directly on the bottom forging of the cask through the schedule 80S pipe. The two scalloped 1/2-inch thick support plates and the base plate of each basket module provide lateral support and maintain the fuel configuration in the side drop orientation.

Heat rejection from the DIDO fuel and basket structure is augmented by six aluminum shunts and two heat transfer shells. Each shunt is mechanically attached to the center stainless steel fuel

tube. The heat transfer shell wraps around the 6 outer fuel tubes and is mechanically attached to the drain tube guide bars. The heat shunts are machined to match the outer diameter of the center fuel tube and are held in place by two shunt posts and shunt retainers. The shunt post at the bottom of each basket module is assembled with a tight fit between the shunt post, shunt retainer and base plate to provide a good conductive heat transfer path. The shunt post at the top of the basket is assembled with a slotted hole in the shunt to permit unrestricted differential thermal expansion between the fuel tube and thermal shunt. The aluminum sheet heat transfer shell is held in place against the outside fuel tubes by bolting the edge of the aluminum sheet to the drain tube guide bars. The heat shunts and heat transfer shell are not structural components and are not included in the structural analysis as load carrying components. The mass of the heat shunts and heat transfer shell have been included as loads in the structural analysis.

2.6.12.8.1 DIDO Fuel Basket Cask Interface Analysis

Structural analysis of the DIDO modular fuel basket and the MTR modular fuel basket are similar. DIDO fuel baskets and MTR fuel baskets are made from the same type of stainless steel. The contact points between the basket structure and the cask inner shell and between the basket structure and the cask bottom forging are similar. DIDO fuel baskets have an additional lateral support ring, reducing the side drop bearing stresses. A loaded DIDO fuel basket base module weighs approximately 250 lbs, assuming each DIDO assembly weighs 15 lbs. Loaded top and intermediate modules weigh approximately 247.4 lbs each. A full cask load of six DIDO basket modules represents a total contents weight of 1,487 lbs. The weight of a loaded 28-element MTR basket module is 289 lbs, which bounds the loaded weight of the loaded base DIDO basket module. Therefore, the bearing stress between the basket and the cask inner shell created by the DIDO basket module is bounded by the 28-element MTR fuel basket interface analysis.

The cask contents weight for the loaded 42-element MTR basket is 2,262 lbs, which bounds the cask contents weight of 1,487 lbs for the loaded DIDO basket. Therefore, the bearing stresses between the basket and cask bottom forging and between the basket and the cask lid created by the DIDO fuel baskets, are bounded by the 42-element MTR fuel basket interface analysis.

2.6.12.8.2 DIDO Fuel Basket Structural Analysis

Structural analyses of the DIDO fuel basket for the 1-foot end drop and the 1-foot side drop are performed using a finite element model of one basket module, as shown in Figure 2.6.12-1 and Figure 2.6.12-2, and the ANSYS general purpose computer program. Eight node brick elements (SOLID45) are used to construct the model. Each solid element has the material properties of stainless steel. In each basket module, the elements representing the seven 4.01-inch inner diameter tubes are joined to the base plate and to the two support plates at locations where the

welds are specified to connect the tubes to the plates. By design, the center tube is not connected to any of the six outer tubes. In this evaluation, the center tube is not considered to have any interaction with the outer six tubes, which is conservative, particularly in the side drop orientation where the tube is cantilevered from the base plate.

DIDO Fuel Basket 1-Foot Side Drop Orientation Analysis

The 1-foot side drop analysis of the DIDO fuel basket considers the weight of the center tube and fuel to be transferred to the circular base plate. A bounding fuel assembly weight of 15 pounds is used in the side drop analysis. To model the interaction of the two support plates and the base plate with the 13.375-inch cask inner shell diameter, CONTAC52 elements are used. The CONTACT52 element consists of two nodes, which corresponds to a 3D-line element, limiting transmitted loads to compression. One node of the CONTACT52 element is located on a circular plate, while the second node represents the inner shell, and is constrained in all three degrees of freedom. This boundary condition is considered to be conservative, since it models the inner shell as a rigid surface and minimizes the angle of contact between a circular plate and the cask inner shell, resulting in a more concentrated load at the point of contact. The aluminum heat shunts and aluminum heat transfer shell are not considered to be structural components. The shunts and shells are represented as lumped masses using the MASS21 element. These lumped masses are distributed along the outside of the center tube to represent the distributed weight of the heat shunt. The heat transfer shell is represented with lumped masses distributed along the outer six fuel tubes at the points of contact with the heat transfer shell.

The 1-foot side drop normal condition event is analyzed using an acceleration of 24.3g applied in each of three orientations: 0°, -60°, and -90° with respect to the model's X-axis. Maximum primary membrane stresses for each of the side drop orientations are shown in Table 2.6.12-1. The minimum margin of safety is calculated to be +2.5 for the 0° and 60° orientations. The maximum primary membrane plus bending stresses for each of the side drop orientations are shown in Table 2.6.12-2. The minimum margin of safety is calculated to be + 0.003 for the 60° orientation. Figure 2.6.12-3 presents the location of the maximum primary membrane and the primary membrane plus bending stresses for the side drop load.

DIDO Fuel Basket 1-Foot End Drop Analysis

For the end drop analysis, the finite element model load orientation and boundary conditions are specified to represent axial loading and consideration of the base basket module supporting five stacked modules above it. Equivalent pressure was applied to the area inside of the fuel tube at the top surface of the base plate to represent the fuel in each of the fuel tube locations in each basket module. The weight of the five loaded fuel basket modules, which rest on the base fuel basket module, multiplied by the equivalent acceleration, is applied as an equivalent pressure to

the top edges of the fuel tubes in the base module. A bounding DIDO fuel assembly weight of 15 pounds is used in the end drop analysis. The bounding assembly weight accounts for the fuel assembly and the tube spacer and variations in the weight of either. The total weight resting on the top of the base module is approximately 1,237 pounds. This load was applied as a pressure load on the ends of the fuel tubes.

Total end area of tubes = $7 \times \pi/4 \times (4.25^2 - 4.01^2) = 10.9$ in^2

Equivalent pressure = 1237 lbs/10.9 in^2 = 113.5 psi

The end drop finite element model reflects the base basket design shown on the drawings provided in Section 1.0. The height of the base skirt below the bottom support is 0.5 inch. Four full height drain slots are cut into the base skirt.

For the 1-foot end drop condition, the equivalent pressure load is increased to represent the maximum acceleration of 15.8 g. The maximum primary membrane stress for the end drop orientation is 11.4 ksi (shown in Table 2.6.12-1) resulting in a minimum margin of safety of +0.75. The maximum primary membrane plus bending stress is 13.2 ksi (shown in Table 2.6.12-2) resulting in a minimum margin of safety of + 1.27. Figure 2.6.12-6 presents the location of the maximum primary membrane and the primary membrane plus bending stresses for the end drop load.

Based on these results, it is concluded that the DIDO fuel basket is structurally adequate for normal transport conditions.

2.6.12.8.3 Fuel Assembly Spacer Structural Evaluation

During a top end drop, the spacer would be loaded by the weight of the fuel and the tube spacer. A bounding analysis of the DIDO fuel spacer post and top disk, based on hypothetical accident condition g-loads, is performed. The DIDO fuel assembly weight of 15 lbs is considered to include the weight of the tube spacer. The post is analyzed by determining the membrane stress due to the weight of the fuel assembly and tube spacer acting concentrically on the post. The top disk of the spacer is analyzed as a circular plate with a uniform load acting over the entire surface of the disk. The results, showing the spacer design is adequate to sustain the hypothetical accident top end drop analysis, are:

Component	Primary Membrane Stress (psi)	Allowable Stress (psi) @ Temp.	Margin of Safety	Primary Membrane + Bending (psi)	Allowable Stress (psi) @ Temp.	Margin of Safety
Pin	1,140	46,200	Large	5,082	66,000	12.0
Disk	N/A	46,200	N/A	10,980	66,000	5.0

Figure 2.6.12-3 DIDO Fuel Basket Module Structural Model – Top View

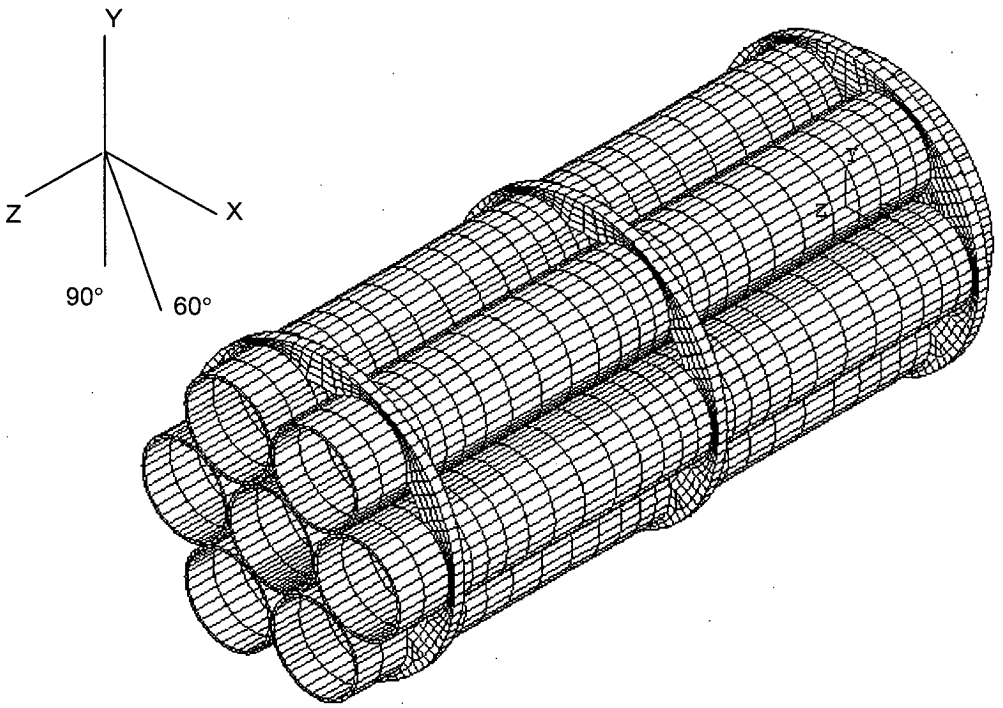

Figure 2.6.12-4 DIDO Fuel Basket Module Structural Model – Bottom View

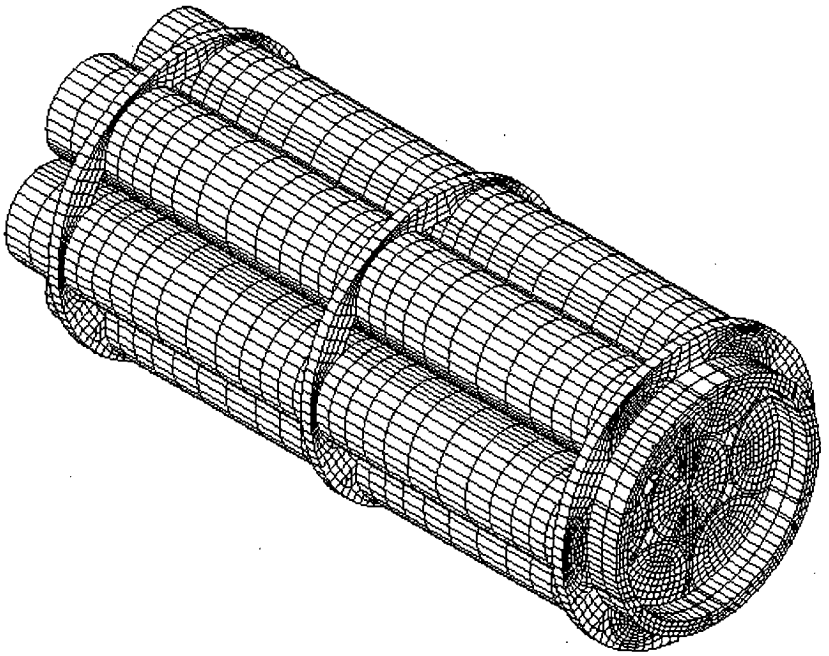

Figure 2.6.12-5 DIDO Fuel Basket Module Maximum Stress Locations for the Side Drop Orientation

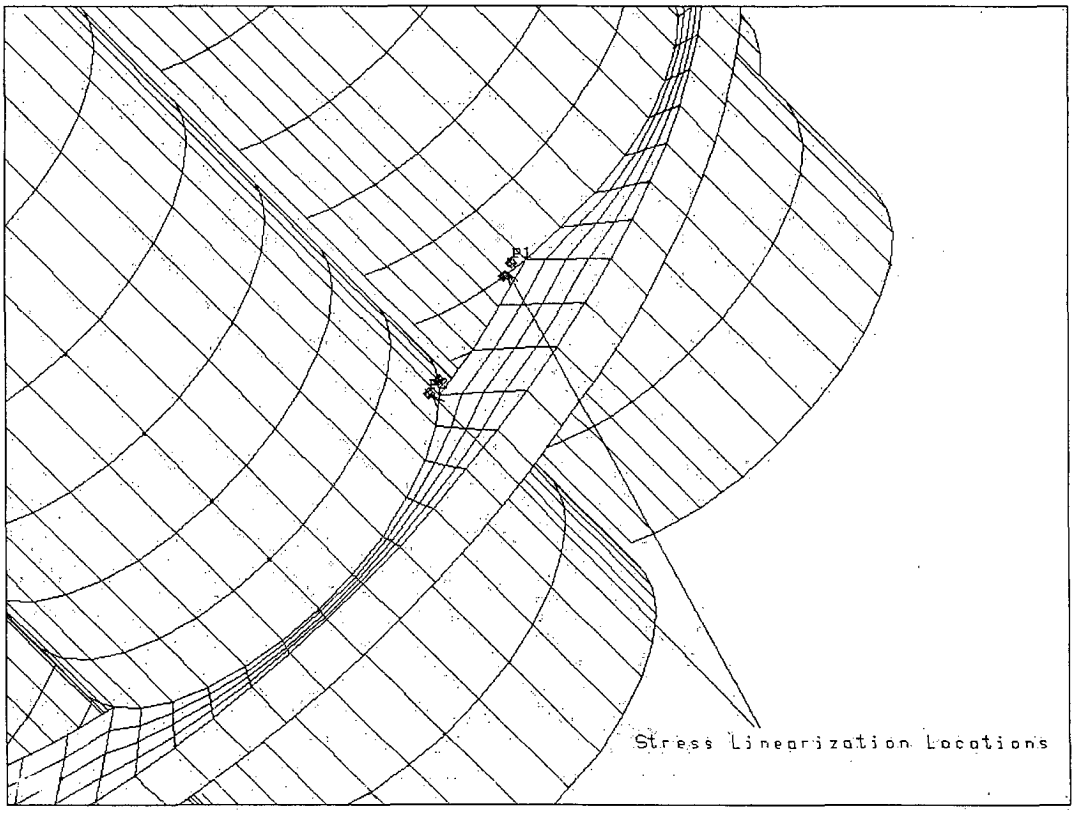

Figure 2.6.12-6 DIDO Fuel Basket Module Maximum Stress Locations for the End Drop Orientation

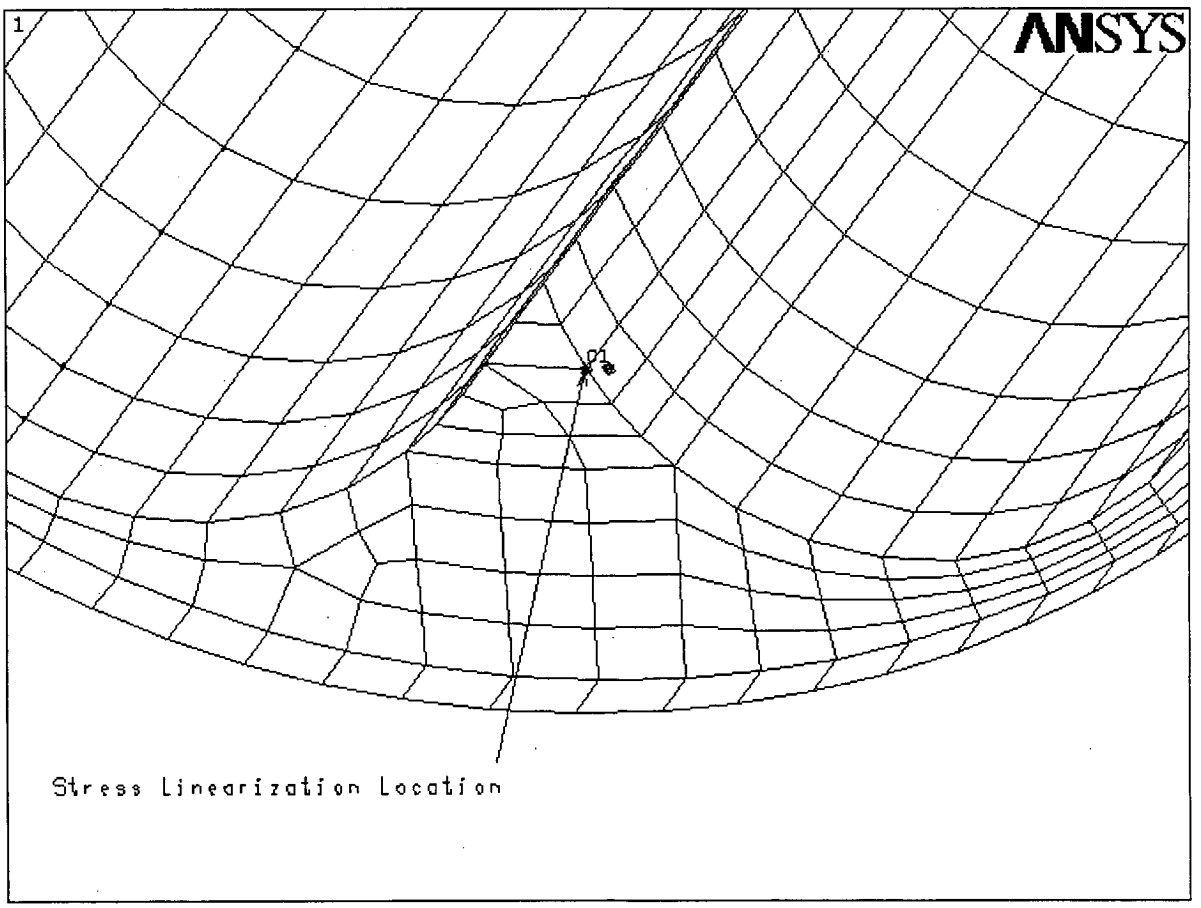

Table 2.6.12-1 Maximum Primary Membrane Stress for the 1-Foot Drop (DIDO Basket)

Location	Load Case 1-ft drop	Membrane (ksi)	Allowable (ksi) [1]	Margin of Safety [2]
Fuel Tube Wall	Side @ 0 Deg[3]	5.7	20.0	2.5
Fuel Tube Wall	Side @ 60 Deg[3]	5.7	20.0	2.5
Fuel Tube Wall	Side @ 90 Deg[3]	5.2	20.0	2.8
Fuel Tube Wall	End drop	11.4[4]	20.0	0.75

Table 2.6.12-2 Maximum Primary Membrane Plus Bending Stress for the 1-Foot Drop (DIDO Basket)

Location	Load Case 1-ft drop	Membrane + Bending (ksi)	Allowable (ksi) [5]	Margin of Safety [2]
Fuel Tube Wall	Side @ 0 Deg[3]	29.6[6]	30.0	0.01
Fuel Tube Wall	Side @ 60 Deg[3]	29.9[6]	30.0	0.003
Fuel Tube Wall	Side @ 90 Deg[3]	24.4[6]	30.0	0.23
Fuel Tube Wall	End drop	13.2[4]	30.0	1.27

1 $P_m \leq S_m$.
2 Margin of safety = (Allowable-Stress/Actual Stress) – 1.
3 Angle orientation shown on Figure 2.6.12-1.
4 The linearized stresses for the end drop case are scaled by the ratio of 360/178.65, which is the full arc-to-arc length of the tube welded to the base plate.
5 $P_m + P_b \leq 1.5S_m$.
6 These stresses are maximum local tube wall stresses and may be considered secondary stresses. They are conservatively considered primary membrane plus bending stresses and are located as shown in Figure 2.6.12-3.

2.6.12.9 General Atomics IFM Basket Construction

The General Atomics Irradiated Fuel Material (IFM) basket consists of a top module assembly designed to carry two IFM Fuel Handling Units (FHUs). Each IFM FHU is associated with RERTR or HTGR fuel materials. A spacer assembly is used to permit the top module assembly to be positioned next to the transport cask lid.

The top module is 43.7 inches long and is made up of two fuel tubes and three support plates. All components are made from ASME SA240 Type 304 stainless steel. The fuel tubes have a 6.0-inch outer diameter and a 0.25-inch wall thickness. Two of the support plates are 0.50-inch thick and the third, center plate, is 1.0-inch thick. The support plates are welded to the fuel tubes with 1/8-inch bevel welds.

Two types of IFM FHU are carried by the top module. One FHU carries irradiated HTGR fuel material and is 5.25 inches in diameter (0.12-inch thick wall) and 39.0 inches long. The other FHU contains irradiated RERTR fuel material, is 4.75 inches in diameter (0.12-inch thick wall), and is 37.25 inches long.

Each end of the FHU is comprised of a 0.25-inch thick plate welded to the container shell. The weld connecting the end plate to the container shell is labeled as a full-penetration butt weld. The dimensions of the end plate and the container shell provide a minimal gap (2 mils when considering maximum tolerances) to permit the end plate to be inserted into the container end. The close tolerances ensure that the two components are effectively in contact along the 0.5-inch common interface length of the end plate and the container. Once the end plate is inserted, a fusion weld procedure is employed to weld the lip of the end plate to the wall of the container. The depth of the weld along the interface between the end plate and the container is equal to approximately 70% of the thickness of the end plate lip or the container lip.

Due to the location of the weld for the end plate, the weld does not transfer any load for the drop conditions. Additionally, since the heat loads are insignificant (13w) and the backfill for the FHU and the cask cavity are limited to atmospheric pressure, the pressure differential across the welded plates is insignificant. Each of these FHUs also has an additional smaller container, which holds the fuel. In these evaluations, the inner container is neglected.

The spacer assembly is 133.0 inches in length, excluding guide pins. The assembly is comprised of one spacer tube and five support plates. The spacer tube consists of a Type 304 stainless steel 8-inch Schedule 80S pipe. The tube has an outside diameter of 8.63 inches and a wall thickness of 0.50 inch. The spacer plates are 1.0-inch thick and are welded to the tube with 1/8-inch bevel welds. Two guide pins are located at the top of the spacer assembly to facilitate alignment with the top module.

2.6.12.9.1 General Atomics IFM Basket Interface Analysis

The structural evaluation of the top module assembly is performed using classical hand calculations. The weight of the top module is bounded by 200 lbs, and the maximum weight of one FHU and its fuel contents is 76 lbs. Therefore, the total weight of a loaded top module system is 200 + 2(76) or 352 lbs. The weight of the spacer assembly is 760 lbs. The total loaded system weight is 1,112 lbs, and this weight is bounded by the design basis contents weight for the LWT system. Therefore, no analysis of the LWT cask body is required.

2.6.12.9.2 General Atomics Top Module Structural Analysis

Structural analyses for the top module for the 1-foot end drop and 1-foot side drop are performed using classical hand calculations.

General Atomics 1-Foot Side Drop Analysis

Top Module:

During a 1-foot side drop, the distributed load on one fuel tube is:

$$W = \frac{\left(76 + 0.291 \times \frac{\pi\left(6.0^2 - 5.5^2\right)}{4} \times 43.7\right)}{43.7} = 3.1 \text{ lb/in}$$

where:

weight of fuel = 76 lbs

length of tube = 43.7 inches

outer diameter = 6.0 inches

inner diameter = 5.5 inches

The maximum bending moment in tube is:

$$M = \frac{3.1 \times 20.35^2}{8} = 160 \text{ in - lbs}$$

The maximum bending stress in the fuel tube for 1g loading is:

$$I = \frac{\pi\left(6.0^4 - 5.5^4\right)}{64} = 18.7 \text{ in}^4$$

$$S_b = \frac{160 \times 3}{18.7} = 26 \text{ psi}$$

The margin of safety for tube bending for a 1-foot side drop (25g) is:

$$MS = \frac{1.5S_m}{S_b} - 1 = \frac{1.5 \times 19350}{25 \times 26} - 1 = +\underline{\text{Large}}$$

During a 1-foot side drop, the support plates bear up against the inner shell of the LWT cask. The center plate will carry the maximum weight. The bearing load on the center plate is:

$$W = \frac{10 \times \frac{[(2 \times 76) + 200]}{40.7} \times 20.35}{8} = 220 \text{ lbs}$$ (Page 2-299, #12, Manual of Steel Construction)

The bearing stress is maximum for the center disk.

The bearing stress is (Item 2c, Table 33, Young):

LWT cask cavity diameter, D1 = 13.375 inches

Support plate diameter, D2 = 13.265 inches

$$K_D = \frac{D_1 D_2}{D_1 - D_2} = 1{,}613$$

$$C_E = \frac{1 - 0.31^2}{26.75e6} + \frac{1 - 0.31^2}{8.29e6} = 1.42e-7$$

$$S_c = 0.798\sqrt{\frac{p}{K_D C_E}} = 0.798\sqrt{\frac{220}{1613 \times 1.42e-7}} = 782 \text{ psi, 1g loading}$$

where:

p = 220/(1.0) = 220 lbs/in

E = 26.75e6 psi @ 350°F

Effective 'E' of LWT shells with lead:

$$E = \frac{0.75 \times 26.75e6 + 1.25 \times 26.75e6 + 5.75 \times 1.87e6}{7.75} = 8.29e6 \text{ psi}$$

The margin of safety for bearing for a 1-foot side drop (25g) is:

$$MS = \frac{S_y}{25 \times S_c} = \frac{21600}{25 \times 782} - 1 = +0.10$$

During a side drop, the top and bottom support plate welds are in shear. The load on the weld due to 1g is:

$$W = \frac{3 \times \frac{[(2 \times 76) + 200]}{40.7} \times 20.35}{8} = 66 \text{ lbs}$$ (Page 2-299, #12, Manual of Steel Construction)

The weld length is:

$$L = 2(\pi d_{tube} - r_{tube}\theta)$$
$$= 2(\pi \times 6.0 - 3.0 \times 1.57) = 28.3 \text{ inches}$$
$$\theta = \text{non welded arc length} = 90 \text{ deg} = 1.57 \text{ radians}$$

The support disk/ tube weld is a 1/8-inch bevel weld. The stress in the weld for 1g is:

$$S = \frac{66}{(28.3 \times 0.125 \times 0.7071)} = 26.4 \text{ psi, 1g loading}$$

For visual inspection, the weld factor is 0.25 per ASME Section III, Subsection NG-3352. The margin of safety for shear is:

$$MS = \frac{0.25 \times 0.6 S_m}{25S} - 1 = \frac{0.25 \times 0.6 \times 19350}{25 \times 26.4} - 1 = +3.4$$

Spacer Assembly:

During a 1-foot side drop, the distributed load on the tube is:

$$W = \frac{760}{129.5} = 5.9 \text{ lb/in, use } 6.0 \text{ lb/in}$$

The maximum bending moment in tube, conservatively assuming a simply supported beam, is:

$$M = \frac{6 \times 32.0^2}{8} = 768 \text{ in - lbs}$$

The bending stress in tube for a 1g loading is:

$$I = \frac{\pi(8.63^4 - 7.63^4)}{64} = 106 \text{ in}^4$$
$$S_b = \frac{768 \times (8.63/2)}{106} = 31 \text{ psi}$$

The margin of safety for bending in the 1-foot side drop (25g) is:

$$MS = \frac{1.5 S_m}{S_b} - 1 = \frac{1.5 \times 19350}{25 \times 31} - 1 = + \text{Large}$$

During a 1-foot side drop, the support plates bear up against the inner shell of the LWT cask. The maximum load on a support plate during a side drop is:

$$W = 1.143 \times \frac{760}{128.0} \times 32.0 = 217 \text{ lbs}$$ (Page 2-309, #39, Manual of Steel Construction)

The bearing stress is (Item 2c, Table 33, Young):

LWT cask cavity diameter $D_1 = 13.375$ inches

Support plate diameter $D_2 = 13.265$ inches

$$K_D = \frac{D_1 D_2}{D_1 - D_2} = 1{,}613$$

$$C_E = \frac{1 - 0.31^2}{26.75e6} + \frac{1 - 0.31^2}{8.29e6} = 1.42e-7$$

$$S_c = 0.798\sqrt{\frac{p}{K_D C_E}} = 0.798\sqrt{\frac{217}{1613 \times 1.42e-7}} = 777 \text{ psi}$$

where:

$p = 217 / 1.0 = 217$ lb/in

$E = 26.75e6$ psi @ 350°F

Effective 'E' of LWT shells with lead:

$$E = \frac{0.75 \times 26.75e6 + 1.25 \times 26.75e6 + 5.75 \times 1.87e6}{7.75} = 8.29e6 \text{ psi}$$

The margin of safety for bearing is:

$$MS = \frac{S_y}{25 \times S_c} = \frac{21600}{25 \times 777} - 1 = +0.11$$

During a side drop, the top and support plate weld is in shear. The load on the weld is:

$$W = 0.393 \times \frac{760}{128.0} 32.0 = 75 \text{ lbs}$$ (Page 2-309, #39, Manual of Steel Construction)

The weld length is:

$$L = \pi \times 8.63 = 27.1 \text{ inches}$$

The weld between the support disk and tube is a 1/8-inch bevel weld. The stress in the weld for 1g is:

$$S = \frac{75}{(27.1 \times 0.125 \times 0.7071)} = 31 \text{ psi, 1g loading}$$

For visual inspection, the weld factor is 0.25 per ASME Section III, Subsection NG-3352. The margin of safety for shear is:

$$MS = \frac{0.25 \times 0.6S_m}{25S} - 1 = \frac{0.25 \times 0.6 \times 19350}{25 \times 31} - 1 = 2.7$$

Fuel Handling Units (FHU)

The FHUs are analyzed in accordance with ASME Section III, Subsection NG. The bounding weight of a loaded fuel container is 76 lbs.

The side drop is analyzed assuming a circular ring under an external compressive load using Roarks Table 17, Item 1 (Young). The stress in the container shell is:

$$\alpha = \frac{I}{AR^2} = \frac{\pi(2.125^3) \times (0.12)}{\pi(2.125^2 - 2.0^2) \times 2.125^2} = 0.49$$

$$k_2 = 1 - \alpha = 1 - 0.49 = 0.51$$

$$M = (0.5 - 0.3183k_2)WR = [0.5 - 0.3183(0.51)]\frac{76}{35.5}2.125 = 1.5 \text{ in - lb}$$

$$S = \frac{6(1.5)}{0.12^2} = 0.63 \text{ ksi}$$

The margin of safety is:

$$MS = \frac{1.5S_m}{25S} - 1 = \frac{1.5 \times 19.35}{25 \times 0.63} - 1 = +0.84$$

General Atomics 1-Foot End Drop Analysis

Top Module:

During an end drop, the stress in the fuel tubes is calculated as follows.

The cross-sectional area of a tube is:

$$A = \frac{\pi(6.0^2 - 5.5^2)}{4} = 4.52 \text{ in}^2$$

Using a top module weight of 200 lbs, fuel weight not included, the stress in the two fuel tubes is:

$$S = \frac{200}{2 \times 4.52} = 22 \text{ psi}$$

The margin of safety is:

$$MS = \frac{S_m}{20S} - 1 = \frac{19350}{20 \times 22} - 1 = +\underline{Large}$$

Since the axial compression stress in the tubes is minimal, no buckling evaluation is required.

The top end drop is the bounding end drop because the top end has significantly less bearing area than the bottom end, and the weight of the spacer is included.

The bearing area for the top end is assumed to be the two fuel tubes, conservatively neglecting the lifting components. The cross-sectional area is:

$$A = 2\left[\frac{\pi\left(6.0^2 - 5.5^2\right)}{4} - 3.22 \times 0.25\right] = 7.42 \text{ in}^2$$

where:

outer diameter = 6.0 inches

inner diameter = 5.5 inches

cut out arc length = 3.22 inches

$$S = r\theta = 2.875 \times 1.12 = 3.22 \text{ inches}$$

$$\theta = 2 \times \tan^{-1}\left(\frac{1.72}{2.75}\right) = 64.05^\circ = 1.12 \text{ radians}$$

The bearing stress, fuel weight not included, in the module for a 1g loading is:

$$S_{brg} = \frac{200 + 760}{7.42} = 129 \text{ psi}$$

The margin of safety is:

$$S_{brg} = 20 \times 129 = 2.58 \text{ ksi}$$

$$MS = \frac{S_y}{S_{brg}} - 1 = \frac{21.6}{2.58} - 1 = +7.37$$

During an end drop, the self-weight of the center support plate has to be carried by the welds. The weight of the center support plate is:

$$W = 0.291\left\{1.0\left[\frac{\pi \times 13.265^2}{4} - 2\left(\frac{\pi \times 6.0^2}{4}\right)\right]\right\} = 24 \text{ lbs (use 30 lbs)}$$

where:

0.291 lbs/in^3 is the density of 304 stainless steel

1.0 inch is the disk thickness

13.265 inches is the disk diameter

6.0 inches is the cutout diameter

The weld length is:

$$L = 2(\pi d_{tube} - r_{tube}\theta)$$
$$= 2(\pi \times 6.0 - 3.0 \times 1.57) = 28.3 \text{ in.}$$
$$\theta = \text{nonwelded arc length} = 90 \text{ deg} = 1.57 \text{ radians}$$

The welds are 1/8-inch bevel welds on both sides of the disk. The stress in the weld for 1g is:

$$S = \frac{30}{2(28.3 \times 0.125 \times 0.7071)} = 6.0 \text{ psi}$$

For visual inspection, the weld factor is 0.25 per ASME Section III, Subsection NG-3352. The margin of safety for normal conditions is:

$$MS = \frac{0.25 \times 0.6 S_m}{20S} - 1 = \frac{0.25 \times 0.6 \times 19350}{20 \times 6} - 1 = +\underline{\text{Large}}$$

Spacer Assembly:

During an end drop, the stress in the tube is calculated as follows.

The cross-sectional area of a tube is:

$$A = \frac{\pi(8.63^2 - 7.63^2)}{4} = 12.77 \text{ in}^2$$

The stress in the tube is:

$$S = \frac{760 + 200 + 2 \times 76}{12.77} = 87 \text{ psi}$$

The margin of safety is:

$$MS = \frac{S_m}{20S} - 1 = \frac{19350}{20 \times 87} - 1 = +\underline{\text{Large}}$$

Since the axial stress in the tube is minimal, no buckling evaluation is required.

For a top and bottom end drop, the bearing stresses for 1g are:

$$A_{top} = 2(9.9 \times 0.3125) = 6.19 \text{ in}^2$$

$$S_{brg} = \frac{760}{6.19} = 123 \text{ psi}$$

$$A_{bot} = \frac{\pi(8.63^2 - 7.63^2)}{4} - (4 \times 1.0 \times 0.5) = 10.77 \text{ in}^2$$

$$S_{brg} = \frac{760 + 200 + 2 \times 76}{10.77} = 103 \text{ psi}$$

The margin of safety is:

$$S_{brg} = 20 \times 123 = 2.46 \text{ ksi}$$

$$MS = \frac{S_y}{S_{brg}} - 1 = \frac{21.6}{2.46} - 1 = +7.78$$

During an end drop, the weight of a support plate has to be carried by the welds to the tube.

The weight of the support plate is:

$$W = 0.291\left(\frac{\pi\left(13.265^2 - 8.63^2\right)}{4} \times 1.0\right) \approx 25 \text{ lbs}$$

The weld length is:

$$L = \pi \times 8.63 = 27.1 \text{ inches}$$

$$S = \frac{25}{2(27.1 \times 0.125 \times 0.7071)} = 5.2 \text{ psi}$$

Since the weld stress is less than the weld stress in the support disks in the top module, no additional analysis is required.

Fuel Handling Unit:

The maximum bearing stress occurs in the top end drop orientation. The bearing area for the handle supports is:

$$A = 2 \times 0.5^2 = 0.5 \text{ in}^2$$

The bearing stress is:

$$S_{brg} = \frac{76}{0.5} = 152 \text{ psi}$$

The margin of safety is

$$S_{brg} = 20 \times 152 = 3.0 \text{ ksi}$$

$$MS = \frac{S_y}{S_{brg}} - 1 = \frac{21.6}{3.0} - 1 = +6.2$$

The top lid and bottom plates sit on a lip in the container shell. The cross-sectional area of the lip is:

$$A = \frac{\pi\left(4.124^2 - 4.0^2\right)}{4} = 0.79 \text{ in}^2$$

Since the area is greater than the handle support area above, no additional analysis is required.

The cross-sectional area of the tube is:

$$A = \frac{\pi\left(4.25^2 - 4.0^2\right)}{4} = 1.62\,\text{in}^2$$

For a 20g end drop, normal conditions, the stress in the tube is:

$$S = \frac{20 \times 76}{1.62} = 0.94\,\text{ksi}$$

$$MS = \frac{S_m}{S} - 1 = \frac{19.35}{0.94} - 1 = +\underline{\text{Large}}$$

Since the axial compression stresses in the tube are minimal, no buckling evaluation is required.

2.6.12.10 TPBAR Basket Analysis

The TPBAR basket is a modified NAC-LWT PWR basket with increased free volume that is fabricated from 6061-T651 aluminum alloy. Figure 2.6.12-7 shows the cross-section of the TPBAR basket. A 13.25-inch outside diameter, 8.25-inch long stainless steel alternate upper fitting is bolted to the top of the basket body. This fitting provides lifting points for removing the basket from the cask. Additionally, this alternate upper fitting prevents the basket from applying load to the TPBAR contents during the top-end drop. A stainless steel lower fitting is bolted to the bottom of the basket body. The lower fitting assembly supports the fuel basket and contents longitudinally. An additional spacer assembly is bolted to the cask lid to prevent the TPBAR contents from shifting axially and rotationally within the basket. A groove on the periphery of the basket body provides for the cask drain tube. The drain tube is connected to a fitting on the cask body for draining or filling the cask during wet cask loading or unloading operations.

The TPBAR basket accommodates two TPBAR content configurations. The first TPBAR content configuration is the shipment of up to 300 production TPBARs (of which two can be prefailed) contained in an open consolidation canister with optional top insert. The consolidation canister body is fabricated from Type 304 stainless steel and the bail is fabricated from Type 7-4 precipitation hardened stainless steel. The consolidation canister is used to load and unload the TPBARs into and from the NAC-LWT cask configured with a TPBAR basket assembly.

The second TPBAR content configuration is the shipment of up to 55 segmented TPBARs, following post-irradiation examinations (PIE), contained in a welded sealed waste container. The waste container is welded to an extension weldment to provide the identical length as the consolidation canister to assure fit-up in the TPBAR basket assembly. The waste container and extension are fabricated from Type 316L stainless steel.

Following placement of the consolidation canister or the waste container with extension in the TPBAR basket, and installation and bolting of the lid, the TPBAR basket and contents are evaluated without consideration of the strength of the consolidation canister or waste container. The TPBAR basket provides a boundary for support on all sides of the consolidation canister and TPBARs for the full length of the canister. The cylindrical TPBAR waste container (external diameter 8.6 inches) is sized to fit within the square cross-section (8.8 inches) of the TPBAR basket. The TPBAR upper end-fitting spacer guides do not permit the consolidation canister to be loaded by the TPBAR basket in any drop orientation. The TPBAR spacer assembly attached to the bottom of the cask lid restricts the movement of the TPBARs in the axial direction and prevents rotation of the TPBAR waste container. Therefore, no additional evaluations are required for the TPBAR consolidation canister or TPBAR waste container and extension weldment.

2.6.12.10.1 TPBAR Basket Body

Structural analyses of the TPBAR basket for 1-foot side and end drops are performed using classical hand calculations. The analyzed weight of the loaded TPBAR consolidation canister is 1,000 lbs, which bounds the loaded weight of the TPBAR waste container and extension of 700 lbs. Therefore, the analyses provided for the consolidation canister are bounding.

TPBAR Basket Body 1-Foot Side Drop Analysis

The TPBAR basket body is constructed of four machined segments held together with aluminum bands at five locations along the axial length of the basket; as well as the top and bottom fittings, which are bolted to the aluminum basket. During a side drop, the TPBAR basket is subjected to bending and bearing stresses. The maximum bending stress occurs at Location 'A' as shown in the following sketch and is due to the content weight. The maximum bending stress is calculated using a cantilevered beam. This is conservative, since it neglects any support of the load due to the edges of the basket being supported by the cask inner shell. The maximum bending stress is:

$$S_b = \frac{6M}{t^2} = \frac{6 \times 152}{0.5^2} = 3.6 \text{ ksi}$$

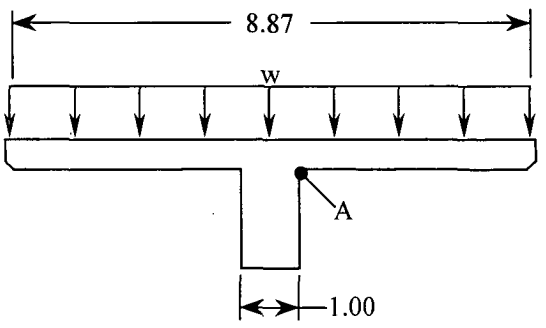

where:

$$w = \frac{W_c \times g}{L \times b} = \frac{1000 \times 25}{144 \times 8.87} = 19.6 \text{ psi}$$

(distributed load of the TPBAR consolidation canister)

W_c = 1,000 lbs, bounding TPBAR canister weight (with TPBARs)

L = 144 inches, length of consolidation canister

b = 8.87 inches, TPBAR basket opening width

g = 25g, bounding side drop acceleration

$$M = w \times \left(\frac{b}{2} - \frac{1}{2}\right) \times \frac{1}{2}\left(\frac{b}{2} - \frac{1}{2}\right)$$

$$= 19.6 \times \left(\frac{8.87}{2} - \frac{1}{2}\right) \times \frac{1}{2}\left(\frac{8.87}{2} - \frac{1}{2}\right) = 152 \text{ in-lb/in, the maximum bending moment}$$

t = 0.5 in, thickness of the flange

The margin of safety is:

$$MS = \frac{1.5S_m}{S_b} - 1 = \frac{1.5 \times 8.4}{3.6} - 1 = +2.5$$

where:

S_m = 8.4 ksi, stress intensity of 6061-T651 aluminum @300°F

The bearing stress in the basket is:

$$S_{brg} = \frac{P}{A} = \frac{47{,}500}{1.00 \times 161.5} = 294 \text{ psi} \approx 0.3 \text{ ksi}$$

where:

P = $g \times (W_c + W_b) = 25 \times (1{,}000 \text{ lbs} + 900 \text{ lbs}) = 47{,}500$ lbs, total side drop load

W_b = 900 lbs, the bounding weight of the TPBAR basket

A = is the minimum bearing area of the basket

The margin of safety is:

$$MS = \frac{S_y}{S_{brg}} = \frac{26.9}{0.3} - 1 = +\underline{\text{Large}}$$

where:

S_y = 26.9 ksi, yield strength of 6061-T651 aluminum @300°F

TPBAR Basket 1-Foot End-Drop Analysis

During an end drop, the maximum compressive stress on the minimum cross-section of the basket body is:

$$S_{comp} = \frac{g \times W_b}{A} = \frac{20 \times 900}{32.26} = 558 \text{ psi} \approx 0.6 \text{ ksi}$$

where:

A = $9.87^2 - 8.87^2 + 4(1.00 \times (13.25 - 9.87)) = 32.26\,in^2$, the minimum cross-sectional area of the basket (see Figure 2.6.12-7)

g = 20g, bounding end drop acceleration

W_b = 900 lbs, bounding weight of the TPBAR basket

The margin of safety is:

$$MS = \frac{S_y}{S_{comp}} - 1 = \frac{26.9}{0.6} - 1 = +\underline{Large}$$

where:

S_y = 26.9 ksi, yield strength of 6061-T651 aluminum @300°F

2.6.12.10.2 TPBAR Basket Upper Fitting

The upper fitting prevents the basket from loading the consolidation canister and TPBARs during a top-end drop. Four (4) spacer guides of the upper fitting are provided for this purpose. The spacer guides have a length of 7.63 inches, a width of 2.0 inches, and a thickness of 1.00 inch with a 45° × 0.25-inch chamfer. A bounding weight of 900 lbs is used for the TPBAR basket analysis. The temperature of the lid and upper region of the NAC-LWT cask body during TPBAR shipment is conservatively assumed to be 300°F. From Chapter 3, a temperature of 300°F bounds the maximum temperature of the upper LWT region for a maximum heat load of 1.05 kW. Since the maximum heat load for the TPBAR shipment is less than 1.0 kW, using 300°F for the analysis of the TPBAR upper fitting is conservative.

TPBAR Basket Upper Fitting 1-Foot Side Drop

During a side drop, the welds that hold the spacer guides to the top fitting are in shear and bending. The shear load on the welds is:

P = $(b \times t \times L) \times \rho \times g = (2.0 \times 1.0 \times 7.63) \times 0.288 \times 25 = 110$ lbs

where:

b = 2.0 inches, spacer guide width

t = 1.0 in, spacer guide thickness

L = 7.63 inches, spacer guide length

ρ = 0.288 lb/in^3, density of Type 304 stainless steel

g = 25g, side drop acceleration

The welds for the spacer are ⅛-inch fillet welds on three sides. The shear stress in the welds is:

$$\tau = \frac{P}{A} = \frac{110}{0.354} = 311 \text{ psi} = 0.3 \text{ ksi}$$

where:

$A = 0.125 \times 0.707 \times (2.0 + 2 \times 1.0) = 0.354 \text{ in}^2$, weld area

The bending moment is:

$$M = \frac{wL^2}{2} = \frac{(b \times t \times \rho \times g) \times L^2}{2} = \frac{(2 \times 1 \times 0.288 \times 25) \times 7.63^2}{2} = 419 \text{ in-lb}$$

The stress in the weld due to bending is:

$$S = \frac{M}{t \times S_w} = \frac{419}{(0.125 \times 0.707) \times 0.56} = 8.5 \text{ ksi}$$

where:

$$S_w = \frac{d^2(2b + d^2)}{3(b + d)} = \frac{1^2(2 \times 2 + 1^2)}{3(2 + 1)} = 0.56 \text{ in}^2, \text{ section modulus of weld (Blodgett)}$$

The maximum shear stress, τ_{max}, in the weld which, is equivalent to the stress intensity divided by two is:

$$\tau_{max} = \frac{\sqrt{S^2 + 4\tau^2}}{2} = \frac{\sqrt{8.5^2 + 4 \times 0.3^2}}{2} = 4.26 \text{ ksi}$$

The margin of safety is:

$$MS = \frac{0.6S_y}{\tau_{max}} - 1 = \frac{0.6 \times 22.5}{4.26} - 1 = +2.17$$

where:

$S_y = 22.5$ ksi, yield strength of Type 304 stainless steel @300°F

TPBAR Basket Upper Fitting 1-Foot Top-End Drop

For a top-end drop the weight of the TPBAR basket will load the four spacer guides. The membrane stress in the spacer guide is:

$$S = \frac{W_b \times g}{A} = \frac{900 \times 20}{(2.0 \times 1.0) \times 4} = 2.3 \text{ ksi}$$

where:

$W_b = 900$ lbs, bounding TPBAR basket weight

$A = (2.0 \times 1.0) \times 4 = 8 \text{ in}^2$, cross sectional area of the spacer guide

g = 20g, bounding end drop acceleration

The margin of safety is:

$$MS = \frac{S_y}{S} - 1 = \frac{22.5}{2.3} - 1 = +8.8$$

where:

S_y = 22.5 ksi, yield strength of Type 304 stainless steel @300°F

The bearing stress is:

$$S = \frac{W_b \times g}{A} = \frac{900 \times 20}{6} = 3.0 \text{ ksi}$$

where:

A = $(2.0 \times 0.75) \times 4 = 6$ in^2, bearing area of the spacer guide

The margin of safety is:

$$MS = \frac{S_y}{S} - 1 = \frac{22.5}{3.0} - 1 = +6.5$$

The critical buckling load for the spacer is determined by using Euler's buckling equation. The critical buckling load is:

$$W_{cr} = K_c \frac{EI}{L^2} = 2.47 \frac{27 \times 10^6 (0.1667)}{7.63^2} \approx 190.9 \text{ kip}$$

where:

E = 27×10^6 psi, modulus of elasticity of Type 304 stainless steel @ 300°F

K_c = 2.47, buckling constant (Blake, Table 10.3)

I = $\frac{bt^3}{12}$ = 0.1667 in^4, minimum moment of inertia for cross section

b = 2.0 inches, spacer guide width

t = 1.0 in, spacer guide thickness

L = 7.63 inches, length of spacer guide

The margin of safety against buckling of the four spacer guides is:

$$MS = \frac{190{,}900}{20 \times 900/4} - 1 = + \underline{\text{Large}}$$

2.6.12.10.3 TPBAR Basket Lower Fitting

The TPBAR basket lower fitting is identical to the lower fitting of the PWR basket. The weight of the loaded TPBAR basket is less than the weight of the loaded PWR basket. Therefore, no further analysis is required.

2.6.12.10.4 TPBAR Spacer

The TPBAR Spacer is designed to limit the movement of the TPBAR contents during transport and to prevent the consolidation canister from loading the TPBARs during a top-end drop. The spacer is constructed of a circular base plate, two triangular spacer bases, two tubes, and two triangular top plates. The circular base plate forms the attachment of the spacer to the lower surface of the NAC-LWT cask closure lid. The circular base plate is attached with Type 304 stainless steel bolts. The two triangular spacer bases are bolted to the circular base plate. The tubes, constructed of 3-inch schedule 80 pipes, are welded to the spacer base and the triangular top plates that provide the interface with the TPBAR contents. The triangular top plates are arranged to form a square with a gap that fits over the consolidation canister or waste container bail and above the consolidation canister contents or the welded top of the waste container. Figure 2.6.12-8 shows the top view of the triangular top plate and tube. The calculated weight of the spacer assembly is 115 lbs. The analyzed loaded weight of the consolidation canister is 1,000 lbs, which bounds the loaded weight of the waste container (700 lbs). During the top-end drop condition, the weight of the consolidation canister is supported by the bail and directly transmitted into the NAC-LWT cask lid. Therefore, only the weight of the TPBARs is supported by the spacer for top-end drop conditions. The temperature of the lid and upper region of the NAC-LWT cask body during TPBAR transport is conservatively assumed to be 300°F. From Chapter 3, a temperature of 300°F bounds the maximum temperature of the upper LWT region for a maximum heat load of 1.05 kW. Since the maximum heat load for the transport of the TPBAR consolidation canister shipment is less than 0.7 kW, using 300°F for the analysis of the TPBAR spacer is conservative. The heat load of the TPBAR waste container is 0.127 kW and, therefore, the evaluated temperatures for the consolidation canister are bounding.

TPBAR Spacer 1-Foot Side Drop

Bolts

During 1-foot side-drop conditions, the weight of the spacer applies a shearing and tensile load to the bolts. The tensile load is due to the moment generated by the cantilever action of the spacer.

The shear stress is:

$$\tau = \frac{P}{A_t} = \frac{719}{0.1419} = 5.1\,\text{ksi}$$

where:

$$P = \frac{W \times g}{4} = \frac{115 \times 25}{4} = 719 \text{ lbs}$$

W = 115 lb, spacer assembly weight abbreviations

g = 25g, side-drop acceleration

$A_t = 0.7854\left(D - \frac{0.9743}{n}\right)^2 = 0.7854\left(0.5 - \frac{0.9743}{13}\right)^2 = 0.1419 \text{ in}^2$, tensile area of screw thread with ultimate strength up to 100 ksi

For ½-13UNC bolts (Machinery's Handbook)

n = 13, number of threads per inch

D = 0.50 in, bolt diameter

Kn_{max} = 0.434 in, maximum minor diameter of internal thread

Es_{min} = 0.4435 in, minimum major diameter of external thread

En_{max} =0.4565 in, maximum pitch diameter of internal thread

Ds_{min} =0.4876 in, minimum major diameter of external thread

L_e = 1.0 in, Thread engagement

$$P = \frac{M}{d} = \frac{16{,}891}{2 \times 4.95} = 1{,}706 \text{ lbs}$$, the tensile load

d = 9.9 in, maximum distance between bolts

$$M = \frac{wL^2}{2} \times g = \frac{\left(\frac{115}{11.75}\right)\left(11.75^2\right)}{2} \times 25 = 16{,}891 \text{ in - lb}$$, the prying moment generated by the cantilever action of the spacer

The bolt tensile stress due to the moment, M, is:

$$S = \frac{P}{A_t} = \frac{1706}{0.1419} = 12.0 \text{ ksi}$$

The membrane stress intensity on the fastener is:

$$SI = \sqrt{S^2 + 4\tau^2} = \sqrt{12.0^2 + 4 \times 5.1^2} = 15.7 \text{ ksi}$$

The margin of safety is:

$$MS = \frac{S_y}{SI} - 1 = \frac{22.5}{15.7} - 1 = +0.43$$

where:

S_y = 22.5 ksi, yield strength of Type 304 stainless steel @300°F

The shear stress on the external threads is:

$$\tau = \frac{P}{A_S} = \frac{1706}{0.7789} = 2.2 \text{ ksi}$$

where:

$$A_S = 3.1416 n L_e Kn_{max}\left[\frac{1}{2n} + 0.57735(Es_{min} - Kn_{max})\right]$$

$$= 3.1416(13)(1.00)(0.434)\left[\frac{1}{2(13)} + 0.57735(0.4435 - 0.434)\right]$$

= 0.7789 in^2, shear area of the bolt threads

The margin of safety is:

$$MS = \frac{0.6S_y}{\tau} - 1 = \frac{0.6 \times 22.5}{2.2} - 1 = +6.14$$

Spacer Welds

Using a bounding weight (W) of 25 pounds for the tube and triangular plates, the shear load on the welds is:

$$P = W \times g = 25 \times 25 = 625 \text{ lbs}$$

where:

g = 25 g, side-drop acceleration

The welds for the spacer are ¼-inch fillet weld. The shear stress in the weld is:

$$\tau = \frac{P}{t_w 0.707 \pi d} = \frac{625}{0.25 \times 0.707 \times (\pi \times 3.5)} = 322 \text{ psi}$$

where:

t_w = 0.25 in, weld size

d = 3.5 inches, outside diameter of 3-inch schedule-80 pipe

The stress in the weld due to bending is:

$$S = \frac{M}{t \times S_w} = \frac{5{,}263}{(0.25 \times 0.707)9.62} = 3.1 \text{ ksi}$$

where:

$M = wL = 25 \times 25 \times 8.42 = 5{,}263$ in - lb, the bending moment

$S_w = \frac{\pi d^2}{4} = \frac{\pi \times 3.5^2}{4} = 9.62\ \text{in}^2$, section modulus of the weld (Blodgett)

The maximum shear stress (τ_{max}) in the weld, which is equivalent to the stress intensity divided by two, is:

$$\tau_{max} = \frac{\sqrt{S^2 + 4\tau^2}}{2} = \frac{\sqrt{3.1^2 + 4 \times 0.3^2}}{2} = 1.6\ \text{ksi}$$

The margin of safety is:

$$MS = \frac{0.6S_y}{\tau_{max}} - 1 = \frac{0.6 \times 22.5}{1.6} - 1 = +7.4$$

where:

S_y = 22.5 ksi, yield strength of Type 304 stainless steel @300°F

TPBAR Spacer 1-Foot Top-End Drop

When loaded in the consolidation canister, the TPBARs (held in the shape of a square) load the spacer tubes via the triangular top plates during top-end drop conditions. The compressive load applied to the tubes during the top-end drop is the weight of the TPBARs, 795 lbs (300 TPBARs at a bounding weight of 2.65 lbs per TPBAR), times the bounding acceleration of 20g (actual 15.8 g). For this analysis, W=1,000 lbs, is conservatively used.

Tube

The compressive stress in the tubes is:

$$S = \frac{W \times g}{A} = \frac{1000 \times 20}{2 \times \left(\frac{\pi}{4}\left(3.5^2 - 2.9^2\right)\right)} = 3.3\ \text{ksi}$$

where:

A = the cross sectional area of a 3-inch schedule-80 pipe with an outer diameter of 3.5 inches and a thickness of 0.3 inch

The margin of safety is:

$$MS = \frac{S_y}{S} - 1 = \frac{22.5}{3.3} - 1 = +5.8$$

where:

S_y = 22.5 ksi, yield strength of Type 304 stainless steel @300°F

Triangular Top Plate

Referring to the dimensions provided in Figure 2.6.12-8, the pressure applied to a triangular plate is

$$P_{TP} = \frac{1}{2} \times \frac{1000}{0.5 \times 7.43 \times 7.43} \times 20 = 362 \text{ psi}$$

The bending moment in the top plate is (see Line A in Figure 2.6.12-6)

$$M = 362 \times \left(0.5 \times 4.18^2\right) \times \left(\frac{1}{3} \times 4.18\right) = 4406 \text{ in-lb}$$

The bending stress in the plate is:

$$S = \frac{6M}{bt^2} = \frac{6 \times 4{,}406}{4.18 \times 0.75^2} = 11.2 \text{ ksi}$$

The margin of safety is:

$$MS = \frac{1.5S_m}{S} - 1 = \frac{1.5 \times 20.0}{11.2} - 1 = +1.68$$

where:

S_m = 20.0 ksi, stress intensity of Type 304 stainless steel @300°F

TPBAR Spacer 1-Foot Bottom-End Drop

During the one-foot bottom-end drop, the inertial load of the spacer is applied to the bolts that affix the spacer to the NAC-LWT cask lid and the welds used to fabricate the spacer assembly. The maximum bottom-end drop acceleration is 20g.

Bolts

Four bolts (½-13UNC, Type 304 stainless steel) hold the spacer assembly to the bottom of the NAC-LWT cask lid and six bolts hold the spacer base to the circular base plate. For this evaluation, only the four spacer assembly bolts are considered since the individual bolt load is higher and the thread engagement length is shorter. The Internal lid thread evaluation is not required since high strength Helicoil inserts are utilized. Using the spacer assembly weight of 115 lbs and an acceleration of 20g, the critical bolt load is:

$$P = \frac{115 \times 20}{4} = 575 \text{ lbs}$$

The tensile stress is:

$$S = \frac{P}{A_t} = \frac{575}{0.1419} = 4.1\,\text{ksi}$$

The margin of safety is:

$$MS = \frac{S_y}{S} - 1 = \frac{22.5}{4.1} - 1 = +4.49$$

where:

S_y = 22.5 ksi, yield strength of Type 304 stainless steel @300°F

The shear stress in the bolt thread is:

$$\tau = \frac{P}{A_S} = \frac{575}{0.7789} = 0.74\,\text{ksi}$$

The margin of safety is:

$$MS = \frac{0.6S_y}{\tau} - 1 = \frac{0.6(22.5)}{0.74} - 1 = +\underline{\text{Large}}$$

Spacer Welds

During a 1-foot bottom-end drop (20g), the spacer weld is loaded by the inertial load of the spacer tube and the triangular top plate (25 lbs bounding). The weld is a ¼-inch fillet weld. The weld stress is:

$$S_w = \frac{W \times g}{t(0.707)(\pi d)} = \frac{25 \times 20}{0.25 \times 0.707 \times (\pi \times 3.5)} = 257\,\text{psi} = 0.3\,\text{ksi}$$

where:

d = 3.5 in, outside diameter of 3-inch schedule 80 pipe
t = 0.25 in, weld size

The margin of safety is:

$$MS = \frac{0.6S_y}{S_w} - 1 = \frac{0.6(22.5)}{0.3} - 1 = +\underline{\text{Large}}$$

where:

S_y = 22.5 ksi, yield strength of Type 304 stainless steel @300°F

Figure 2.6.12-7 Cross-Section of TPBAR Basket

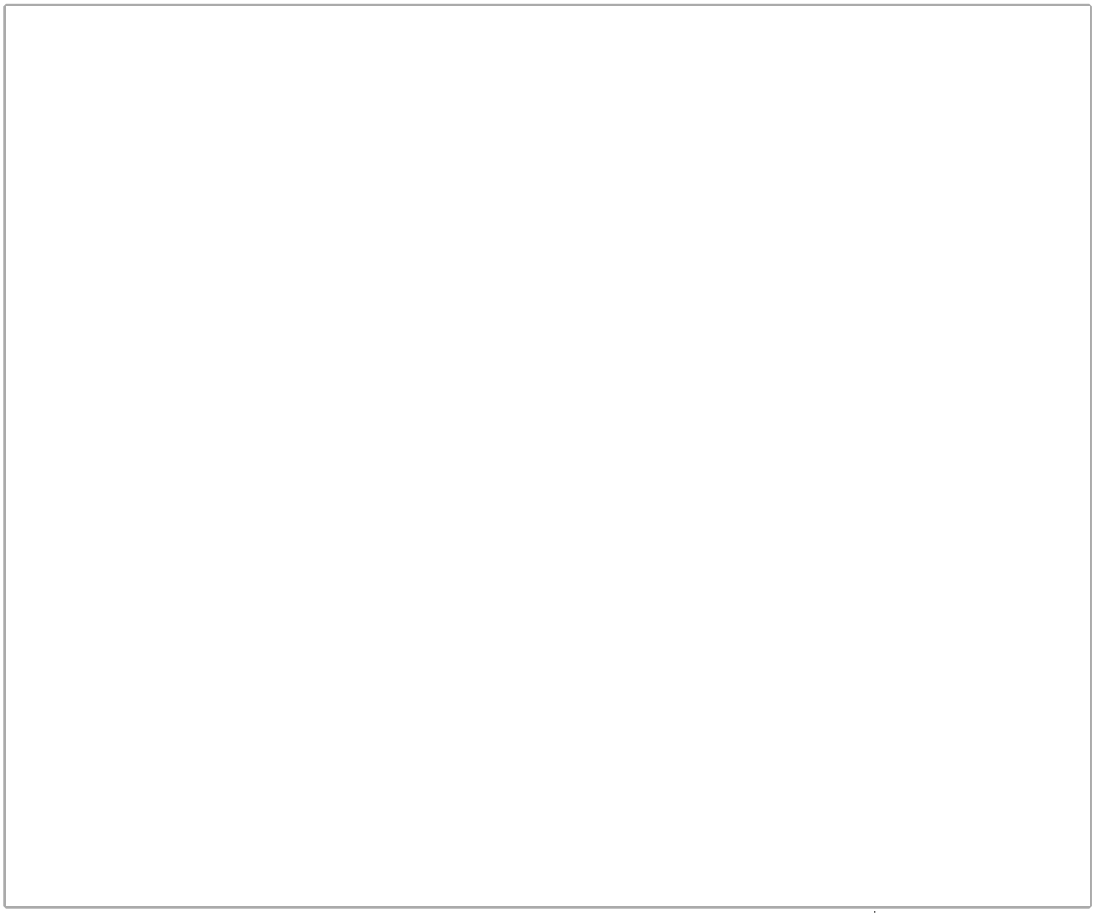

Figure 2.6.12-8 TPBAR Spacer Schematic Triangular Top Plate and Tube

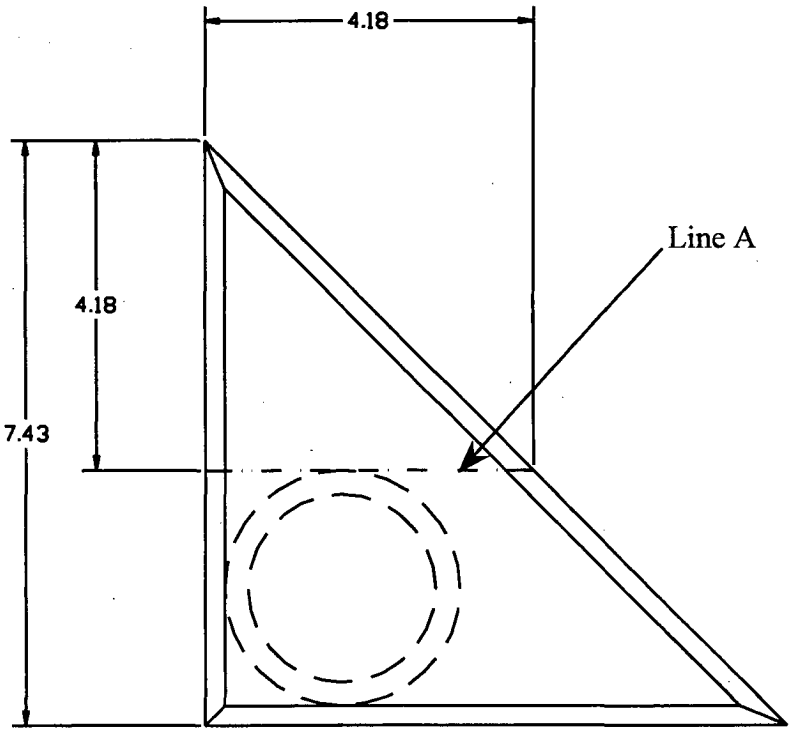

(Unit = inches)

2.6.12.11 ANSTO Basket Analysis

The ANSTO modular basket assembly consists of a top module, four intermediate modules, and a base module. The top and base modules are each 29.8 inches long; each of the four intermediate modules is 29.3 inches long (not including guide pins); and all six modules have an outer diameter of 13.27 inches. Each module is capable of holding up to seven spiral fuel assemblies or MOATA plate bundles. Each module is a weldment made up of a 13.27-inch-diameter, 1/2-inch-thick base plate and six 13.27-inch-diameter, 1/2-inch-thick support plates scalloped on the inner diameter to fit around six peripheral fuel tubes. The weldment structure, fuel tubes, and base and support plates are fabricated from Type 304 stainless steel. Each of the seven fuel tubes in each module has an outer diameter of 4.375 inches and a wall thickness of 0.125 inch. The bottom of each fuel tube is welded to the 1/2-inch-thick base plate. At the bottom of each fuel tube, where it is welded to the base plate, there is a 0.3-inch slot to permit water to drain from the tube. The base plate supports the fuel assembly/bundle in the end drop orientation. The base module sits on a 0.5-inch-high, 10-inch-diameter ring that is welded in segments to the base plate. The total weight of the ANSTO basket assembly bears directly on the bottom forging of the cask through the ring. The six scalloped 1/2-inch-thick support plates and the base plate of each basket module provide lateral support and maintain the fuel configuration in the side drop orientation.

2.6.12.11.1 ANSTO Basket Body 1-Foot Side Drop Analysis

Structural analyses of the ANSTO basket for 1-foot side and end drops are performed using classical hand calculations.

The inertia load of the LWT cask for a 1-foot side drop is 25g. A conservative loading condition of a diametrically loaded ring (Table 17, Case 1, Roark) is considered, which neglects any load distribution. Also, it is conservative to assume that there are three loaded fuel tubes acting on the top of a fuel tube since, in reality, there are only two of them. The stresses in the circumferential direction and in the longitudinal direction are added without regard to their signs. Since the circumferential direction and the longitudinal direction also correspond to the direction of the principal stresses, the addition of the two magnitudes reflects the possibility of the principal stresses being of opposite signs.

The maximum applied load to a fuel tube for the circumferential bending stress is:

$$P_s = (3W_{FT} + 3W) \times 25 = 2{,}415 \text{ lbs}$$

where:

W_{FT} = 14.2 lbs, maximum fuel tube weight

W = 18.0 lbs, maximum average fuel assembly weight

The bending moment in the fuel tube is:

$$M = \frac{wRk_2}{\pi} = \frac{84 \times 2.13 \times 1.00}{\pi} = 57 \text{ in-lb/in}$$ (Table 17, Case 1, Roark)

where:

$$w = \frac{P_s}{L_t} = 84 \text{ lb/in}$$

L_t = 28.81 inches, shortest fuel tube length

R = 2.13 inches, mean radius of fuel tube

k_2 = 1-α =1.00

$$\alpha = \frac{I}{A \times R^2} = \frac{bt^3/12}{b \times t \times R^2} = 2.87 \times 10^{-4}$$

b = 1.0 in, unit length

t= 0.125 in, tube wall thickness

The circumferential bending stress in the fuel tube is:

$$\sigma c = \frac{6M}{bt^2} = \frac{6 \times 57}{1 \times 0.125^2} = 21.9 \text{ ksi}$$

The stress in the fuel tube in the longitudinal direction is calculated assuming the fuel tube acts like a beam. The maximum bending moment occurs at the top of the basket where the fuel tube acts like a cantilever beam. (The maximum moment for a cantilevered beam with a uniform loading of w (lb/in) and length (l) is $wl^2/2$, as compared to the maximum moment $wl^2/8$ for a simply supported beam.) The bending moment in the tube is:

$$M = \frac{wl^2}{2} = \frac{84 \times 4.0^2}{2} = 672 \text{ in-lb}$$

where:

l = 4.0 inches, the length of the tube extending beyond the support plates

The bending stress is:

$$\sigma_l = F\frac{Mc}{I} = \frac{672 \times 2.19}{3.77} \approx 1.1 \text{ ksi}$$

where:

c = 2.19 inches, distance to extreme outer fiber of tube from centroid of tube

I = 3.77 in^4, tube moment of inertia

F = 2.725, factor to account for the effect of the small diameter-to-length ratio on bending for a cantilevered tube. This is obtained for a uniformly loaded beam in Article 7.10 in Roark.

The maximum stress in the tube is:

$$\sigma_b = 21.9 + 1.1 = 23.0 \text{ ksi}$$

The margin of safety is:

$$MS = \frac{1.5S_m}{\sigma_b} - 1 = +0.26$$

where:

S_m = 19.4 ksi, design stress intensity, Type 304 stainless steel, 350°F

The bearing stress on the support plate is calculated using Table 33, Case 2c from Roark.

The maximum weight of a loaded module is the weight of the base module, W_{BM} = 280 lbs. The weight of the loaded basket is supported by the six support plates and the base plate (i.e., total of seven). The bearing stress on a support plate is:

$$\sigma_{brg} = 0.591\sqrt{\frac{pE}{K_D}} = 3.6 \text{ ksi}$$

where:

$$p = \frac{W}{7t_d}g = \frac{280}{7 \times 0.5} \times 25 = 2{,}000 \text{ lb/in, bearing load for 25g side drop}$$

t_d = 0.5 in, support disk thickness

g = 25g, side drop inertia load

$$K_D = \frac{D_1 D_2}{D_1 - D_2} = 1{,}366.81$$

D_1 = 13.395 inches, LWT cask inner diameter

D_2 = 13.265 inches, support disk diameter

E = 25.7×10^6 psi, modulus of elasticity, Type 304 stainless steel, 350°F

The margin of safety is:

$$MS = \frac{S_y}{\sigma_{brg}} - 1 = +5.06$$

where:

S_y = 21.8 ksi, yield strength, Type 304 stainless steel, 350°F

2.6.12.11.2 ANSTO 1-Foot End Drop Evaluation

The inertia load for the LWT for a 1-foot end drop is 20g. The applied load to the ANSTO basket is:

$$P = W_{total} \times 20 = 35{,}400 \text{ lbs}$$

where:

W_{total} = 1,770 lbs, total weight of loaded basket, which bounds the calculated weight of 1,667 lbs

The minimum cross-sectional area is at the base of the fuel tubes where the cutouts for water drainage are located. The cross-sectional area is:

$$A = \frac{\left[\frac{\pi}{4}\left(D_o^2 - D_i^2\right) \times 6\right]}{2} + \left[\frac{\pi}{4}\left(D_o^2 - D_i^2\right) - 6 \times l_c \times t_t\right] = 5.93 \text{ in}^2$$

where:

D_o = 4.375 inches, tube outer diameter

D_i = 4.125 inches, tube inner diameter

l_c = 1.00 in, cutout length in center tube

t_t = 0.125 in, tube wall thickness

The membrane stress in the basket is:

$$\sigma = \frac{P}{A} = \frac{35{,}400}{5.93} = 5.97 \text{ ksi}$$

The margin of safety is:

$$MS = \frac{S_m}{\sigma} - 1 = +2.2$$

where:

S_m = 19.4 ksi, design stress intensity, Type 304 stainless steel, 350°F

The support plates are welded to the fuel tube with 1/16-inch bevel welds on both sides of the plate. The area of the weld is:

$$A_W = \frac{6(\pi D_o)}{2} \times 2t_w = 5.15 \text{ in}^2$$

where:

D_o = 4.375 inches, outer diameter of tube

t_w = 1/16 in, weld thickness

The bounding weight of the support plates is 20.1 lbs; and the bounding g-load factor is 60. A weld quality factor of 0.25 for a surface visual examination is divided into the calculated stress. This factor corresponds to the largest stress reduction factor in Table NG-3352-1 of the ASME Code. Therefore, the stress in the weld is:

$$\sigma_w = \frac{20.1 \times 60}{A_w (0.25)} = 936 \text{ psi}$$

The margin of safety using normal conditions allowable is:

$$MS = \frac{0.6S_m}{\sigma_w} - 1 = +\underline{\text{Large}}$$

where:

S_m = 19.4 ksi, design stress intensity, Type 304 stainless steel, 350°F

2.6.12.11.3 ANSTO Thermal Stress Evaluation

Thermal stress caused by a temperature gradient in the basket is calculated in this section. The thermal stress is minimal since the basket is free to expand. The thermal stress occurs as the hotter tubes expand radially against the basket support plates, which are at a lower temperature.

The maximum thermal stress of the fuel tube is back-calculated from the displacement computed using equations for circular rings from Table 17, Case 1, Roark.

The diametrical displacements caused by the thermal expansions for the center tube (Δ_1) and the tube adjacent to it (Δ_2) are calculated as:

$$\Delta_1 = \alpha \times \Delta T \times R_t = 4.58 \times 10^{-3} \text{ in}$$

where:

$\alpha = 9.1 \times 10^{-6}$ /°F, coefficient of thermal expansion, Type 304 stainless steel, 350°F

ΔT= 230°F (300-70), T_{max} of the basket is conservatively considered to be 300°F

70°F is room temperature

R_t = 2.19 inches (4.375/2), radius of the fuel tube outer surface

$$\Delta_2 = \alpha \times \Delta T \times D_t = 9.17 \times 10^{-3} \text{ in}$$

where,

$\alpha = 9.1 \times 10^{-6}$ /°F, coefficient of thermal expansion, Type 304 stainless steel, 350°F

ΔT= 230°F (300-70), T_{max} of the basket is conservatively considered to be 300°F

70°F is room temperature

D_t = 4.375, diameter of the fuel tube

The displacement caused by the thermal expansions for the outer surface of the support plate (Δ_S) is calculated as:

$$\Delta_S = \alpha \times \Delta T \times R_S = 8.58 \times 10^{-3} \text{ in}$$

where,

$\alpha = 9.1 \times 10^{-6}$ /°F, coefficient of thermal expansion, Type 304 stainless steel, 350°F

ΔT= 144°F (214-70), T_{max} of the inner shell

70°F is room temperature

R_S = 6.55 inches (13.1/2), radius of the support plate

Note: 214°F is conservatively used to result in a minimum Δ_S in order to maximize the thermal stress.

The deformation that results in thermal stress is -5.17×10^{-3} inch ($\Delta_S - \Delta_1 - \Delta_2$). Therefore, the fuel tube will experience a reduction in diameter due to the differential thermal expansion of the fuel tubes and support plates. It is conservative to assume that all deformation occurs at the center tube. Using Case 1 in Table 17 of Roark, the change in the diameter of the circular ring, D_V, and the moment, M_A, are given by:

$$D_V = 0.1488\times\frac{WR^3}{EI} \quad \text{and} \quad M_A = \frac{WR\times k_2}{\pi}$$

therefore:

$$M_A = \frac{D_V\times EI}{0.1488\times R^2}\times\frac{k_2}{\pi}$$

where:

W is the load due to differential thermal expansion

$D_V = 5.17\times10^{-3}$ inch, change in the diameter due to thermal stress

R = 2.13 inches, mean radius of fuel tube

$E = 25.7 \times 10^6$ psi, modulus of elasticity, Type 304 stainless steel, 350°F

$I = bt^3/12$, inertial of the cross-section

b = 1.0 in, unit length

t = 0.125 in, tube wall thickness

$k_2 = 1-\alpha = 1.00$

$$\alpha = \frac{I}{A\times R^2} = \frac{bt^3/12}{b\times t\times R^2} = 2.87\times10^{-4}$$

The thermal stress is:

$$\sigma = \frac{6M_A}{bt^2} = \frac{D_V E t k_2}{0.2976\pi R^2} = \frac{5.17\times10^{-3}\times25.7\times10^6\times0.125\times1.0}{0.2976\times\pi\times2.13^2} = 3{,}916 \text{ psi}$$

The maximum P+Q stress in the basket is conservatively calculated by combining the bending stress and thermal stress in the basket. The P+Q stress is:

$$\sigma_{pq} = \sigma_b + \sigma_{th} = 23.0 + 3.9 = 26.9 \text{ ksi}$$

The margin of safety is:

$$MS = \frac{3S_m}{\sigma_{pq}} - 1 = +1.16$$

where:

S_m = 19.4 ksi, design stress intensity, Type 304 stainless steel, 350°F

2.6.12.12 TPBAR Basket with the PWR/BWR Rod Transport Canister

This section provides the structural analysis for the shipment of up to 25 individual TPBARs in the PWR/BWR Rod Transport Canister, the PWR insert and the TPBAR basket. Section 2.6.12.10 provides the structural evaluation of the TPBAR basket, with 300 TPBARs, considering a slightly lower contents weight (1800 lbs) than the TPBARs in the PWR/BWR Rod Transport Canister configuration (1901 lbs). The effects of the increased weight loading for the TPBAR basket are addressed in this section. The structural evaluation of the PWR/BWR Rod Transport Canister and the PWR insert is performed in Section 2.6.7.10.

TPBAR Basket Body 1-Foot Side Drop Analysis – Normal Condition

The TPBAR basket body is constructed of four machined segments that are held together with aluminum bands at five locations along the axial length of the basket, as well as the top and bottom fittings, which are bolted to the aluminum basket. During a side drop, the TPBAR basket is subjected to bending and bearing stresses. The maximum bending stress occurs at Location 'A' in the following figure and is due to the content weight. The maximum bending stress is calculated using a cantilevered beam. This is conservative since it neglects any support of the load due to the edges of the basket being supported by the cask inner shell. The maximum bending stress is:

$$S_b = \frac{6M}{t^2} = \frac{6 \times 226}{0.5^2} = 5.42 \text{ ksi}$$

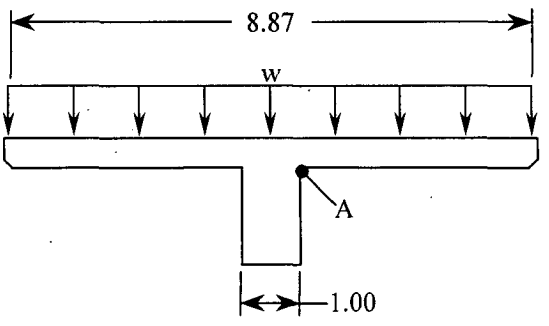

where:

$$w = \frac{W_c \times g}{L \times b} = \frac{1{,}650 \times 25}{159.5 \times 8.87} = 29.2 \text{ psi},$$

the distributed load transfer by the PWR insert on the TPBAR basket

W_c = 1,650 lb, bounding TPBAR contents weight (with TPBARs, PWR/BWR Rod Transport Canister and the PWR insert)

L = 159.5 in, loadable length of the TPBAR basket

b = 8.87 in, TPBAR basket opening width

g = 25g, bounding side drop acceleration

$$M = w\times\left(\frac{b}{2}-\frac{1}{2}\right)\times\frac{1}{2}\left(\frac{b}{2}-\frac{1}{2}\right)$$

$$= 29.2\times\left(\frac{8.87}{2}-\frac{1}{2}\right)\times\frac{1}{2}\left(\frac{8.87}{2}-\frac{1}{2}\right)=226 \text{ in-lb/in, the maximum bending moment}$$

t = 0.5 in, thickness of the flange

The margin of safety is

$$MS = \frac{1.5S_m}{S_b}-1=\frac{1.5\times 8.4}{5.42}-1=+1.32$$

where:

S_m = 8.4 ksi, stress intensity of 6061-T6 aluminum @ 300°F

The bearing stress in the basket is

$$S_{brg} = \frac{P}{A}=\frac{63{,}750}{1.00\times 161.5}=395 \text{ psi}=0.4 \text{ ksi}$$

where:

P = $g \times (W_c + W_b) = 25 \times (1{,}650 \text{ lb} + 900 \text{ lb}) = 63{,}750$ lb, total side drop load

W_b = 900 lb, the bounding weight of the TPBAR basket

A = is the minimum bearing area of the basket

The margin of safety is

$$MS = \frac{S_y}{S_{brg}}=\frac{26.9}{0.4}-1=+\text{large}$$

where:

S_y = 26.6 ksi, yield strength of 6061-T6 aluminum @ 300°F

TPBAR Basket – End Drop

In an end drop scenario, the basket is only loaded by its own weight. The TPBAR basket weight is bounded by what was considered for the end drop analysis of the TPBAR basket in Section 2.6.12.10. Additionally, the assumed component temperatures remain conservative. Therefore, the results of section 2.6.12.10 are bounding and no further analysis is required.

TPBAR Basket Upper Fitting

The TPBAR basket upper fitting is identical to what was analyzed for the TPBAR basket in Section 2.6.12.10. The TPBAR basket weight and component temperatures considered in Section 2.6.12.10 are conservative. Therefore, the results of the Section 2.6.12.10 are bounding and no further analysis is required.

TPBAR Basket Lower Fitting

The TPBAR basket lower fitting is identical to the lower fitting of the PWR basket. The weight of the loaded TPBAR basket is less than the weight of the loaded PWR basket. Therefore, no further analysis is required.

PWR Insert

The PWR insert contains the PWR/BWR Rod Transport Canister assembly for insertion into the TPBAR basket. The PWR insert is not a structural component and, therefore, an analysis of its performance under normal conditions is not required.

PWR/BWR Rod Transport Canister Assembly Analysis

The PWR/BWR Rod Transport Canister is identical to the configuration analyzed in Section 2.6.7.10. The fuel weight considered in the Section 2.6.7.10 analysis for the PWR/BWR fuel (350 lbs) bounds the fuel weight of 25 TPBARs in the PWR/BWR Rod Transport Canister (66 lbs). Therefore, no further analysis is required for the canister.

Internal Spacer

The internal spacer for the PWR/BWR Rod Transport Canister is identical to what was analyzed in Section 2.6.7.10. The fuel weight considered in the Section 2.7.1.7 analysis for the PWR/BWR fuel (350 lbs) bounds the fuel weight of 25 TPBARs in the PWR/BWR Rod Transport Canister (66 lbs). Therefore, no further analysis is required for the internal spacer.

4×4 and 5×5 Inserts

The 4×4 and 5×5 inserts for the PWR/BWR Rod Transport Canister are identical to what was analyzed in Section 2.6.7.10. The fuel weight considered in the Section 2.7.1.7 analysis for the PWR/BWR fuel (350 lbs) bounds the fuel weight of 25 TPBARs in the PWR/BWR Rod

Transport Canister (66 lbs). Therefore, no further analysis is required for the 4×4 and 5×5 inserts.

2.6.12.13 Conclusion

Loads generated during normal operations conditions for each basket assembly design result in total equivalent stresses, which each basket body can adequately sustain. Analyses show that all basket-bearing stresses during a side drop are much less than the material yield strength. Column analyses demonstrate that each basket assembly is self-supporting during an end drop. The minimum Margin of Safety, for all basket designs, is +0.10 as reported in Section 2.6.12.7.4 for the TRIGA basket; +0.003 as shown in Table 2.6.12-2 for the DIDO basket; +0.10 as reported in Section 2.6.12.9.2 for the GA fuel basket; and +0.26 as reported in Section 2.6.12.11.1 for the ANSTO basket. Therefore, it can be concluded that all basket designs have sufficient structural integrity for adequate service during normal conditions of transport.

2.7 Hypothetical Accident Conditions

The 10 CFR 71.73 requires the NAC-LWT cask to be structurally adequate for the free drop, puncture, fire and water immersion hypothetical accident scenario. In the free drop analyses, the cask impact orientation evaluated is that which inflicts the maximum damage to the cask. The 10 CFR 71.73 also requires the cask accident assessment to be at the most unfavorable ambient temperature in the range from –20°F to 100°F. The NAC-LWT cask is evaluated for structural integrity for the hypothetical accident conditions in this section.

2.7.1 Free Drop (30 Feet)

The NAC-LWT cask is required by 10 CFR 71.73(c)(1) to demonstrate structural adequacy for a free drop through a distance of 30 feet onto a flat, unyielding, horizontal surface. The cask strikes the surface in an orientation that inflicts maximum damage. In determining which orientation produces the maximum damage, the NAC-LWT cask is evaluated for impact orientations in which the cask strikes the impact surface on its top end, top end oblique, side, bottom end, and bottom end oblique. The impact limiters and the impact limiter attachments are evaluated in Section 2.6.7.4 for all loading conditions.

Impacts with the maximum and minimum weights of contents are considered. The environmental temperature for the drop is between -20°F and 100°F. Internal heat generation from the contents and insolation are also considered. Regarding internal pressure, the maximum or minimum normal operations pressure is applied to produce the critical stress condition in conjunction with the other loads previously discussed. Closure lid bolt preload and fabrication stresses are also considered. The analyses for the end and oblique drop accidents are conservatively based on a cask outer shell thickness of 1.12 inches. The side drop analyses are based on the cask outer shell thickness of 1.20 inches.

The following method and assumptions are adopted in all of the drop analyses:

1. The finite element method is utilized to do the impact analyses. The analyses are performed by the ANSYS computer program.
2. The analyses assume linearly elastic behavior of the cask.
3. The impact loads calculated in Section 2.6.7.4 are statically applied to the impact surface of the cask. The dynamic wave propagation produced by the impact is assumed to spread throughout the cask body simultaneously.
4. The finite element model of the NAC-LWT cask includes only the major structural components of the cask body; thus, the weight of the modeled cask body, 37,519 lbs, does not include the weight of the neutron shield material, the neutron shield shell nor the contents. However, the applied loads on the cask model are based on a cask design weight of 52,000 lbs.
5. To account for the lead slump during the drops and the differential thermal expansion between the cask stainless steel shells and lead shell, gap elements are used in the finite element model.
6. Although the 10 CFR 71.73 only requires the cask accident drop assessment to be at the most unfavorable ambient temperature in the range from –20°F to 100°F, the NAC-LWT cask is conservatively evaluated in all cases except the side drop for the ambient temperature in the range from -40°F to 130°F. The side drop evaluation uses an ambient temperature range of –40°F to 100°F.

Four accident conditions were identified for a detailed finite element stress presentation:

1. A 30-foot top end drop (drop orientation = $\phi = 0°$, where ϕ is defined as the impact orientation; that is, the angle between the impact direction and the cask centerline), 130°F ambient temperature, maximum decay heat load.
2. A 30-foot top corner drop (drop orientation $\phi = 15.74°$), 130°F ambient temperature, maximum decay heat load.
3. A 30-foot top oblique drop (drop orientation = $\phi = 60°$), 130°F ambient temperature, maximum decay heat load.
4. A 30-foot side drop (drop orientation = $\phi = 90°$), 100°F ambient temperature, maximum decay heat load.

The top end ($\phi = 0°$), top corner ($\phi = 15.74°$), top oblique ($\phi = 60°$) and side ($\phi = 90°$) drops envelope all of the drop orientations.

The types of loading involved in the four accident conditions include: (1) thermal, (2) internal pressure, (3) closure lid bolt preload, and (4) impact and inertial loads resulting from the impact event. These loadings and the boundary conditions, used in the finite element analyses, are discussed in Sections 2.7.1.1.2 through 2.7.1.3.2. Appendix 2.10.10 gives a thorough look at the procedures, analysis and stress results for the 30-foot drop accident conditions. The stress results, calculated for each individual loading at the 123 nodal points on the cask, are tabulated in Tables 2.10.10-6 through 2.10.10-15. Both the stress components and the principal stresses are included.

Note that the fabrication stresses are considered negligible as explained in Section 2.6.11. The puncture analysis is performed using classical hand calculations, as shown in Section 2.7.2.

2.7.1.1 End Drop

2.7.1.1.1 Discussion

The NAC-LWT cask is evaluated for the hypothetical accident end drop conditions to demonstrate its structural adequacy in accordance with the requirements of 10 CFR 71.73. The event scenario is that the NAC-LWT cask, equipped with impact limiters, falls through a distance of 30 feet onto a flat, unyielding, horizontal surface. The cask strikes the surface in a vertical position and, consequently, an end impact on the bottom or the top of the cask occurs. The types of loading involved in an end drop accident include (1) closure lid bolt preload, (2) internal pressure, (3) thermal, (4) inertial body load, and (5) impact load due to the end drop. There are six credible end impact conditions to be considered, according to Regulatory Guide 7.8:

1. Bottom end drop with 130°F ambient temperature and maximum decay heat load
2. Bottom end drop with -40°F ambient temperature and maximum decay heat load
3. Bottom end drop with -40°F ambient temperature and no decay heat load
4. Top end drop with 130°F ambient temperature and maximum decay heat load
5. Top end drop with -40°F ambient temperature and maximum decay heat load
6. Top end drop with -40°F ambient temperature and no decay heat load

The finite element analysis method is utilized to perform the end drop stress evaluation for the NAC-LWT cask.

2.7.1.1.2 Analysis Description

The detailed geometry and finite element model of the NAC-LWT cask are thoroughly described in Section 2.10.2. The cask is modeled as an axisymmetric structure assembly of ANSYS STIF42 isoparametric elements.

The dynamic wave propagation produced by the impact is assumed to spread throughout the cask body simultaneously. In addition, the equivalent static method is adopted to do the impact evaluations. The analyses assume linearly elastic behavior of the cask and that the fabrication stresses are negligible.

Based on the previous assumptions and discussions, the applied loads on the finite element model are as follows:

1. Closure lid bolt preload

   The required total preload of 250,000 lbs, as calculated in Section 2.6.7.6, is converted to an initial strain of 0.0021361 inch/inch/radians and is applied to the bolt, which is modeled as a vertical beam element.

2. Internal pressure

   The cask internal pressure is temperature dependent and is evaluated in Section 3.4.4. Pressures of 50 psig and 12 psig are applied on the interior surfaces of the cask cavity for the hot ambient and cold ambient cases, respectively.

3. Thermal

   There are three thermal conditions.

   A. The heat transfer analysis performed in Section 3.4.2 determined the cask temperatures for the hot environment (130°F temperature) with maximum insolation and maximum decay heat load. See Section 2.10.3.1 for the resulting isothermal temperature plot.

B. Similarly, the heat transfer analysis performed in Section 3.4.3 calculated the cask temperatures for the cold environment (-40°F ambient) with maximum decay heat load and no insolation. See Section 2.10.3.2 for the resulting isothermal temperature plot.

C. The third thermal condition evaluates the cask subjected to an ambient temperature of -40°F with no decay heat load and no insolation.

4. Inertial body load

   Applying D'Alembert's principle, the inertial effects created by an impact can be represented by equivalent static forces. In the analyses, a 76.8 g inertial load is vertically applied on the mass of the cask modeled. The 76.8 g value is derived from the multiplication of 60 g (shown in Table 2.6.7-34) and the factor of $\frac{48,000}{37,519}$, where 48,000 lbs is the cask body design weight and 37,519 lbs is the finite element model weight (The 60-g value is conservatively based on a 3,850-psi maximum crush strength of aluminum honeycomb, although the design maximum crush strength is only 3,675 psi).

   The inertial load resulting from the 4,000-pound contents weight is simulated as an equivalent static pressure load (1,708 psi) uniformly applied on the interior surface of the cask impact end.

5. Impact load

   The impact load is assumed to be uniformly applied over the impact surface of the cask. A uniform pressure of 4,852 psi is applied on the model. This pressure is obtained by dividing the total impact load ($60 \times 52,000$ lb $= 3.12 \times 10^6$ lb) by the impact area, 643 in^2 which is the bottom (or top end) surface area of the cask (Refer to note in 4).

Boundary conditions that are imposed on the model of the cask to restrain rigid body motion include: (1) the nodes located on the vertical centerline are restrained from moving radially, and (2) vertical restraints are imposed on the edge nodes located on the free surface; that is, the nonimpact end.

2.7.1.1.3 Results and Conclusions

The stresses throughout the finite element model are calculated for the combined load conditions. Based on the design criteria presented in Section 2.1.2 and Regulatory Guide 7.6, the calculated stresses are categorized into P_m , $P_m + P_b$, and total stress categories. The secondary stresses (thermal) are conservatively included in the primary stress categories and the margin of safety calculations.

As demonstrated in Section 2.10.3.3, procedures have been implemented to determine the critical Pm, Pm + Pb, and total stresses for each cask component. The calculated stresses are conservatively based on an outer shell thickness of 1.12 inches, although the design outer shell thickness is 1.20 inches. The most critical sections for each component during a particular loading condition are shown in Figure 2.7.1-1 through Figure 2.7.1-5. The critical Pm, Pm + Pb, and total stresses for each component are documented in Table 2.7.1-1 through Table 2.7.1-15. Additionally, the stresses at representative sections throughout the cask are presented in the tables in Section 2.10.7. These tables document the maximum stress locations tabulated for each component. Appendix 2.10.10 presents tabulated detailed stresses for the individual load conditions for the stress points at each section selected for analysis. Tabulations are also presented for the various combinations of the individual load cases.

The allowable stresses for the cask components are determined based on 300°F. Note that the maximum cask temperature is below 300°F for all of the conditions considered and the allowable stresses are, therefore, conservative.

Comparing the analyses results from loading condition 2, as documented in Table 2.7.1-4 through Table 2.7.1-6 and in Table 2.7.1-10 through Table 2.7.1-12, it is evident that the most critical Pm, Pm + Pb, and total stresses are comparable for the bottom and the top end drops. Furthermore, the margins of safety are very large. It is, therefore, expected that the top end drop under loading condition 3 will produce results similar to those for the bottom end drop under loading condition 3. Thus, analyzing the top end drop under loading condition 3 is considered to be unnecessary and is not performed.

The analyses demonstrate that all margins of safety are positive for all of the end drop accident conditions.

The documentation of the NAC-LWT cask adequacy in satisfying the buckling criteria for the stresses of the end drop conditions is presented in Section 2.10.6. The NAC-LWT cask maintains its containment capability and satisfies the 10 CFR 71 requirements for the end drop accident condition.

2.7.1.2 Side Drop

2.7.1.2.1 Discussion

This section presents the evaluation of the structural adequacy of the NAC-LWT cask for the hypothetical accident, 30-foot drop, side impact condition. The event scenario is that the NAC-LWT cask, with an impact limiter attached over each end, experiences a free drop through a distance of 30 feet onto a flat, unyielding surface and strikes the surface in the horizontal position. The types of loading involved in a side drop accident are similar to those discussed in

Section 2.7.1.1 for the end drop accident condition. However, for the side drop accident condition, both the inertial load and the side impact load are nonaxisymmetric and require special consideration for them to be applied on an axisymmetric model using the ANSYS harmonic elements.

There are three credible side impact conditions to be evaluated and discussed: (1) side drop with 100°F ambient temperature and maximum decay heat load, (2) side drop with -40°F ambient temperature and maximum decay heat load, and (3) side drop with -40°F ambient temperature and no decay heat load. Finite element analyses were performed for these side impact evaluations.

2.7.1.2.2 Analysis Description

The NAC-LWT cask is modeled as an axisymmetric structure utilizing the ANSYS STIF25 elements. The finite element mesh is illustrated in Section 2.10.2.

The analyses utilize linearly elastic structural behavior of the cask and the fabrication stresses are negligible.

There are five loads applied on the finite element model - closure lid bolt preload, internal pressure, thermal, inertial body load and impact load. The first three loads are the same as those described in Section 2.7.1.1. The inertial body load and the side impact load are nonaxisymmetric and require further discussion.

The 63.56-g inertial load is transversely applied on the mass of the cask model. The 63.56 g is determined from the side impact acceleration 49.7 g (determined in Section 2.6.7.4) multiplied by the weight factor of 48,000 / 37,519, where 48,000 lbs is the cask body design weight and 37,519 lbs is the cask finite element model weight.

The inertial load produced by the contents is applied as an equivalent static pressure (177.1 psi) on the interior surface of the cask; to be specific, the pressure is uniformly distributed along the cavity length with a circumferential variation. The method used to calculate the pressure of the contents is identical to that for the determination of the impact load pressure.

The impact load applied on the finite element model is nonaxisymmetric and localized. Consequently, it requires special consideration. The cask body (excluding the neutron shield shell) is conservatively assumed to resist the entire impact load due to the side drop accident. This impact load is calculated as $49.7 \times 52{,}000 = 2.58 \times 10^6$ pounds, where the factor 49.7 g was previously explained. The impact load is applied to the finite element model as a distributed pressure over the impact surface of the cask. The distribution of impact pressure is assumed to be uniform, in the longitudinal direction, but sinusoidally varied in the circumferential direction. A cosine-shaped pressure distribution is selected, which is peaked at the center and spread over a

90-degree arc in the circumferential direction as shown in Figure 2.7.1-6. The region of the applied pressure (a 90° arc) is defined based on the "crush" geometry of an impact limiter designed to limit the impact force for a 30-foot drop. The assumption of a "peaked" pressure distribution is a conservative, classical, stress analysis procedure. Variations in the shape and/or magnitude of the applied pressure distribution are expected to produce a localized stress variation in the pressure-applied region. Since the cask body is massive in this region, the variation in stress level is negligible.

Based on the previous discussion, a cosine-shaped pressure distribution, p(θ), in the circumferential direction (Figure 2.7.1-6) is selected as:

$$p(\theta) = \begin{cases} \bar{p} \cos 2\theta, & \text{for } -45° \le \theta \le 45° \\ 0, & \text{for } 315° > \theta > 45° \end{cases} \qquad (1)$$

where $\bar{p}$ represents the peaked value at the 0-degree orientation and is determined from the following equation,

$$P = \left[\int_0^{2\pi} p(\theta) \cos\theta \; r \; d\theta\right] \ell$$

$$= 0.5 \; (2.58 \times 10^6) = 1.29 \times 10^6 \text{ lb} \qquad (2)$$

where:

r = outside radius of outer shell = 14.3075 in

ℓ = interface lengths between the cask and the impact limiters, 11.88 inches are actually engaged with both the bottom and the top impact limiters. In the calculation, 11.25 inches is conservatively used for the bottom engagement and 11.00 inches is conservatively used for the top.

P = side drop impact force at each end of the cask

Thus, the impact pressures, $\bar{p}$, applied on the finite element model are 8,498 psi near the bottom end and 8,691 psi near the top end. These pressures are uniformly distributed element pressures along the longitudinal direction.

In order to use an axisymmetric finite element model to analyze a nonaxisymmetric loading, it is necessary to use the ANSYS harmonic element and harmonic function capability. This is

achieved by defining the pressure distribution, as shown in equation (1), in terms of a Fourier series of harmonic functions, as:

$$p(\theta) = A_o + A_1\cos\theta + A_2\cos2\theta + A_3\cos3\theta + A_4\cos4\theta + A_5\cos5\theta \qquad (3)$$

Note that, since the impact load is centered at the 0-degree orientation, all loading terms are of the form cos iθ. Each term of the series represents an individual axisymmetric load mode and is defined by the load coefficient (A_i), the number of harmonic waves in the mode shape, and the symmetry condition (cos iθ). The analytical results for the defined nonaxisymmetric loading are the summation of the results of each of the individual axisymmetric load term analyses. The load coefficients, A_i, are determined by the ANSYS PREP6 routine, and equation (3) becomes

$$p(\theta) = \bar{p}\,[0.1590 + 0.2999\cos\theta + 0.2498\cos2\theta + 0.1799\cos3\theta + 0.1059\cos4\theta + 0.0427\cos5\theta] \qquad (4)$$

Equations (1) and (4) are illustrated in Figure 2.7.1-7. The figures indicate that the Fourier series function contains six terms. The combination of these six terms adequately represents the desired impact pressure distribution. Consequently, six loading mode analyses are required to evaluate the effect on the cask body resulting solely from the impact load during the side impact event.

In summary, the finite element analysis of the side drop condition considers the combined loads resulting from internal pressure, bolt preload, thermal, inertia and impact. Nine loading mode analyses are developed such that their combination evaluates the effects previously mentioned. Table 2.7.1-16 summarizes the load analyses and their descriptions.

To combine the stress results produced by the nine loading mode analyses; the following steps are performed:

1. Utilize the Fourier series coefficients, as reported in equation (4), to multiply the results obtained from load mode analyses 4 through 9. This provides the stresses that result from the impact load.
2. Combine the results obtained from Step 1 and load mode analyses 1 and 3. This provides the stresses caused by the combined effects of internal pressure, bolt preload, inertial, and impact. The resulting stresses are used to calculate the P_m stress intensities and the $P_m + P_b$ stress intensities.
3. Combine the results from Step 1 and load mode analyses 2 and 3. This provides the results to be used to calculate the total stress intensities.

The boundary conditions imposed upon the model of the cask to restrain rigid body motions are defined as follows:

1. The top node located on the vertical centerline is restrained from moving radially.
2. The bottom node located on the vertical centerline is fixed completely.
3. A displacement constrained condition is imposed on the interface surface at the bolt location between the lid and the upper ring. This constrained condition is only imposed for the analysis of the impact load case and the inertial body load case.

2.7.1.2.3 Results and Conclusions

To balance the demands of analytical accuracy and computational efficiency, it is conservatively assumed that the sliding coefficient is zero between the lead/steel interface in the finite element analysis. This significantly minimizes the total number of iterations required for the analysis to converge; yet, it provides conservative analysis results because the horizontal shear resistance at the lead/steel interface is ignored, making the cask structure more flexible under bending. The stresses calculated by the finite element analysis are compared with the hand-calculated stress results. The finite element method indicates that the maximum bending stress, 1,373 psi, occurs at the midpoint of the cask outer shell due to a 1 g inertial load. The hand calculation considers the cask structure as a hollow, circular cross section beam, simply supported at each end, which gives 1,353 psi at the midpoint of the cask outer shell for a 1 g inertial load. The finite element and hand-calculated results agree extremely well. The hand-calculated results are presented in Table 2.10.11-2.

Since the material properties of the cask structure are temperature-dependent, varying environmental temperatures will produce changes in the calculated stresses in the cask for the thermal load cases; but they will not change the calculated stresses in the cask produced by the other types of loads. This is verified by comparing the finite element results for the NAC-LWT cask subjected to a gravity load for different temperature conditions. Also, the stress levels produced by the following different thermal conditions were evaluated: (1) 100°F ambient temperature with maximum decay heat load, (2) -40°F ambient temperature with maximum decay heat load, and (3) -40°F ambient temperature with no decay heat load. The combination effect of the thermal loads with other load types (e.g., inertial body load) has also been studied. It is determined that the side drop event with 100°F ambient temperature represents the worst case for the 30-foot side drop accident condition. Therefore, only the stress results produced by a 30-foot side drop with 100°F ambient temperature are reported.

Stress components and stress intensities are calculated throughout the finite element model for the combined loads due to internal pressure, bolt preload, thermal, inertial, and impact.

The critical sections for each cask component are shown in Figure 2.7.1-8. Table 2.7.1-17 through Table 2.7.1-19 report the P_m stress intensities, the $P_m + P_b$ stress intensities, and the total stress intensities for each cask component, which are obtained from the finite element side drop

analysis. The total P_m and $P_m + P_b$ stresses at representative sections throughout the cask are presented in the tables in Appendix 2.10.7. These tables document the maximum stress locations tabulated for each component. Appendix 2.10.10 presents tabulated detailed stresses for the individual load conditions for the stress points at each section selected for analysis. Tabulations are also presented for the various combinations of the individual load cases.

As mentioned previously, the finite element cask model conservatively ignores the effect of the neutron shield shell on the overall bending of the cask structure.

The margins of safety in Table 2.7.1-17 and Table 2.7.1-18 are positive for all cask components.

The documentation of the NAC-LWT cask adequacy in meeting the buckling criteria for the stresses of the side drop is presented in Section 2.10.6.

It has been demonstrated that all margins of safety are positive for the 30-foot side drop conditions. The NAC-LWT cask maintains its containment capability and satisfies the 10 CFR 71 requirements for the 30-foot side drop accident condition.

2.7.1.3 Oblique Drops

2.7.1.3.1 Discussion

This section presents the structural evaluation of the NAC-LWT cask for the hypothetical accident 30-foot oblique drops. In this event, the NAC-LWT cask, equipped with an impact limiter over each end, falls through a distance of 30 feet onto a flat, unyielding surface. According to NRC Regulatory Guide 7.8, "The center of gravity is usually considered to be directly above the impact area; however, evaluations of other oblique drop orientations are requested 'when appropriate'." An impact at an orientation angle of 15.74 degrees is defined as a corner impact, i.e., the center of gravity of the cask is vertically above the impacting edge of the cask. The NAC-LWT cask is evaluated for four oblique drop orientations (15.74, 30, 45, and 60 degrees) under varying ambient conditions. The types of loading involved in an oblique drop accident are similar to those described in Sections 2.7.1.1 and 2.7.1.2; the inertial loading and the impact loading are nonaxisymmetric and must be applied to the axisymmetric finite element model using the ANSYS harmonic elements. This method is similar to that used for the side drop analyses.

Four credible oblique impact orientations (15.74, 30, 45, and 60 degrees) are considered. For each oblique impact orientation, four combinations of ambient temperature, decay heat load, and cask end loading are evaluated:

1. Top end oblique drop, 130°F ambient temperature, maximum decay heat load.
2. Top end oblique drop, -40°F ambient temperature, maximum decay heat load.

3. Top end oblique drop, -40°F ambient temperature, no decay heat load.
4. Bottom end oblique drop, 130°F ambient temperature, maximum decay heat load.

The finite element analysis method is used for the oblique impact evaluations.

The hypothetical accident oblique drop initial impacts are followed by a secondary impact or "slapdown" of the cask on the end opposite the initially impacted end. The secondary impact is addressed in Section 2.10.4; the energy dissipation requirements for slapdown are shown to be well within the energy absorption capabilities of the NAC-LWT cask impact limiters. Thus, slapdown is not a limiting case for the cask and is not considered any further.

2.7.1.3.2 Analysis Description

Similar to the side impact analysis, the ANSYS STIF25 element is utilized to model the NAC-LWT cask. The finite element model is illustrated in Section 2.10.2.

The oblique drop analyses assume that the cask exhibits linear elastic behavior and that the fabrication stresses are negligible. There are five loads applied on the finite element model – closure lid bolt preload, internal pressure, thermal, inertial body load and impact load. The first three loads are the same as those described in Section 2.7.1.1. The inertial body load and the oblique impact load are nonaxisymmetric and require further discussion.

The inertial body load is the same as that discussed in Section 2.7.1.2, with an additional consideration in the oblique impact analysis. Both lateral and longitudinal inertial loads are applied on the cask. Unique g loads are applied on the mass of the cask model. Table 2.7.1-20 summarizes the applied g loads and their components (lateral and axial) for the different drop orientations. Refer to Section 2.6.7.4 for the detailed calculations of the g loads for the different oblique drop orientations. The g loads are conservatively based on a 3,850-psi maximum crush strength of aluminum honeycomb, although the design maximum crush strength is only 3,675 psi.

The cavity contents force components are applied to the inside of the cask body finite element model. The lateral component of the inertial load produced by the contents is applied to the cask model similarly to the side impact analysis, i.e., uniformly along the cavity length with a cosine-shaped distribution over a 2θ arc (the same sector of the cask on which the lateral impact load is applied) in the circumferential direction. The axial component of the inertial load due to the contents is applied on the end of the cavity of the cask model with the same cosine-shaped distribution over a 2θ arc as that described previously, and with a uniform distribution in the radial direction from the inside diameter of the cask cavity to its axial centerline. Table 2.7.1-21 summarizes the applied contents pressures used in the analyses.

The impact load condition is applied to the cask model similarly to the inertial body load. The lateral component of the impact load is applied to the side of the cask model at the impacting end, uniformly over the 11.25-inch long impact limiter region with a cosine-shaped distribution in the circumferential direction along a 2θ arc. The axial component of the impact load is applied to the impacting end of the cask model with a cosine-shaped distribution in the circumferential direction along an arc of 2θ (the same sector of the cask on which the lateral impact load component is applied) and with a uniform distribution in the radial direction from the outside diameter of the end of the cask to its axial centerline. Table 2.7.1-21 summarizes the pressures produced by the impact loads, which are calculated using the same method as presented in Section 2.7.1.2.

These load distributions of the impact force components and the cavity contents force components on the cask model are selected as being realistic, yet conservative, representations of the actual loadings on the cask for an oblique impact. Variations from actual load distributions are expected to be negligible. In addition, at locations on the cask away from the loading region, the stress results are not affected by the shape of the load distributions.

As shown in the side drop analysis (Section 2.7.1.2), six loading mode analyses are adequate to evaluate the effect on the cask body of the impact load during the oblique impact event. The modal coefficients for the oblique impact are determined by the ANSYS PREP6 routine and reported in Table 2.7.1-22.

In summary, the finite element analyses of the oblique drop conditions consider the combined loads due to internal pressure, bolt preload, thermal, inertia, and impact. Sixteen loading analyses are developed such that the various combinations of the defined load conditions are all considered. The sixteen loading combinations are summarized in Table 2.7.1-23.

To combine the analysis results produced by the sixteen loading mode analyses, the following steps are performed:

1. Utilize the Fourier series coefficients, as reported in Table 2.7.1-22, to multiply the results obtained from load analyses 5 through 16. This provides the stress results due to the oblique impact load.
2. Combine the results obtained from step 1 and load mode analyses 1, 3, and 4. This provides the stresses due to the effects of internal pressure, bolt preload, inertia, and impact. The resulting stresses are used to calculate the P_m stress intensities and the $P_m + P_b$ stress intensities.
3. Combine the results from step 1 and load mode analyses 2, 3, and 4. This gives the results which are used to calculate the total stress intensities.

The boundary conditions that are imposed upon the model of the cask to restrain rigid body motions are defined as follows:

1. On the vertical centerline of the cask, the node on the end opposite the impact is completely fixed.
2. On the vertical centerline of the cask, the node on the end near the impact is restrained from moving radially.
3. On the outside radius of the model, the node on the end opposite the impact is fixed in the radial direction to prevent rigid body rotation, but it is free to move axially.
4. A displacement constrained condition is imposed on the interface surface at the bolt location between the lid and the upper ring. This constrained condition is only imposed for the analyses of the impact load case and the inertial body load case.

2.7.1.3.3 Results and Conclusions

Similar to the discussion presented in Section 2.7.1.2.3, the friction coefficient at the interface between the lead and the stainless steel shells is conservatively assumed to be zero. The stress results produced by the following three oblique impact conditions are reported:

1. Top end oblique drop, 130°F ambient temperature, maximum decay heat load.
2. Top end oblique drop, -40°F ambient temperature, no decay heat load.
3. Bottom end oblique drop, 130°F ambient temperature, maximum decay heat load.

These three oblique drop conditions represent the bounding cases for all of the 30-foot oblique drop accident conditions. Four oblique orientations of the cask (15.74, 30, 45, and 60 degrees) are analyzed for each of the ambient temperature/heat load bounding conditions.

The stresses throughout the cask body are calculated for the combined load conditions. Based on the design criteria presented in Section 2.1.2 and Regulatory Guide 7.6, the calculated stresses are categorized into P_m, $P_m + P_b$, and total stress categories.

As demonstrated in Section 2.10.3.3, procedures have been implemented to determine the critical P_m, $P_m + P_b$, and total stresses for each cask component. The most critical sections for each component during a particular loading condition are shown in Figure 2.7.1-10 through Figure 2.7.1-21. The critical P_m, $P_m + P_b$, and total stresses for each component are documented in Table 2.7.1-24 through Table 2.7.1-59, with the following additional considerations: (1) the boundary effect on the finite element analysis results; and (2) the boundary effect on stress results. The calculated stresses are conservatively based on an outer shell thickness of 1.12 inches, although the design outer shell thickness is 1.20 inches. Additionally, the stresses at representative sections throughout the cask are presented in the tables in Section 2.10.7. These tables document the maximum stress locations tabulated for each component. Appendix 2.10.10 presents tabulated detailed stresses for the individual load conditions for the stress points at each section selected for analysis. Tabulations are also presented for the various combinations of the individual load cases.

Boundary Effect on Finite Element Analyses Results

As discussed previously, the oblique drop condition induces an eccentric (angular) momentum, which causes a rigid body rotation of the cask and a slapdown onto the unyielding surface. To eliminate this rigid body rotation in the oblique drop evaluation, certain displacement restraints are imposed on the finite element model. These restraints cause localized peak stresses in the immediate vicinity of boundary conditions. This boundary effect attenuates very rapidly at locations slightly away from the boundary region. Component 7 (bottom closure plate) exhibits this boundary effect; refer to P_m and $P_m + P_b$ stress intensities reported in Table 2.7.1-51, Table 2.7.1-52, Table 2.7.1-54, Table 2.7.1-55, Table 2.7.1-57 and Table 2.7.1-58. The case reported in Table 2.7.1-58 is selected to illustrate the attenuation of the boundary effect, because the stresses produced by the 60 degree oblique drop condition are most critical. Figure 2.7.1-22 shows the plot of the sectional stresses versus radial location with respect to the axial centerline of the cask. It is obvious that the structural behavior of the bottom cover plate is disturbed in the region from node 1 to node 3, because the calculated $P_m + P_b$ stress intensity is less than the P_m stress intensity. Consequently, these stresses are considered to be unrealistic and are disregarded.

This decision is justified by observing the stress plots shown in Figure 2.7.1-23 and Figure 2.7.1-24. In Figure 2.7.1-23, three curves are shown for the cask bottom (refer to Figure 2.7.1-25 for the location) for the 30-foot bottom oblique drop condition:

1. Curve 1 represents the P_m stress intensities versus the radial location, which are produced by the total loading, i.e., the combined result from load analyses 1 and 3 through 16. (See Table 2.7.1-23 for load analyses identification.)
2. Curve 2 is similar to curve 1, but is produced by a partial loading, i.e., the combined result from load analyses 3, 4, 5, 6, 11, and 12 only.
3. Curve 3 is identical to curve 2, except that the boundary restraint is moved to node 3; it was at node 1 for curves 1 and 2.

The close agreement between curves 1 and 2 indicates that the partial loading case is adequate to simulate the structural behavior of the cask produced by the total loading case. Comparing the stress values represented by curves 2 and 3, the curves clearly indicate that the stresses are greatly reduced in the vicinity of the boundary by changing the location of the displacement restraint from node 1 to node 3. This documents the statement that the stresses in the vicinity of the boundary restraint are unrealistic and are disregarded. Similarly, the plot of $P_m + P_b$ stress intensity (Figure 2.7.1-24) indicates the stress reduction, which results from shifting the location of the boundary restraint. Consequently, the stress results (excluding the boundary effect region; i.e., from section cut d through the rest of component 7; Figure 2.7.1-25) obtained from the finite element analyses are evaluated and reported. This criterion is applicable to all of the other drop orientation cases.

Figure 2.7.1-26 and Figure 2.7.1-27 show the same boundary effect on the stress results for the 30-degree and 45-degree impact orientations (in the vicinity of the boundary in the bottom closure plate of the cask) as is indicated in Figure 2.7.1-25. Thus, the criterion developed for the 60 degree orientation is applicable.

The following tables report the stress results excluding the boundary effect: Table 2.7.1-51, Table 2.7.1-52, Table 2.7.1-54, Table 2.7.1-55, Table 2.7.1-57 and Table 2.7.1-58.

Boundary Effect on Stress Results

The stresses reported in Table 2.7.1-49 indicate that the maximum $P_m + P_b$ stress intensity of component 1 is 69.74 ksi. Again, this is as a result of the boundary effect at this section cut (node 2561). This value of 69.74 ksi is unrealistically high. The next highest $P_m + P_b$ stress intensity for component 1 is 6.79 ksi, located at the section next to the section containing the boundary restraint. (Note that the stress value is one order of magnitude lower).

The method described in Section 2.7.1.3.2 to determine the stresses in the vicinity of the free end of the NAC-LWT cask for the oblique drops is conservative. Inertia loads on the cask, which are responsible for dynamic equilibrium during an oblique drop impact, consist of translational deceleration, the angular deceleration and the centrifugal deceleration. The crushing force generated by the limiter and the translational decelerations are determined from RBCUBED (Section 2.10.1.2) for the particular drop of interest. Results from RBCUBED are used to determine the input into ANSYS for the deceleration of the cask body and the pressure load for the contents. The remaining inertia forces representing the angular deceleration and the centrifugal deceleration are established by the imposed displacement boundary conditions at node 1 (at the center line of the model at the bottom end) and node 2561 (at the center line at the top end). While the actual physical loading is distributed over the body, the analysis procedures cause the boundary restraint to behave as a point load. This produces a concentration of the load in the free end of the cask and results in unrealistically large stresses in this region.

The stresses in the end region can also be determined by using the analysis results from the end drop and the side drop. In each case the effect of the geometrical discontinuities are present since the physical boundaries coincide. The manner in which the forces are developed in an oblique drop can be expressed as a combination of the end drop and side drop. The end drop represents the loads generated by the axial translational deceleration. The load path of the axial load in the end drop is the same as for the oblique drop. In the side drop, the loads generated by the cask body and contents must be reacted by the impact limiter crush forces. In the oblique drop, however, the lateral angular deceleration balances the translational deceleration. This represents some conservatism since the limiter load is concentrated in the end region (for the side drop), while the angular deceleration is not (for the oblique drop).

The actual superposition of the side drop results and end drop results is accomplished by applying a separate factor to the component stresses for each load case prior to the algebraic combination.

The factor for the end drop results is the ratio of the axial translational decelerations which is the only nonhomogeneous boundary condition applied to the model. This factor is expressed as:

$$K1 = \frac{Aao}{Aae} \quad (1)$$

where:

Aao = axial deceleration component for the oblique drop

Aae = axial deceleration for the end drop

The factor for the side drop results is the ratio of the lateral translational decelerations, which again is the only nonhomogeneous boundary condition applied to the model. This factor is:

$$K2 = \frac{Alo}{Als} \quad (2)$$

where:

Alo = lateral deceleration component for the oblique drop

Als = lateral deceleration for the side drop

Since superposition requires the stress components to be added, the stress intensity (maximum principal stress difference) must be recomputed once the component stresses have been determined for the combined case. Thus for each "superimposed" stress component,

$$Sij = K1(S'ij) + K2(S"ij) \quad (3)$$

where:

S'ij the stress component for the end drop (i = x, y, z, xy)

S"ij the stress component for the side drop (i = x, y, z, xy)

The stresses are to be evaluated for the end region and for portions of the cask shell itself. The factors for the different angles are specified below.

Angle of Drop(degrees)	K1	K2
15.74 (corner)	0.970	0.330
30	0.785	0.547
45	0.517	0.624
60	0.370	0.775

These factors are applied to the $P_m + P_b$ stresses, the S_n stresses, and stress ranges on a stress component level. This implies that the factors are applied to thermal stresses in the stress summaries. Since Kl + K2 is greater than unity for any angle, this method will provide some conservatism. All principal stresses and stress intensities are based on the revised stress components. For the critical stress summaries, the maximum stress components listed for the side drop (for the affected cask components only) are combined with the maximum stress components listed for the end drop. This ensures that the maximum stress for the oblique drops is truly the maximum for the component listed in the critical stress summary.

A measure of how far the combined stress methodology should extend axially along the cask shell is given by a fraction of the shell wave length. The formula used is:

$$L' = 2.4\,(rt)^{0.5} \qquad (4)$$

where:

r = mean radius

t = thickness

The value of r for the NAC-LWT cask is taken to be 14.5 inches. The outer shell comprises approximately 80 percent of the effective cross-sectional bending rigidity (See Section 2.10.11 for this computation). For computational purposes the thickness for the outer shell, which is 1.2 inches, is used. The estimated distance along the shell is determined to be 10 inches. This corresponds to a position between section cut "J" and section cut "L" of the cask shell in Figure 2.10.7-1 for the top end drop. For the bottom drop, this places the boundary of the re-evaluated stresses near section cut "T" for the top. It should be noted that the section cuts identifiers start with A at the center line of the bottom end and progresses to Z at the center line at the top end. The node numbers begin with "1" at the center line of the cask at the bottom and monotonically increase to 2561 at the center line at the top center line. This nodal numbering pattern allows the region of affected stresses to be identified by a node number. The location of the stresses to be revised by the superposition method for the top end drops and the bottom end drops are identified on the following page.

Impact End	Section Cuts[1]	Node Numbers[2]
Top	A through J	1 through 698
Bottom	S through Z	1481 through 2561

[1] The section cuts are identified in Figure 2.10.7-1 and their coordinates are listed in Table 2.10.7-1.

[2] The node numbers versus nodal coordinates are specified in Table 2.10.2-1.

Conclusion

The documentation of the NAC-LWT cask adequacy in meeting the buckling criteria for the stresses of the oblique drop is presented in Section 2.10.6.

It has been demonstrated that all margins of safety are positive for the 30-foot oblique drop conditions. The NAC-LWT cask maintains its containment capability and satisfies 10 CFR 71 requirements for the 30-foot oblique drop accident condition.

2.7.1.4 Shielding for Lead Slump Accident

Following the 30-foot free drop, the lead region may experience slumping resulting in a reduction in the shielding capabilities of the cask. The shielding evaluation of the lead slump accident was performed in a series of steps. Initially, QAD-CG was used to model the cask without any lead to see if this simple model would give a reasonable dose rate. It was determined that a more detailed analysis was required. This included calculating the lead gap that was formed because of contraction following the lead pour. The HEATING5 computer program (Turner) is used to calculate the temperatures throughout the cask assuming no gap. The resulting maximum temperature of the lead was 245°F. The gap was calculated based on this temperature. This gap value is then used to find the amount that the lead slumps at either the top or the bottom, depending on the cask drop orientation. The calculation is performed as follows:

$$V_1 = \pi[(r_o - s)^2 - r_i^2]h_1$$

$$V_2 = \pi[r_o^2 - r_i^2]h_2$$

Setting $V_1 = V_2$ and solving for h_2:

$$h_2 = \frac{[(r_o - s)^2 - r_i^2]h_1}{r_o^2 - r_i^2}$$

$$= \frac{[(13.19 - .0417)^2 - (7.45)^2](175.0)}{(13.19)^2 - (7.45)^2}$$

$$= 173.37 \text{ in}$$

therefore:

$$\Delta h = h_1 - h_2 = 175.0 - 173.37 = 1.63 \text{ inches}$$

where:

V_1 = volume of the lead after contraction (in^3)

V_2 = volume of the lead following the pour (in^3)

r_o = outside radius of lead region (in)

r_i = inside radius of lead region (in)

h = height of lead region (in)

s = gap (in) (Section 3.2)

The lead slump calculated using this method (1.63 inches) is much larger than the lead slump determined in the finite element analysis (Section 2.10.5), which makes the resulting dose rates conservative. At this point, another model is created using QAD-CC to determine the final dose rates 1 meter from the surface of the cask through this "window" in the lead shielding (Details of the models are found in Figures 5.3.3-3 through 5.3.3-5). This process is followed for both the top and bottom end-fittings of a PWR assembly and the bottom end-fitting of a BWR assembly. The BWR bottom end-fitting is analyzed since it is larger and has a higher Co 60 source than the PWR bottom end-fitting. The analysis is not performed for the BWR top end-fitting because it is smaller and, therefore, has a lower source strength than the PWR top end-fitting.

The resulting dose rates are less than the 49 CFR 73 limits, and can be found in Table 5.1.1-6. The analysis shows that the loss of lead shielding resulting from a lead slump accident will not result in a substantial loss in shielding effectiveness and that the dose rates from this accident are small when compared to the loss of neutron shield accident evaluated in Section 2.7.2.5.

2.7.1.5 Bolts - Closure Lid (Hypothetical Accident - Free Drop)

Section 2.6.7.6 provides a general description of the analysis approaches employed to demonstrate structural integrity of the NAC-LWT cask closure system for both normal conditions of transport and hypothetical accident conditions.

A complete range of impact orientations is evaluated, from an end impact at 0 degrees to a flat side impact at 90 degrees, and at 5-degree increments in between. Loads are derived from the hypothetical accident impact accelerations summarized within Table 2.6.7-34 and Table 2.7.1-20. Where necessary, impact accelerations have been interpolated at 5-degree increments from those values given in Table 2.6.7-34.

The details of this analytic evaluation are described and performed within Section 2.10.9 for both normal conditions of transport and hypothetical accident conditions. Hypothetical accident condition results are summarized in Table 2.7.1-60 and Table 2.7.1-61, corresponding to a "hot"

initial condition and a "cold" initial condition, respectively. The hot initial condition bolt temperature is taken at 227°F, as summarized in Table 3.4-2. The cold initial condition bolt temperature is assumed to be -20°F, per regulatory requirements. Physical properties for the SA-453, Grade 660 bolts are conservatively taken at 300°F and room temperature (70°F) for hot and cold conditions, respectively. As defined within Table 2.1.2-1, allowable bolt stress is taken as S_y, leading to an allowable direct tension stress of 81.9 ksi and 85.0 ksi, at 300°F and 70°F respectively. Based on this thorough evaluation, the closure bolts incur a maximum stress intensity of 64,511 psi, which result in a minimum margin of safety of 27 percent. See Table 2.7.1-60 (at 5°):

$$MS = 81.9/64.511 - 1$$
$$= +\underline{0.27}$$

Bolt engagement may be evaluated by computing shear stresses within the SA-336, Type 304, and forging material. At 300°F, the allowable shear stress is 0.5 S_U, or 33 ksi, according to Tables 2.1.2-1 and 2.3.1-1. The maximum tensile load is found as the product of the maximum bolt stress intensity, noted above, and the bolt stress area, or (64,511 psi) (0.6051) = 39,036 lbs. The shear area per inch of engagement for a 1 - 8 UNC internal thread is 2.325 in^2/in ("Table Speeds Calculation of Strength of Threads"). The resultant shear stress and margin of safety within the top body forging is:

$$\tau = P/A = (39{,}036) / [(2.325)(1.875)]$$
$$= 8{,}954 \text{ psi}$$

$$MS = 33.0/8.954 - 1$$
$$= +\underline{2.69}$$

Using consistently conservative assumptions, the NAC-LWT cask lid bolted closure is shown to satisfy the performance and structural integrity requirements of 10 CFR 71.73(c)(1) for hypothetical accident conditions.

2.7.1.6 Crush

The dynamic crush test required by 10 CFR 71.73 (c) (2) does not apply to the NAC-LWT cask. The mass of the NAC-LWT exceeds 500 kg and the overall package density is greater than 1,000 kg/m^3.

2.7.1.7 Rod Shipment Can Assembly Analysis

2.7.1.7.1 Discussion

The NAC-LWT rod shipment can assembly is analyzed for structural adequacy in accordance with the requirements of 10 CFR 73 for a 30-foot drop (hypothetical accident condition). The structural evaluation is performed by classical elastic analysis methods. The components evaluated include the can weldment, internal spacer, 4×4 and 5×5 inserts, and the PWR insert. The analysis follows the same methodology as that used for the normal conditions analysis contained in Section 2.6.7.10.

2.7.1.7.2 Analysis Description

Geometry

The geometry of the can assembly is shown in Drawing 315-40-098. Note that the tube component of the can assembly is fabricated from a 6-in. × 6-in. × 0.5-in.-thick tube that is machined to the final dimensions of 5.5-in. × 5.5-in. × 0.25-in.-thick. The can assembly is positioned within the basket during transport of the cask. If the cask is equipped with a PWR basket, the PWR insert is required to provide correct positioning within the basket. The can assembly is constructed of Type 304 stainless steel with the exception of the PWR insert, which is constructed of 6061 Aluminum.

Loadings

The magnitude of the impact force varies according to the drop height and drop orientation. As calculated in Section 2.6.7.4, the g-loads for the 30-foot end and side drops are 60 and 49.7 g, respectively.

Detailed Analysis

Can Weldment

The can body is contained within the basket assembly and is not subjected to bending stresses in the side-drop case.

For the end drop, the can weldment is loaded by its own weight. The can contents bear against the bottom or top of the can assembly, depending on drop orientation.

LWT Can Weldment Compressive Stress

Under hypothetical accident conditions, the tube is evaluated for a 60 g acceleration for the end drop. The compressive load (P) on the tube is the combined weight of the lid and tube body. times the 60 g factor.

The compressive load (P) is:

$$P = 310 \times 60 = 18{,}600 \text{ lbs}$$

The compressive stress (S_c) in the tube body is:

$$S_c = \frac{P}{A} = \frac{18{,}600}{4.98} \cong 3{,}735 \text{ psi}$$

The margin of safety (MS) is then:

$$MS = \frac{0.7S_u}{S_c} - 1 = \frac{0.7(63{,}100)}{3{,}735} - 1 = +10.8$$

LWT Can Weldment Bolt Stresses

During the top end drop, the can assembly impacts on the lid handle. The insert and fuel rods strike the lid and the internal spacer strikes the flange. The resulting lid and flange deformations could result in prying forces on the lid bolts. To compute the force in the lid bolts due to a 30-foot top end drop, a 3-D finite element model of the lid, lid handle, flange, and can tube is constructed. The lid, lid handle, flange, and can tube are modeled using solid elements (SOLID45). The bolts are included in the model using beam elements (BEAM4) originating at the top of the lid and terminating at the top of the flange. The interface between the lid and flange uses contact element (COMBIN40) to model the interaction at this joint. The model represents 1/4 of the can assembly cross section. A uniform pressure load is applied to the inner lid surface to represent the weight of the fuel rods (350 lbs) and insert (75 lbs) multiplied by the 60g-accident acceleration loading. Nodal forces applied to the edge of the flange represent the weight of the internal spacer (240 lbs) multiplied by the 60g-accident acceleration. A plot of the model along with the applied loads follows.

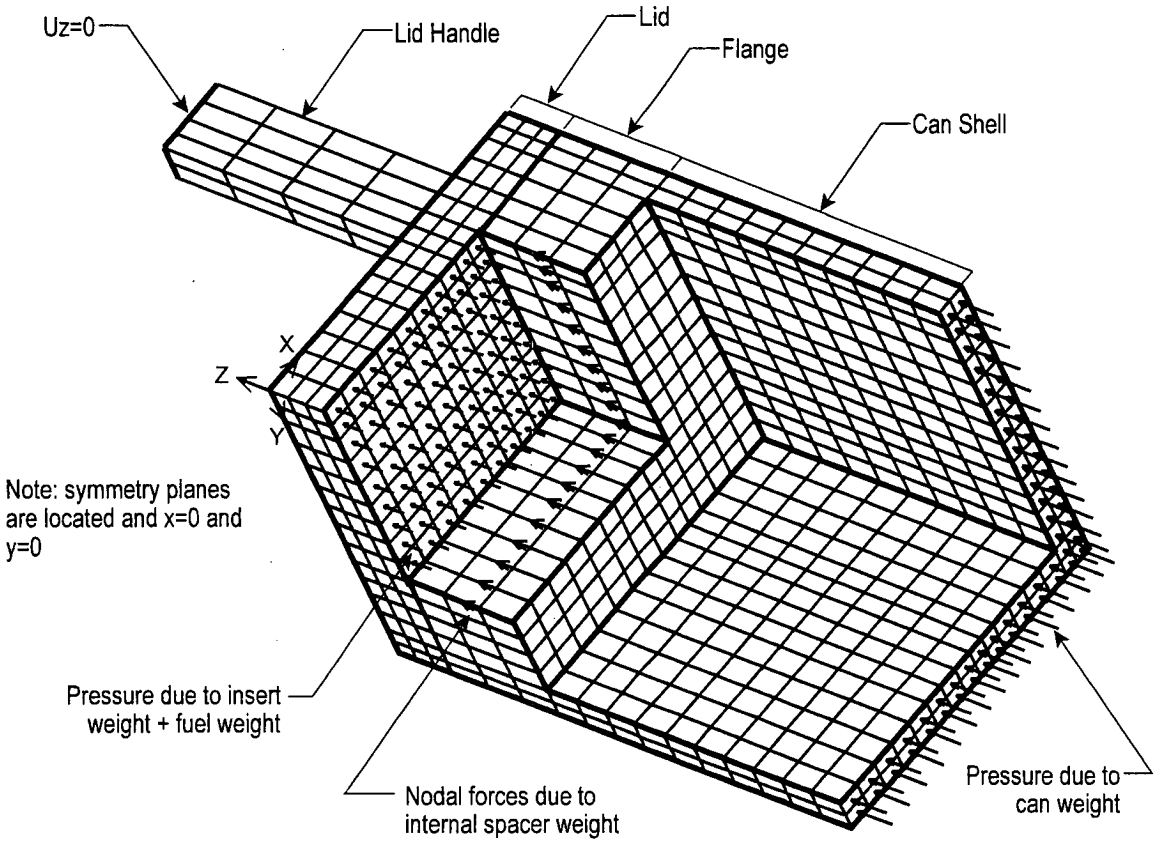

Since the entire can is not modeled, the weight of the can (310 lbs) multiplied by the 60g-accident acceleration is applied using a uniform pressure applied to the "cut surface" on the can shell. Because internal pressure opposes the impact force, thus reducing the bolt tensile load, its effect is not included in the analysis. Symmetry boundary conditions are applied at x = 0 and y = 0 positions on the model. The axial load is reacted at the top of the handle by restraining the Uz degree of freedom at this surface.

An initial strain is applied to the bolt beam elements to simulate the bolt preload. The bolt tension due to the bolt preload is calculated from the following relation. Each lid bolt is initially installed with a torque of 35 ± 5 in.-lb. The tensile force (P_B) in the bolt due to the maximum installation torque (T = 40 in.-lbs) is:

$$P_B = \frac{T}{\left(\frac{l}{2\pi} + \frac{d_2\mu_1}{2\cos\alpha} + \frac{(d + b\mu_2)}{4}\right)} = 635 \text{ lbs}$$ (Machinery's Handbook, equation 22)

where:

l = 0.0556 in, thread lead = 1/n

d_2 = 0.2732 in, pitch diameter

d = 0.3125 in, nominal bolt diameter

b = 0.5 in, nominal diameter of bolt head contact surface

α = 30°, 1/2 thread angle

$\mu_1 = \mu_2 = 0.15$, friction coefficient

From the finite element analysis, the maximum bolt tensile load (F), including preload and impact load, is 904 lbs. The maximum bolt stress is:

$$S = F / A = 904/((\pi/4)\ (0.25)^2) = 18.42 \text{ ksi}$$

Where F is the resulting bolt tensile force and A is the bolt cross-sectional area. The allowable bolt stress for pressure containing structures is S_y.

At 575°F, the yield stress for 316 stainless steel SA-479 is 19.1 ksi and the ultimate stress is 71.8 ksi. Therefore, the allowable stress is19.1 ksi. The resulting margin of safety is:

$$MS = \frac{S_y}{S} - 1 = \frac{19.1}{18.42} - 1 = +0.03$$

Therefore, the lid bolts maintain structural integrity during the end drop.

During the end impact, puncture of the can ends is possible by the fuel rods, an insert tube, or the lid handle. Since the lid is half the thickness of the can bottom plate, only puncture of the lid will be considered. Conservatively considering that the fuel rod weight and insert weight impacts the lid, the resulting shear stress is calculated as:

$$S = \frac{F}{A} = \frac{(350 + 75)x60}{\pi(0.6875)(0.5)} = 23.6 \text{ ksi}$$

where F is the weight of the fuel (350 lbs) and insert (75 lbs) and A is the shear area of the insert tube. The allowable for a pure shear loading during accident drop conditions is 0.5 S_u or 0.5 (63.7 ksi) = 31.85 ksi at 575°F for the 304 SS lid. The resulting margin of safety is:

$$MS = \frac{0.5S_u}{S} - 1 = \frac{31.85}{23.6} - 1 = +0.35$$

Considering puncture due to the lid handle,

$$S = \frac{F}{A} = \frac{(350 + 75 + 310)\ x\ 60}{2(1.25x2 + 2x0.625)(0.5)} = 11.76 \text{ksi}$$

where F is the weight of the fuel (350 lbs), insert (75 lbs), and can (310 lbs) and A is the shear area of handle at the lid intersection. The resulting margin of safety is:

$$MS = \frac{0.5S_u}{S} - 1 = \frac{31.85}{11.76} - 1 = +1.71$$

Can Internal Pressure

Can weldment internal pressure is considered insignificant in the end-drop and side-drop cases because it will tend to reduce the compressive loads on the can tube sides.

The effect of internal pressure is evaluated for the bending stress that the pressure imposes on the can weldment sides. Conservatively, a one-inch-wide section of the tube wall, equal in length to the outside dimension of the tube (L = 5.5 in) is analyzed as a simply supported beam with a uniform load.

The maximum moment (M) is determined by the following relation:

$$M = \frac{wL^2}{8} = \frac{(140 - 14.7)(5.5^2)}{8} \cong 474 \text{ in.-lb}$$

where w is the maximum differential pressure across the can wall due to the fire accident temperature (assumes that the cask internal pressure is atmospheric).

The bending stress (σ) in the tube wall is:

$$\sigma = \frac{Mc}{I} = \frac{(474 \text{ in.} - \text{lb})(0.125 \text{ in})}{0.0013 \text{ in.}^4} \cong 45.58 \text{ ksi}$$

The margin of safety (MS) is:

$$MS = \frac{3.6S_m}{\sigma} - 1 = \frac{56.16 \text{ ksi}}{45.58 \text{ ksi}} - 1 = +0.23$$

Can Lid Bolt Analysis

The tensile force (F_p) on each lid bolt due to internal pressure is:

$$F_p = \frac{PA}{n} = \frac{(140 - 14.7)(3.75^2)}{8} \cong 220.3 \text{ lbs}$$

where:

P = the pressure differential across the can wall (100% rod failure with fire temperature and assuming atmospheric pressure in the cask)

A = 3.75 inches × 3.75 inches, the area of the can lid exposed to pressure

n = 8, number of bolts

The total tensile force on each lid bolt is F_p + the initial preload force, F_i = 635 lbs

The lid bolt tensile stress (σ) is:

$$\sigma = \frac{F_p + F_i}{A_t} = \frac{855.3}{0.049} = 17.46 \text{ ksi}$$

where:

At = 0.049 in^2, the bolt tensile stress area $\frac{\pi}{4}(0.25^2)$

The margin of safety (MS) for the hypothetical accident condition is:

$$MS = \frac{S_y}{\sigma} - 1 = \frac{19.1}{17.46} - 1 = +0.09$$

Can Tube Buckling

The critical buckling load was calculated (see Section 2.6.7.10) as 698 × 10^3 pounds. Since the actual compressive load of 310 × 60 = 18,600 lbs is much less than the critical buckling load, the tube has adequate resistance to buckling.

Internal Spacer

The internal spacer is contained within the can assembly and is not subjected to bending in the side drop condition.

The compressive stress in the internal spacer rails during the side drop is determined as follows:

$$\sigma_b = \frac{Wg}{A} = \frac{665 \text{ x } 49.7}{123.7} \cong 267.2 \text{ psi}$$

where:

W = total load = 350 (fuel) + 240 (internal spacer) + 75 (4x4 insert) = 665 lbs

g = 49.7 (hypothetical accident condition side drop)

A = 123.7 in^2 cross-sectional area of spacer rails, 4 × 0.188 × (165.25 – 2 x 0.38)

The resulting margin of safety is Large.

Internal Spacer Compressive Stress

For the end drop, the internal spacer shell is loaded by its own weight. The insert rail stiffness is conservatively neglected in the strength.

Under hypothetical accident conditions, the spacer is evaluated for a 60 g acceleration. The compressive load (P) on the shell is due to the weight of the internal spacer. The entire weight of the internal spacer times the 60 g factor is used to calculate the compressive load.

The compressive load (P) is:

$$P = 240 \times 60 = 14{,}400 \text{ lbs}$$

The compressive stress (S_c) in the spacer body is:

$$S_c = \frac{P}{A} = \frac{14{,}400}{1.69} \cong 8{,}521 \text{ psi}$$

The margin of safety (MS) is then:

$$MS = \frac{0.7S_u}{S_c} - 1 = \frac{0.7(63{,}100)}{8{,}521} - 1 = +4.18$$

Internal Spacer Buckling

The critical buckling load was calculated (see Section 2.6.7.10) as 190×10^3 pounds. Since the actual compressive load ($240 \times 60 = 14{,}400$ lbs) is much less than the critical buckling load, the tube has adequate resistance to buckling.

4×4 and 5×5 Inserts

The 4×4 and 5×5 inserts are contained within the internal spacer. The 4×4 inserts are supported by straps on 10-inch spacing. These straps provide a clearance of 0.31 inches and will allow bending of the tubes to occur. The 5×5 insert tubes are evaluated for a diametrically opposed load due to the weight of the adjacent tubes during the side drop.

The 4×4 insert lower tube will be evaluated as a fixed-fixed beam over a 10-inch span. The weight of the 3 tubes above (as well as lower tube self-weight) will be considered in the analysis. The stiffness of the tubes above the lower tube will conservatively be neglected. The combined weight (P) of the fuel pins and insert tubes are considered as a uniformly distributed load over the 10-inch span. In addition, the weights are scaled by the 60 g deceleration factor.

The maximum bending stress (f_b) is determined as follows:

$$f_b = \frac{Wlg}{12\ Z} = \frac{5.8(10.0)49.7}{12x0.0092} \cong 26{,}111 \text{ psi}$$

where:

W = load on 10-inch section = (14 + 9.5) × 4 × 10/163.0 = 5.8 lbs

l = 10 inch (span of tube)

g = 49.7 (accident condition side drop)

Z = $\pi/32\ (0.6875^4 - 0.6315^4) / 0.6875 = 0.0092\ in^3$ (section modulus of the tube)

The margin of safety (MS) is:

$$MS = \frac{1.0\ S_u}{\sigma_{max}} - 1 = \frac{1.0(48{,}160)}{26{,}111} - 1 = +0.84$$

The bending moment due to the diametrically opposed line load on the 5x5 insert is calculated by the following:

$$M_b = \frac{WRg}{\pi} = \frac{70/163.0 \times 0.344 \times 49.7}{\pi} \cong 2.34\ lb-in$$

where:

W = total load = 14 x 4 (fuel) + 70/5 (tube) = 70 lbs

g = 49.7 (hypothetical accident condition side drop)

R = 0.6875/2 = 0.344 in (radius of insert tube)

The resulting bending stress is:

$$f_b = \frac{6M_b}{t^2} = \frac{6 \times 2.34}{0.028^2} \cong 17{,}908\ psi$$

The margin of safety (MS) is:

$$MS = \frac{1.0\ S_u}{\sigma_{max}} - 1 = \frac{1.0(48{,}160)}{17{,}908} - 1 = +1.69$$

4×4 and 5×5 Insert Tube Compressive Stress

Under hypothetical accident conditions, the tube is evaluated for a 60 g acceleration. The compressive load (P) on the shell is due to the weight of the tube. The entire weight of the tube is calculated as:

The compressive load (P) is:

P = 2.72 x 60 = 163.2 lbs

The compressive stress (S_c) in the tube body is:

$$S_c = \frac{P}{A} = \frac{163.2}{0.058} \cong 2{,}814\ psi$$

where:

$A = \pi/4\ (0.6875^2 - 0.6315^2) = 0.058\ in^2$

The margin of safety (MS) is then:

$$MS = \frac{0.7S_u}{S_c} - 1 = \frac{0.7(48{,}160)}{2{,}814} - 1 = +11.0$$

PWR Insert

The PWR insert contains the can assembly for insertion into the PWR basket. The PWR insert comprises a square box section with smooth sides. Therefore, no bending stresses will be introduced in the side drop condition.

PWR Insert Body Compressive Stress

Under accident conditions, the tube is evaluated for a 60 g acceleration. The compressive load (P) on the body is due to the weight of the PWR insert. The entire weight of the PWR insert times the 60 g factor will conservatively be used to calculate the compressive load.

The compressive load (P) is:

$P = 650 \times 60 = 39{,}000$ lbs

The compressive stress (S_c) in the tube body is:

$$S_c = \frac{P}{A} = \frac{39{,}000}{39.2} \cong 995 psi$$

where:

$A = (8.5^2 - 5.75^2) = 39.2\ in^2$

The margin of safety (MS) is then:

$$MS = \frac{0.7S_u}{S_c} - 1 = \frac{0.7(25{,}800)}{995} - 1 = +17.2$$

PWR Insert Tube Buckling

The critical buckling load was calculated (see Section 2.6.7.10) as 3.86×10^6 pounds. Since the maximum compressive load (650 x 60 = 39,000 lbs) is much less than the critical buckling load (3.86×10^6 lb), the PWR insert has adequate resistance to buckling.

Figure 2.7.1-1 30-Foot Bottom End Drop with 130°F Ambient Temperature and Maximum Decay Heat Load

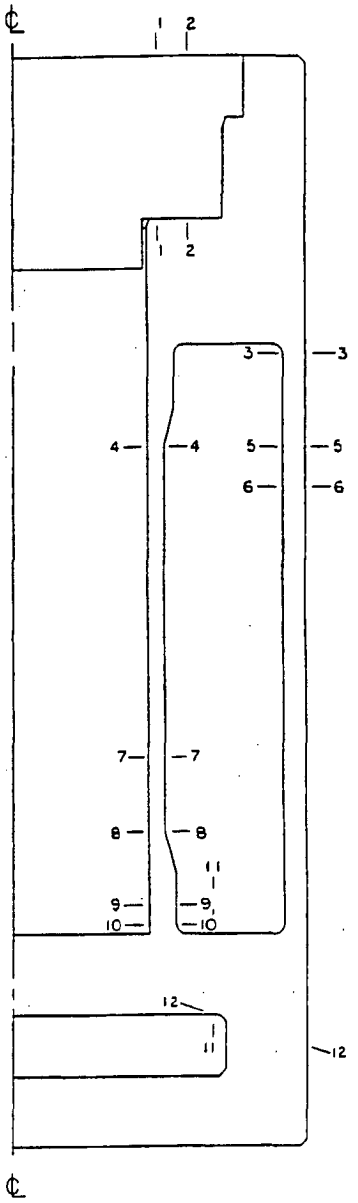

Figure 2.7.1-2 30-Foot Bottom End Drop with -40°F Ambient Temperature and Maximum Decay Heat Load

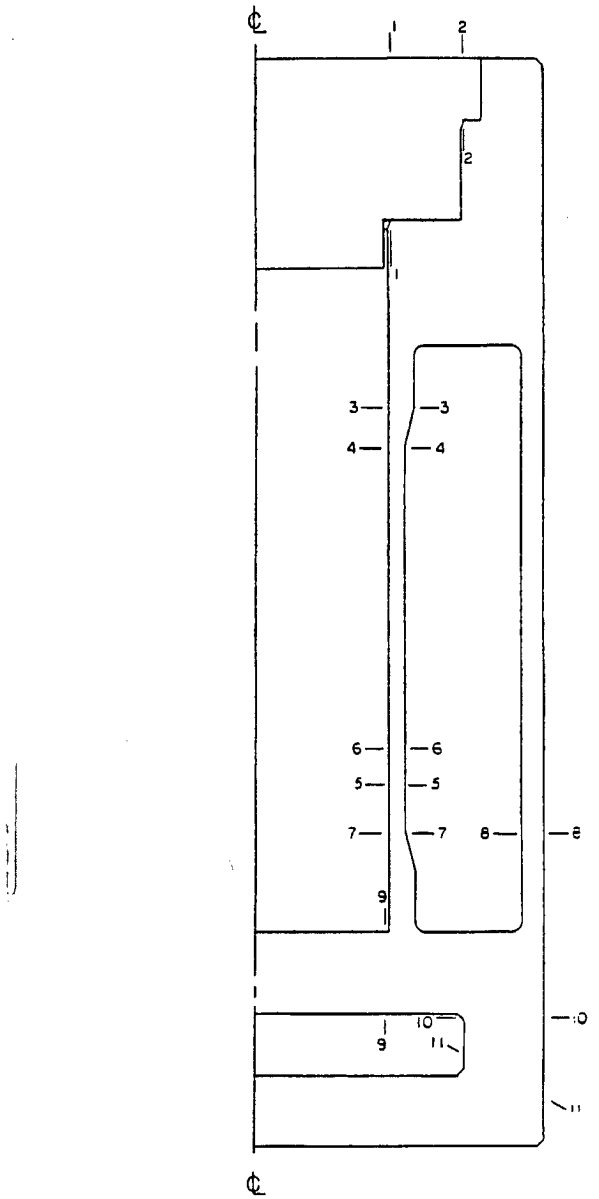

Figure 2.7.1-3 30-Foot Bottom End Drop with -40°F Ambient Temperature and No Decay Heat Load

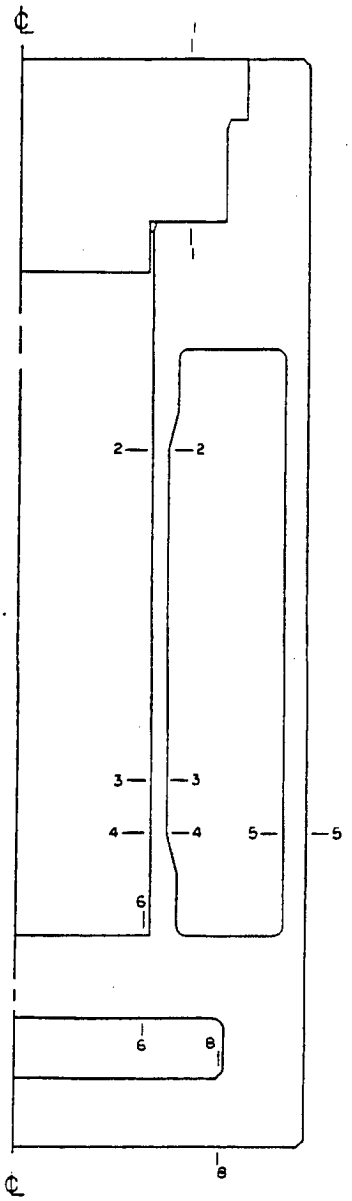

Figure 2.7.1-4 30-Foot Top End Drop with 130°F Ambient Temperature and Maximum Decay Heat Load

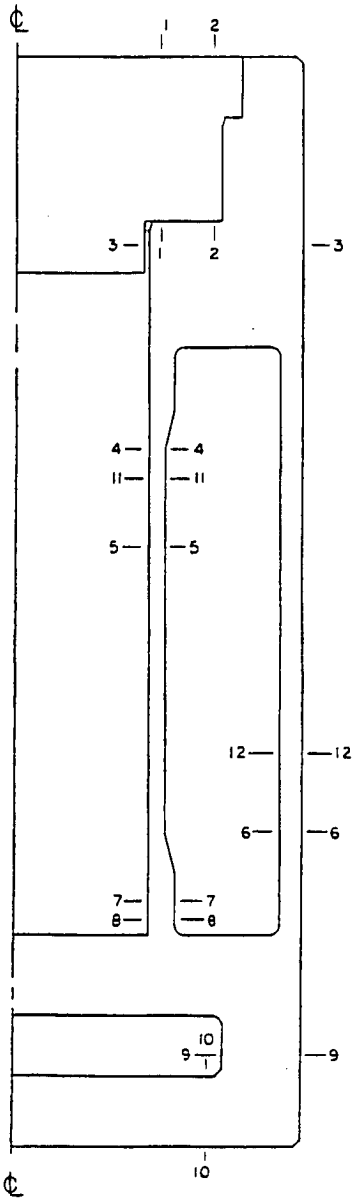

Figure 2.7.1-5 30-Foot Top End Drop with -40°F Ambient Temperature and Maximum Decay Heat Load

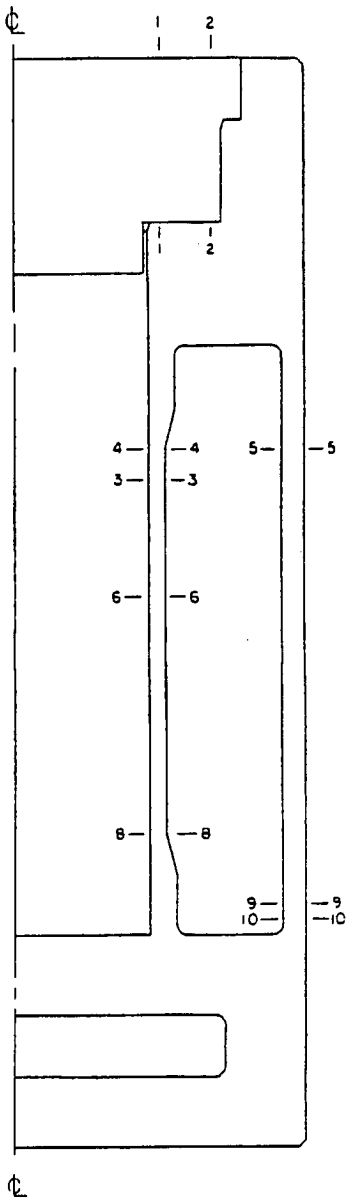

Figure 2.7.1-6 Circumferential Load Distribution for Cask Side Drop Impact

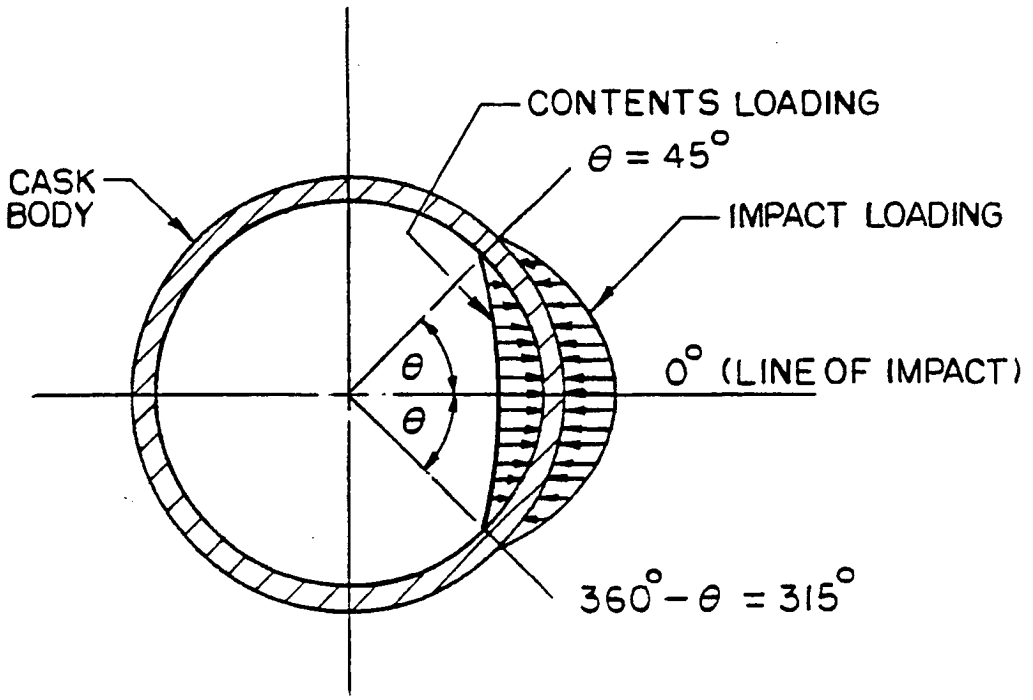

Figure 2.7.1-7 Six Term Fourier Series Representation of Circumferential Load Distribution for Cask Side Drop Impact

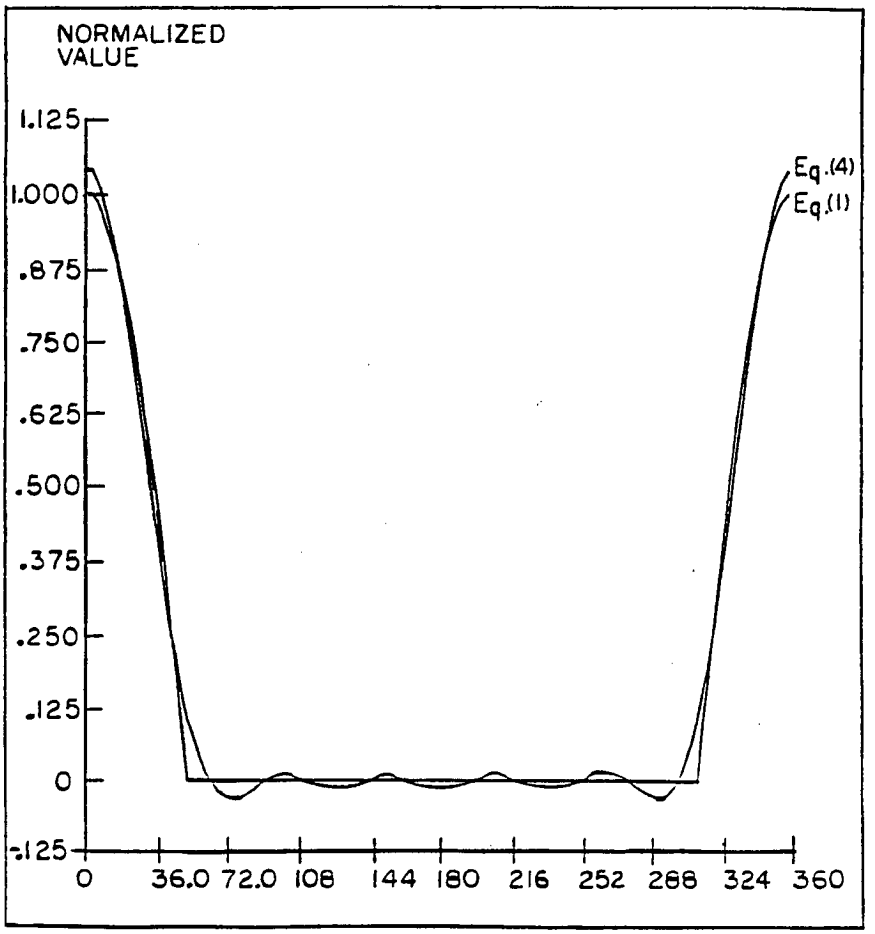

Figure 2.7.1-8 NAC-LWT Cask Critical Sections (30-Foot Side Drop with 100°F Ambient Temperature)

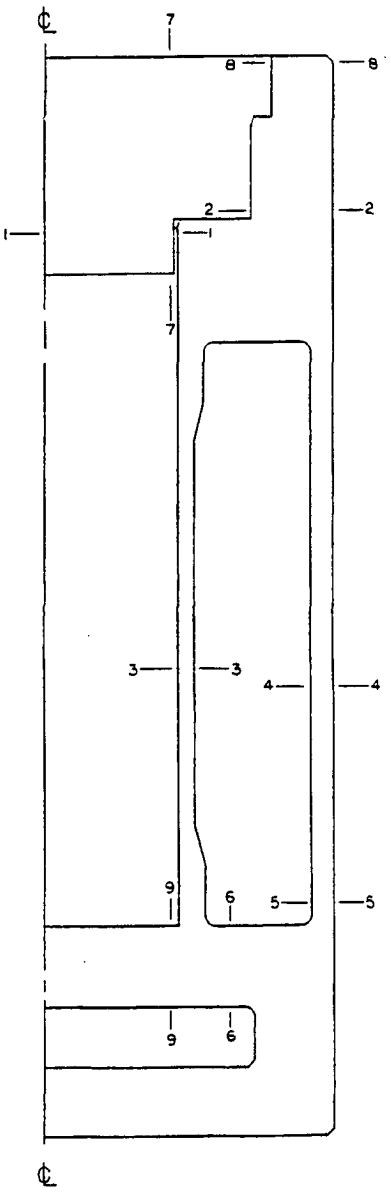

Figure 2.7.1-9 Circumferential Load Distribution for Cask Oblique Drop Impact

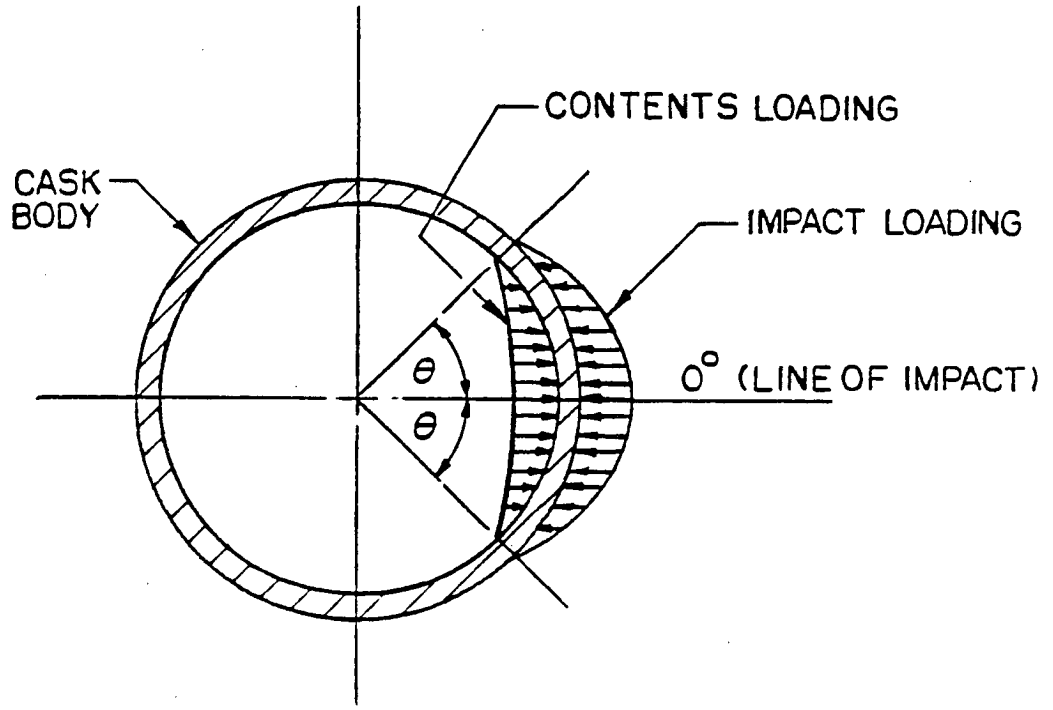

Figure 2.7.1-10 30-Foot Top Corner Drop with 130°F Ambient Temperature - Drop Orientation = 15.74 Degrees

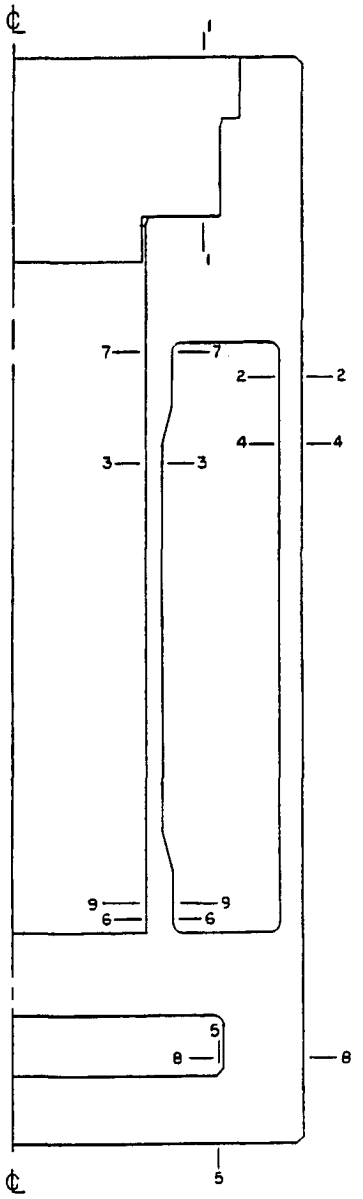

Figure 2.7.1-11 30-Foot Top Oblique Drop with 130°F Ambient Temperature - Drop Orientation = 30 Degrees

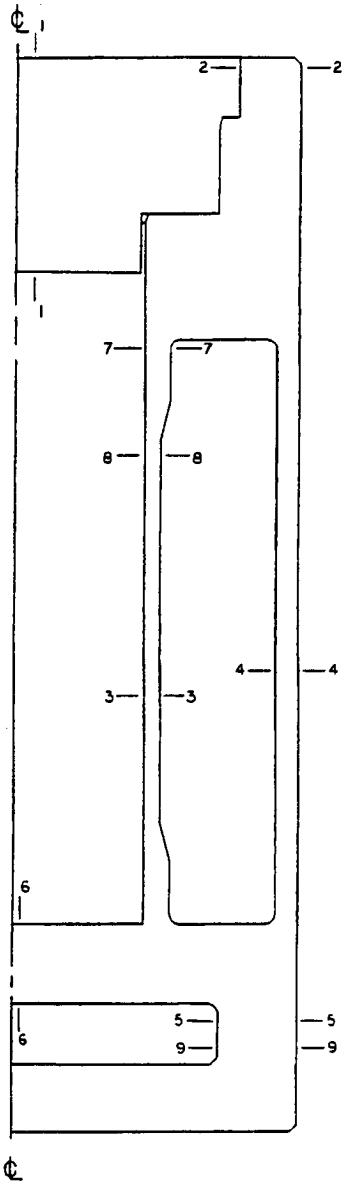

Figure 2.7.1-12 30-Foot Top Oblique Drop with 130°F Ambient Temperature - Drop Orientation = 45 Degrees

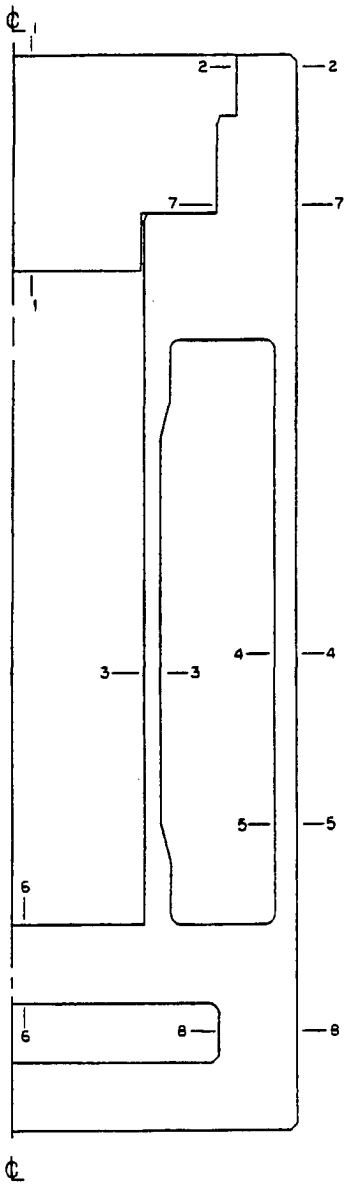

Figure 2.7.1-13 30-Foot Oblique Drop with 130°F Ambient Temperature - Drop Orientation = 60 Degrees

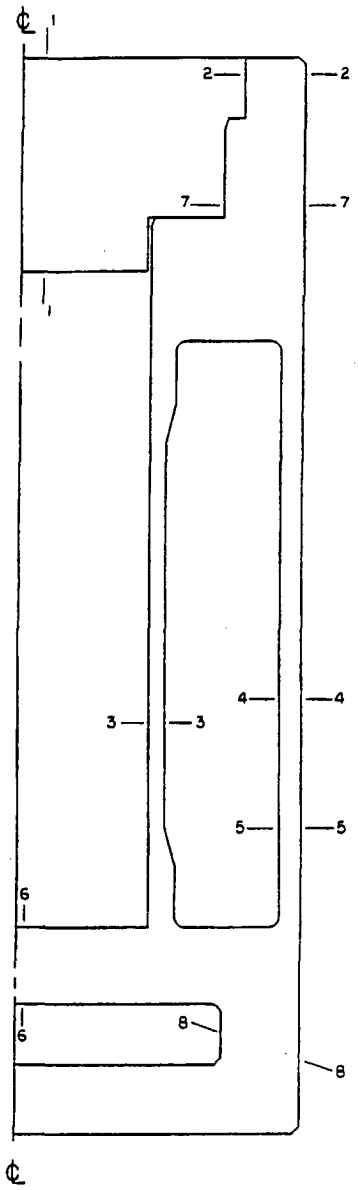

Figure 2.7.1-14 30-Foot Top Corner Drop with -40°F Ambient Temperature - Drop Orientation = 15.74 Degrees

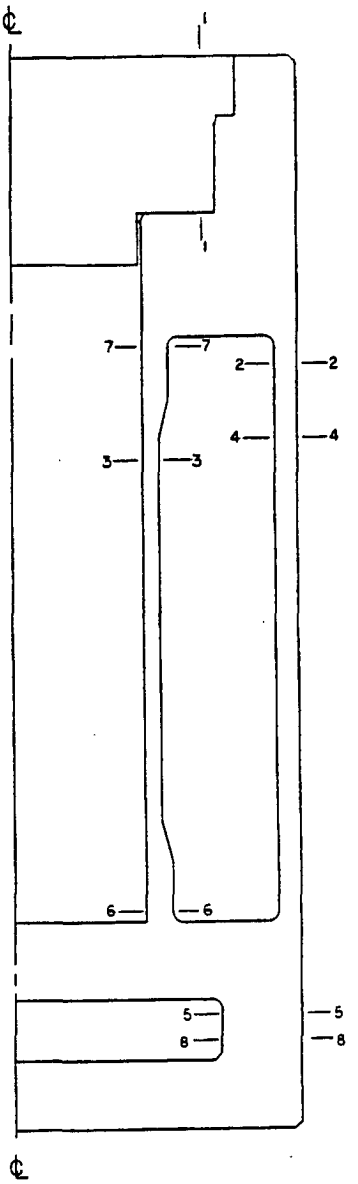

Figure 2.7.1-15 30-Foot Top Oblique Drop with -40°F Ambient Temperature - Drop Orientation = 30 Degrees

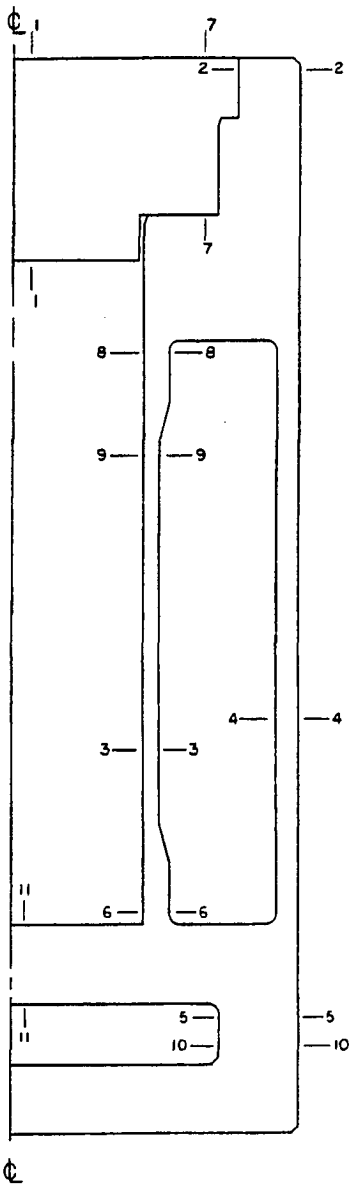

Figure 2.7.1-16 30-Foot Top Oblique Drop with -40°F Ambient Temperature - Drop Orientation = 45 Degrees

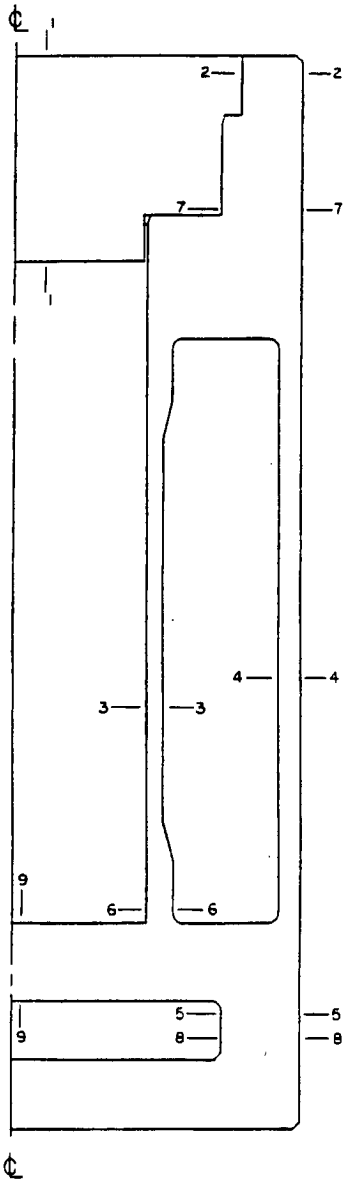

Figure 2.7.1-17 30-Foot Top Oblique Drop with -40°F Ambient Temperature - Drop Orientation = 60 Degrees

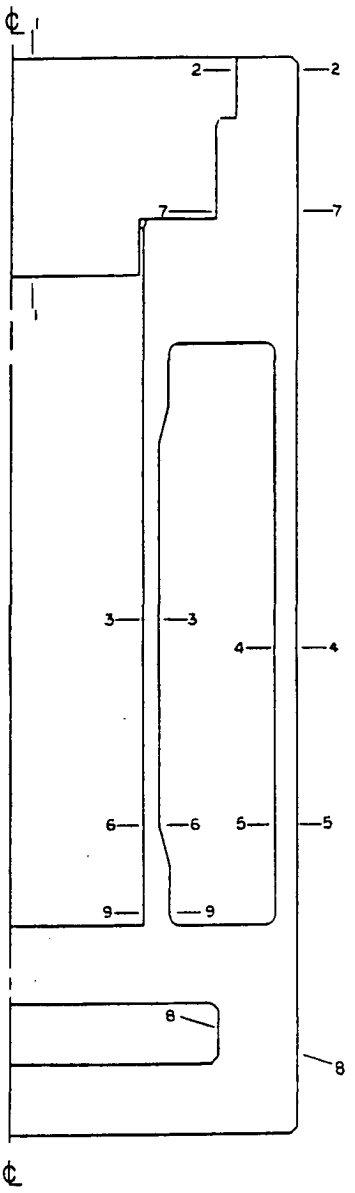

Figure 2.7.1-18 30-Foot Bottom Oblique Drop with 130°F Ambient Temperature – Drop Orientation = 15.74 Degrees

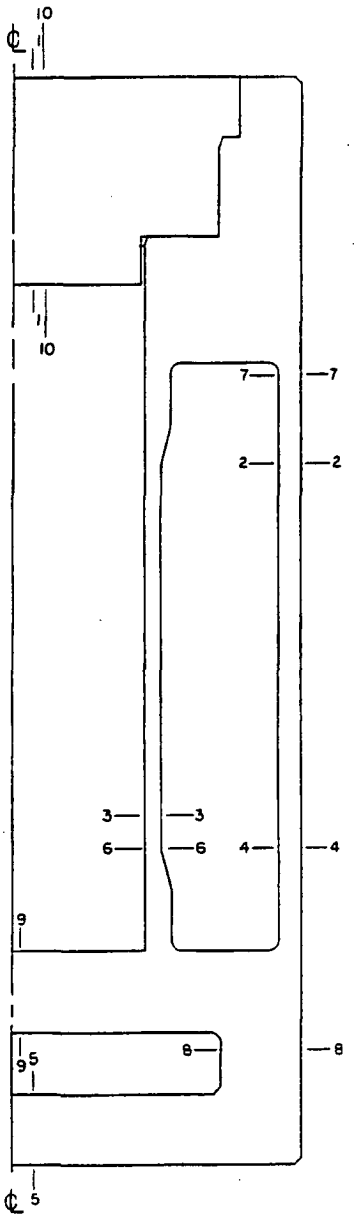

Figure 2.7.1-19 30-Foot Bottom Oblique Drop with 130°F Ambient Temperature - Drop Orientation = 30 Degrees

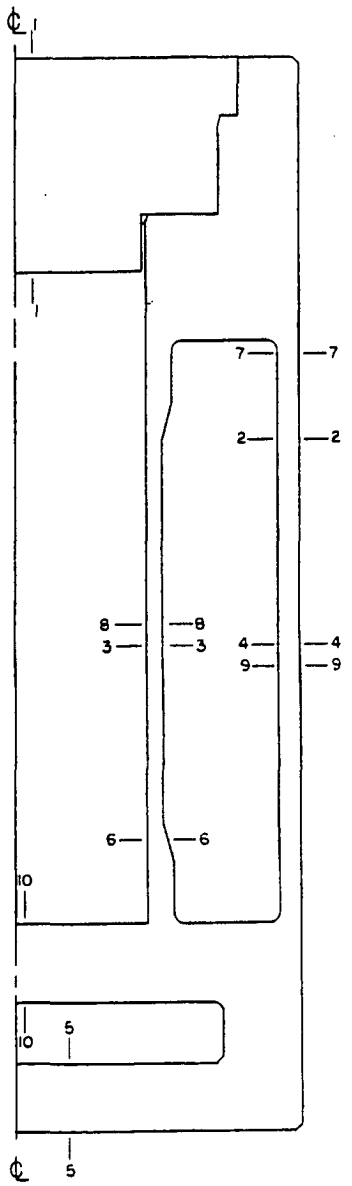

Figure 2.7.1-20 30-Foot Bottom Oblique Drop with 130°F Ambient Temperature - Drop Orientation = 45 Degrees

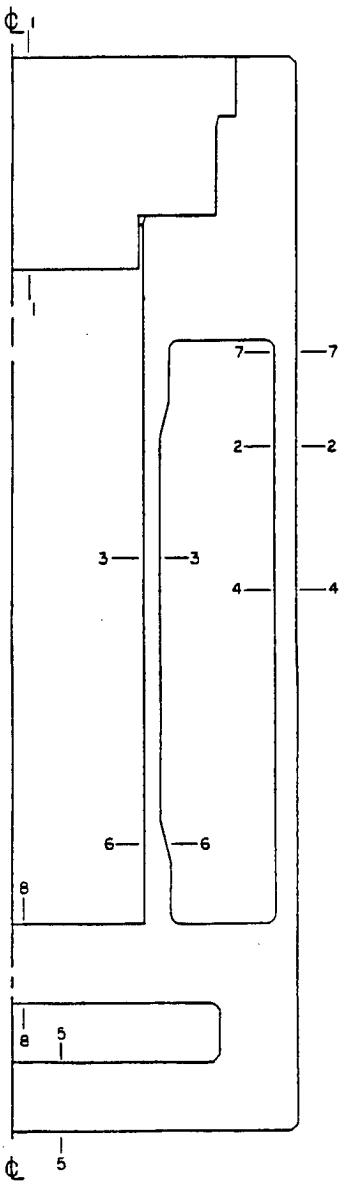

Figure 2.7.1-21 30-Foot Bottom Oblique Drop with 130°F Ambient Temperature - Drop Orientation = 60 Degrees

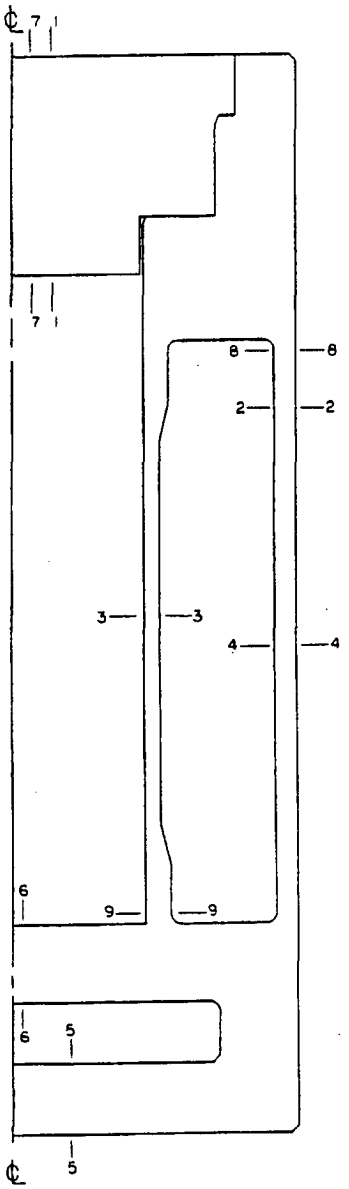

Figure 2.7.1-22 Sectional Stress Plot - 30-Foot Bottom Oblique Drop with 130°F Ambient Temperature - Drop Orientation = 60 Degrees

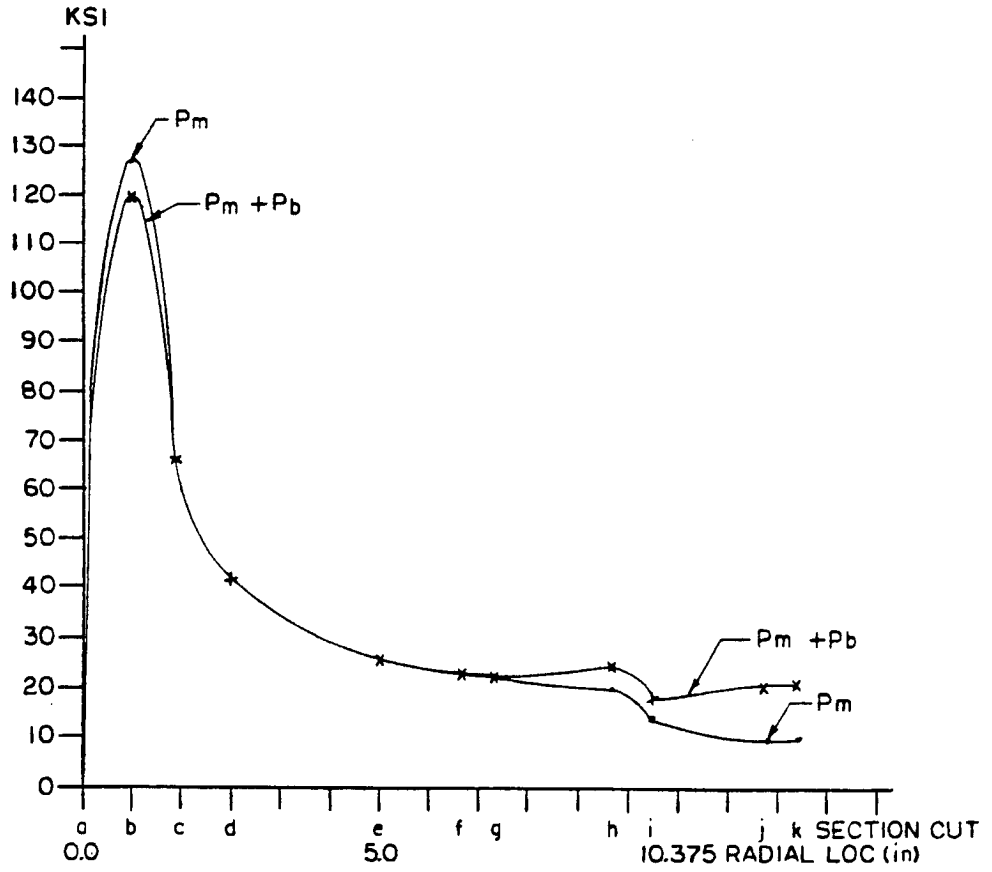

Note: Refer to Figure 2.7.1-25 for identification of the section cut.

Figure 2.7.1-23 Sectional Stress Plot (P_m) – 30-Foot Bottom Oblique Drop with 130°F Ambient Temperature - Drop Orientation = 60 Degrees

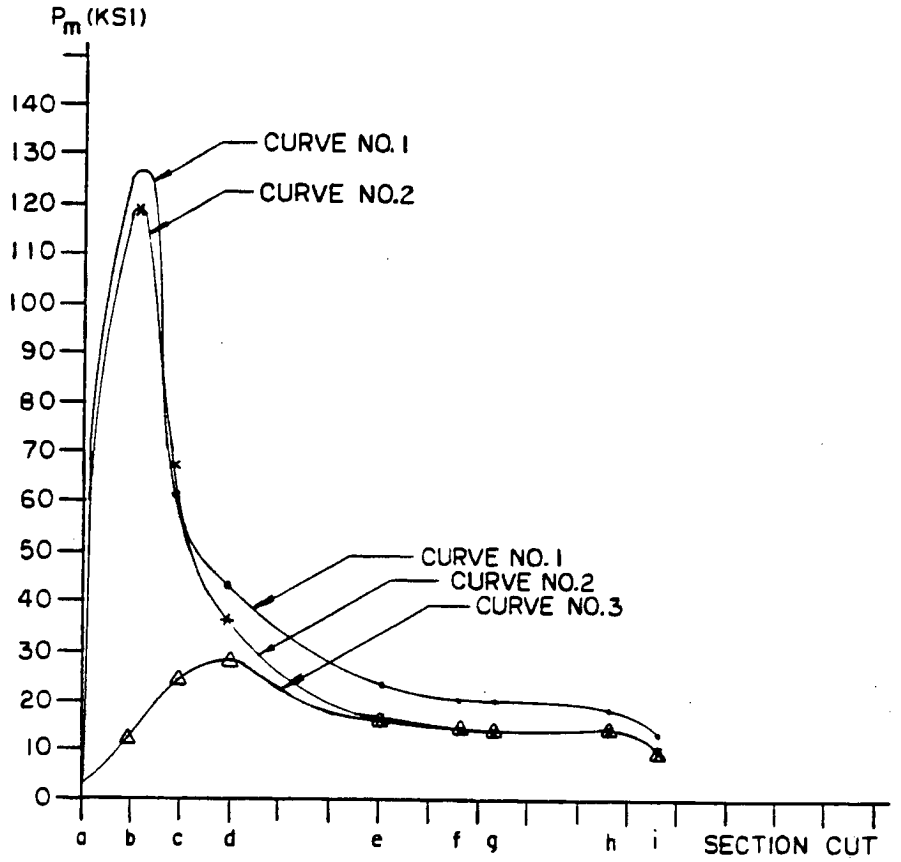

Note: Refer to Figure 2.7.1-25 for identification of the section cut.

Figure 2.7.1-24 Sectional Stress Plot ($P_m + P_b$) - 30-Foot Bottom Oblique Drop with 130°F Ambient Temperature - Drop Orientation = 60 Degrees

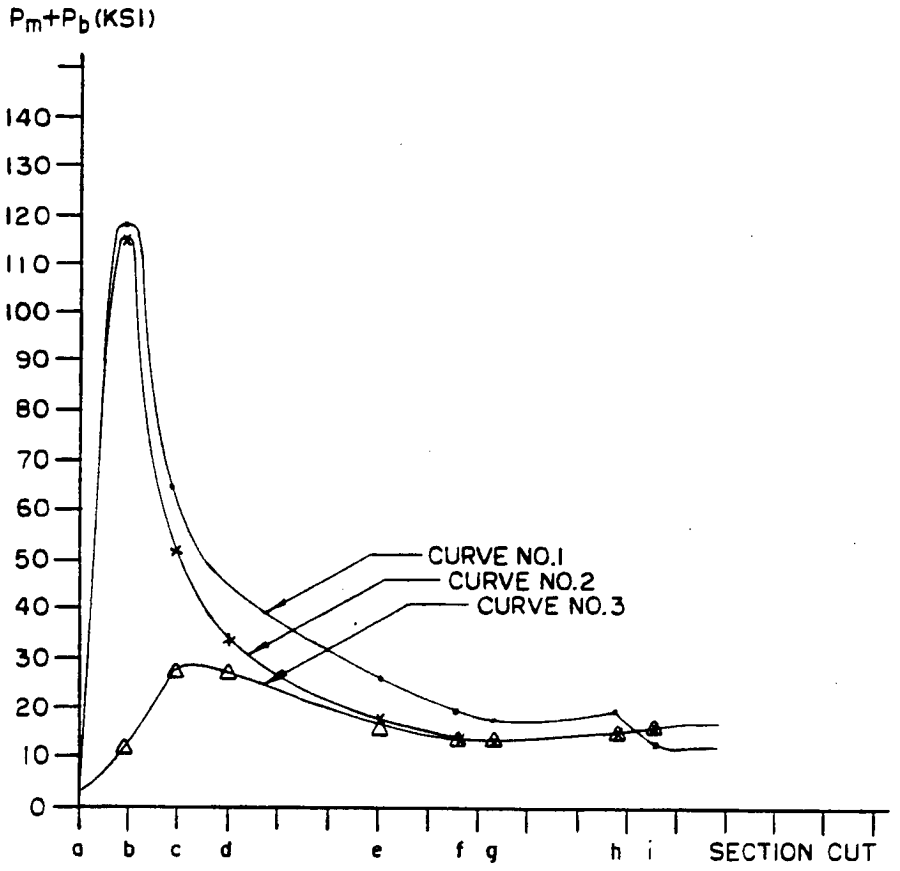

Note: Refer to Figure 2.7.1-25 for identification of the section cut.

Figure 2.7.1-25 Bottom Closure Plate - Section Cut Identification

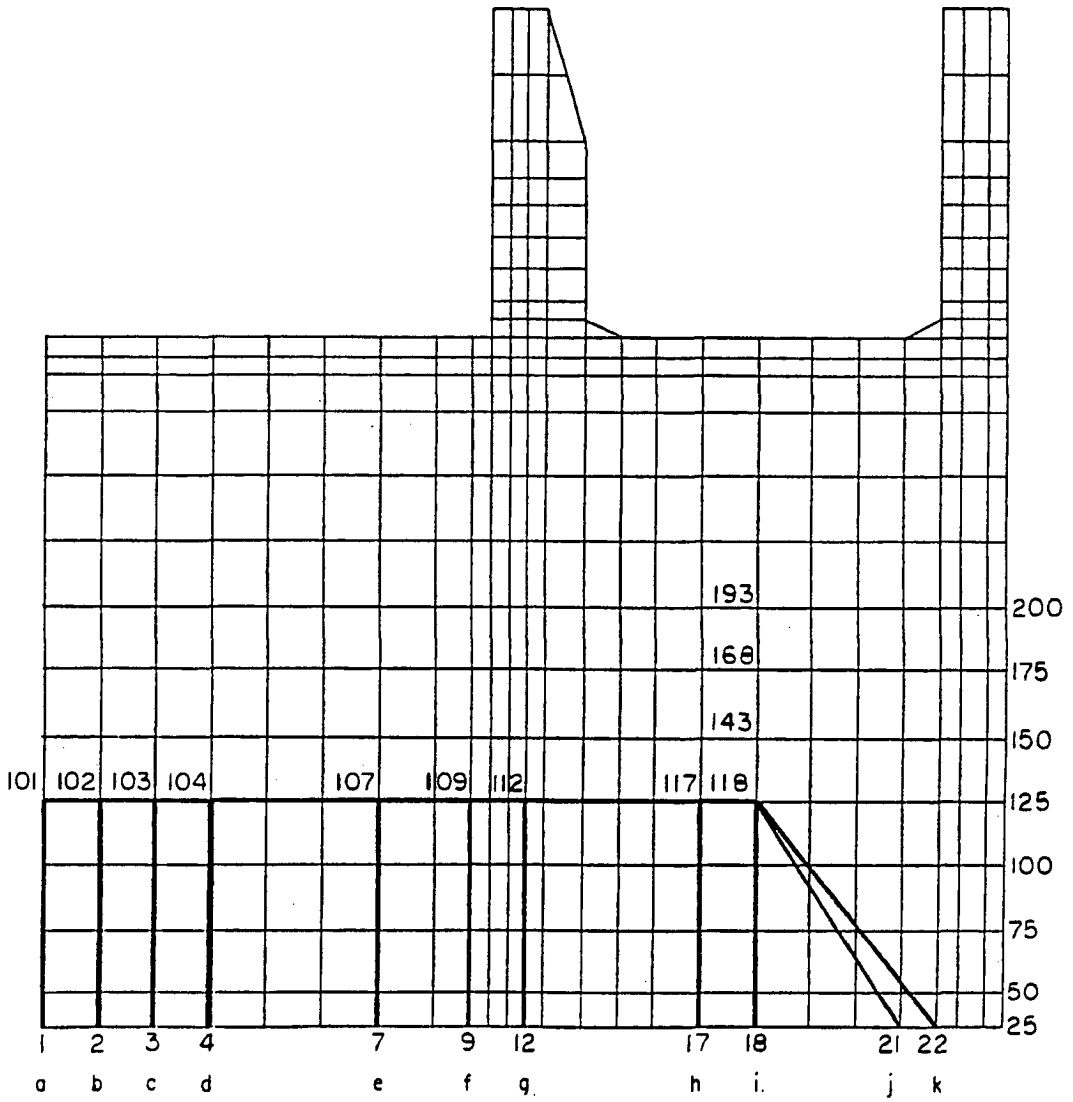

Figure 2.7.1-26 Sectional Stress Plot - 30-Foot Bottom Oblique Drop with 130°F Ambient Temperature - Drop Orientation = 45 Degrees

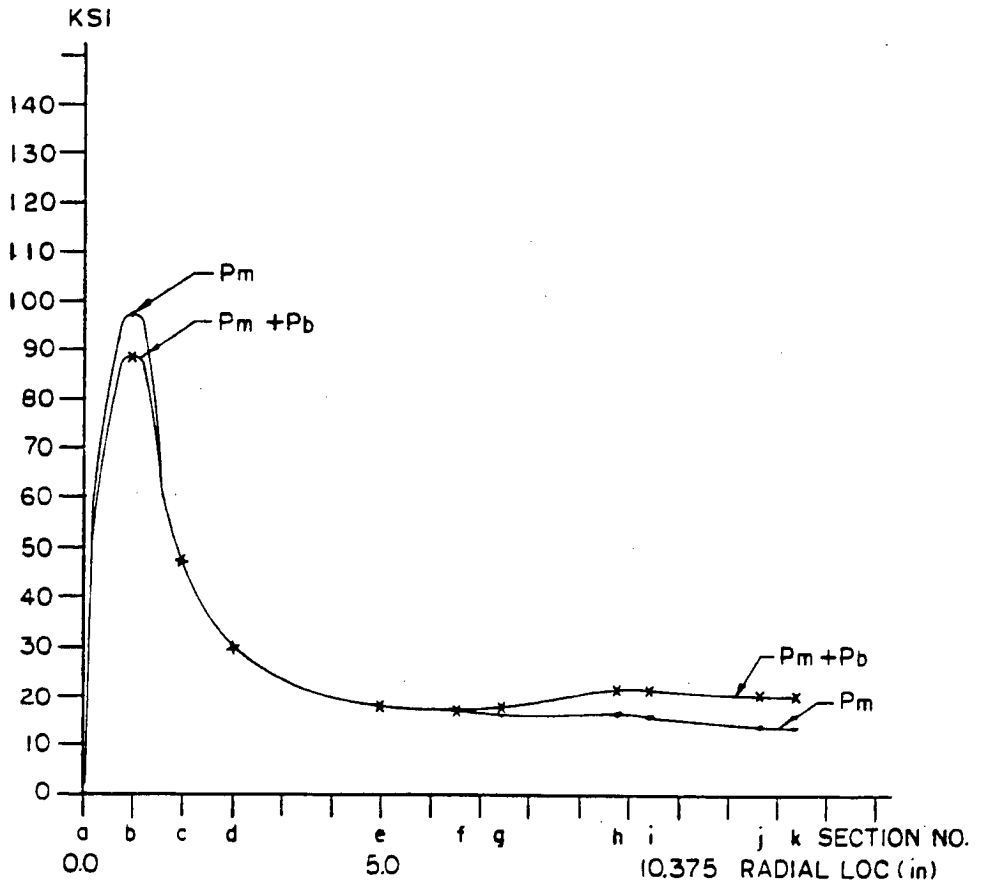

Note: Refer to Figure 2.7.1-25 for identification of the section cut.

Figure 2.7.1-27 Sectional Stress Plot - 30-Foot Bottom Oblique Drop with 130°F Ambient Temperature - Drop Orientation = 30 Degrees

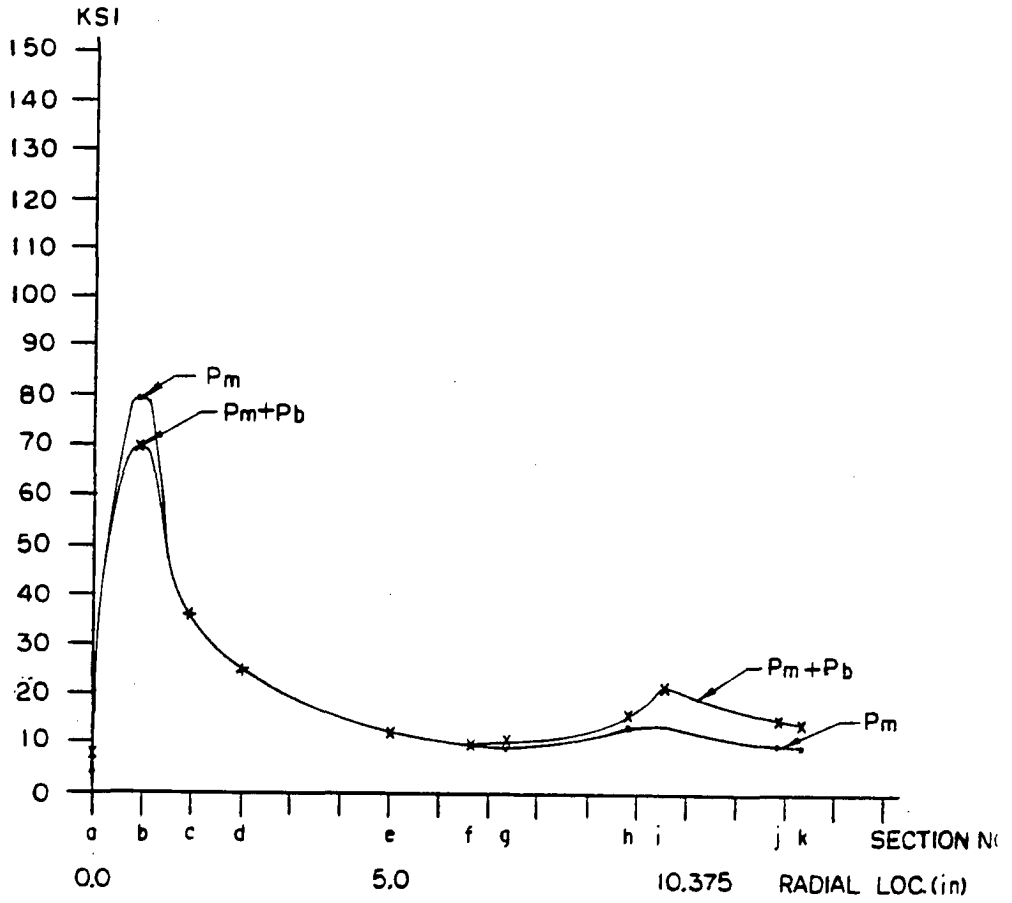

Note: Refer to Figure 2.7.1-25 for identification of the section cut.

Table 2.7.1-1 Critical Stress Summary (30-Foot Bottom End Drop) – Loading Condition 1 – P_m

Loading Condition 1: 130°F Ambient Temperature and Maximum Decay Heat Load

		P_m Stresses** (ksi)				Principal Stresses					
Comp. No.*	Section Cut Node to Node	S_x	S_y	S_z	S_{xy}	S_1	S_2	S_3	S.I.	Allow. Stress 0.7 S_u	Margin of Safety
	2-2										
1	2375 to 2575	-0.17	-0.23	0.62	0.40	0.62	0.2	-0.6	1.22	46.2	Large
	4-4										
3	1581 to 1584	-0.1	-4.54	-0.16	-0.14	-0.1	-0.16	-4.55	4.45	46.2	+9.38
	7-7										
4	701 to 704	-0.03	-8.44	0.51	-0.02	0.51	-0.03	-8.44	8.94	66.0	+6.38
	6-6										
6	1515 to 1518	0.00	1.98	-0.16	-0.04	1.98	0.00	-0.16	2.14	66.0	Large
	11-11										
7	192 to 342	-6.50	1.18	1.28	1.69	1.54	1.28	-6.85	8.39	46.2	+4.51
	10-10										
8	361 to 365	0.77	-5.40	3.89	-0.99	3.89	0.92	-5.55	9.44	46.2	+3.89

* Refer to Figure 2.10.2-9 for component identification.

** Conservatively based on a 1.12-inch thick outer shell and on a 3,850-psi crush strength aluminum honeycomb impact limiter (Section 2.7.1.1).

Table 2.7.1-2 Critical Stress Summary (30-Foot Bottom End Drop) – Loading Condition 1 - $P_m + P_b$

Loading Condition 1: 130°F Ambient Temperature and Maximum Decay Heat Load

		$P_m + P_b$ Stresses** (ksi)				Principal Stresses					
Comp. No.*	Section Cut Node to Node	S_x	S_y	S_z	S_{xy}	S_1	S_2	S_3	S.I.	Allow. Stress 1.0 S_u	Margin of Safety
	1-1										
1	2371 to 2571	-3.91	-0.35	0.11	0.00	0.11	-0.35	-3.91	4.01	66	Large
	3-3										
3	1835 to 1838	-0.1	4.66	2.25	0.29	4.68	2.25	-0.1	4.76	66	Large
	8-8										
4	621 to 624	0.15	-10.37	-1.16	0.28	0.16	-1.16	-10.38	10.54	94.3	+8.94
	5-5										
6	1595 to 1598	-0.01	3.03	0.57	0.00	3.03	0.57	-0.01	3.04	94.3	Large
	12-12										
7	150 to 193	9.25	-5.21	2.76	0.63	9.27	2.76	-5.24	14.51	66	+3.54
	9-9										
8	381 to 385	-0.21	-13.14	2.03	-1.07	2.03	-0.12	-13.23	15.26	66	+3.33

* Refer to Figure 2.10.2-9 for component identification.

** Conservatively based on a 1.12-inch thick outer shell and on a 3,850-psi crush strength aluminum honeycomb impact limiter (Section 2.7.1.1).

Table 2.7.1-3 Critical Stress Summary (30-Foot Bottom End Drop) – Loading Condition 1 - Total Range

Loading Condition 1: 130°F Ambient Temperature and Maximum Decay Heat Load

		Total Stress Range** (ksi)				Principal Stresses			Stress Differences		
Comp. No.*	Node	S_x	S_y	S_z	S_{xy}	S_1	S_2	S_3	S_1-S_2	S_2-S_3	S_3-S_1
1	2376	0.80	-4.48	-0.22	-0.31	0.82	-0.22	-4.50	1.04	4.28	-5.32
3	1805	-0.19	-5.27	-2.19	-0.78	-0.07	-2.19	-5.39	2.12	3.20	-5.32
4	604	-0.69	-12.07	-1.65	0.61	-0.66	-1.65	-12.10	0.99	10.45	-11.44
6	1595	-0.02	2.93	0.48	0.00	2.93	0.48	-0.02	2.45	0.50	-2.95
7	192	12.54	-7.35	3.46	-3.90	13.28	3.46	-8.09	9.82	11.55	-21.37
8	361	-0.03	-16.44	0.82	-1.4	0.82	0.09	-16.56	0.73	16.65	-17.38

* Refer to Figure 2.10.2-9 for component identification.

** Conservatively based on a 1.12-inch thick outer shell and on a 3,850-psi crush strength aluminum honeycomb impact limiter (Section 2.7.1.1).

Table 2.7.1-4 Critical Stress Summary (30-Foot Bottom End Drop) – Loading Condition 2 – P_m

Loading Condition 2: -40°F Ambient Temperature and Maximum Decay Heat Load

		P_m Stresses** (ksi)				Principal Stresses					
Comp. No.*	Section Cut Node to Node	S_x	S_y	S_z	S_{xy}	S_1	S_2	S_3	S.I.	Allow. Stress 0.7 S_u	Margin of Safety
	2-2										
1	2478 to 2578	0.03	-0.11	1.28	0.02	1.28	0.03	-0.11	1.39	46.2	Large
	4-4										
3	1581 to 1584	-0.15	-7.90	-0.93	-0.26	-0.14	-0.93	-7.91	7.77	46.2	Large
	6-6										
4	701 to 704	-0.02	-12.08	0.20	-0.03	0.20	-0.02	-12.08	12.28	66.0	+4.37
	8-8										
6	615 to 618	0.00	-2.85	0.80	0.00	0.80	0.00	-2.85	3.65	66.0	Large
	11-11										
7	100 to 143	-3.18	-4.19	2.15	2.18	2.15	-1.45	-5.93	8.07	46.2	Large
	7-7										
8	601 to 604	-0.23	-11.12	-1.21	0.46	-0.21	-1.21	-11.13	10.93	46.2	Large

* Refer to Figure 2.10.2-9 for component identification.

** Conservatively based on a 1.12-inch thick outer shell and on a 3,850-psi crush strength aluminum honeycomb impact limiter (Section 2.7.1.1).

Table 2.7.1-5 Critical Stress Summary (30-Foot Bottom End Drop) – Loading Condition 2 - $P_m + P_b$

Loading Condition 2: -40°F Ambient Temperature and Maximum Decay Heat Load

		$P_m + P_b$ Stresses** (ksi)				Principal Stresses					
Comp. No.*	Section Cut Node to Node	S_x	S_y	S_z	S_{xy}	S_1	S_2	S_3	S.I.	Allow. Stress 1.0 S_u	Margin of Safety
	1-1										
1	2371 to 2571	-4.10	-0.43	0.14	0.00	0.14	-0.43	-4.10	4.24	66	Large
	3-3										
3	1701 to 1705	0.04	-8.08	-1.59	-0.34	0.05	-1.59	-8.10	8.15	66	+7.10
	5-5										
4	621 to 624	0.18	-13.91	-1.67	0.32	0.19	-1.67	-13.91	14.10	94.3	+5.68
	8-8										
6	615 to 618	0.03	-4.12	0.63	0.00	0.63	0.03	-4.12	4.75	94.3	Large
	10-10										
7	193 to 200	3.76	-9.04	1.83	-0.76	3.81	1.83	-9.09	12.89	66	+4.12
	9-9										
8	185 to 335	-12.66	-0.38	-0.11	1.93	-0.09	-0.11	-12.96	12.87	66	+4.13

* Refer to Figure 2.10.2-9 for component identification.

** Conservatively based on a 1.12-inch thick outer shell and on a 3,850-psi crush strength aluminum honeycomb impact limiter (Section 2.7.1.1).

Table 2.7.1-6 Critical Stress Summary (30-Foot Bottom End Drop) – Loading Condition 2 - Total Range

Loading Condition 2: -40°F Ambient Temperature and Maximum Decay Heat Load

		Total Stress Range** (ksi)				Principal Stresses			Stress Differences		
Comp. No.*	Node	S_x	S_y	S_z	S_{xy}	S_1	S_2	S_3	S_1-S_2	S_2-S_3	S_3-S_1
1	2376	0.67	-4.03	0.05	-0.35	0.7	0.05	-4.06	0.65	4.11	-4.75
3	1805	-0.32	-9.36	-3.82	-1.34	-0.12	-3.82	-9.56	3.70	5.74	-9.44
4	604	-0.90	-15.99	-2.51	0.80	-0.86	-2.51	-16.03	1.65	13.52	-15.17
6	618	0.03	-4.2	0.57	0.00	0.57	0.03	-4.20	0.54	4.23	-4.77
7	143	-5.58	-14.56	-1.04	0.55	-1.04	-5.55	-14.59	4.51	9.05	-13.55
8	361	0.01	-14.97	-0.81	-1.62	0.18	-0.81	-15.14	0.99	14.33	-15.33

* Refer to Figure 2.10.2-9 for component identification.

** Conservatively based on a 1.12-inch thick outer shell and on a 3,850-psi crush strength aluminum honeycomb impact limiter (Section 2.7.1.1).

Table 2.7.1-7 Critical Stress Summary (30-Foot Bottom End Drop) – Loading Condition 3 – P_m

Loading Condition 3: -40°F Ambient Temperature and No Decay Heat Load

		P_m Stresses** (ksi)				Principal Stresses					
Comp. No.*	Section Cut Node to Node	S_x	S_y	S_z	S_{xy}	S_1	S_2	S_3	S.I.	Allow. Stress 0.7 S_u	Margin of Safety
	1-1										
1	2375 to 2575	-0.21	0.00	-0.03	0.18	0.1	-0.03	-0.31	0.41	46.2	Large
	2-2										
3	1581 to 1584	-0.22	-3.78	-5.48	-0.28	-0.19	-3.80	-5.48	5.29	46.2	+7.73
	3-3										
4	621 to 624	0.04	-7.76	-1.05	0.24	0.04	-1.05	-7.77	7.81	66.0	+7.45
	5-5										
6	615 to 618	0.00	-6.85	-0.13	0.00	0.00	-0.13	-6.85	6.85	66.0	Large
	8-8										
7	18 to 118	-10.02	-0.60	-2.86	2.62	0.08	-2.86	-10.70	10.78	46.2	+3.29
	4-4										
8	601 to 604	-0.16	-7.07	-0.78	0.34	-0.14	-0.78	-7.09	6.95	46.2	+5.65

* Refer to Figure 2.10.2-9 for component identification.

** Conservatively based on a 1.12-inch thick outer shell and on a 3,850-psi crush strength aluminum honeycomb impact limiter (Section 2.7.1.1).

Table 2.7.1-8 Critical Stress Summary (30-Foot Bottom End Drop) – Loading Condition 3 - $P_m + P_b$

Loading Condition 3: -40°F Ambient Temperature and No Decay Heat Load

		$P_m + P_b$ Stresses** (ksi)				Principal Stresses					
Comp. No.*	Section Cut Node to Node	S_x	S_y	S_z	S_{xy}	S_1	S_2	S_3	S.I.	Allow. Stress 1.0 S_u	Margin of Safety
	1-1										
1	2375 to 2575	-1.99	0.00	-0.03	0.18	0.01	-0.03	-2.01	2.02	66	Large
	2-2										
3	1581 to 1584	0.01	-3.30	-5.65	-0.28	0.03	-3.33	-5.65	5.68	66	Large
	3-3										
4	621 to 624	0.12	-8.99	-1.30	0.24	0.13	-1.30	-9.00	9.13	94.3	+9.32
	5-5										
6	615 to 618	0.00	-7.06	-0.19	0.00	0.00	-0.19	-7.06	7.06	94.3	Large
	8-8										
7	18 to 118	-20.14	-0.6	-2.86	2.62	-0.25	-2.86	-20.49	20.23	66	+2.26
	6-6										
8	185 to 335	-8.83	1.55	1.16	2.22	2.0	1.16	-9.29	11.29	66	+4.85

* Refer to Figure 2.10.2-9 for component identification.

** Conservatively based on a 1.12-inch thick outer shell and on a 3,850-psi crush strength aluminum honeycomb impact limiter (Section 2.7.1.1).

Table 2.7.1-9 Critical Stress Summary (30-Foot Bottom End Drop) – Loading Condition 3 - Total Range

Loading Condition 3: -40°F Ambient Temperature and No Decay Heat Load

		Total Stress Range** (ksi)				Principal Stresses			Stress Differences		
Comp. No.*	Node	S_x	S_y	S_z	S_{xy}	S_1	S_2	S_3	S_1-S_2	S_2-S_3	S_3-S_1
1	2376	0.96	-3.75	-0.64	-0.11	0.96	-0.64	-3.75	1.60	3.11	-4.71
3	2176	3.74	-17.36	-1.84	-2.41	4.01	-1.84	-17.63	5.85	15.79	-21.64
4	604	-0.58	-10.47	-1.81	0.56	-0.55	-1.81	-10.50	1.26	8.69	-9.95
6	615	0.00	-7.05	-0.19	0.00	0.00	-0.19	-7.05	0.19	6.86	-7.05
7	143	0.08	-23.96	-3.03	-2.73	0.39	-3.03	-24.27	3.42	21.24	-24.65
8	361	-0.02	-10.55	0.26	-1.38	0.26	0.16	-10.73	0.10	10.89	-10.99

* Refer to Figure 2.10.2-9 for component identification.

** Conservatively based on a 1.12-inch thick outer shell and on a 3,850-psi crush strength aluminum honeycomb impact limiter (Section 2.7.1.1).

Table 2.7.1-10 Critical Stress Summary (30-Foot Top End Drop) – Loading Condition 1 – P_m

Loading Condition 1: 130°F Ambient Temperature and Maximum Decay Heat Load

		P_m Stresses** (ksi)				Principal Stresses					
Comp. No.*	Section Cut Node to Node	S_x	S_y	S_z	S_{xy}	S_1	S_2	S_3	S.I.	Allow. Stress 0.7 S_u	Margin of Safety
	2-2										
1	2377 to 2577	-7.46	-0.06	0.09	0.15	0.09	-0.05	-7.46	7.55	46.2	+5.12
	4-4										
3	1581 to 1584	-0.20	-7.58	-0.57	-0.33	-0.18	-0.57	-7.60	7.42	46.2	+5.29
	5-5										
4	1481 to 1484	-0.03	-8.19	0.52	0.02	0.52	-0.03	-8.19	8.71	46.2	+6.57
	12-12										
6	695 to 698	0.00	2.39	-0.10	0.04	2.40	0.00	-0.10	2.50	46.2	Large
	10-10										
7	17 to 117	-1.04	1.54	2.36	-2.84	3.37	2.36	-2.87	6.23	46.2	+6.42
	7-7										
8	401 to 405	-0.03	-2.63	1.89	-0.39	1.89	0.03	-2.69	4.58	46.2	+9.09

* Refer to Figure 2.10.2-9 for component identification.

** Conservatively based on a 1.12-inch thick outer shell and on a 3,850-psi crush strength aluminum honeycomb impact limiter (Section 2.7.1.1).

Table 2.7.1-11 Critical Stress Summary (30-Foot Top End Drop) – Loading Condition 1 - $P_m + P_b$

Loading Condition 1: 130°F Ambient Temperature and Maximum Decay Heat Load

		$P_m + P_b$ Stresses** (ksi)				Principal Stresses					
Comp. No.*	Section Cut Node to Node	S_x	S_y	S_z	S_{xy}	S_1	S_2	S_3	S.I.	Allow. Stress 1.0 S_u	Margin of Safety
	1-1										
1	2371 to 2571	-12.69	-0.13	-0.22	-1.01	-0.05	-0.22	-12.77	12.72	66.0	+4.19
	3-3										
3	1941 to 1956	0.84	-10.28	-3.31	0.03	0.84	-3.31	-10.28	11.12	66.0	+4.94
	11-11										
4	1561 to 1564	0.12	-9.50	-0.89	-0.22	0.13	-0.89	-9.51	9.64	94.3	+8.78
	6-6										
6	615 to 618	-0.02	3.50	0.78	0.00	3.50	0.78	-0.02	3.52	94.3	Large
	9-9										
7	143 to 150	-7.68	6.60	1.37	1.33	6.72	1.37	-7.80	14.52	66.0	+3.55
	8-8										
8	381 to 385	-0.15	-6.77	0.67	-0.49	0.67	-0.12	-6.81	7.47	66.0	+7.84

* Refer to Figure 2.10.2-9 for component identification.

** Conservatively based on a 1.12-inch thick outer shell and on a 3,850-psi crush strength aluminum honeycomb impact limiter (Section 2.7.1.1).

Table 2.7.1-12 Critical Stress Summary (30-Foot Top End Drop) – Loading Condition 1 - Total Range

Loading Condition 1: 130°F Ambient Temperature and Maximum Decay Heat Load

		Total Stress Range** (ksi)				Principal Stresses			Stress Differences		
Comp. No.*	Node	S_x	S_y	S_z	S_{xy}	S_1	S_2	S_3	S_1-S_2	S_2-S_3	S_3-S_1
1	2371	2.76	-10.30	0.04	3.56	3.67	0.04	-11.21	3.63	11.25	-14.88
3	1962	-1.54	-12.69	-5.46	-1.00	-1.45	-5.46	-13.05	4.01	7.59	-11.60
4	1584	-0.62	-10.96	-1.54	-0.54	-0.59	-1.54	-10.99	0.95	9.45	-10.40
6	615	-0.01	3.43	0.72	-0.01	3.43	0.72	-0.01	2.71	0.73	-3.44
7	143	-7.68	6.79	1.34	2.96	7.37	1.34	-8.26	6.03	9.60	-15.63
8	361	-0.07	-8.76	-0.09	-0.78	0.00	-0.09	-8.83	0.09	8.74	-8.83

* Refer to Figure 2.10.2-9 for component identification.

** Conservatively based on a 1.12-inch thick outer shell and on a 3,850-psi crush strength aluminum honeycomb impact limiter (Section 2.7.1.1).

Table 2.7.1-13 Critical Stress Summary (30-Foot Top End Drop) – Loading Condition 2 – P_m

Loading Condition 2: -40°F Ambient Temperature and Maximum Decay Heat Load

		P_m Stresses** (ksi)				Principal Stresses					
Comp. No.*	Section Cut Node to Node	S_x	S_y	S_z	S_{xy}	S_1	S_2	S_3	S.I.	Allow. Stress 0.7 S_u	Margin of Safety
	2-2										
1	2377 to 2577	-7.42	-0.08	0.30	0.18	0.30	-0.08	-7.42	7.72	46.2	+4.98
	4-4										
3	1581 to 1584	-0.24	-10.89	-1.33	-0.44	-0.22	-1.33	-10.91	10.69	46.2	+3.32
	6-6										
4	1481 to 1484	-0.02	-11.17	0.24	0.04	0.24	-0.02	-11.77	12.01	66.0	+4.59
	5-5										
6	1595 to 1598	0.01	-2.37	1.0	0.02	1.0	0.01	-2.37	3.37	66.0	Large
	10-10										
7	375 to 378	-1.35	1.92	2.97	-0.61	2.97	2.03	-1.45	4.42	46.2	+9.45
	8-8										
8	601 to 604	-0.13	-7.55	-0.80	0.27	-0.12	-0.80	-7.56	7.44	46.2	+5.21

* Refer to Figure 2.10.2-9 for component identification.

** Conservatively based on a 1.12-inch thick outer shell and on a 3,850-psi crush strength aluminum honeycomb impact limiter (Section 2.7.1.1).

Table 2.7.1-14 *Critical Stress Summary (30-Foot Top End Drop) – Loading Condition 2 - $P_m + P_b$*

Loading Condition 2: -40°F Ambient Temperature and Maximum Decay Heat Load

		$P_m + P_b$ Stresses** (ksi)				Principal Stresses					
Comp. No.*	Section Cut Node to Node	S_x	S_y	S_z	S_{xy}	S_1	S_2	S_3	S.I.	Allow. Stress 1.0 S_u	Margin of Safety
	1-1										
1	2371 to 2571	-12.88	-0.21	-0.19	-1.02	-0.13	-0.19	-12.96	12.84	66.0	+4.14
	4-4										
3	1581 to 1584	-0.52	-12.05	-1.44	-0.45	-0.51	-1.44	-12.07	11.56	66.0	+4.71
	3-3										
4	1561 to 1564	0.17	-13.22	-1.52	-0.30	0.17	-1.52	-13.23	13.40	94.3	+6.03
	5-5										
6	1595 to 1598	0.04	-3.78	0.86	0.02	0.86	0.04	-3.78	4.64	94.3	Large
	9-9										
7	395 to 398	-0.18	7.35	4.97	-0.78	7.42	4.97	-0.26	7.69	66.0	+7.58
	8-8										
8	601 to 604	-0.18	-7.94	-0.67	0.27	-0.18	-0.67	-7.95	7.78	66.0	+7.48

* Refer to Figure 2.10.2-9 for component identification.

** Conservatively based on a 1.12-inch thick outer shell and on a 3,850-psi crush strength aluminum honeycomb impact limiter (Section 2.7.1.1).

Table 2.7.1-15 Critical Stress Summary (30-Foot Top End Drop) – Loading Condition 2 - Total Range

Loading Condition 2: -40°F Ambient Temperature and Maximum Decay Heat Load

		Total Stress Range** (ksi)				Principal Stresses			Stress Differences		
Comp. No.*	Node	S_x	S_y	S_z	S_{xy}	S_1	S_2	S_3	S_1-S_2	S_2-S_3	S_3-S_1
1	2371	2.56	-10.43	0.01	3.61	3.50	0.01	-11.37	3.49	11.38	-14.87
3	1962	-1.54	-12.88	-5.92	-1.05	-1.44	-5.92	-12.98	4.48	7.06	-11.54
4	1584	-0.85	-15.19	-2.48	-0.76	-0.81	-2.48	-15.23	1.67	12.75	-14.42
6	1598	0.02	-3.94	0.76	0.02	0.76	0.02	-3.94	0.74	3.96	-4.70
7	378	-0.19	7.42	4.95	-0.07	7.42	4.95	-0.19	2.47	5.14	-7.61
8	361	-0.02	-7.21	-1.7	-1.0	0.16	-1.70	-7.38	1.86	5.68	-7.54

* Refer to Figure 2.10.2-9 for component identification.

** Conservatively based on a 1.12-inch thick outer shell and on a 3,850-psi crush strength aluminum honeycomb impact limiter (Section 2.7.1.1).

Table 2.7.1-16 Side Drop Load Analysis Description

Load Analysis No.	Description	ANSYS Mode No.**
1	Bolt Preload + Internal Pressure	0
2	Thermal + Bolt Preload + Internal Pressure	0
3	Inertial Body Load (excluding content load)	1
4	Impact Load + Content Load*	0
5	Impact Load + Content Load*	1
6	Impact Load + Content Load*	2
7	Impact Load + Content Load*	3
8	Impact Load + Content Load*	4
9	Impact Load + Content Load*	5

* The same circumferential distribution arc is applied to both the impact load and content load.

** ANSYS Mode No. "0" indicates loading type is axisymmetric, while other positive numbers indicate loading types are nonaxisymmetric.

Table 2.7.1-17 Critical Stress Summary (30-Foot Side Drop) – Loading Condition 1 - P_m

Loading Condition 1: 100°F Ambient Temperature and Maximum Decay Heat Load

		P_m Stresses (ksi)				Principal Stresses					
Comp. No.*	Section Cut Node to Node	S_x	S_y	S_z	S_{xy}	S_1	S_2	S_3	S.I.	Allow. Stress 0.7 S_u	Margin of Safety
	1-1										
1	2361 to 2370	-6.94	-0.61	0.13	-0.53	0.13	-0.57	-6.99	7.12	46.2	+5.49
	2-2										
3	1969 to 1976	-20.74	3.86	-9.26	-3.37	4.32	-9.26	-21.20	25.51	46.2	+0.81
	3-3										
4	1141 to 1144	-0.22	31.55	0.52	0.00	31.55	0.52	-0.22	31.77	66.0	+1.08
	4-4										
6	1115 to 1118	-0.10	65.09	2.67	0.00	65.09	2.67	-0.10	65.19	66.0	+0.01
	5-5										
7	395 to 398	-4.44	8.30	-11.27	1.59	8.49	-4.64	-11.27	19.76	46.2	+1.34
	6-6										
8	192 to 342	-11.19	-0.72	-6.26	0.36	-0.71	-6.26	-11.20	10.50	46.2	+3.40

* Refer to Figure 2.10.2-9 for component identification.

Table 2.7.1-18 Critical Stress Summary (30-Foot Side Drop) – Loading Condition 1 - $P_m + P_b$

Loading Condition 1: 100°F Ambient Temperature and Maximum Decay Heat Load

		$P_m + P_b$ Stresses (ksi)				Principal Stresses					
Comp. No.*	Section Cut Node to Node	S_x	S_y	S_z	S_{xy}	S_1	S_2	S_3	S.I.	Allow. Stress 1.0 S_u	Margin of Safety
	7-7										
1	2301 to 2561	-1.60	0.12	1.68	8.10	7.40	1.68	-8.88	16.29	66.0	+3.05
	8-8										
3	2150 to 2156	-8.99	-0.17	-41.23	0.03	-0.17	-8.99	-41.23	41.06	66.0	+0.61
	3-3										
4	1141 to 1144	-0.15	33.56	1.75	0.00	33.56	1.75	-0.15	33.71	94.3	+1.80
	4-4										
6	1115 to 1118	0.02	68.25	3.06	0.00	68.25	3.06	0.02	68.23	94.3	+0.38
	5-5										
7	395 to 398	-2.27	32.90	-1.83	1.59	32.97	-1.83	-2.34	35.31	66.0	+0.87
	9-9										
8	177 to 327	-16.88	-3.68	0.56	-3.01	0.56	-3.03	-17.54	18.10	66.0	+2.65

* Refer to Figure 2.10.2-9 for component identification.

Table 2.7.1-19 Critical Stress Summary (30-Foot Side Drop) – Loading Condition 1 - Total Range

Loading Condition 1: 100°F Ambient Temperature and Maximum Decay Heat Load

		Total Stress Range** (ksi)				Principal Stresses			Stress Differences		
Comp. No.*	Node	S_x	S_y	S_z	S_{xy}	S_1	S_2	S_3	S_1-S_2	S_2-S_3	S_3-S_1
1	2561	0.13	0.04	2.72	31.16	31.25	2.72	-31.07	28.53	33.79	-62.32
3	1815	3.52	50.86	7.38	15.09	55.33	7.38	-0.94	47.95	8.32	-56.27
4	1144	-0.15	35.89	1.96	0.00	35.89	1.96	-0.15	33.93	2.11	-56.27
6	1118	0.02	77.67	3.29	0.00	77.67	3.29	0.02	74.38	3.27	-77.65
7	395	-2.26	46.39	2.66	3.07	46.59	2.66	-2.46	43.93	5.12	-49.05
8	177	-46.95	-2.35	-18.78	-1.66	-2.25	-18.78	-47.05	16.53	28.27	-44.80

* Refer to Figure 2.10.2-9 for component identification.

Table 2.7.1-20 G Loads – Oblique Drop

Drop Orientation	G Load*	Adjusted G Load**	Lateral Component	Axial Component
15.74°	60.4	77.27	20.96	74.37
30.0°	54.4	69.59	34.80	60.27
45.0°	43.8	56.03	39.62	39.62
60.0°	44.4	56.80	49.19	28.40

* Refer to Section 2.6.7.4 for g load calculations. The g loads are conservatively based on a maximum crush strength of 3850 psi for the aluminum honeycomb impact limiters, although the design maximum crush strength is 3675 psi.

** Adjusted g load = (g load)(cask body weight/model weight)
= (g load)(48,000/37,519)

Table 2.7.1-21 Impact and Contents Pressures – Oblique Drop

Impact Location	Drop Orientation	θ Angle*	Impact Pressure* (psi)		Content Pressure* (psi)	
			Lateral	Axial	Lateral	Axial
Top	15.74°	90.00°	3370	14768	35	5298.8
Top	30.0°	83.34°	5834	12925	60.6	4637.5
Top	45.0°	65.32°	7812	10840	81.2	3889.4
Top	60.0°	52.88°	11470	9599	119.3	3444.1
Bottom	15.74°	90.00°	3292	14768	34.9	5199.8
Bottom	30.0°	87.59°	5549	12294	58.8	4328.7
Bottom	45.0°	68.35°	7389	10359	78.3	3647.4
Bottom	60.0°	55.22°	10820	9191	114.7	3236.2

* The angle 2θ determines the pressure distribution arc in the circumferential direction (Figure 2.7.1-9). The same arc is chosen for both impact pressure and content pressure to be applied.

Table 2.7.1-22 Fourier Series Modal Coefficients – Oblique Drop

		Fourier Series Coefficents for Each Loading Mode					
Impact Location	Drop Orientation	Mode 0	Mode 1	Mode 2	Mode 3	Mode 4	Mode 5
Top	15.74°	0.318334	0.500064	0.212287	0.000064	-0.042393	0.000064
Top	30.0°	0.294779	0.479776	0.236186	0.030107	-0.041325	-0.015759
Top	45.0°	0.230640	0.407149	0.271864	0.119183	0.009851	-0.031607
Top	60.0°	0.186891	0.344502	0.266534	0.165172	0.070325	0.004581
Bottom	15.74°	0.318334	0.500064	0.212287	0.000064	-0.042393	0.000064
Bottom	30.0°	0.309638	0.493021	0.221703	0.010632	-0.043160	-0.005739
Bottom	45.0°	0.241699	0.421390	0.269221	0.104574	-0.003428	-0.034201
Bottom	60.0°	0.195189	0.357110	0.239495	0.158298	0.058632	-0.005100

Table 2.7.1-23 Oblique Drop Load Analysis Description

Load Analysis No.	Description	ANSYS Mode No.*
1	Bolt Preload + Internal Pressure	0
2	Thermal + Bolt Preload + Internal Pressure	0
3	Inertial Body Load (Lateral Direction)	1
4	Inertial Body Load (Axial Direction)	0
5	Impact Load + Content Load (Lateral)	0
6	Impact Load + Content Load (Lateral)	1
7	Impact Load + Content Load (Lateral)	2
8	Impact Load + Content Load (Lateral)	3
9	Impact Load + Content Load (Lateral)	4
10	Impact Load + Content Load (Lateral)	5
11	Impact Load + Content Load (Axial)	0
12	Impact Load + Content Load (Axial)	1
13	Impact Load + Content Load (Axial)	2
14	Impact Load + Content Load (Axial)	3
15	Impact Load + Content Load (Axial)	4
16	Impact Load + Content Load (Axial)	5

* ANSYS Mode No. "0" indicates loading type is axisymmetric, while other positive numbers indicate loading types are nonaxisymmetric.

Table 2.7.1-24 Critical Stress Summary (30-Foot Top Corner Drop) – Loading Condition 1 - P_m – Drop Orientation = 15.74 Degrees

Loading Condition 1: 130°F Ambient Temperature and Maximum Decay Heat Load

		P_m Stresses (ksi)**				Principal Stresses					
Comp. No.*	Section Cut Node to Node	S_x	S_y	S_z	S_{xy}	S_1	S_2	S_3	S.I.	Allow. Stress 0.7 S_u	Margin of Safety
	1-1										
1	2377 to 2577	-24.38	-1.69	-3.35	-0.98	-1.65	-3.35	-24.42	22.78	46.2	+1.03
	2-2										
3	1775 to 1778	-0.26	-21.63	2.63	0.06	2.63	-0.26	-21.63	24.26	46.2	+0.90
	3-3										
4	1561 to 1564	0.12	-17.16	-2.01	-0.63	0.14	-2.01	-17.18	17.32	66.0	+2.81
	4-4										
6	1595 to 1598	-0.03	-19.40	2.58	0.13	2.58	-0.03	-19.40	21.98	66.0	+2.00
	5-5										
7	18 to 118	-2.47	4.23	-1.43	-2.23	4.91	-1.43	-3.15	8.05	46.2	+4.74
	6-6										
8	361 to 365	-3.72	-2.79	-0.23	-0.26	-0.23	-2.72	-3.79	3.56	46.2	Large

* Refer to Figure 2.10.2-9 for component identification.

** Conservatively based on a 1.12-inch thick outer shell and on a 3,850-psi maximum crush strength aluminum honeycomb impact limiter (Section 2.7.1.3).

Table 2.7.1-25 Critical Stress Summary (30-Foot Top Corner Drop) – Loading Condition 1 - $P_m + P_b$ – Drop Orientation = 15.74 Degrees

Loading Condition 1: 130°F Ambient Temperature and Maximum Decay Heat Load

		$P_m + P_b$ Stresses (ksi)**				Principal Stresses					
Comp. No.*	Section Cut Node to Node	S_x	S_y	S_z	S_{xy}	S_1	S_2	S_3	S.I.	Allow. Stress 1.0 S_u	Margin of Safety
	1-1										
1	2377 to 2577	-27.51	-1.69	-3.35	-0.98	-1.65	-3.35	-27.55	25.90	66.0	+1.55
	2-2										
3	1775 to 1778	0.08	-20.95	7.55	1.47	7.55	0.18	-21.05	28.60	66.0	+1.31
	3-3										
4	1561 to 1564	0.33	-22.71	-4.58	-0.63	0.35	-4.58	-22.72	23.07	94.3	+3.09
	4-4										
6	1595 to 1598	0.04	-19.76	2.23	0.13	2.23	0.04	-19.77	22.00	94.3	+3.29
	8-8										
7	143 to 150	-8.20	17.26	0.73	1.81	17.39	0.73	-8.33	25.72	66.0	+1.57
	9-9										
8	381 to 385	-5.72	-7.78	0.83	-1.47	0.83	-4.95	-8.54	9.38	66.0	+6.04

* Refer to Figure 2.10.2-9 for component identification.

** Conservatively based on a 1.12-inch thick outer shell and on a 3,850-psi maximum crush strength aluminum honeycomb impact limiter (Section 2.7.1.3).

Table 2.7.1-26 Critical Stress Summary (30-Foot Top Corner Drop) – Loading Condition 1 – Total Range – Drop Orientation = 15.74 Degrees

Loading Condition 1: 130°F Ambient Temperature and Maximum Decay Heat Load

		Total Stress Range** (ksi)				Principal Stresses			Stress Differences		
Comp. No.*	Node	S_x	S_y	S_z	S_{xy}	S_1	S_2	S_3	S_1-S_2	S_2-S_3	S_3-S_1
1	2561***	2.74	-6.25	-3.49	215.9	214.19	-3.49	-217.70	217.68	214.21	-431.89
3	1815	-1.46	-18.25	2.52	0.59	2.52	-1.44	-18.27	3.96	16.83	-20.79
4	1584	-1.38	-23.60	-4.79	-1.37	-1.30	-4.79	-23.68	3.49	18.89	-22.39
6	1595	-0.06	-7.75	3.43	2.38	3.43	0.62	-8.43	2.81	9.04	-11.86
7	2	-8.20	21.90	2.18	3.88	22.39	2.18	-8.69	20.21	10.87	-31.08
8	361	-15.56	-9.27	-6.28	-1.30	-6.28	-9.01	-15.82	2.73	6.81	-9.54

* Refer to Figure 2.10.2-9 for component identification.

** Conservatively based on a 1.12-inch thick outer shell and on a 3,850-psi maximum crush strength aluminum honeycomb impact limiter (Section 2.7.1.3).

*** Stresses at node 2561 are unrealistic, resulting from the boundary effect. See Section 2.7.1.3.3 for the discussion of the boundary effect on the stress results.

Table 2.7.1-27 Critical Stress Summary (30-Foot Top Oblique Drop) – Loading Condition 1 - P_m – Drop Orientation = 30 Degrees

Loading Condition 1: 130°F Ambient Temperature and Maximum Decay Heat Load

		P_m Stresses (ksi)**				Principal Stresses					
Comp. No.*	Section Cut Node to Node	S_x	S_y	S_z	S_{xy}	S_1	S_2	S_3	S.I.	Allow. Stress 0.7 S_u	Margin of Safety
	1-1										
1	2302 to 2562	-18.88	-13.60	2.04	-10.79	2.04	-5.13	-27.35	29.39	46.2	+0.57
	2-2										
3	2150 to 2156	-3.01	-12.69	-26.09	0.09	-3.01	-12.69	-26.09	23.07	46.2	+1.00
	3-3										
4	941 to 944	-0.07	14.41	0.82	0.00	14.41	0.82	-0.07	14.48	66.0	+3.56
	4-4										
6	1035 to 1038	-0.05	30.01	1.60	0.00	30.01	1.60	-0.05	30.06	66.0	+1.20
	5-5										
7	168 to 175	-3.25	5.75	-4.31	-1.36	5.95	-3.45	-4.31	10.26	46.2	+3.50
	6-6										
8	176 to 326	-6.14	-2.46	-1.94	-0.11	-1.94	-2.46	-6.15	4.21	46.2	+9.98

* Refer to Figure 2.10.2-9 for component identification.

** Conservatively based on a 1.12-inch thick outer shell and on a 3,850-psi maximum crush strength aluminum honeycomb impact limiter (Section 2.7.1.3).

Table 2.7.1-28 Critical Stress Summary (30-Foot Top Oblique Drop) – Loading Condition 1 - $P_m + P_b$ – Drop Orientation = 30 Degrees

Loading Condition 1: 130°F Ambient Temperature and Maximum Decay Heat Load

		$P_m + P_b$ Stresses (ksi)**				Principal Stresses					
Comp. No.*	Section Cut Node to Node	S_x	S_y	S_z	S_{xy}	S_1	S_2	S_3	S.I.	Allow. Stress 1.0 S_u	Margin of Safety
	1-1										
1	2302 to 2562	2.72	-13.60	2.04	-10.79	8.09	2.04	-18.97	27.06	66.0	+1.44
	7-7										
3	1821 to 1825	0.06	-20.55	7.79	1.54	7.79	0.17	-20.66	28.46	66.0	+1.32
	8-8										
4	1561 to 1564	0.29	-18.93	-3.81	-0.57	0.30	-3.81	-18.95	19.25	94.3	+3.90
	4-4										
6	1035 to 1038	0.01	31.34	1.65	0.00	31.34	1.65	0.01	31.33	94.3	+2.00
	9-9										
7	143 to 150	-7.27	23.18	0.07	1.91	23.80	0.07	-7.39	30.69	66.0	+1.15
	6-6										
8	176 to 326	-9.35	-7.33	0.83	-2.03	0.83	-6.07	-10.61	11.44	66.0	+4.77

* Refer to Figure 2.10.2-9 for component identification.

** Conservatively based on a 1.12-inch thick outer shell and on a 3,850-psi maximum crush strength aluminum honeycomb impact limiter (Section 2.7.1.3).

Table 2.7.1-29 Critical Stress Summary (30-Foot Top Oblique Drop) – Loading Condition 1 – Total Range – Drop Orientation = 30 Degrees

Loading Condition 1: 130°F Ambient Temperature and Maximum Decay Heat Load

		Total Stress Range** (ksi)				Principal Stresses			Stress Differences		
Comp. No.*	Node	S_x	S_y	S_z	S_{xy}	S_1	S_2	S_3	S_1-S_2	S_2-S_3	S_3-S_1
1	2561***	2.57	-5.32	-2.66	423.0	421.64	-2.66	-424.39	424.30	421.73	-846.04
3	1856	0.38	-7.44	3.51	-0.14	3.51	0.38	-7.44	3.13	7.83	-10.95
4	1584	-1.14	-19.57	-3.72	-1.19	-1.06	-3.72	-19.65	2.66	15.93	-18.58
6	1038	0.01	41.20	1.89	0.00	41.20	1.89	0.01	39.31	1.88	-41.19
7	25	-7.27	30.71	2.51	4.00	31.12	2.51	-7.68	28.62	10.19	-38.81
8	177	-25.74	-8.16	-10.34	-1.52	-8.03	-10.34	-25.87	2.31	15.52	-17.84

* Refer to Figure 2.10.2-9 for component identification.

** Conservatively based on a 1.12-inch thick outer shell and on a 3,850-psi maximum crush strength aluminum honeycomb impact limiter (Section 2.7.1.3).

*** Stresses at node 2561 are unrealistic, resulting from the boundary effect. See Section 2.7.1.3.3 for the discussion of the boundary effect on the stress results.

Table 2.7.1-30 Critical Stress Summary (30-Foot Top Oblique Drop) – Loading Condition 1 - P_m – Drop Orientation = 45 Degrees

Loading Condition 1: 130°F Ambient Temperature and Maximum Decay Heat Load

		P_m Stresses (ksi)**				Principal Stresses					
Comp. No.*	Section Cut Node to Node	S_x	S_y	S_z	S_{xy}	S_1	S_2	S_3	S.I.	Allow. Stress 0.7 S_u	Margin of Safety
	1-1										
1	2302 to 2562	-20.53	-16.65	3.19	-13.28	3.19	-5.17	-32.01	35.21	46.2	+0.31
	2-2										
3	2150 to 2156	-3.91	-10.88	-30.14	0.10	-3.91	-10.88	-30.14	26.23	46.2	+0.76
	3-3										
4	961 to 964	-0.09	17.88	0.84	0.01	17.88	0.84	-0.09	17.97	66.0	+2.67
	4-4										
6	1055 to 1058	-0.06	37.32	1.84	0.00	37.32	1.84	-0.06	37.38	66.0	+0.77
	5-5										
7	615 to 618	-3.31	5.98	-5.81	-0.48	6.00	-3.33	-5.81	11.81	46.2	+2.91
	6-6										
8	176 to 326	-7.00	-1.81	-2.93	0.02	-1.81	-2.93	-7.00	5.19	46.2	+7.90

* Refer to Figure 2.10.2-9 for component identification.

** Conservatively based on a 1.12-inch thick outer shell and on a 3,850-psi maximum crush strength aluminum honeycomb impact limiter (Section 2.7.1.3).

Table 2.7.1-31 Critical Stress Summary (30-Foot Top Oblique Drop) – Loading Condition 1 - $P_m + P_b$ – Drop Orientation = 45 Degrees

Loading Condition 1: 130°F Ambient Temperature and Maximum Decay Heat Load

		$P_m + P_b$ Stresses (ksi)**				Principal Stresses					
Comp. No.*	Section Cut Node to Node	S_x	S_y	S_z	S_{xy}	S_1	S_2	S_3	S.I.	Allow. Stress 1.0 S_u	Margin of Safety
	1-1										
1	2302 to 2562	7.92	-16.65	3.19	-13.28	13.73	3.19	-22.45	36.18	66.0	+0.82
	7-7										
3	1969 to 1996	-44.85	-17.81	-11.30	0.12	-11.30	-17.81	-44.85	33.55	66.0	+0.97
	3-3										
4	961 to 964	-0.03	19.01	1.30	0.01	19.01	1.30	-0.03	19.05	94.3	+3.95
	4-4										
6	1055 to 1058	0.01	39.00	1.96	0.00	39.00	1.96	0.01	38.99	94.3	+1.41
	8-8										
7	143 to 150	-5.39	23.94	-0.43	1.68	24.04	-0.43	-5.48	29.52	66.0	+1.24
	6-6										
8	176 to 326	-10.61	-5.80	0.70	-2.13	0.70	-4.99	-11.42	12.11	66.0	+4.45

* Refer to Figure 2.10.2-9 for component identification.

** Conservatively based on a 1.12-inch thick outer shell and on a 3,850-psi maximum crush strength aluminum honeycomb impact limiter (Section 2.7.1.3).

Table 2.7.1-32 Critical Stress Summary (30-Foot Top Oblique Drop) – Loading Condition 1 – Total Range – Drop Orientation = 45 Degrees

Loading Condition 1: 130°F Ambient Temperature and Maximum Decay Heat Load

		Total Stress Range** (ksi)				Principal Stresses			Stress Differences		
Comp. No.*	Node	S_x	S_y	S_z	S_{xy}	S_1	S_2	S_3	S_1-S_2	S_2-S_3	S_3-S_1
1	2561***	2.31	-3.96	-1.76	508.3	507.48	-1.76	-509.13	509.24	507.37	-1016.62
3	1969	-47.18	-32.83	-18.27	5.25	-18.27	-30.95	-49.06	12.68	18.11	-30.79
4	964	-0.02	21.80	1.65	0.02	21.80	1.65	-0.02	20.15	1.67	-21.82
6	1058	0.01	48.86	2.21	0.00	48.86	2.21	0.01	46.65	2.20	-48.85
7	25	-5.38	32.46	2.35	3.45	32.77	2.35	-5.69	30.42	8.04	-38.46
8	177	-29.33	-6.00	-11.77	-1.44	-5.91	-11.77	-29.42	5.86	17.66	-23.51

* Refer to Figure 2.10.2-9 for component identification.

** Conservatively based on a 1.12-inch thick outer shell and on a 3,850-psi maximum crush strength aluminum honeycomb impact limiter (Section 2.7.1.3).

*** Stresses at node 2561 are unrealistic, resulting from the boundary effect. See Section 2.7.1.3.3 for the discussion of the boundary effect on the stress results.

Table 2.7.1-33 Critical Stress Summary (30-Foot Top Oblique Drop) – Loading Condition 1 - P_m – Drop Orientation = 60 Degrees

Loading Condition 1: 130°F Ambient Temperature and Maximum Decay Heat Load

		P_m Stresses (ksi)**				Principal Stresses					
Comp. No.*	Section Cut Node to Node	S_x	S_y	S_z	S_{xy}	S_1	S_2	S_3	S.I.	Allow. Stress 0.7 S_u	Margin of Safety
	1-1										
1	2302 to 2562	-24.77	-21.65	4.65	-17.41	4.65	-5.72	-40.69	45.35	46.2	+0.02
	2-2										
3	2150 to 2156	-5.64	-9.89	-36.97	0.13	-5.63	-9.90	-36.97	31.34	46.2	+0.47
	3-3										
4	981 to 984	-0.15	23.48	0.65	0.03	23.48	0.65	-0.15	23.63	66.0	+1.79
	4-4										
6	1075 to 1078	-0.08	49.11	2.30	0.00	49.11	2.30	-0.08	49.19	66.0	+0.34
	5-5										
7	615 to 618	-3.83	7.00	-7.86	0.18	7.01	-3.83	-7.86	14.87	46.2	+2.11
	6-6										
8	176 to 326	-8.68	-1.53	-4.15	0.13	-1.53	-4.15	-8.69	7.16	46.2	+5.45

* Refer to Figure 2.10.2-9 for component identification.

** Conservatively based on a 1.12-inch thick outer shell and on a 3,850-psi maximum crush strength aluminum honeycomb impact limiter (Section 2.7.1.3).

Table 2.7.1-34 Critical Stress Summary (30-Foot Top Oblique Drop) – Loading Condition 1 - $P_m + P_b$ – Drop Orientation = 60 Degrees

Loading Condition 1: 130°F Ambient Temperature and Maximum Decay Heat Load

		$P_m + P_b$ Stresses (ksi)**				Principal Stresses					
Comp. No.*	Section Cut Node to Node	S_x	S_y	S_z	S_{xy}	S_1	S_2	S_3	S.I.	Allow. Stress 1.0 S_u	Margin of Safety
	1-1										
1	2302 to 2562	14.65	-21.65	4.65	-17.41	21.66	4.65	-28.65	50.31	66.0	+0.31
	7-7										
3	1969 to 2016	-62.10	-19.16	-9.36	2.21	-9.36	-19.05	-62.22	52.86	66.0	+0.25
	3-3										
4	981 to 984	-0.09	24.96	1.44	0.03	24.96	1.44	-0.09	25.06	94.3	+2.76
	4-4										
6	1075 to 1078	0.01	51.35	2.56	0.00	51.35	2.56	0.01	51.33	94.3	+0.84
	8-8										
7	125 to 168	-4.60	27.94	-0.91	1.72	28.03	-0.91	-4.69	32.72	66.0	+1.02
	6-6										
8	176 to 326	-13.14	-5.36	0.68	-2.51	0.68	-4.62	-13.88	14.56	66.0	+3.53

* Refer to Figure 2.10.2-9 for component identification.

** Conservatively based on a 1.12-inch thick outer shell and on a 3,850-psi maximum crush strength aluminum honeycomb impact limiter (Section 2.7.1.3).

Table 2.7.1-35 Critical Stress Summary (30-Foot Top Oblique Drop) – Loading Condition 1 – Total Range – Drop Orientation = 60 Degrees

Loading Condition 1: 130°F Ambient Temperature and Maximum Decay Heat Load

		Total Stress Range** (ksi)				Principal Stresses			Stress Differences		
Comp. No.*	Node	S_x	S_y	S_z	S_{xy}	S_1	S_2	S_3	S_1-S_2	S_2-S_3	S_3-S_1
1	2561***	1.60	-3.05	-0.43	655.2	654.48	-0.43	-655.93	654.91	655.50	-1310.41
3	1969	-67.53	-43.53	-23.94	-1.29	-23.94	-43.46	-67.60	19.52	24.14	-43.66
4	984	-0.08	27.75	1.78	0.03	27.75	1.78	-0.08	25.97	1.86	-27.83
6	1078	0.02	61.20	2.81	0.00	61.20	2.81	0.02	58.39	2.79	-61.18
7	25	-4.59	38.46	2.56	3.47	38.74	2.56	-4.87	36.19	7.43	-43.61
8	177	-36.41	-5.06	-14.59	-1.58	-4.98	-14.59	-36.49	9.60	21.90	-31.51

* Refer to Figure 2.10.2-9 for component identification.

** Conservatively based on a 1.12-inch thick outer shell and on a 3,850-psi maximum crush strength aluminum honeycomb impact limiter (Section 2.7.1.3).

*** Stresses at node 2561 are unrealistic, resulting from the boundary effect. See Section 2.7.1.3.3 for the discussion of the boundary effect on the stress results.

Table 2.7.1-36 Critical Stress Summary (30-Foot Top Corner Drop) – Loading Condition 3 - P_m – Drop Orientation = 15.74 Degrees

Loading Condition 3: -40°F Ambient Temperature and No Decay Heat Load

		P_m Stresses (ksi)**				Principal Stresses					
Comp. No.*	Section Cut Node to Node	S_x	S_y	S_z	S_{xy}	S_1	S_2	S_3	S.I.	Allow. Stress 0.7 S_u	Margin of Safety
	1-1										
1	2377 to 2577	-23.41	-1.57	-3.70	-1.18	-1.50	-3.70	-23.48	21.97	46.2	+1.1
	2-2										
3	1775 to 1778	-0.30	-20.30	3.03	0.08	3.03	-0.30	-20.30	23.33	46.2	+1.0
	3-3										
4	1561 to 1564	0.14	-13.57	-2.03	-0.54	0.16	-2.03	-13.59	13.75	66.0	+3.80
	4-4										
6	1595 to 1598	-0.03	-18.20	2.61	0.15	2.61	-0.03	-18.20	20.82	66.0	+2.17
	5-5										
7	168 to 175	-2.77	4.60	-0.84	-0.07	4.60	-0.84	-2.78	7.38	46.2	+5.26
	6-6										
8	381 to 385	-3.82	-7.56	-2.84	0.38	-2.84	-3.78	-7.60	4.76	46.2	+8.71

* Refer to Figure 2.10.2-9 for component identification.

** Conservatively based on a 1.12-inch thick outer shell and on a 3,850-psi maximum crush strength aluminum honeycomb impact limiter (Section 2.7.1.3).

Table 2.7.1-37 Critical Stress Summary (30-Foot Top Corner Drop) – Loading Condition 3 - $P_m + P_b$ – Drop Orientation = 15.74 Degrees

Loading Condition 3: -40°F Ambient Temperature and No Decay Heat Load

		$P_m + P_b$ Stresses (ksi)**				Principal Stresses					
Comp. No.*	Section Cut Node to Node	S_x	S_y	S_z	S_{xy}	S_1	S_2	S_3	S.I.	Allow. Stress 1.0 S_u	Margin of Safety
	1-1										
1	2377 to 2577	-27.21	-1.57	-3.70	-1.18	-1.51	-3.70	-27.27	25.75	66.0	+1.56
	7-7										
3	1821 to 1825	0.20	-21.52	7.75	1.92	7.75	0.37	-21.69	29.45	66.0	+1.24
	3-3										
4	1561 to 1564	0.29	-18.60	-4.46	-0.54	0.30	-4.46	-18.61	18.92	94.3	+3.98
	4-4										
6	1595 to 1598	0.04	-18.68	2.26	0.15	2.26	0.04	-18.68	20.94	94.3	+3.50
	8-8										
7	143 to 150	-0.92	17.99	4.22	-0.23	17.99	4.22	-0.93	18.92	66.0	+2.49
	6-6										
8	381 to 385	-5.74	-8.92	-0.47	-0.73	-0.47	-5.58	-9.08	8.61	66.0	+6.66

* Refer to Figure 2.10.2-9 for component identification.

** Conservatively based on a 1.12-inch thick outer shell and on a 3,850-psi maximum crush strength aluminum honeycomb impact limiter (Section 2.7.1.3).

Table 2.7.1-38 Critical Stress Summary (30-Foot Top Corner Drop) – Loading Condition 3 – Total Range – Drop Orientation = 15.74 Degrees

Loading Condition 3: -40°F Ambient Temperature and No Decay Heat Load

		Total Stress Range** (ksi)				Principal Stresses			Stress Differences		
Comp. No.*	Node	S_x	S_y	S_z	S_{xy}	S_1	S_2	S_3	S_1-S_2	S_2-S_3	S_3-S_1
1	2561***	0.53	-5.77	-5.37	196.6	194.01	-5.37	-199.25	199.38	193.88	-393.25
3	1815	-1.78	-34.09	-0.31	1.13	-0.31	-1.74	-34.13	1.43	32.39	-33.82
4	1584	-1.07	-13.54	-7.81	-1.49	-0.89	-7.81	-13.72	6.92	5.91	-12.82
6	1598	-0.07	-22.77	2.35	0.07	2.35	-0.07	-22.77	4.42	22.70	-25.12
7	2	-0.93	22.51	5.68	0.95	22.54	5.68	-0.97	16.86	6.65	-23.51
8	385	-15.51	-7.77	-7.85	-1.52	-7.48	-7.85	-15.80	0.36	7.95	-8.32

* Refer to Figure 2.10.2-9 for component identification.

** Conservatively based on a 1.12-inch thick outer shell and on a 3,850-psi maximum crush strength aluminum honeycomb impact limiter (Section 2.7.1.3).

*** Stresses at node 2561 are unrealistic, resulting from the boundary effect. See Section 2.7.1.3.3 for the discussion of the boundary effect on the stress results.

Table 2.7.1-39 Critical Stress Summary (30-Foot Top Oblique Drop) – Loading Condition 3 - P_m – Drop Orientation = 30 Degrees

Loading Condition 3: -40°F Ambient Temperature and No Decay Heat Load

		P_m Stresses (ksi)**				Principal Stresses					
Comp. No.*	Section Cut Node to Node	S_x	S_y	S_z	S_{xy}	S_1	S_2	S_3	S.I.	Allow. Stress 0.7 S_u	Margin of Safety
	1-1										
1	2302 to 2562	-16.20	-12.40	1.94	-9.53	1.94	-4.59	-24.02	25.96	46.2	+0.78
	2-2										
3	2150 to 2156	-2.78	-11.71	-24.46	0.10	-2.78	-11.71	-24.46	21.68	46.2	+1.13
	3-3										
4	941 to 944	-0.01	11.94	0.15	0.00	11.94	0.15	-0.01	11.95	66.0	+4.52
	4-4										
6	1035 to 1038	-0.04	27.17	1.33	0.00	27.17	1.33	-0.04	27.21	66.0	+1.49
	5-5										
7	168 to 175	-3.49	6.05	-3.83	0.39	6.06	-3.50	-3.83	9.90	46.2	+3.67
	6-6										
8	381 to 385	-6.22	-6.32	-4.05	0.41	-4.05	-5.86	-6.68	2.63	46.2	+16.56

* Refer to Figure 2.10.2-9 for component identification.

** Conservatively based on a 1.12-inch thick outer shell and on a 3,850-psi maximum crush strength aluminum honeycomb impact limiter (Section 2.7.1.3).

Table 2.7.1-40 Critical Stress Summary (30-Foot Top Oblique Drop) – Loading Condition 3 - $P_m + P_b$ – Drop Orientation = 30 Degrees

Loading Condition 3: -40°F Ambient Temperature and No Decay Heat Load

		$P_m + P_b$ Stresses (ksi)**				Principal Stresses					
Comp. No.*	Section Cut Node to Node	S_x	S_y	S_z	S_{xy}	S_1	S_2	S_3	S.I.	Allow. Stress 1.0 S_u	Margin of Safety
	1-1										
1	2377 to 2577	-27.70	-2.51	-3.18	-2.00	-2.35	-3.18	-27.86	25.51	66.0	+1.59
	8-8										
3	1821 to 1825	0.23	-21.21	8.11	2.18	8.11	0.45	-21.43	29.54	66.0	+1.23
	9-9										
4	1561 to 1564	0.23	-13.23	-3.71	-0.43	0.24	-3.71	-13.25	13.49	94.3	+5.99
	4-4										
6	1035 to 1038	0.01	28.33	1.36	0.00	28.33	1.36	0.01	28.32	94.3	+2.33
	10-10										
7	143 to 150	-1.38	23.77	2.90	0.26	23.77	2.90	-1.39	25.15	66.0	+1.62
	11-11										
8	176 to 326	-9.37	-8.25	-0.22	-1.43	-0.22	-7.27	-10.35	10.13	66.0	+5.51

* Refer to Figure 2.10.2-9 for component identification.

** Conservatively based on a 1.12-inch thick outer shell and on a 3,850-psi maximum crush strength aluminum honeycomb impact limiter (Section 2.7.1.3).

Table 2.7.1-41 Critical Stress Summary (30-Foot Top Oblique Drop) – Loading Condition 3 – Total Range – Drop Orientation = 30 Degrees

Loading Condition 3: -40°F Ambient Temperature and No Decay Heat Load

		Total Stress Range** (ksi)				Principal Stresses			Stress Differences		
Comp. No.*	Node	S_x	S_y	S_z	S_{xy}	S_1	S_2	S_3	S_1-S_2	S_2-S_3	S_3-S_1
1	2561***	0.55	-4.91	-4.43	388.2	286.03	-4.43	-390.39	390.36	386.06	-776.42
3	1821	0.41	-23.19	9.86	0.65	9.86	0.43	-23.21	9.43	23.64	-33.07
4	1584	-0.72	-7.54	-6.57	-1.20	-0.52	-6.57	-7.74	6.05	1.17	-7.23
6	1038	0.01	24.74	1.37	0.00	24.74	1.37	0.01	23.37	1.36	-24.73
7	25	-1.39	31.20	5.34	1.62	31.28	5.34	-1.47	25.94	6.81	-32.75
8	385	-25.70	-6.95	-11.61	-1.69	-6.79	-11.61	-25.85	4.81	14.24	-19.06

* Refer to Figure 2.10.2-9 for component identification.

** Conservatively based on a 1.12-inch thick outer shell and on a 3,850-psi maximum crush strength aluminum honeycomb impact limiter (Section 2.7.1.3).

*** Stresses at node 2561 are unrealistic, resulting from the boundary effect. See Section 2.7.1.3.3 for the discussion of the boundary effect on the stress results.

Table 2.7.1-42 Critical Stress Summary (30-Foot Top Oblique Drop) – Loading Condition 3 - P_m – Drop Orientation = 45 Degrees

Loading Condition 3: -40°F Ambient Temperature and No Decay Heat Load

		P_m Stresses (ksi)**				Principal Stresses					
Comp. No.*	Section Cut Node to Node	S_x	S_y	S_z	S_{xy}	S_1	S_2	S_3	S.I.	Allow. Stress 0.7 S_u	Margin of Safety
	1-1										
1	2302 to 2562	-18.06	-15.24	2.98	-11.92	2.98	-4.65	-28.65	31.63	46.2	+0.46
	2-2										
3	2150 to 2156	-3.61	-10.04	-28.16	0.10	-3.61	-10.04	-28.16	24.55	46.2	+0.88
	3-3										
4	981 to 984	-0.01	14.90	0.16	0.00	14.90	0.16	-0.01	14.91	66.0	+3.43
	4-4										
6	1055 to 1058	-0.05	33.61	1.52	0.00	33.61	1.52	-0.05	33.66	66.0	+0.96
	5-5										
7	168 to 175	-3.47	6.17	-5.50	0.68	6.22	-3.52	-5.50	11.72	46.2	+2.94
	6-6										
8	381 to 385	-7.05	-4.35	-4.32	0.36	-4.30	-4.32	-7.10	2.79	46.2	+15.54

* Refer to Figure 2.10.2-9 for component identification.

** Conservatively based on a 1.12-inch thick outer shell and on a 3,850-psi maximum crush strength aluminum honeycomb impact limiter (Section 2.7.1.3).

Table 2.7.1-43 Critical Stress Summary (30-Foot Top Oblique Drop) – Loading Condition 3 - $P_m + P_b$ – Drop Orientation = 45 Degrees

Loading Condition 3: -40°F Ambient Temperature and No Decay Heat Load

		$P_m + P_b$ Stresses (ksi)**				Principal Stresses					
Comp. No.*	Section Cut Node to Node	S_x	S_y	S_z	S_{xy}	S_1	S_2	S_3	S.I.	Allow. Stress 1.0 S_u	Margin of Safety
	1-1										
1	2302 to 2562	7.23	-15.24	2.98	-11.92	12.38	2.98	-20.38	32.76	66.0	+1.01
	7-7										
3	1969 to 1996	-41.18	-16.23	-10.45	0.25	-10.45	-16.23	-41.19	30.74	66.0	+1.15
	3-3										
4	981 to 984	0.00	15.70	0.16	0.00	15.70	0.16	0.00	15.70	94.3	+5.01
	4-4										
6	1055 to 1058	0.01	35.09	1.62	0.00	35.09	1.62	0.01	35.08	94.3	+1.69
	8-8										
7	143 to 150	-1.51	24.33	1.43	0.59	24.34	1.43	-1.52	25.87	66.0	+1.55
	9-9										
8	176 to 326	-10.63	-6.40	0.00	-1.74	0.00	-5.78	-11.25	11.25	66.0	+4.87

* Refer to Figure 2.10.2-9 for component identification.

** Conservatively based on a 1.12-inch thick outer shell and on a 3,850-psi maximum crush strength aluminum honeycomb impact limiter (Section 2.7.1.3).

Table 2.7.1-44 Critical Stress Summary (30-Foot Top Oblique Drop) – Loading Condition 3 – Total Range – Drop Orientation = 45 Degrees

Loading Condition 3: -40°F Ambient Temperature and No Decay Heat Load

		Total Stress Range** (ksi)				Principal Stresses			Stress Differences		
Comp. No.*	Node	S_x	S_y	S_z	S_{xy}	S_1	S_2	S_3	S_1-S_2	S_2-S_3	S_3-S_1
1	2561***	0.57	-3.66	-3.33	467.6	466.1	-3.33	-469.2	469.4	465.82	-935.21
3	1969	-43.14	-27.23	-17.08	2.69	-17.08	-26.79	-43.58	9.71	16.80	-26.50
4	984	-0.93	6.36	-8.61	0.00	6.36	-0.93	-8.61	7.29	7.68	-14.97
6	1058	0.01	31.49	1.62	0.00	31.49	1.62	0.01	29.87	1.61	-31.48
7	25	-1.51	32.78	4.22	1.88	32.89	4.22	-1.61	28.67	5.83	-34.50
8	385	-29.31	-5.19	-12.60	-1.55	-5.09	-12.60	-29.41	7.50	16.81	-24.31

* Refer to Figure 2.10.2-9 for component identification.

** Conservatively based on a 1.12-inch thick outer shell and on a 3,850-psi maximum crush strength aluminum honeycomb impact limiter (Section 2.7.1.3).

*** Stresses at node 2561 are unrealistic, resulting from the boundary effect. See Section 2.7.1.3.3 for the discussion of the boundary effect on the stress results.

Table 2.7.1-45 Critical Stress Summary (30-Foot Top Oblique Drop) – Loading Condition 3 - P_m – Drop Orientation = 60 Degrees

Loading Condition 3: -40°F Ambient Temperature and No Decay Heat Load

		P_m Stresses (ksi)**				Principal Stresses					
Comp. No.*	Section Cut Node to Node	S_x	S_y	S_z	S_{xy}	S_1	S_2	S_3	S.I.	Allow. Stress 0.7 S_u	Margin of Safety
	1-1										
1	2302 to 2562	-22.17	-19.88	4.31	-15.80	4.31	-5.18	-36.87	41.18	46.2	+0.12
	2-2										
3	2150 to 2156	-5.21	-9.13	-34.47	0.13	-5.20	-9.13	-34.47	29.27	46.2	+0.58
	3-3										
4	1021 to 1024	-0.01	19.85	0.18	0.00	19.85	0.18	-0.01	19.86	66.0	+2.32
	4-4										
6	1075 to 1078	-0.06	44.14	1.89	0.00	44.14	1.89	-0.06	44.20	66.0	+0.49
	5-5										
7	615 to 618	-3.94	7.14	-7.64	1.01	7.23	-4.03	-7.64	14.87	46.2	+2.11
	6-6										
8	601 to 604	-8.72	-3.35	-5.15	0.38	-3.32	-5.15	-8.75	-5.42	46.2	+7.52

* Refer to Figure 2.10.2-9 for component identification.

** Conservatively based on a 1.12-inch thick outer shell and on a 3,850-psi maximum crush strength aluminum honeycomb impact limiter (Section 2.7.1.3).

Table 2.7.1-46 Critical Stress Summary (30-Foot Top Oblique Drop) – Loading Condition 3 - $P_m + P_b$ – Drop Orientation = 60 Degrees

Loading Condition 3: -40°F Ambient Temperature and No Decay Heat Load

		$P_m + P_b$ Stresses (ksi)**				Principal Stresses					
Comp. No.*	Section Cut Node to Node	S_x	S_y	S_z	S_{xy}	S_1	S_2	S_3	S.I.	Allow. Stress 1.0 S_u	Margin of Safety
	1-1										
1	2302 to 2562	13.46	-19.88	4.31	-15.80	19.76	4.31	-26.18	45.94	66.0	+0.44
	7-7										
3	1969 to 2016	-56.85	-17.63	-8.69	2.13	-8.69	-17.51	-56.97	48.28	66.0	+0.37
	3-3										
4	1021 to 1024	0.00	20.91	0.18	0.00	20.91	0.18	0.00	20.92	94.3	+3.51
	4-4										
6	1075 to 1078	0.01	46.11	2.12	0.00	46.11	2.12	0.01	46.10	94.3	+1.05
	8-8										
7	125 to 168	-1.83	28.22	0.42	0.94	28.25	0.42	-1.86	30.10	66.0	+1.19
	9-9										
8	381 to 385	-13.15	-5.79	0.19	-2.23	0.19	-5.17	-13.77	13.96	66.0	+3.73

* Refer to Figure 2.10.2-9 for component identification.

** Conservatively based on a 1.12-inch thick outer shell and on a 3,850-psi maximum crush strength aluminum honeycomb impact limiter (Section 2.7.1.3).

Table 2.7.1-47 Critical Stress Summary (30-Foot Top Oblique Drop) – Loading Condition 3 – Total Range – Drop Orientation = 60 Degrees

Loading Condition 3: -40°F Ambient Temperature and No Decay Heat Load

		Total Stress Range** (ksi)				Principal Stresses			Stress Differences		
Comp. No.*	Node	S_x	S_y	S_z	S_{xy}	S_1	S_2	S_3	S_1-S_2	S_2-S_3	S_3-S_1
1	2561***	0.06	-2.82	-1.96	603.5	602.12	-1.96	-604.88	604.08	602.92	-1207.00
3	1969	-62.00	-37.03	-22.36	1.03	-22.36	-36.99	-62.04	14.63	25.05	-39.68
4	1024	-0.93	11.58	-8.59	0.00	11.58	-0.93	-8.59	12.51	7.66	-20.17
6	1078	0.01	42.52	2.12	0.00	42.52	2.12	0.01	40.40	2.11	-42.51
7	25	-1.82	38.70	3.89	2.35	38.83	3.89	-1.96	34.94	5.85	-40.79
8	177	-36.39	-4.49	-15.18	-1.66	-4.40	-15.18	-36.48	10.78	21.30	-32.08

* Refer to Figure 2.10.2-9 for component identification.

** Conservatively based on a 1.12-inch thick outer shell and on a 3,850-psi maximum crush strength aluminum honeycomb impact limiter (Section 2.7.1.3).

*** Stresses at node 2561 are unrealistic, resulting from the boundary effect. See Section 2.7.1.3.3 for the discussion of the boundary effect on the stress results.

Table 2.7.1-48 Critical Stress Summary (30-Foot Bottom Oblique Drop) – Loading Condition 1 - P_m – Drop Orientation = 15.74 Degrees

Loading Condition 1: 130°F Ambient Temperature and Maximum Decay Heat Load

		P_m Stresses (ksi)**				Principal Stresses					
Comp. No.*	Section Cut Node to Node	S_x	S_y	S_z	S_{xy}	S_1	S_2	S_3	S.I.	Allow. Stress 0.7 S_u	Margin of Safety
	1-1										
1	2301 to 2561	-2.46	-0.42	-0.64	0.21	0.64	-0.40	-2.48	3.12	46.2	+13.80
	2-2										
3	1595 to 1598	-6.94	-3.13	-3.21	-1.25	-2.76	-3.21	-7.31	4.56	46.2	+9.14
	3-3										
4	621 to 624	0.07	-16.15	-1.45	0.48	0.09	-1.45	-16.17	16.26	66.0	+3.05
	4-4										
6	615 to 618	-0.05	-24.26	1.38	-0.17	1.38	-0.05	-24.26	25.64	66.0	+1.57
	5-5										
7	2 to 102	-29.38	-17.87	-0.14	13.44	-0.14	-9.01	-38.25	38.11	46.2	+0.21
	6-6										
8	601 to 604	-0.37	-14.99	-0.87	0.68	-0.34	-0.87	-15.02	14.68	46.2	+2.15

* Refer to Figure 2.10.2-9 for component identification.

** Conservatively based on a 1.12-inch thick outer shell and on a 3,850-psi maximum crush strength aluminum honeycomb impact limiter (Section 2.7.1.3).

Table 2.7.1-49 Critical Stress Summary (30-Foot Bottom Oblique Drop) – Loading Condition 1 - $P_m + P_b$ – Drop Orientation = 15.74 Degrees

Loading Condition 1: 130°F Ambient Temperature and Maximum Decay Heat Load

		$P_m + P_b$ Stresses (ksi)**				Principal Stresses					
Comp. No.*	Section Cut Node to Node	S_x	S_y	S_z	S_{xy}	S_1	S_2	S_3	S.I.	Allow. Stress 1.0 S_u	Margin of Safety
	1-1										
1	2301 to 2561	-4.32	-0.30	0.66	2.67	1.03	0.66	-5.65	6.69	66.0	+8.87
	7-7										
3	1815 to 1818	-3.06	4.46	-11.42	0.29	4.48	-3.07	-11.42	15.90	66.0	+3.15
	3-3										
4	621 to 624	0.27	-20.83	-3.90	0.48	0.28	-3.90	-20.84	21.12	94.3	+3.46
	4-4										
6	615 to 618	-0.11	-25.58	1.47	-0.17	1.47	-0.11	-25.58	27.05	94.3	+2.48
	8-8										
7	168 to 175	45.23	-16.97	-0.74	-1.45	45.26	-0.74	-17.01	62.27	66.0	+0.06
	9-9										
8	176 to 326	-32.63	0.00	-4.06	0.00	0.00	-4.06	-32.63	32.63	66.0	+1.02

* Refer to Figure 2.10.2-9 for component identification.

** Conservatively based on a 1.12-inch thick outer shell and on a 3,850-psi maximum crush strength aluminum honeycomb impact limiter (Section 2.7.1.3).

Table 2.7.1-50 Critical Stress Summary (30-Foot Bottom Oblique Drop) – Loading Condition 1 – Total Range – Drop Orientation = 15.74 Degrees

Loading Condition 1: 130°F Ambient Temperature and Maximum Decay Heat Load

		Total Stress Range** (ksi)				Principal Stresses			Stress Differences		
Comp. No.*	Node	S_x	S_y	S_z	S_{xy}	S_1	S_2	S_3	S_1-S_2	S_2-S_3	S_3-S_1
1	2561	0.82	-4.33	0.68	9.98	8.55	0.68	-12.07	7.87	12.75	-20.62
3	1815	0.98	11.67	0.31	4.22	13.14	0.31	-0.49	12.83	0.80	-13.63
4	604	-1.35	-22.40	-4.09	1.23	-1.28	-4.09	-22.47	2.81	18.38	-21.19
6	615	-0.03	-14.25	2.26	-0.28	2.26	-0.02	-14.26	2.28	14.23	-16.52
7	1***	-0.49	-6.30	-9.12	-213.50	210.12	-9.12	-216.91	219.24	207.79	-427.04
8	361	0.02	-28.18	2.01	-2.18	2.01	0.19	-28.35	1.82	28.54	-30.36

* Refer to Figure 2.10.2-9 for component identification.

** Conservatively based on a 1.12-inch thick outer shell and on a 3,850-psi maximum crush strength aluminum honeycomb impact limiter (Section 2.7.1.3).

*** Stresses at node 1 are unrealistic, resulting from the boundary effect. See Section 2.7.1.3.3 for the discussion of the boundary effect on the stress results.

Table 2.7.1-51 Critical Stress Summary (30-Foot Bottom Oblique Drop) – Loading Condition 1 - P_m – Drop Orientation = 30 Degrees

Loading Condition 1: 130°F Ambient Temperature and Maximum Decay Heat Load

		P_m Stresses (ksi)**				Principal Stresses					
Comp. No.*	Section Cut Node to Node	S_x	S_y	S_z	S_{xy}	S_1	S_2	S_3	S.I.	Allow. Stress 0.7 S_u	Margin of Safety
	1-1										
1	2301 to 2561	-3.93	-0.51	0.56	0.02	0.56	-0.51	-3.93	4.49	46.2	+9.30
	2-2										
3	1595 to 1598	-11.42	-1.45	-5.19	-1.95	-1.08	-5.19	-11.79	10.71	46.2	+3.31
	3-3										
4	1261 to 1264	-0.06	16.36	0.81	0.00	16.36	0.81	-0.06	16.42	66.0	+3.02
	4-4										
6	1195 to 1198	-0.05	29.57	1.48	0.00	29.57	1.48	-0.05	29.62	66.0	+1.22
7	2 to 102	-48.76	-30.81	5.29	31.95	5.29	-6.60	-72.97	78.26***	46.2	***
	6-6										
8	501 to 505	-0.06	-11.36	0.85	0.81	0.85	0.00	-11.42	12.27	46.2	+2.77

* Refer to Figure 2.10.2-9 for component identification.

** Conservatively based on a 1.12-inch thick outer shell and on a 3,850-psi maximum crush strength aluminum honeycomb impact limiter (Section 2.7.1.3).

*** This stress is unrealistic and is disregarded. See Section 2.7.1.3.3 for the discussion of the boundary effect on the stress results. The critical section and its stresses for component 7 are:

Section Cut Node to Node	S_x	S_y	S_z	S_{xy}	S_1	S_2	S_3	S.I.	0.7 S_u	MS
5-5 4 to 104	-11.36	-24.02	-2.05	4.49	-2.05	-9.93	-25.45	23.40	46.2	+0.97

Table 2.7.1-52 Critical Stress Summary (30-Foot Bottom Oblique Drop) – Loading Condition 1 - $P_m + P_b$ – Drop Orientation = 30 Degrees

Loading Condition 1: 130°F Ambient Temperature and Maximum Decay Heat Load

		$P_m + P_b$ Stresses (ksi)**				Principal Stresses					
Comp. No.*	Section Cut Node to Node	S_x	S_y	S_z	S_{xy}	S_1	S_2	S_3	S.I.	Allow. Stress 1.0 S_u	Margin of Safety
	1-1										
1	2301 to 2561	-3.94	-0.21	1.01	4.43	2.73	1.01	-6.89	9.62	66.0	+5.86
	7-7										
3	1815 to 1818	-5.00	3.57	-20.79	0.24	3.57	-5.00	-20.79	24.36	66.0	+1.71
	8-8										
4	1241 to 1244	-0.02	17.27	1.03	0.00	17.27	1.03	-0.02	17.29	94.3	+4.45
	9-9										
6	1175 to 1178	0.00	30.88	1.52	0.00	30.88	1.52	0.00	30.88	94.3	+2.04
7	2 to 102	-1.21	-30.81	5.29	31.95	19.20	5.29	-51.22	70.43***	66.0	***
	10-10										
8	176 to 326	-26.38	0.00	-3.46	0.00	0.00	-3.46	-26.38	26.38	66.0	+1.50

* Refer to Figure 2.10.2-9 for component identification.

** Conservatively based on a 1.12-inch thick outer shell and on a 3,850-psi maximum crush strength aluminum honeycomb impact limiter (Section 2.7.1.3).

*** This stress is unrealistic and is disregarded. See Section 2.7.1.3.3 for the discussion of the boundary effect on the stress results. The critical section and its stresses for component 7 are:

Section Cut Node to Node	S_x	S_y	S_z	S_{xy}	S_1	S_2	S_3	S.I.	1.0 S_u	MS
5-5 4 to 104	-13.71	-24.02	-2.05	4.49	-2.05	-12.03	-25.70	23.65	66.0	+1.79

Table 2.7.1-53 Critical Stress Summary (30-Foot Bottom Oblique Drop) – Loading Condition 1 – Total Range – Drop Orientation = 30 Degrees

Loading Condition 1: 130°F Ambient Temperature and Maximum Decay Heat Load

		Total Stress Range** (ksi)				Principal Stresses			Stress Differences		
Comp. No.*	Node	S_x	S_y	S_z	S_{xy}	S_1	S_2	S_3	S_1-S_2	S_2-S_3	S_3-S_1
1	2561	0.70	-3.49	1.32	16.80	15.53	1.32	-18.33	14.22	19.64	-33.86
3	1815	1.78	23.68	2.32	7.64	26.09	2.32	-0.63	23.77	2.94	-26.71
4	604	-1.10	-18.18	-3.00	1.02	-1.04	-3.00	-18.24	1.96	15.24	-17.20
6	1178	0.01	40.71	1.75	0.00	40.71	1.75	0.01	38.96	1.74	-40.70
7	1***	-1.03	-5.20	-6.73	-423.50	420.39	-6.73	-426.62	427.12	419.89	-847.01
8	177	-39.92	-4.9	-27.40	-3.15	-4.62	-27.40	-40.20	22.78	12.80	-35.58

* Refer to Figure 2.10.2-9 for component identification.

** Conservatively based on a 1.12-inch thick outer shell and on a 3,850-psi maximum crush strength aluminum honeycomb impact limiter (Section 2.7.1.3).

*** Stresses at node 1 are unrealistic, resulting from the boundary effect. See Section 2.7.1.3.3 for the discussion of the boundary effect on the stress results.

Table 2.7.1-54 Critical Stress Summary (30-Foot Bottom Oblique Drop) – Loading Condition 1 - P_m – Drop Orientation = 45 Degrees

Loading Condition 1: 130°F Ambient Temperature and Maximum Decay Heat Load

		P_m Stresses (ksi)**				Principal Stresses					
Comp. No.*	Section Cut Node to Node	S_x	S_y	S_z	S_{xy}	S_1	S_2	S_3	S.I.	Allow. Stress 0.7 S_u	Margin of Safety
	1-1										
1	2301 to 2561	-4.42	-0.50	0.40	-0.12	0.40	-0.50	-4.42	4.82	46.2	+8.58
	2-2										
3	1595 to 1598	-12.99	0.06	-5.86	-2.18	0.41	-5.86	-13.35	13.76	46.2	+2.36
	3-3										
4	1241 to 1244	-0.09	19.42	0.87	0.00	19.42	0.87	-0.09	19.51	66.0	+2.38
	4-4										
6	1175 to 1178	-0.06	36.99	1.79	0.00	36.99	1.79	-0.06	37.04	66.0	+0.78
7	2 to 102	-55.62	-36.07	9.42	40.01	9.42	-4.65	-87.03	96.45***	46.2	***
	6-6										
8	501 to 505	-0.06	-8.84	1.04	0.67	1.04	-0.01	-8.89	9.93	46.2	+3.65

* Refer to Figure 2.10.2-9 for component identification.

** Conservatively based on a 1.12-inch thick outer shell and on a 3,850-psi maximum crush strength aluminum honeycomb impact limiter (Section 2.7.1.3).

*** This stress is unrealistic and is disregarded. See Section 2.7.1.3.3 for the discussion of the boundary effect on the stress results. The critical section and its stresses for component 7 are:

Section Cut Node to Node	S_x	S_y	S_z	S_{xy}	S_1	S_2	S_3	S.I.	0.7 S_u	MS
5-5 4 to 104	-10.17	-27.98	0.97	6.07	0.97	-8.3	-29.85	30.82	46.2	+0.50

Table 2.7.1-55 Critical Stress Summary (30-Foot Bottom Oblique Drop) – Loading Condition 1 - $P_m + P_b$ – Drop Orientation = 45 Degrees

Loading Condition 1: 130°F Ambient Temperature and Maximum Decay Heat Load

		$P_m + P_b$ Stresses (ksi)**				Principal Stresses					
Comp. No.*	Section Cut Node to Node	S_x	S_y	S_z	S_{xy}	S_1	S_2	S_3	S.I.	Allow. Stress 1.0 S_u	Margin of Safety
	1-1										
1	2301 to 2561	-3.02	-0.11	1.11	5.05	3.70	1.11	-6.82	10.52	66.0	+5.27
	7-7										
3	1815 to 1818	-5.66	2.30	-24.56	0.17	2.31	-5.67	-24.56	26.87	66.0	+1.46
	3-3										
4	1241 to 1244	-0.03	20.58	1.32	0.00	20.58	1.32	-0.03	20.62	94.3	+3.57
	4-4										
6	1175 to 1178	0.00	38.64	1.74	0.00	38.64	1.74	0.00	38.64	94.3	+1.44
7	2 to 102	3.28	-36.07	9.42	40.01	28.20	9.42	-60.98	89.18***	66.0	***
	8-8										
8	176 to 326	-17.26	0.00	-1.15	0.00	0.00	-1.15	-17.26	17.26	66.0	+2.82

* Refer to Figure 2.10.2-9 for component identification.

** Conservatively based on a 1.12-inch thick outer shell and on a 3,850-psi maximum crush strength aluminum honeycomb impact limiter (Section 2.7.1.3).

*** This stress is unrealistic and is disregarded. See Section 2.7.1.3.3 for the discussion of the boundary effect on the stress results. The critical section and its stresses for component 7 are:

Section Cut Node to Node	S_x	S_y	S_z	S_{xy}	S_1	S_2	S_3	S.I.	1.0 S_u	MS
5-5 4 to 104	-12.31	-27.98	0.97	6.07	0.97	-10.23	-30.06	31.03	66.0	+1.13

Table 2.7.1-56 Critical Stress Summary (30-Foot Bottom Oblique Drop) – Loading Condition 1 – Total Range – Drop Orientation = 45 Degrees

Loading Condition 1: 130°F Ambient Temperature and Maximum Decay Heat Load

		Total Stress Range** (ksi)				Principal Stresses			Stress Differences		
Comp. No.*	Node	S_x	S_y	S_z	S_{xy}	S_1	S_2	S_3	S_1-S_2	S_2-S_3	S_3-S_1
1	2561	0.49	-2.29	1.58	19.28	18.44	1.58	-20.23	16.85	21.82	-38.67
3	1815	2.10	29.01	3.47	9.01	31.75	3.47	-0.64	28.28	4.11	-32.39
4	1244	-0.03	23.31	1.61	0.00	23.31	1.61	-0.03	21.70	1.64	-23.34
6	1178	0.01	48.47	1.97	0.00	48.47	1.97	0.01	46.50	1.96	-48.46
7	1***	0.06	-3.93	-3.64	-509.70	507.77	-3.64	-511.64	511.41	508.00	-1019.41
8	177	-40.74	-4.08	-23.25	-2.37	-3.88	-23.25	-40.94	19.37	17.69	-37.06

* Refer to Figure 2.10.2-9 for component identification.

** Conservatively based on a 1.12-inch thick outer shell and on a 3,850-psi maximum crush strength aluminum honeycomb impact limiter (Section 2.7.1.3).

*** Stresses at node 1 are unrealistic, resulting from the boundary effect. See Section 2.7.1.3.3 for the discussion of the boundary effect on the stress results.

Table 2.7.1-57 Critical Stress Summary (30-Foot Bottom Oblique Drop) – Loading Condition 1 - P_m – Drop Orientation = 60 Degrees

Loading Condition 1: 130°F Ambient Temperature and Maximum Decay Heat Load

		P_m Stresses (ksi)**				Principal Stresses					
Comp. No.*	Section Cut Node to Node	S_x	S_y	S_z	S_{xy}	S_1	S_2	S_3	S.I.	Allow. Stress 0.7 S_u	Margin of Safety
	1-1										
1	2302 to 2562	-5.44	-0.56	0.33	-0.26	0.33	-0.54	-5.46	5.79	46.2	+6.99
	2-2										
3	1595 to 1598	-16.11	1.31	-7.24	-2.66	1.71	-7.24	-16.51	18.22	46.2	+1.54
	3-3										
4	1221 to 1224	-0.12	24.94	0.91	-0.02	24.94	0.91	-0.12	25.06	66.0	+1.63
	4-4										
6	1155 to 1158	-0.07	48.97	2.27	0.00	48.97	2.27	-0.07	49.04	66.0	+0.34
7	2 to 102	-69.10	-45.77	14.35	52.94	14.35	-3.22	-111.6	126.00***	46.2	***
	6-6										
8	177 to 327	-3.61	-11.52	1.18	0.46	1.18	-3.58	-11.55	12.73	46.2	+2.63

* Refer to Figure 2.10.2-9 for component identification.

** Conservatively based on a 1.12-inch thick outer shell and on a 3,850-psi maximum crush strength aluminum honeycomb impact limiter (Section 2.7.1.3).

*** This stress is unrealistic and is disregarded. See Section 2.7.1.3.3 for the discussion of the boundary effect on the stress results. The critical section and its stresses for component 7 are:

Section Cut Node to Node	S_x	S_y	S_z	S_{xy}	S_1	S_2	S_3	S.I.	0.7 S_u	MS
5-5										
4 to 104	-10.12	-35.55	3.96	8.66	3.96	-7.45	-38.22	42.18	46.2	+0.10

Table 2.7.1-58 Critical Stress Summary (30-Foot Bottom Oblique Drop) – Loading Condition 1 - $P_m + P_b$ – Drop Orientation = 60 Degrees

Loading Condition 1: 130°F Ambient Temperature and Maximum Decay Heat Load

		$P_m + P_b$ Stresses (ksi)**				Principal Stresses					
Comp. No.*	Section Cut Node to Node	S_x	S_y	S_z	S_{xy}	S_1	S_2	S_3	S.I.	Allow. Stress 1.0 S_u	Margin of Safety
	7-7										
1	2301 to 2561	-2.69	-0.04	1.34	6.28	5.05	1.34	-7.78	12.83	66.0	+4.14
	8-8										
3	1815 to 1818	-7.00	1.59	-31.12	0.13	1.59	-7.01	-31.12	32.72	66.0	+1.02
	3-3										
4	1221 to 1224	-0.06	26.49	1.66	-0.02	26.49	1.66	-0.06	26.55	94.3	+2.55
	4-4										
6	1155 to 1158	0.01	51.14	2.18	0.00	51.14	2.18	0.01	51.13	94.3	+0.84
7	2 to 102	8.63	-45.77	14.35	52.94	40.94	14.35	-78.09	119.00***	66.0	***
	9-9										
8	381 to 385	-0.82	-14.41	-3.80	0.98	-0.75	-3.80	-14.48	13.74	66.0	+3.80

* Refer to Figure 2.10.2-9 for component identification.

** Conservatively based on a 1.12-inch thick outer shell and on a 3,850-psi maximum crush strength aluminum honeycomb impact limiter (Section 2.7.1.3).

*** This stress is unrealistic and is disregarded. See Section 2.7.1.3.3 for the discussion of the boundary effect on the stress results. The critical section and its stresses for component 7 are:

Section Cut Node to Node	S_x	S_y	S_z	S_{xy}	S_1	S_2	S_3	S.I.	1.0 S_u	MS
5-5										
4 to 104	-12.00	-35.55	3.96	8.66	3.96	-9.16	-38.40	42.4	66.0	+0.56

Table 2.7.1-59 Critical Stress Summary (30-Foot Bottom Oblique Drop) – Loading Condition 1 – Total Range – Drop Orientation = 60 Degrees

Loading Condition 1: 130°F Ambient Temperature and Maximum Decay Heat Load

		Total Stress Range** (ksi)				Principal Stresses			Stress Differences		
Comp. No.*	Node	S_x	S_y	S_z	S_{xy}	S_1	S_2	S_3	S_1-S_2	S_2-S_3	S_3-S_1
1	2561	0.40	-1.63	2.03	24.03	23.44	2.03	-24.67	21.41	26.70	-48.11
3	1815	2.66	37.47	4.91	11.41	40.87	4.91	-0.75	35.96	5.66	-41.62
4	1224	-0.05	29.24	1.96	-0.02	29.24	1.96	-0.05	27.28	2.01	-29.29
6	1158	0.01	60.98	2.42	0.00	60.98	2.42	0.01	58.56	2.41	-60.97
7	1***	-0.88	-3.07	-0.83	-655.60	653.63	-0.83	-657.58	654.46	656.75	-1311.20
8	177	-46.34	-4.01	-22.03	-2.06	-3.91	-22.03	-46.46	18.39	24.16	-42.55

* Refer to Figure 2.10.2-9 for component identification.

** Conservatively based on a 1.12-inch thick outer shell and on a 3,850-psi maximum crush strength aluminum honeycomb impact limiter (Section 2.7.1.3).

*** Stresses at node 1 are unrealistic, resulting from the boundary effect. See Section 2.7.1.3.3 for the discussion of the boundary effect on the stress results.

Table 2.7.1-60 NAC-LWT Cask Hot Bolt Analysis Hypothetical Accident Conditions

Nominal Diameter (in):	1.00	
Number of Bolts:	12	
Service Stress, Sy (ksi):	81.9	at a 300
Bolt Expansion (in/in):	9E-06	degree-F
Bolt Modulus (ksi):	26700	Service
Lid Expansion (in/in):	9E-06	Temperature
Lid Modulus (ksi):	27000	
Stress Area (in2):	0.6051	
Grip Length (in):	7.99	
Maximum Pressure (psi):	50	
Seal Diameter (in):	15.750	
Preload Torque (ft-lbs):	260	at RT
Nominal Room Temp, RT:	70	deg-F
Bolt Circle Diameter (in):	17.88	
Lid Diameter (in):	22.50	

Longitudinal Weight (lbs):	4941
Lateral Weight (lbs):	941
Service DT (degrees):	157
[default value =]	230

CALCULATED LOADS & STIFFNESS

Bolt Thermal Load (lbs):	1423
Bolt Preload (lbs):	34770
Bolt Pressure Load (lbs):	812
Bolt Stiffness (lbs/in):	1.9E+06
Lid Stiffness (lbs/in):	2.1E+07

Angle wrt Vert. (Deg)	Impact Accel. (g)	<**** LOADS (lbs.) **** Impact Tension	Impact Shear	Bolt Tension Applied	Bolt Tension Net	<**** STRESSES (psi) **** Direct Tension	Principal Shear	Principal Sig-1	Principal Sig-2	Stress Intens.	Margin of Safety
0 End	15.80	6506	0	7317	36795	60808	0	0	60808	60808	0.35
5 (+)	14.69	8216	100	9028	36936	61041	166	0	61041	61042	0.34
10 (+)	13.57	7506	185	8318	36877	60944	305	-2	60946	60947	0.34
15.7 Corner	12.30	6650	261	7462	36807	60828	431	-3	60831	60834	0.35
20 (+)	12.99	6858	349	7670	36824	60856	576	-5	60862	60867	0.35
25 (+)	13.80	7025	457	7837	36838	60879	756	-9	60888	60898	0.34
30 (+)	14.61	7106	573	7918	36845	60890	947	-15	60905	60919	0.34
35 (+)	15.42	7093	693	7905	36843	60888	1146	-22	60910	60931	0.34
40 (+)	16.22	6980	818	7792	36834	60873	1352	-30	60903	60933	0.34
45 (+)	17.03	6764	944	7576	36816	60844	1561	-40	60884	60924	0.34
50 (+)	17.84	6440	1072	7252	36790	60800	1771	-52	60851	60903	0.34
55 (+)	18.65	6007	1198	6819	36754	60741	1980	-64	60805	60870	0.35
60 (+)	19.45	5463	1321	6275	36709	60667	2183	-78	60745	60824	0.35
65 (+)	20.26	4809	1440	5621	36656	60578	2380	-93	60671	60765	0.35
70 (+)	21.07	4047	1553	4859	36593	60474	2566	-109	60583	60692	0.35
75 (+)	21.88	3180	1657	3992	36522	60356	2739	-124	60480	60604	0.35
80 (+)	22.68	2212	1752	3024	36442	60225	2895	-139	60364	60503	0.35
85 (+)	23.49	1150	1835	1962	36355	60080	3033	-153	60233	60386	0.36
90 Side	24.30	0	1906	812	36260	59924	3149	-165	60089	60254	0.36

Minimum Margin of Safety: 0.34

Table 2.7.1-61 NAC-LWT Cask Cold Bolt Analysis Hypothetical Accident Conditions

Nominal Diameter (in):	1.00	
Number of Bolts:	12	
Service Stress, Sy (ksi):	85	at a 70
Bolt Expansion (in/in):	8E-06	degree-F
Bolt Modulus (ksi):	27800	Service
Lid Expansion (in/in):	8E-06	Temperature
Lid Modulus (ksi):	28300	
Stress Area (in2):	0.6051	
Grip Length (in):	7.99	
Maximum Pressure (psi):	50	
Seal Diameter (in):	15.750	
Preload Torque (ft-lbs):	260	at RT
Nominal Room Temp, RT:	70	deg-F
Bolt Circle Diameter (in):	17.88	
Lid Diameter (in):	22.50	

Longitudinal Weight (lbs):	4941
Lateral Weight (lbs):	941
Service DT (degrees):	-90
[default value =]	0
CALCULATED LOADS & STIFFNESS	
Bolt Thermal Load (lbs):	-594
Bolt Preload (lbs):	34770
Bolt Pressure Load (lbs):	812
Bolt Stiffness (lbs/in):	2.0E+06
Lid Stiffness (lbs/in):	2.2E+07

Angle wrt Vert. (Deg)	Impact Accel. (g)	<**** LOADS (lbs.) Impact Tension	Impact Shear	Bolt Tension Applied	Bolt Tension Net ****	<**** STRESSES (psi) Direct Tension	Direct Shear	Principal Sig-1	Principal Sig-2	Stress Intens. ****	Margin of Safety
0 End	15.80	6506	0	7317	34775	57469	0	0	57469	57469	0.48
5 (+)	14.69	8216	100	9028	34914	57700	166	0	57701	57701	0.47
10 (+)	13.57	7506	185	8318	34856	57604	305	-2	57606	57607	0.48
15.7 Corner	12.30	6650	261	7462	34786	57489	431	-3	57492	57495	0.48
20 (+)	12.99	6858	349	7670	34803	57517	576	-6	57522	57528	0.48
25 (+)	13.80	7025	457	7837	34817	57539	756	-10	57549	57559	0.48
30 (+)	14.61	7106	573	7918	34824	57550	947	-16	57566	57581	0.48
35 (+)	15.42	7093	693	7905	34823	57548	1146	-23	57571	57594	0.48
40 (+)	16.22	6980	818	7792	34813	57533	1352	-32	57565	57597	0.48
45 (+)	17.03	6764	944	7576	34796	57504	1561	-42	57546	57589	0.48
50 (+)	17.84	6440	1072	7252	34769	57460	1771	-55	57515	57569	0.48
55 (+)	18.65	6007	1198	6819	34734	57402	1980	-68	57470	57538	0.48
60 (+)	19.45	5463	1321	6275	34689	57328	2183	-83	57411	57494	0.48
65 (+)	20.26	4809	1440	5621	34636	57240	2380	-99	57339	57437	0.48
70 (+)	21.07	4047	1553	4859	34574	57137	2566	-115	57252	57367	0.48
75 (+)	21.88	3180	1657	3992	34503	57020	2739	-131	57151	57282	0.48
80 (+)	22.68	2212	1752	3024	34424	56889	2895	-147	57036	57183	0.49
85 (+)	23.49	1150	1835	1962	34337	56745	3033	-162	56907	57069	0.49
90 Side	24.30	0	1906	812	34243	56590	3149	-175	56765	56939	0.49

Minimum Margin of Safety: 0.47

2.7.2 Puncture

The puncture accident outlined in 10 CFR 71 Subpart F requires that the NAC-LWT cask suffer no loss of containment as a result of a 40-inch free fall onto an upright 6-inch diameter mild steel bar (puncture pin), which is supported on an unyielding surface. The impact orientation of the cask is required to be such that maximum damage is inflicted upon the cask.

Locations of cask impact with the puncture pin, which will cause maximum cask damage, are direct impact on the (1) cask side - midpoint, (2) center of the cask lid, (3) center of the cask bottom, and (4) cask port covers. Since an impact at any other location is less severe, the NAC-LWT cask is analyzed for the required puncture accident at these four locations.

2.7.2.1 Puncture - Cask Side Midpoint

2.7.2.1.1 Discussion

The NAC-LWT cask is analyzed for structural adequacy in accordance with the requirements of 10 CFR 71.73(c)(2), puncture (hypothetical accident condition). The cask is assumed to be in a horizontal position and dropped through a distance of 40 inches onto a 6-inch diameter, mild steel bar oriented vertically on an unyielding surface. The static structural evaluation of the cask is performed by classical analysis and the use of relations derived from destructive testing.

2.7.2.1.2 Analysis Description

Figure 2.7.2-1 illustrates the local cask midpoint section that has been evaluated for this analysis. It is composed of the initial 1.12-inch design thickness, Type XM-19 stainless steel outer shell, a 5.75-inch thick chemical copper lead middle shell, and a 0.75-inch thick, Type XM-19, stainless steel inner shell. The final design outer shell thickness is 1.20 inches. The additional thickness will only serve to enhance the ability of the NAC-LWT cask to resist the puncture event at the cask side midpoint.

During impact, the puncture pin is considered to apply a force (due to its assumed 47,000 psi dynamic flow stress) of 1.329×10^6 lbs to the cask outer shell midpoint in the inward normal direction. The neutron shield tank is conservatively not considered.

2.7.2.1.3 Detailed Analysis

For an impact occurring on the cask side, the required local cask outer shell thickness (t_r) for puncture integrity is calculated according to the Nelms equation (Shappert) as:

$$t_r = \left[\frac{W}{S_u} \right]^{0.71} = 0.655 \text{ in}$$

where:

W = cask design weight = 52,000 lbs

S_u = cask outer shell ultimate tensile strength at 300°F

= 94,300 psi

From the free body diagram in the sketch that follows, it can be determined that:

$$\text{Deceleration} = \frac{\text{Applied Load}}{\text{Cask Design Weight}} = \frac{1.329 \times 10^6}{52,000} = 25.57 \text{ g}$$

letting $W_B = W_L$

W_B = (weight of bottom assembly and limiter) × 25.57 g

= 94,865 lbs

W_L = (weight of cask lid and upper limiter) × 25.57 g

= 94,865 lbs

P = distributed linear load (lb/in)

$$= \frac{(52,000)(25.57) - (2)(94,865)}{199.75}$$

= 5706.7 lb/in

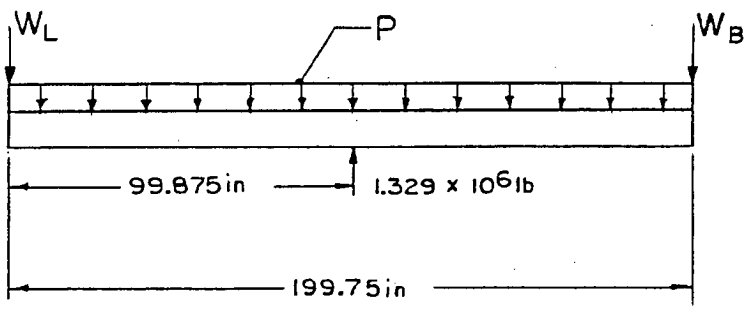

Cask Side Midpoint Puncture - Free Body Diagram

Then the maximum moment and shear are:

$$M_{max} = 99.875\ W_L + 0.50\ P\ (99.875)^2 = 3.80 \times 10^7\ \text{in-lb}$$

$$V_{max} = (1.329 \times 10^6)(0.50) = 6.645 \times 10^5\ \text{lb}$$

Since this loading is bounded by the 30-foot side drop loading (i.e., a cask deceleration force of 2.71×10^6 lbs, which produces $M_{max} = 6.36 \times 10^7$ in-lb and $V_{max} = 1.355 \times 10^6$ lbs; Section 2.7.1.2), the overall cask stresses are bounded by the 30-foot side drop, disregarding the local stresses in the area of the puncture pin. Since the outer shell thickness is 1.12 inches, the margin of safety, based on thickness, is +0.71.

2.7.2.1.4 Conclusion

For the pin puncture event at the cask midpoint, local deformation may occur in the region of the impact; however, the cask is demonstrated to have sufficient thickness to resist puncture. Therefore, the NAC-LWT cask satisfies the requirements of 10 CFR 71 for consideration of puncture at the cask midpoint.

2.7.2.2 Puncture - Center of Cask Closure Lid

2.7.2.2.1 Discussion

The NAC-LWT cask closure lid is analyzed for structural adequacy in accordance with the requirements of 10 CFR 71.73(c)(2), puncture (hypothetical accident condition). The cask is assumed to be inverted, with the lid downward, when dropped through a distance of 40 inches onto a 6-inch diameter, mild steel bar oriented vertically on an unyielding surface. The structural evaluation of the cask lid is performed by classical elastic analysis and the use of relations derived from destructive testing.

2.7.2.2.2 Analysis Description

The cask lid geometry is shown in Figure 2.7.2-2. It is fabricated of Type 304 stainless steel. The temperature-dependent material properties presented in Section 2.3 are used in this analysis.

During the impact, the puncture pin is considered to apply a pressure of 47,000 psi (assumed dynamic flow stress of mild steel) on the cask lid at the centerline of the exterior surface in the inward normal direction. The presence of an impact limiter is conservatively ignored.

The cask lid is vertically restrained at its mating surface with the cask body, which is located 8 inches below the top of the lid. For this analysis, the rotational restraint provided by the lid bolts is conservatively ignored.

2.7.2.2.3 Detailed Analysis

For the loading and displacement boundary conditions previously described, the bending behavior of the cask lid can be assessed by applying formulas from Case 2 (Roark, page 216) for a simply supported circular plate, concentrically loaded with a uniform load (q) over radius (r). The maximum radial and tangential stresses at the center of the plate are:

$$S_r = S_t = \frac{3qr^2}{2mt^2}\left[m + (m+1)\log\left(\frac{a}{r}\right) - (m-1)\frac{r^2}{4a^2}\right]$$

$$= 13{,}953 \text{ psi}$$

where:

r = 3 inches

a = 6.6875 inches

ν = Poisson's Ratio = 0.275

m = $1/\nu$ = 3.636

q = 47,000 psi

t = 8.0 inches

then

$$M.S. = \frac{S_y}{S_r} - 1 = \underline{+0.61}$$

where:

S_y = 22,500 psi at 300°F

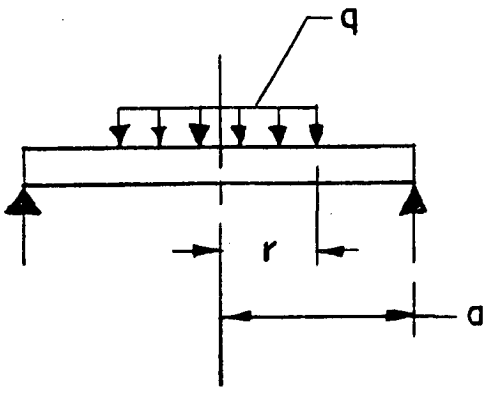

Lid Plate Loading Diagram

Neglecting all end restraint (from the bolts), the slope θ at the edge is:

$$\theta = \frac{3qr^2a\,(m-1)}{Emt^3}$$

$$= 0.00045 \text{ radians } (0.0258°)$$

where:

$E = 27 \times 10^6$ psi

The distance from the assumed support to the outer seal is 1.4 inches. The maximum vertical displacement (D) at the outer seal is assessed from the slope (θ) and the closure lid geometry.

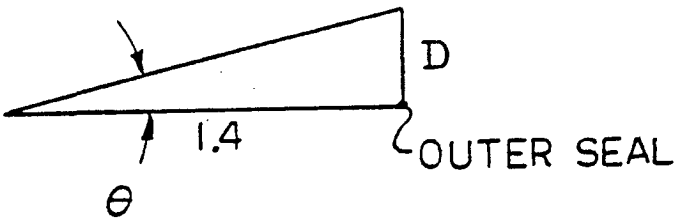

Displacement Geometry

$D = 1.4 \tan \theta = 0.0006$ in

Since this value represents a negligible loss of seal pressure (five times less than machine tolerance), the seals are unaffected by the puncture impact at the lid centerline.

It is obvious by inspection that the puncture pin does not penetrate the cask lid. The puncture pin load applied to the cask is:

$$F_{pp} = \pi r^2 S_{DFS}$$

$$= 1.329 \times 10^6 \text{ lbs}$$

where:

$r = 3.0$ inches (pin radius)

$S_{DFS} = 47{,}000$ psi (assumed dynamic flow stress)

Then for static equilibrium, the cask deceleration force is a maximum of 1.329×10^6 lbs. Since this loading is bounded by the 30-foot top end drop loading (a cask deceleration force of 3.12×10^6 lbs; Section 2.7.1.1), the cask stresses are bounded by the 30-foot top end drop stress calculations.

2.7.2.2.4 Conclusion

For a pin puncture impact on the cask closure lid, local deformation may occur in the region of the impact. However, using conservative loading and displacement boundary conditions, it is determined that (1) the minimum margin of safety is +0.61, (2) containment is maintained by the seals, (3) the cask lid puncture resistance exceeds puncture requirements, and (4) overall cask stresses are enveloped by the 30-foot top end drop analysis. Therefore, the NAC-LWT cask satisfies the requirements of 10 CFR 71 for consideration of puncture on the cask closure lid.

2.7.2.3 Puncture - Center of Cask Bottom

2.7.2.3.1 Discussion

The NAC-LWT cask bottom is analyzed for structural adequacy in accordance with the requirements of 10 CFR 71.73(c)(2), puncture (hypothetical accident condition). The cask is assumed to be vertical and upright when dropped through a distance of 40 inches onto a 6-inch diameter, mild steel bar oriented vertically on an unyielding surface. The structural evaluation of the cask bottom is performed by classical elastic analysis and the use of relations derived from destructive testing.

2.7.2.3.2 Analysis Description

The cask bottom geometry shown in Figure 2.7.2-3 depicts a 10.50-inch thick cylindrical composite of chemical copper lead and Type 304 stainless steel. The temperature-dependent material properties in Section 2.3 are used in this analysis.

During the impact, the puncture pin is considered to apply a pressure of 47,000 psi (assumed dynamic flow stress of mild steel) on the cask bottom exterior surface in the inward normal direction. The presence of an impact limiter is conservatively ignored.

Vertical and rotational restraint is provided at the 21.00-inch diameter for the composite section by the stainless steel ring with an inside diameter of 21.00 inches and an outside diameter of 28.62 inches.

2.7.2.3.3 Detailed Analysis

For the loading and displacement boundary conditions described, the bending behavior of the bottom 3.50-inch thick plate can be assessed by applying formulas from Case 7 (Roark, page 218) for a fixed edge circular plate, with a concentric uniform load (q) over a circular area of radius (r). Conservatively neglecting the strength of the lead backing, the maximum radial, tangential, and shear stresses at the fixed edge of the bottom 3.50-inch thick plate are:

$$S_r = \frac{3qr^2}{2t^2}\left[1 - \frac{r^2}{2a^2}\right] = 49{,}682 \text{ psi (extreme fiber bending)}$$

$$S_t = \frac{S_r}{m} = 13{,}664 \text{ psi}$$

$$S_s = \frac{qr^2}{2at} = 5{,}755 \text{ psi}$$

where:

q= 47,000 psi (assumed dynamic flow stress of puncture pin)

t= 3.50 inches

r= 3 inches

a= 10.50 inches radius

m = 1/ν = 1/Poisson's ratio = 3.636

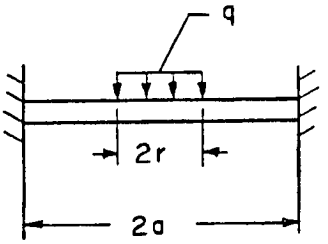

Bottom Plate Loading Diagram

Since the maximum temperature of the cask bottom is less than 300°F for the 130°F ambient temperature hot case (Section 3.4.2), the minimum ultimate strength (S_u) and design stress intensity (S_m) are 66,000 and 20,000 psi, respectively. For accident conditions, the section stress intensity resulting from $P_m + P_b$ stresses must not exceed 66,000 psi (lesser value of 3.6 S_m or S_u); the section stress intensity resulting from P_m stress must not exceed 46,200 psi (lesser value

of 2.4 S_m or 0.7 S_u). Averaging the radial bending stress, the fixed edge cross-section primary bending stress is:

$$S_r' = \frac{S_r}{2} = 24,841 \text{ psi}$$

Conservatively, the maximum shear stress is:

$$S_{smax} = \left[\frac{(S_r' + S_t)^2}{2} + S_s^2\right]^{0.5} = 27,815 \text{ psi}$$

Then the maximum stress intensity and margin of safety associated with $P_m + P_b$ stresses are:

$$S.I. = 2S_{smax} = 55,630 \text{ psi}$$

$$M.S. = \frac{S_u}{S.I.} - 1 = \underline{+0.186}$$

Clearly, the addition of S_s and S_t for the P_m stress intensity is less critical than the above stress combination.

The required local bottom plate thickness (t_r) for puncture integrity is calculated according to Shappert as:

$$t_r = \left[\frac{W}{S_u}\right]^{0.71} = 0.844 \text{ in}$$

where:

W = cask design weight = 52,000 lbs

S_u = 66,000 psi (bottom plate ultimate tensile strength at 300°F)

$$M.S. = \frac{1.12}{0.844} - 1 = \underline{+0.327}$$

The puncture pin load applied to the cask is:

$$F_{pp} = \pi r^2 S_{DFS}$$
$$= 1.329 \times 10^6 \text{ lbs}$$

where:

r = 3.0 inches (pin radius)

S_{DFS} = 47,000 psi (assumed dynamic flow stress)

Then for static equilibrium, the cask deceleration force is a maximum of 1.329×10^6 lbs. Since this loading is bounded by the 30-foot bottom end drop loading (i.e., a cask deceleration force of 3.12×10^6 lbs; Section 2.7.1.1), the cask stresses are bounded by the 30-foot bottom end drop stress calculations.

2.7.2.3.4 Conclusion

For a pin puncture impact on the cask bottom, local deformation may occur in the region of the impact. However, using conservative loading, it is determined that (1) the minimum margin of safety is +0.186, (2) the bottom plate puncture resistance exceeds puncture requirements, and (3) overall cask stresses are enveloped by the 30-foot bottom end drop analysis. Therefore, the NAC-LWT cask satisfies the requirements of 10 CFR 71 for consideration of puncture on the cask bottom.

2.7.2.4 Puncture - Port Cover

The port cover of the NAC-LWT cask is analyzed for structural adequacy in accordance with the requirements of 10 CFR 71.73(c)(3), puncture (hypothetical accident condition). The cask is assumed to be in a horizontal position and dropped through a distance of 40 inches onto a 6-inch diameter, mild steel bar oriented vertically on an unyielding surface. The structural evaluation of the port cover is performed by classical elastic analysis methods.

2.7.2.4.1 Analysis Description

The port cover geometry shown in Figure 2.7.2-4 is typical for the two port cover locations on the cask. Each cover centerline is located 11 inches axially below the top of the cask. In this region, the cask body is a Type 304 stainless steel ring in excess of 6 inches thick. The port cover material is SA-705, Grade 630, precipitation-hardened stainless steel. The temperature-dependent material properties presented in Section 2.3 are used in this analysis.

During the impact, the puncture pin is considered to apply a pressure of 47,000 psi (assumed dynamic flow stress of mild steel) on the port cover and the surrounding exterior surface of the cask in the inward normal direction. The existence of the top impact limiter is conservatively ignored.

The port cover rotation at its mating surface with the cask body is restrained by the bolted flange configuration of the cover. The port cover is also restrained from rotation in its flange region due to the puncture pin pressure acting on its exterior surface.

2.7.2.4.2 Detailed Analysis

Local Impact Region - Port Cover

For the loading and displacement boundary conditions described, the bending behavior of the port cover is assessed by applying formulas from Case 6 (Roark, page 217) for a uniformly loaded circular plate with fixed edges. The maximum radial stresses and the inward deflection of the port cover are, respectively:

$$S_r = \frac{3qa^2}{4t^2} = 74{,}569 \text{ psi}$$

$$y = \frac{3qa^4(1 - \nu^2)}{16Et^3} = 0.0013 \text{ in}$$

where:

q = 47,000 psi

a = 1.469 inches

t = 1.01 inches

E = 27.6×10^6 psi (at 200°F)

ν = Poisson's ratio = 0.287

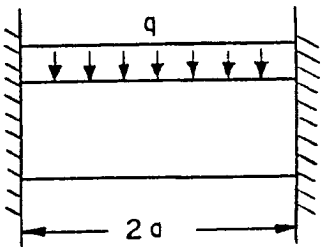

Port Cover Plate Loading Diagram

Since the maximum port cover temperature is less than 300°F for the 130°F ambient temperature hot case (Section 3.4.2), the yield strength of the port cover (conservatively based on 300°F) is 93,100 psi. Therefore, the minimum margin of safety is +0.25. Since the clearance between the port cover and the valve exceeds 0.0013 inch, the port cover does not contact the valve during impact.

Local Impact Region - Upper Ring

Locally, the potential puncture pin force due to its dynamic flow stress is:

$$F_{pp} = (3)^2 \pi(47{,}000) = 1.329 \times 10^6 \text{ lbs}$$

This force acting on the 7-inch thick stainless steel cask body produces a maximum shear stress:

$$S_s = F_{pp} / [6\pi(7)] = 10{,}071 \text{ psi.}$$

On the annular ring surrounding the port cover (i.e., from 4.53-inch to 6.00-inch diameter), the bearing stress on the cask is:

$$S_{br} = F_{pp} / \pi [(6.00)^2 - (4.53)^2] = 109{,}317 \text{ psi.}$$

If deformation of the cask and/or pin permits the pin to impact the top of the port cover, the bearing area increases to:

$$A_b = 0.25\pi [(6.00)^2 - (4.53)^2 + (4.50)^2 - (2.875)^2] - 0.75\pi (.45)^2$$

$$= 21.09 \text{ in}^2$$

Then, the bearing stress is:

$$S_{br} = \frac{F_{pp}}{A_b} = 63{,}016 \text{ psi}$$

The stress at the cask seal area is less because the load (F_{pp}) distributes over a larger area. The allowable dynamic yield bearing stress of Type 304 stainless steel is 65,130 psi, i.e., 1.67 (MIL-HDBK-5A) x 39,000 psi dynamic yield strength. The allowable dynamic ultimate bearing stress of Type 304 stainless steel is 132,000 psi, i.e., 2.0 (MIL-HDBK-5A) x 66,000 psi ultimate tensile strength. Thus, the minimum yield margin of safety is +0.03 and the ultimate margin of safety is +1.09 for the bearing stress state at the cask and port cover mating surface.

Cask Body Stresses

The NAC-LWT cask is analyzed for structural adequacy during a puncture pin impact on a port cover. The cask is assumed to be in a horizontal position and dropped through a distance of 40 inches, impacting the pin on a port cover, which is located near the upper end of the cask. The static structural evaluation of the cask is performed by classical elastic analysis methods.

During an impact, the puncture pin is considered to apply a total force of 1.329×10^6 lbs (Figure 2.7.2-5) to the cask at the port cover in the inward normal direction assuming a pin dynamic flow

stress of 47,000 psi. Vertical restraint is provided by the bottom impact limiter and the puncture pin located 11 inches from the top of the cask.

For the loading and displacement boundary conditions described, the free body diagram (Figure 2.7.2-5) is evaluated. For static equilibrium, the cask deceleration force (F_g) and reaction (R_r) are determined by solving the following simultaneous equations:

$$1.329 \times 10^6 - F_g + R_r = 0$$

$$F_g (89.15) - 182.75 R_r = 0$$

then

$F_g = 2.595 \times 10^6$ lbs, and

$R_r = 1.266 \times 10^6$ lbs

Since this loading is bounded by the 30-foot side drop loading (a cask deceleration force of 3.12×10^6 lbs; Section 2.7.1.2), the cask stresses for the puncture pin impact are bounded by the 30-foot side drop accident.

2.7.2.4.3 Alternate Port Cover – Puncture

Analyses presented evaluate the consequences of the puncture event on the port cover, attachment bolts stresses and the inertial load acting on the port cover to reduce the compressive load on the primary O-ring. Also, a bounding analysis evaluating the effect of thermal expansion on the port cover bolt stress and compressive load on the primary O-ring due to extreme temperatures acting on the cask is presented in the section titled "Alternate Port Cover Differential Thermal Expansion."

The alternate port cover design is shown in Figure 2.6.10.3. The alternate port cover design includes the primary O-ring between the inner face of the port cover barrel and the sealing surface located in the cask top forging. The secondary (test) O-ring is located in a groove on the barrel of the port cover body. Both O-rings are manufactured from Viton®. The alternate port cover body is fabricated from Type 630, 17-4 PH precipitation-hardened stainless steel. The alternate port cover bolts are SA-193 GR B6 (Type 410 stainless steel) socket-head cap screws.

The analysis presented in the section titled "Local Impact Region – Port Cover" evaluates the load created by a mild steel pin impinging directly on a portion of the port cover. While the analysis is conservative, it does demonstrate the adequacy of the alternate port cover; it does not represent how the cask is expected to be configured at the time of the puncture event. A more representative analysis includes the cask impact limiters, which would be installed at the time of the puncture event.

The puncture accident is the third in the succession of hypothetical accidents that the cask must sustain. The impact limiters remain attached subsequent to the 30-foot free drop, as shown in Section 2.6.7.4. It is concluded in Section 2.7.1.6 that the hypothetical crush accident does not apply to the NAC-LWT cask. Therefore, the impact limiters will be attached to the cask prior to the cask dropping onto the mild steel pin. Both port covers are located near the top of the cask, underneath the impact limiter. When the top impact limiter strikes the mild steel pin, it will support the top end of the cask, while the bottom of the cask continues to translate then begin to rotate about the mild steel pin as a pivot point, until the bottom impact limiter contacts the unyielding surface. The bottom impact limiter will then absorb the cask's remaining kinetic energy. There is a load on the top of the cask that is assumed to be equivalent to the cask's weight. Furthermore, it is assumed to act directly on the alternate port cover, when in actuality, it will load the impact limiter immediately above the alternate port cover. The impact limiter will act to spread the load of the pin on the cask, reducing the actual load on the alternate port cover.

The bearing load (S_b) on the alternate port cover seal surface is:

$$S_b = W_c/A_s = 18{,}500 \text{ psi}$$

where:

W_c = Design basis weight of the loaded NAC-LWT cask = 52,000 lbs

A_s = Total concentric ring bearing area at inner face of port cover = 2.81 in^2

Inner ring: $A_i = \pi/4((D_{outer})^2 - (D_{inner})^2)$

$= \pi/4((2.065 \text{ in})^2 - (1.63 \text{ in})^2) = 1.26 \text{ in}^2$

Outer ring: $A_o = \pi/4((D_{outer})^2 - (D_{inner})^2)$

$= \pi/4((2.77)^2 - (2.387 \text{ in})^2) = 1.55 \text{ in}^2$

$A_s = 2.81 \text{ in}^2$

The maximum port cover temperature is less than 300°F for the 130°F ambient temperature hot case, shown in Section 3.4.2; the yield strength of Type 304 stainless steel, the material of the top forging, is 22,500 psi at 300°F. The port covers are installed in the upper forging. Under these conditions, the minimum margin of safety is +0.17. Therefore, the load on the bearing surface is within the elastic range. The bolt preload will maintain the necessary load on the Viton® O-ring, thereby maintaining the containment seal.

It is also postulated that when the package is in a horizontal orientation and the port cover is oriented toward the impact surface, a g-load is applied to the port cover that would reduce the load on the inner end O-ring during deceleration from a 30-ft free drop. To evaluate this

condition, a three-dimensional finite element model of the port cover is used. The resulting load on the bolts is then calculated, including bolt preload, and the resulting sealing force evaluated.

Two loading cases are evaluated. One load case includes the bolt preload force, normal pressure, and the 60 g inertia load with the material temperatures assumed to be 250°F. The second load case evaluates the bolt preload and the accident pressure with the materials at 845°F. This second load case postulates the cask post-fire accident conditions containing a design basis fuel assembly with 100% of the fuel rods ruptured, as described in Section 3.5.4. The maximum cavity pressure acts on the inner face of the port cover to reduce the compressive load on the O-ring.

The results are summarized as:

Load Case	Preload + Normal Pressure + 60 g	Preload + Accident Pressure
Evaluation Temperature (°F)	250	845
Calculated Seal Force (lbs)	808	676
Percent O-ring compression (20-30% compression to maintain seal)	25.2[1]	25.2[1]
Bolt Tensile Force (lbs)	1794	1541
Bolt Stress (based on Tensile Stress Area) (psi)	28,931	24,850
Bolt Margin of Safety	1.72	1.66

[1] Maximum compression possible due to metal-to-metal contact with O-ring fully compressed in O-ring groove.

This table presents a summary of the port cover bolt stresses resulting from the cask operating in two environmental extremes. In the extreme cold case, the "preload + normal pressure + 60 g inertial" bolt stress was added to the thermal stress as a worst case condition. In the fire case, only the containment pressure load is assumed to act on the port cover and load the bolts.

Alternate Port Cover Differential Thermal Expansion

The alternate port cover primary containment sealing surfaces are located at the inner end of the port cover, where it interfaces with the top forging of the cask. The coefficients of thermal expansion of Type 304 stainless steel and Type 630, 17-4 PH precipitation hardened stainless steel are sufficiently different to warrant examination of the consequences of extreme temperature differences on the compressive load on the primary O-ring and on the port cover bolt stresses. The port cover bolt material SA193 B6 has a coefficient of thermal expansion that is essentially equal to that of Type 304 stainless steel. Also, for the purposes of the analyses presented, the cask is assumed to be loaded at 70°F.

Extreme Cold

The coefficient of thermal expansion for the Type 304 stainless steel top forging is greater than that of the 17-4 PH precipitation hardened stainless steel port cover. When the cask temperature is reduced to -40°F, after loading at a 70°F ambient temperature, the cask top forging will contract at a greater rate than does the port cover. Since the top forging contracts more than the port cover, the compressive load between the port cover and the top forging will increase. However, since the top forging and port cover bolts contract more than the port cover, the port cover will be pushing against the port cover bolts, increasing the bolt tensile stress. Figure 2.7.2-6 presents a sketch of the port cover dimensions used in this analysis. The change in length of the port cover is:

$$\Delta L_{pc} = \Delta T\, \alpha\, L = 110°F \text{ x } (5.88E\text{-}6 \text{ in/in-°F}) \text{ x } 2.62 \text{ inches} = 1.695E\text{-}3 \text{ inches}$$

where:

ΔT = the change in temperature from 70°F to –40°F,

α = the thermal expansion coefficient,

L = the length of the section.

The top forging decreases in length:

$$\Delta L_{cask} = 110 \times (8.13E\text{-}6 \text{ in/in-°F}) \text{ x } 2.62 = 2.343E\text{-}3 \text{ inches}$$

The change in length of the port cover bolt is then:

$$\Delta L = 2.343E\text{-}3 - 1.695E\text{-}3 = 6.48E\text{-}4 \text{ inches}$$

The uniform strain in the bolt shank is then:

$$e_b = \Delta L / L = 6.48E\text{-}4 \text{ inches}/1.19 \text{ inches} = 5.445E\text{-}4 \text{ in/in}$$

where:

L is the length of the shank of the bolt.

The resulting bolt tensile stress is:

$$\sigma = e_b E = 5.445E\text{-}4 \times 30.3E6 \text{ psi} = 16{,}500 \text{ psi}$$

where:

E = the bolt Modulus of Elasticity.

The increase in tensile stress, due to differential thermal expansion between the port cover and the bolt and top forging is presented in a summary table at the end of this section. A margin of safety of +0.87 is maintained for the port cover bolts.

Extreme Heat

When the cask is heated from the 70°F ambient temperature at cask loading, the top forging and the port cover bolts will expand more than the port cover, resulting in the primary O-ring having to seal a small gap between the inner end of the port cover and the top forging. The bounding condition for minimum surface contact is during the accident fire condition. Figure 3.5-13 shows the peak temperature of the port cover bolt threads is 807°F, which occurs at 30 minutes into the fire accident event. The corresponding temperature of the primary containment O-ring at 30 minutes is 472°F. The average temperature (807°F + 472°F) of 640°F is considered representative of the temperature change expected for the port cover.

$$\Delta L_{pc} = \Delta T \, \alpha \, L = 570°F \times (5.93E\text{-}6 \text{ in/in-°F}) \times 2.62 \text{ inches} = 8.9E\text{-}3 \text{ inches}$$

where ΔT is the change in temperature from 70°F to 640°F, α is the thermal expansion coefficient, and L is the length of the section. For the top forging, the change in length is:

$$\Delta L_{cask} = 570°F \times (9.56E\text{-}6 \text{ in/in-°F}) \times 2.62 = 1.43E\text{-}2 \text{ inches}$$

The gap resulting between the bottom of the port cover and the bottom of the port cover housing is then:

$$\text{Gap} = 1.43E\text{-}2 - 8.9E\text{-}3 = 5.40E\text{-}3 \text{ inches.}$$

The inner end of the port cover and the sealing surface in the top forging are not in contact during the maximum temperature condition reached in the fire accident. However, the O-ring, located in a groove at the inner end of the port cover fills the 0.0054-inch gap because the O-ring remains under compressive load. The seal groove has a nominal depth of 0.104 inches. The calculated gap between the metallic sealing surfaces during the fire transient is 0.0054 inch. The O-ring fills this gap and is compressed between the O-ring groove and the top forging. The total depth available for the O-ring to occupy is 0.104 + 0.0054 = 0.1094 inch. The O-ring nominal diameter is 0.139 inch. The percent O-ring compression that remains is:

$$\% \text{ Compression} = [(0.139 - 0.1094)/ 0.139] \times 100 = 21.3\%$$

Conservatively, thermal expansion of the O-ring during heating is ignored. According to the O-ring manufacturer's design data, O-ring compression between 20% and 30% is satisfactory to ensure that a seal is maintained. In addition, according to the O-ring manufacturers design data, the O-ring can withstand pressure in excess of 1,000 psi. The maximum hypothetical accident pressure in the cask is calculated to be 168 psig. Therefore, the primary containment O-ring is adequate to retain the maximum hypothetical accident condition pressure.

The changes in port cover bolt stresses due to extreme changes in temperature are presented as follows.

Load Case	Extreme Cold	Fire Accident
Evaluation Temperature (°F)	-40	847
Thermal Stress on Bolt (psi)	16,500	0
Bolt Stress (based on Tensile Stress Area) (psi)	45,431	5,855
Bolt Margin of Safety	0.87	10.3[1]

[1] Extrapolated bolt yield strength of 66.1 ksi at 845°F.

2.7.2.4.4 Conclusion

For the pin puncture event, local deformation may occur in the region of impact. However, it is demonstrated by use of conservative loading that (1) a positive margin of safety for the alternate port cover for local stresses is provided; (2) containment is maintained by the O-rings; and (3) cask bending stresses are enveloped by the 30-foot side drop analysis. Therefore, the NAC-LWT cask satisfies the requirements of 10 CFR 71 for a puncture impact on the cask at the port cover location.

2.7.2.5 Puncture Accident - Shielding Consequences

In order to comply with 10 CFR 71, calculations were performed for the hypothetical accident described in Section 2.7. In this case, a puncture occurs, which causes a reduction in the cask shielding resulting from a total loss of the liquid neutron shield. The resulting dose rates do not exceed the limits of 49 CFR 173. Details of the shielding analysis are presented in Section 5.4.

2.7.2.6 Puncture - Conclusion

The analyses of Section 2.7.2 demonstrate the structural and shielding adequacy of the NAC-LWT cask for a puncture pin impact on the (1) cask side midpoint, (2) center of cask closure lid, (3) center of cask bottom, and (4) cask port cover. Therefore, the NAC-LWT cask satisfies the structural requirements of 10 CFR 71.73(c)(2) and the shielding requirements of 49 CFR 173 for the puncture event.

Figure 2.7.2-1 NAC-LWT Cask Midpoint Section

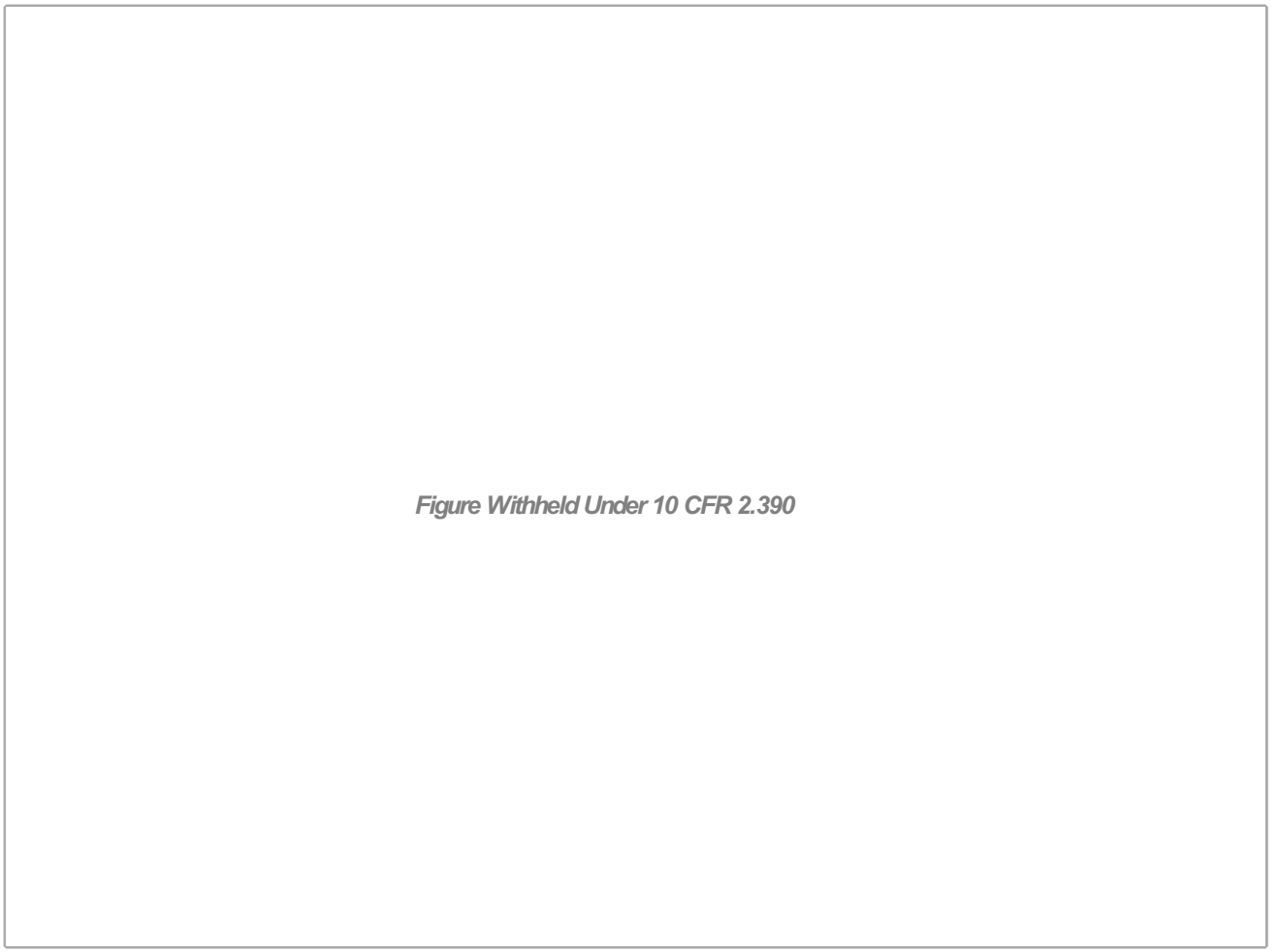

* The outer shell thickness conservatively used in the analysis was 1.12 inches. This yields conservative results since the actual outer shell thickness is 1.20 inches.

Figure 2.7.2-2 Cask Lid Configuration

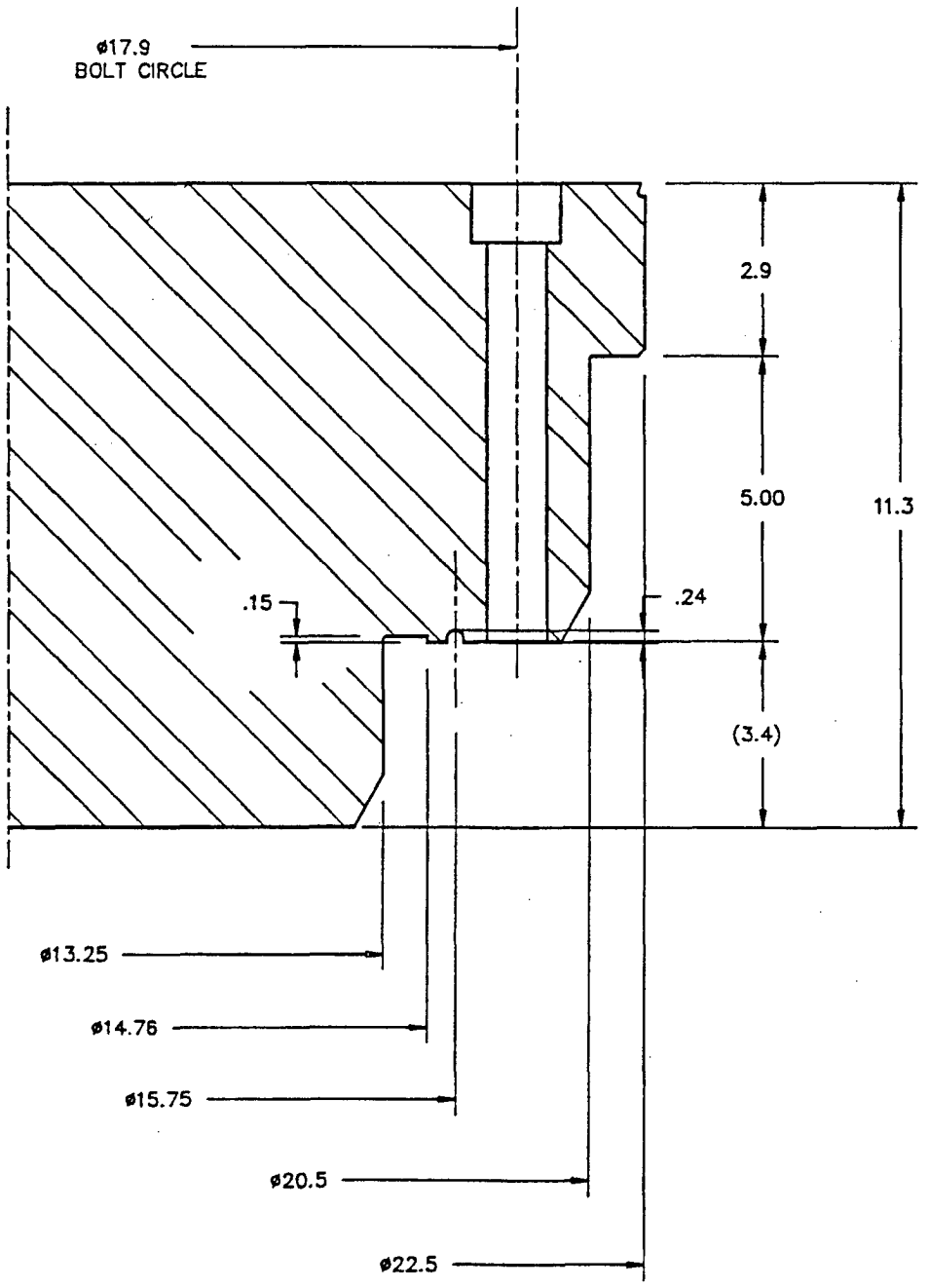

Figure 2.7.2-3 NAC-LWT Cask Bottom Design Configuration

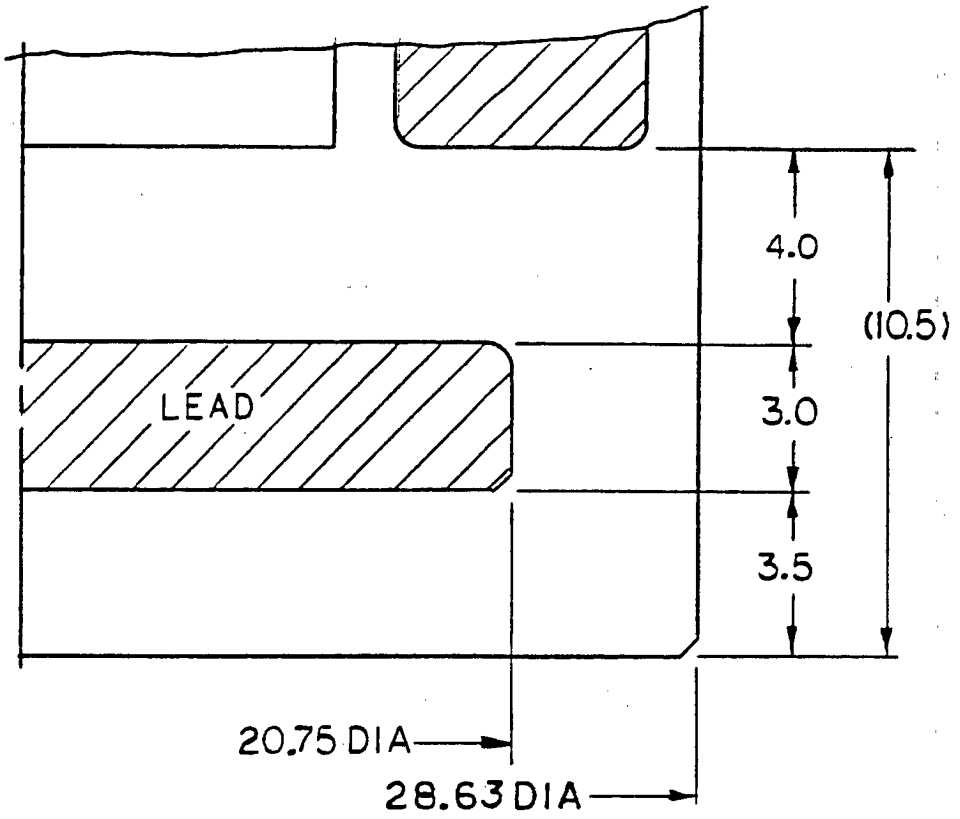

Figure 2.7.2-4 Port Cover Geometry

Figure 2.7.2-5 Puncture of Cask at Valve Cover Region

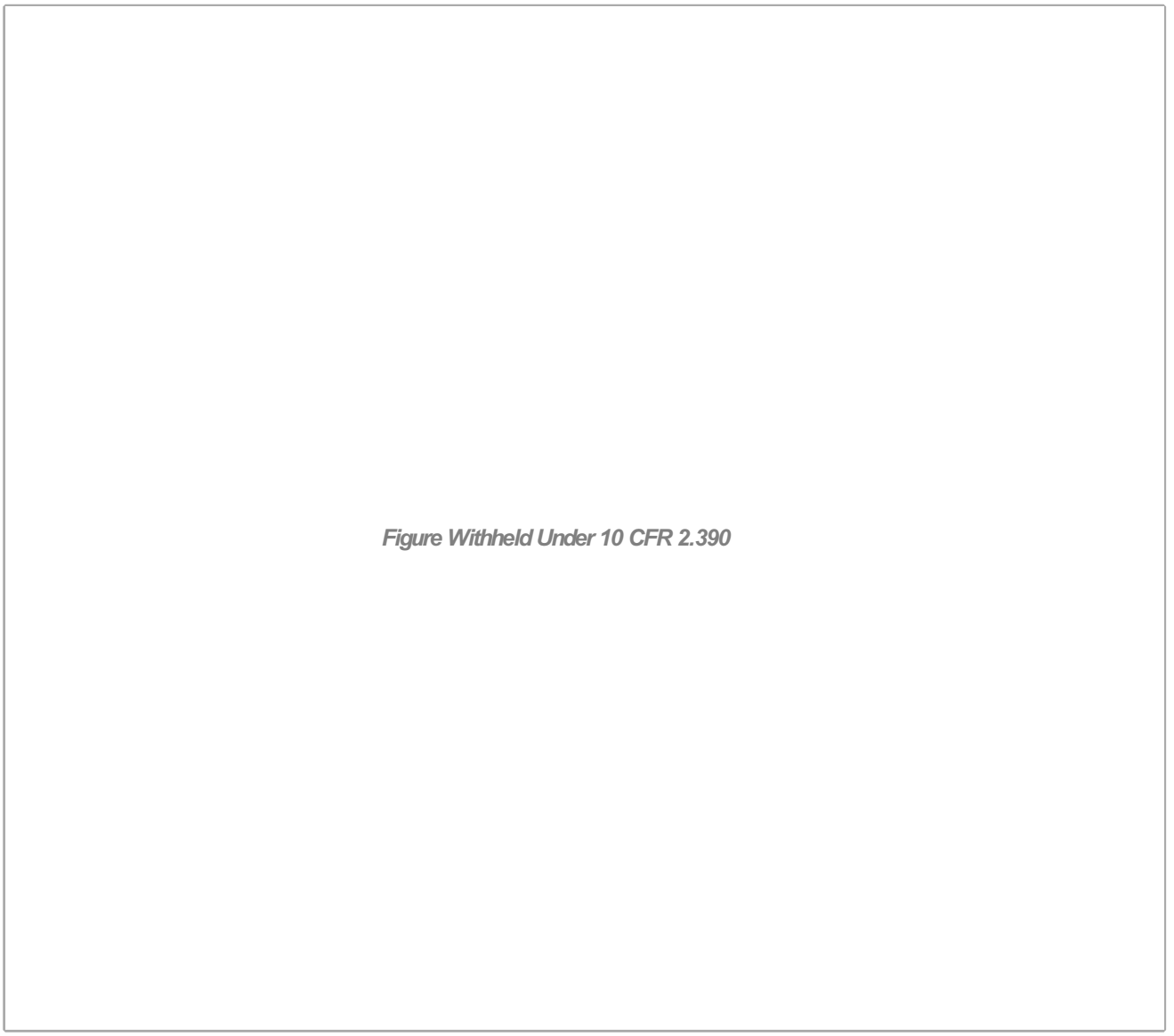

Figure 2.7.2-6 Alternate Port Cover Thermal Analysis Geometry

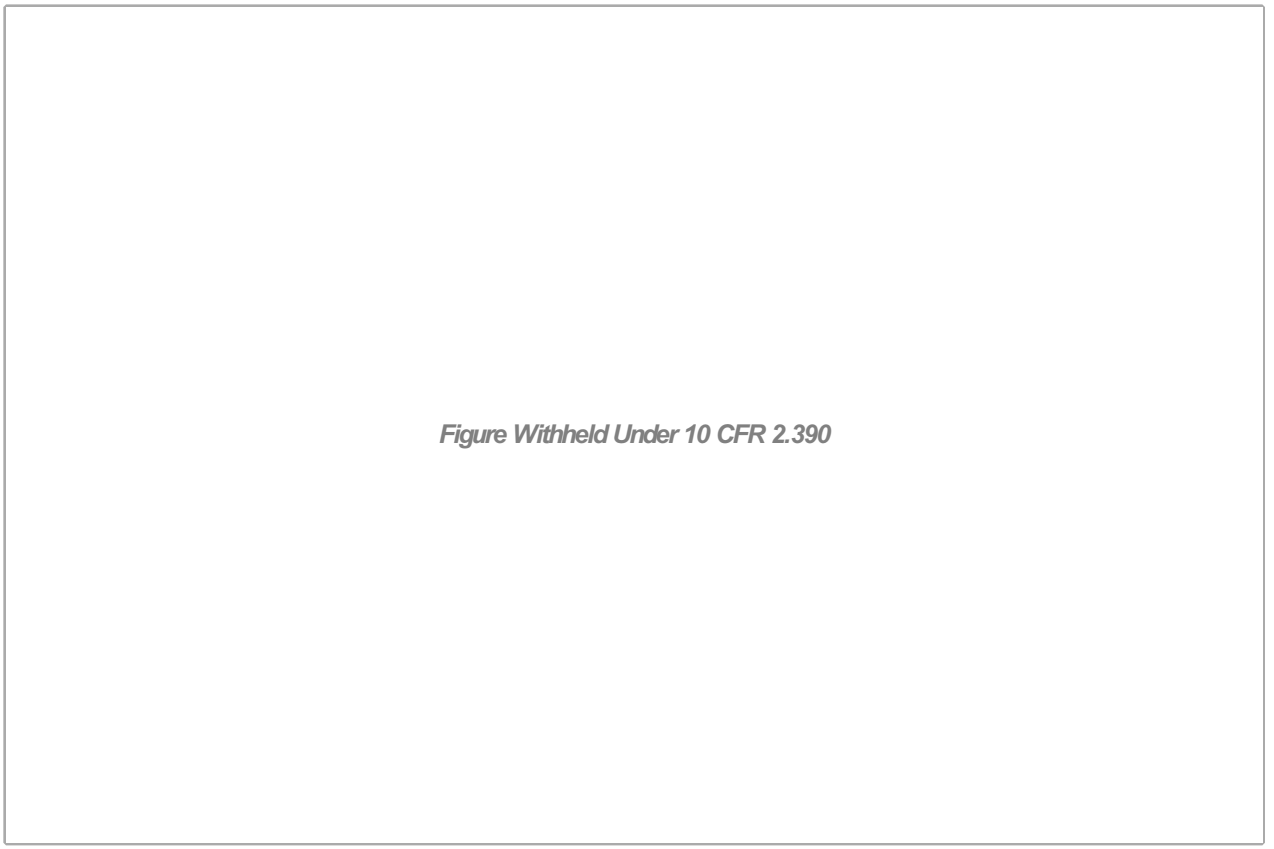

2.7.3 Fire

2.7.3.1 Discussion

The NAC-LWT is analyzed for structural adequacy in accordance with the requirements of 10 CFR 71.73 (c)(3) fire (hypothetical accident condition). The cask is assumed to be subjected to a surrounding environment of 1,475°F for a period of 30 minutes. The structural evaluation of the cask is performed using a linear elastic finite element model.

2.7.3.2 Thermal Stress Evaluation

Differential thermal expansion stresses and through-thickness thermal gradient stresses are induced in the NAC-LWT as a result of the thermal (fire) accident event. All of these thermal stresses are classified as secondary, displacement-limited stresses according to the ASME Code. Limits on secondary stresses do not apply for accident conditions (Table 2.1.2-1); the secondary stresses, in themselves, do not compromise the integrity of the cask. To satisfy the requirement regarding the extreme total stress intensity range as specified in Paragraph C.7 of Regulatory Guide 7.6 (as discussed in Section 2.1.3.3), a finite element analysis is performed to determine the maximum stresses associated with the thermal (fire) accident event.

The thermal analysis of the NAC-LWT for the fire accident event is performed using an ANSYS two-dimensional, axisymmetric finite element model described in Section 3.5. For the corresponding structural analyses, the elements are changed to be PLANE42, a two-dimensional structural element. The thermal stress model includes the lead, with the lead allowed to expand against the walls of the cavity that contains the lead. No gap is considered to exist between the lead and stainless steel walls. The elastic modulus is used for lead as this results in a pressure being applied to the inner and outer shell walls that is conservative. Displacement boundary conditions were added to prevent rigid body motion from occurring.

To ensure that the maximum thermal stress is calculated, the temperatures for each time step are employed to compute the corresponding stresses. A uniform temperature of 70°F is input as the initial stress free condition of the structural finite element model. Temperature dependent material properties allow the ANSYS model to use the correct properties for each nodal temperature. The temperature dependent material properties are obtained from the ASME Code, Section III, Division 1, Appendix I. Material properties from the ASME Code, Section III, Subsection NH (1995 Edition), Appendix I-14 are used for temperatures greater than 800°F. The material properties of XM-19 at elevated temperatures are not listed in Subsection NH. Since Type 304 and Type 316 stainless steel belong to the same austenitic stainless steel group as

XM-19 and exhibit the same mechanical behavior, the material properties of Type 304 and Type 316 stainless steel are used at elevated temperatures.

The maximum primary plus secondary nodal stress intensity, calculated for the containment vessel by the ANSYS model for all the time steps considered in the fire accident, is 165 ksi, which occurs at the outer shell surface near the bottom of the trunnion.

To conservatively evaluate the stress states, the maximum primary plus secondary (P+Q) stress intensity in the containment vessel (165 ksi) is used. It is demonstrated in other sections of the SAR that the maximum combined primary membrane plus primary bending stress intensities for all of the other normal conditions of transport and hypothetical accident conditions satisfy Regulatory Guide 7.6, i.e., they are less than 1.0 S_u. It is, therefore, conservative to assume that the maximum allowable value for the primary stresses, 1.0 S_u, actually develops within the NAC-LWT containment vessel.

The maximum S_u value for the containment vessel material is 100.0 ksi (type XM-19 stainless steel). Adding this value to the maximum P+Q stress intensity calculated for the thermal accident, the maximum total primary plus secondary stress intensity is 165 + 100 = 265 ksi. The maximum possible stress intensity range, S_n, is conservatively assumed to be twice this value, or S_n = (2) (265) = 530 ksi. The appropriate alternating stress intensity, S_{alt}, is one-half of this value, or S_{alt} = (0.5)(530) = 265 ksi. To account for the temperature effects, the variation in modulus of elasticity of the material is factored into the calculation of S_{alt} as:

$$S_{alt}(1250°F) = (E_{70}/E_{1250})(S_{alt})$$
$$= [28.3 \times 10^6/20.8 \times 10^6](265)$$
$$= 360.6 \text{ ksi}$$

At 1,250°F, Appendix T-1420 of the ASME Code, Section III, Subsection NH (1995 Edition with Addenda through 1997), limits the 10-cycles fatigue strain, ε_t, to 0.0316 inch/inch for 304 stainless steel and to 0.0266 inch/inch for Type 316 stainless steel. In accordance with Appendix I-14 of Subsection NH of the ASME Code, Section III (1995 Edition with Addenda through 1997), the modulus of elasticity for Type 304 and Type 316 stainless steel at 1,250°F is 20,800 ksi. Therefore, the adjusted ASME allowable alternating stress, S_{alt}, for austenitic stainless steel at 10 cycles at 1,250°F is limited to (0.0266)(20,800 ksi) or 553.3 ksi.

The margin of safety is:

$$MS = (553.3/360.6) - 1 = +0.53$$

Considering the conservative assumptions used in the evaluation, i.e., (1) use of the allowable primary stress rather than the actual value; (2) assuming fully reversing primary and secondary stress states to determine stress intensity ranges; and (3) assuming the worst case fire transient stresses, the actual margin of safety is considered to be significantly larger than +0.53. Thus, the requirements of Paragraph C.7 of Regulatory Guide 7.6 are satisfied.

2.7.3.3 Bolts - Closure Lid (Hypothetical Accident - Fire)

During the hypothetical fire accident, the NAC-LWT cask closure and lid bolts are conservatively predicted to experience a temperature of 642°F, which is the maximum average temperature of the lid bolts. To evaluate the bolt stress, a temperature of 750°F is conservatively used. Mating surfaces between the cask lid and cask body maintain contact since the coefficient of thermal expansion for the lid is larger than the coefficient of thermal expansion for the bolts. The cask closure lid and body (top forging) are forgings of SA-182, Type 304 stainless steel, whereas the lid bolts are SA-453, Grade 660 high alloy steel bolting material. Considering the temperature increase in the fire accident, the maximum thermal stress induced in a lid bolt resulting from the lid and bolt expansion is:

$$S_{th} = \Delta T[E_{\ell}\alpha_{\ell} - E_b\alpha_b]$$

$$= 14{,}500 \text{ psi}$$

where:

ΔT = 680°F, thermal differential (750°F - 70°F); the fire temperature less the ambient temperature when the bolts were torqued

$E_t = 24.4 \times 10^6$, lid modulus at 750°F

$\alpha_t = 9.76 \times 10^{-6}$, lid expansion coefficient at 750°F

$E_b = 23.8 \times 10^6$, bolt modulus at 750°F

$\alpha_b = 9.11 \times 10^{-6}$, bolt expansion coefficient at 750°F

Bolt preload is 57,497 psi (Section 2.1.3.2.2) and the pressure stress for a 168 psig internal pressure is:

$$S_p = 3.36 \times 1342 = 4{,}509 \text{ psi}$$

where:

3.36 is the ratio of the pressures, (168 psi/ 50 psi)

1,342 is the stress at 50 psi (Table 2.7.1-60)

The total bolt tension stress is the sum of preload stress, thermal stress and pressure stress:

$$S_t = S_i + S_{th} + S_p$$

$$= 76{,}506 \text{ psi}$$

Based upon a bolt yield stress, S_y = 80.1 ksi, extrapolated at 750°F, the margin of safety is:

$$MS = 80.1/76.5 - 1 = +0.05$$

Under hypothetical fire accident conditions, containment integrity is maintained as required by 10 CFR 71.73(c)(3).

2.7.3.4 Inner Shell Evaluation

During a hypothetical fire accident, assuming 100% fuel failure, the internal pressure of the cask is calculated to be 125.8 psia (Section 3.5.4). Conservatively, 168 psig is used in the inner shell stress calculation. Neglecting the strength of the lead liner and the outer shell, the load generated by the internal pressure, from Roark, 5th Edition Table 29, Case 1c, is:

$$S_r = \text{radial stress} = -168 \text{ psi}$$

$$S_a = \frac{P_f \times \pi \times (r_i - t_i)^2}{\pi \times \left(r_i^2 - (r_i - t_i)^2\right)} = 700 \text{ psi}$$

$$S_t = \frac{P_f \times 2 \times r_i}{2 \times t_i} = 1{,}647 \text{ psi}$$

where:

P_f=168 psig r_i=7.45 inches t_i=0.76 in

The resulting stress intensities are:

$$|S_a - S_t| = 947 \text{ psi} \qquad |S_t - S_r| = 1{,}815 \text{ psi} \qquad |S_r - S_a| = 868 \text{ psi}$$

The allowable primary membrane stress in the accident condition for XM-19 stainless steel at 500°F is the lesser of:

$2.4\ S_m = (2.4)(29.7) = 71.28$ ksi $\qquad 0.7S_u = (0.7)(89.1) = 62.37$ ksi

$$\text{Margin of Safety} = \frac{62{,}370}{1{,}815} - 1 = +\underline{\text{Large}}$$

The allowable primary membrane plus bending stress for XM-19 stainless steel at 500°F is the lesser of:

$3.6\ S_m = (3.6)(29.7) = 106.92$ ksi $\qquad S_u = 89.1$ ksi

$$\text{Margin of Safety} = \frac{89{,}100}{1{,}815} - 1 = +\underline{\text{Large}}$$

Therefore, the inner shell of the transport cask maintains its structural integrity under an internal pressure of 168 psig caused by a hypothetical fire accident with 100% fuel failure.

2.7.3.5 Conclusion

The NAC-LWT cask shells, bottom, and closure lid bolts are demonstrated to be structurally adequate, providing a minimum margin of safety of +0.05 against loss of containment. Therefore, the NAC-LWT cask satisfied the structural requirements of 10 CFR 71 for the fire accident event.

2.7.4 Immersion – Fissile Material

The criticality evaluation of the NAC-LWT cask presented in Chapter 6 considers the effect of water inleakage; therefore, the requirement of 10 CFR 71.73(c)(4) is satisfied.

2.7.5 Immersion-Irradiated Nuclear Fuel Packages

The NAC-LWT cask has been designed to withstand immersion in water at an external pressure of 2 MPa (290 psi) for at least one hour as prescribed in 10 CFR 71.61. This pressure corresponds to a depth of water of 200 meters. As demonstrated in this section, the containment seal remains intact, and the minimum margin of safety for the cask structure is + 20.7.

This evaluation bounds the 0.9 meter water immersion required for fissile material packages in accordance with 10 CFR 71.73 (c) (5) and the 15 meter water immersion required for all packages in accordance with 10 CFR 71.73 (c) (6).

2.7.5.1 Method of Analysis

Three types of loads are present on a submerged NAC-LWT cask: (1) thermal due to decay heat of contained fuel; (2) internal pressure due to decay heat of contained fuel; and (3) external pressure due to submersion in water. The maximum decay heat load for the contained fuel is 2.5 kW. The secondary (thermal) stresses are not considered in the accident condition primary stress analyses. Stresses in the cask due to the low internal pressure are very small and are conservatively neglected. Thus, the external pressure load on the cask is the only load considered in the primary stress analyses for this accident event.

Classical methods are used to calculate the stress intensities resulting from the external pressure. These stress intensities are evaluated with respect to the accident condition allowable stresses presented in Tables 2.1.2-1 and 2.1.2-2.

2.7.5.2 Closure Lid Stresses

The external pressure principal stresses at the center of the closure lid are calculated from Table X, Case 1 in Roark, 4th Edition, for a flat circular plate (13.4 inches OD) with the outer edge simply supported under loading of uniform pressure. The hydrostatic pressure, P_h, is 290 psi.

The weight of the water is calculated as:

$W = P_h(\pi/4)\ (13.4)^2 = 41{,}000$ lbs

The stress is calculated as:

$$S_r = S_t = \frac{3W}{8\pi mt^2}(3m+1) = 257 \text{ psi}$$

where:

$m = 1/\nu = 3.636$

$t = 7.9$ inches

$S_a = -290$ psi

The stress intensities are calculated as:

$| S_a - S_t | = 547$ psi

$| S_t - S_r | = 0$

$| S_r - S_a | = 547$ psi

Considering the accident condition containment structure allowable stresses for primary membrane and primary membrane plus primary bending, Table 2.1.2-1, the margin of safety for the lid primary membrane stress, subjected to the 200 meter immersion, is:

$$\text{Margin of Safety} = \frac{48{,}000}{547} = +\underline{\text{Large}}$$

Where the allowable primary membrane stress for 304 stainless steel at 200°F is the lesser of:

$2.4\ S_m = (2.4)\ (20.0) = 48.0$ ksi

or

$0.7\ S_u = (0.7)\ (71.0) = 49.7$ ksi

Allowable primary membrane plus bending stress for 304 stainless steel at 200°F is the lesser of:

$3.6\ S_m - (3.6)\ (20.0) = 72.0$ ksi

or

$S_u = 71.0$ ksi

thus

$$\text{Margin of Safety} = \frac{71{,}000}{547} = +\underline{\text{Large}}$$

2.7.5.3 Outer Bottom Head Forging Stresses

The principal stresses due to the external pressure at the inner diameter of the bottom forging are calculated from Table X, Case 6 on Roark, 4th Edition, for a flat circular plate with the outer edge fixed under a uniform pressure load. The diameter of the bottom forging is 20.75 inches.

$W = (P_h)\ (\pi/4)\ (20.75)^2 = 98{,}400$ lbs

$S_a = -290$ psi

$$S_t = \frac{3W}{4\pi mt^2} = 527 \text{ psi}$$

$$S_r = \frac{3W}{4mt^2} = 1{,}657 \text{ psi}$$

where:

$m = 3.636$

$t = 3.5$ inches

The stress intensities are calculated as:

$| S_a - S_t | = 818$ psi

$| S_t - S_r | = 1{,}130$ psi

$| S_r - S_a | = 1{,}948$ psi

The margin of safety for the outer bottom head forging based on the accident condition allowable stress for primary membrane, Table 2.1.2-2 is:

$$\text{Margin of Safety} = \frac{48{,}000}{1{,}948} = + \underline{\text{Large}}$$

The margin of safety for the primary membrane plus bending stress, using the allowable values from Table 2.3.1-1, is:

$$\text{Margin of Safety} = \frac{71{,}000}{1{,}948} - 1 = + \underline{\text{Large}}$$

2.7.5.4 Cask Cylindrical Shell Stresses

The stresses generated in the shells of the cask in the 200 meter water immersion (290 psi) are evaluated using the formula for elastic stability from Table 35, Case 20 in Roark, 5th Edition.

The relevant dimensions, material properties, and the design basis of the cask are:

$t_i = 0.76$ in (inner shell thickness)

$t_l = 5.73$ inches (lead shell thickness)

$t_o = 1.2$ inches (outer shell thickness)

$r_i = 7.45$ inches (inner shell, outer radius)

$r_o = 14.38$ inches (outer shell, outer radius)

L = 160.3 inches (unsupported length of the inner shell)

E = 27.6 x 10^6 psi (modulus of elasticity for XM-19 at 200°F)

S_u = 99.5 ksi (ultimate stress at 200°F)

S_m = 33.2 ksi (allowable stress at 200°F)

P_h = - 290 psi (hydrostatic pressure under 200 meter of water)

Neglecting the strength of the lead and the outer shell in resisting the load generated by the external pressure, the stresses in the inner shell are:

S_r = radial stress = - 290 psi

$$S_a = \text{axial stress} = \frac{P_h \cdot \pi \cdot r_o^2}{\pi \cdot [r_i^2 - (r_i - t_i)^2]} = -5{,}580 \text{ psi}$$

$$S_t = \text{tangential stress} = \frac{P_h \cdot 2 \cdot r_i}{2 \cdot (t_i)} = -2{,}843 \text{ psi}$$

The stress intensities are:

$| S_a - S_t |$ = 2,737 psi

$| S_t - S_r |$ = 2,553 psi

$| S_r - S_a |$ = 5,290 psi

The allowable primary membrane stress for XM-19 stainless steel at 200°F is the lesser of:

2.4 S_m = (2.4)(33.2) = 79.7 ksi, or

0.7 S_u = (0.7) (99.5) = 69.7 ksi

Therefore, the margin of safety for primary membrane stress is:

$$\text{Margin of safety} = \frac{69{,}700}{5{,}290} - 1 = +\underline{\text{Large}}$$

The allowable primary membrane plus bending stress for XM-19 stainless steel at 200°F is the lesser of:

3.6 S_m = (3.6)(33.2) = 119.5 ksi, or

S_u = 99.5 ksi

Therefore, the margin of safety for primary membrane plus bending stress is conservatively calculated as:

$$\text{Margin of Safety} = \frac{99{,}500}{5{,}290} - 1 = +\underline{\text{Large}}$$

Conservatively assuming that the outer shell in not functional and only the inner shell exists, the containment boundary is evaluated for buckling using the formula for elastic stability from Roark, 5th Edition, Table 35, Case 20:

$$\text{The ratio of: } \left(\frac{L}{r_i}\right)^2\left(\frac{r_i}{t_i}\right) = 4{,}538 > 300$$

Therefore, the critical pressure, q′, can be approximated by:

$$q' = \frac{0.92E}{\left(\frac{L}{r_i}\right)\left(\frac{r_i}{t_i}\right)^{2.5}} = 3{,}923 \text{ psi}$$

Using Roark's recommended design external pressure that is 80% of the theoretical critical pressure and a factor of safety of 1.34 for buckling:

$$q' = 0.8 \times \frac{3{,}923}{1.34} = 2{,}342 \text{ psi.}$$

The margin of safety is:

$$\text{Margin of Safety} = \frac{2{,}342}{290} - 1 = +\underline{\text{Large}}$$

2.7.5.5 Containment Seal Evaluation

Immersion of the NAC-LWT cask in 200 meters of water subjects the cask and closure system to an external pressure load of 290 psi. The external pressure produces additional compression force on the sealing surfaces of the cask.

Increasing the sealing surface compression load without increasing cask internal loads results in an increase in seal margins and does not challenge design conditions. Therefore, the containment seals are acceptable for cask immersion to 200 meters.

2.7.6 Damage Summary

The analysis results reported in Sections 2.7.1 through 2.7.5 are summarized in Table 2.7.6-1 through Table 2.7.6-3.

They indicate that the damage incurred by the NAC-LWT cask during the hypothetical accident is minimal and does not diminish its ability to maintain the containment boundary. The 30-foot fall or the 40-inch fall onto the pin may cause the failure of the neutron shield tank and resultant loss of the neutron shielding. However, the gamma shielding remains intact to provide the required shielding following the accident.

Also, in a 30-foot hypothetical drop accident, the impact limiters may crush to a maximum depth of 15.70 inches and the lead may slump to a maximum of 0.33 inch. These potential consequences have no adverse structural effects.

Based on the analyses of Section 2.7, the NAC-LWT cask fulfills the structural requirements of 10 CFR 71 and the shielding requirements of 49 CFR 173 for all of the hypothetical accident conditions.

Table 2.7.6-1 Summary of Maximum Calculated Stresses – 30-Foot Drop

30-Foot Drop	Conditions*						Maximum Calculated Stress		Allowable Stress		Margin of Safety
	1		2	3	4	5	Type	Value (ksi)	Type	Value (ksi)	
	130°F	-40°F									
Containment** (on end)		✓		✓	✓	✓	P_m	12.28	$0.7\ S_u$	66.0	+4.37
	✓		✓	✓	✓	✓	$P_m + P_b$	14.10	$1.0\ S_u$	94.3	+5.68
Noncontainment*** (on end)		✓					P_m	10.93	$0.7\ S_u$	46.2	+3.22
		✓					$P_m + P_b$	20.23	$1.0\ S_u$	66.0	+2.26
Containment** (on side)	100°F		✓	✓	✓	✓	P_m	31.77	$0.7\ S_u$	66.0	+1.08
	100°F		✓	✓	✓	✓	$P_m + P_b$	33.71	$1.0\ S_u$	94.3	+1.80
Noncontainment*** (on side)	100°F		✓	✓	✓	✓	P_m	65.19	$1.0\ S_u$	66.0	+0.01
	100°F		✓	✓	✓	✓	$P_m + P_b$	68.23	$1.0\ S_u$	94.3	+0.38
Containment** (oblique)	✓		✓	✓	✓	✓	P_m	45.35	$0.7\ S_u$	46.2	+0.02
	✓		✓	✓	✓	✓	$P_m + P_b$	60.21	$1.0\ S_u$	66.0	+0.10
Noncontainment*** (oblique)		✓		✓	✓	✓	P_m	44.20	$0.7\ S_u$	66.0	+0.49
		✓		✓	✓	✓	$P_m + P_b$	63.73	$1.0\ S_u$	66.0	+0.04

* 1. Ambient Temperature
2. Insolance
3. Decay Heat
4. Internal Pressure
5. Weight of Contents

** The containment structure includes the lid, upper ring, inner shell, and bottom closure plate. See Figure 2.10.2-5 for component identification.

*** The noncontainment structure includes the outer shell and the cask bottom.

Table 2.7.6-2 Summary of Maximum Calculated Stresses – 40-Inch Free Drop

40-Inch Free Drop	Conditions*					Maximum Calculated Stress		Allowable Stress		Margin of Safety
	1		2	3	4	5	Type	Value (ksi)	Type	Value (ksi)	
	130°F	-40°F									
Containment** (on lid center)	✓		✓			✓	$P_m + P_b$	13.95	S_y	22.5	+0.61
		✓				✓					
Noncontainment*** (on mid-length)	✓		✓			✓	-	-	-	-	+0.71****
		✓				✓					
Noncontainment** (on bottom center)	✓		✓			✓	$P_m + P_b$	55.63	1.0 S_u	66.0	+0.19
		✓				✓					

* 1. Ambient Temperature
2. Insolance
3. Decay Heat
4. Internal Pressure
5. Weight of Contents

** The containment structure includes the lid, upper ring, inner shell, and bottom closure plate. See Figure 2.10.2-5 for component identification.

*** The noncontainment structure includes the outer shell and the cask bottom.

**** Result obtained from the displacement criteria, not from the stress criteria.

Table 2.7.6-3 Summary of Maximum Calculated Stresses - Fire

Fire	Conditions*					Maximum Calculated Stress		Allowable Stress		Margin of Safety
	1 130°F	2 -40°F	3	4	5	Type	Value (ksi)	Type	Value (ksi)	
Containment** (inner shell)			✓	✓	✓	$P_m + P_b + Q$	36.67	$2.4\ S_m$	70.1	+0.91
Noncontainment*** (outer shell)			✓	✓	✓	$P_m + P_b + Q$	38.51	$2.4\ S_m$	70.1	+0.82
Bottom			✓	✓	✓	$P_m + P_b + Q$	31.51	S_u	64.0	+1.03
Lid Bolts			✓	✓	✓	$P_m + Q$	53.25	S_y	70.0	+0.31

* 1. Ambient Temperature
2. Insolance
3. Decay Heat
4. Internal Pressure
5. Weight of Contents

** The containment structure includes the lid, upper ring, inner shell, and bottom closure plate. See Figure 2.10.2-5 for component identification.

*** The noncontainment structure includes the outer shell and the cask bottom.

2.7.7 Fuel Basket Accident Analysis

2.7.7.1 Discussion

Aluminum and stainless steel fuel baskets support NAC-LWT cask contents and retain them in a subcritical and safe geometry. Nine fuel basket designs are analyzed for accident condition loads: the PWR basket (Section 2.7.7.2); the BWR basket (Section 2.7.7.4); the metallic fuel basket (Section 2.7.7.5); the MTR basket (Section 2.7.7.6); the failed metallic fuel basket (Section 2.10.13); the TRIGA fuel basket (Section 2.7.7.9); the DIDO basket (Section 2.7.7.10); the GA IFM basket (Section 2.7.7.11); and the TPBAR basket (Section 2.7.7.12). Side and end impact orientations are the two limiting accident cases. In the side drop orientation, the basket is supported in bearing on the inner shell, and all structural loads are transmitted to the cask structure. Analysis shows that the structural load occurring during the end drop will not cause the basket assemblies or the analyzed spacers to buckle.

2.7.7.2 PWR Basket Construction

The PWR basket is cylindrical in shape, and constructed from 6061-T6 aluminum. A central hollow, square cavity supports the cask contents during transport. An aluminum spacer assembly is welded to the bottom of the PWR basket. It supports the fuel basket and contents longitudinally and limits their movement within the cask cavity. Additional spacers may be bolted to the cask lid as required by the length of the contents. A complete description of the basket and its construction is provided in Section 2.6.12. For the shipment of up to 25 individual PWR rods, a spacer canister will be utilized to position the PWR rods within the PWR or BWR basket. The PWR rods and canister are bounded by the PWR basket analyses of Section 2.7.7.3.

2.7.7.3 PWR Basket Analysis

The NAC-LWT cask maximum inner shell diameter is 13.405 inches at 70°F. The basket body outside diameter is 13.25 inches at 70°F. Except when the cask is empty, the cask cavity temperature is always higher than 70°F. The 6061-T6 aluminum alloy expands approximately 1.5 times more per degree Fahrenheit than does stainless steel. During the -40°F ambient, high heat load, normal transport condition, the average inner cavity wall temperature is 151°F. Accounting for the thermal response of the basket, the diameter of the basket body is 13.26 inches. The maximum as-designed gap between the basket and the cavity, when the basket is centered in the cavity, is 0.094 inch (both inner baskets are considered to be at 70°F). The basket is assumed to be in bearing contact with the inner shell during a side drop accident. All loads from the contents are transmitted through the basket to the inner shell and the cask structure.

2.7.7.3.1 Bearing Stress Calculation - Side Drop

The bearing stress is calculated using Case 6 (Roark, page 320), which models the cylindrical basket in a circular groove. The maximum compressive stress is calculated using:

$$S_{c_{max}} = 0.798 \left[\frac{\frac{P(D_1 - D_2)}{D_1 D_2}}{\frac{1 - \nu_1^2}{E_1} + \frac{1 - \nu_2^2}{E_2}} \right]^{0.5}$$

$$= 2242 \text{ psi}$$

where the material properties at 250°F are:

Stainless Steel

D_1 = 13.405

E_1 = 27.3×10^6 psi

ν_1 = 0.275

Aluminum (6061-T6)

D_2 = 13.25 inches

E_2 = 9.4×10^6 psi

ν_2 = 0.334

contents + basket weight = 4,000 lbs

P_{lg} = 4,000 lb/178 in = 22.5 lb/in

$P_{49.7g}$ = (22.5 lb/in)(49.7 g) = 1,118 lbs/in

The side drop g load, 49.7 g, is determined in Section 2.6.7.4.

The allowable bearing stress is the lesser value of the yield strength of aluminum or of stainless steel, which is 23,800 psi; the yield strength (S_y) of Type 304 stainless steel at 250°F. The margin of safety is calculated as:

$$M.S. = \frac{S_y}{S_{c_{max}}} - 1 = \underline{+Large}$$

2.7.7.3.2 Compressive Buckling Stress Calculations - End Drop

The PWR basket and inner cavity length are designed to ensure that there is very limited movement of the basket and contents relative to the cask during transport. Spacers are attached to the cask lid or placed at the bottom of the basket prior to fuel loading, if the contents do not fill the cavity. However, adequate clearance is maintained so that differential thermal expansion does not produce longitudinal loads on the basket body. The basket must be able to support itself during an end drop accident. To determine if the basket is self-supporting, it is treated like a column, acted upon by its own weight. The basket weighs 840 lbs. During the end drop accident, the basket weight is decelerated at 58.2 g (Table 2.6.7-34), for a total compressive force, P_c = 48,890 lbs. The compressive force acts over the 59.2-square inch basket body cross section. The compressive stress (S_c) acting on the basket is 826 psi (48,890 lb/59.2 in^2), which is negligible. An Euler column analysis is used to determine the critical buckling load of the basket. Assuming that the impacting end is fixed and the other is free, the critical buckling stress (Shigley, page 116) is calculated:

$$P_{cr} = \frac{n\pi^2 EI}{L^2}$$

$$= 670,700 \text{ psi}$$

where:

n = 0.25, end fixity coefficient

$E_{Al_{250°F}}$ = 9.4×10^6 psi

$I_{basket\ body}$ = 870 in^4 (Roark, Case 10, page 75)

L = inner cavity length = 178 inches

$$M.S. = \frac{P_{cr}}{P_c} - 1 = \underline{+Large}$$

2.7.7.4 BWR Basket Construction

The BWR basket is cylindrical in shape, and constructed from 6061-T6 aluminum. A central, hollow, rectangular cavity is divided into two square cavities by an aluminum plate, which supports the basket contents during transport. A complete description of the basket and its construction is provided in Section 2.6.12.4.

2.7.7.4.1 BWR Basket Analysis

The BWR basket is constructed from the same aluminum material as the PWR basket. Therefore, it displays similar thermal expansion characteristics. Similar to Section 2.7.7.3, the BWR basket is in contact bearing with the inner shell, and all loads from the contents are transmitted through the basket to the inner shell and the cask structure.

2.7.7.4.2 Bearing Stress Calculation - Side Drop

The bearing stress is calculated using Case 6 (Roark, page 320), which models the cylindrical basket in a circular groove. The maximum compressive stress is calculated using:

$$S_{c_{max}} = 0.798 \left[\frac{\frac{P(D_1 - D_2)}{D_1 D_2}}{\frac{1 - \nu_1^2}{E_1} + \frac{1 - \nu_2^2}{E_2}} \right]^{0.5}$$

$$= 1969 \text{ psi}$$

where the material properties at 250°F are:

Stainless Steel

D_1 = 13.405

E_1 = 27.3×10^6 psi

ν_1 = 0.275

Aluminum (6061-T6)

D_2 = 13.25 inches

E_2 = 9.4×10^6 psi

ν_2 = 0.334

contents + basket weight = 2,624 lbs

P_{lg} = 2,624 lb/178 in = 14.7 lb/in

$P_{49.7g}$ = (14.7 lb/in)(49.7 g) = 733 lb/in

The side drop g load, 49.7 g, is obtained from Table 2.6.7-34.

The allowable bearing stress is the lesser value of the yield strength of aluminum or of stainless steel, which is 23,800 psi; the yield strength (S_y) of Type 304 stainless steel at 250°F. The margin of safety is calculated as:

$$M.S. = \frac{S_y}{S_{c_{max}}} - 1 = \underline{+Large}$$

2.7.7.4.3 Compressive Buckling Stress Calculations - End Drop

The BWR basket and inner cavity length are designed to ensure that there is very limited movement of the basket and its contents relative to the cask during transport. However, adequate clearance is maintained to ensure that differential thermal expansion does not produce longitudinal loads on the basket body. The basket must be able to support itself during an end drop accident. To determine if the basket is self-supporting, it is treated like a column, acted upon by its own weight. The basket weighs 1,124 lbs. During the end drop accident, the basket weight is decelerated at 58.2 g (Table 2.6.7-34), for a total compressive force, P_c = 65,417 pounds. The compressive force acts over the 72.5-square inch basket body cross section. The compressive stress (S_c) acting on the basket is 65,417 lb/72.5 in = 902 psi, which is negligible. An Euler column analysis is used to determine the critical buckling stress of the basket. Assuming that the impacting end is fixed and the other is free, the critical buckling stress (Shigley, page 116) is calculated:

$$P_{cr} = \frac{n\pi^2 EI}{L^2}$$

$$= 1.0 \times 10^6 \text{ psi}$$

where:

n = 0.25, end fixity coefficient

$E_{Al_{250°F}} = 9.4 \times 10^6$ psi

$I_{basket\ body}$ = 1,298 in^4 (Roark, Case 10, page 75)

L = inner cavity length = 178 inches

$$M.S. = \frac{P_{cr}}{P_c} - 1 = \underline{+Large}$$

2.7.7.5 Metallic Fuel Basket Analysis

The metallic fuel basket consists of three aluminum tubes held in position by five 0.25-inch bulkhead plates, forming a cylindrical shape. The tube centers are hollow cavities, which support the fuel contents during transport. A complete description of the basket and its construction is provided in Section 2.6.12.5.

The metallic fuel basket is constructed from aluminum as is the PWR basket. Therefore, it displays similar thermal expansion characteristics. Similar to Section 2.7.7.3, the metallic fuel basket is in contact bearing with the cask inner shell; thus, all loads from the contents are transmitted through the basket to the cask inner shell.

2.7.7.5.1 Bearing Stress Calculation - Side Drop

The bearing stress between the cask inner shell and the basket bulkhead plates is calculated using Case 6 (Roark, page 320), which models the cylindrical basket in a circular groove. The maximum compressive stress is calculated using:

$$S_{c_{max}} = 0.798 \left[\frac{\frac{P(D_1 - D_2)}{D_1 D_2}}{\frac{1 - \nu_1^2}{E_1} + \frac{1 - \nu_2^2}{E_2}} \right]^{0.5}$$

$$= 19{,}537 \text{ psi}$$

where the material properties at 250°F are:

Stainless Steel

D_1 = 13.405

E_1 = 27.3×10^6 psi

ν_1 = 0.275

Aluminum (6061-T6)

D_2 = 13.25 inches

E_2 = 9.4×10^6 psi

ν_2 = 0.334

contents + basket weight = 2,208 lbs

P_{lg} = 2,208 lb/1.25 in = 1,766 lb/in

$P_{49.7g}$ = (1,766 lb/in)(49.7 g) = 87,790 lb/in

The side drop g load, 49.7 g, is obtained from Table 2.6.7-34.

The allowable bearing stress is the lesser value of the yield strength of aluminum or of stainless steel, which is 23,800 psi; the yield strength (S_y) of Type 304 stainless steel at 250°F. The margin of safety is calculated as:

$$M.S. = \frac{S_y}{S_{c_{max}}} - 1 = \underline{+0.22}$$

2.7.7.5.2 Compressive Buckling Stress Calculations - End Drop

The metallic fuel basket and inner cavity length are designed to minimize the movement of the basket and its contents relative to the cask. The basket length is designed to provide adequate clearance to ensure that differential thermal expansion will not produce longitudinal loads on the basket body. The basket is self-supporting during an end drop accident. Therefore, the basket components are examined for compressive column stability, to ensure that the basket structure is adequate. The fuel tubes are considered to support the weight of the metallic fuel basket (128 lbs) in a top end drop. The spacer tube supports the basket and contents (2,208 lbs) during a bottom end drop. The maximum end drop load results from a 58.2 g cask deceleration. The fuel tubes have a total cross-sectional area of 6.48 square inches; therefore, the accident compressive stress ($S_{c_{fuel}}$) in each tube is (128 lbs)(58.2 g)/6.48 in^2 = 1,150 psi. During a bottom end drop, the spacer tube sustains a compressive stress ($S_{c_{spacer}}$) of (2,208)(58.2)/6.87 = 18,705 psi.

An Euler column analysis is used to determine the critical buckling stress of the basket fuel tubes and the spacer. Assuming that the impacting end is fixed and the other is free, the critical buckling stress (Shigley, page 116) is calculated:

Fuel Tubes (3)

P_{max} = (128)(58.2) = 7450 lbs

Spacer Tube

P_{max} = (2,208)(58.2) = 128,506 lbs

Fuel Tubes (3)

$$P_{cr} = \frac{n\pi^2 EI}{L^2}$$

= 26,930 lbs

Spacer Tube

$$P_{cr} = \frac{n\pi^2 EI}{L^2}$$

= 1,754,000 lbs

where:

n = 0.25, end fixity coefficient

$E_{AL250°F} = 9.4 \times 10^6$ psi

$I_{fuel\ tubes} = 45.8\ in^4$

L = 145.3 in, fuel tube length

$MS = P_{cr} / P_{max} - 1 = +LARGE$

n = 0.25, end fixity coefficient

$E_{AL250°F} = 9.4 \times 10^6$ psi

$I_{spacer\ tube} = 65.8\ in^4$

L = 29.5 in, spacer tube length

$MS = P_{cr} / P_{max} - 1 = +LARGE$

2.7.7.6 MTR Fuel Basket Construction

The MTR modular basket assembly has four configurations. One configuration is for intact fuel; the second is for 35 partially cut fuel elements that have had portions of the upper and lower end fittings removed; the third configuration is for 42 MTR fuel assemblies with the end fittings removed; and the fourth is for PULSTAR fuel elements loaded in the 28 MTR basket. The PULSTAR fuel elements may be intact fuel assemblies, intact fuel elements (rods) loaded in a fuel rod insert or a PULSTAR can, or failed fuel elements loaded in a PULSTAR failed fuel can or a PULSTAR screened fuel can. Each basket configuration consists of one base module, one top module, and either two, three or four intermediate modules for the 28-, 35- and 42-element configurations, respectively. Each 28 MTR basket module is capable of holding up to seven MTR type fuel assemblies or up to seven PULSTAR fuel assemblies.

The hypothetical accident analyses for the MTR fuel baskets are not affected by the specific fuel element design or enrichment as long as the fuel characteristics are in compliance with the fuel characteristics listed in Table 1.2-4.

Each module, fabricated from Type 304 stainless steel, is a weldment made up of two 1/2-inch thick, 13.625-inch diameter, and circular plates at each end of the longitudinal divider plates creating seven MTR fuel assembly compartments. The outside wall of the four symmetric outermost fuel tubes is fabricated from 11- gage Type 304 stainless steel sheet. The 1/2-inch thick plate at the top end of the MTR basket module is welded to all webs and divider plates. The 1/2-inch thick baseplate is continuously welded to the 1/4-inch thick divider plates and the 5/16-inch thick web plates. The 11-gage sheet metal and the 5/16-inch intermediate webs are discontinued at 1/4 inches from the surface of the baseplate to provide full tube drainage. The 5/16-inch plate material may be machined to a minimum thickness of 0.28 inch. In addition, a 1-inch diameter hole is located at the center of each of the compartments in each basket module. The MTR basket base module sits on a 1.5-inch long, 10-inch schedule 80S pipe welded to the

1/2-inch thick baseplate. The 10-inch schedule 80S pipe carries the total weight of the MTR basket assembly and bears directly on the bottom forging of the cask.

The MTR fuel basket base module and intermediate modules have guide pins fixed to the surface of the top support plate. The guide pins fit into holes in the base plate of the top and intermediate modules and provide controlled alignment of the basket assembly. A groove slot on the outside of each basket unit support plate is provided for the cask drain tube clearance and to provide for the basket assembly circumferential alignment.

2.7.7.6.1 MTR Fuel Basket Analysis

The MTR basket assembly and the inner shell are both fabricated from Type 304 stainless steel material. The nominal radial gap between the MTR basket assembly and the cask inner shell is 0.055 inch. The nominal radial gap between the basket and the inner shell is 0.0531 inch at the design base fuel normal operation steady state temperature. As defined for other NAC-LWT fuel-specific basket designs, since the gap between the basket and cask inner shell wall is small, it is assumed that there is no relative motion between the basket and the cask, and that the basket is in contact bearing on the inner shell during a side drop. The basket bearing loads are transmitted to the inner shell and cask structure.

2.7.7.6.2 Bearing Stress Calculation - Bottom Forging

The MTR basket assembly, when in the vertical position, is supported by a, 0.5-inch thick, 10-inch nominal diameter schedule 80S pipe. The 1.5-inch long pipe is welded to the baseplate of the base unit. The compressive stress is calculated as:

$$S_c = gW/A = 8{,}430 \text{ psi}$$

where:

A = Cross-sectional area of base pipe support = 16.1 in^2

W = Weight of MTR basket assembly and contents = 2,262 lbs

g = Dynamic load factor (31-foot end drop) = 60

The allowable stress, S_y, of Type 304 stainless steel at a conservative maximum operating temperature envelope of 600°F is 18,200 psi. The margin of safety is calculated as follows:

$$\text{Margin of Safety} = S_y/S_c - 1 = +1.16$$

2.7.7.6.3 Compressive Stress Calculation - Fuel Tubes (Cask End Drop)

The MTR basket assembly and the inner cavity length are designed to ensure that there is limited longitudinal movement of the basket assembly relative to the cask cavity. The base module of the MTR basket assembly supports itself and the weight of other basket units, including fuel assemblies, during an end drop. The accident condition load compressive stress developed in the basket tube wall is:

$$\sigma_c = \frac{g \times W}{A} = 23{,}576 \text{ psi}$$

where:

W = Maximum weight of MTR basket with contents (PULSTAR) = 3,222 lbs

g = 31-foot end drop acceleration = 60 g

A = Total compartment cross-sectional area at baseplate (Figure 2.6.12.6-2) = 8.20 in^2

The allowable compressive stress, $0.7S_u$, is 44,450 psi conservatively evaluated for Type 304 stainless steel at 600°F. The margin of safety is:

$$MS = \frac{0.7S_u}{\sigma_c} - 1 = +0.89$$

The Euler elastic buckling load formulation is used to determine the critical buckling load of the MTR base module. The base module is conservatively treated as simply supported, which results in an effective length that is twice the actual length, thus reducing the critical buckling load by a factor of 4.0. The basket base module buckling load is:

$$P_{cr} = \frac{\pi^2 EI_i}{(L_e)^2} = 1.55 \times 10^6 \text{ lbs}$$

The margin of safety is:

$$MS = \frac{P_{cr}}{P_c} - 1 = +8.0$$

where:

P_c = Compressive load = 60g × W = 193,320 lbs

I_i = Basket inertia moment = 47.92 in^4

E = Elastic modulus (@ 600°F) = 25.3 × 106 psi.

L_e = Effective length of 28 assembly basket = 2 × 44.0 in = 88 inches

2.7.7.6.4 Lateral Stress Calculation

The baseplate at the end of a typical MTR basket module supports the weight of seven MTR fuel assemblies when the cask is in the vertical orientation (0 degree drop). With the cask in the horizontal orientation (90 degree drop), the fuel tubes support the entire length of the MTR fuel. The baseplate and the fuel tubes share in the support the MTR fuel at any drop orientation between a 0 degree drop and a 90 degree drop.

Baseplate Stresses (Cask End Drop)

The support plate at the top end of the basket modules is continuously welded to the outside periphery of the fuel tubes. The baseplate of a typical basket module is continuously welded to the two 11.57-inch wide, 5/16-inch (minimum 0.28-inch considering machining tolerance) thick web plates and two 3.44-inch wide, 1/4-inch thick divider plates. The ½-inch thick baseplate supports up to seven MTR fuel assemblies or PULSTAR fuel assemblies and is conservatively assumed to be supported by the main longitudinal webs mentioned above during a cask end drop. Two separate load cases are examined. The maximum stress for each case is then combined to obtain the total stress on the baseplate. Figure 2.6.12.6-2 details the baseplate support.

The first case, Case I, examines a 3.44-inch square plate with two adjacent sides fixed and the other two sides free. The applied pressure over the entire plate is uniform (Roark, 6th Ed., Table 26, Case 11a). The bending stress is:

$$\sigma_I = \frac{-g\beta_I P b^2}{at^2} = -33{,}975 \text{ psi}$$

where:

P = fuel weight = 80.0 lbs

g = 31-foot end drop acceleration = 60.0

a = Area of plate = $(3.44 \text{ in})^2 = 11.83 \text{ in}^2$

t = Plate thickness = 0.5 inch

b = Plate width = 3.44 inches

β_I = Boundary condition stress factor = 1.769

The second case, Case II, examines a rectangular plate, 11.57 inches by 3.44 inches, fixed along the long edges, free along the short edges and uniformly loaded (Roark, 5th Ed., Table 26, Case 6).

The configuration of the baseplate and supports is shown in Figure 2.6.12.6-2 (Roark's, 6th Ed., Table 26, Case 6a). The bending stress is:

$$\sigma_{II} = \frac{-g\beta_{II}Pb^2}{at^2} = -2{,}837 \text{ psi}$$

where:

a = Area of plate = 11.57×3.44 inch = 39.8 in^2

β_{II} = Boundary condition stress factor = 0.497

The total bending stress is conservatively obtained by adding the individual stresses:

$$\sigma = \sigma_I + \sigma_{II} = -36{,}812 \text{ psi}$$

The allowable stress, S_u, is 63,500 psi for Type 304 stainless steel at the conservative maximum temperature envelope of 600°F. The margin of safety is:

$$MS = \frac{63{,}500}{36{,}812} - 1 = +0.73$$

Fuel Tube Stresses (Cask Side Drop)

The maximum stress in the fuel tubes occurs in the 0.12-inch thick, 11-gage sheet metal fuel tubes, which support the entire length of the MTR fuel assembly or the PULSTAR fuel assembly, cans or fuel rod insert. The design basis MTR fuel has a rectangular cross-section with slotted aluminum plates on each of the opposite sides of the assembly. The aluminum plates hold a nominal 18, aluminum clad fuel plates to create an assembly. There are two cases to consider. In the first case, the weight of the fuel contents is transmitted to the tube through the two aluminum plates at the sides of the fuel assembly. As shown in Figure 2.6.12.6-1, this load path creates a uniform line load along the length of the tube located about 0.315 inch from the corners. The tube is analyzed as a simple beam, 1 inch wide, 0.12 inch thick, and 3.44 inches long with a concentrated load at 0.315 inch from the ends. The maximum bending moment, M_I, is:

$$M_I = \frac{(8Pa + WL^2) \times g}{8} = 28.7 \text{ in-lb/in}$$

where:

W = Unit tube body weight = $0.288 \times t = 0.0346$ lb/in^2

L = Length = 3.44 inches

P = Bounding fuel load = $P_f / (2 \times L_f) = 1.67$ lb/in

P_f = Fuel weight = 80.0 lbs

L_f = Shortest length over which fuel load is applied = 24 inches

a = Distance from applied load, P to support = 0.315 inch

g = 31-foot side drop acceleration = 49.7g

In the second case, the weight of the fuel assembly is transmitted to the tube as a uniform load. The load path is shown in Figure 2.6.12.6-1. The maximum bending moment for this case, M_{II}, is:

$$M_{II} = \frac{(2PL^2 + WL^3)\times g}{8L} = 73.9 \text{ in-lb/in}$$

The maximum bending stress, σ, is:

$$\sigma = \frac{6M_{II}}{t^2} = 30{,}792 \text{ psi}$$

where:

t = Fuel tube thickness = 0.12 inch

The stress allowable, S_u, is 63,500 psi for Type 304 stainless steel at 600°F. The margin of safety is:

$$MS = \frac{63{,}500}{30{,}792} - 1 = +1.06$$

The 11-gage (0.12 inch) sheet metal tube is continuously welded to the adjacent divider plates with a ⅛-inch fillet weld. This weld resists shear developed in the simple beam analyzed above.

$$V = \frac{(2P + WL)\times g}{L} = 50.0 \text{ lb/in}$$

The shear stress, τ, is:

$$\tau = \frac{V}{t} = 417 \text{ psi.}$$

The "throat" thickness of the weld is 0.088 inch. The ratio of the plate thickness (0.12 inch) to the weld "throat" thickness (0.088 inch) is 1.36. The maximum stress of 417 psi calculated above is adjusted by a factor of 1.36 to obtain the maximum stress in the weld for the 31-foot side drop (49.7g). Maximum stress in the weld, S_w, is:

$S_w = 1.36 \times \tau = 567$ psi

The ASME Code, Subsection NG-3352 recommends that the allowable stress for a fillet weld with PT or MT surface examination be decreased by the quality factor, n, of 0.4. The stress allowable, S_y, of the base metal, Type 304 stainless steel, is 18,200 psi at a conservative operating temperature envelope of 600°F. The margin of safety for the fillet weld is:

$$MS = \frac{S_y \times n}{S_w} - 1 = +\underline{Large}$$

Fuel Tube Stresses (Cask Oblique Drop)

Table 2.6.7-34 summarizes the cask drop equivalent g load factors for six drop orientations: the cask end drop (0 degrees), the cask corner drop (15.74 degrees), the cask oblique drops (30, 45 and 60 degrees) and the cask side drop (90 degrees). According to Table 2.6.7-34, the maximum axial dynamic load factor of 58.2 g (1.8g less than the g load experienced for the 31-foot end drop) occurs at the 30-degree drop orientation for any of the 31-foot oblique drops. The maximum lateral dynamic load factor of 38.5 g (11.2 g less than the g load experienced for the 31-foot side drop) occurs at the 60-degree drop orientation for any of the 31-foot oblique drops. As reported in Section 2.7.7.6.3, the maximum stress in the longitudinal dividers (fuel tubes) is 16,551 psi for the 60 g 31-foot end drop. The maximum stress of 10,467 psi is also reported in the section titled "Fuel Tube Stresses (Cask Side Drop) for the 0.12-inch thick, 11-gage sheet metal tubes for the 49.7 g 31-foot side drop.

To conservatively envelop the maximum stresses expected for all the 31-foot oblique drops, the calculated stresses of 23,576 psi in Section 2.7.7.6.3 for the end drop and 30,792 psi for the side drop in Section 2.7.7.6.4 are added as absolute values. The maximum stress in the MTR basket that envelops the maximum stresses expected for any 31-ft oblique drop is 54,368 psi. The margin of safety, against the stress allowable, S_u, of 63,500 psi, at 600°F, is:

$$MS = \frac{63,500}{54,368} - 1 = +0.17$$

2.7.7.6.5 Fuel Cans in the MTR Basket for PULSTAR Fuel

PULSTAR Damaged Fuel Can

The PULSTAR damaged fuel can is a modification of the existing failed fuel can for TRIGA fuel. The TRIGA fuel can is provided in two different lengths. The PULSTAR fuel can has the same cross-section (can width and wall thickness) as the TRIGA fuel can and is approximately four inches longer than the shorter TRIGA fuel can. The material of construction is identical for both the TRIGA and the PULSTAR fuel cans. As shown in Section 2.7.7.9.5 the TRIGA fuel can is evaluated for a maximum weight of 59.6 lbs, which includes a can weight of 20 lbs and a

payload of 39.6 lbs. The weight of the PULSTAR fuel can and the payload is approximately 15 lbs and 35 lbs, respectively. The maximum internal pressure for the PULSTAR can is 59.2 psig. The calculation for the TRIGA can in Section 2.7.7.9.5 used a value of 168 psig, which bounds the maximum accident condition pressure for the PUSTAR can. Therefore, the evaluation presented in Section 2.7.7.9.5 for the TRIGA fuel can bounds the evaluation for the PULSTAR fuel can. The PULSTAR fuel can is structurally adequate for hypothetical accident conditions of transport. No additional analysis is required.

PULSTAR Screened Fuel Can

The PULSTAR screened can is a modification of the existing damaged fuel can for TRIGA fuel, which has two different design lengths. The PULSTAR screened fuel can has the same cross-section (can width and wall thickness) as the TRIGA screened fuel can and is approximately four inches longer than the shorter TRIGA screened fuel can design. Identical materials of fabrication are used for both TRIGA and PULSTAR fuel cans. As shown in Section 2.7.7.9.4, the TRIGA fuel can is evaluated for a maximum weight of 71 lbs, which includes a maximum can weight of 17 lbs and a payload of 54 lbs. The weights of the PULSTAR screened fuel can and its maximum payload are 12 lbs and 54 lbs, respectively, for a maximum total weight of 66 lbs. Therefore, the evaluation presented in Section 2.7.7.9.4 for the TRIGA screened fuel can bounds the evaluation for the PULSTAR screened fuel can, and it may be concluded that the PULSTAR screened fuel can is structurally adequate for accident conditions of transport. No additional analysis is required.

PULSTAR Fuel Rod Insert and Spacer

Intact PULSTAR fuel elements (rods) can be placed into the PULSTAR fuel rod insert. This insert is identical to the TRIGA fuel rod insert evaluated in Section 2.7.7.9.8. The weight of an individual PULSTAR fuel element is 1.31 lbs, which is bounded by the weight of an individual TRIGA rod of 1.44 lbs reported in Section 2.6.12.7.9. Therefore no additional evaluation for the PULSTAR fuel rod insert is required.

2.7.7.6.6 MTR Plate Canister Analysis

In this section, the NAC-LWT MTR Plate Canister (canister) is evaluated and found to be structurally adequate for the hypothetical accident condition. Analysis methodology is the same as that used for the normal operating conditions analysis presented in Section 2.6.12.6.6.

Stresses developed during the hypothetical accident condition meet all appropriate allowable criteria with positive margins.

Classical hand calculations are used to determine the stresses in the canister. Calculated stresses are compared to allowable stresses for non-containment structures shown in Table 2.1.2-2, "Allowable Stress Limits for Noncontainment Structures."

Design deceleration (g) factors used in the canister analysis are shown in Table 2.6.7-34, "Summary of Cask Drop Equivalent G Load Factors."

A temperature of 295°F bounds the highest calculated canister temperature and is used for both normal and accident condition analyses.

Stresses for corner and oblique drops are considered to be enveloped by the stresses produced by the end and side drops.

Side Drop

The canister is contained within the NAC-LWT MTR 42 element basket assembly in the side-drop case. Because of the support provided by the basket, only the uppermost canister plate is subjected to bending. Bending of the plate is analyzed by considering a 1-inch section as a fixed-fixed beam equal in length to the width of the plate and uniformly loaded by the plate weight times the appropriate acceleration (g).

Hypothetical Accident Condition (30-foot drop)

With the 0.125-in thick plate uppermost:

The maximum moment (M_{max}) is:

$$M_{max} = \frac{wL^2}{12} = \frac{(0.61)(3.3^2)}{12} = 0.553 \text{ in-lb}$$

$$S_b = \frac{Mc}{I} = \frac{(0.553)(0.0625)}{1.63\times10^{-4}} = 212 \text{ psi for the hypothetical accident condition}$$

where:

$$w = 0.125 \times 1.0 \times 1.0 \times 0.098 \times 49.7g = 0.61 \text{ lb/in}$$

With the 0.24-in-thick plate uppermost:

The maximum moment (M_{max}) is:

$$M_{max} = \frac{wL^2}{12} = \frac{(1.17)(3.3^2)}{12} = 1.06 \text{ in-lb}$$

$$S_b = \frac{Mc}{I} = \frac{(1.06)(0.125)}{1.15\times10^{-3}} = 115 \text{ psi for the hypothetical accident condition}$$

where:

$$w = 0.24 \times 1.0 \times 1.0 \times 0.098 \times 49.7g = 1.17 \text{ lb/in}$$

$$I = \frac{bh^3}{12} = \frac{(1.0)(0.24^3)}{12} = 1.15 \times 10^{-3} \text{ in}^4$$

$$MS = \frac{S_u}{S_b} - 1 = \frac{38{,}000}{212} - 1 = \text{ +Large for the hypothetical accident condition}$$

Side Plate Buckling

The 0.125-in thick side plates are evaluated as axially loaded compression members.

The allowable load (P_a) as calculated in Section 2.6.12.6.6 is:

$$P_a = S_a \times A = 5{,}882 \text{ psi} \times 0.125 \text{ in}^2 = 735 \text{ lbs}$$

The load (P) imposed by the hypothetical accident, 30-foot side drop is:

$$P = 0.24 \times 1.0 \times 3.3 \times 0.098 \times 49.7g \cong 4 \text{ lbs}$$

This 4-pound load is conservative because the load from the thicker plate is actually shared between the two thinner plates.

Because the calculated compressive loads are much less than the allowable buckling load P_a = 735 lbs, the canister side plates are not expected to buckle under the load imposed by the hypothetical accident side drop.

End Drop

For the end drop, the can weldment is loaded by its own weight. The canister contents bear against the bottom or top of the canister, depending on drop orientation.

Under accident conditions, the canister body weldment is evaluated for a 60 g acceleration.

The compressive load (P) is:

$$P = 10 \text{ lb} \times 60g = 600 \text{ lbs}$$

The compressive stress (S_c) in the canister body weldment is:

$$S_c = \frac{P}{A} = \frac{600 \text{ lbs}}{2.24 \text{ in}^2} \cong 268 \text{ psi}$$

The margin of safety (MS) is then:

$$MS = \frac{0.7S_u}{S_c} - 1 = \frac{0.7(38{,}000) \text{ psi}}{268 \text{ psi}} - 1 = \text{+large for accident conditions}$$

Canister Body Buckling

The critical buckling load (P_{cr}) as calculated in Section 2.6.12.6.6 is 77,292 lbs.

Because the maximum compressive load (10 lbs × 60 g = 600 lbs under the accident condition) is much less than the critical buckling load (77,292 lbs), the canister body has adequate resistance to buckling.

Lifting Bail Compressive Stress

Under accident conditions, the lifting bail is evaluated for a 60 g acceleration.

The compressive load (P) is:

$$P = 30 \text{ lbs} \times 60 \text{ g} = 1{,}800 \text{ lbs}$$

The compressive stress (S_c) in the lifting bail is:

$$S_c = \frac{P}{A} = \frac{1{,}800 \text{ lbs}}{0.965 \text{ in.}^2} = 1{,}865 \text{ psi}$$

The margin of safety (MS) is then:

$$MS = \frac{0.7S_u}{S_c} - 1 = \frac{0.7(38{,}000) \text{ psi}}{1{,}865 \text{ psi}} - 1 = + \text{Large for accident conditions.}$$

2.7.7.7 Conclusion

The minimum margin of safety of + 1.16 is reported in Section 2.7.7.6.2 for the MTR basket and 30.0 lbs fuel element. Column analyses establish that each basket component is structurally stable during an end drop. Thus, all of the basket components have sufficient structural integrity to meet the requirements of 10 CFR 71.

2.7.7.8 PWR Spacer

2.7.7.8.1 Top Spacer

The top spacer for the NAC-LWT cask containing the PWR basket is shown in Figure 2.7.7-1. The spacer is subject to an impact load during an accidental drop of the cask. The most critical load occurs during a corner drop, where the axial component of the deceleration (Table 2.6.7-34) is:

$$a_{axial} = 60.4 \text{ g} \cos 15.74° = 58.2 \text{ g}$$

The design weight of the PWR basket (840 lbs) and its contents (1500 lbs) is 2340 lbs. The impact load on the spacer is:

$P_T = 2,340\ (58.2) = 136,188$ lbs

Top Plate

The top plate of the top spacer on which the weight of the basket and its contents impact during an accident is in direct contact with the cask lid. Load is transferred through the plate to the support legs without bending the plate; therefore, the plate is structurally adequate.

Support Legs

The four support legs of the top spacer are made from SA-312, Type 304 stainless steel bars. The yield strength of these bars is 22,500 psi at 300°F. The maximum compressive stress in the support legs from impact of the fuel assembly during a drop accident occurs at the area of the leg in contact with the fuel assembly basket, $A_b = (1.25)^2 - (0.5)(0.375)^2 = 1.492$ in^2. The maximum stress is calculated as follows:

$$S_{cb} = P_T/4A_b = 136,188/4(1.492) = 22,485 \text{ psi}$$

The margin of safety on the yield strength is:

$$MS = (S_y/S_{cb} - 1) = +0.00$$

The average compressive stress in the bar, to be compared with the buckling stress, is determined by computing the average area as follows:

A_a = area of bar at start of the taper = $(1.50)^2 = 2.25$ in^2

L_a = length of uniform section = 4.94 inches

L_b = length of tapered section = 4.00 inches

$$A_{avg} = [A_aL_a + (A_a + A_b)L_b/2]/(L_a + L_b)$$

$$= [(2.25)(4.94) + (2.25 + 1.492)(4.00)/2]/(4.94 + 4.00) = 2.080 \text{ in}^2$$

The average stress in the member is:

$$S_{cavg} = P_T/4A_{avg} = 136,188/4(2.080) = 16,369 \text{ psi}$$

The slenderness ratio must be determined to select the method of analyzing the member's buckling strength. The member is analyzed for block compression if its slenderness ratio is less than $(L'/\rho)_{min}$ between $(L'/\rho)_{min}$ and $(L'/\rho)_{max}$ is considered to be a short-column, and greater than $(L'/\rho)_{max}$ requires a long-column analysis. The value for $(L'/\rho)_{min}$ equals 12 (Peery, page 253). The value for $(L'/\rho)_{max}$ is calculated from the straight-line short-column formula $(L'/\rho)_{max} = \pi [(3)(27 \times 10^6)/22,500]^{0.5} = 188.5$.

The slenderness ratio of the member is calculated by the equation $L'/\rho = L/\rho\ (c)^{0.5}$, where L = 11.82 inches, c = 2.04 (Peery, page 352), and $\rho = (I/A)^{0.5}$. The value of ρ is determined by using the average section properties for the square bar, calculated as follows:

$$b = (A_{avg})^{0.5} = (2.080)^{0.5} = 1.442 \text{ inches}$$

$$I = b^4/12 = (1.442)_4/12 = 0.360 \text{ in}^4$$

$$A = A_{avg} = 2.080 \text{ in}^2$$

$$\rho = (I/A)^{0.5} = (0.360/2.080)^{0.5} = 0.416 \text{ in}$$

$$L'/\rho = 11.82/0.416(2.04)^{0.5} = 19.893$$

The member is considered to be in the short-column range because the slenderness ratio falls between $(L'/\rho)_{min}$ and $(L'/\rho)_{max}$.

The straight-line formula, the most conservative for a short-column (Peery, page 354), is used to calculate the buckling strength (S_{cr}) as follows:

$$S_{cr} = S_{co}\ [1 - 0.385(L'/\rho)/\ \pi\ (E/S_{co})^{0.5}]$$

$$= 22{,}500[1 - 0.385(19.893)/\ \pi\ [(27 \times 10^6)/22{,}500]^{0.5}]$$

$$= 20{,}831 \text{ psi}$$

The margin of safety on buckling is:

$$MS = (S_{cr}/S_{cavg}) - 1 = +0.27$$

2.7.7.8.2 Bottom Spacer

The bottom PWR spacer for the NAC-LWT cask is shown in Drawing No. 315-40-10 (Section 1.4). The top plate, which is shown as 7/8-inch thick in the bill of materials in the reference drawing, is to be machined to a 3/4-inch final thickness. The bottom spacer is subject to the same load as the top spacer (Section 2.7.7.1).

Top Plate

The top plate for the bottom spacer is 0.75-inch thick, SA-240, Type 304 stainless steel. The maximum stress due to the fuel assembly impact is (Roark, Case 15, page 220):

$$S_b = (3W/2\pi mt^2)\left[2a^2(m + 1)[\log(c/d)]/(a^2 - b^2)\right.$$

$$\left. + (m - 1)(c^2 - d^2)/(a^2 - b^2)\right]$$

$$= 4{,}859 \text{ psi}$$

where:

W = 136,188 lbs

m = $1/\nu$ = 1/0.275 = 2.636

t = 0.75 in

a = 6.63 inches

b = 2.25 inches

c = 4.24 inches

d = 4.19 inches

The margin of safety against yield at 300°F is:

$MS = (S_y/S_b) - 1 = \underline{+Large}$

Column Support

The column support for the bottom spacer is an 8-inch schedule 80, A-312, Type 304 pipe. The net area, deducting the area removed for the openings at the base, is:

$A_{net} = 12.8 - 4(1.2)(0.50) = 10.4 \text{ in}^2$

The compressive stress is:

$S_c = 136{,}188/10.4 = 13{,}095$ psi

The margin of safety is:

$MS = (S_y/S_c) - 1 = \underline{+0.76}$

The buckling stress is (Baker, page 230):

$S_{cr} = \gamma C_c \eta E t/R = 1{,}675{,}000$ psi

where:

γ = 0.84 for R/t = 4.06/0.50 = 8.1

C_c = 0.6

η = 1.0 for elastic bucking

E = 27×10^6 psi at 300°F

t = 0.50 in

R = 4.06 inches

The margin of safety for buckling is:

$$MS = (S_{cr}/S_c) - 1 = \underline{+Large}$$

Thus, the PWR spacers, whose length is less than 27 inches, satisfy the yield strength criteria. (If spacer lengths exceed 27 inches, the Euler column equation must be applied.)

Figure 2.7.7-1 PWR Spacer Geometry

2.7.7.9 TRIGA Fuel Basket Thirty-Foot Drop Evaluation

This section evaluates the stresses developed in the TRIGA fuel basket assembly described in Section 2.6.12.7 as a result of the 30-foot drop hypothetical accident conditions. As indicated in Section 2.6.12.7, the loading produced by the TRIGA fuel cluster rods and fuel rod insert are bounded by those produced by the TRIGA fuel elements.

The weights of the TRIGA basket assembly and modules are shown below. The weight includes the weight of 140 of the heaviest fuel elements that could be installed in the module, and failed fuel can in the top and bottom modules. The calculated weight of each top and bottom module is increased by 70 lbs to account for the poison plates and to conservatively bound the analysis. Similarly, the calculated weight of the intermediate module is increased by 140 lbs.

Component	Weight of Fuel (lb) 140 Elements	Weight of Module(s)[1] (lb)	Total Weight (lb)	Length of Module(s) (in)
Bottom Module	247	356	603	34.70
3 Intermediate Modules	741	957	1,698	31.50
Top Module	370	460	830	48.30
Weight of Empty Basket		1,773		
Loaded Weight of Basket			3,131	

[1] Includes the weight of the failed fuel cans plus additional weight for conservative design evaluation.

2.7.7.9.1 NAC-LWT Bottom Forging Bearing Stress

The TRIGA basket assembly, when in the vertical position, is supported by a 0.5-inch thick 10-inch nominal diameter schedule 80S pipe. The 1.5-inch long pipe is welded to the baseplate of the base unit. The compressive stress is:

$$S_c = \frac{g \times W}{A} = 11{,}688\,\text{psi}$$

where:

g = 60, Dynamic load factor for the 30-foot end drop

W = 3,131 lbs, Total weight of the basket

A = 16.1 in^2, Area of 10-inch diameter schedule 80S pipe

The allowable stress, S_u = 63,500 psi at 600°F.

Therefore:

$$MS = \frac{63,500}{11,688} - 1 = +\underline{4.44}$$

2.7.7.9.2 TRIGA Basket Compressive Stress Analysis

The TRIGA fuel basket is designed to ensure that there is very limited longitudinal movement of the basket relative to the cask inner cavity. The fuel contents are not attached to the basket and do not impart any longitudinal structural load on the basket body. However, the basket must support itself during an end drop accident. The basket is analyzed as a column, acted upon by a structural (weight) compressive load.

The compressive stress developed in the basket compartment wall is:

$$S_c = \frac{g \times W}{A} = 22,910 \quad \text{psi}$$

where:

g = 60, Dynamic load factor for the 30-foot end drop

W = 3,131 lbs, Total weight of the basket

A = 8.20 in^2, Total compartment cross-section area at base plate

The allowable stress, S_u = 63,500 psi at 600°F.

Therefore:

$$MS = \frac{63,500}{22,910} - 1 = +\underline{1.77}$$

The Euler elastic buckling load formulation is used to determine the critical buckling load (P_{cr}) of the 10-inch diameter Schedule 80S pipe and the base module. The pipe and base module are conservatively treated as simply supported, which results in an effective length that is twice the actual length, reducing the critical buckling load by a factor of 4.0. For the 10-inch pipe, the critical buckling load is:

$$P_{cr} = \frac{\pi^2 EI}{L_e^{\,2}} = 5.88 \times 10^9 \text{ lbs}$$

where:

E = 25.3×10^6 psi at 600°F

I = 212 in^4, inertia moment

L_e = 2 x 1.5 = 3.0 in., effective length (2L)

The calculated compressive stress is:

$P_c = W \times g = 3{,}131 \times 60 = 187{,}860$ lbs

where:

g = 60, Dynamic load factor for the 30-foot end drop

W = 3,131 lbs, Total weight of the basket

Therefore:

$$MS = \frac{P_{cr}}{P_c} - 1 = \frac{5.88 \times 10^9}{187{,}860} - 1 = +\underline{\text{Large}}$$

The critical buckling load for the base module is calculated using the same equation as above, by applying the moment of inertia of the fuel support structure. The fuel web and divider support structure is shown in the following figure in Section 2.7.7.9.3.

The moment of inertia for the support structure is:

Item	$(I_o)_{yy}$	A	h	Ah^2	$(I_o)_{xx}$
2-11.57" x 0.28" web plate	0.0	6.48	1.86	22.42	72.28
2-3.44" x 0.25" divider plate	1.7	1.72	3.72	23.80	0.0
Total	1.7			46.22	72.28

$(I_o)_{yy} = I_o + \Sigma\, Ah^2 = 1.7 + 46.22 = 47.92\ in^4$

$(I_o)_{xx} = \Sigma\, I_o = 72.28\ in^4$

Choosing the smaller moment of inertia, $(I_o)_{yy}$, as I:

$I = 47.92\ in^4$

$$P_{cr} = \frac{\pi^2 EI}{L_e^{\,2}} = \frac{\pi^2 \times 25.3 \times 10^6 \times 47.92}{(2 \times 33.2)^2} = 2.71 \times 10^6 \text{ lbs}$$

where:

L_e = 2 x 33.2 inches

P_c = W x g = 3,131 x 60 = 187,860 lbs

g = 60, Dynamic load factor for the 30 foot end drop

W = 3,131 lbs, Total weight of the basket

The margin of safety is:

$$M.S. = \frac{P_{cr}}{P_c} - 1 = \frac{2.71 \times 10^6}{187{,}860} - 1 = +\underline{\text{Large}}$$

2.7.7.9.3 TRIGA Basket Lateral Stress Analysis

The base plate at the end of a typical TRIGA basket module supports the weight of up to 28 TRIGA fuel elements when the cask is in the vertical orientation (0 degree drop). With the cask in the horizontal orientation (90 degree drop), the fuel cell divider plates support the entire length of the TRIGA fuel. The base plate and the divider plates share in the support of the TRIGA fuel at drop orientations between 0 and 90 degrees.

Baseplate Stress Due to End Drop

The support plate at the top end of the modules is continuously welded to the outside periphery of the plates, including the support plates that form the fuel cells. The baseplate of the basket module is continuously welded to the two 11.57-inch wide, 5/16-inch thick web plates (0.28 inches, minimum thickness), and to the two 3.44-inch wide, 1/4-inch thick divider plates as shown below.

The baseplate supports up to 28 fuel elements and is conservatively assumed to be supported by the main longitudinal support plates during a cask end drop. Two separate load cases are evaluated. The maximum stresses for each case are combined to obtain the total stress on the baseplate.

The first case (Case I), evaluates a 3.44-inch square plate with adjacent sides fixed and the other sides free. The applied pressure over the entire plate is uniform (Young, page 471, case 11). The second case, Case II, examines a rectangular plate, 11.57 inches by 3.44 inches, fixed along the long edges, free along the short edges and uniformly pressurized (Young, page 462, case 6).

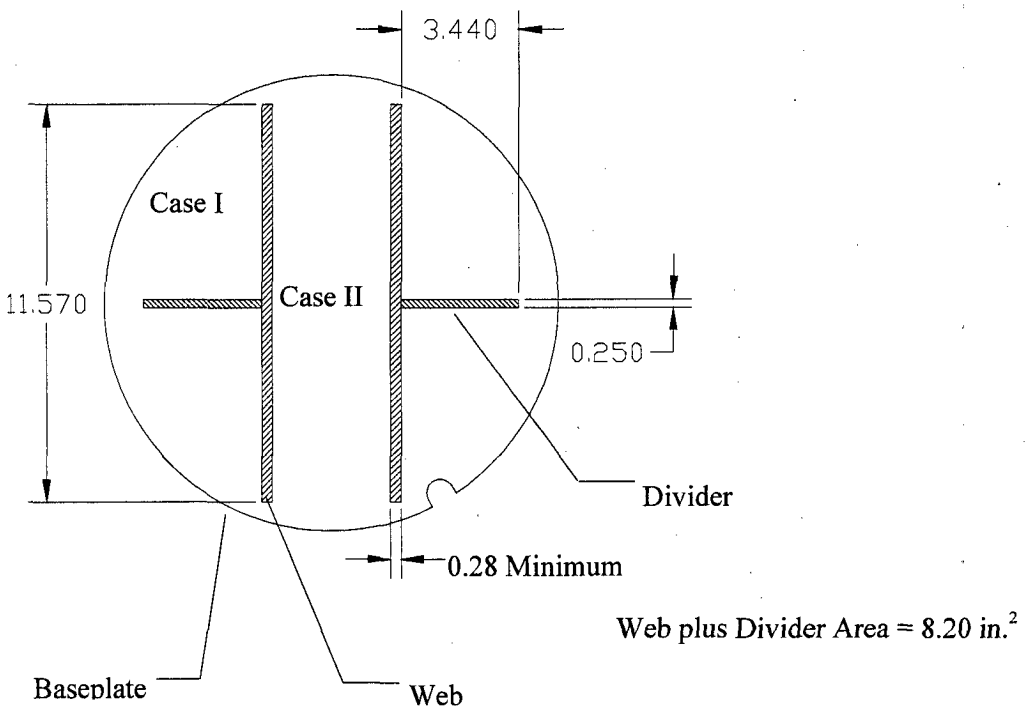

For Case I, the 3.44-inch square plate is analyzed as a cantilevered plate supported at two adjacent sides with the other two sides free. Load is assumed uniform over the area of the plate. The bounding fuel weight is applied. The maximum stress is expressed as (Young, page 471, case 11):

$$S_I = \frac{-g \times B_I \times P \times b^2}{A \times t^2} = -33{,}965\,\text{psi}$$

where:

g = 60, Dynamic load factor for the 30-foot end drop

B_I = 1.769, Boundary condition stress factor

P = 80 lbs, Bounding module fuel weight

b = 3.44 inches, Width of plate

A = $(3.44)^2$ sq. inches, Plate area

t = 0.5 in, Plate thickness

Case II, evaluates a plate 3.44-inch by 3.44-inch (width x length), fixed on two opposite sides, with the other two sides free. The maximum stress is expressed as (Young, page 462, case 6):

$$S_{II} = \frac{-g \times B_{II} \times P \times b^2}{A \times t^2} = -9{,}600 \quad \text{psi}$$

where:

g = 60, Dynamic load factor for the 30-foot end drop

B_{II} = 0.5, Boundary condition stress factor

P = 80 lbs, Bounding module fuel weight

b = 3.44 inches, Width of plate

A = $(3.44)^2$ sq. inches, Plate area

t = 0.5 in., Plate thickness

Total bending stress from Case I and Case II is:

$S_{total} = S_I + S_{II} = -43{,}565$ psi $< S_u = 63{,}500$ psi

Therefore:

$$MS = \frac{63{,}500}{43{,}565} - 1 = +\underline{0.46}$$

Support Plate Stress Due to the Screened Failed Fuel Can in the Side Drop

The maximum stress in the support plates that form the fuel cells occurs in the 0.12-inch thick 11 gage sheet metal tubes which support the entire length of the TRIGA fuel element. The weight of the TRIGA fuel element is transmitted through the can walls to the support plates that form the fuel cell. This load path creates a uniform pressure load over the entire area as shown below.

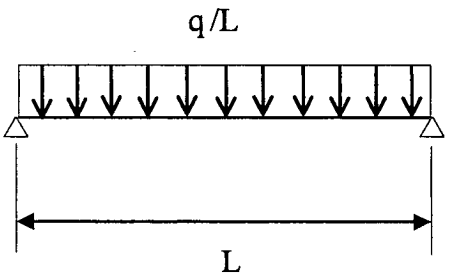

The fuel weight per unit length for all fuel types is presented in Section 2.6.12.7.4.

The intact fuel bounding load, q_i, along the length of the tube is:

$$q_i = \frac{W_i}{L_s} = 1.850 \quad \text{lb / in}$$

The uniform pressure load for the shorter (L_s) failed fuel in the screened can is:

$$q_f = \frac{W_f}{L_s} = 1.950 \quad lb/in$$

The uniform pressure load of the longer (L_L) failed fuel in the screened can is:

$$q_f = \frac{W_f}{L_L} = 1.778 \quad lb/in$$

where:

L_s = 29.88 inches = length of short fuel element

L_L = 45 inches = length of long fuel element

Weight of long failed fuel can = 17 lbs

Weight of short failed fuel can = 13 lbs

Added weight for fuel can calculation = 10 lbs

The weight calculation below includes 4 fuel elements, added weight, plus the screened failed fuel can.

W_f = 58.28 lbs for fuel can with fuel elements having a length of 29.88 inches (L_s)

W_f= 80 lbs for fuel can with fuel elements having a length of 45 inches (L_L)

W_i = 55.28 lbs for fuel can with intact fuel

The bounding load for TRIGA fuel is 1.950 lb/in.

The maximum bending moment is:

$$M_{max} = \frac{(q_f + w) \times gL}{8} = 44.21 \quad in - lb$$

where:

q_f = 1.950 lb/in

g = 49.7

t = 0.12 (11 gage)

L = 3.44 inches = width of side support plate (11 gage)

w = 0.288 x 3.44 × t = 0.1185 lb/in, steel beam weight

$$S = \frac{6 \times M_{max}}{t^2} = 18{,}544 \quad \text{psi}$$

Therefore:

$$MS = \frac{63{,}500}{18{,}544} - 1 = +\underline{2.42}$$

The 11 gage sheet metal is continuously welded to the adjacent divider plates with a 1/8-inch fillet weld. This weld resists the shear developed in the simple beam analysis above.

$$V = \frac{(W_f + wL_s) \times g}{2 \times L_s} = 51.41 \text{ lbs}$$

where:

$W_f = 58.28$ lbs

$L_s = 29.88$ inches

and,

$$S_v = \frac{V}{t \times 1} = 430 \text{ psi}$$

The throat thickness of 1/8-inch fillet weld is $0.707 \times 0.125 = 0.088$ in. The square of the ratio of the plate thickness (0.12 in) to the weld throat thickness (0.088 in) is 1.86. ASME Code Subsection NG - 3352 recommends that the calculated stress in a fillet weld be increased by a factor of $1/0.35 = 2.86$.

The maximum weld stress is:

$S_w = S_v\ (1.86)\ (2.86) = 2{,}287$ psi

The allowable stress is $0.42S_u = 26{,}670$ psi at 600°F.

Therefore,

$$MS = \frac{26{,}670}{2{,}287} - 1 = +\underline{\text{Large}}$$

Support Plate Stress Due To Side Drop For Sealed Failed Fuel Can

The stress of the support plates on the LWT-TRIGA basket is checked when the support plate is loaded with the sealed failed fuel can. The total bounding weight of the sealed can is 59.6 lbs, which includes 20 lbs for the canister and 39.6 lbs for the follower control elements.

The maximum stress in the support plates occurs in the 0.12-inch thick (11 gage) sheet metal tubes which supports the entire length of the sealed can. Since the can is cylindrical, its weight is transmitted as a line load over the entire length to the supporting plate. For a unit cross-section of the supporting plate, the line load is treated as a concentrated load over the supporting plate as shown in the following loading diagram.

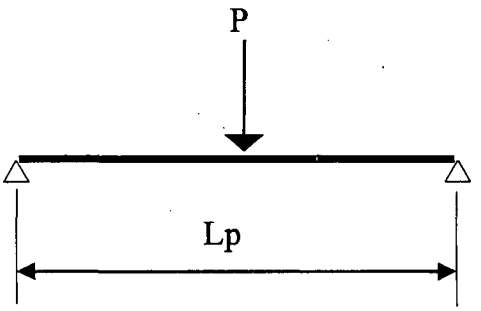

The load of the sealed can and its contents is represented by a uniformly distributed line load along the basket length that is in contact with the can. For a unit length, the concentrated load is:

For the longer can: $$P = \frac{W_f \times g}{L} = 77.12 \text{ lb/in.}$$

where:

W_f = 59.6 lbs, weight of the long sealed can (20 lbs) and follower control elements (39.6 lbs)

g = 49.7, dynamic load factor for 30-foot side drop

L = 38.41 inches, length of the longer tube body

For the shorter can: $$P = \frac{W_f \times g}{L} = 92.53 \text{ lb/in.}$$

where:

W_f = 43.4 lbs, weight of the short sealed can (17 lbs) and three fuel elements (26.4 lbs)

g = 49.7, dynamic load factor for 30-foot side drop

L = 23.31 inches, length of the shorter tube body

The concentrated load from the shorter can (P = 92.53 lb/in.), enveloping both the longer can and short can, is used to calculate the maximum bending moment. The unit length of the basket supporting plate with the 92.53 lbs concentrated force in the middle is treated as a simply supported beam. The maximum bending moment is:

$$M_{max} = \frac{P \times L_p}{4} = 79.58 \quad in - lb$$

where:

P = 92.53 lbs, concentrated load

L_p = 3.44 inches, width of the 11 gage support plate

The maximum bending stress is:

$$S = \frac{6 \times M_{max}}{t^2} = 33{,}380 \text{ psi}$$

where:

M_{max} = 79.58 in-lb, maximum bending moment

t = 0.12 in (thickness of the 11 gage support plate)

The margin of safety is:

$$MS = \frac{S_u}{S} - 1 = \frac{63{,}500}{33{,}380} - 1 = +0.9$$

The 11 gage sheet metal is continuously welded to the adjacent divider plates with a 1/8-inch fillet weld. This weld resists shear developed in simple beam analyzed above.

$$S_v = \frac{P}{t \times 1} = 774 \quad psi$$

where:

P = 92.53 lbs, load of unit length

t = 0.12 in., thickness of 11 gage support plate

The throat thickness of 1/8-inch fillet weld is 0.707 × 0.125 = 0.088-inch. The square of the ratio of the plate thickness (0.12-inch) to the weld throat thickness (0.088-inches) is 1.86. ASME Code Subsection NG - 3352 recommends that the calculated stress in a fillet weld be increased by a factor of 1/0.35 = 2.86.

Maximum weld stress is the calculated stress in the material times these factors:

$S_w = S_v (1.86) (2.86) = (774)(1.86)(2.86) = 4{,}117$ psi

The allowable stress = $0.42S_u$= 26,670 psi @ 600°F.

The margin of safety is:

$$MS = \frac{26,670}{4,117} - 1 = +\underline{Large}$$

Maximum Basket Stress Due To Oblique Drop

As shown in the side drop calculations presented in the two previous sections, between the two different configurations of failed fuel cans, the sealed failed fuel can induces greater stress to the basket supporting plates due to its cylindrical cross-section. Therefore, the maximum stress in the basket is bounded by the stress induced by the sealed can.

The maximum stress in the basket during oblique drop is found by absolutely combining the maximum stresses found in the basket during side drop and end drop determined in the previous sections. Although the stresses in the two different drop configurations do not occur in the same location, the stress combination method conservatively envelopes the maximum possible stress states during the oblique drop.

The maximum calculated stresses for the 30-foot end drop and the 30-foot side drop are:

Maximum stress = 22,910 psi for end drop

Maximum stress = 33,380 psi for side drop

Adding the two stress values above to obtain oblique drop stress, the maximum oblique drop stress = 22,910 + 33,380 = 56,290 psi

Allowable stress = S_u = 63,500 psi @ 600°F,

$$MS = \frac{63,500}{56,290} - 1 = +\underline{0.13}$$

2.7.7.9.4 Screened Failed Fuel Can

This section evaluates the stresses in the screened failed fuel can as a result of the 30-foot drop hypothetical accident condition. The screened failed fuel can is described in Section 2.6.12.7. The screened failed fuel can is analyzed for side and end drop during transportation.

Screened Failed Fuel Can Compressive Stress Analysis

The fuel contents are not attached to the screened failed fuel can, and do not impart any longitudinal structural load on the screened can. The can must support itself during an end drop accident. It is analyzed as a column acted upon by a structural (weight) compressive load consisting of the weight of the can and its contents. The screened failed fuel can for fuel

follower control rods is used since it is heavier, carries a heavier load, and bounds the shorter screened failed fuel can.

The compressive stress developed in the screened can wall is:

$S_c = Wg/A = 4,347$ psi

where:

W = 71 lbs, weight of can and contents

g = 60.0, dynamic load factor for 30-foot end drop

A = 0.98 sq. inch, cross-section area of can

The allowable stress, $0.7S_u$, = 44,450 psi at 600°F.

Therefore:

MS = (44,450/4,347) - 1 = +Large

The Euler elastic buckling load formulation is used to determine the critical buckling load (P_{cr}) of the screened failed fuel can. The screened failed fuel can is conservatively treated as simply supported, which results in an effective length that is twice the actual length. For the screened failed fuel can, the critical buckling load is:

$P_{cr} = (\pi^2)EI/(L_e)^2 = 49,262$ lbs

where:

E = 25,300,000 psi at 600°F

I = 1.68 in^4

L_e = 2 x 46.14 = 92.28 in., effective length (2L)

The calculated compressive stress is:

$P_c = gW = 60 \times 71 = 4,260$ lbs

where:

g = 60, dynamic load factor for 30 foot end drop

W = 71 lbs, total weight of screened can and contents

Therefore:

MS = (49,262/4,260) - 1 = +Large

Screened Failed Fuel Can Plate Stress Due to Side Drop

The plate making up the screened can is analyzed for bending as a result of loads applied resulting from a side drop. To bound the analysis, the weight of the longer can is used and this load is distributed over the length of the shorter fuel can to determine the load acting on a one inch wide strip of the fuel can cross-section. This total load on a 1-inch strip is conservatively applied to the area between fuel elements (1.5-inches). This is the longest span of plate subject to bending from a side drop.

The bending moment in the plate is:

$$M = gPL/8 = 21.1 \text{ in.-lb.}$$

where:

g = 49.7, dynamic load factor for 30 foot side drop

P = 2.26 lbs, total load on one-inch wide strip

L = 1.5 inches, spacing between fuel elements

The section modulus of the cross-section resisting the bending moment is:

$$S = t^2/6 = 0.00093 \text{ in}^3$$

where:

t = 0.075 in, thickness of plate making up the can

The bending stress is:

$$S_b = M/S = 22{,}646 \text{ psi}$$

The allowable stress is, $S_u = 63{,}500$ psi

Therefore:

$$MS = (63{,}500/22{,}646) - 1 = +1.80$$

2.7.7.9.5 Sealed Failed Fuel Can

This section evaluates the stresses in the sealed failed fuel can as a result of the hypothetical accident 30-foot end and side drops. The sealed can is described in Section 2.6.12.7.

Sealed Failed Fuel Can Compressive Stress Analyses Due to End Drop

This section analyzes the compressive stress and buckling load of the fuel tube, bottom tube and lifting lugs. The bounding weight of the sealed can used in this analysis is 59.6 lbs, which includes 20 lbs for the canister and 39.6 lbs for the follower control elements.

Fuel Tube

The fuel elements are not attached to the round tube that forms the wall of the can. However, it is conservatively assumed that the shell of the can carries the entire weight of the can and contents. The compressive stress is:

$$\sigma_C = \frac{W \times g}{A} = 5{,}498 \text{ psi}$$

where:

W = 59.6 lbs, total weight of the can and contents

g = 60.0, dynamic load factor for 30-foot end drop

A = $\pi (1.625^2 - 1.56^2) = 0.6504$ in^2, cross-sectional area of the can

For the 30-foot end drop, the dynamic load applied by its contents and a conservative 11.4 atm external pressure load caused by 100% fuel failure is applied to the sealed can.

Considering the sealed can as a thin wall cylinder with internal pressure of 168 (11.4 ×14.7) psi, the stresses in circumferential, radial and longitudinal directions are:

$$\sigma_\theta = \frac{P \times r}{t} = -4{,}200 \text{ psi}$$

$$\sigma_r = -P = -168 \text{ psi}$$

$$\sigma_Z = \frac{P \times r}{2 \times t} = -2{,}100 \text{ psi}$$

where:

P = 168 psi

r = 3.25/2 inches, the radius of the can

t = 0.065 in, the thickness of the can

Combining the stresses caused by can contents (30-ft end drop) and external pressure, the longitudinal stress becomes:

$$\sigma_Z + \sigma_C = -7{,}598 \text{ psi}$$

The stress intensity is:

$$S_{int} = \sigma_q - (\sigma_Z + \sigma_C) = 11{,}798 \quad psi$$

Margin of safety for 30-foot side drop plus 100% fuel failure is:

$$MS = \frac{3.6\ S_m}{\sigma_C} - 1 = +\underline{4.0}$$

The compressive stress for the bottom tube (2.5-inch OD, 1/8-inch wall tube) is:

$$\sigma_C = \frac{W \times g}{A} = 3{,}834 \ psi$$

where:

W = 59.6 lbs, weight of the can and contents

g = 60.0, dynamic load factor for the 30-foot end drop

A = $\pi (1.25^2 - 1.125^2) = 0.9327$ in^2 cross-section area of bottom tube

The margin of safety is:

$$MS = \frac{2.4S_m}{\sigma_C} - 1 = \frac{39{,}360}{3{,}834} - 1 = +\underline{Large}$$

Lifting Lugs

The can lifting lugs may be subject to compressive or buckling loads in drop accident events. The load is considered evenly distributed to both lugs.

The compressive stress for two lift lugs is:

$$\sigma_C = \frac{W \times g}{A} = 13{,}887 \ psi$$

where:

W = 59.6 lbs, weight of the can and contents

g = 60.0, dynamic load factor for the 30-foot end drop

A = 2 x 0.515 x 0.25 = 0.2575 in.^{2} smallest cross-section area of the two lift lugs

The margin of safety is:

$$MS = \frac{2.4S_m}{\sigma_C} - 1 = \frac{39,360}{13,887} - 1 = +\underline{1.83}$$

Considering the lift lug as a cantilever beam with fixed end, the load is carried by an equivalent moment M, where:

$$M = (P/2) \times d \times 60 = 434 \text{ in-lb}$$

where:

g = 60.0, dynamic load factor for the 30-foot end drop

P = 59.6 lbs, weight of can and contents

d = 0.2425 in, the length of moment arm, measured from the center of the section to the point of load application (0.5 - 0.515/2)

The total stress acting on the neck section is:

$$\sigma = \frac{(M)(c)}{I} + \sigma_C = 53,063 \text{ psi}$$

where:

σ_C is the compressive stress previously calculated, 13,887 psi

M = 434 in-lb, equivalent moment

c = 0.515/2 in., distance from the center of neck section to the edge

I = $0.25 \times (0.515)^3/12 = 2.85 \times 10^{-3}$ in.^{4}, moment of inertia of the cross-section

The margin of safety is:

$$MS = \frac{S_u}{\sigma_C} - 1 = \frac{63,500}{53,063} - 1 = +\underline{0.20}$$

The Euler elastic buckling load formulation is used to determine the critical buckling load of the tube body and bottom tube. The tubes and lugs are conservatively treated as simply supported which results in an effective length that is twice the actual length, thus reducing the critical bucking load by a factor of 4.0.

Buckling of the Sealed Failed Fuel Can

Only the body tube with longer length is analyzed since the shorter one is bounded by the longer tube.

$$P_{cr} = \frac{\pi^2 EI}{L_e^2} = 35{,}324 \text{ lbs}$$

where:

E = 25.3×10^6 psi @ 600 °F

I = $\pi r^3 t = 0.8762$ in^4, inertia moment of body tube

L_e = 2 x 39.35= 78.7 in, effective length (2L)

The compressive load is:

$P_c = W \times g = 3{,}576$ lbs

where:

g = 60.0, dynamic load factor for the 30-foot end drop

W = 59.6 lbs, weight of can and contents

$$MS = \frac{P_{cr}}{P_c} - 1 = \frac{35{,}324}{3{,}576} - 1 = \underline{+\text{Large}}$$

Buckling of the Bottom Tube

The critical buckling load for bottom tube is:

$$P_{cr} = \frac{\pi^2 EI}{L_e^2} = 4{,}615 \times 10^3 \text{ lbs}$$

where:

E = 25.3×10^6 psi @ 600°F

I = $\pi r^3 t = 0.5591$ in^4, inertia moment of body tube

L_e = 2 x 2.75 = 5.50 inches, effective length (2L)

The compressive load is:

$P_c = Wg = 59.6 \times 60.0 = 3{,}576$ lbs

where:

g = 60.0, dynamic load factor for the 30-foot end drop

W = 59.6 lbs, weight of can and contents

$$MS = \frac{P_{cr}}{P_c} - 1 = \frac{4{,}615 \times 10^3}{3{,}576} - 1 = +\underline{\text{Large}}$$

Buckling of the Lifting Lug

The critical buckling load for a lift lug is:

$$P_{cr} = \frac{\pi^2 EI}{L_e^2} = 2{,}319 \text{ lbs}$$

where:

E = 25.3×10^6 psi @ 600°F

I = $0.515 \times .25^3/12 = 6.71 \times 10^{-4}$ in^4, inertia moment of smallest cross section

L_e = 2 x 4.25 = 8.5 in, effective length (2L)

The compressive load is:

$P_c = Wg/2 = 59.6 \times 60/2 = 1{,}788$ lbs

where:

g = 60, dynamic load factor for a 30-foot end drop

W = 59.6 lbs, weight of the can and contents

$$MS = \frac{P_{cr}}{P_c} - 1 = \frac{2{,}319}{1{,}788} - 1 = +\underline{0.30}$$

Sealed Failed Fuel Can Plate Stress Due to Side Drop

For the 30-foot side drop, the load applied to the sealed can is considered as a linearly distributed load over the bottom 120° arc. The radial pressure w_x varies linearly from 0 at beginning to w at the bottom point of the can, as shown in the figure below. The internal pressure of 168 psi is also considered to be acting on the failed fuel can.

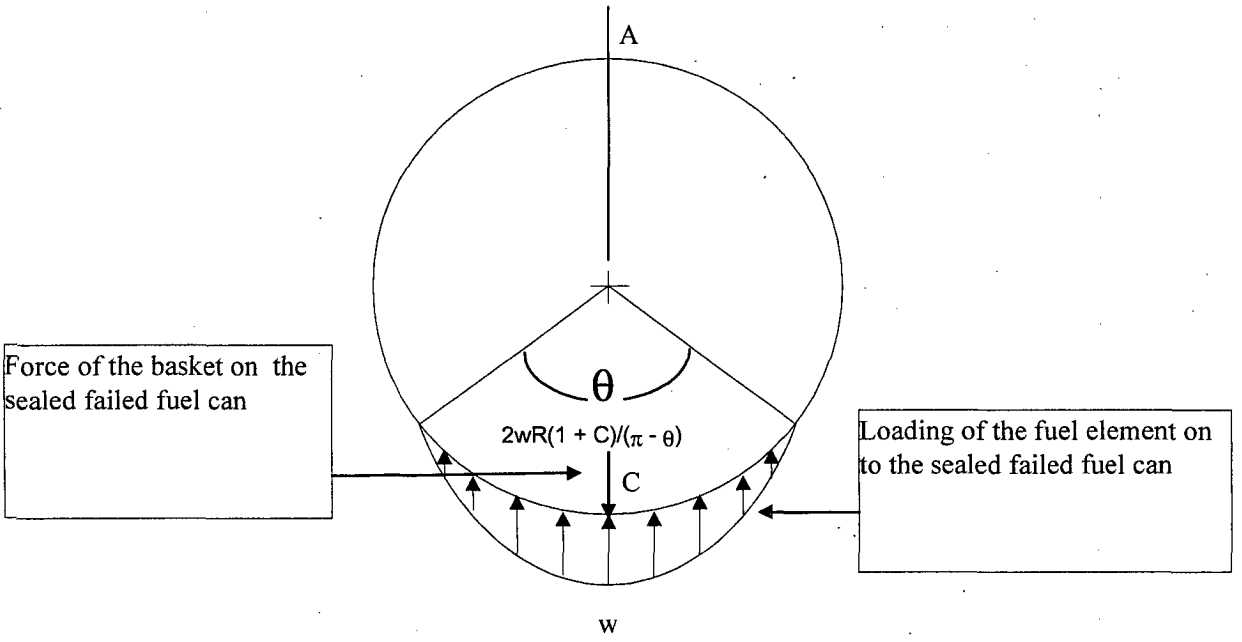

The load is uniformly distributed along the length of the can. For a unit length it can be calculated as:

For the longer can: $p = \frac{W_f \times g}{L} = 51.24$ lb / in.

where:

W_f = 39.6 lbs, conservative fuel weight of three fuel follower control elements

g = 49.7, dynamic load factor for the 30-foot side drop

L = 38.41 inches, length of the longer body tube

For the shorter can: $p = \frac{W_f \times g}{L} = 56.29$ lb / in.

where:

W_f = 24.4 lbs, conservative fuel weight of three fuel elements

g = 49.7, dynamic load factor for the 30-foot side drop

L = 23.31 inches, length of the shorter body tube

To bound both the longer can and short can, p = 56.29 lb/in. is used to calculate the maximum distributed load.

Since (Young, 6th Edition, Table 17, Case 13):

$$p = 2wR(1+C)/(\pi-\theta)$$

$$w = \frac{p\times(\pi-\theta)}{2R\times(1+C)} = 36.27 \text{ lb/in.}$$

where:

p = 56.29 lbs, load on this unit length of the can

θ = 120° = 2π/3, angle

C = cos (θ) = -0.5

R = 3.25/2, radius of the can

The bending moment occurring at location A and C are respectively (Young, 6th Edition, Table 17, Case 13):

$$M_A = \frac{-wR^2}{\pi(\pi-\theta)}\left\{2+2C-s(\pi-\theta)+k_2\left[1+C-\frac{(\pi-\theta)^2}{2}\right]\right\} = -2.603 \text{ in-lb}$$

$$M_C = \frac{-wR^2}{\pi(\pi-\theta)}\left\{\pi(\pi-\theta)-2-2C-s\theta+k_2\left[1+C-\frac{(\pi-\theta)^2}{2}\right]\right\} = -13.311 \text{ in-lb}$$

where:

w = 36.27 lb/in, maximum distributed load

R = 3.25/2 - 0.065/2, radius of the can

θ = 120° = 2π/3, angle

C = cos (θ) = -0.5

s = sin(θ) =0.866

$k_2 = 1 - \alpha = 1$ and $\alpha = \frac{I}{AR^2} = \frac{2.289 \times 10^{-5}}{0.6504\times1.593^2} = 1.388\times10^{-5}$

$I = \frac{1\times0.065^3}{12} = 2.289\times10^{-5}$ in^4, moment of inertia of ring cross-section

$A = \pi(1.625^2 - 1.56^2) = 0.6504$ in^2

The bending stress at location C, for a unit length, is:

$$\sigma_c = \frac{M_C}{t^2/6} = 18.903 \times 10^3 \text{ psi}$$

where:

M_C = 13.311 lb-in., bending moment at location C

t = 0.065 in, thickness of the sealed failed fuel canister

For the 30-foot side drop, the sealed failed fuel can needs to withstand the load applied by its contents and the pressure internal load caused by 100% fuel failure. The internal pressure is taken to be 11.4 atm, which is conservative.

Considering the sealed failed fuel can as a thin wall cylinder with an internal pressure of 168 (11.4 x 14.7) psi, the stresses in circumferential, radial and longitudinal directions are:

$$\sigma_\theta = \frac{P \times r}{t} = 4{,}200 \text{ psi}$$

$$\sigma_r = -P = -168 \text{ psi}$$

$$\sigma_Z = \frac{P \times r}{2 \times t} = 2{,}100 \text{ psi}$$

where:

P = 168 psi, pressure

r = 3.25/2 inches, radius of the can,

t = 0.065 in, thickness of the can,

Combining the stresses caused by the can contents (30 ft side drop) and internal pressure, the circumferential stress is:

$$S + \sigma_\theta = 23{,}103 \text{ psi}$$

The stress intensity is:

$$S_{int} = S + \sigma_\theta - \sigma_r = 23{,}271 \text{ psi}$$

Margin of safety:

$$\text{M.S.} = \frac{3.6\ S_m}{\sigma_C} - 1 = \frac{59{,}040}{23{,}271} - 1 = +1.54$$

Seal Failed Fuel Can Bolt Evaluation

Bolts for the failed fuel can are qualified using worst case loading conditions. For analysis purposes, the maximum differential thermal expansion (from accident), lifting loads, and bolt preload are combined to calculate the maximum bolt stresses.

The detailed bolt evaluation is provided in Section 2.6.12.7.6.3. The analysis shows the sealed failed fuel can closure bolts are adequate for normal and accident loading conditions.

2.7.7.9.6 Borated Stainless Steel Plate Weld Stress

For the purposes of this analysis, the borated stainless steel plate is assumed to be welded along two sides to the divider plates using a 1/16-inch fillet weld. This assumption is conservative, since the borated plate is welded completely around its periphery. For the end drop condition, the only load applied on the weld is the self weight of the plate, which results in a shear stress. For side drop, the load applied on the weld is the self weight of plate, which also results in shear stress. The plate also carries the weight of the fuel, which results in compressive stress.

The welded area for one stainless steel plate is:

Parameter	Base Module	Intermediate Module	Top Module
Weight of Plate (lb)	14.44	13.64	21.61
Length of Plate (in.)	30.45	28.75	45.55
Cross-section Area (in^2)	99.27	93.73	148.49
Weld Area (in^2)	3.81	3.59	5.69

Using the smallest area, 3.59 in^2 and largest weight, 21.61 lbs, the accident condition shear stress is:

$$S_{se} = \frac{g \times W}{A} = 361.17 \text{ psi}$$

where:

g = 60.0, 30-foot end drop load factor

W = 21.61 lbs, bounding poison plate weight

A = 3.59 in^2, bounding weld area

The allowable shear stress for accident conditions is 0.42 S_u = 26,670 psi. The margin of safety is:

$$\text{Margin of Safety} = \frac{26{,}670}{361.17} - 1 = +\underline{\text{Large}}$$

Using the smallest area, 3.59 in^2 and the largest weight, 21.61 lbs, the 30-foot side drop shear stress is:

$$S_{ss} = \frac{g \times W}{A} = 299.17 \text{ psi}$$

where:

g = 49.7, 30-foot side drop load factor

W = 21.61 lbs, bounding poison plate weight

A = 3.59 in^2, bounding weld area

The allowable shear stress for accident conditions is 0.42 S_u = 26,670 psi. The margin of safety is

$$\text{Margin of Safety} = \frac{26{,}670}{299.17} - 1 = +\underline{\text{Large}}$$

The compressive stress is evaluated using a bounding fuel cell weight of 80 lbs and the minimum cross-section area of 93.73 in^2.

$$S_c = \frac{g \times W}{A} = 42.42 \text{ psi}$$

where:

g = 49.7, the 30-foot side drop load factor

W = 80 lbs, bounding fuel cell weight

A = 93.73 in^2, bounding cross-section area

The allowable stress for accident conditions is 0.70 S_u = 44,450 psi. The margin of safety is:

$$\text{Margin of Safety} = \frac{44{,}450}{42.42} - 1 = +\underline{\text{Large}}$$

This evaluation shows that the borated stainless steel plates and welds have large margins of safety for the stresses that could occur in accident conditions.

2.7.7.9.7 TRIGA Fuel Spacer Evaluation

A spacer fabricated from Type 304 stainless steel is used in poisoned TRIGA basket Configuration 2 (base module and 4 intermediate modules). The spacer consists of 8-inch diameter pipe with a 1 inch thick plate welded to the bottom, and a 0.5 inch thick plate welded to the top. The top plate is attached to the underside of the NAC-LWT cask lid using four 1/2-inch diameter SA-193, Grade B6, bolts. The spacer has a calculated weight of 85 lbs.

The spacer and bolts are analyzed for the effects of a normal condition 1-foot side and end drop. The material temperatures and properties are the same as those imposed on the fuel baskets. The compression load is calculated as 192,960 lbs, which results in a calculated stress of 22,971 psi (Margin of Safety = +0.94). The stress on the bolts in combined shear and tension is 24,307 psi. All margins of safety are positive with a minimum Margin of Safety of +1.68 for the bolts in shear and tension as a result of the side drop condition.

2.7.7.9.8 TRIGA Fuel Cluster Rods 30-Foot Drop Evaluation

During the 30-foot side drop, load is transferred to the adjacent 0.75-inch outer diameter 6061-T6 aluminum insert tube. The maximum stress occurring in the 0.75-inch tube will be a bending stress due to the diametrical line loads. This evaluation was also performed for the 1-foot operational side drop using an acceleration of 24.3 g in Section 2.6.12.7.9. For the 30-foot drop, the acceleration is 49.7 g. Since the bending stress is directly proportional to the acceleration, the bending stress for the 30-foot drop is computed by applying a ratio of 49.7/24.3 to the bending stress of 3,969 psi (from Section 2.6.12.7.9), which results in a stress of 8,117 psi for the accident condition. The allowable primary stress for this accident condition is 16,800 (at 400°F), which results in a Margin of Safety of 16,800/8,117-1 or +1.07. This verifies that the aluminum tube maintains acceptable stress during the 30-foot accident condition.

2.7.7.9.9 Conclusion

Loads generated in the TRIGA fuel basket assembly in the hypothetical accident conditions result in stresses, which are below allowable limits. Analyses show that all basket bearing stresses during a postulated 30-foot side drop are less than the material ultimate strength. Column analyses demonstrate that the basket assembly is self-supporting during the postulated 30-foot end drop. The minimum margin of safety is 0.13 (Section 2.7.7.9.3). Therefore, the TRIGA fuel basket has sufficient structural integrity in the hypothetical accident conditions.

2.7.7.10 DIDO Fuel Basket Construction

The DIDO modular basket assembly consists of a top module, four intermediate modules, and a base module. The top module is 29.8 inches long and the intermediate modules are each 29.3 inches long and all have an outer diameter of 13.27 inches. The base module has a length of 29.8 inches and an outer diameter of 13.27 inches. Each module is capable of holding seven DIDO fuel assemblies. Each module is a weldment made up of a 13.27-inch diameter 1/2-inch thick base plate and two 13.27-inch diameter 1/2-inch thick support plates scalloped on the inner diameter to fit around six peripheral fuel tubes. The weldment structure, fuel tubes and base and support plates are fabricated from Type 304 stainless steel. Each fuel tube has an inner diameter of 4.01 inches and a wall thickness of 0.12 inch. The bottom of each fuel tube is welded to the 1/2-inch thick base plate. The bottom of each fuel tube has a slot at the bottom to permit water to drain from the fuel tube. The base plate supports the fuel in the end drop orientation. The base module sits on a 0.5-inch long, 10-inch diameter schedule 80S pipe that is welded to the base plate. The total weight of the DIDO basket assembly bears directly on the bottom forging of the cask through the schedule 80S pipe. The two scalloped 1/2-inch thick support plates and the base plate of each basket module provide lateral support and maintain the fuel configuration in the side drop orientation.

Heat rejection from the DIDO fuel and basket structure is augmented by six aluminum shunts, which are mechanically attached to the center stainless steel fuel tube, and two heat transfer shells, which wrap around the 6 outer fuel tubes. The heat shunts are machined to match the outer diameter of the center fuel tube and are held in place by two shunt posts and shunt retainers. The shunt post at the bottom of each basket module is assembled with a tight fit between the shunt post, shunt retainer and base plate to provide a good conductive heat transfer path. The shunt post at the top of the basket is assembled with a slotted hole in the shunt to permit unrestricted differential thermal expansion between the fuel tube and thermal shunt. The aluminum sheet heat transfer shell is held in place against the outside fuel tubes by bolting the edge of the aluminum sheet to the drain tube guide bars. The heat shunts and heat transfer shell are not structural components and are not included in the structural analysis as load carrying components. The mass of the heat shunts and heat transfer shell has been included as a load in the structural analysis.

2.7.7.10.1 DIDO Fuel Basket Cask Interface Analysis

Structural analysis of the DIDO modular fuel basket and the MTR modular fuel basket are similar. DIDO fuel baskets and MTR fuel baskets are made from the same type of stainless steel. The contact points between the basket structure and the cask inner shell and between the

basket structure and cask bottom forging are similar. DIDO fuel baskets have an additional lateral support ring, reducing the side drop bearing stresses. A loaded DIDO fuel basket base module weighs approximately 250 lbs, assuming each DIDO fuel assembly weighs 15 lbs. The bounding assembly weight accounts for the fuel assembly and tube spacer and any variations in the weight of either. Loaded top and intermediate modules weigh 247.4 lbs each. A full cask load of six DIDO basket modules represents a total contents weight of 1,487 lbs. The weight of a loaded 28-element MTR basket is 289 lbs, which bounds the loaded weight of the loaded base DIDO basket module. Therefore, the bearing stress between the basket and the cask inner shell created by the DIDO basket module is bounded by the 28-element MTR fuel basket interface analysis.

The cask contents weight for the loaded 42-element MTR basket is 2,262 lbs, which bounds the cask contents weight of 1,487 lbs for the loaded DIDO basket. Therefore, the bearing stresses between the basket and cask bottom forging and between the basket and the cask lid created by the DIDO fuel baskets, are bounded by the 42-element MTR fuel basket interface analysis.

2.7.7.10.2 DIDO Fuel Basket Structural Analysis

Structural analyses of the DIDO fuel basket for the 30-foot end drop and the 30-foot side drop are performed using a finite element model, Figure 2.6.12-1 and Figure 2.6.12-2, and the ANSYS general purpose computer program. Eight node brick elements (SOLID45) are used to construct the model. Stainless steel material properties are used for each of the solid elements. The elements representing the seven 4.01-inch inner diameter tubes are joined to the base support plates at locations where the welds are specified to connect the tubes to the plates. All seven tubes are connected to the 1/2-inch thick base plate. By design, the center tube is also connected to the base plate, but it is not connected to any of the six outer tubes. In this evaluation, the center tube is not considered to have any interaction with the outer six tubes, which is conservative, particularly in the side drop orientation where the tube is cantilevered from the base plate.

DIDO Fuel Basket 30-Foot Side Drop Analysis

The 30-foot side drop analysis of the DIDO fuel basket considers the weight of the center tube and fuel to be transferred to the circular base plate. To model the interaction of the two support plates and the base plate with the 13.375-inch cask inner shell diameter, CONTAC52 elements are used. The CONTACT52 element consists of two nodes which correspond to a 3D-line element, limiting transmitted loads to compression. One node of the CONTACT52 element is located on a circular plate, while the second node represents the inner shell, and is constrained in all three degrees of freedom. This boundary condition is considered to be conservative, since it

models the inner shell as a rigid surface and minimizes the angle of contact between a circular plate and the cask inner shell, resulting in a more concentrated load at the point of contact. The aluminum heat shunts and aluminum heat transfer shell are not considered to be structural components. Inclusion of these components in the structural model is limited to their representation as lumped masses using the MASS21 element. These lumped masses are distributed along the outside of the center tube to represent the distributed weight of the heat shunt. The heat transfer shell is represented with lump masses distributed along the outer six fuel tubes at the points of contact with the heat transfer shell.

The 30-foot side drop accident condition is analyzed using an acceleration of 47.9g applied in each of three orientations: 0°, -60°, and -90° with respect to the model's X-axis. Maximum primary membrane stresses for each of the side drop orientations are shown in Table 2.7.7-1. The minimum margin of safety is calculated to be +3.7 for the -60° orientation. The maximum primary membrane plus bending stresses for each of the side drop orientations are shown in Table 2.7.7-2. The minimum margin of safety is calculated to be +0.35 for the -60° orientation.

DIDO Fuel Basket 30-Foot End Drop Configuration

For the 30-foot end drop analysis, the finite element model load orientation and boundary conditions are specified to represent axial loading and consideration of the base basket module supporting five stacked modules above it. Equivalent pressure was applied to the area inside of the fuel tube at the top surface of the base plate to represent the fuel in each of the fuel tube locations in each basket module. The weight of the five loaded fuel basket modules, which rest on the base fuel basket module, multiplied by the equivalent acceleration, is applied as an equivalent pressure to the top edges of the fuel tubes in the base module. Therefore, the total weight resting on the top of the base module is 1,237 pounds. This load was applied as a pressure load on the ends of the fuel tubes.

Total end area of tubes = $7 \times \pi/4 \times (4.25^2 - 4.01^2) = 10.9$ in^2

Equivalent pressure = 1237 lbs/10.9 in^2 = 113.5 psi

The end drop finite element model reflects the base basket design shown on the drawings provided in Section 1.0. The height of the base skirt below the bottom support is 0.5 inches. Four full height drain slots are cut into the base skirt.

For the 30-foot end drop condition, the equivalent pressure load is increased to represent the maximum acceleration of 60g. The maximum primary membrane stress for the end drop orientations is 43.3 ksi (shown in Table 2.7.7-1) results in a minimum margin of safety of +0.07.

The maximum primary membrane plus bending stress is 50.0 ksi (shown in Table 2.7.7-2) results in a minimum margin of safety of +0.32.

Based on these results it is concluded that the DIDO fuel basket is structurally adequate for hypothetical drop accident conditions.

Table 2.7.7-1 Maximum Primary Membrane Stress for the 30-Foot Drop

Location	Load Case 30-ft Drop	Membrane (ksi)	Allowable (ksi) [1]	Margin of Safety [2]
Fuel Tube Wall	Side @ 0 Deg[3]	9.8	46.2	3.70
Fuel Tube Wall	Side @ 60 Deg[3]	9.9	46.2	3.70
Fuel Tube Wall	Side @ 90 Deg[3]	9.6	46.2	3.80
Fuel Tube Wall	End drop	43.3[4]	46.2	0.07

Table 2.7.7-2 Maximum Primary Membrane Plus Bending Stress for the 30-Foot Drop

Location	Load Case 30-ft Drop	Membrane + Bending (ksi)	Allowable (ksi) [1]	Margin of Safety[2]
Fuel Tube Wall	Side @ 0 Deg[3]	48.3	66.0	0.37
Fuel Tube Wall	Side @ 60 Deg[3]	49.0	66.0	0.35
Fuel Tube Wall	Side @ 90 Deg[3]	45.1	66.0	0.46
Fuel Tube Wall	End drop	50.0[4]	66.0	0.32

1 $P_m \leq S_m$.
2 Margin of safety = (Allowable-Stress/Actual Stress) – 1.
3 Angle orientation shown on Figure 2.6.12-1.
4 The linearized stresses for the end drop case are scaled by the ratio of 360/178.65, which is the full arc length to arc length of the tube welded to the base plate.

2.7.7.11 General Atomics IFM Basket Construction

The General Atomics IFM basket consists of a top module assembly designed to carry two IFM FHU. Each fuel container is associated with a RERTR fuel element or HTGR fuel materials. A spacer assembly is used to permit the top module assembly to be positioned next to the transport cask lid.

The top module is 43.7 inches long and is made up of two fuel tubes and three support plates. All components are made from ASME SA240 Type 304 stainless steel. The fuel tubes have a 6.0-inch outer diameter and a 0.25-inch wall thickness. Two of the support plates are 0.50-inch thick and the third, center plate, is 1.0-inch thick. The support plates are welded to the fuel tubes with 1/8-inch bevel welds.

Two types of IFM FHU are carried by the basket. One FHU carries irradiated HTGR fuel material and is 5.25 inches in diameter (0.12-inch thick wall) and is 39.0 inches long. The other FHU contains irradiated RERTR fuel material and is 4.75 inches in diameter (0.12-inch thick wall) and is 37.25 inches long.

Each end of the FHU is comprised of a 0.25-inch thick plate welded to the container shell. The weld connecting the end plate to the container shell is labeled as a full penetration butt weld. The dimensions of the end plate and the container shell provide a minimal gap (2 mils when considering maximum tolerances) to permit the end plate to be inserted into the container end. The close tolerances ensure that the two components are effectively in contact along the 0.5-inch common interface length of the end plate and the container. Once the end plate is inserted, a fusion weld procedure is employed to weld the lip of the end plate to the wall of the container. The depth of the weld along the interface between the end plate and the container is equal to approximately 70% of the thickness of the end plate lip or the container lip.

Due to the location of the weld for the end plate, the weld does not transfer any load for the drop conditions. Additionally, since the heat loads are insignificant (13w) and the backfill for the FHU and the cask cavity is limited to atmospheric pressure, the pressure differential across the welded plates is insignificant. Each of these FHUs also has an additional smaller container, which holds the fuel. In these evaluations, the inner container is neglected.

The spacer assembly is 133.0 inches in length, excluding guide pins. The assembly is made up of one spacer tube and five support plates. The spacer tube consists of a Type 304 stainless steel 8-inch Schedule 80S pipe. The tube has an outside diameter of 8.63 inches and a wall thickness of 0.50 inch. The spacer plates are 1.0-inch thick and are welded to the tube with 1/8-inch bevel welds. Two guide pins are located at the top of the spacer assembly to facilitate alignment with the top module.

2.7.7.11.1 General Atomics IFM Basket Interface Analysis

The structural evaluation of the fuel basket assembly is performed using classical hand calculations. The weight of the top module is bounded by 200 lbs, and the maximum weight of one FHU is 76 lbs (General Atomics, April 2002). Therefore, the total weight of a loaded top module system is 200 + 2(76) or 352 lbs. The weight of the spacer assembly is 760 lbs. The total loaded system weight is 1,112 lbs, and this weight is bounded by the design basis contents weight for the LWT system. Therefore, no analysis of the LWT cask is required.

2.7.7.11.2 General Atomics IFM Basket Structural Analysis

Structural analyses for the General Atomics basket for the 30-foot end drop and 30-foot side drop are performed using classical hand calculations.

General Atomics 30-Foot Side Drop Analysis

Top Module:

Using the 1 g bending stress, 26 psi, calculated in the subsection titled "General Atomics Top Module Structural Analysis," the margin of safety for a 30-foot side drop is:

$$MS = \frac{S_u}{S_b} - 1 = \frac{65200}{55 \times 26} - 1 = +\underline{\text{Large}}$$

During a side drop, the top and bottom support plate welds are in shear. Using the stress in the weld for 1g, 26.4 psi, calculated in the subsection titled "General Atomics Top Module Structural Analysis," and the visual inspection weld factor, the margin of safety for shear, 30-foot side drop (55 g), is:

$$MS = \frac{0.25 \times 0.42 S_u}{55S} - 1 = \frac{0.25 \times 0.42 \times 65{,}200}{55 \times 26.4} - 1 = +3.71$$

Spacer Assembly:

Using the 1g bending stress, 31 psi, calculated in the subsection titled "General Atomics Top Module Structural Analysis," the margin of safety for bending during a 30-foot side drop is:

$$MS = \frac{S_u}{S_b} - 1 = \frac{65{,}200}{55 \times 31} - 1 = +\underline{\text{Large}}$$

During a side drop, the top support plate weld is in shear. From the subsection titled "General Atomics Top Module Structural Analysis," the weld shear stress for a 1 g loading is 31 psi. Using a 0.25-inch weld quality factor, the margin of safety for a 30-foot side drop is:

$$MS = \frac{0.25 \times 0.42 S_u}{55S} - 1 = \frac{0.25 \times 0.42 \times 65{,}200}{55 \times 31} - 1 = +3.0$$

Fuel Handling Unit (FHU):

The FHUs are analyzed in accordance with ASME Section III, Subsection NG. From the subsection titled General Atomics Top Module Structural Analysis, the stress in the FHU for a 1g side drop is 0.63 ksi. For a 30-foot side drop, the margin of safety is

$$MS = \frac{S_u}{55S} - 1 = \frac{65.2}{55 \times 0.63} - 1 = +0.88$$

Because the internal and external pressures on the container are essentially identical, no additional ASME Section III, Subsection NG analysis is required.

General Atomics 30-Foot End Drop Analysis

Top Module:

During an end drop, the stress in the fuel tubes is 22 psi for a 1 g end drop (see subsection titled General Atomics 1-Foot End Drop Analysis). The margin of safety for a 30-foot end drop is:

$$MS = \frac{0.7 S_u}{60S} - 1 = \frac{0.7 \times 65{,}200}{60 \times 22} - 1 = +\underline{\text{Large}}$$

Since the stress in the tubes is significantly below yield, no buckling evaluation is required.

During an end drop, the stress in the support plate weld for a 1g end drop is 6.0 psi (see subsection titled "General Atomics 1-Foot End Drop Analysis"). For a 30-foot end drop, the margin of safety in the weld is:

$$MS = \frac{0.25 \times 0.6 S_m}{20S} - 1 = \frac{0.25 \times 0.6 \times 19{,}350}{20 \times 6} - 1 = +\underline{\text{Large}}$$

Spacer Assembly:

During an end drop, the stress in the tube for a 1 g end drop is 87 psi. For a 30-foot end drop, the margin of safety is:

$$MS = \frac{0.7 S_u}{60S} - 1 = \frac{0.7 \times 65{,}200}{60 \times 87} - 1 = +\underline{\text{Large}}$$

Since the stress in the tube is significantly below yield, no buckling evaluation is required.

During a 1 g end drop, the stress in the support disk weld is 5.2 psi. Since the weld stress is less than the weld stress in the top module support disk, no additional analysis is required.

Fuel Handling Unit:

During a 30-foot end drop, the stress in the tube is:

$$S = \frac{60 \times 76}{1.62} = 2.8 \text{ ksi}$$

$$MS = \frac{0.7S_u}{S} - 1 = \frac{0.7 \times 65.2}{2.8} - 1 = +\underline{\text{Large}}$$

Since the stresses in the tube are significantly below the yield stress allowable, no buckling evaluation is required.

2.7.7.12 TPBAR Basket Analysis

The TPBAR basket is a modified NAC-LWT PWR basket that has had material removed to increase free volume in the cask cavity. The cylindrical basket is fabricated from 6061-T651 aluminum alloy. A central opening, 8.82 inches square, extends the length of the basket and provides lateral support for the two TPBAR content conditions: the TPBAR consolidation canister; and the TPBAR waste canister. A 13.25-inch outside diameter, 8.25-inch long stainless steel upper fitting is bolted to the top of the basket body. This fitting provides lifting points for installation and removal of the basket from the cask. Additionally, this fitting prevents the basket from applying load to the TPBAR consolidation canister or waste container during the top-end drop. The lifting bail for both the consolidation canister and the waste container are fabricated from Type 17-4 precipitation hardened stainless steel. A second stainless steel fitting is bolted to the bottom of the basket body. The lower fitting assembly supports the fuel basket and contents longitudinally and limits movement within the cask. A TPBAR spacer assembly is bolted to the underside of the cask lid to prevent the TPBAR contents from shifting axially within the basket, and maintains the waste container rotational orientation. A groove on the periphery of the basket body provides for the cask drain tube. The drain tube is connected to a fitting on the cask body and is used to drain or fill the cask during cask loading or unloading operations.

The first TPBAR content condition is for the transport of up to 300 production TPBARs in an open (unsealed), Type 304 stainless steel consolidation canister with optional top insert. The canister is considered a nonstructural component and is only used to position the TPBARs within the basket and to handle the TPBARs during loading and unloading operations. The second content condition is for the transport of up to 55 TPBARs, which have been segmented from PIE, in a welded, Type 316L stainless steel waste container. The container is also considered a nonstructural component only used for handling the TPBAR segments and debris during cask

loading and unloading operations. Therefore, for purposes of the basket structural analyses, the canister and container are both considered to fail and to not protect the contents from damage. The effects of damage to the TPBARs are evaluated in other sections of the SAR.

Once the cask lid is bolted to the cask body, the configuration of the TPBAR contents (i.e., consolidation canister or waste container) are maintained by the TPBAR basket without consideration of the strength of the canister or container. The TPBAR basket provides a boundary for support on all sides and for the full length of the contents. The TPBAR basket upper end-fitting spacer guides carry the weight of the basket and prevent the contents from being loaded by the TPBAR basket in any drop orientation. The TPBAR spacer assembly attached to the bottom of the cask lid restricts the axial movement of the contents. Therefore, no additional evaluation is required for either the TPBAR consolidation canister or the TPBAR waste container and extension. The analyses for the loaded consolidation canister weight of 1,000 lbs bounds the loaded weight of the TPBAR waste container (700 lbs).

2.7.7.12.1 TPBAR Basket Body

Structural analyses of the TPBAR basket for 30-foot end and side drops are performed using classical hand calculations.

TPBAR Basket Body 30-Foot Side-drop Analysis

The TPBAR basket body is constructed of four machined segments held together with aluminum bands at five locations along the axial length of the basket, as well as the upper and lower fittings, which are bolted to the aluminum basket. During a side drop, the TPBAR basket is subjected to bending and bearing stresses. The maximum bending stress occurs at Location 'A' shown in the following sketch and is due to the content weight. The maximum bending stress is calculated using a cantilevered beam. This is conservative since it neglects any support of the load due to the edges of the basket being supported by the cask inner shell. The maximum bending stress is:

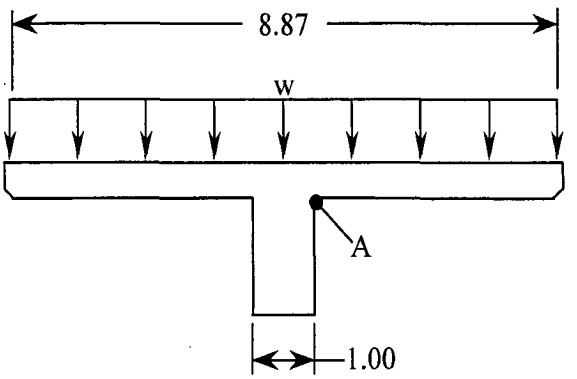

$$S_b = \frac{6M}{t^2} = \frac{6 \times 364}{0.5^2} = 8.7 \text{ ksi}$$

where:

$$M = w \times \left(\frac{b}{2} - \frac{1}{2}\right) \times \frac{1}{2}\left(\frac{b}{2} - \frac{1}{2}\right)$$

$$= 47 \times \left(\frac{8.87}{2} - \frac{1}{2}\right) \times \frac{1}{2}\left(\frac{8.87}{2} - \frac{1}{2}\right) = 364 \text{in-lb/in, the maximum bending moment}$$

$$w = \frac{W_c \times g}{L \times b} = \frac{1000 \times 60}{144 \times 8.87} = 47 \text{ psi}$$, the distributed load of the TPBAR consolidation canister

W_c = 1,000 lbs, bounding TPBAR canister weight (with TPBAR rods)

L = 144 inches, length of consolidation canister

b = 8.87 inches, TPBAR basket opening width

g = 60 g, side-drop acceleration

t = 0.5 in, thickness of the flange

The margin of safety is:

$$MS = \frac{S_u}{S_b} - 1 = \frac{31.5}{8.7} - 1 = +2.6$$

where:

S_u = 31.5 ksi, ultimate strength of 6061-T651 aluminum @300°F

TPBAR Basket Body 30-Foot End Drop Analysis

During end drops, the maximum compressive stress on the minimum cross- section of the basket body is:

$$S_{comp} = \frac{g \times W_b}{A} = \frac{60 \times 900}{32.26} = 1.7 \text{ ksi}$$

where:

W_b = 900 lbs, the bounding weight of the TPBAR basket

g = 60 g, accident end drop acceleration

A = $9.87^2 - 8.87^2 + 4(1.00 \times (13.25 - 9.87)) = 32.26 \text{ in}^2$, the minimum cross-sectional area of the basket

The margin of safety is:

$$MS = \frac{0.7S_u}{S_{comp}} - 1 = \frac{0.7 \times 31.5}{1.7} - 1 = +\underline{\text{Large}}$$

where:

S_u = 31.5 ksi, ultimate strength of 6061-T651 aluminum @ 300°F

2.7.7.12.2 TPBAR Basket Upper Fitting

The upper fitting of the TPBAR basket prevents the basket from loading the TPBAR contents during a top-end drop. Four spacer guides of the upper fitting fabricated from Type 304 stainless steel are provided for this purpose. The spacer guides have a length of 7.63 inches, a width of 2.0 inches, and a thickness of 1.00 inch with a 45° × 0.25-inch chamfer. A bounding weight of 900 pounds is used for the TPBAR basket. The temperature of the lid and upper region of the NAC-LWT cask body during TPBAR shipment is conservatively assumed to be 300°F. From Chapter 3, a temperature of 300°F bounds the maximum temperature of the upper NAC-LWT region for a maximum heat load of 1.05 kW. Since the maximum heat load for the TPBAR shipment is less than 1.0 kW, using 300°F for the analysis of the TPBAR upper fitting is conservative.

TPBAR Basket Upper Fitting 30-foot Side Drop

During a side drop, the welds that hold the spacer guides to the top fitting are in shear and bending. The shear load on the welds is:

$$P = (b \times t \times L) \times \rho \times g = (2.0 \times 1.0 \times 7.63) \times 0.288 \times 60 = 264 \text{ lbs}$$

where:

b = 2.0 inches, spacer guide width

t = 1.0 in, spacer guide thickness

L = 7.63 inches, spacer guide length

ρ = 0.288 lb/in^3, density of Type 304 stainless steel

g = 60 g, side-drop acceleration

The welds for the spacer are ⅛-inch fillet welds on three sides. The shear stress in the welds is:

$$\tau = \frac{P}{A} = \frac{264}{0.354} = 747 \text{ psi} \approx 0.8 \text{ ksi}$$

where:

$$A = 0.125 \times 0.707 \times (2.0 + 2 \times 1.0) = 0.354 \text{ in}^2, \text{ weld area}$$

The bending moment is:

$$M = \frac{wL^2}{2} = \frac{(b \times t \times \rho \times g) \times L^2}{2} = \frac{(2 \times 1 \times 0.288 \times 60) \times 7.63^2}{2} = 1{,}006 \text{ in-lb}$$

The stress in the weld due to bending is:

$$S = \frac{M}{t \times S_w} = \frac{1{,}006}{(0.125 \times 0.707)0.56} = 20.3 \text{ ksi}$$

where:

t = weld throat

$S_w = \frac{d^2(2b+d^2)}{3(b+d)} = \frac{1^2(2\times 2+1^2)}{3(2+1)} = 0.56 \text{ in}^2$, section modulus of weld (Blodgett)

The maximum shear stress, τ_{max}, in the weld that is equivalent to the stress intensity divided by two is:

$$\tau_{max} = \frac{\sqrt{S^2+4\tau^2}}{2} = \frac{\sqrt{20.3^2+4\times 0.8^2}}{2} = 10.2 \text{ ksi}$$

The margin of safety is:

$$MS = \frac{0.5 \times S_u}{SI} - 1 = \frac{0.5\times 66.0}{10.2} - 1 = +2.2$$

where:

S_u = 66.0 ksi, ultimate strength of Type 304 stainless steel @ 300°F

TPBAR Basket Upper Fitting 30-Foot Top-End Drop

For a top-end drop, the weight of the TPBAR basket will load the four spacer guides. The membrane stress in the spacer guide is:

$$S = \frac{W_b \times g}{A} = \frac{900\times 60}{(2.0\times 1.0)\times 4} = 6.8 \text{ ksi}$$

where:

W_b = 900 lbs, bounding TPBAR basket weight

A = $(2.0 \times 1.0) \times 4 = 8 \text{ in}^2$, cross-sectional area of the spacer guide

g = 60 g, end-drop acceleration

The margin of safety is:

$$MS = \frac{0.7 \times S_u}{S} - 1 = \frac{46.2}{6.8} - 1 = +5.8$$

where:

S_u = 66.0 ksi, ultimate strength of Type 304 stainless steel @300°F

The critical buckling load for the spacer is determined by using Euler's buckling equation. The critical buckling load is:

$$W_{cr} = K_c \frac{EI}{L^2} = 2.47 \frac{27 \times 10^6 (0.1667)}{7.63^2} \approx 190.9 \text{ kip}$$

where:

E = 27×10^6 psi, modulus of elasticity of Type 304 stainless steel @ 300°F

K_c = 2.47, buckling constant (Blake, Table 10.3)

I = $\frac{bt^3}{12} = 0.1667$ in^4, minimum moment of inertia for cross-section

b = 2.0 inches, spacer guide width

t = 1.0 in, spacer guide thickness

L = 7.63 inches, length of spacer guide

The margin of safety against buckling of the four spacer guides is:

$$MS = \frac{190{,}900}{60 \times 900/4} - 1 = +\underline{\text{Large}}$$

2.7.7.12.3 TPBAR Basket Lower Fitting

The TPBAR basket lower fitting is identical to the bottom fitting of the PWR basket. The weight of the loaded TPBAR basket is less than the weight of the loaded PWR basket. Therefore, additional analyses are not required.

2.7.7.12.4 TPBAR Spacer

The TPBAR spacer is designed to maintain the location of the TPBARs during transport and to prevent the consolidation canister from loading the TPBAR contents during a top-end drop. The spacer is constructed of a circular base plate, two triangular spacer bases, two tubes, and two triangular top plates. The circular base plate is used to attach the spacer to the lower surface of the NAC-LWT cask closure lid. The circular base plate is attached with Type 304 stainless steel bolts. The two triangular spacer bases are bolted to the circular base plate. The tubes, constructed of 3-inch schedule 80 pipes, are welded to the spacer base and the triangular top plates that provide the interface with the TPBARs. The triangular top plates are arranged to form

a square that fits inside the consolidation canister. A gap between the triangular top plates provides a recess to accommodate the lifting bail of the canister and container. The weight of the spacer assembly is bounded by 115 pounds. The bounding weight of the consolidation canister is 184 lbs (978 lbs when loaded with 300 TPBARs). During top-end drop conditions, the weight of the consolidation canister is carried by the bail and directly transmitted into the NAC-LWT cask lid. Therefore, only the weight of the TPBARs is supported by the spacer for top-end drop conditions. The temperature of the lid and upper region of the NAC-LWT cask body during TPBAR shipment is conservatively assumed to be 300°F. From Chapter 3, a temperature of 300°F bounds the maximum temperature of the upper LWT region for a maximum heat load of 1.05 kW. Since the maximum heat load for the TPBAR shipment is less than 1.0 kW, using 300°F for the analysis of the TPBAR spacer is conservative. In the case of the TPBAR waste container, the entire loaded weight of the container of 700 lbs is conservatively assumed to be supported by the spacer. This loading condition is bounded by the loading of the 794-pound maximum TPBAR weight in the consolidation canister.

TPBAR Spacer 30-foot Side Drop

Bolts

During 30-foot side-drop conditions, the weight of the spacer applies a shearing and tensile load to the bolts. The tensile load is due to the couple reacting out the moment generated by the cantilever action of the spacer. The shear stress is:

$$\tau = \frac{P}{A_t} = \frac{1{,}725}{0.1419} = 12.2 \text{ ksi}$$

where:

$$P = \frac{W \times g}{4} = \frac{115 \times 60}{4} = 1{,}725 \text{ lbs}$$

W = 115 lbs, spacer assembly weight

g = 60 g, side-drop acceleration

$$A_t = 0.7854\left(D - \frac{0.9743}{n}\right)^2 = 0.7854\left(0.5 - \frac{0.9743}{13}\right)^2 = 0.1419 \text{ in}^2, \text{ tensile area}$$

of bolt thread with ultimate strength up to 100 ksi

For ½-13UNC bolts (Machinery's Handbook):

n = 13, number of threads per inch

D = 0.50 in, bolt diameter

Kn_{max} = 0.434 in, maximum minor diameter of internal thread

Es_{min} = 0.4435 in, minimum major diameter of external thread

En_{max} = 0.4565 in, maximum pitch diameter of internal thread

Ds_{min} = 0.4876 in, minimum major diameter of external thread

L_e = 1.0 in, thread engagement

The bolt tensile load is:

$$P = \frac{M}{d} = \frac{40{,}538}{2 \times 4.95} = 4{,}095 \text{ lbs}$$

d = 9.9 inches, maximum distance between bolts

$$M = \frac{wL^2}{2} \times g = \frac{\left(\frac{115}{11.75}\right)(11.75^2)}{2} \times 60 = 40{,}538 \text{ in - lb}$$, the prying moment generated by the cantilever action of the spacer

The bolt tensile stress due to the moment, M, is:

$$S = \frac{P}{A_t} = \frac{4{,}095}{0.1419} = 28.9 \text{ ksi}$$

The membrane stress intensity on the bolt is:

$$SI = \sqrt{S^2 + 4\tau^2} = \sqrt{28.9^2 + 4 \times 12.2^2} = 37.8 \text{ ksi}$$

The margin of safety is:

$$MS = \frac{0.7\,S_u}{SI} - 1 = \frac{0.7(66.0)}{37.8} - 1 = +0.22$$

where:

S_u = 66.0 ksi, yield strength of Type 304 stainless steel @ 300°F

The shear stress on the external threads is:

$$\tau = \frac{P}{A_S} = \frac{4{,}095}{0.7789} = 5.3 \text{ ksi}$$

where:

$$A_s = 3.1416 n L_e Kn_{max} \left[\frac{1}{2n} + 0.57735(Es_{min} - Kn_{max})\right]$$

$$= 3.1416(13)(1.00)(0.434)\left[\frac{1}{2(13)} + 0.57735(0.4435 - 0.434)\right]$$

$$= 0.7789 \text{ in}^2, \text{ shear area of the bolt threads}$$

The margin of safety is:

$$MS = \frac{0.5S_u}{\tau} - 1 = \frac{0.5(66.0)}{5.3} - 1 = +5.23$$

where:

S_u = 66.0 ksi, ultimate strength of Type 304 stainless steel @ 300°F

Spacer Welds

Using a bounding weight (W) of 25 pounds for the tube and triangular plates, the shear load on the welds is:

$$P = W \times g = 25 \times 60 = 1{,}500 \text{ lbs}$$

where:

g = 60 g, side-drop acceleration

The welds for the spacer are ¼-inch fillet weld. The shear stress in the weld is:

$$\tau = \frac{P}{t_w 0.707 \pi d} = \frac{1{,}500}{0.25 \times 0.707 \times (\pi \times 3.5)} = 772 \text{ psi} = 0.77 \text{ ksi}$$

where:

t_w = 0.25 in, weld size

d = 3.5 inches, outside diameter of 3 inch schedule 80 pipe

The stress in the weld due to bending is:

$$S = \frac{M}{t \times S_w} = \frac{12{,}630}{(0.25 \times 0.707)9.62} = 7.4 \text{ ksi}$$

where:

$M = wL = 25 \times 60 \times 8.42 = 12{,}630 \text{ in - lb}$, the bending moment

$S_w = \frac{\pi d^2}{4} = \frac{\pi \times 3.5^2}{4} = 9.62 \text{ in}^2$, section modulus of the weld (Blodgett)

The maximum shear stress (τ_{max}) in the weld, which is equivalent to the stress intensity divided by two, is:

$$\tau_{max} = \frac{\sqrt{S^2 + 4\tau^2}}{2} = \frac{\sqrt{7.4^2 + 4 \times 0.77^2}}{2} = 3.8 \text{ ksi}$$

The margin of safety is:

$$MS = \frac{0.5S_u}{SI} - 1 = \frac{0.5 \times 66.0}{3.8} - 1 = +7.7$$

where:

S_u= = 66 ksi, ultimate strength of Type 304 stainless steel @ 300°F

TPBAR Spacer 30-Foot Top-End Drop

The maximum content of 300 TPBARs is retained in the consolidation canister in the shape of a square and this configuration loads the spacer tubes via the triangular top plates during top-end drop conditions. The compressive load applied to the tubes during the top-end drop is the weight of the TPBARs, 794 lbs (300 × 2.65 lb/TPBAR), times the bounding acceleration of 60 g. For this analysis, W_c = 1,000 lbs, is conservatively used. This conservatively bounds the loaded weight of the TPBAR waste container of 700 lbs.

Tube

The compressive stress in the tubes is:

$$S = \frac{W_c \times g}{A} = \frac{1000 \times 60}{2 \times \left(\frac{\pi}{4} \left(3.5^2 - 2.9^2 \right) \right)} = 9.9 \text{ ksi}$$

where:

A = the cross-sectional area of a 3-inch schedule 80 pipe with an outer diameter of 3.5 inches and a thickness of 0.3 inch

The margin of safety is:

$$MS = \frac{0.7S_u}{S} - 1 = \frac{46.2}{9.9} - 1 = +3.7$$

where:

S_u = 66.0 ksi, ultimate strength of Type 304 stainless steel @ 300°F

Triangular Top Plate

Referring to the dimensions provided in Figure 2.6.12-6, the pressure applied to a triangular plate is:

$$p_{TP} = \frac{1}{2} \times \frac{1000}{0.5 \times 7.43 \times 7.43} \times 60 = 1{,}087 \text{ psi}$$

The bending moment in the top plate is (see Line A in Figure 2.6.12-6):

$$M = 1{,}087 \times \left(0.5 \times 4.18^2\right) \times \left(\frac{1}{3} \times 4.18\right) = 13{,}231 \text{ in-lbs}$$

The bending stress in the plate is:

$$S = \frac{6M}{bt^2} = \frac{6 \times 13{,}231}{4.18 \times 0.75^2} = 33.8 \text{ ksi}$$

The margin of safety is:

$$MS = \frac{S_u}{S} - 1 = \frac{66.0}{11.2} - 1 = +0.95$$

where:

S_u = 66.0 ksi, ultimate strength of Type 304 stainless steel @300°F

TPBAR Spacer 30-Foot Bottom-End Drop

During the 30-foot bottom-end drop, the inertial load of the spacer is applied to the bolts that affix the spacer to the NAC-LWT cask lid and the welds used to fabricate the spacer assembly. The maximum bottom-end drop acceleration is 60 g.

Bolts

Four bolts (½-13UNC, Type 304 stainless steel bolts) hold the spacer assembly to the bottom of the NAC-LWT cask lid and six fasteners hold the two spacer bases to the circular base plate. For this evaluation, only the four spacer assembly bolts are considered since the individual bolt load is higher and the thread engagement length is shorter. Internal lid threads are not required since high- strength Helicoils are utilized. Using the spacer assembly weight of 115 lbs and an acceleration of 60 g, the critical bolt load is:

$$P = \frac{115 \times 60}{4} = 1{,}725 \text{ lbs}$$

The tensile stress is:

$$S = \frac{P}{A_t} = \frac{1{,}725}{0.1419} = 12.2 \text{ ksi}$$

The margin of safety is:

$$MS = \frac{0.7\,S_u}{S} - 1 = \frac{0.7(66.0)}{12.2} - 1 = +2.79$$

where:

S_u = 66.0 ksi, ultimate strength of Type 304 stainless steel @300°F

The shear stress in the bolt thread is:

$$\tau = \frac{P}{A_S} = \frac{1{,}725}{0.7789} = 2.2\ \text{ksi}$$

The margin of safety is:

$$MS = \frac{0.5S_u}{\tau} - 1 = \frac{0.5(66.0)}{2.2} - 1 = +\underline{\text{Large}}$$

where:

S_u = 66.0 ksi, ultimate strength of Type 304 stainless steel @ 300°F

Spacer Welds

During a 30-foot bottom-end drop (60 g), the spacer weld is loaded by the inertial load of the spacer tube and the triangular top plate (25 lbs bounding). The weld is a ¼-inch fillet weld. The weld stress is:

$$S_w = \frac{W \times g}{t(0.707)(\pi d)} = \frac{25 \times 60}{0.25 \times 0.707 \times (\pi \times 3.5)} = 772\ \text{psi} \approx 0.8\ \text{ksi}$$

where:

d = 3.5 inches, outside diameter of 3-inch schedule 80 pipe

t = 0.25 in, weld size

The margin of safety is:

$$MS = \frac{0.5S_u}{S_w} - 1 = \frac{0.5(66.0)}{0.8} - 1 = +\underline{\text{Large}}$$

where:

S_u = 66.0 ksi, ultimate strength of Type 304 stainless steel @ 300°F

2.7.7.13 ANSTO Basket Analysis

The ANSTO modular basket assembly consists of a top module, four intermediate modules, and a base module. The top and base modules are each 29.8 inches long; each of the four intermediate modules is 29.3 inches long; and all six modules have an outer diameter of 13.27 inches. Each module is capable of holding up to seven spiral fuel assemblies or MOATA plate bundles. Each module is a weldment made up of a 13.27-inch-diameter 1/2-inch-thick base plate and six 13.27-inch-diameter, 1/2-inch-thick support plates scalloped on the inner diameter to fit around six peripheral fuel tubes. The weldment structure, fuel tubes, and base and support plates are fabricated from Type 304 stainless steel. Each of the seven fuel tubes in each module has an outer diameter of 4.375 inches and a wall thickness of 0.125 inch. The bottom of each fuel tube is welded to the 1/2-inch-thick base plate. At the bottom of each fuel tube, where it is welded to the base plate, there is a 0.3-inch slot to permit water to drain from the tube. The base plate supports the fuel in the end drop orientation. The base module sits on a 0.5-inch-long, 10-inch-diameter ring that is welded to the base plate. The total weight of the ANSTO basket assembly bears directly on the bottom forging of the cask through the ring. The six scalloped 1/2-inch-thick support plates and the base plate of each basket module provide lateral support and maintain the fuel configuration in the side drop orientation.

2.7.7.13.1 ANSTO Basket Body 30-Foot Side Drop Analysis

Structural analyses of the ANSTO basket for 30-foot side and end drops are performed using classical hand calculations.

The inertia load for the LWT for a 30-foot side drop is 60 g. A conservative loading condition (Table 17, Case 1, Roark) is considered, which neglects any load distribution. Also, it is conservative to assume that there are three loaded fuel tubes acting on the top of a fuel tube since, in reality, there are only two of them. The stresses in the circumferential direction and in the longitudinal direction are added without regard to their signs. Since the circumferential direction and the longitudinal direction also correspond to the direction of the principal stresses, the addition of the two magnitudes reflects the possibility of the principal stresses being of opposite signs.

The maximum applied load to a fuel tube for the circumferential bending stress is:

$$P_s = (3W_{FT} + 3W) \times 60 = 5{,}796 \text{ lbs}$$

where:

W_{FT} = 14.2 lbs, maximum fuel tube weight

W = 18.0 lbs, maximum fuel assembly weight

The bending moment in the fuel tube is:

$$M = \frac{wRk_2}{\pi} = \frac{201 \times 2.13 \times 1.0}{\pi} = 136 \text{ in-lb/in} \quad \text{(Table 17 Case 1, Roark)}$$

where:

$w = \frac{P_s}{L_t} = 201$ lb/in

L_t = 28.81 inches, shortest fuel tube length

R = 2.13 inches, mean radius of fuel tube

k_2 = $1-\alpha = 1.00$

$$\alpha = \frac{I}{A \times R^2} = \frac{bt^3/12}{b \times t \times R^2} = 2.87 \times 10^{-4}$$

b = 1.0 in, unit length

t = 0.125 in, tube wall thickness

The circumferential bending stress in the fuel tube is:

$$\sigma_c = \frac{6M}{bt^2} = \frac{6 \times 136}{1 \times 0.125^2} = 52.2 \text{ ksi}$$

where:

b = 1.0 in, unit length

t = 0.125 in, tube wall thickness

The stress in the fuel tube in the longitudinal direction is calculated assuming the fuel tube acts like a beam. The maximum bending moment occurs at the top of the basket where the fuel tube acts like a cantilever beam. (The maximum moment for a cantilevered beam with a uniform loading of w (lb/in) and length (l) is $wl^2/2$, as compared to the maximum moment $wl^2/8$ for a simply supported beam.) The bending moment in the tube is:

$$M = \frac{wl^2}{2} = \frac{201 \times 4.^2}{2} = 1{,}608 \text{ in-lb}$$

where:

l = 4.0 inches, the length of the tube extending beyond the support plates

The bending stress is:

$$\sigma_1 = F\frac{Mc}{I} = \frac{1{,}608 \times 2.19}{3.77} = 2.5 \text{ ksi}$$

where:

c = 2.19 inches, distance to extreme outer fiber of tube from centroid of tube

I = 3.77 in^4, tube moment of inertia

F = 2.725, factor to account for the effect of the small diameter to length ratio on bending for a cantilevered tube. This is obtained for a uniformly loaded beam in Article 7.10 in Roark.

The maximum stress in the tube is:

$$\sigma_b = 52.2 + 2.5 = 54.7 \text{ ksi}$$

The margin of safety is:

$$MS = \frac{S_u}{\sigma_b} - 1 = +0.20$$

where:

S_u = 65.6 ksi, ultimate strength, Type 304 stainless steel, 350°F

2.7.7.13.2 ANSTO Basket Body 30-Foot End Drop Analysis

The inertia load for the LWT for a 30-foot end drop is 60g. The applied load to the ANSTO basket is:

$$P = W \times 60 = 106{,}200 \text{ lbs}$$

where:

W = 1,770 lbs, total weight of the loaded basket, which bounds the calculated value of 1,667 lbs

The minimum cross-sectional area is at the base of the fuel tubes where the cutouts for water drainage are located. The cross-sectional area is:

$$A = \frac{\left[\frac{\pi}{4}\left(D_o^2 - D_i^2\right) \times 6\right]}{2} + \left[\frac{\pi}{4}\left(D_o^2 - D_i^2\right) - 6 \times l_c \times t_t\right] = 5.93 \text{ in}^2$$

where:

D_o = 4.375 inches, tube outer diameter

D_i = 4.125 inches, tube inner diameter

l_c = 1.00 in, cutout length in center tube

t_t = 0.125 in, tube wall thickness

The membrane stress in the basket is:

$$\sigma = \frac{P}{A} = \frac{106{,}200}{5.93} = 17.9 \text{ ksi}$$

The margin of safety is:

$$MS = \frac{0.7S_u}{\sigma} - 1 = +1.5$$

where:

S_u = 65.6 ksi, ultimate strength, Type 304 stainless steel, 350°F

The welds between the support plates and the fuel tube, and the welds between the base plate and the fuel tube for the accident condition are qualified in Section 2.6.12.11.2

Localized buckling of a fuel tube is evaluated using the methodology presented in Blake. The critical stress is:

$$S_{CR} = E\frac{0.605 - 10^{-7}m^2}{m(1+0.004\phi)} = 160.0 \text{ ksi}$$

where:

E = 25.7×10^6 psi, modulus of elasticity, Type 304 stainless steel, 350°F

$$m = \frac{r_m}{t} = \frac{2.125}{0.125} = 17$$

r_m = 2.125 inches, mean radius of fuel tube

t = 0.125 in, fuel tube thickness

$$\phi = \frac{E}{S_y} = \frac{25.7\times10^6}{21{,}800} = 1{,}179$$

S_y = 21.8 ksi, yield strength, Type 304 stainless steel, 350°F

This critical stress, which is required to result in tube buckling, is much larger than the stress of 17.9 ksi for the fuel tube during the 30-foot end drop condition. Therefore, the fuel tube remains stable during the drop.

2.7.7.14 TPBAR Basket with the PWR/BWR Rod Transport Canister

This section provides the structural analysis for the shipment of up to 25 individual TPBARs in the PWR/BWR Rod Transport Canister, the PWR insert and the TPBAR basket under accident conditions. Section 2.7.7.12 provides the structural evaluation of the TPBAR basket with 300 TPBARs, considering a slightly lower content weight (1800 lbs) than the TPBARs in the PWR/BWR Rod Transport Canister configuration (1901 lbs). The effects of the increased weight loading for the TPBAR basket are addressed in this section. The structural evaluation of the PWR/BWR Rod Transport Canister and the PWR insert is presented in Section 2.7.1.7.

TPBAR Basket Body 30-Foot Side Drop Analysis – Accident Condition

The TPBAR basket body is constructed of four machined segments that are held together with aluminum bands at five locations along the axial length of the basket, as well as the top and bottom fittings, which are bolted to the aluminum basket. During a side drop, the TPBAR basket is subjected to bending and bearing stresses. The maximum bending stress occurs at Location 'A' in the following figure and is due to the content weight. The maximum bending stress is calculated using a cantilevered beam. This is conservative since it neglects any support of the load due to the edges of the basket being supported by the cask inner shell. The maximum bending stress is:

$$S_b = \frac{6M}{t^2} = \frac{6 \times 542}{0.5^2} = 13 \text{ ksi}$$

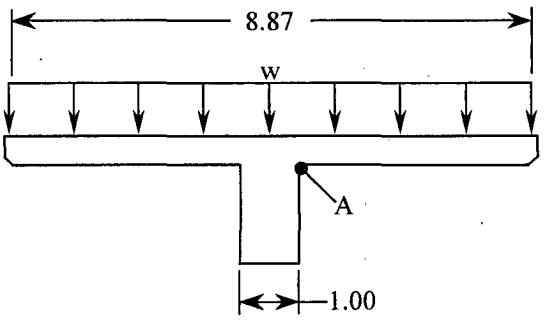

where:

$$w = \frac{W_c \times g}{L \times b} = \frac{1{,}650 \times 60}{159.5 \times 8.87} = 70 \text{ psi}$$, the distributed load of the TPBAR consolidation canister

W_c = 1,650 lb, bounding TPBAR contents weight (with TPBARs, PWR/BWR Rod Transport Canister assembly and the PWR insert)

L = 159.5 in, loadable length of the TPBAR basket

b = 8.87 in, TPBAR basket opening width

g = 60g, side drop acceleration

$$M = w \times \left(\frac{b}{2} - \frac{1}{2}\right) \times \frac{1}{2}\left(\frac{b}{2} - \frac{1}{2}\right)$$

$$= 70\times\left(\frac{8.87}{2}-\frac{1}{2}\right)\times\frac{1}{2}\left(\frac{8.87}{2}-\frac{1}{2}\right)=542 \text{ in-lb/in, the maximum bending moment}$$

t = 0.5 in, thickness of the flange

The margin of safety is

$$MS = \frac{S_u}{S_b}-1=\frac{31.5}{13}-1=+1.42$$

where:

S_u = 31.5 ksi, ultimate strength of 6061-T6 aluminum @300°F

TPBAR Basket – End Drop

In an end drop scenario, the basket is only loaded by its own weight. The TPBAR basket weight is bounded by what was considered for the end drop analysis of the TPBAR basket in Section 2.7.7.12.1. Therefore, the results of the previous analysis are bounding and no further analysis is required.

TPBAR Basket Upper Fitting

The TPBAR basket upper fitting is identical to what was analyzed for the TPBAR basket in Section 2.7.7.12. The TPBAR basket weight and component temperatures considered in Section 2.7.7.12 are conservative. Therefore, the results of the 2.7.7.12 are bounding and no further analysis is required.

TPBAR Basket Lower Fitting

The TPBAR basket lower fitting is identical to the lower fitting of the PWR basket. The weight of the loaded TPBAR basket is less than the weight of the loaded PWR basket. Therefore, no further analysis is required.

PWR Insert

The PWR insert contains the PWR/BWR Rod Transport Canister assembly for insertion into the TPBAR basket. The PWR insert is not a structural component and, therefore, an analysis for accident conditions is not required.

PWR/BWR Rod Transport Canister Assembly Analysis

The PWR/BWR Rod Transport Canister is identical to what was analyzed in Section 2.7.1.7. The fuel weight considered in the Section 2.7.1.7 analysis for the PWR/BWR fuel (350 lbs) bounds the weight of 25 TPBARs in the PWR/BWR Rod Transport Canister (66 lbs). Therefore, no further analysis is required for the PWR/BWR Rod Transport Canister.

Internal Spacer

The internal spacer for the PWR/BWR Rod Transport Canister is identical to what was analyzed in Section 2.7.1.7. The fuel weight considered in the Section 2.7.1.7 analysis for the PWR/BWR fuel (350 lbs) bounds the fuel weight of 25 TPBARs in the PWR/BWR Rod Transport Canister (66 lbs). Therefore, no further analysis is required for the internal spacer.

4×4 and 5×5 Inserts

The 4×4 and 5×5 inserts for the PWR/BWR Rod Transport Canister are identical to what was analyzed in Section 2.7.1.7. The fuel weight considered in the Section 2.7.1.7 analysis for the PWR/BWR fuel (350 lbs) bounds the weight of up to 25 TPBARs in the PWR/BWR Rod Transport Canister (66 lbs max.). Therefore, no further analysis is required for 4×4 and 5×5 inserts.